SEDIMENT AND ASSOCIATED PHOSPHORUS DYNAMICS IN MEANDERING FLOODPLAIN WETLANDS IN THE TSITSA RIVER CATCHMENT: IMPLICATIONS FOR FLOODPLAIN SYSTEMS IN SOUTH AFRICA

A thesis submitted in fulfilment of the requirements for the degree of

DOCTOR OF PHILOSOPHY

of

RHODES UNIVERSITY

by

PIPPA SCHLEGEL

Supervisor: Dr B van der Waal

Co-supervisors: Dr S Grenfell and Dr J Tanner

RHODES UNIVERSITY
Where leaders learn

GEOGRAPHY
RHODES UNIVERSITY

NRF National Research Foundation

ABSTRACT

A key function of floodplain wetlands systems is their ability to remove and store sediments and associated particulates (such as nutrients, organic carbon, and contaminants) from water, thus improving water quality for downstream ecosystems and water users. Increases in sediment and nutrient inputs to drainage networks pose a serious challenge to integrated resource management. These issues can be partly mitigated through natural buffering solutions along drainage networks, such as preserving essential wetland systems like floodplains. However, their trapping efficiency and storage timescales are uncertain. Although a large body of international knowledge and literature has advanced our understanding of river-floodplain systems and the ecosystem services that they provide, the factors determining their likelihood and effectiveness in supplying those regulatory ecosystem services have not been extensively and scientifically tested in floodplain systems in South Africa. This research aimed to describe and quantify the regulatory ecosystem services related to sediment and phosphorus buffering dynamics of two meandering floodplain systems in the Eastern Cape, South Africa. The study examined the geomorphology, sedimentology, and historical rates of sediment and associated phosphorus accumulation and release in the two floodplain systems. These systems varied in their morphometric features, size, catchment location, and predominant land use, providing a diverse range of characteristics. A comparative analysis was conducted between the two systems to understand the influence of local and catchment-scale factors.

Time-averaged suspended sediment samples from the two wetlands were used to compare suspended sediment and associated total phosphorous fluxes over annual scales. Although both floodplains were net depositional during the study period, contemporary suspended sediment mass balance calculations suggested that the relatively larger Minnehaha floodplain system (~1.5 km²) situated in a significantly smaller catchment (~40 km²) had notably higher sediment and associated phosphorus trapping efficiencies of 44 % and 49 % respectively, compared to 16 % and 8 % for the relatively small Gatberg floodplain system (~0.3 km2) situated in a much larger catchment (~135 km²). This variability is attributed to the interaction between annual rainfall regimes, sediment supply, sediment composition, relative wetland size to catchment area and wetland geomorphic character. To test the hypothesis that the suspended sediments and associated total phosphorus were retained by the adjacent floodplain system and to determine which parts of the two floodplains were most effective for retaining suspended sediments and phosphorus, concurrent measurements of sediment accretion were made at 6 sites in different geomorphic features in each of the floodplains. This was achieved using Cesium-137 and Lead-

210 (Hereinafter referred to as ^{137}Cs and ^{210}Pb) dating techniques. In-field observations suggested that all geomorphic units are still active and are frequently inundated during overbank flood flows.

The average overbank sediment deposition and total phosphorus accumulation rates were 9376.9 g-sediment m^{-2} yr^{-1}, 0.8 g-TP m^{-2} yr^{-1} for the Gatberg floodplain and 11802.8 g-sediment m^{-2} yr^{-1}, 1.0 g-TP m^{-2} yr^{-1} for the Minnehaha floodplain. Deposition rates were temporally and spatially highly variable and dependent on the sediment supply, microtopographic relief, sinuosity, distance from the channel, the mode of inundation, and the extent of retention pondage. Overall, high average deposition rates were associated closest to the channel within the proximal floodplain zone (9712.1 g-sediment m^{-2} yr^{-1}, 1.0 g-TP m^{-2} yr^{-1} for the Gatberg floodplain; 13541.1 g-sediment m^{-2} yr^{-1}, 1.0 g-TP m^{-2} yr^{-1} for the Minnehaha floodplain) where the highest D_{50} particle sizes (25.4 µm for the Gatberg and 32.8 µm for the Minnehaha) and percentage sand fractions (15 % and 21 %, respectively) were found. This may reflect the coarse nature of the sediment and the frequent connectivity to the channel, suggesting rapid accumulation is linked to a larger particle size which was deposited more readily in this zone. In the Gatberg system, the backswamp zone had one of the highest sedimentation rates and second highest phosphorus accumulation rates (13806.8 g-sediment m^{-2} yr^{-1}, 0.9 g-TP m^{-2} yr^{-1}). This was attributed to the additional coarse sediment inputs from the uncapped gravel forestry road that runs adjacent to the floodplain margin. In contrast, the backswamp zone within the Minnehaha River floodplain system had the lowest sedimentation rates (2005.9 g-sediment m^{-2} yr^{-1}, 0.1 g-TP m^{-2} yr^{-1}, which is what would be expected for the zone furthest away from the channel. In both floodplains, oxbows were important fine-sediment and phosphorus retention features (7126.0 g-sediment m^{-2} yr^{-1}, 0.6 g-TP m^{-2} yr^{-1} for the Gatberg floodplain; 10101.0 g-sediment m^{-2} yr^{-1}, 1.1 g-TP m^{-2} yr^{-1}). Phosphorus distribution patterns were mainly attributed to variations in organic matter content and iron concentrations in fine-grained sediment deposits, while particle size distributions were less important.

Using a mass balance approach the trapping efficiencies of the two floodplain systems were estimated. The average trapping efficiency for the Gatberg River floodplain accounts for 16 % of the suspended sediment yield (1317.5 tonnes-sediment yr^{-1}) and 8 % of the suspended sediment-associated total phosphorus yield (0.093 tonnes-TP yr^{-1}). Deposition on the Minnehaha floodplain accounts for an average of 44 % (1073.6 tonnes-sediment yr^{-1}) and 49 % of the suspended sediment-associated total phosphorus yield (0.098 tonnes-TP yr^{-1}). Within the Gatberg and Minnehaha River floodplain systems, the sediment sinks (oxbow and backswamp geomorphic zones) accounted for 13 % and 6 % (1070.6 tonnes-sediment yr^{-1} and 0.069 tonnes-TP yr^{-1}); and 28 % and 33 % (683.2 tonnes-sediment yr^{-1} and 0.066 tonnes-TP yr^{-1}),

respectively, of the mean proportion of the total sediment and associated phosphorus yield. The zone of potential exchange (the proximal floodplain geomorphic zone) within the Gatberg floodplain system was calculated to trap 3 % (247.1 tonnes-yr^{-1}) of the mean proportion of the total sediment yield and 2 % (0.023-tonnes yr^{-1}) of the mean proportion of the total associated-phosphorus yield. Within the Minnehaha floodplain, this zone was estimated to trap 16 % (390.4 tonnes-sediment yr^{-1} and 0.032 tonnes-TP yr^{-1}) of the mean proportion of both the total sediment and associated total phosphorus yield. These results indicate the importance of the distal floodplain reaches and oxbows as sediment and phosphorus storage hotspots.

While floodplains mainly result from the accumulation of sediment, they're often modified and altered by erosion processes. Channel erosion and avulsions (e.g. meander bend cutoff events) are natural dynamic processes and form two of the principal processes of meandering river migration. During two wet seasons, both Gatberg and Minnehaha River floodplain areas experienced a mix of deposition and erosion, with slightly higher erosion observed in the Gatberg River reach. Channel bed scouring was prevalent in most cross-sections, suggesting limited sediment accumulation within the main channel beds. Volumetric estimates of sediment loss from meander migration were calculated by analysing cross-sectional data from 2019 and 2021 surveys to determine median and maximum eroded volumes, which were then converted to mass and scaled to tonnes per year for each river's eroded meander bends. The eroded sediment volumes were estimated as 520 tonnes yr^{-1} for the Gatberg and 360 tonnes yr^{-1} for the Minnehaha. The time sequence analysis using historical aerial images (between 1958, 1966, 1993, and 2015) revealed a few channel planform changes due to meander bend cutoff events in both river reaches. These events influence river morphology, increasing local channel slope, reducing sinuosity, and limiting floodplain access while impacting sediment and phosphorus flux. In the Gatberg system, changes in land use, such as increased road density from commercial forestry activities, likely drove channel straightening to accommodate higher sediment and bed loads. In the Minnehaha system, agricultural practices and livestock tracks likely increased sediment loads and hillslope-channel connectivity, driving channel changes. The results from the geochronology of two nested oxbows on the Gatberg floodplain estimated lateral migration rates of ~0.03 m yr^{-1}. The floodplain reworking rates of the Gatberg River floodplain are low compared to other systems in humid regions around the world, although, the Gatberg system compares well with migration rates of rivers in dryland regions.

This study highlights the potential for floodplains undergoing regular flooding to be effective natural buffers along the sediment and phosphorus cascade in dryland landscapes. It enhances our

comprehension of how sediment accumulates over time on floodplains within South African river systems, shedding light on both spatial and temporal patterns. These insights can contribute to better methodologies for evaluating the services provided by floodplain wetlands. These results can inform management decisions by offering a deeper understanding and allowing for the quantification of the cost-benefit of floodplain restoration and preservation actions in South Africa.

Keywords

Sediment processes, total phosphorus dynamics, sediment storage, phosphorus trapping, regulatory ecosystem services, drylands, South Africa.

DECLARATION

I declare that the work contained therein is my original work and that I am the sole author (save to the extent explicitly stated). Neither the whole, nor any part of the thesis, has been, is being, or will be submitted for a higher degree from any other university.

Signature:

Philippa Kirsten Schlegel (Pippa)

ACKNOWLEDGEMENTS

I would like to thank the following people and organisations for their generosity and support, without which, this research would not have been possible:

Firstly, my supervisor, Dr B van der Waal, is sincerely thanked for his support, practicality, curiosity, and questions about the natural world, for giving his time so generously, and for his words of encouragement.

My co-supervisors, Dr SE Grenfell, thank you for creating this opportunity, kindness and encouraging words. Dr J Tanner, thank you for stepping into this process, for your comments and reassurance, and for helping me with funds for the extra time needed to complete this research.

A very special thanks to Emeritus Professor Ian Foster and Dr Atish Vadher of Northampton University for doing the Pb and Cs lab analysis and answering my questions on the subject.

The National Research Foundation, for funding me for the duration of my research.

Thanks must also be made to local landowners, specifically Mr Ty, Mr and Mrs Bouwer, and Mr and Mrs Sephton.

Mr. Dlamini, from the South African Weather Service, and Mr. Volschenk, from the Department of Water and Sanitation, for assisting me in gathering weather data and flow records for the research areas.

Those who helped me collect data in the field; Nicholaus Huchzermeyer, Sibu Pakati, Kenwinn Wiener, and Faeeza Fortune, thank you for persevering and exploring the depths and breadths of these systems with me.

My parents and sister, for their unfaltering love, kindness, and support. Thank you for always believing in me and my abilities.

Nicholaus Huchzermeyer, for your kind words, strength, and love when it was most needed.

TABLE OF CONTENTS

LIST OF FIGURES

LIST OF TABLES

ACRONYMS

^{14}C	Carbon-14
^{137}Cs	Ceasium-137
^{210}Pb	Lead-210
^{222}Rn	Radon-222
^{226}Ra	Radium-226
AI	Aridity Index
Al	Aluminium
AMS	Accelerator Mass Spectrometry
ANOVA	Analysis of variance
ARC-ISCW	The Agricultural Research Council – Institute for Soil, Climate and Weather
BEMLAB	BEMLAB is a SANAS accredited environmental and agricultural laboratory
BP	Before present
Ca	Calcium
CRS	Constant Rate of Supply
Cs	Caesium
CV	Coefficient of Variation
D_{16}	Particle size at which 16% of material is smaller
D_{50}	Average particle size
D_{84}	Particle size at which 84% of material is smaller
DFFE	Department of Forestry, Fisheries, and the Environment
DGPS	Differential Global Positioning System
EDTA	Ethylenediaminetetraacetic acid
Fe	Iron
GIS	Geographic Information System
ICP-OES	Inductively coupled plasma-optical emission spectrometer
KeV	Kiloelectron volt
MAP	Mean Annual Precipitation
MEA	Millennium Ecosystem Assessment
Mg	Magnesium

NFEPA	National Freshwater Ecosystem Priority Area
OP	Organic phosphorus
TP	Total phosphorus
Pb	Lead
PET	Potential Evapotranspiration
R	South African Rand
SANLC	South African National Land Cover
SSY	Suspended sediment yield
UK	United Kingdom
UNEP	United Nations Environment Programme
USA	United States of America
USACE	The United States Army Corps of Engineers

%	Percentage
°	Degree
°C	Degrees Celsius
µm	Micrometre
Bq g^{-1}	Becquerel per gram
cm	Centimetre
cm yr^{-1}	Centimetre per year
g cm^{-2} yr^{-1}	Grams per square centimetre per year
g kg^{-1}	Grams per kilogram
g m^{-2} yr^{-1}	Grams per square meter per year
km^2	Squared kilometre
m	Metre
m.a.s.l	Metres above sea level
m^3s^{-1}	Metres cubed per second
Ma	Million years
mg kg^{-1}	Milligram per kilogram
mm	Millimetre

mm hr^{-1}	Millimetre per hour
r^2	Coefficient of determination
t yr^{-1}	Tonnes per year
US$	United States Dollar
yr	Year

CHAPTER 1 : GENERAL INTRODUCTION

This chapter outlines the motivation for the research, the aims and objectives, and provides a thesis overview.

1.1 INTRODUCTION

Wetlands provide a wide range of functions that benefit downstream ecosystems and society (Millennium Ecosystem Assessment (MEA) 2005), accounting for up to 40 % of the financial benefits, of global ecosystem services (Costanza et al. 1997; Zedler and Kercher 2005; de Groot et al. 2012). Provisioning (e.g., water, fibre, and food supply), regulating (e.g., flood mitigation, water quality improvements, sediment, and nutrient retention), and cultural services (e.g., tourist and recreational activities) are the three broad categories of ecosystem services provided by wetlands (MEA 2005). According to de Groot et al. (2012), a single hectare of palustrine wetland has an annual value of more than US$ 25 600. While the economic valuation of wetlands has been useful in developing legislation for the protection and management of wetlands (e.g., Ramsar Convention) there is a distinct lack of in-depth empirical understanding of key wetland processes and the relationship between ecosystem service provision, especially in South Africa. This has likely contributed to the exploitation and deterioration of wetlands in South Africa (Ellery et al. 2009; Maltby and Acreman 2011; Maila et al. 2017). This trajectory is expected to deteriorate further due to projected water shortages, population expansion, and increased demands on water sources in dryland regions.

The bulk of wetlands in southern Africa are linked with fluvial systems (i.e., alluvial wetlands) due to the macro-scale geomorphic setting (i.e., super-elevated land surface and steep river profiles) and a dry climate (Partridge and Maud 1987; Ellery et al. 2016). This is characteristic of dryland habitats, where high evapotranspiration rates and minimal rainfall prevent the establishment of fluvially disconnected wetlands such as blanket bogs. River systems and the wetlands linked to them are dynamic components of the landscape, playing crucial roles in ecosystem processes. Although rivers are conveyors of sediment and sediment-associated nutrients and contaminants to the oceans, rivers also retain sediment and its associations within the riparian ecosystems along alluvial wetlands, such as floodplains. Floodplains have the potential to act as long-term ($> 10^2$ y) storage.

Floodplain systems in Drylands (Aridity index < 0.65) are dynamic landforms and hotspots of ecosystem service delivery (Tooth et al. 2015; Grenfell et al. 2022), including flood attenuation and water quality improvement by trapping and storing sediment, sediment-associated nutrients, and contaminants.

Floodplain systems also play an important role in the sediment and nutrient budget of the catchment. The ability of wetland systems to provide ecosystem services such as sediment trapping and nutrient assimilation is linked to their geomorphic structure, hydrological circumstances, topographic location, and capacity to retain sediment and its associated components (Brinson et al. 1995; Kotze et al. 2009). Among the various services provided by alluvial wetlands, the regulatory functions related to water quality improvements (such as the sequestration of sediment, nutrients, and contaminants) have been known for many years (Brinson et al. 1984; Johnston 1991; Fisher and Acreman 2004). However, most research on the function of water quality improvement by wetlands has generally concentrated on the chemistry of surface water (Verhoeven et al. 2006; Rebelo et al. 2018; Uwimana et al. 2018). The sediment's regulatory role in water quality improvement has been largely overlooked and remains insufficiently understood particularly in South Africa (de Villiers and Thiart 2007).

Floodplains are formed by the fluvially controlled movement of water and sediment via a river corridor, and the floodplain mosaic and structure governs the exchanges of water, solutes, sediment, and associated nutrients and contaminants between the surface and subsurface, as well as between the surrounding landscape and the floodplain (Wohl 2021). However, accelerated erosion due to catchment mismanagement, land use changes, and climate change has increased the sediment supply in rivers which poses a serious management challenge due to impacts on the physical aspect of rivers and floodplains (e.g., siltation of wetlands) and ecological processes (e.g., habitat mosaics, fish spawning and macroinvertebrate abundance) (Owens et al. 2005; Bilotta and Brazier 2008; Collins et al. 2011).

Fine-cohesive sediments, which include clay and silt-sized particles, are the most chemically active sediment fraction in rivers and wetlands, influencing the removal, storage, and transfer of nutrients (e.g., nitrogen and phosphates) and toxicants (such as herbicides, pesticides, and heavy metals) (Horowitz 1991; Johnston 1991). Nutrient and contaminant concentrations associated with fine sediment are typically several orders of magnitude higher than dissolved elemental concentrations (Horowitz and Elrick 1987; Horowitz 1991), with serious implications for ecological processes and human well-being (Owens et al. 2005). Therefore, the extent to which regulatory functions, such as nutrient and toxicant removal, along with carbon storage, are carried out depends on how effectively floodplains trap sediment and the quality of available sediment (for instance, its organic, geochemical, and textural composition). Given that increasing sediment and associated contaminant fluxes in rivers have become a global problem because of anthropogenic activities (Owens et al. 2005), the role of floodplains and other wetland types in regulating these fluxes between the surrounding landscape, upstream, and downstream systems is

critical, especially in dryland environments where water resources are scarce and heavily utilised. However, despite the general perception that floodplains trap and store sediments along with their associated nutrients and contaminants, few empirical studies have been conducted in South Africa.

1.2 MOTIVATION FOR RESEARCH

Despite extensive global research and literature enhancing our understanding of river-floodplain systems and the ecosystem services that they provide, such as sediment trapping and nutrient assimilation, there hasn't been thorough scientific testing of the factors influencing the probability and efficacy of these regulatory ecosystem services in South African floodplain systems.

This thesis research concentrates on sediment deposition and the associated nutrients, particularly phosphorus, within two floodplain systems: one along the Gatberg River and the other along the lower Minnehaha River in the Eastern Cape of South Africa. These rivers are situated in the upper regions of the Tsitsa River catchment, which is a part of the broader Umzimvubu River catchment. The selection of this research and study area is motivated by several factors:

- Water source areas are those geographical regions that supply a disproportionate amount of mean annual rainfall and runoff that support the growth and development of a large area. The deterioration of water quality and the reduction of flow quantity (due to abstraction or climate change) in these regions can have excessive detrimental impacts on local and downstream ecosystems, users, and economies (Viviroli et al. 2007). Appropriate management of these regions, which often make up a small percentage of the land surface, can help ensure the sustainability of downstream water quality and quantity. In South Africa, this is particularly important due to the country's limited water resources and growing water quality issues. In these areas, wetlands play a vital and critical role. Once thought of as wastelands with no value, wetlands are now seen as natural assets and green infrastructure with many vital functions and services. Wetland conservation and rehabilitation should be the heart of water management. It is necessary to prioritise South Africa’s remaining wetlands such that those that offer valuable ecosystem services and are least impacted by current pressures or threats are offered immediate attention to avoid further loss, conversion, or degradation. To do this, extensive qualitative research must be done.
- The Umzimvubu River System has been nationally ranked as one of the few remaining 'near natural rivers' (NFEPA Assessment 2011); however, it is classified as vulnerable due to high degradation rates in the catchment. The Umzimvubu River catchment has been prioritised as an

important “strategic water source area” and is one of South Africa’s last remaining free-flowing rivers. The catchment of the Tsitsa River (a tributary of the Umzimvubu River) is severely affected by soil erosion, with large areas underlain by dispersive soils and subject to gullying (Le Roux et al. 2008a; 2008b; 2015; Msadala et al. 2010). Overgrazing and frequent fires may have aggravated the problem (Gordon et al. 2013). The communities of the Tsitsa River catchment depend heavily on natural resources and infrastructure. Wetlands and the ecosystem services they provide are vital to improving the quality of water within this catchment. Quantifying and understanding the services provided by wetlands will help prioritise and fund management, protection, and rehabilitation programs.

- National efforts in wetland research have predominantly been focused on mapping and categorising the different wetlands across the country. The different hydrogeomorphic types of wetlands are known to provide a variety of ecosystem services, which justifies such an approach. Undeniably, research has repeatedly demonstrated that ecosystem services have significant economic value, with estimations by de Groot et al. (2012) reaching over US$ 25 600 per year for a single hectare of inland wetlands. Although economic estimates are remarkable, wetland ecosystem services have vital, practical results that have long-term impacts on the lives of those who live adjacent to or downstream of a wetland system. The WET-Ecoservices tool is currently the most widely used assessment methodology in South Africa to estimate the potential of a specific wetland to provide individual services, with the underlying assumption that the range of ecosystem services provided by each wetland is determined by the wetland hydrogeomorphic type (Kotze et al. 2009). To determine the effectiveness of a particular wetland in providing a service, several biophysical parameters (for example, hydroperiod, vegetation type, and cover) are used. However, factors that impact the likelihood and performance of many ecosystem services outlined in the WET-Ecoservices tool have never been empirically verified in South African wetlands. This is the next key step in wetland research in South Africa.
- Geomorphic wetland research in South Africa has focused on understanding the origin and formation of wetlands to increase our knowledge of the long-term development of wetlands in the landscape. The goal of the WET-rehabilitation (part of the larger WET-Management series which includes background information about wetlands and natural resource management, tools that can be used to guide decisions around wetland management, and an evaluation of rehabilitation outcomes in several case studies in South Africa) research initiative was to anticipate the potential efficacy of various rehabilitation measures in specific wetland systems

using knowledge of controls on wetland origin (Dada et al. 2007). Although this strategy has proved itself, we still know relatively little about the geomorphic processes that occur within wetlands, the spatial variability, and the temporal scales at which these processes occur within a wetland.

This data scarcity has created the opportunity for this research to fill this gap in the context of two meandering floodplain systems in the Eastern Cape of South Africa.

1.3 RESEARCH AIM

The research project's overall aim was to understand the sediment and phosphorus dynamics in two dryland meandering floodplain systems in the Eastern Cape, South Africa.

1.4 RESEARCH OBJECTIVES

The following specific objectives were established for the research:

- Classify, map, and characterise potential sediment and phosphorus sources and buffers and their connectivity in the two river catchments, to create a spatial understanding of the potential sediment and phosphorus dynamics upstream of the two floodplain systems.
- Investigate the spatial variability of sediment and phosphorus composition of the riverbeds, banks, and recently deposited floodplain sediment, to explore the relationship of these factors with the geomorphological characteristics of the two floodplain systems.
- Quantify and characterise the historical sedimentation and phosphorus storage rates and trapping efficiencies and the effect that geomorphology has on these values within the two floodplain systems, to make a partial sediment and phosphorus budget with a historical dimension.
- Estimate and describe the contemporary channel erosion and deposition, explore the historical channel change, estimate lateral migration rates, and investigate the channel's potential for future change and how this affects sediment and phosphorus patterns and dynamics in the two floodplains.

1.5 THESIS STRUCTURE

Chapter 1 defines the research project by outlining the circumstances that drove the research activities, as well as the challenges that moulded the methodology and activities conducted to obtain the targeted aim and objectives.

Chapter 2 covers the literature on factors and processes that may influence sediment and associated nutrient (phosphorus) deposition on floodplains and forms the basis on which the research project was built. This chapter includes a published literature review journal article (Wiener et al. 2022).

Chapter 3 describes the attributes of the study area, providing the environmental and socio-economic context for the research.

Chapter 4 analyses the potential sources of sediment and phosphorus, connectivity, and buffers in the Gatberg and Minnehaha River catchments.

Chapter 5 describes the spatial variability of sediment and phosphorus composition of the channels' beds and banks (cut banks and point bars) and the recently deposited sediment exploring the relationships and patterns between the sediment characteristics within the two meandering channels and across the surface of the two floodplain systems.

Chapter 6 focuses on characterising and quantifying sediment and phosphorus storage within the two floodplain systems and allocates storage amounts based on depositional geomorphic units within the floodplains. This chapter also quantifies the trapping efficiencies of the two floodplain systems based on the sediment and phosphorus yield values.

Chapter 7 estimates and describes contemporary channel erosion and deposition, explores the historical channel change, estimates lateral migration rates, and investigates the potential of the two channels for future change.

Chapter 8 synthesises the literature review and the findings of Chapters 4 to 7. Chapter 8 highlights the contribution of this research to understanding sediment trapping and phosphorus assimilation ecosystem services, as well as their dynamics along the Transkei Drakensberg Escarpment, gives the limitations of this research, and highlights recommendations for further research.

CHAPTER 2 : LITERATURE REVIEW AND KEY CONCEPTS

Published review paper: Wiener, KD; Schlegel, PK; Grenfell, SE; van der Waal, B. 2022. Contextualising sediment trapping and phosphorus removal regulating services: a critical review of the influence of spatial and temporal variability in geomorphic processes in alluvial wetlands in drylands. Wetlands Ecology and Management. https://doi.org/10.1007/s11273-022-09861-9. Author Contributions Conceptualization: KW and SG; Writing- original draft preparation: KW (all sections except 2.3) and PS (Sect. Sediment trapping in meandering river floodplains: processes of accretion and erosion); Writing- review and editing: SG, BvdW, PS and KW; Funding acquisition: SG; Supervision: SG and BvdW. All authors have read and given approval for the publication of the manuscript. The work in this thesis is original work.

2.1 INTRODUCTION

River systems are active elements of the landscape, playing vital roles in ecosystem processes. Although rivers are conveyors of sediment and sediment-associated nutrients and contaminants to the oceans, rivers also retain sediment and its associations within the riparian ecosystems along floodplains. Floodplains have the potential to act as long-term (> 10^2 y) storage.

Floodplain systems in Drylands are dynamic landforms and hotspots of ecosystem service delivery, including flood attenuation, and water quality improvement by trapping and storing sediment and sediment-associated nutrients and contaminants. Floodplain systems also play an important role in the sediment budget of the catchment. This review focuses on meandering floodplain systems in drylands with particular attention to the long-term resilience of ecosystem services associated with sediment trapping and storage in these systems. First, this review will examine the mechanisms and factors influencing sediment and sediment-associated nutrient deposition and storage. Then erosion and sediment recycling will be explored. The global rates of sediment accretion within meandering floodplain systems will be critically evaluated, where a comparison will be drawn between humid/ temperate zones and their drier counterparts. The biochemical cycling of sediment-associated phosphorus in floodplain systems will be considered. In conclusion, the effects of drylands on sediment trapping and sediment-associated phosphorus attenuation will be explored.

2.2 FLOODPLAIN FORMS

Rivers are primarily hydrological units that redistribute water across the Earth's surfaces and deliver most of this water to the oceans (Phillips 2009). Sediment dynamics as such are a by-product of hydrological processes, however, the role of rivers in entraining, transporting, and storing sediment is of key interest to geomorphologists. This sediment redistribution maintains or changes the morphology of the land

surfaces of the Earth. Floodplains are integral components of alluvial river systems. Where water and sediment interact with the terrestrial environment affecting the rivers' conveyance system of water and sediment. The floodplain part of the river system is activated when water overtops the channel banks, exceeding the capacity of the channel, and flows across the adjacent land surface. Areas adjacent to the channel banks are often referred to as the proximal floodplain, while areas furthest from the channel, adjacent to the valley margins, are termed the distal floodplain (Figure 2.1). In between the two areas, where deposits of fine sediments settle after a flood, creating a marsh-like environment, is called the backswamp. Floodplains are often poorly drained, acting as settling basins in which fine-grained suspended-load sediments settle out from overbank flows and are stored on the land surface.

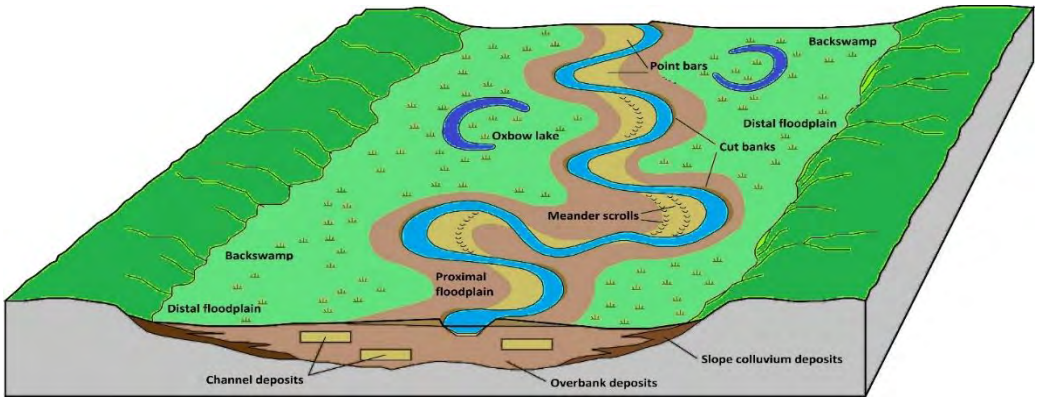

Figure 2.1 General floodplain features (adapted from Gabler et al. 2007)

The occurrence of floodplains along a longitudinal profile indicates a change in the dominant processes along an energy gradient. This change reflects a shift from source-zone activity, of within-channel processes of erosion and transport of materials with sporadic short-term stores of coarse sediment, to transfer-zone activity, in which out-of-channel processes create floodplain sediment stores (Schumm 1977). Sediment settles out of suspension and is stored on floodplain surfaces due to the low gradient that characterises floodplains and the greater accommodation space. These two characteristics, as well as highly vegetated surfaces, promote the reduction of energy, allowing suspended-load materials time to settle out and be stored within the floodplain. In the transfer zone along a river corridor, floodplains typically occur as isolated pockets within partly confined valleys with low gradients (Wohl 2021). Initially, floodplain pockets can be controlled by bedrock, where sediments are trapped behind bedrock outcrops or at sites of local valley widening (e.g., at tributary confluences) (McCarthy et al. 2002; Tooth et al. 2002; Ellery et al. 2009; Grenfell et al. 2010). Eventually, these pockets alternate, as the river switches from one side of the valley to the other, creating planform-controlled floodplain pockets within partly confined

valley settings. There may be significant pocket-to-pocket variability in floodplain forms due to a range of localised controls such as changes in the nature/degree of valley confinement or differing flow alignments over floodplain surfaces in response to changes in valley or channel alignment. As the slope decreases downstream and the valley widens further, floodplain pockets become more frequent, eventually becoming continuous along both banks in laterally unconfined valleys of the accumulation zone. In these settings, the river flows within its deposits (i.e., fully alluvial rivers).

2.3 SEDIMENT ACCRETION MECHANISMS IN MEANDERING RIVER SYSTEMS

Floodplain systems can be made up of a composite of different types of sediment (Nanson and Croke 1992). Firstly, the basal parts of floodplains usually are made up of bedload deposits, and larger-sized sediments such as boulders, pebbles, or gravels. These materials may be launched onto floodplain surfaces during high-energy flood events, or they may be deposited within the river as channel bars. Suspended-load deposits of well-sorted sand-sized sediments, transported by saltation, are regularly deposited above the bedload deposits and are transported further onto the floodplain surface. Finally, suspended-load deposits of fine-grained sediment (silt, clay, fine sand, as well as any particles that are associated with fine materials, for example, organics, nutrients, or contaminants) comprise the bulk of most floodplain deposits. These sediments settle out from suspension in backwater areas and low-velocity zones on the floodplain such as old floodplain features (e.g., oxbows or abandoned channels), or the backswamp. Lateral and vertical accretion (see sections 2.3.1 and 2.3.4) are the primary processes that form and maintain floodplain systems (Rhoads 2020). Related to this, the less prominent mechanisms include oblique accretion (see section 2.3.2; Page et al. 2003), counterpoint accretion (see section 2.3.3; Nanson and Croke 1992; Smith et al. 2009), and accretion that occurs in old floodplain features (section 2.3.5; Toonen et al. 2012). Each of these floodplain accretion processes is described below (Figure 2.2). The degree to which these different processes influence floodplain development varies both with differences in fluvial morphology and with temporal variability in discharge and sediment supply (Rhoads 2020).

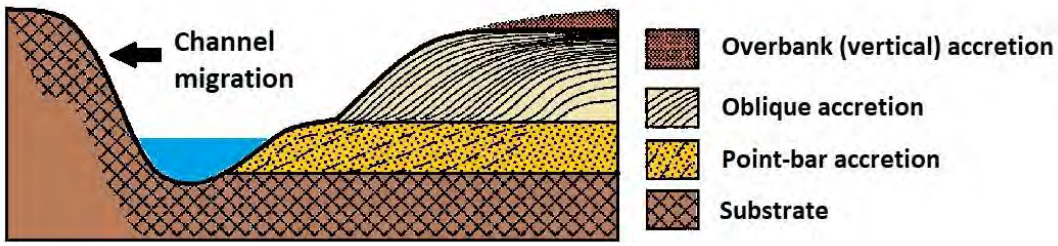

Figure 2.2 Schematic floodplain cross-section showing the different depositional processes (from Page et al. 2003)

2.3.1 LATERAL ACCRETION

Lateral accretion occurs when the bedload or suspended load is deposited in the low energy margins of the channel banks and is incorporated into the floodplain surface through progressive lateral and downstream migration of meandering rivers. Lateral accretion can occur below the bankfull stage because it involves deposition on within-channel bars (Rhoads 2020). In meandering rivers, progressive migration of the outer bank through erosion is typically balanced by deposition on the inner bank as point bars (Sundborg 1956; Wolman and Leopold 1957; Ritter et al. 1975; Jackson 1976; Nanson 1980).

Research has shown that flow velocities along meander bends are nonuniform, where higher velocities and erosion are typically concentrated along the bank of the convex (outer) bend, and deposition and slower velocities are concentrated along the inner concave bank creating helicoidal flow (Hooke 1975; Bridge and Jarvis 1976; Dietrich et al. 1979; Dietrich and Smith 1983, 1984). The power of the helicoidal flow depends on water depth, bend radius and friction of the banks and bed. This results in sections of flow being deflected from the thalweg as the flow travels around the bend. This creates a shear stress zone along the convex (outer) bank, which transports sediment from the thalweg to the point bar. Generally, the point bar consists of a sloping face that extends into the thalweg flattening out closer to the inner bank (Nanson 1980). Usually, point bars lie slightly below the elevation of the floodplain surface. The sedimentological structure of point bars begins with the aggradation of relatively coarse-grained sediment at the bar head that fines as you move through the sequence and the lateral accretion of migrating transverse unit bars (Lewin 1978; Peakall et al. 2007). This leads to the distinctive stratigraphy of point bars which are characterised by large-scale inclined strata (Bridge et al. 1995; Leclerc and Hickin 1997; Sambrook Smith et al. 2016). Experimental studies by van de Lageweg et al. (2014), showed that lateral accretion of the point bar occurs largely in response to the erosion of the outer bank, which results in local widening of the channel and deposition of bedload on the point bar face. Scroll bars develop when the point bar is inundated at flows slightly below or near the bankfull stage. Vertical accretion by migrating bedforms (Jackson 1976; Bridge et al. 1986) or by deposition of suspended sand (Nanson 1980) builds a scroll bar, on the point bar platform during these events. This variation can lead to a range of floodplain morphologies, from minimal surface variation to intricately formed scroll patterns (Nanson 1980).

2.3.2 OBLIQUE ACCRETION

In slowly meandering river systems, both lateral and oblique accretion occur on the concave gentle-sloping channel margins when suspended sediment settles out. However, oblique accretion deposits occur as predominantly clay and silt in low-energy systems where deposits are draped over lateral

deposits and are in a sense transitional between lateral and vertical deposits (Page et al. 2003). Successive deposition of alternating layers of sand and muddy fines on the inner bank as the channel migrates creates highly inclined (> 20°) layers (Rhoads 2020). Oblique accretion in some floodplain systems can be very effective at trapping suspended sediment prone to deposition near the channel margin. This limits vertical accretion to distal parts of the floodplain surface. Page et al. (2003) showed that in the Murrumbidgee River oblique accretion contributes more than 65 % of the floodplain sediments. Nanson and Croke (1992) and Page et al. (2003) further suggest that this could be the case for other low-energy, mixed-load, and suspended sediment-load alluvial rivers.

2.3.3 COUNTERPOINT ACCRETION

Another form of lateral accretion called counterpoint accretion (Nanson and Croke 1992) or counter-point-bar deposition (Smith et al. 2009), can also occur along the outer bank upstream of the apex of sharp bends in conjunction with the occurrence of low-velocity flow or stagnation at this location (Carey 1969; Woodyer 1975; Hickin 1979; Thome and Lewin 1979; Page and Nanson 1982; Lewin 1983; Makaske and Weerts 2005; Smith et al. 2009, 2011). This depositional process produces fine-grained concave bank benches, which, once formed, usually become vegetated. Bench growth is further enhanced by the establishment of vegetation, which increases the likelihood of suspended sediment deposition (Page and Nanson 1982; Schnauder and Sukhodolov 2012). The benches, which consist mainly of a mixture of silt, clay, or fine sand, and organic material resulting from the deposition of suspended sediment within a low-velocity environment, may eventually increase in height to just below the level of the floodplain (Page and Nanson 1982). Studies conducted by Makaske and Weerts (2005) and Smith et al. (2009) showed that counterpoint bar formation often takes place under conditions where a river encounters erosion-resistant material in an outer bank in a sharp meander bend.

2.3.4 VERTICAL ACCRETION

Vertical accretion requires flow to exceed bankfull capacity for sediment to be transported over the bank and deposited on the floodplain surface. Research has shown that vertical accretion is the dominant process along various low-gradient single-thread channels (Beckinsale and Richardson 1964; Schumm 1968; Ritter et al. 1975; Rose et al. 1980; Nanson and Young 1981; Burrin and Scaife 1984; Burrin 1985) and some anastomosing channels (Smith 1971, 1974; Smith and Smith 1980) where channel migration is restricted due to insufficient stream power (Nanson and Croke 1992). The most active vertical accretion environments occur along high-energy channels with sandy floodplains that can be destroyed

catastrophically by large floods and subsequently reconstructed predominantly by overbank deposition (Schumm and Lichty 1963; Burkham 1972; Nanson 1986).

Two primary processes contribute to the transport of suspended sediment onto floodplains: lateral turbulent diffusion and lateral advection. Lateral turbulent diffusion occurs due to significant variations in velocity and sediment concentration between the main channel flow and the flow across the floodplain. This difference creates a shear layer at the channel-floodplain interface, where turbulent vortices transfer momentum and sediment between the channel and floodplain (Knight and Shiono 1990; Carling et al. 2002; Rhoads 2020). Due to the greater sediment-transport capacity and suspended sediment concentration within the main channel, a net transport of suspended sediment occurs toward the floodplain (Rhoads 2020). The reduced transport capacity of the unconfined sheet-like flow on the floodplain relative to the deeper and faster flow in the main channel, in turn, leads to the deposition of suspended sediment. The deposition of suspended load materials vertically builds the floodplain over time. In general, these fine-grained, horizontally bedded, suspended-load materials dominate floodplain sequences beyond the active channel zone. In many instances, vertical accretion deposits overlie lateral accretion deposits.

Two forms of sediment sorting patterns commonly characterise vertical accretion deposits: distal and vertical fining. When the flow overtops the channel banks, the coarsest suspended-load sediments are deposited at the channel margins within the proximal floodplain. Finer-grained sediments are progressively deposited with distance from the channel due to the decreasing transport capacity of the flow, which is consistent with observations in the Tshwane-Pienaars River (Larkin et al. 2017), the Waal River (Walling et al. 2010), and the Strickland River (Swanson 2013). This proximal-distal gradation in sediment particle size is described as distal fining (He and Walling 1996; Walling et al. 1996, 1998, 2003; Wang et al. 2020). Vertical accretion deposits also grade with depth. This process is typically illustrated by repeated cycles of flood couplets that fine upward. Each flood event leaves behind deposits that mirror the rising and falling stages of flow across the floodplain. Analysing these sediment sequences enables the interpretation of flow conditions during overbank events, providing insights into the history and rate of floodplain accumulation (Rhoads 2020).

Vertical accretion of a floodplain is a self-limiting process as ongoing accretion builds elevation which reduces the frequency of floodplain inundation and overbank sedimentation (Wolman and Leopold 1957; Moody and Troutman 2000). However, as lateral channel migration occurs, bank erosion can reintroduce

sediment into the channel, offsetting bar accretion on the opposite bank and thereby counteracting overbank deposition elsewhere.

2.3.5 Old floodplain features accretion

Old floodplain feature accretion occurs when overbank deposits accumulate vertically in floodplain features such as paleochannels, cutoffs, and oxbows, during overbank flow. The primary mechanism of meander bend abandonment is neck cutoff. Neck cutoff occurs late in the development of meander bends. This occurs by cutting a new channel across the narrow neck of the meander bend or through the capture of one bend by the next upstream. The end of the cutoff is rapidly filled by bedload sediment to create an oxbow. These features have well-defined morphologies. Overbank flows generate upward-fining particle size trends within abandoned channel fills. Over time, progressively larger flows are required to fill the abandoned channel. The nature of the sediment that fills abandoned channels, especially clay plugs, can resist subsequent movement of the channel, affecting the morphology of the meander bend and the migratory pathways on the valley floor (Toonen et al. 2012). In general, once an oxbow is created, sedimentation rates within the oxbow depend on the connectivity between the main channel and the oxbow, the depth of water in the oxbow, the alignment of the oxbow to the main channel, the geometry and position of the oxbow on the floodplain, the overbank flow frequency, the sediment concentration of the overbank flows, and the distance of different locations within the oxbow from the main channel. Sedimentation in oxbows usually consists of finer sediments (silts and clays; Fisk 1947; Saucier 1994; Toonen et al. 2012; Ishii and Hori 2016), however, sand deposits are not uncommon (Erskine et al. 1992; Hooke 1995). In many instances, abandoned channel fills can be excavated to reconstruct paleo-channel dimensions in river evolution analyses.

The rates of infilling of floodplain features range from a few millimetres per year to several centimetres per year. Generally, rates decline over time as the floodplain features fill with sediment (Hooke 1995). Migration of the river away from an oxbow can decrease sedimentation rates, while changes in land use, such as clearing of forests and implementation of agriculture on floodplains, which increases the frequency of overbank flows, can increase sedimentation rates (Erskine et al. 1992; Wren et al. 2008).

2.4 Factors influencing sediment and nutrient deposition and storage

Information on floodplain processes is essential to understand the geomorphic origin and evolution of floodplains and to restore, maintain, and manage floodplain ecosystems. Overbank sedimentation influences downstream sediment loads and sediment-associated nutrients and contaminants (Walling

and Owens 2003). The accumulation of the loads of fine sediment on floodplains increases floodplain elevations and modifies the frequency of inundation and the capacity of channel conveyance (Benjankar and Yager 2012). Furthermore, sediment deposition creates important riparian habitats and replenishes sediment-associated nutrients (Noe and Hupp 2009).

Overbank floodplain sedimentation rates are influenced by floodplain topography, distance from the channel, local hydraulics, vegetation characteristics (density, height, and growth form), flood characteristics (frequency and duration), sediment supply (suspended sediment concentration) and depositional processes (Nicholas and Walling 1997, 1998).

Floodplain microtopography, consisting of hummocks and hollows (Barry et al. 1996; Day et al. 2008), can have a significant impact on the elevation of the floodplain, which in turn affects the spatial and temporal flood patterns, frequency, and duration across a floodplain surface. Research done in floodplain forests in North Carolina by Bledsoe and Shear (2000) found that a change in elevation of as little as 10 cm resulted in a 20 % difference in flooding frequency during the growing season. Microtopography creates spatial and temporal variability in plant communities and productivity (Titus 1990), soil types and properties (Stolt et al. 2001), biogeochemical processes (Schilling and Lockaby 2005), and nutrient cycling (Courtwright and Findley 2011; Bannister et al. 2014). Hummocks and other higher-elevation microsites are important areas for the colonisation of woody species (Titus 1990; Vivian-Smith 1997).

In a study comparing various floodplain plant types on sediment deposition, Olde Venterink et al. (2006) observed higher rates of deposition on floodplains dominated by *Phragmites australis* reed beds compared to those covered by agricultural grassland and woodlands. This difference was attributed to the robust nature, density, and height of the reeds. A two-year study conducted by Sánchez-Carrillo et al. (2001) on a semiarid floodplain wetland in Central Spain revealed that seasonal variations in vegetation growth and fluctuations in vegetation coverage aligned with patterns of sediment accumulation and storage. Additionally, the authors noted that changes in water levels and flow accounted for only a relatively small proportion of the variation in sediment accumulation and storage. Research conducted by Batson et al. (2015) demonstrated strong connections between vegetation and nutrient and sediment cycling processes at both the plot and longitudinal scales in a forested floodplain in Piedmont, Virginia, USA. However, these connections were not reflected in the relationships between these aspects and floodplain geomorphic features, such as levees, backswamp, and toe-slopes. Furthermore, the study revealed that sediment trapping increased with higher coverage of herbaceous plants and lower density of tree canopy, indicative of a vegetation community more tolerant to water. Despite the impact of

urbanisation on hydrology, the forested floodplain was found to function as an effective sediment and nutrient trap (Batson et al. 2015).

Another well-established factor that affects sediment deposition and in turn sedimentation rates is the distance from the sediment source, the channel. Research has shown that sediment deposition rates decrease across the floodplain with distance from the channel (consistent with observations in the Tshwane-Pienaars River (Larkin et al. 2017), the Waal River (Walling et al. 2011), and the Strickland River (Swanson et al. 2008). In a study in southeast France by Brunet et al. (1994), it was found that deposition of sediment was 50 times higher in the riparian zone, between 10 - 50 m from the channel than further away from the channel.

Patterns of floodplain sedimentation rates are influenced by sediment supply, flood frequency and duration, and flood water residence time. An increase in all the factors mentioned will increase the amount of sediment that is deposited on the floodplain (Walling and He 1997; He and Walling 1998; Middelkoop and Van der Perk 1998; Van Der Lee et al. 2004; Kronvang et al. 2007). High deposition rates will occur at low elevations that are frequently fluvially inundated for long periods (Nicholas and Walling 1998; Aalto et al. 2003), until a certain threshold when erosion is initiated or if the floodplain is filled with water, which in turn will create a shear layer hindering sediment from settling out of suspension.

2.5 ACCRETION RATES IN FLOODPLAIN SYSTEMS

The study of floodplain deposition has gained interest due to the increasing awareness of the geological, geomorphological, environmental, and social significance of sediment deposition, transport, and storage. Floodplain deposition is now known as a key component in the sediment budgets of catchments because floodplains form key interrupters of the sediment conveyance system, whereby suspended sediment may be stored for significant lengths of time (Walling 1983; Walling et al. 1998). Previous studies of sediment accretion rates in wetlands have focused mainly on floodplain wetlands in humid climatic regions (Aridity index (AI) > 0.65); whereas there are only a few studies in dryland regions (AI < 0.65; UNEP 1997). The Aridity Index, adopted by the United Nations Environmental Program (UNEP) in 1992), is a numerical measure of how dry the climate is at a specific location and is defined as the ratio between average annual precipitation and potential evapotranspiration.

Contemporary floodplain sedimentation rates (for the last ~100 years) reported in the literature generally range from a few millimetres to a couple of centimetres per year, and maximum values have been observed during extreme flood events (see Simm 1995; Terry et al. 2002). Significant differences in

sedimentation rates can be observed for floodplain surfaces in dryland regions, ranging from 0.01 to 1.21 cm yr^{-1}, and humid regions, ranging from 0.01 to 5.99 cm yr^{-1} (Table 2.1). Sedimentation rates in floodplain features, such as abandoned channels, cutoffs, and oxbows, depict considerable variety (Table 2.2). Values for sedimentation rates within floodplain features range from 0.003 to 3 cm yr^{-1} (Table 2.2). However, upon examination of the variety in sedimentation rates, for example in South African systems (within a narrow climate band with AI ranging from 0.27 to 0.28) sedimentation rates range from 0.01 to 1.15 cm yr^{-1} (Table 2.2), it suggests that vertical sediment accretion rates are not solely controlled by climate variability. Other floodplain factors such as distance from the channel, microtopography of the floodplain, local base level, catchment area, valley slope, sediment supply, vegetation structure and composition, lateral migration and bank erosion may play a significant role in the variability of sedimentation rates (Tooth et al. 2007; Keen-Zebert et al. 2013). Similarly, Craft et al. (2017) found that long-term sediment accumulation in Midwestern USA floodplain wetlands was up to 50 % higher than the rates measured in a floodplain wetland in the South Bohemian Region of Czechia, despite similar climates. This was ascribed to the differences in catchment land use intensity and the resulting suspended sediment supply. Another factor that may contribute to variable sedimentation rates is the wide range and accuracy of dating and field sampling techniques.

Humans and their impacts on the environment have changed the sediment deposition rates of many floodplain systems around the world. Research conducted on forested floodplains in the humid lowlands and foothills of eastern USA observed long-term sedimentation rates (> 100 years) ranging from 0.001 to 0.3 g cm^{-2} yr^{-1} (Kleiss 1996; Craft and Casey 2000; Bannister et al. 2015). Whereas contemporary accumulation rates for the same region ranged between 0.01 to 2.67 g cm^{-2} yr^{-1} (Hupp et al. 2013; Gillespi et al. 2018). This could be attributed to widespread changes in land use and anthropogenic changes in catchments, rivers, and floodplains where local hydrodynamics (e.g., runoff and flow patterns) and sediment regimes have been modified.

Dryland floodplain systems have a considerably lower and narrower range of accumulation rates compared to humid regions. This may be attributed to high seasonality and interannual variability in flow, variable sediment supply and higher evapotranspiration, which in turn decreases inundation extent and duration, and discontinuities in downstream water and sediment transport due to climate (McCarthy et al. 2011).

Although sedimentation deposition rates are frequently low and, in some cases, almost indiscernible, substantial amounts may be deposited when large areas, which usually characterise floodplain systems,

are involved (Walling and Owens 2003). As a result of the overbank deposition, floodplains may trap and store a significant part of the suspended sediment load of a river system. Several existing studies have shown that between 10 and 60 % of suspended sediments in the annual load entering the river system do not reach the outlet (e.g., Trimble 1983; Lambert and Walling 1986; Phillips 1989; Walling and Quine 1992; Campo and Desloges 1994; Mertes 1994; Allison et al. 1998; Goodbred and Kuehl 1998; Owens et al. 1999; Walling et al. 2003). When excluding anthropogenic storage units (e.g., reservoirs), this discrepancy can be accounted for by lateral accretion (point bar, scroll bar and oblique accretion). Research by Moody (2019) on the Powder River in South-eastern Montana, USA, found that point bars are about two times more efficient in trapping sediment than floodplains. Likewise, Walling et al. (1998) and Owens et al. (1999) estimated that channel storage was between 10 and 50 % of the annual suspended sediment load delivered to the main channel for the Ouse, Wharfe and Tweed rivers, in the United Kingdom. In contrast with channel-bed storage where the residence time of sediments is usually in the order of a year to a couple of years, sediment deposited on the floodplain may remain stored for decades to centuries before re-entering the river system due to channel migration or floodplain surface erosion (see section 2.6).

Table 2.1 Published sedimentation rates for floodplain wetlands ordered according to UNEP aridity index

Region	Source	Location	Aridity Index	Rates (cm yr^{-1})
Dryland regions (Aridity Index <0.65)	Omengo et al. (2016)	Lower Tana River, Kenya	0.18	1.15-1.21
	Cabezas et al. (2010)	Ebro River, Spain	0.25	0.57
	McCarthy et al. (2011)	Nyl River, South Africa	0.27	0.01
	Larkin et al. (2017)	Tshwane-Pienaars River, South Africa	0.28	0.02-1.15
	Hughes et al. (2009)	Theresa Creek, Australia	0.28	0.07 (±0.02)- 0.21 (±0.01)
	Xu (1998)	Yellow River, China	0.45	0.2-0.3
Humid regions (Aridity Index >0.65)	He and Walling (1996)	River Stour, United Kingdom	0.72	0.83
	Knox (2006)	Upper Mississippi River	0.76	0.2-2
	Saxena et al. (2002)	Yamuna River, India	0.76	2.48-5.99
	Owens et al. (1999)	River Ouse, United Kingdom	0.78	0.11-1.04
	Owens et al. (2013)	James River, Missouri, USA	0.90	0.19-0.69
	Hobo et al. (2010)	Lower Rhine River, Netherlands	0.92	0.02-2.5
	Wallinga et al. (2010)	River Waal, Netherlands	0.96	0.3-0.8
	Walling et al. (1996)	River Culm, United Kingdom	1.09	0.32
	Goodbred and Kuehl (1998)	Ganges-Brahmaputra River, Bangladesh	1.11	0.03 (0.06)- 0.27 (0.13)
	He and Walling (1996)	River Severn, United Kingdom	1.17	0.86
	He and Walling (1996)	River Exe, United Kingdom	1.24	0.45
	Saint-Laurent et al. (2010)	St Lawrence River, southern Québec	1.50	0.01-0.1
	Froehlich and Walling (2006)	Teesta River, India	1.95	0.21-3.56
	Aalto et al. (2008)	Strickland River, Papua New Guinea	2.15	1.6
	Swanson (2013) Day et al. (2008)	Fly River, Papua New Guinea	2.30	0.13-0.2

Table 2.2 Published sedimentation rates for oxbows and other floodplain surface features ordered according to UNEP aridity index

Region	Source	Location	Aridity Index	Rates (cm yr^{-1})
Dryland regions (Aridity Index <0.65)	Gell et al. (2005; 2006)	Oxbows on the Murray River, Australia	0.12	0.09-3
	Cabezas et al. (2010)	Oxbows on the Ebro River, Spain	0.25	1.57-2.07
	Larkin et al. (2017)	Abandoned channels on the Tshwane-Pienaars River, South Africa	0.28	0.3-0.74
	Gell and Little (2006)	Oxbows on the Murrumbidgee River, Australia	0.33	0.6
	Keen-Zebert et al. (2013)	Abandoned channels on the Klip River, South Africa	0.34	0.003-0.008
	Erskine et al. (1992)	Four oxbow cutoffs along the lower Hunter River in Australia	0.35	0.45-1.4
Humid regions (Aridity Index >0.65)	Davidson et al. (2004)	Oxbows on the Upper Mississippi River	0.76	0.02-1.3
	McGlue et al. (2011)	Floodplain lakes on the Pantanal, Upper Paraguay River, Brazil	0.78	0.11-0.24
	Piegay et al. (2009)	14 cutoffs, Ain River, France	1.20	0.065-0.24
	Citterio and Piegay (2009)	39 cutoffs in south-eastern France	1.40	0-0.26
	Ishii and Hori (2016)	Four cutoffs, Ishikari, lowland, Japan	1.50	0.04-0.09
	Oestreicher et al. (2016)	Floodplain lakes on the Tapajós River (Tributary of the Amazon River), Brazil	3.50	0.11-1.25
	Lewis and Lewin (1983)	92 cutoffs in Wales, UK		0.03-0.71

2.6 EROSION AND RECYCLING

Although floodplains develop through the accumulation of alluvium, and as such are depositional features along the river system, they are often shaped and modified by erosional processes once formed (Rhoads 2020). Main floodplain erosional processes involve: i) lateral migration of cut banks and associated shaving of floodplains, ii) stripping of floodplain surfaces, iii) carving of secondary channels into floodplain surfaces, and iv) avulsion of the main flow to another area on the floodplain. As with depositional processes, the efficacy of erosional processes varies geographically, with river type, climate, vegetation cover, geomorphology, and critical fluvial parameters (e.g., gradient, sediment particle size, stream power and shear stress; Hupp et al. 2009). Floodplains of rivers with high stream power, that transport coarse bed material, are more likely to experience an erosional change in shorter temporal scales in comparison to rivers with low stream power, transporting and depositing suspended sediment (Rhoads 2020). Erosional processes have a multitude of impacts on floodplain systems, for example, the building of the sediment stratigraphy (Paola et al. 2001; Martin et al. 2009; Straub et al. 2013), the storage time of sediment on floodplains (Nakamura and Kikuchi 1996; Bradley and Tucker 2013; Torres et al. 2017) or in the creation or removal of fluvial terraces (Limaye and Lamb 2016; Malatesta et al. 2017). The erosion of the floodplain directly affects habitats (Shields et al. 2002), land use potential, and flooding hazards (Hutton and Haque 2004).

2.6.1 LATERAL MIGRATION

Lateral migration of a river often governs the spatial pattern and rate of sediment deposition and delivery (Aalto et al. 2008), and as such, it has important consequences for geochemical cycling (Billen et al. 1991) and nutrient and contaminant remobilisation and transport (Marcus et al. 2001; Papacostas et al. 2008).

Two key processes involved in river bend migration are floodplain shaving and bend extension (Lauer and Parker 2008). These two processes transfer sediment from floodplains to the channels. Floodplain shaving occurs due to the height difference between the inner (lateral deposition) bank and the outer (vertical accretion and cut) bank along bends (Rhoads 2020). The inner bank is typically lower than the outer bank, due to vertical growth by long-term overbank deposition. As the higher, outer bank is eroded, floodplain sediment is transported to the channel that is not directly replaced on the inner bank by lateral and vertical accretion (Rhoads 2020). In conjunction, the crust of the floodplain is 'shaved' off along the inner bend.

The second process of lateral migration is bend-extension. Bend extension elongates the channel, and if the channel width and depth are kept constant, it increases the volume of sediment eroded by the channel, reducing floodplain storage. Floodplain erosion by bend extension is restricted by meander bend cutoff events, which shorten the length of a meandering river. However, meander bend cutoff events frequently develop quickly and large amounts of sediment from the floodplain are eroded (Zinger et al. 2011), whereas the deposition and accretion of oxbows take much longer (centuries to millennia; Dieras et al. 2013). Lauer and Parker (2008) estimated that for four rivers in the USA, an average of 22 % of the total outer bank erosion was due to shaving and extension.

2.6.2 STRIPPING, SECONDARY CHANNELS AND AVULSIONS

Floodplain erosion, also referred to as floodplain 'stripping,' can occur when large floods generate shear stresses on the floodplain surface that surpass the erosional resistance of floodplain sediments. Erosional floodplain stripping is most common within steep, narrow valleys that concentrate flood flows creating overbank flows that have high stream power (Nanson 1986; Warner 1997; Hauer and Habersack 2009; Tranmer et al. 2015). In some extreme events, stripping can remove almost the entire floodplain. In other instances, such as, on floodplains of large, low-gradient meandering rivers, floodplain stripping can occur locally where overbank flow moves perpendicular to topographic gradients associated with old floodplain features, such as meander scars. Goodwell et al. (2014) observed, during the 2011 flood along the Mississippi River, the creation of upstream-migrating gullies due to intentional levee breaches where flow

energy increased as it crossed the relict outer bank of a meander scar. Scour can also occur within secondary channels on the floodplain surface as flow is concentrated during floods (Riquier et al. 2017).

River avulsion is the process by which flow is diverted from the main channel to a new course on the adjacent floodplain (Slingerland and Smith 2004). Avulsions occur mostly on aggrading floodplains. Flood-induced avulsions that carve out a new channel or secondary channel are common floodplain erosional processes (Rhoads 2020). The recurrence interval of avulsions varies widely, as certain internal and external thresholds must be crossed before an avulsion can occur. Recurrence intervals, based on available data from a few rivers, range from as low as 28 years for the Kosi River (India) to up to 1400 years for the Mississippi (Fisk 1944; Stouthamer and Berendsen 2000).

2.6.3 IN-CHANNEL EROSION

A growing body of literature suggests that in-channel sources can represent a significant source of both suspended sediment and phosphorus to river loads (Simon and Darby 1999; Sekely et al. 2002; Evans et al. 2006; Wilson et al. 2008; Miller et al. 2014; Fox et al. 2016). Studies from across the United States have suggested that channel banks can contribute from 23 to as much as 95 % of the total catchment's sediment yield (USACE 1983; Simon and Hupp 1986; Odgaard 1987; Rondeau et al. 2000; Simon et al. 2002; Simon and Thomas 2002; Simon et al. 2004; Thoma et al. 2005; Wilson et al. 2008). Research from the United Kingdom calculated that the contribution to the suspended sediment load from channel banks was between 7 and 37 % (Ashbridge 1995; Bull 1997; Walling et al. 1999; Collins and Walling 2007) which is significantly lower than contributions calculated across the United States. A recent study, done by Pulley and Collins (2024), found that the contributions of channel bank erosion in the UK to be much higher than agricultural topsoil contributions. They conclude that the previous studies done on this subject underestimated the contributions of channel bank erosion in the UK. In Gelbæk River, Denmark, Kronvang et al. (1997) suggest that in-channel (channel banks and bed) is the primary source of catchments suspended sediment yield, contributing 92 %.

Significant, yet highly variable, channel bank contributions have also been documented for total phosphorus annual loads (Kronvang et al. 1997; Sekely et al. 2002; Thoma et al. 2005; Walling et al. 2008; Miller et al. 2014). In some Danish rivers, it has been calculated that bank erosion contributes up to 90 % of the overall phosphorus loads (Kronvang et al. 1997). Although a wide range has been observed, estimates have generally been lower in the Midwestern United States. In Minnesota, Sekely et al. (2002) suggested that bank erosion contributed 7 - 10 % of the total phosphorus load. Meanwhile, in an Illinois study, Roseboom (1987), estimated that up to 56 % of the total phosphorus load resulted from channel

bank erosion. Despite the potential significance of channel bank erosion as a contributor to channel phosphorus loads, published literature has relatively little information on the concentrations of total phosphorus within channel banks (Fox et al. 2016). According to the assessment by Fox et al. (2016), the evidence currently available generally indicates that the total phosphorus concentrations in channel bank material may exceed 250 mg kg^{-1}. However, Beck et al. (2018) in Iowa, USA, reported quantities as low as 171 mg kg^{-1}, whereas Granger et al. (2022) in the upper River Taw in southwest England found amounts ranging from 130 to 1207 mg kg^{-1}. It is difficult to accurately estimate total phosphorus loads at a strategic scale for catchment management and policy support without a solid understanding of the concentrations of total phosphorus in channel banks, given that they have the potential to be a significant source of catchment sediment.

Studies measuring the total phosphorus and suspended sediment contribution from channel banks are still few and regionally underrepresented (Fox et al. 2016). Suspended sediment and total phosphorus loading from channel bank erosion are frequently excluded from local and regional water quality policies intended to reduce nutrient loading due to the relative scarcity and high variability of data, although improved simulation models are taking steps to help overcome these issues (Janes et al. 2018).

2.6.3.1 MECHANISMS

Subaerial processes (processes that take place on land and occur above the waterline), fluvial erosion (refers to the removal of material from the riverbed and its banks), and mass wasting are all components of the cyclical process known as channel bank erosion (Simon et al. 1999; Couper and Maddock 2001; Couper 2003; Fox and Wilson 2010). Fluvial erosion is influenced by the amount of applied shear stress, the sinuosity of the channel, the stream power or river discharge, and the soil resistance of the riverbanks to the fluvial force (Thorne 1981, 1982; Morisawa 1985). A linear excess shear stress equation is most frequently used to represent fluvial erosion. This equation depends on the applied shear stress as well as two erodibility parameters: the critical shear stress and the erodibility coefficient. In addition, several other factors affect the applied shear stress placed on channel bank materials, including i) river flow rates, which are closely related to land use and management in the catchment (Ramos-Scharron and MacDonald 2005); ii) channel properties, including roughness (grain roughness on the channel bed, bedform roughness due to bedforms, and boundary roughness), slope, and cross-sectional area of the channel (Shore et al. 2016); and iii) degree of sinuosity or meandering as channel banks along the outside of a meander bend experience higher shear stress (Daly et al. 2015a). If the applied shear stress is greater than the critical shear stress of the soil, continual fluvial erosion may occur. Once the applied shear reaches the

critical shear stress, the rate at which detachment due to fluvial erosion occurs depends on the streambank sediment's erodibility coefficient. The critical shear stress and erodibility coefficient typically have an inverse relationship, with more sandy and erodible soils having a higher erodibility coefficient and lower critical shear stress and more clay and less erodible soils having a lower erodibility coefficient and higher critical shear stress (Hanson and Simon 2001). Nonetheless, significant diversity is frequently noted surrounding this inverse association (Daly et al. 2015a, b).

Gravity may cause mass wasting (Bowie 1982; Thorne 1982), typically caused by a decrease in the upper bank's internal strength due to saturation, undermining, or foundation deterioration from seepage (Harmel et al. 1999, Fox and Wilson 2010). Mass wasting, unlike fluvial erosion, is episodic. Subaerial erosion is linked to climate and occurs when soil strength is reduced because of subaerial processes, resulting in direct erosion or an increased risk of erosion (Fox et al. 2006; Daly et al. 2015a). These three processes are all interdependent. Subaerial erosion can weaken a bank initially, making it more vulnerable to erosion (Midgley et al. 2013). Fluvial erosion can then easily undercut the bank or scour the bed, resulting in increased instability and, eventually, mass wasting (Fox and Wilson 2010; Midgley et al. 2012). Indeed, the most severe erosive events occur when banks are predisposed to fail due to high soil water content in the bank (Fox and Wilson 2010; Daly et al. 2015a). High flows that occur as isolated events may transport a significant amount of bed load or suspended load in the river but may result in limited bank retreat.

2.6.3.2 CHANNEL BANK PHOSPHORUS CONCENTRATIONS AND LOADS

The variation of phosphorus concentrations in riverbanks and their implications for catchment phosphorus concentrations and loads are important topics of investigation. Alluvial material that has been eroded and deposited can form riverbanks, giving them distinct physical and chemical characteristics derived and fluvially sorted from the upstream catchment and soils. Catchment land use and management practices, as such, have an impact on these physical and chemical characteristics. Miller et al. (2014) reported along the Barren Fork Creek in eastern Oklahoma, a longitudinal profile in several of these chemical characteristics (pH and EC). When the riverbank sediment qualities differed from the catchment soil chemical properties, it was postulated that these longitudinal variations in soil chemical properties may have been caused by excessive fertiliser applications in the catchment (Miller et al. 2014). Studies on channel bank phosphorus loading require more data on soil physical and chemical parameters and other soil characteristics including mineralogy and redox conditions. Additionally, riparian buffers may cause

sedimentation and deposition of sediment-associated phosphorus in adjacent soils, thereby, potentially increasing the channel bank phosphorus contributions (Hoffman et al. 2009).

Since most of the phosphorus in soils is solid-phase phosphorus (primarily found associated with the fine fraction of the sediment), it will be incorporated into surface water along with riverbank sediment (Shore et al. 2016). The sediment may operate as a sink or a source of phosphorus, meaning phosphorus might easily be released into the system, depending on the soil phosphorus concentration, receiving water phosphorus concentration, solid: solution ratio, period of contact, and numerous chemical variables. Studies have linked increased sediment loading with elevated river phosphorus concentrations (Kroening and Andrews 1997; Engstrom et al. 2009). The modelling and prediction of sediment loading from channel bank erosion and, consequently, estimations for phosphorus loading from these banks, will be more accurate if fluvial processes are understood and the dynamics of in-channel suspended sediment can be observed and estimated (Sherriff et al. 2015).

2.7 EROSION AND RECYCLING RATES IN FLOODPLAIN SYSTEMS

Several studies of floodplain systems provide insights regarding lateral migration rates. The reported migration rates in humid and dryland settings are summarised in Table 2.3. For humid regions with an Aridity Index greater than 0.65, research has revealed that lateral migration is an active and dominant process within these systems with a recorded range of between 5 m for the Strickland River in Papua New Guinea (Aalto et al. 2008) and 140 m yr^{-1} maximum movement for a bend on the Amazon River (Mertes et al. 1996). Comparatively floodplain systems occurring in dryland regions with an Aridity Index of less than 0.65, research has revealed that lateral migration is a much slower process with a recorded range between 0.034 and 3.74 m yr^{-1} (Table 2.3). This could be due to the irregular nature and short period of floods that are big enough to initiate bend movement within dryland settings.

Table 2.3 Published erosion and recycling rates for floodplain wetlands ordered according to UNEP aridity index

Region	Source	Location	Aridity Index	Lateral migration rates (m yr^{-1})
Dryland regions (Aridity Index <0.65)	Magdaleno and Fernandez-Yuste (2011)	Ebro River, Spain	0.25	3.74: 1927-1956 0.87: 1957-2003
	Larkin et al. (2017)	Tshwane-Pienaars River, South Africa	0.28	<1
	Tooth et al. (2014)	Blood River, South Africa	0.31	0.2 (cutoff development)
	Owens (1998)	Murrumbidgee River, Australia	0.33	0.08
	Rodnight et al. (2005)	Klip River, South Africa	0.34	0.05-0.16
	Ellery et al. (2003)	Mkuze River, South Africa	0.42	0.034, 0.036, 0.049
	Liu and Liu (2019)	Baihe River tributary of the Yellow River, in China	0.45	0.38-6.10
	Grenfell (2007)	Nsonge River, South Africa	0.61	<1
Humid regions (Aridity Index >0.65)	Drago (1990)	Parana River, Argentina	1.30	50-200
	Coleman (1969)	Ganges–Brahmaputra River, Bangladesh	1.11	60-420
	Black et al. (2010)	Winooski River, Vermont, USA	1.25	0.7
		Connecticut River, Stratford, USA	1.20	3.1
		Genesee River, central New York State, USA	1.20	4.7
	Herndon (1853); Bates (1962)	Fonte Boa, Cayhiarhy (tributary) of the Amazon River	0.90	25

2.8 NUTRIENT DYNAMICS AND STORAGE

Water chemistry is a primary determinant of the ecological quality of rivers. Among the parameters measured to assess water quality is the nutrient phosphorus, which holds particular significance for managing river systems and their floodplains. Phosphorus, as well as Nitrogen, are the two macronutrients that are essential components of all organisms and are connected to the aquatic carbon cycle, establishing both the primary production and the microbial mineralisation of organic matter in river systems (Weigelhofer et al. 2018). However, industrialisation and intensification of farming production have led to excessive loadings of sediment and phosphorus to river systems and have resulted in decreasing water quality and eutrophication of many of the world's aquatic systems (Grizetti et al. 2011).

Several studies have shown that wetlands, including floodplains, can improve downstream water quality by removing and storing nutrients and contaminants (e.g., Blackwell et al. 2002; Fisher and Acreman 2004; Rebelo et al. 2018). Research has shown that the retention of the total phosphorus loads by wetland systems is in the range of 5 to 80 % (Brunet and Astin 1997; van der Lee et al. 2004; Gillespie et al. 2018). Phosphorus and other nutrients and contaminants are primarily transported and stored in association with fine sediment (< 63 microns (µm); Allan 1986; Horowitz 1991; Richardson and Craft 1993; Walling et al. 1997). This is mainly attributed to the negative charge and large surface area structure of colloidal particles, particularly the clay fractions (< 3.9 µm; Horowitz 1991). Fundamentally, the sediment composition and accretion rates determine the nutrient and contaminant transport and storage capacity

of alluvial wetland systems (van der Lee et al. 2004). These, in turn, are determined by sediment supply, wetland type, hydrogeomorphic characteristics, and vegetation composition (type, density and height; Johnston et al. 1984; Sánchez-Carrillo et al. 2001; Kronvang et al. 2007). Accumulation rates of sediment and nutrients in humid-region floodplains with various catchment land uses were compared by Noe and Hupp (2005). The results from the study showed that phosphorus accumulation is intrinsically linked to mineral sedimentation and that the accumulation rates of sediment and phosphorus among the different floodplains displayed the same pattern. However, there can be notable spatial and temporal differences in accumulation rates within a single floodplain. This is because of the variability in local hydro-geomorphic drivers, topography, vegetation characteristics, sediment sorting processes and localised hydraulics that occur across both temporal and spatial scales (Thoms 1998; Axt and Walbridge 1999; Bridgham et al. 2001; Johnston et al. 2001; Bruland and Richardson 2004; Olde Venterink et al. 2006; Odhiambo et al. 2016).

2.9 CONCLUSION AND SIGNIFICANCE OF THE RESEARCH

Floodplains provide a variety of physical and biological roles, which are intricately linked. Floodplains' primary physical function is to attenuate water flows as well as dissolved material, sediment, and organic matter conveyed by water. Although floodplain storage is a physical process, floodplain biogeochemical processes and biotic communities have a major effect on essential aspects of storage such as amount, calibre, duration, and spatial distribution. A floodplain is a dynamic ecosystem located at the aquatic-terrestrial interface. Whatever the climate and flow regime, a floodplain alternates between a submerged surface with lotic or lentic water and an exposed area with hydrologic conditions more akin to nearby uplands than to the river channel. A floodplain is not a homogenous ecosystem, either spatially or temporally, and different parts of it, such as abandoned cutoff meanders, natural levees, and backswamp regions, can have significantly varied hydrologic, sedimentological, and biological conditions.

Floodplains are primarily depositional fluvial landforms that store significant volumes of sediment. The major depositional processes of floodplain formation are 1) lateral accretion of point bars and 2) vertical accretion on floodplain surfaces, which includes overbank sedimentation, levee construction, splay formation, and channel infilling. Because of these processes floodplain's primary function is to attenuate fluxes of sediment, associated nutrients and contaminants, and organic matter transported by flood water. This buffering function supplied by floodplains can influence downstream fluxes within the river conveyance corridor (Harvey and Gooseff 2015).

The interactions between fluxes of material and floodplain storage are substantially influenced by the floodplain's physical properties, particularly spatial variability. The relevant spatial scales of floodplain heterogeneity may vary depending on the kind of storage studied, but they are most likely hierarchical (Wohl 2021). Floodplains can be longitudinally discontinuous at the scale of a river network, especially in mountainous areas, with river beads (river segments with floodplains) interspersed longitudinally with river strings (laterally confined reaches lacking floodplains) (Bellmore and Baxter 2014; Wohl et al. 2018). The disturbance regime caused by water and sediment fluxes generates distinct geomorphic units such as the active channel, natural levees, cutoff meanders, and backswamp deposits (Dunne and Aalto 2013). Each of these geomorphic units is distinct and differs from the others in terms of their characteristics such as topography, sediment particle size, organic matter content, phosphorus content, hydraulics, hydrological regime, and sedimentation rates. The interactions between water, sediment and associated materials and the floodplain ecosystem across temporal and spatial scales suggest that floodplain storage is the consequence of a dynamic, integrative system.

While there have been studies on sediment dynamics in floodplain systems, there is a lack of empirical studies on floodplain systems in drylands, such as South Africa. Wetlands in drylands unique hydroclimatic, geomorphological, and sedimentological features are expected to have an impact on sediment transport and biogeochemical processes, thus changing sedimentation rates, trapping efficiencies, and the rates at which phosphorus is sequestered in these systems. In addition, little is known about the relationship between the dynamics of sediment and phosphorus flux and these unique wetland features. Furthermore, there is still a dearth of knowledge regarding the quantitative feedback processes and connections between the biophysical elements and processes that regulate the rates and amounts of sediment trapping and phosphorus absorption in floodplain wetlands in dryland environments. As a result, this research will concentrate on two interconnected ecosystem services: sediment trapping and storage and phosphate assimilation using two case studies in South Africa. This study contributes to the efforts of better understanding and quantifying floodplain processes and regulatory ecosystem services within dryland environments.

CHAPTER 3 : THE STUDY AREAS

3.1 INTRODUCTION

The following chapter provides a description and analysis of the broader catchment area and the two study sites, encompassing aspects such as locality, climate, hydrology, topography, land cover and usage, geology and soils, and erosion status.

3.2 BROADER CATCHMENT DESCRIPTION

The Umzimvubu River system lies along the northern boundary of the Eastern Cape and extends for over 200 kilometres from its source in the steep Maloti-Drakensberg Escarpment (approximately 2 700 m.a.s.l) to the estuary at Port St. Johns where it flows into the Indian Ocean (Figure 3.1). The river drains a catchment area of approximately 20 000 km². This river system has been nationally prioritised as one of the few remaining near-natural and free-flowing rivers; however, it is categorised as vulnerable due to the rapid rates of degradation in the catchment. In addition, the adjacent template of grassland, forest, thicket, wetlands, and dune vegetation are some of the most biodiverse in the world (Environmental and rural solutions 2011). These habitats support numerous species of flora and fauna and provide a range of ecosystem services such as water provision, erosion control, sediment trapping, infrastructure protection, fodder for livestock and food security, and materials for household and community use. The Tsitsa River is a large tributary of the Umzimvubu River. The research in this thesis focuses on floodplain systems in the Gatberg River and the Minnehaha River. The two rivers are in the upper regions of the Tsitsa River catchment. Maclear and Ugie are the two urban towns closest to the systems and are indicated on Figure 3.1.

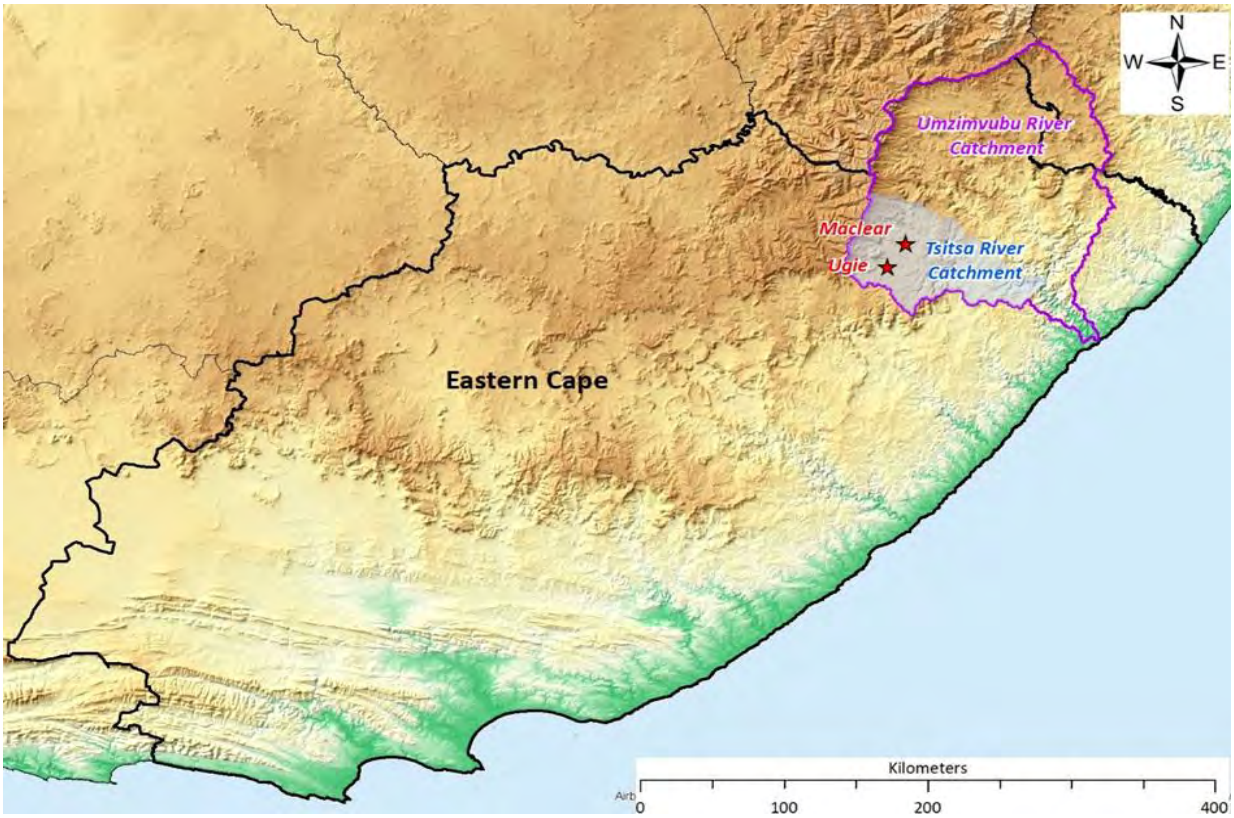

Figure 3.1 The landscape setting of Maclear and Ugie in relation to the Tsitsa River catchment within the broader Umzimvubu River catchment in the Eastern Cape province (based map: Airbus, USGS, NGA, NASA, CGIAR, NLS, OS, NMA Geodatastyrelsen, GSA, GSI and the GIS user community)

3.2.1 TSITSA RIVER CATCHMENT DESCRIPTION

3.2.1.1 LOCATION

The main stem of the Umzimvubu River has four major tributaries; the Tsitsa, Tina, Kinira, and Mzintlava Rivers, all of which have their headwaters in the Maloti-Drakensberg Mountains. The study sites for this research fall within the upper Tsitsa River catchment. The upper Tsitsa River catchment (Quaternary Catchment T35 A-K) drains an area of approximately 4 300 km² (Figure 3.2). Approximately 45 % of the Tsitsa River catchment lies in traditional council areas (found mostly in the middle and lower parts of the catchment) of the former Transkei homeland where much of the population resides in low-density rural villages, often situated on the mid-slopes of hillsides. Land use in traditional council areas is dominated by rural subsistence livestock (cattle, sheep, and goats) farming and subsistence vegetable gardens. The slightly larger portion (55 %) of the middle and upper catchment is privately owned land and consists of bigger commercial farms and plantations with urban and peri-urban centres scattered around the catchment (Kakembo and Rowntree 2003). Although there are some urban centres, commercial farms,

and plantations, the Tsitsa catchment is one of the poorest and least developed regions of South Africa (Calmeyer and Muruven 2015). During the Apartheid era, communal land was part of the Transkei homeland where population density was high, and livelihoods were dependent on migrant labour, grants, and subsistence farming (Fabricius et al. 2016). Even though the homeland policy was abolished in 1994 the area remains poor with a shortage of infrastructure and employment opportunities. The rural communities depend heavily on the natural environment in which they are situated and depend on river water during dry periods. Wetlands in the catchment play an important role in supporting good water quality and quantity (Kakembo and Rowntree 2003; Blignaut et al. 2010; van der Waal 2015; van der Waal and Rowntree 2018; Schlegel et al. 2019).

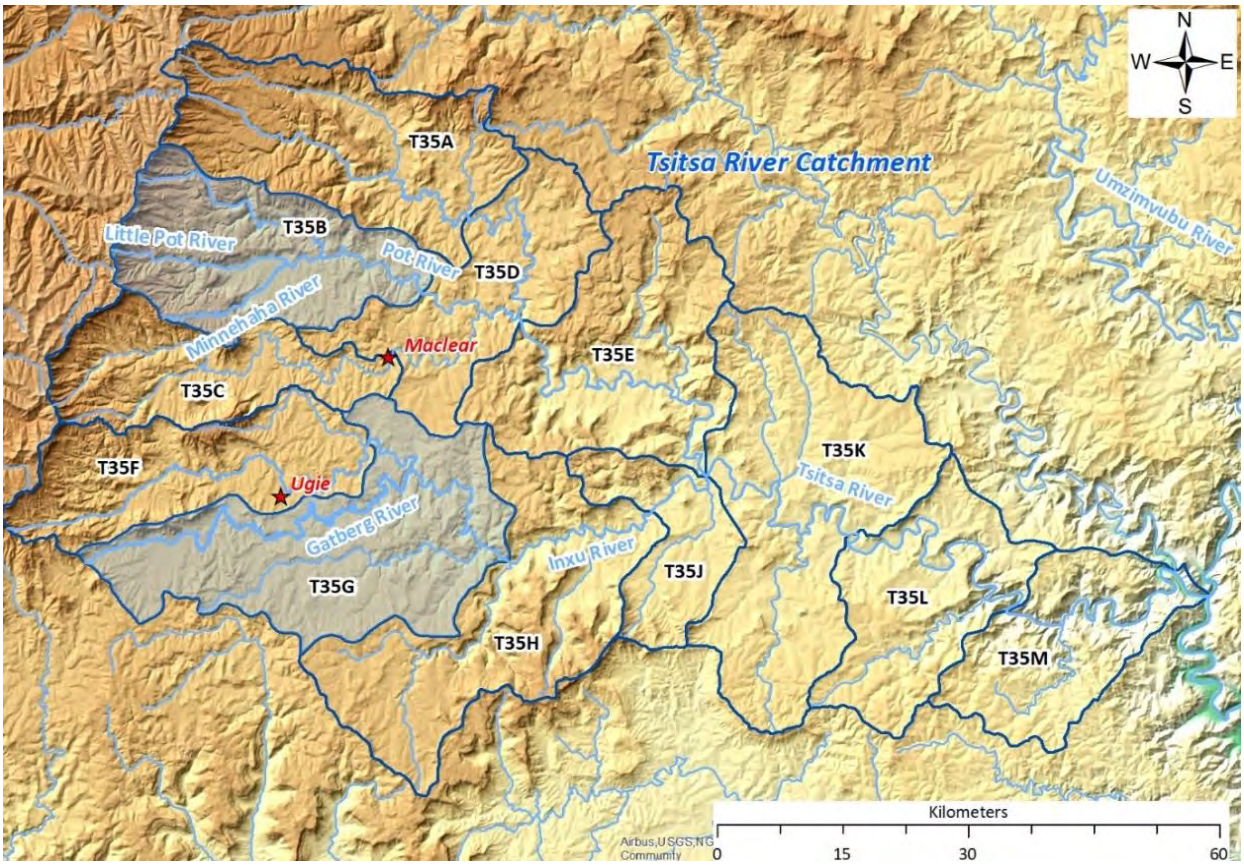

Figure 3.2 The two study area catchments (Gatberg River and Minnehaha River) located within the Tsitsa River catchment with all major rivers and Maclear and Ugie shown

3.2.1.2 TOPOGRAPHY

The Tsitsa River has its headwaters in the Great Escarpment geomorphic province, here the landscape is dissected by an intricate drainage network, characterised by deep and narrow cross-valley profiles. Longitudinal profiles of the river and its tributaries are very steep and stepped in places where they intercept hard resistant geological barriers (e.g., dolerite intrusions, Figure 3.3Figure 3.4). Partridge et al. (2010) categorised this area predominantly as a low to very low (MV- medium average macro-reach valley width to very steep average macro-reach slope and NV- narrow average macro-reach valley width to very steep average macro-reach slope) sediment storage surrogate description. The Tsitsa River flows from its headwaters in the Great Escarpment at approximately 1 300 m.a.s.l and flows onto an elevated platform margin of the Cedarville Flats. The river then flows through the Southeastern coastal hinterland geomorphic province (Partridge et al. 2010) to its confluence with the Umzimvubu River. Here the landscape is steep, transforming into hilly to rolling hills with V-shaped valleys and limited sediment deposition space. The most significant constraint on the rivers of this area were two post-Cretaceous epeirogenic uplift events in the Neogene (the first at approximately 20 Ma and the second at around 5 Ma) that were concentrated along the Ciskei–Swaziland axis, 80 km inland from the coast (McCarthy and Rubidge 2005). Uplift totalled between 800 and 1 100 m, elevating the eastern section of southern Africa, and thus magnifying the relief between the Great Escarpment and the Southeastern coastal hinterland geomorphic province. The uplift produced large-scale (asymmetrical) arching, steepening of the lower courses of rivers, entrenchment, and rapid down-cutting of pre-existing meander systems. Due to the presence of dolerite sills, dykes, and other hard lithologies in an area of considerable geological diversity, the longitudinal profiles of the Tsitsa River and its tributaries are stepped (Figure 3.3 and Figure 3.4).

The Tsitsa River transitions between a bedrock and mixed bedrock-alluvial river. The long profile of the river is strongly influenced by the type of rock, where steeper sections form on more resistant bedrock (such as basalt and dolerite) and gentler sections form on sandstones, mudstones, and mudrocks (Figure 3.5). Along the steeper escarpment zones, the riverbeds are dominated by bedrock with rapids and waterfalls. Instream vegetation is generally absent, with riparian vegetation dominated by alien invader tree species. In many places, channels are deep to very deeply incised in the alluvial plains and are locally characterised by flood benches, meanders, and oxbows (van der Waal and Rowntree 2018). Below the upper Tsitsa waterfall, the Tsitsa River passes through a deep and largely inaccessible gorge as it crosses the middle escarpment. The Mooi River, having been joined by the Pot River, converges with the Tsitsa River within this gorge. Below the gorge, the river opens into a mixed alluvial river with large sediment

deposits and sand beds in low-gradient areas. The Gatberg and Minnehaha rivers are both found in the upper Tsitsa River catchment. The Gatberg River is a tributary of the Inxu River, which is a tributary of the Tsitsa River (Figure 3.4). The Minnehaha River is a tributary of the Little Pot River (Figure 3.3).

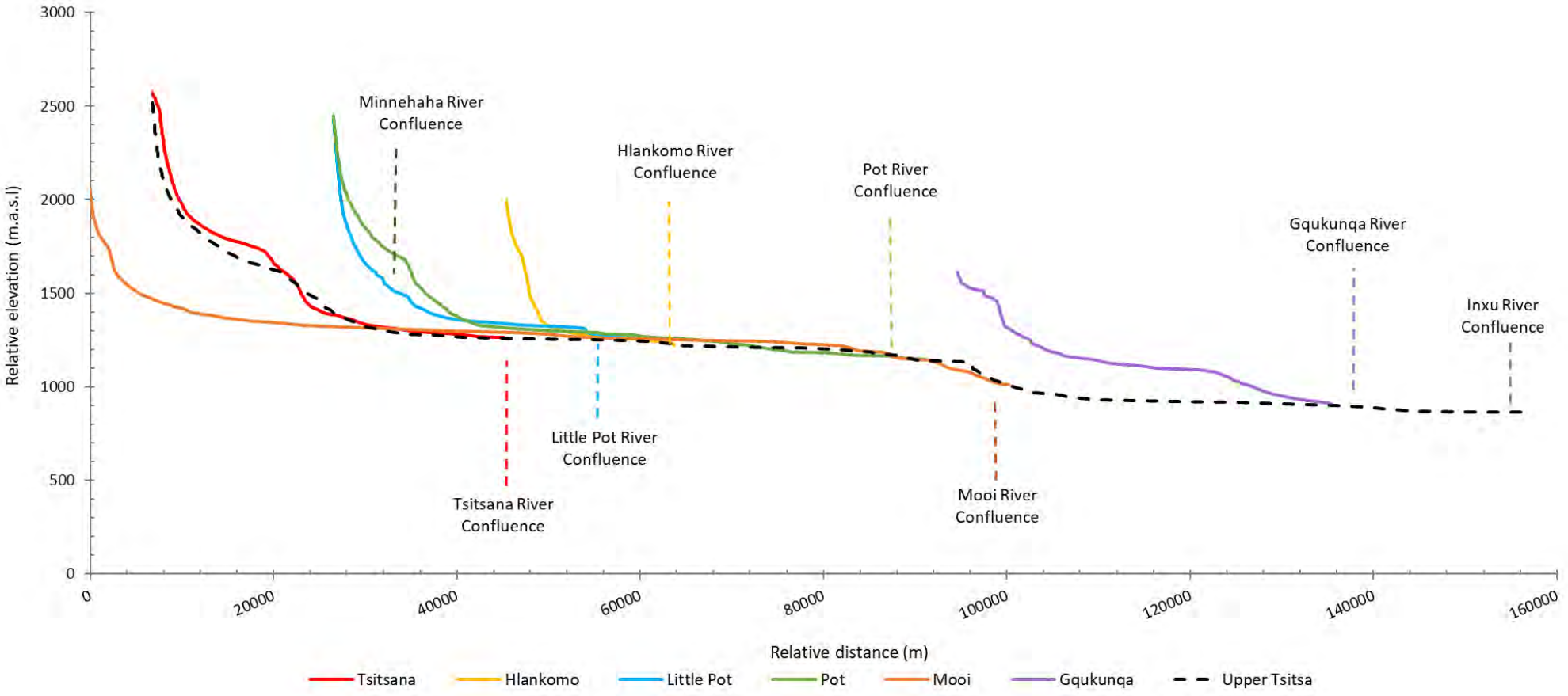

Figure 3.3 Longitudinal profile of the upper Tsitsa River and its major tributaries from their headwaters to the confluence with the Inxu River

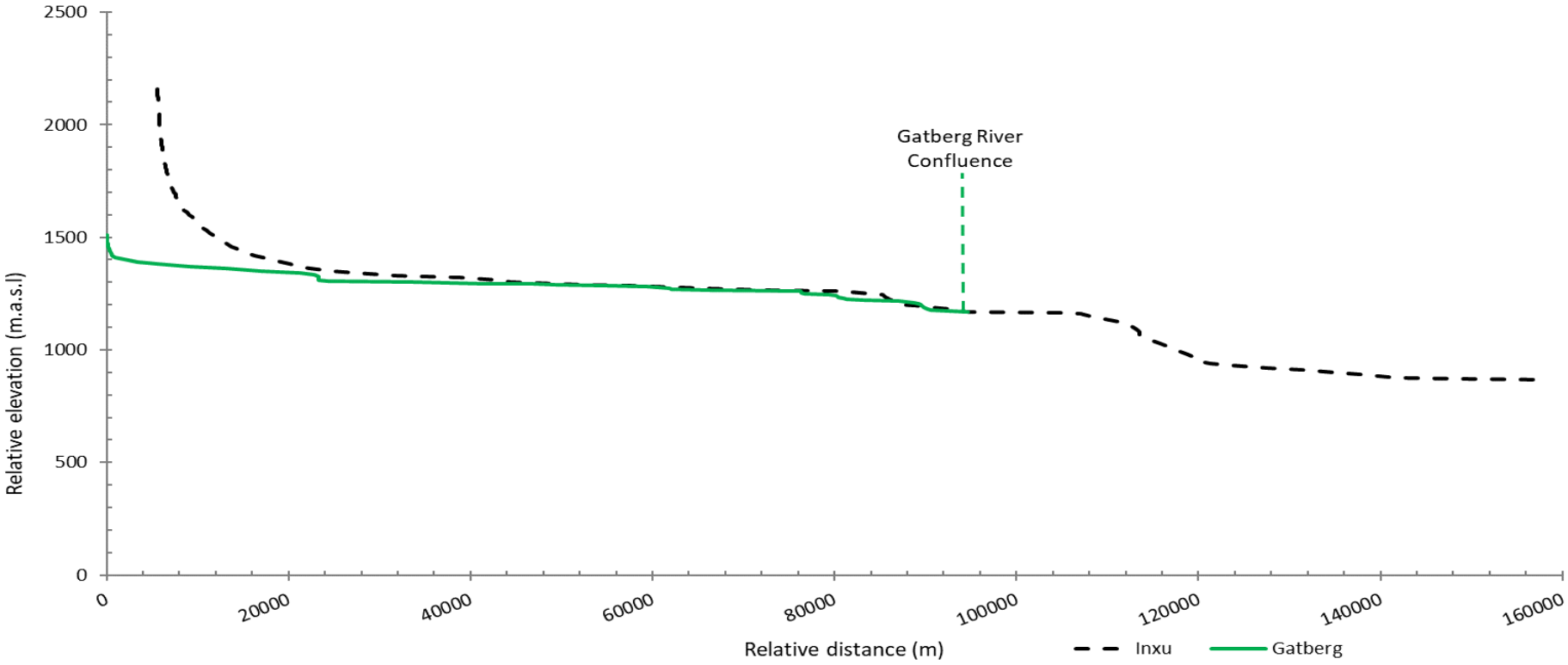

Figure 3.4 Longitudinal profile of the Gatberg River in relation to the longitudinal profile of the Inxu River

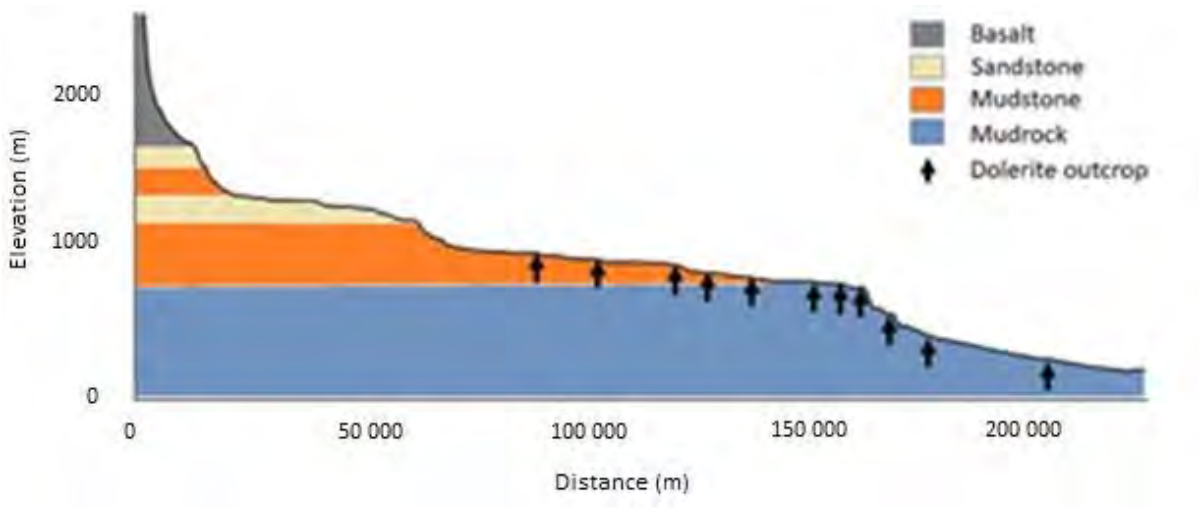

Figure 3.5 Longitudinal profile of the Tsitsa River showing generalised rock types and dolerite outcrops (from Huchzermeyer et al. 2019)

3.2.1.3 GEOLOGY AND SOILS

The geological composition of the catchment plays a crucial role in shaping its landscape, groundwater characteristics, and soil composition, which in turn affects the vegetation types and how the land is utilised. These factors interact to determine the hydrological and sedimentological regime of the catchment. Moreover, geology also affects the sediment yields and the specific properties (physical or chemical) of that sediment (Lambert and Walling 1986).

The upper parts of the catchment area are underlain by basic mafic lavas of the Drakensberg formation. Moving downward, the catchment is underlain with intercalated arenaceous and argillaceous strata. The lower sedimentary sequence consists of the sandstones of the Clarens, mudstones of the Elliot, sandstones of Molteno, highly dispersive mudstones of the Tarkastad Formations and alluvium in the valley bottoms. Intrusions of Karoo pyroclastic rocks or dolerite dykes can be found throughout the catchment, mostly in lines indicating previous fissures in the base material (Figure 3.6; Le Roux et al. 2015). The strata have remained structurally intact since their deposition, and the typical dip of the layer ranges from 2 to 70 degrees west. A description of each of the geological formations adapted from de Decker (1981) is detailed below.

- The Drakensberg Formation, which comprises a basalt cap up to 1 200 m thick, generates the escarpment. Basalt was generated by a sequence of basalt flows of varying thicknesses that range from resistant crystalline rock (thick flows) to softer vesicular forms (thinner flows) that give the

basalt its layered appearance. Clarens sandstones may be incorporated in the basal portion. Many cracks occurred in the terrain, as shown by the many dolerite dykes that protrude from it. The majority are orientated northwest-southeast and stand out as large steep ridges.

- The Clarens Formation is dominated by well-sorted, fine-grained feldspathic sandstones of light orange colour and aeolian origin. Between the sandstone layers are minor mudstone strata. This formation was deposited during the Triassic Era (McCarthy and Rubidge 2005) in an arid climate. The formation is up to 275 m thick and can build magnificent cliffs with cave structures.
- Red and purple mudstones dominate the Elliot Formation, with subordinate strata of medium-grained feldspathic sandstone that are not laterally persistent. Upward fining sequences (sand to mudstone) are common; this formation was probably formed by meandering streams. The red colours of the mudstones are due to oxidised iron, which relates to the presence of drier conditions during their development. This layer can be as thick as 370 m.
- The Molteno Formation is the lowest geological formation in the Stormberg Group. The formation is composed of fine, medium, and coarse-grained sandstones, as well as greyish mudstone strata. Trough cross-bedding structures are seen in the coarser sandstones. Siltstones are also found in the mudstones. Secondary quartz overgrowths and clasts in the sandstones give them a characteristic sparkling aspect. Finer-grained sandstones exist throughout the lower deposits of the Molteno Formation, becoming coarser toward the top parts. The Molteno Formation was deposited during the mid-Triassic Era in a warm and humid climate. This layer indicates a transitional era from a warm and humid to a desert climate which dominated the formation of the later Elliot and Clarens Formations (Bordy et al. 2004).
- The oldest layer found in this area is the Tarkastad formation of the Beaufort Group. The formation is composed primarily of sandstones and mudstones deposited in the late Triassic Era. The formation can be up to 250 m thick with alternative layers of coarse sandstone and fine-grained mudstones (Botha and Singh 2012). This formation was likely formed in fluvial-lacustrine environments in a semi-arid environment with highly variable rainfall (Botha and Singh 2012)
- Quaternary deposits can be found in valley bottoms as colluvial and river deposits. The soils are dark, with sandstone and basalt debris at the edges.

The existence of harder strata (e.g., sandstones, which are more resistant to erosion) contributes to the stepped structure of the terrain. Erosion removes the softer layers, such as mudstone, exposing the harder strata and forming the steps.

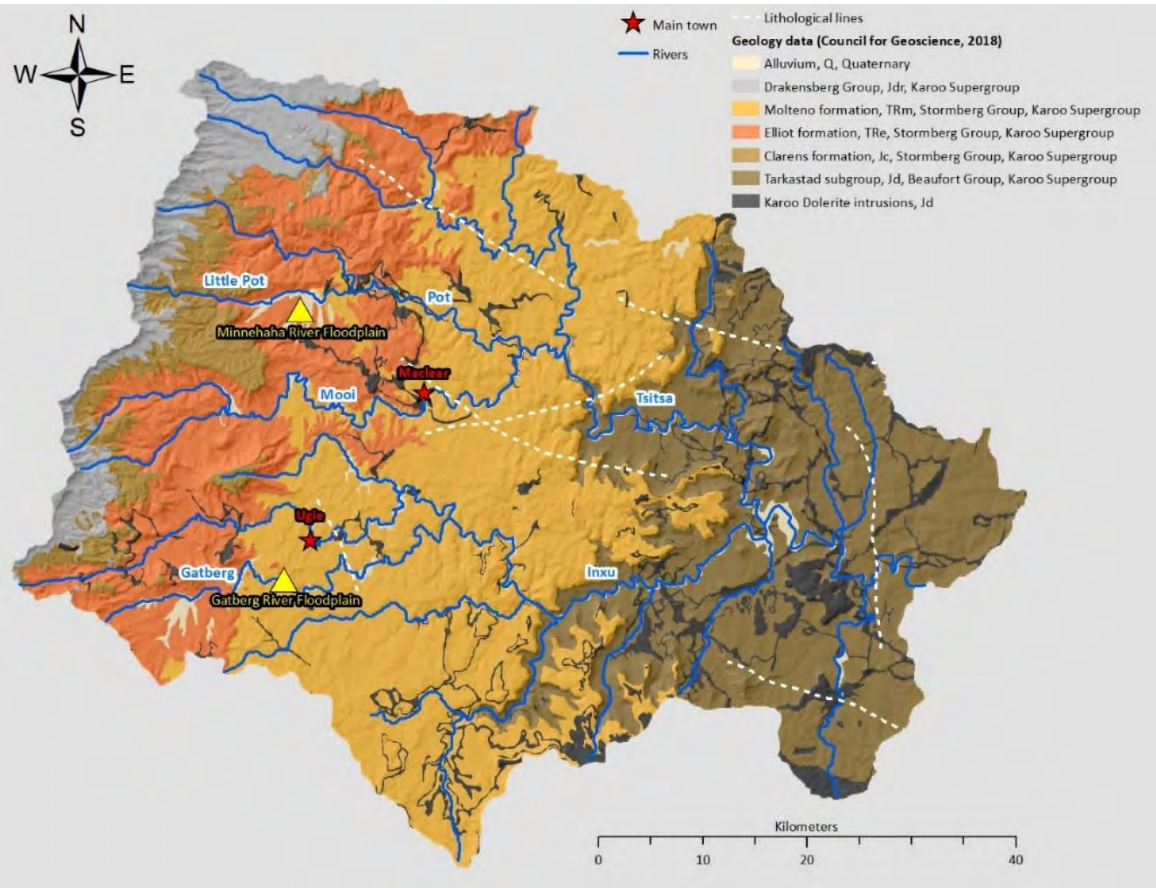

Figure 3.6 Geological map of the Tsitsa River Catchment. The study area catchments (Gatberg and Minnehaha River), all major rivers, and Maclear and Ugie are shown

Soils throughout the catchment vary significantly, but the most prominent soil forms include poorly drained and shallow to moderately deep loams usually with minimal soil development on hard or weathering rock (Land Type Survey Staff 2012). Less common in the catchment are soils of moderately deep to deep sandy loams. Most of the soil types found in the catchment are highly acidic because of the siliceous nature of the lithology that the soils derive from (Huyssteen et al. 2005). Soils that develop on the Tarkastad, Molteno and Elliot Formations, found in the central part of the catchment area, are associated with duplex and dispersive soils which are particularly vulnerable to the formation of soil pipes (Figure 3.7) and subsequent gullying (Le Roux et al. 2015). The most noticeable aspect of these soils is a significant increase in clay content from the topsoil to the subsoil horizon, with an abrupt transition in texture, structure, and consistency between the two (Samadi et al. 2005). These soils are commonly found with vertical, melanic and/or plinthic soils. As a result, these soils impede root growth and reduce infiltration, increasing runoff and erosion. Large gully networks are a prominent feature of this catchment.

Figure 3.7 A photograph of a gully pipe network, a common feature of areas with duplex soils

3.2.1.4 VEGETATION

The Tsitsa River Catchment is dominated by grassland which varies from Lesotho Highland Basalt Grassland (1 900 – 2 900 m.a.s.l), Southern Drakensberg Highland Grassland (1 720 – 1 900 m.a.s.l), East Griqualand Grassland (920 – 1 720 m.a.s.l), Drakensberg Foothill Moist Grassland (880 – 1 860 m.a.s.l), Eastern Valley bushveld, Mthatha Moist Grassland (600 – 1 080 m.a.s.l), Eastern Temperate Freshwater Wetlands, and small pockets of Southern Mistbelt Forests (800 – 1 400 m.a.s.l) in ravines (Mucina and Rutherford 2006). Natural vegetation is fundamentally influenced by aspect, catena, slope, geology, soil type, altitude, and fire occurrences (which in some areas occur as frequently as every year (Snyman 2020)). Invader species, especially the Australian *Acacia sp.,* occur in large stands and are present along most drainage lines within the catchment.

Mucina et al. (2006) define these vegetation categories and associated environmental parameters as follows:

- Lesotho Highland Basalt Grassland is short grass-veld with patches of shrubland (*Leucosidea sericea*), usually associated with disturbance. Basalt underpins this type of vegetation, and soils are basalt-derived with almost equal parts coarse sand, fine sand, silt, clay, and organic material. Organic material is the consequence of the gradual decomposition of the grassroots that holds a lot of precipitation and slowly releases it in the form of seeps. The average monthly minimum and maximum temperatures vary from -10.5 to 31.4°C, with frost persisting all winter.
- The Southern Drakensberg Highland Grassland occur on steep, moist slopes with thick tussock grasslands dominating and a tall shrub component (*Leucosidea sericea*). The soil is usually deep and fine-grained. It has a cool temperate climate (mean temperature of 13°C) with 30 - 90 days of frost each year, which increases with elevation.
- The East Griqualand Grassland dominates on the hilly terrain, with grassland predominant and *Leucosidea sericea* growing on damp slopes. The associated soils are formed from mudstones and sandstones that are 500 - 800 mm deep, well-drained, and rich in clay. The average annual temperature is 14.7°C, with frost occurring around 30 days per year.
- Drakensberg Foothill Moist Grassland cover the moderately rolling and mountainous areas with drier vegetation types, forb-rich grasslands with short tussock grasses (*Themeda triandra and Tristchya leucothrix*) and small patches of forest in the moist ravines. Associated soils are formed from mudstones, sandstones and dolerite intrusions that are more than 800 mm deep, well-

drained, and rich in clay. The average annual temperature is 14.6°C, with frost occurring ~26 days per year.

- The Mthatha Moist Grassland covers the plains between the coastline and the foot slopes, excluding the river valleys. This vegetation type occurs in undulating plains and hills supporting species-poor, sour, wiry grassland dominated by *Eragrostis plana* and *Sporobolus africanus*. Associated with highly leached mudstones. Frost occurs between 2 and 14 days per year.
- Southern Mistbelt Forests occur in fire-shadow habitats on south- or southeast-facing slopes and ravines. This type of vegetation is characterised by tall forests and multilayered understory. Some of the soils associated with this type of vegetation are deep and loamy with high amounts of nutrients developed in dolerite intrusions or mudstones, shales, and sandstones.

3.2.1.5 LAND COVER AND USE

The interactive factors of soils, vegetation and land use often determine the physical and chemical properties of suspended sediment.

According to the National Land Cover (2020), in the Tsitsa River catchment (Figure 3.8), natural vegetation exceeds 2 200 km² (61 %) of the catchment area, including grassland (55 %), and woody vegetation including thicket, indigenous forest, woody alien species and shrubland/ fynbos (5 %). The lower slopes are mainly used for grazing and agricultural practices. The main land use is degraded or unimproved grasslands used for subsistence grazing with minority land uses including agriculture (15 %) and forest plantations (11 %). Relatively large waterbodies such as farm dams and wetlands occupy roughly 112 km² (3 %) of the catchment area. Urban areas cover the remaining 270 km² (6 %) of the catchment area. The two towns of importance to this research, Maclear and Ugie, are also shown.

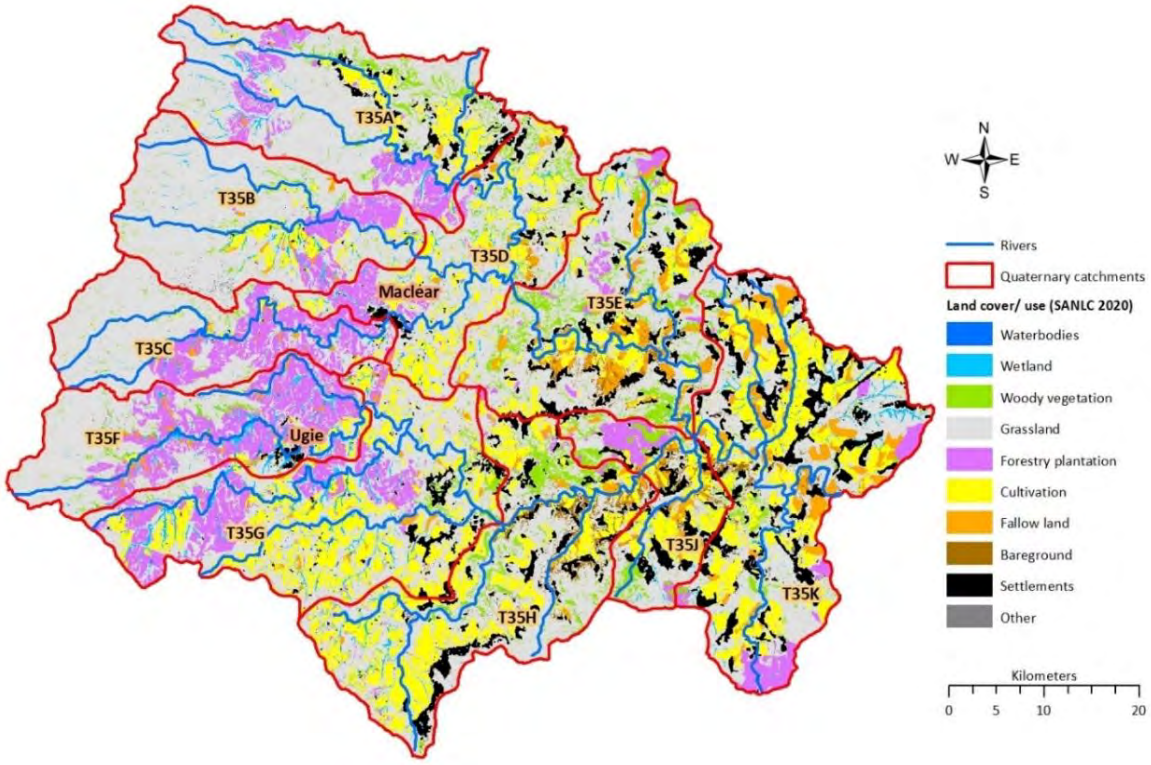

Figure 3.8 Land cover and use in the Tsitsa River Catchment

3.2.1.6 CLIMATE

The predominant climate patterns in the area when integrated with other physical factors, determine the hydrological response of the catchment area, affecting flood frequency and magnitude, as well as the transport, quantity, and quality of suspended sediment.

The climate for most of the Tsitsa River catchment, according to the Köppen-Geiger climate classification, is warm and temperate with warm summers and dry winters with an Aridity Index between 0.5 and 0.65 (Mucina and Rutherford 2006). The catchment receives summer rainfall (between October and April), often in the form of afternoon thunderstorms (Mucina and Rutherford 2006). There is a distinct rainfall gradient, with the mean annual rainfall ranging from 625 mm in the lower catchment to 1 327 mm in the upper catchment closer to the escarpment (Le Roux et al. 2015). The average maximum hourly rainfall rate is 13 mm hr^{-1} with the maximum occurring in September (Agrometeorology Staff. 1984-2008). These are described as high-intensity rainfall events and result in high erosion rates (Fraser et al. 1999). Spatiotemporal variability in rainfall is due to the varied topography across the catchment (Base et al. 2007; Mucina and Rutherford 2006). The driest and coldest month is July, with monthly average rainfall

and temperature of ~13 mm and ~0°C respectively (Mucina and Rutherford 2006). Snowfalls can be expected during the winter months along the Escarpment and may occur less frequently in the lower regions of the catchment.

3.2.1.6.1 Maclear rainfall

The average annual rainfall for Maclear, the closest major town to the Minnehaha River Catchment, rainfall calculated using rainfall data from 1978 to 2012 (The Agricultural Research Council – Institute for Soil, Climate and Weather (ARC-ISCW); Moore 2016), is ~824 mm, which ranges from a low of 503 mm to a high of 1 144 mm (Figure 3.9). The average monthly rainfall for Maclear shows that January has the highest monthly rainfall with ~133 mm, and July has the lowest monthly rainfall with ~15 mm. The average monthly rainfall for Maclear is ~69 mm (Figure 3.10).

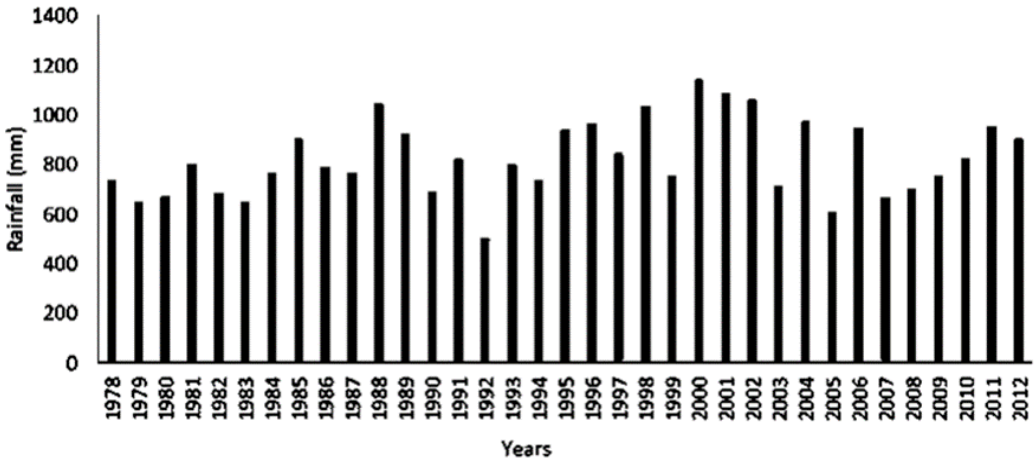

Figure 3.9 Annual rainfall (mm) for Maclear from 1978 to 2012 (adapted from Moore 2016)

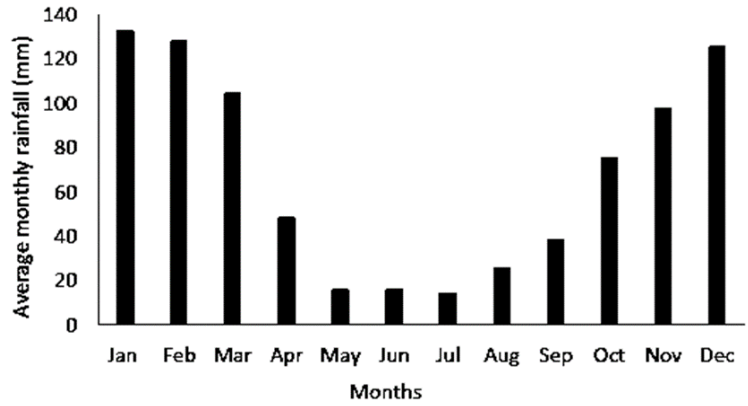

Figure 3.10 Monthly rainfall (mm) for Maclear from 1978 to 2012 (adapted from Moore 2016)

3.2.1.6.2 Discharge

The Tsitsa River at the Xonknxa monitoring station (Latitude: -31.23805; Longitude: 28.85222) has an average daily discharge of approximately 24 m^3s^{-1} (1951- 2021) and the highest recorded discharge was 947 m^3s^{-1} (Department of Water and Sanitation: Verified flow data). The highest average daily discharges mainly occur during the summer season (wet season from November to April) with the peak flows occurring in February (Figure 3.11). The Mooi River, which is a tributary of the Tsitsa River, has an average daily discharge of approximately 3 m^3s^{-1} at the Maclear monitoring station (Latitude: -31.07166; Longitude 28.35361). The peak discharge recorded was 323 m^3s^{-1} (Figure 3.12). Like the Tsitsa River, the Mooi River's average daily discharges are highest in the wet season, peaking in February. Figure 3.13 shows the annual peak water levels with the 2- and 10-year return periods for the Tsitsa River at Xonknxa from 1951 to 2022. In the 71 years recorded 35 years were above the two-year return period, and of those 6 were recorded above the 10-year return period.

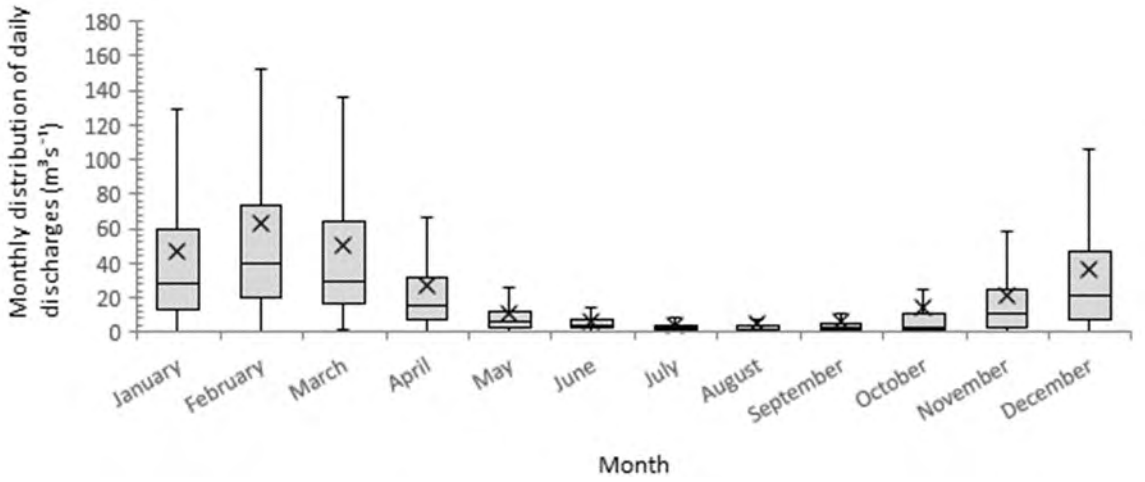

Figure 3.11 The distribution of average daily Tsitsa River discharges per month at Xonknxa from 1951 to 2021 showing the median, mean (x), upper and lower quartiles

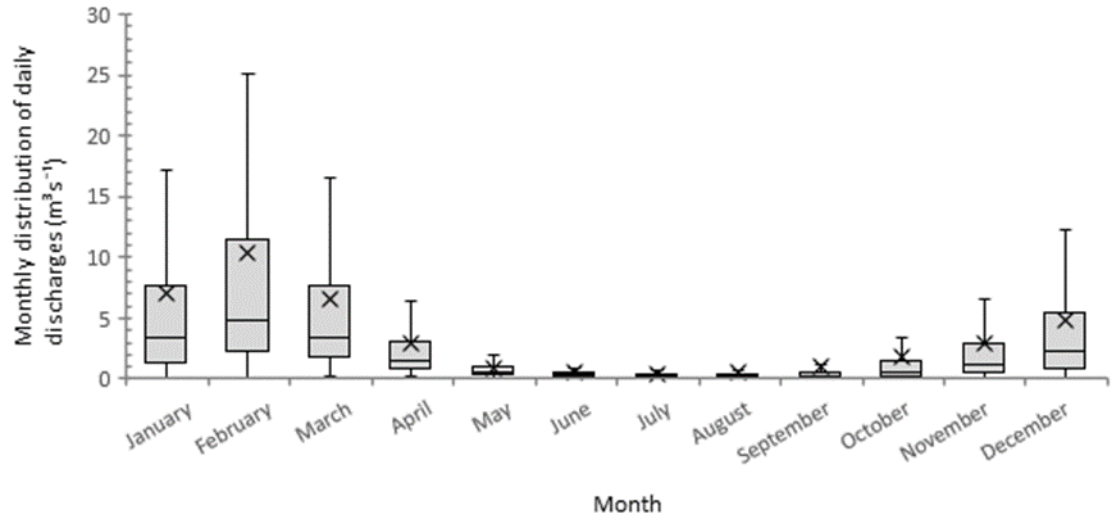

Figure 3.12 The distribution of daily Mooi River discharges per month at Maclear from 1964 to 2021. showing the median, mean (x), upper and lower quartiles

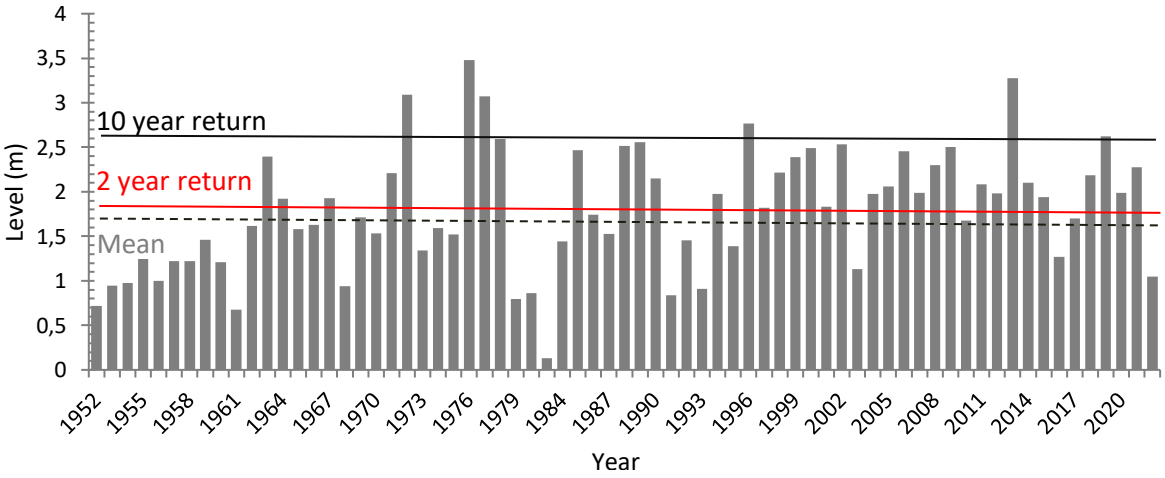

Figure 3.13 Annual water level peaks for the Tsitsa River at Xonkonxa monitoring station 1951-2022

3.2.2 STUDY SITES

3.2.2.1 GATBERG FLOODPLAIN SYSTEM

3.2.2.1.1 LOCATION

The Gatberg floodplain wetland system on the Gatberg River is in the Quaternary Catchment T35G close to the settlement of Ugie in the Eastern Cape (Figure 3.14) and falls within the Elundini Local Municipality. The wetland is situated on the privately-owned farms of Belmount, and Mount Elton surrounded by commercial forestry. The wetland can be accessed through the network of forestry roads with permission from the forestry company, PG Bison, and the landowner.

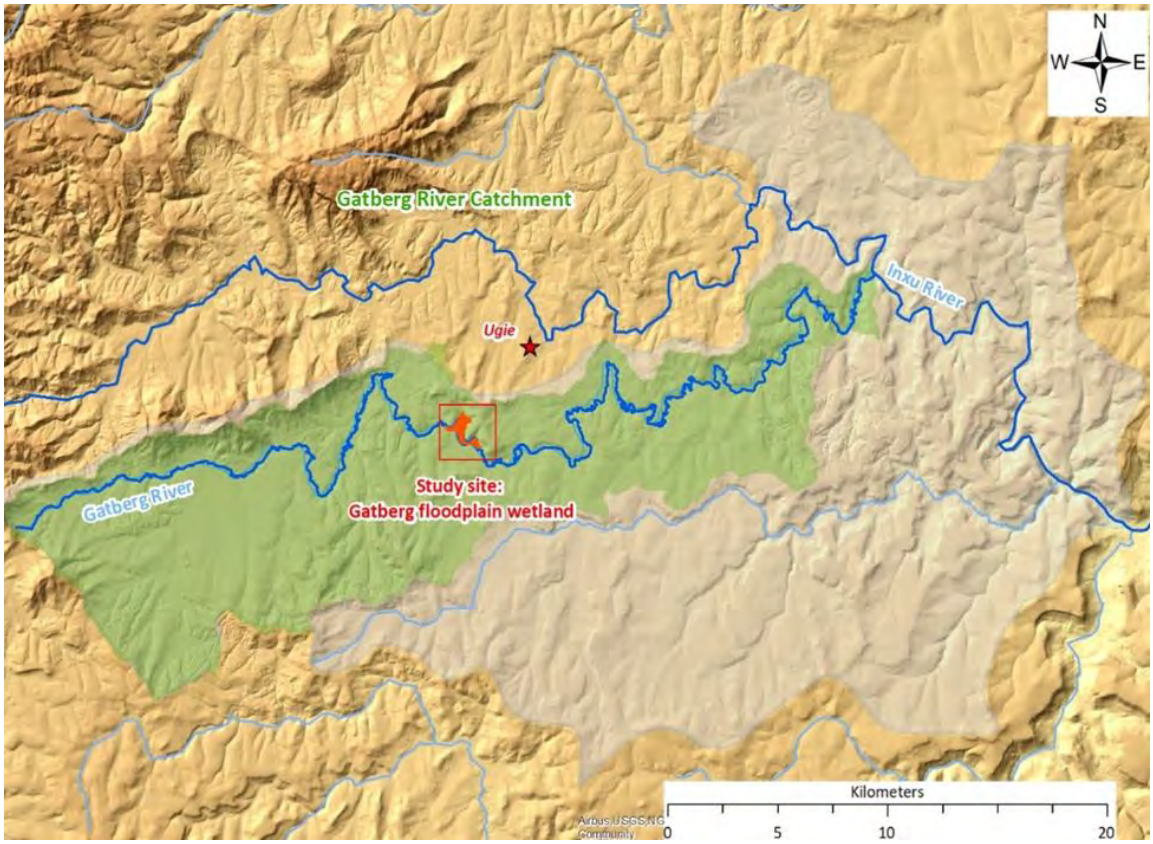

Figure 3.14 The location of the Gatberg floodplain system (study site) within the Gatberg River catchment

3.2.2.1.2 DESCRIPTION

The Gatberg floodplain wetland system is a relatively small wetland pocket (~0.3 km²) within a large catchment (~135 km²). It is connected to the main drainage system of the Gatberg River which drains into the Inxu River, a tributary of the Tsitsa River. The Quaternary catchment has a Mean Annual Precipitation (MAP) of 795 mm and potential Evapotranspiration (PET; refers to the quantity of water that would be evaporated and transpired by a particular crop, soil, or ecosystem under conditions of sufficient water availability) of 1655 mm. A climate ratio (P/E_P) of 0.48 classifies this area within the semiarid climate type. The wetland is situated on alluvium and underlain by the alternating sandstones, mudstones, and shale of the Molteno Formation (Beaufort Group of the Karoo Supergroup geology), with the higher ground being comprised of the Elliot Formation (Beaufort Group of the Karoo Supergroup geology). These soils are generally well-drained with a clay content ranging from 15 to 55 % (Mucina and Rutherford 2006).

The dominant vegetation type in the surrounding area (that has not been transformed to commercial forestry) is East Griqualand Grassland (Gs12), with Drakensberg Foothill Moist Grassland (Gs10) occurring closer to the escarpment and Southern Drakensberg Highland Grassland (Gd4) on the higher slopes in the upper region of the catchment (Mucina and Rutherford 2006). East Griqualand Grassland is considered Vulnerable while the Drakensberg Foothill Moist Grassland and Southern Drakensberg Highland Grassland are considered Least Threatened (Mucina and Rutherford 2006). All types are dominated by grassland species, herbaceous plants, and low shrubs. The vegetation in the wetland itself is still in a nearly natural state, although at the species level, it may be transformed due to selective grazing by cattle and an annual burning regime.

During the dry season (Figure 3.15A), the wetland receives some subsurface and lateral water inputs from the surrounding hillslopes, this has likely been altered by anthropogenic landscape transformation such as commercial forestry and road networks. During the wet season, large and cumulative storm events result in the Gatberg River overtopping its banks and inundating the surrounding floodplain (Figure 3.15B).

Figure 3.15 Aerial images showing the Gatberg floodplain system in A) the dry season and B) the wet season

3.2.2.1.3 RAINFALL (2019-2021)

Rainfall was measured in the Mooi River catchment (PG Bison Training Centre, -31.07454 and 28.21382; Figure 3.16), using a 150 mm funnel tipping bucket rain gauge and a HOBO® pendent event logger. The rain gauge was installed in 2015 under the Tsitsa Project (Huchzermeyer et al. 2021).

Figure 3.17 shows the daily rainfall recorded for the study period (2019-2021). The corresponding flood events recorded for the Gatberg River are highlighted. The maximum daily rainfall recorded was 65.5 mm. The 2019/2020 wet season had fewer storm events, with less rain falling within those events than in 2020/2021.

Figure 3.16 Google Earth image showing the location of the PG Bison rain gauge in relation to the two study sites

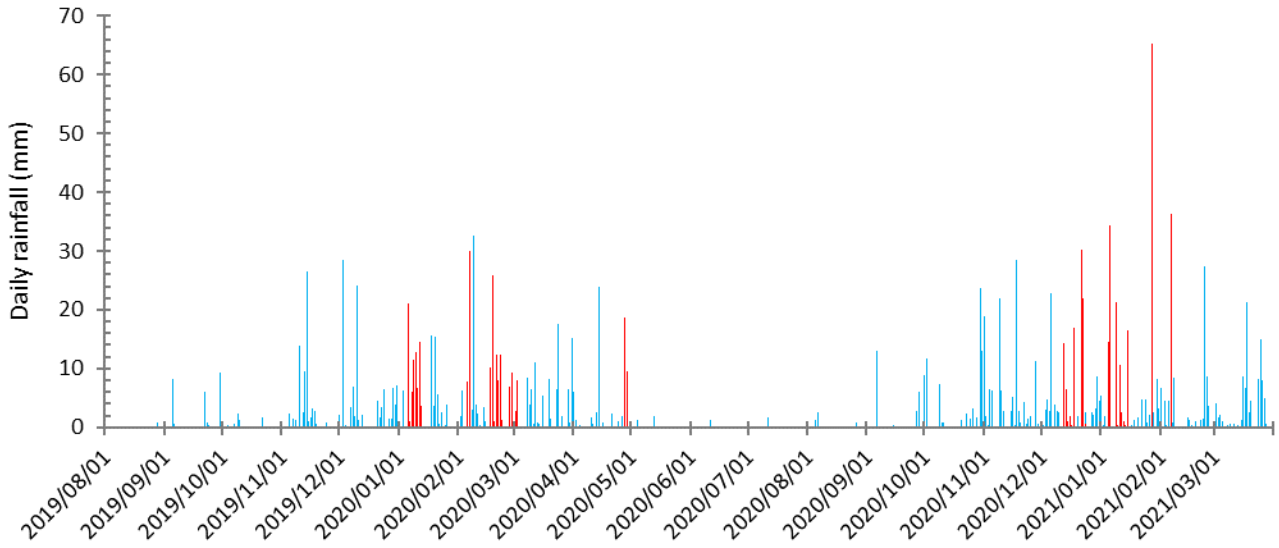

Figure 3.17 Daily rainfall recorded at PG Bison for the research period (2019-2021). Events highlighted in red correspond to the recorded flood events presented in the following section

3.2.2.1.4 River flow and floodplain inundation (2019-2021)

Discharge is a significant driver of channel response and floodplain dynamics over time (Rowntree and Wadeson 1999). Significant sediment entrainment and transport necessitate high flows. In rivers and their floodplain systems, higher and overbank flow (frequency, magnitude, and residence time) drives and maintains morphology (Shields Jr et al. 2000), biological processes (Amoros and Bornette 2002; Thoms 2003), habitat formation (Ward et al. 1999), nutrient cycling (Meyer and Likens 1979; Junk et al. 1989; Thoms et al. 2004) and sediment storage (Erskine and Livingstone 1999; Walling et al. 1999; Fryirs et al. 2007). The degree of connectivity between the channel and its floodplain will be determined by the magnitude of the flood and the form of the channel. Smaller magnitude events occur more frequently than larger magnitude events (Wolman and Miller 1960; Pickup and Warner 1976; Fryirs et al. 2007).

In this section the frequency of overbank connectivity is considered for the Gatberg River floodplain system. Measured water level data for two wet seasons were assessed to evaluate the observed inundation frequency of the floodplain.

A Solinst pressure transducer logger was installed, on cross-sectional transect 2, in the channel to monitor water levels across two wet seasons. The pressure logger was set to a 10-minute time interval to record the water level data. In the channel, the logger was placed into a metal cover that was attached to a metal pole. The metal pole was hammered as close to the channel bed as possible. Logger and thalweg elevation

were noted with a Differential Global Positioning System (DGPS) for calibration for the next field visit. The Solinst system recorded both a temperature and a pressure transducer. The total pressure transducer combines the sum of the water and air pressure above the sensor when installed. Following that, atmospheric pressure changes must be calibrated to calculate the actual elevation of the water column above the pressure transducer. To accommodate for the absolute water level elevation, a barometric correction was performed using a Solinst Barologger installed near the wetland.

To map the extent of identified overbank flooding events, 3 m resolution multispectral PlanetScope satellite imagery (Planet Team 2017) was imported into ArcMap 10.8.2. A Normalised Difference Vegetation Index (NDVI) was created from the imagery, and the values corresponding with water, and verified with in-field observations, were extracted.

Figure 3.18 shows the water levels measured in the Gatberg River from August 2019 to October 2021. The dotted line depicts the channel bank height on the same transect as the logger. This was used to estimate the number of overbank floods that occurred over the two wet seasons. During the measurement period 11 floods were recorded that were higher than the channel bank elevation, 5 in the 2020 hydrological year and 6 in the 2021 hydrological year (hydrological years run from October to September). The first flood event recorded for the 2020 hydrological year was on the 12th of January 2020 and the last on the 29th of April 2020. The first flood event recorded for the 2021 hydrological year was on December 17th, 2020, and the last on February 6th, 2021.

Figure 3.19 and Figure 3.20 show the mapped flood extents across the floodplain surface for 4 flood events identified in the water level analysis. These extents would also include collected rain and previous flood waters that had not yet evaporated on the floodplain surface. The satellite images used were a couple of days older than when the flood events occurred due to cloud cover obscuring the wetland. Oxbows and lower-lying areas on the floodplain surface collected water first, however within the wet season most of the floodplain had at least some water on it. From field observations, it was noted that some of the oxbows were permanently filled with water. Table 3.1 shows the summary of the details of the overbank floods that occurred during the two wet seasons. The table shows the magnitude and frequency of flood peaks within the Gatberg River floodplain, floods over-top their banks multiple times every year.

Sections of floodplains become inundated at different rates and times due to floodwater travel time, attenuation and lag, and site-specific morphological and vegetation characteristics. Pondage times after floodwater recession depends upon the rate of stage rise and microtopography, and more particularly the connectivity of the floodplain and the geomorphic unit mosaic. Thus, once overbank spillage occurs, there

is a dramatic reduction in floodwater transmission capacity caused by frictional factors, such as vegetation and microtopography, and shallower floodwater depths, with important implications for sediment deposition and storage.

Measuring suspended sediment fell out of the scope of this study. However, other research on rivers of the upper Tsitsa River catchment (Huchzermeyer 2016; Bannatyne 2018; Bannatyne pers comm.) shows the timing of sediment load transport through these rivers is highly variable. Baseflows typically don't carry much sediment. Most of the sediment is transported, almost exclusively, in the wet season, except for isolated winter rain or snowmelt events. High flows generally carry more sediment, but the relationship between discharge and suspended sediment concentrations typically has a very weak correlation ($r^2 < 0.3$) because of the positive hysteresis. From the data, suspended sediment concentrations and discharge, time series for the Pot River, the upper section of the Tsitsa River, the Gqukunqa River and the Tsitsa River below the tributaries, no general trends in terms of beginning, middle or end of the season could be identified (Bannatyne pers comm). However, the research focussed on annual loads and yields rather than sediment dynamics within the wet seasons. Suspended sediment concentrations seem to be dependent on changing sediment sources within the catchment within and between rainfall events, rainfall erosivity, antecedent conditions and vegetation.

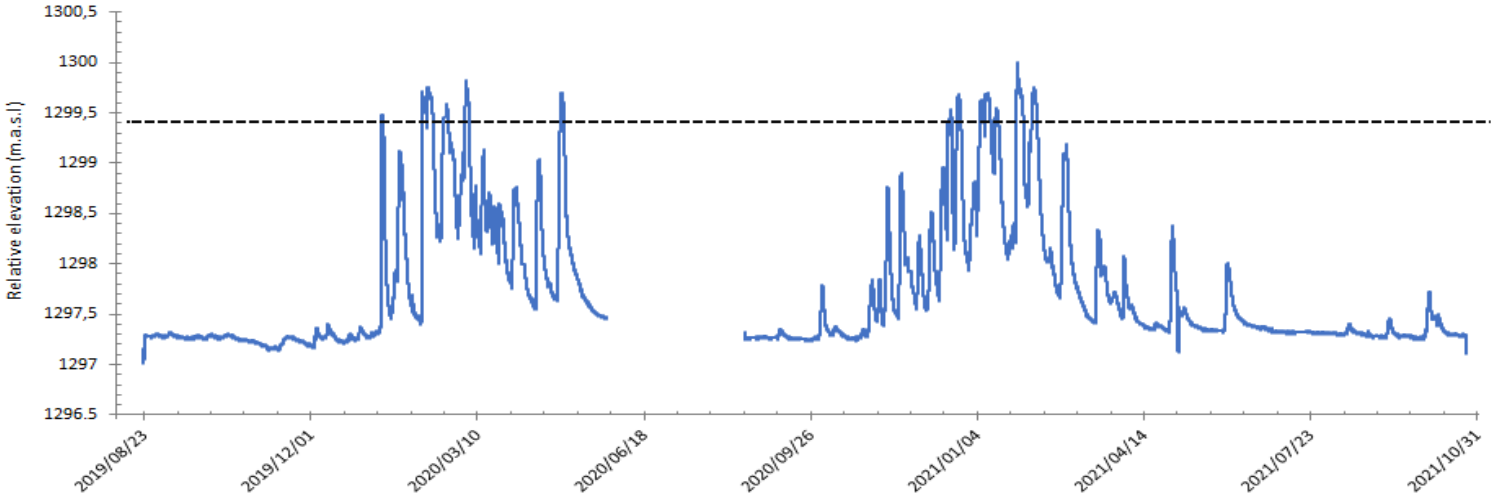

Figure 3.18 Ten-minute compensated water level recorded by the pressure logger. The black dotted line indicates the channel bank elevation. The gap in the data occurred over the dry season in 2019 due to being unable to get into the field due to Covid-19

Table 3.1 Summary of the flood events during the study period

Hydrological year	Storm number	Storm and overbank flood dates (yy/mm/dd)	Date of flood peak (yy/mm/dd)	Time of flood peak (hh:mm:ss)	Peak water level above channel bank (m)
2020	1	2020/01/12 - 2020/01/13	2020/01/13	00:10:00	0.12
	2	2020/02/06 - 2020/02/13	2020/02/09	14:50:00	0.39
	3	2020/02/19 - 2020/02/21	2020/02/20	10:20:00	0.23
	4	2020/03/02 - 2020/03/05	2020/03/03	04:30:00	0.46
	5	2020/04/29 - 2020/05/01	2020/04/29	21:40:00	0.34
2021	6	2020/12/17 - 2020/12/20	2020/12/19	13:20:00	0.18
	7	2020/12/23 - 2020/12/25	2020/12/24	03:10:00	0.32
	8	2021/01/06 - 2021/01/12	2021/01/10	06:00:00	0.34
	9	2021/01/14 - 2021/01/17	2021/01/15	14:40:00	0.18
	10	2021/01/27 - 2021/02/01	2021/01/28	07:50:00	0.64
	11	2021/02/06 - 2021/02/09	2021/02/07	06:00:00	0.39

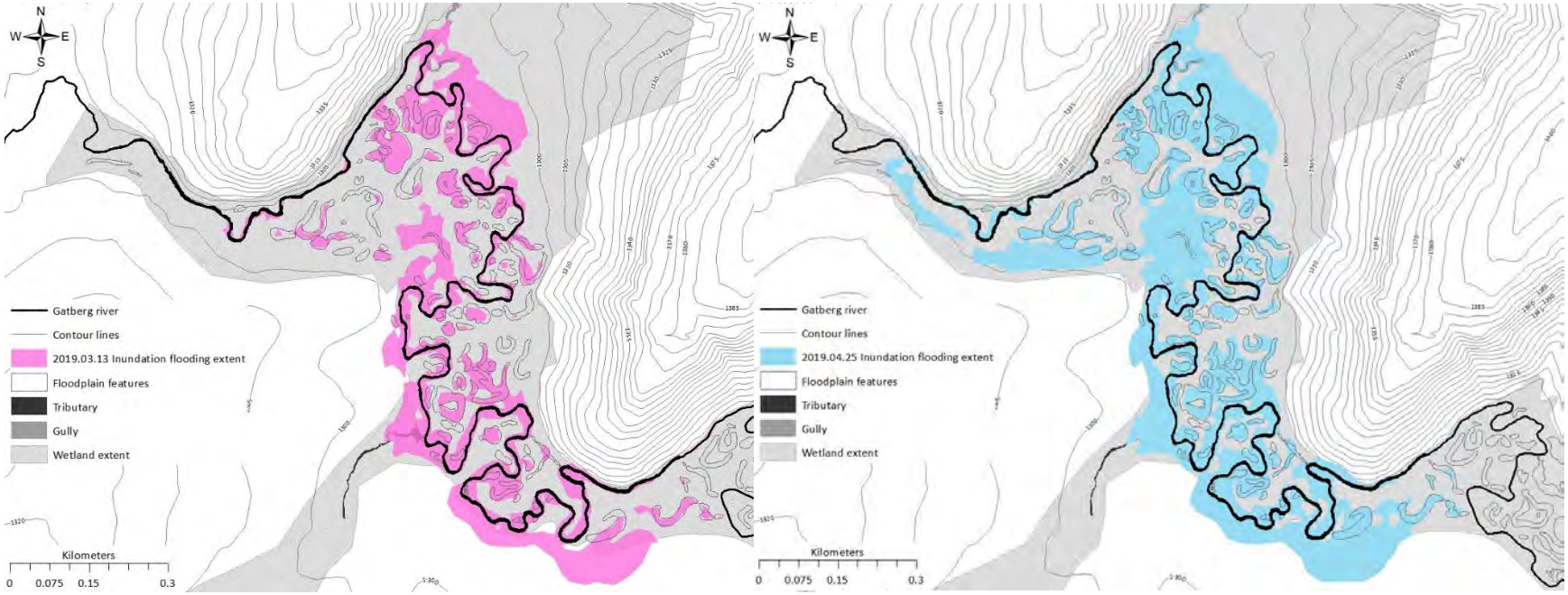

Figure 3.19 Flood water extents mapped by NDVI analysis for 2019.03.13 (pink) and 2019.04.25 (blue)

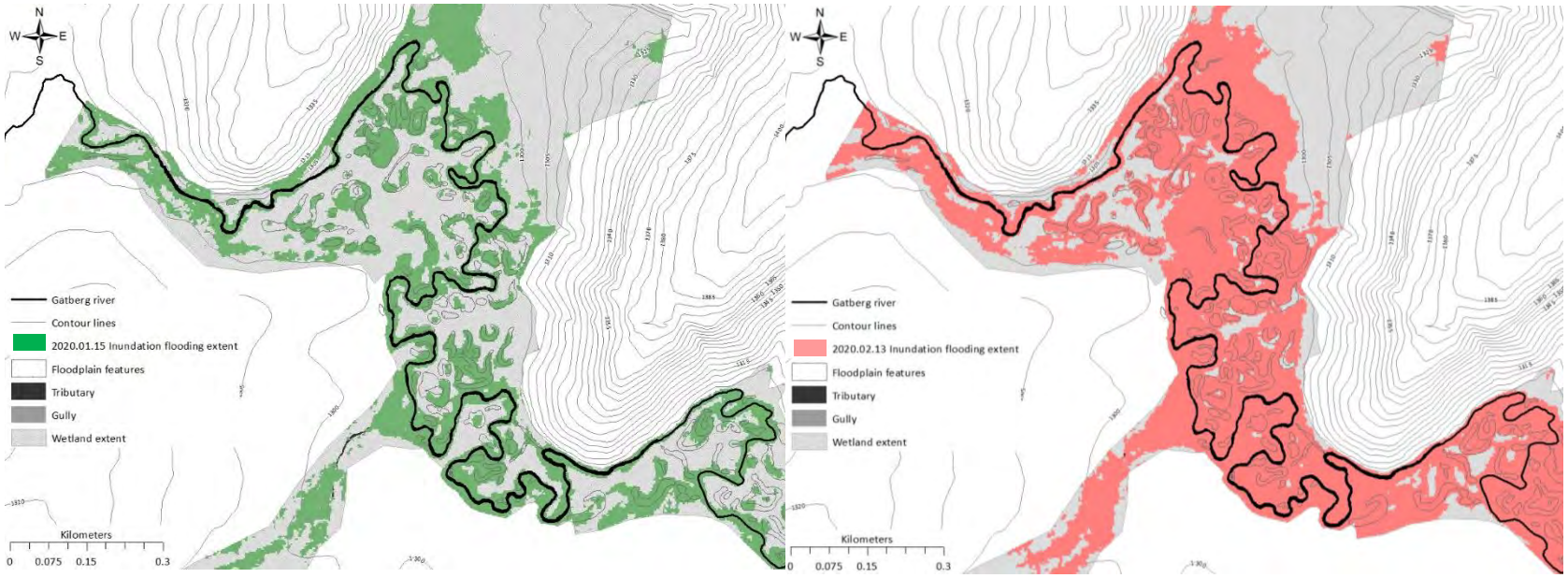

Figure 3.20 Flood water extents mapped by NDVI analysis for 2020.01.15 (green) and 2020.02.13 (salmon)

3.2.2.2 MINNEHAHA FLOODPLAIN WETLAND SYSTEM

3.2.2.2.1 LOCATION

The Minnehaha floodplain wetland system on the Minnehaha River, a tributary of the Little Pot River, is in Quaternary Catchment T35B, 14 km northwest of the settlement of Maclear in the Eastern Cape (Figure 3.21). It falls within the Elundini Local Municipality. The wetland is situated on the privately owned farms of Cornlands, Lower Cornlands, and Minnehaha. The wetland can be accessed via the network of farm roads with permission from the landowners.

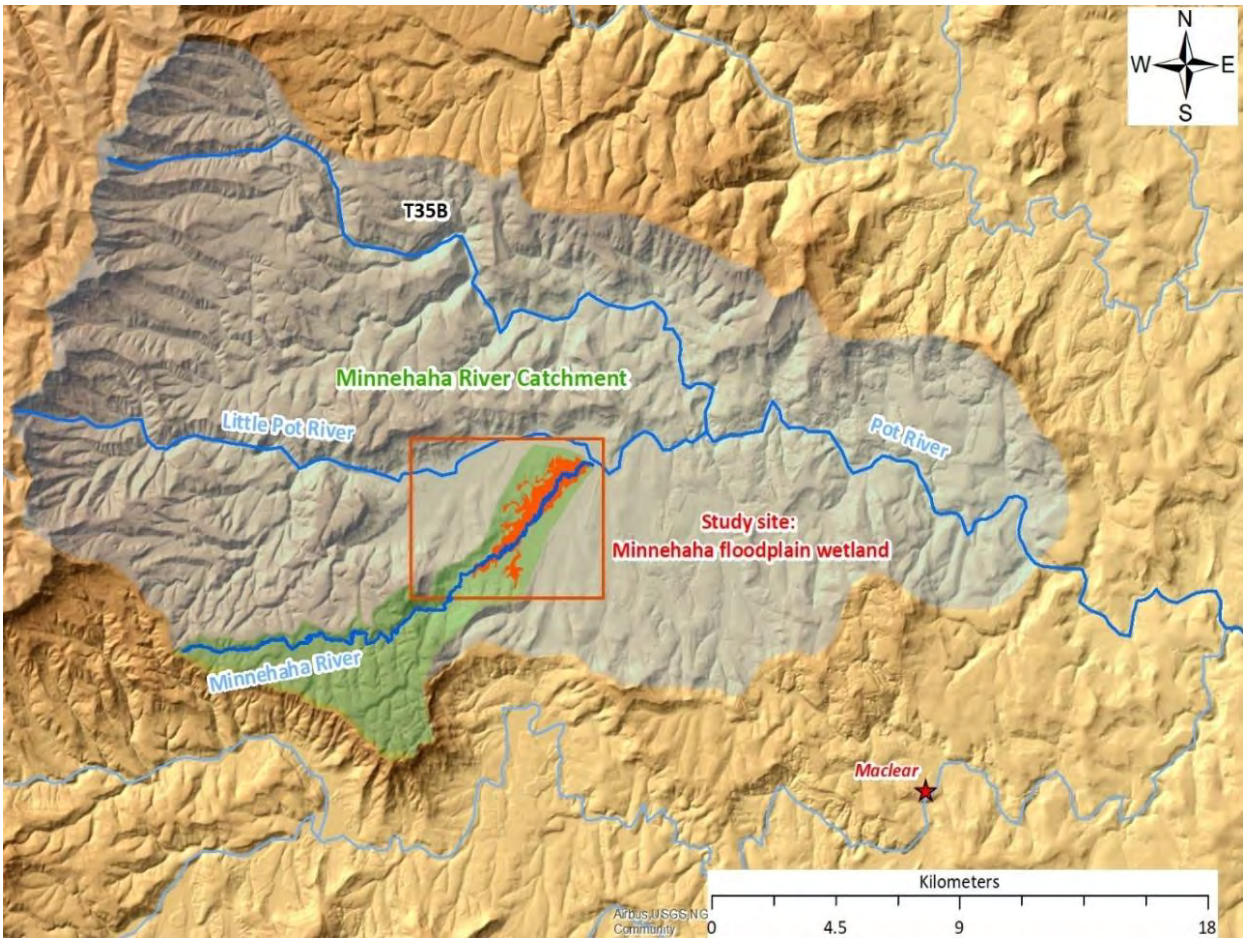

Figure 3.21 The location of the Minnehaha floodplain system (study site) within the Pot River catchment

3.2.2.2.2 DESCRIPTION

The Minnehaha floodplain wetland system is relatively large (~1.5 km²) within its catchment (~ 40 km²). It is connected to the main drainage system of the Minnehaha River which drains into the Little Pot River, a tributary of the Pot River. The Quaternary catchment has a Mean Annual Precipitation (MAP) of 915 mm

and Potential Evaporation (PET) of 1442 mm. A climate ratio (P/E_P) of 0.64 classifies this area within the semiarid climate type. The wetland is in alluvium and is underlain by the alternating sandstones and mudstones of the Elliot Formation (Beaufort Group of the Karoo Supergroup geology) with the higher ground being comprised of the Clarens Formation (fine-grained sandstone and siltstone of the Beaufort Group of the Karoo Supergroup geology). These soils are generally well-drained with a clay content ranging from 15 to 55 % (Mucina and Rutherford 2006).

The dominant vegetation type in the area is East Griqualand Grassland (Gs12) and Southern Drakensberg Highland Grassland (Gd4) on the higher slopes in the upper region of the catchment (Mucina and Rutherford 2006). East Griqualand Grassland is considered vulnerable while the Southern Drakensberg Highland Grassland is considered least threatened (Mucina and Rutherford 2006). All types are typified by grassland species, herbaceous plants, and low shrubs. The vegetation in the wetland itself is still in an almost natural state, although at the species level, it may be transformed due to selective grazing by cattle and sheep.

During the dry season (Figure 3.22A), the wetland receives some subsurface and lateral water inputs from the surrounding hillslopes, this has likely been decreased by anthropogenic landscape transformation such as some agricultural fields and the construction of farm dams in the adjacent area surrounding the wetland. During the wet season (Figure 3.22B) large and cumulative storm events result in the Minnehaha River overtopping its banks and inundating the surrounding floodplain.

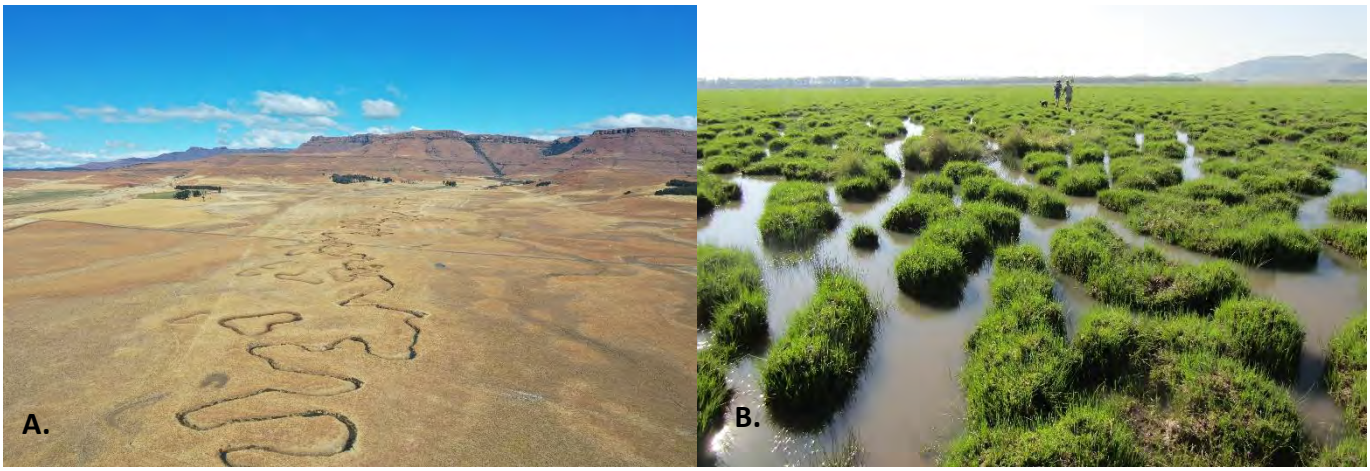

Figure 3.22 Photographs showing the Minnehaha floodplain system in A) the dry season and B) the wet season

3.2.2.2.3 RAINFALL (2019-2021)

Figure 3.23 shows the daily rainfall recorded for the study period (2019-2021). The corresponding flood events recorded for the Minnehaha River are highlighted. The maximum daily rainfall recorded was 65.5 mm. The 2019/2020 wet season had fewer storm events with lower rainfall within those events than 2020/2021.

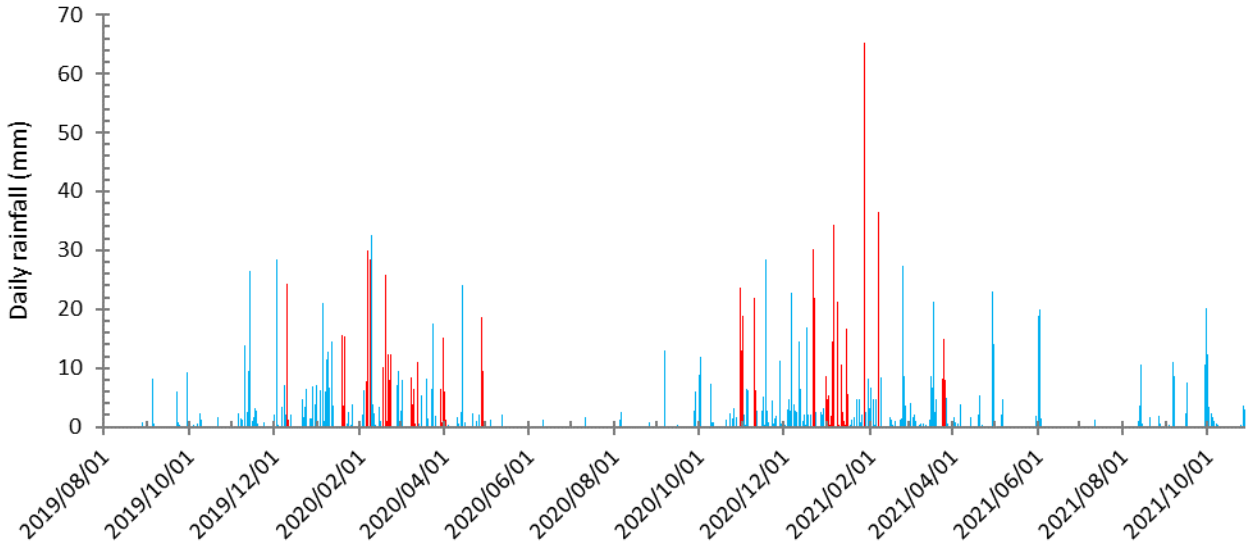

Figure 3.23 Daily rainfall recorded at PG Bison for the research period (2019-2021). Events highlighted in red correspond to the recorded flood events presented in the following section

3.2.2.2.3 RIVER FLOW AND FLOODPLAIN INUNDATION (2019-2021)

Figure 3.24 shows the water levels measured in the Minnehaha River from August 2019 to October 2021. The dotted line depicts the channel bank height on the same transect as the logger. This was used to estimate the number of overbank floods that occurred over the two wet seasons. Over the measurement period 19 floods were recorded that were higher than the channel bank elevation, 9 in the 2020 hydrological year and 10 in the 2021 hydrological year (hydrological years run from October to September). The first flood event recorded for the 2020 hydrological year was on the 11th of December 2019 and the last on the 28th of April 2020. The first flood event recorded for the 2021 hydrological year was on the 1st of November 2020 and the last on the 26th of March 2021. Table 3.2 shows the summary of the details of the overbank floods that occurred during the two wet seasons.

Figure 3.25 shows the extent of the mapped floods across the floodplain surface for 2 flood events identified in the water level analysis. These extents would also include rain collected and previous flood waters that had not evaporated yet on the floodplain surface. The satellite images used were a couple of days after the flood events due to cloud cover over the wetland. Oxbows and lower-lying areas on the floodplain surface collected water first, however within the wet season most of the floodplain had at least some water on it. From field observations, it was observed that the floodplain was covered by water from the lower area behind the channel levees to the backswamp at the floodplain margin.

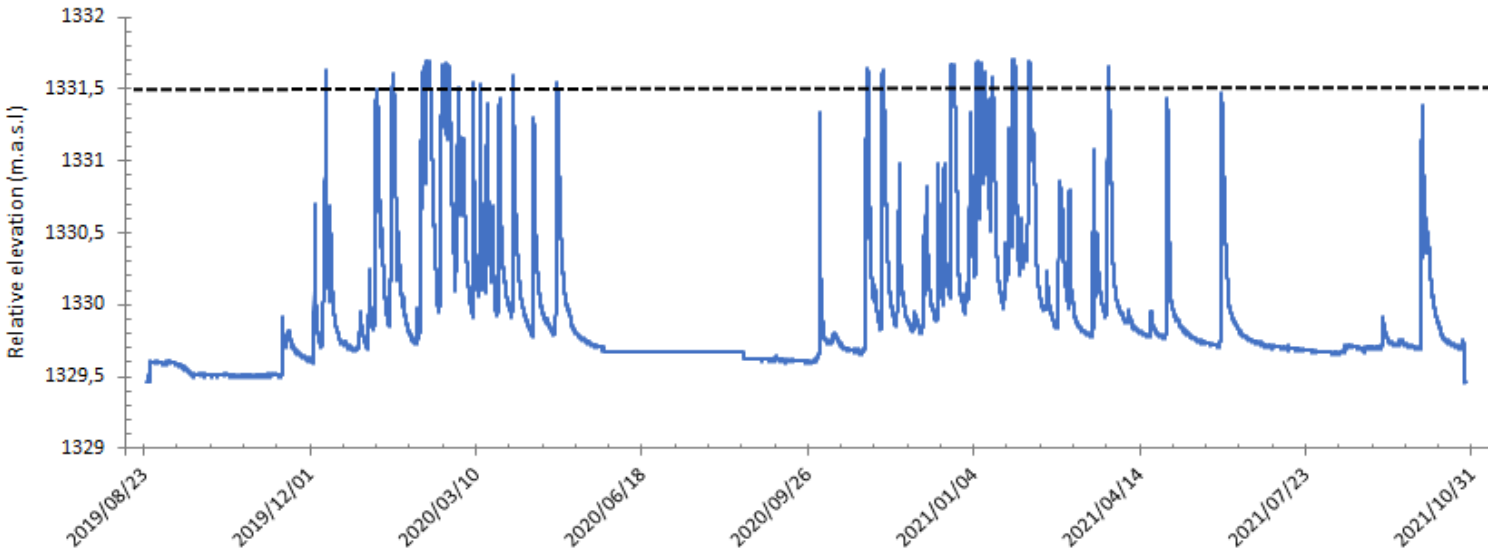

Figure 3.24 Ten-minute compensated water level recorded by the pressure logger. The black dotted line indicates the channel bank elevation

Table 3.2 Summary of the flood events during the study period

Hydrological year	Storm number	Storm and overbank flood dates (yy/mm/dd)	Date of flood peak (yy/mm/dd)	Time of flood peak (hh:mm:ss)	Peak water level above channel bank (m)
2020	1	2019/12/11- 2019/12/11	2019/12/11	05:30:00	0.44
	2	2020/01/20 - 2020/01/20	2020/01/20	02:20:00	0.42
	3	2020/02/07 - 2020/02/11	2020/02/09	22:00:00	0.51
	4	2020/02/19 - 2020/02/19	2020/02/19	05:10:00	0.48
	5	2020/02/21 - 2020/02/23	2020/02/21	21:30:00	0.49
	6	2020/03/08 - 2020/03/08	2020/03/08	20:10:00	0.36
	7	2020/03/13 - 2020/03/13	2020/03/13	07:20:00	0.34
	8	2020/04/02 - 2020/04/02	2020/04/02	12:10:00	0.41
	9	2020/04/28 - 2020/04/28	2020/04/28	16:10:00	0.35
2021	10	2020/11/01 - 2020/11/02	2020/11/01	18:30:00	0.45
	11	2020/11/10 - 2020/11/11	2020/11/11	00:50:00	0.44
	12	2020/12/21 - 2020/12/23	2020/12/23	03:00:00	0.48
	13	2021/01/05 - 2021/01/06	2021/01/06	00:10:00	0.50
	14	2021/01/08 - 2021/01/09	2021/01/08	23:10:00	0.49
	15	2021/01/11 - 2021/01/11	2021/01/11	06:20:00	0.43
	16	2021/01/15 - 2021/01/15	2021/01/15	14:50:00	0.39
	17	2021/01/27 - 2021/01/29	2021/01/27	18:00:00	0.51
	18	2021/02/06 - 2021/02/07	2021/02/06	17:30:00	0.51
	19	2021/03/26 - 2021/03/26	2021/03/26	07:40:00	0.46

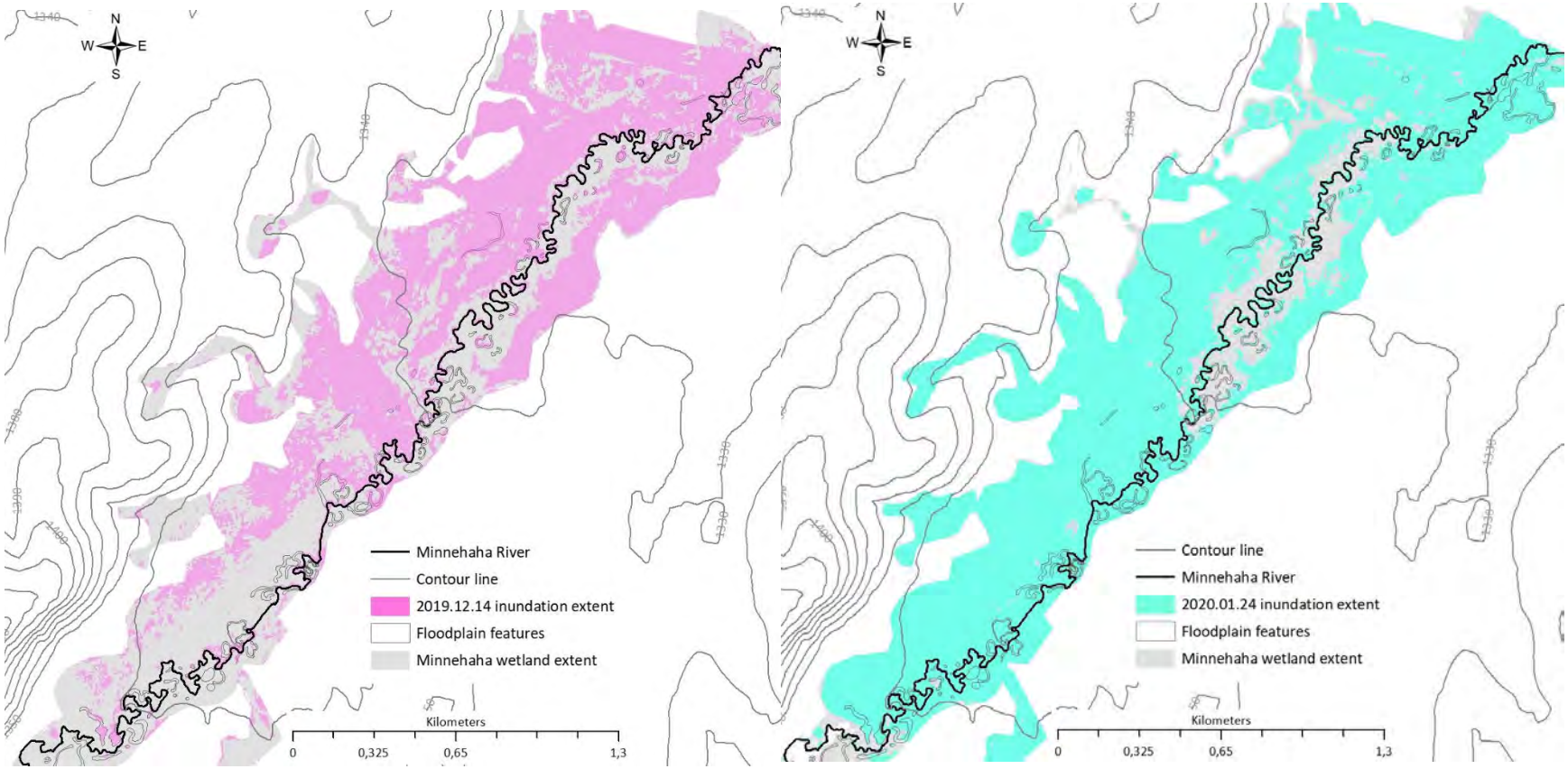

Figure 3.25 Flood water extents mapped by NDVI analysis for 2019.12.14 (pink) and 2020.01.24 (blue)

3.3 CONCLUSION AND CHAPTER SUMMARY

The study area was in a remote part of one of South Africa's least developed provinces, with high levels of unemployment and low levels of education. Many livelihoods are closely tied to ecological infrastructure and services. The Umzimvubu River and its tributaries have been nationally prioritised as one of the few remaining free-flowing, near-pristine rivers; yet it is classified as vulnerable due to the catchment's high rate of degradation.

The Gatberg and Minnehaha Rivers are both found in the upper Tsitsa River catchment, one of the main tributaries of the Umzimvubu River, in the Eastern Cape, South Africa. The Gatberg River is a tributary of the Inxu River, which is a tributary of the Tsitsa River. The Minnehaha River is a tributary of the Little Pot River, which flows into the Pot River, which joins the Tsitsa River and ultimately the Umzimvubu River.

The Gatberg and Minnehaha River catchments are predominantly natural grassland, commercial forestry, and privately owned farms (mostly used for livestock farming (cattle and sheep) and some pastures and agriculture). The soils in the two catchments are primarily derived from sandstone and mudstone from the Elliot, Clarens, and Molteno Formations of the Karoo Supergroup. Shallow, easily weathered soils are found on the steep slopes. Duplex soils, which contain highly dispersive clay soils, are found on lower slopes.

Both the Gatberg and Minnehaha River catchments display characteristics typical of dryland climates, with mean annual precipitation lower than potential evapotranspiration rates, indicating a delicate balance between water input and loss. Hydrologically, both floodplain systems show dynamic responses to seasonal rainfall patterns. Wet season inundation results from localised high-intensity storm events. Analysis of rainfall and flood events over two consecutive wet seasons reveals variations in event frequency and intensity, highlighting the influence of climate variability on hydrological processes and thus sediment transport and trapping within these systems. Measurement of water levels and mapping of flood extents provide valuable data for assessing overbank flooding frequencies and the extent of inundation across the floodplain surfaces. Both the Gatberg and Minnehaha floodplains are inundated every year. According to the analysis of the water levels, both systems experience multiple floods that overtop (a potential source of sediment and phosphorus) the respective channel banks a year. These observations underscore the importance of maintaining connectivity between river channels and their floodplains.

In conclusion, the Gatberg and Minnehaha floodplain systems are integral components of their catchment ecosystems, serving as important reservoirs of ecosystem services and contributing to downstream water quality and flow regulation.

3.3.1 MOTIVATION FOR SELECTION OF THE TWO FLOODPLAIN SYSTEMS

The two floodplain systems were chosen because both are typical meandering floodplain systems, in a nearly pristine state with no man-made structures, and few tributary influences. The Gatberg floodplain wetland system was chosen as it was a floodplain system that fell well within the semi-arid climate index and represents a 'typical' system found on the Gatberg River. It is a small floodplain wetland within a confined valley, where the wetland is controlled by dolerite protrusions. The Minnehaha floodplain wetland system was chosen as it was a floodplain system that fell on the upper limit of the semiarid climate index and represents a larger wetland system with a wide valley where the wetland is controlled by the trunk river (Little Pot River).

CHAPTER 4 : POTENTIAL SEDIMENT AND PHOSPHORUS SOURCES, CONNECTIVITY AND BUFFERS IN THE GATBERG AND MINNEHAHA RIVER CATCHMENTS

4.1 INTRODUCTION

The physical characteristics and functioning of a river are predominantly a product of, and determined by, the movement of water and sediment through the catchment (Rosgen 1994). Sediment input from the catchment is determined by the amount of sediment available and the paths or links (connectivity) required to transport the sediment to the river (Owens 2005). The term 'connectivity' can refer both to i) structural - the physical structure of the landscape and ii) functional - the movement of water, sediment, and other materials (or species) through it. As a result, connectivity is extremely useful in studies of sediment and sediment-associated nutrient dynamics. A well-connected system allows for the movement of energy and materials, as well as mutual adjustment of system components (Harvey 1997; Brierley et al. 2006; Farraj and Harvey 2010). At the catchment scale, the main active geomorphic zones are hillslopes and channels, and the main fluxes are within and between these two components (Bracken et al. 2015).

Connectivity is offset by storage units, such as buffers, barriers, and blankets, within the catchment that allows sediment and water to be retained or stored within the system (Fryirs et al. 2007). The role of sediment sources and connectivity both within the broader catchment and within a floodplain system is vital when trying to understand the dynamics of sediment and nutrients within a floodplain system.

Field observations revealed that the Gatberg and Minnehaha River catchments were characterised by high sediment concentrations during rainfall events. This thesis focuses on two key components of landscape connectivity: firstly, the potential sources, connectivity, and storage units within the upstream catchment, and secondly, those within each floodplain system. Both aspects will be addressed in this analysis. The focus objectives are as follows:

1. Describe the general characteristics of the catchment in terms of the longitudinal profile of the Gatberg and Minnehaha Rivers.
2. Classify, map, and characterise potential sources of sediment and phosphorus within the broader catchment of the two rivers.
3. Classify, map, and characterise potential sediment and phosphorus buffers and barriers within the broader catchment of the two rivers.
4. Classify, map, and characterise potential sediment and phosphorus sources within the two floodplain systems.

The methods for mapping and assessing sources, connectivity, and storage are discussed below.

4.2 METHODS

This section describes the methods that were used to meet the objectives set for this analysis. The methods were based largely on a desktop study using a Geographical Information System (GIS), with field visits to ground truth a selection of the features. High-resolution images and spatial datasets are useful to identify recent sediment sources and the pathways that connect the source areas to the channel. The characteristics of the source areas and the pathways were derived from aerial images (0.5 m resolution; 2021) interpretation and a terrain analysis (based on 10 m contours). Details of the methods used are given below.

4.2.1 DESKTOP ANALYSIS

The desktop analysis was conducted to facilitate a comparison between the Gatberg River floodplain system and the Minnehaha River floodplain system, as well as to offer a catchment-scale and regional context for the two study sites.

4.2.1.1 LONGITUDINAL PROFILES AND CATCHMENT CHARACTERISTICS (POTENTIAL SEDIMENT AND PHOSPHORUS SOURCES, BUFFERS, AND BARRIERS)

This section describes the methods that were used to assess the longitudinal profiles and characteristics of the Gatberg and Minnehaha River catchments to determine the potential sources, buffers, and barriers of sediment and phosphorus (Fryirs et al. 2007). The methods were largely based on a desktop study using a Geographical Information System (GIS), with field observations to verify the characteristics. High-resolution aerial images were used to identify recent sediment sources and the pathways (drainage lines, roads, tracks, and gullies) that connect the source areas to the channel (Owens 2005). Characteristics of the source, buffers, barriers, and pathways were derived from aerial photo interpretation and terrain analysis (based on 10 m contours; Kheir et al. 2007).

Longitudinal profiles of the entire Gatberg and Minnehaha Rivers were compiled using 1:10 000 orthophotographs obtained from the South African Surveyor General, and contours with 10 m intervals. The spatial datasets from the South African National Land Cover (SANLC) 2020, the national wetlands map v5 (2018) and locally relevant vector data (dams, rehabilitation structures, changes in land use, floodplain systems and tributaries) were marked on the aerial imagery along the longitudinal profile to assess potential sediment storage units and additional sediment sources along the profile upstream of the study sites.

A 1:250 000 geological map was obtained from the Council of Geoscience of South Africa, and this was cropped to the location of the study sites and used in the area calculations for each of the geological provinces.

Potential phosphorus sources in the study area were identified using the spatial datasets from the South African National Land Cover (SANLC) 2020; Surveyor General; Council of Geoscience; Tsitsa Project and confirmed using 2022 Google Earth images (© Maxar Technologies, Google Earth 2024). The main sediment phosphorus sources include cultivated fields (agricultural), fallow land, previously cultivated fields (agriculture) and bare ground, gullies, roads and tracks, towns, villages, residential areas, and commercial forestry.

Areas characterised by rectangular or trapezoidal shapes with linear edges, where the vegetation within the boundaries consisted of crops and differed from that outside, were classified as agricultural fields. Agricultural fields that have not been cultivated recently (with plough lines visible) and lacked fencing were categorised as previously cultivated fields. All cultivated lands currently or previously, act as sediment sources to a certain extent (Fryirs and Brierley 1999; Kakembo and Rowntree 2003; Koulouri and Giourga 2007; López-Vicente *et al.* 2013). Currently, cultivated lands are ploughed annually, resulting in a disturbance of the soil structure and low vegetation cover for large parts of the year, resulting in easier entrainment and transport of sediment. Partly used fields are ploughed on a less regular basis but the initial disturbance of the soil structure results in the continual transport of sediment from these areas. Previously cultivated fields were observed to have depleted soils and low vegetation cover and as such are sediment source areas.

The gullies were considered large (> 2 m), incised linear erosional features with steep sidewalls that concentrate flow and sediment predominantly downslope. Roads (gravel) were easily recognisable, as they were larger features (> 2 m wide) of constant width, usually followed the contour and linked homes, farms, or residential areas, and traversed the commercial forestry. Livestock tracks were observed to be narrow (< 2 m wide) linear features, largely following the contours (traversing the slopes) or mountain slopes or concentrating towards water and feed points. Currently and previously cultivated fields, fallow land, bare ground, gullies, towns, villages, residential areas, and commercial forestry were captured as polygons. Roads and livestock tracks were captured as line features. To calculate the area for roads and livestock tracks, the lengths were multiplied by the average width of 4.04 m and 0.79 m respectively (averages based on calculations by van der Waal 2015 in a neighbouring catchment). These widths were

reasonable averages based on field and aerial image observations for the Gatberg and Minnehaha River catchments.

Statistics that described the topographic character of the catchment, each of the geological provinces (regions), and the various types of sediment and phosphorus sources (in terms of the whole catchment and the individual geological provinces) were calculated using ArcMap 10.8.2 GIS. Statistics included: the area of features, percentage of total area (catchment and geological provinces), slope, aspect (Le Roux and Sumner 2012), connectedness to the river network, the percentage of fields that were recently cultivated and the percentage of features located on the agricultural fields.

Each river catchment boundary was established based on 10 m contours (national dataset), and the underlying geology was digitised from a 1:250 000 geological map. A 10 m DEM was created using the *Interpolate* tool and the 10 m contour data. Using the Surface toolset, a slope and aspect raster were generated from the 10 m DEM. To minimise the number of slope classes, only three were classified: gentle (< 6°), moderate (> 6° - 25°) and steep (> 25°) to reflect the stepped nature of the landscape. The steep (> 25°) category represents the very steep sections, often including vertical cliffs; the moderate category represents lower talus slopes and more gentle areas above the steep sections; the gentle category represents the near flat areas found between the 'moderate' sections on top of the mountains (mountain plateaus) or along the valley fill adjacent to the rivers. From the aspect raster, the north-facing slopes (0° - 23° and 338° - 360°) were extracted. North-facing slopes were measured and extracted due to erosion patterns and soil instability. North-facing slopes in the southern hemisphere usually have less vegetation due to sunlight and moisture differences this results in north-facing slopes experiencing more erosion than south-facing slopes. North-facing slopes can contribute more sediment to the river system. Slope and aspect data were extracted for source polygons using the *Extract by Mask* tool. Other attributes, such as geology, connectedness, and location relative to a field, were assigned to each polygon using the *Intersect* tool. Connectivity was assigned according to whether a feature was intersected by a continuous gully or a drainage line (both identified as physical features in the landscape). The same was done for features that were located on fields. The databases were copied to Microsoft Excel for further interpretation.

4.2.1.2 CLASSIFY, MAP AND CHARACTERISE POTENTIAL FLOODPLAIN STORAGE UNITS

Large-scale (1:1 000) geomorphological maps of the Gatberg and Minnehaha valley fill features were created based on high-resolution colour aerial images (0.5 m resolution; 2021) and topographic surveys. An Epoch 35 Differential Global Positioning System (sub-centimetre accuracy) was used to survey

floodplain cross-sections and along the river channel, noting clear breaks in slope, floodplain geomorphic features, and changes in sediment composition. Five transects were surveyed along both floodplain study sites. A detailed map of both floodplain systems was drawn by overlaying the surveyed transects and features on a high-resolution aerial image in ArcMap 10.8.2. The features were classified according to the results of the survey and field observations. Field observations such as slope, sediment composition, and size of features were used, together with changes in vegetation, to extrapolate field-based evidence onto the map.

The following floodplain storage units were identified: proximal floodplain (inner and outer meander bend), oxbow and backswamp areas. The proximal floodplain in this study refers to the floodplain surface immediately adjacent to the channel, it may include levees and the lower elevated floodplain surface beyond the levee, up to 6 m from the channel banks. This is an area of potential sediment and phosphorus exchange, where lateral deposition from the channel may be stored or exchanged. The proximal floodplain deposits are usually formed by large to fine sediment size fractions and have higher sedimentation rates compared to other floodplain zones (Asselman and Middlekoop 1995; Bridge 2009; Swanson 2013; Pizzuto 2016; Wiener et al. 2022). Oxbows are those features common to floodplain systems that are round, near round or u-shaped pools that form when a meander loop is cut off, by neck cutoff or chute cutoff mechanisms, creating a free-standing body of water. Oxbows store sediment and sediment-associated phosphorus from overbank flows that transport material across the floodplain when the flow overtops the active channels' banks. The sediment that is stored in the oxbows is usually the fine sediment fraction. Sedimentation rates depend on a multitude of factors (i.e., flood characteristics, distance from the channel, oxbow morphology, etc.). Backswamp zones are low-lying areas close to the valley margin and are usually inundated less frequently than the proximal floodplain.

4.3 RESULTS

The sections that follow provide GIS and field-based information and statistics for the two catchments, the potential sediment sources, storage units, and pathways. The data could not be displayed meaningfully on a single map because of the huge area and high definition of the mapped source, storage areas, and connectors. Small-scale maps are provided in the text; however, larger versions are included in Appendix 1.

4.3.1 LONGITUDINAL RIVER PROFILES AND CATCHMENT CHARACTERISTICS

The longitudinal profiles of the Gatberg River, the Minnehaha River, and their floodplain sections are illustrated in Figure 4.1 and Figure 4.2. Figure 4.1 illustrates the Gatberg River profile from its headwaters to the Gatberg River floodplain system (research site), while Figure 4.2 shows the slope of the Minnehaha River from its headwaters to the Minnehaha River floodplain system (research site).

The Gatberg catchment is a typical representation of the steep headwater areas of the Drakensberg Escarpment (De Decker 1981; Mucina et al. 2006) with steep slopes dominating the upper catchment and tier edges of the lower parts of the catchment.

The longitudinal profile of the Gatberg River is initially logarithmic (Figure 4.1), with the upper reach having a steep initial slope of 10 % (0 to 991 m) that transitions to a slope of 0.66 % (991 to 5 546 m), then to a slope of 0.26 % (5 546 to 21 212 m). Subsequently, a steep step that has a slope of 5 % and an approximate height of 25 m interrupts the logarithmic trend of the profile, with the step being formed at the boundary between the alternating layers of sandstone, mudstone and shale of the Molteno Formation and the mudstones of the Elliot Formation. This step ends at about 23 km along the profile and after this, the profile becomes more planar continuing with an average slope of 0.04 % which terminates at 46.8 km at the toe of the study site Gatberg floodplain system. The average slope of the Gatberg River upstream of the research site is 0.6 %. Floodplain pockets or 'beads' occur along the longitudinal profile of the Gatberg River. These seem to be linked to changes in valley width or geological composition (dolerite intrusions).

The soil properties (Dijkshoorn et al. 2008) for the catchment are shown in Figure 4.3. The catchment is characterised by Eutric Regosols soils (6 % of the total catchment), Haplic Acrisols (15 %), Eutric Leptosols (19 %) and Gleyic Acrisols (33 %). According to Fey (2010), regosols are characterised by shallow, medium- to fine-textured, unconsolidated parent material that may be of alluvial origin and lack significant soil horizons. Leptosols are soils with a very shallow soil profile and often contain large amounts of gravel. They are especially susceptible to erosion, desiccation, or waterlogging, depending on climate and topography. Acrisols are characterised by clay-rich subsoil.

Gentle (66 %) to moderate (31 %) slopes dominate the catchment (Table 4.1), with a larger proportion of the steeper slopes on the Elliot Formation (Figure 4.4A). A large proportion (14 %) of the slopes were north-facing, with the most (9 %) occurring within the Elliot Formation. The shift from steeper slopes for higher-lying areas indicates the expected trend along the river profile, where the river headwaters are

steeper compared to the gentler landscapes of the lower reaches of the river. There are 9 major tributaries which feed into the Gatberg River upstream of the study site, 5 from the left bank and 4 from the right bank. Numerous valley bottom wetlands (13) feed into the Gatberg River. Due to the erodibility of the soils, intense rainstorms and land use several rehabilitation structures (black arrows in Figure 4.1) have been built along the Gatberg River as part of the Working for Wetlands Gatberg River rehabilitation program to preserve the numerous floodplain systems and other types of wetlands occurring along the river. None of these structures are situated within the Gatberg study site. A large impoundment has been constructed on the Gatberg River in its headwaters (991 m). Several smaller impoundments have been constructed on the tributaries and valley bottom wetlands entering the Gatberg River for water storage and as a resource for fire emergencies for commercial forestry companies or private farms.

The longitudinal profile of the Minnehaha River (Figure 4.2) is initially planar, with the upper reach having a gradual initial slope of 1.3 % (0 to 11 997 m). Subsequently, a steep step that has a slope of 21.4 % and an approximate height of 310 m interrupts the planar trend of the profile. This step ends at about 13.8 km along the profile and after this, the profile becomes planar again continuing with an average slope of 0.3 % which terminates at 29.8 km at the toe of the study site Minnehaha floodplain system. Gentle (66 %) to moderate (31 %) slopes dominate the catchment (Table 4.1), with a larger proportion of the steeper slopes on the Elliot Formation. The soil properties (Dijkshoorn et al. 2008) for the catchment are shown in Figure 4.3. The catchment is characterised by Eutric Regosols soils (48 % of the total catchment) and Haplic Acrisols (52 %). A large proportion (14 %) of the slopes were north-facing, with the most (9 %) occurring within the Elliot Formation.

16 tributaries feed into the Minnehaha River upstream of the study site, 3 from the left and 13 from the right. Four valley bottom wetlands feed into the Minnehaha River. There is also another large floodplain system above the study site upstream of the waterfall. Several smaller farm impoundments have been constructed on the tributaries and valley bottom wetlands that enter the Minnehaha River.

Table 4.1 Area, slope, and aspect (north-facing) for the Gatberg and Minnehaha River catchments

Catchment	Formation	Area Km²	Slope % gentle	% moderate	% steep	Aspect % north-facing
Gatberg River	Total	205	66	31	3	14
	Elliot	126	65	31	4	14
	Molteno	80	68	31	1	13
Minnehaha River	Total	40	48	45	7	18
	Clarens	18	39	56	11	22
	Elliot	22	56	36	5	14

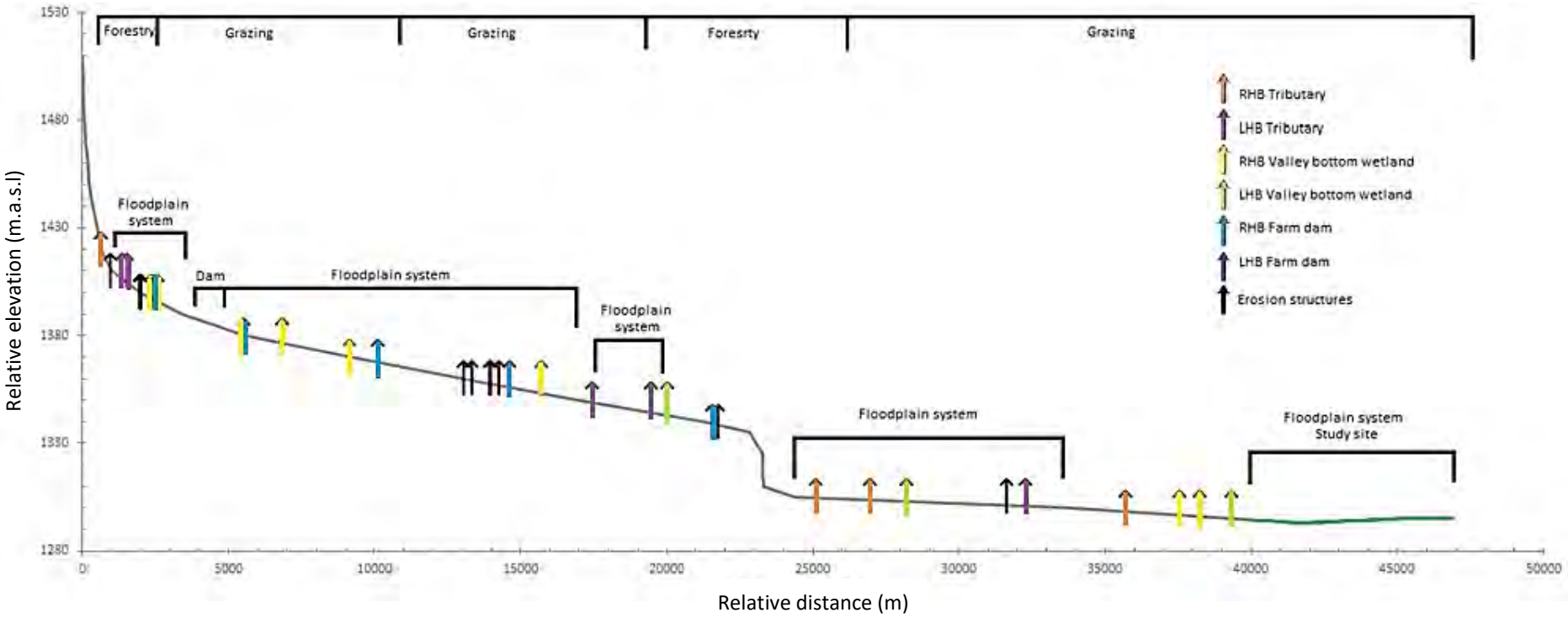

Figure 4.1 The Gatberg River longitudinal profile from its headwaters to the toe of the Gatberg River floodplain system (study site). Dominate land use, tributaries (RHB- right-hand bank and LHB- left-hand bank), floodplain and valley bottom wetlands, dams and erosion structure's locations are marked along the profile

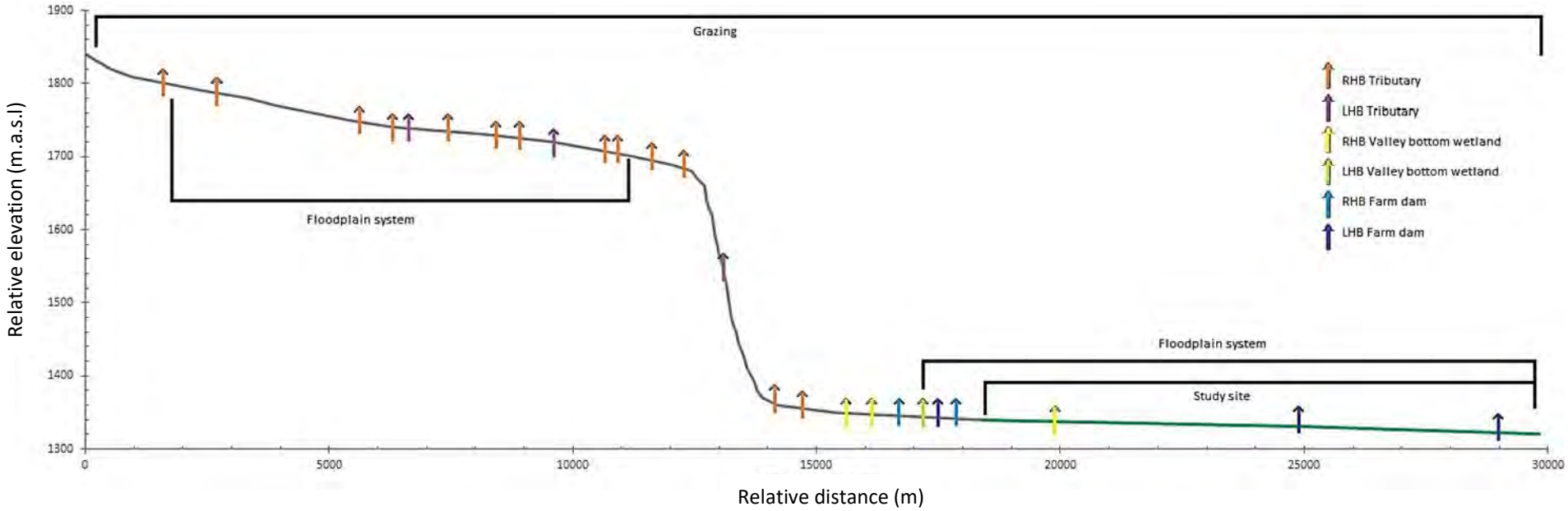

Figure 4.2 The Minnehaha River longitudinal profile from its headwaters to the toe of the Minnehaha River floodplain system (study site). Dominate land-use, tributaries, floodplain and valley bottom wetlands and dam locations are marked along the profile

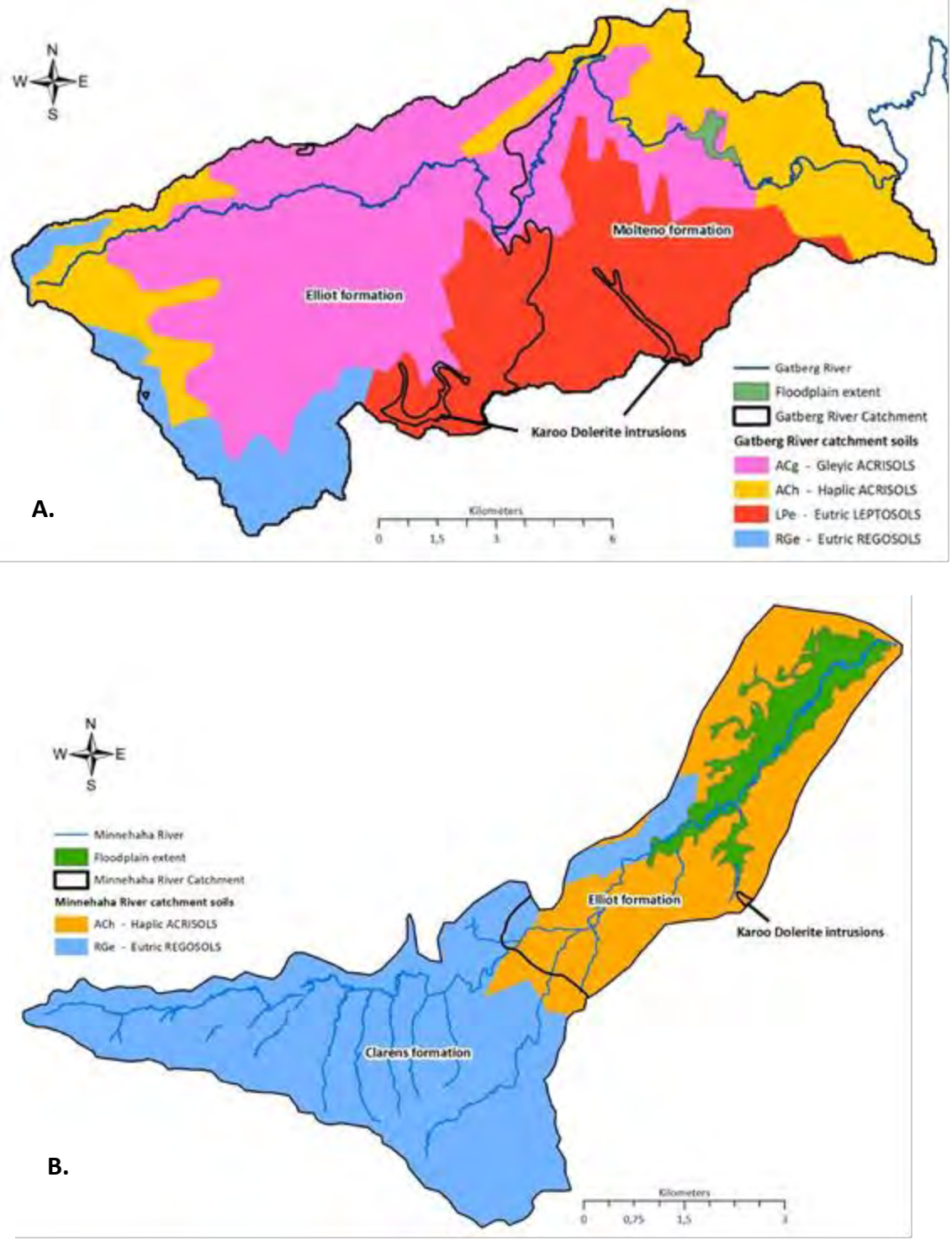

Figure 4.3 Soil properties for the A) Gatberg River catchment and B) Minnehaha River catchment (spatial dataset from Dijkshoorn et al. 2008)

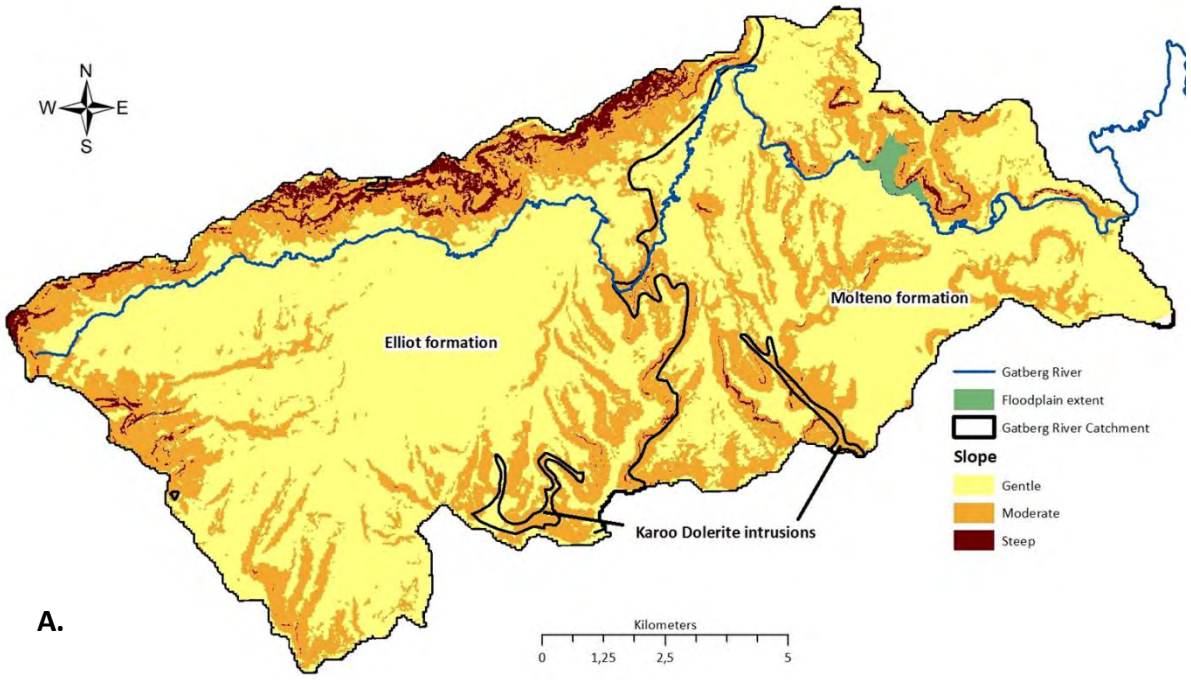
N
W
E
S
Elliot formation
Molteno formation
Karoo Dolerite intrusions
Gatberg River
Floodplain extent
Gatberg River Catchment
Slope
Gentle
Moderate
Steep
Kilometers
0
1,25
2,5
5

A.

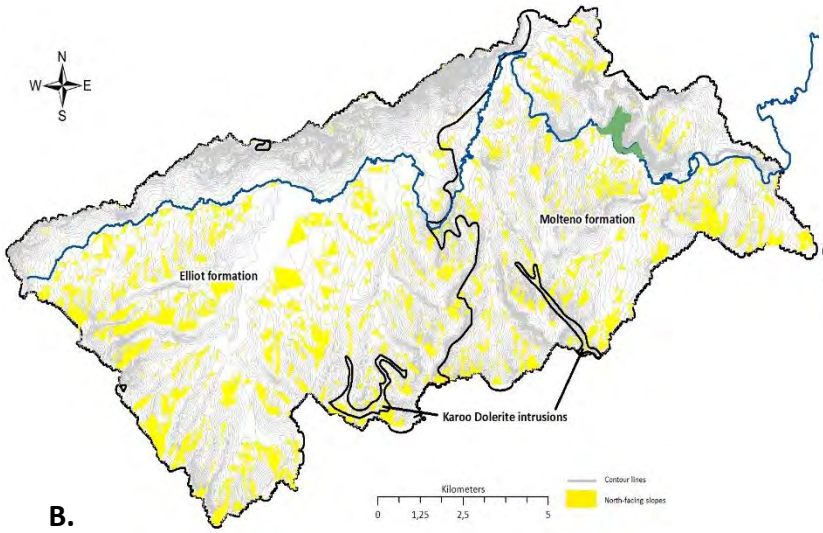
N
W
E
S
Elliot formation
Molteno formation
Karoo Dolerite intrusions
Kilometers
0 1,25 2,5 5
Contour lines
North-facing slopes

B.

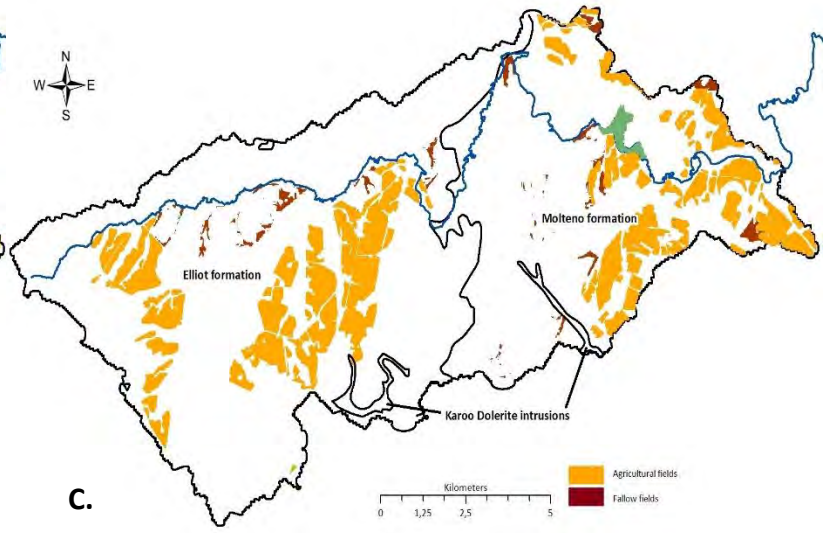
N
W
E
S
Elliot formation
Molteno formation
Karoo Dolerite intrusions
Kilometers
0 1,25 2,5 5
Agricultural fields
Fallow fields

C.

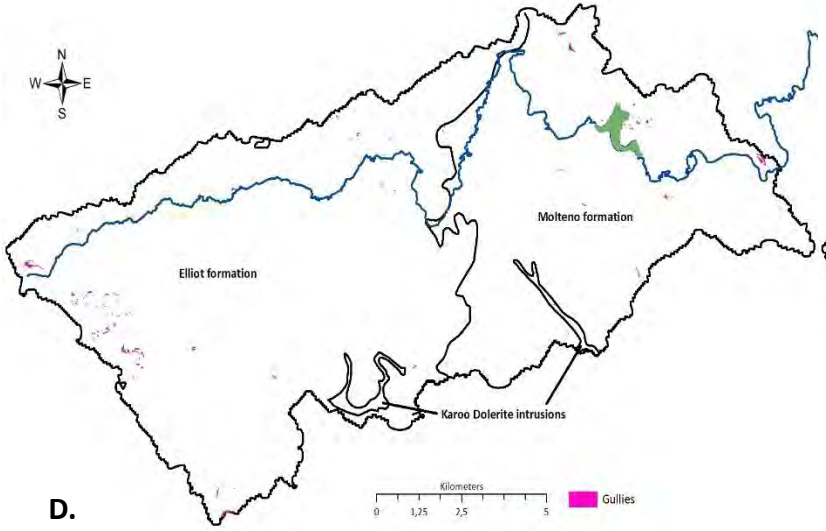
N
W
E
S
Elliot formation
Molteno formation
Karoo Dolerite intrusions
Kilometers
0 1,25 2,5 5
Gullies

D.

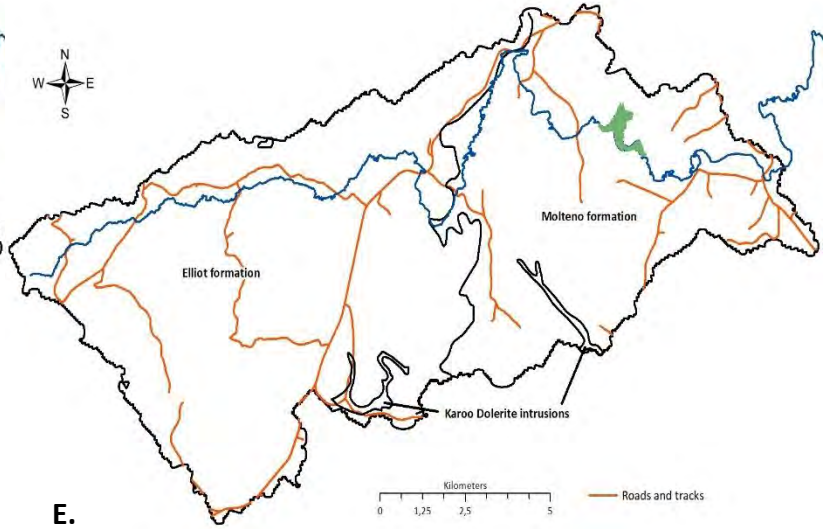
N
W
E
S
Elliot formation
Molteno formation
Karoo Dolerite intrusions
Kilometers
0 1,25 2,5 5
Roads and tracks

E.

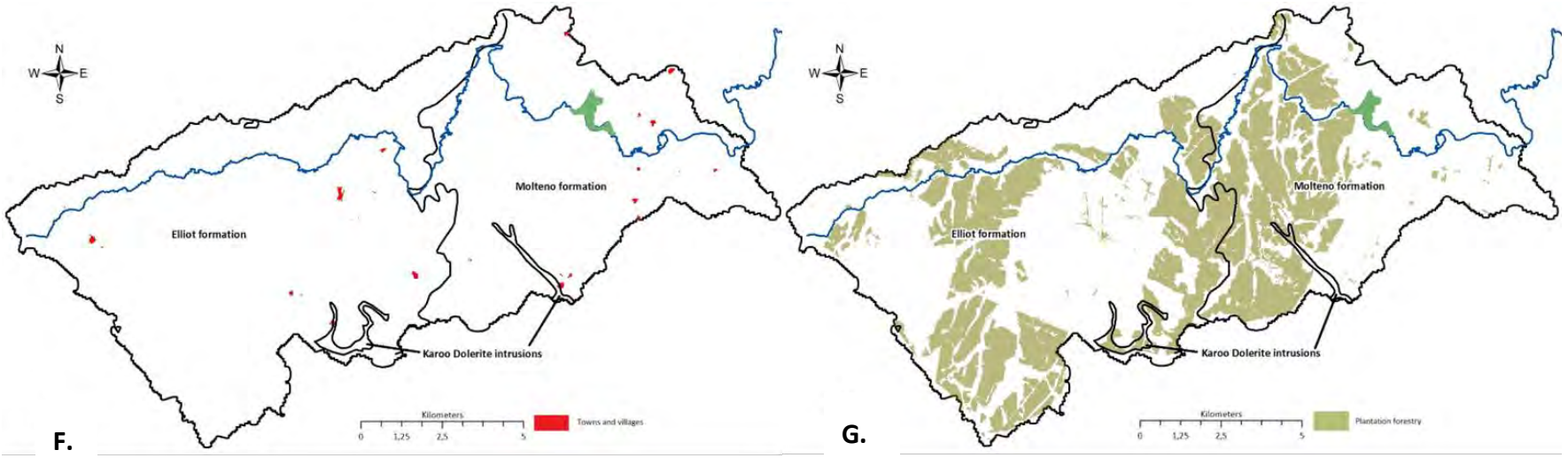

Figure 4.4 A) A slope map indicating gentle (< 5°), moderate (5-20°) and steep (> 20°) slopes for the Gatberg River catchment. Also indicated are the geological provinces. The potential sediment and phosphorus source maps of the Gatberg River catchment are displayed indicating B) North-facing slopes, C) Cultivated fields (currently and previously) and fallow land, D) Gullies, E) Roads, F) Towns and villages and G) Commercial forestry. All maps are included at a higher resolution in Appendix 1

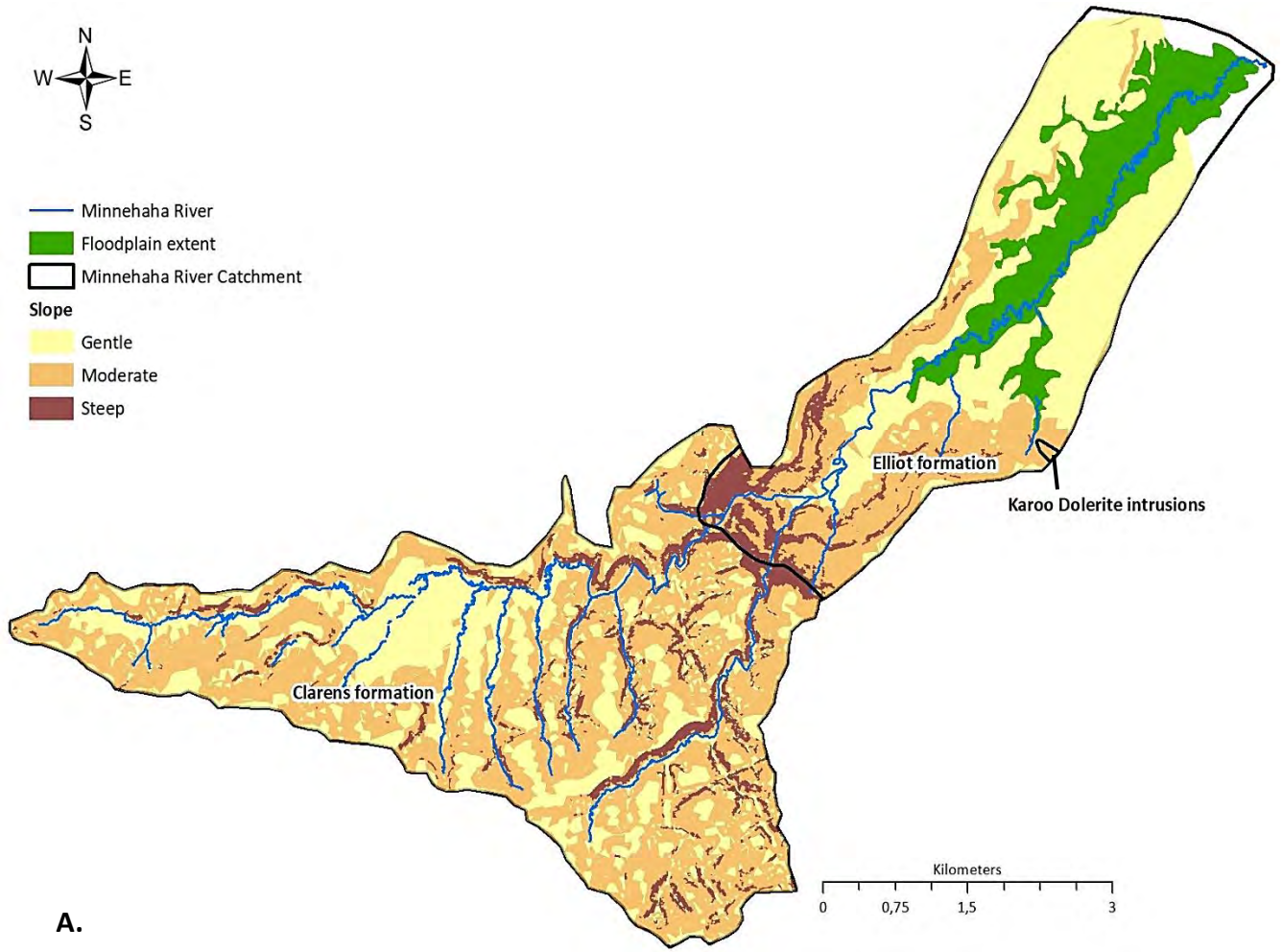
N
W
E
S
Minnehaha River
Floodplain extent
Minnehaha River Catchment
Slope
Gentle
Moderate
Steep
Elliot formation
Karoo Dolerite intrusions
Clarens formation
Kilometers
0
0,75
1,5
3

A.

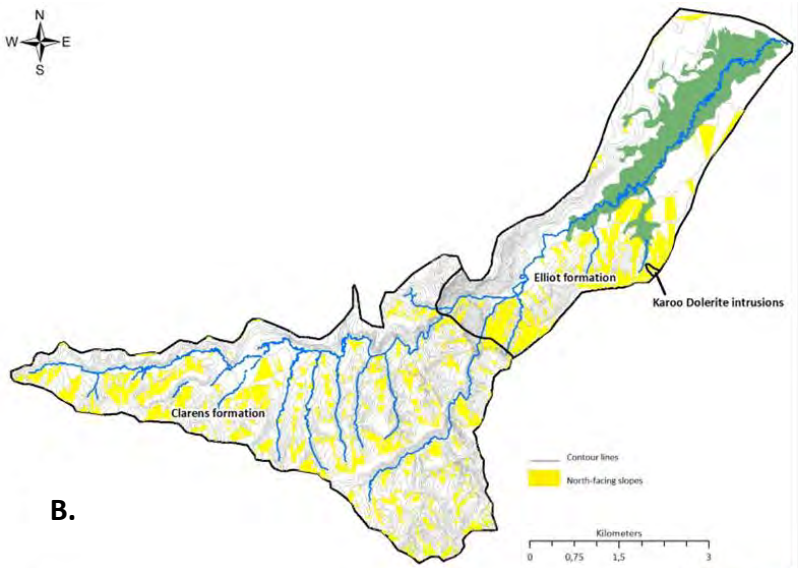
N
W
E
S
Elliot formation
Karoo Dolerite intrusions
Clarens formation
Contour lines
North-facing slopes
Kilometers
0
0,75
1,5
3

B.

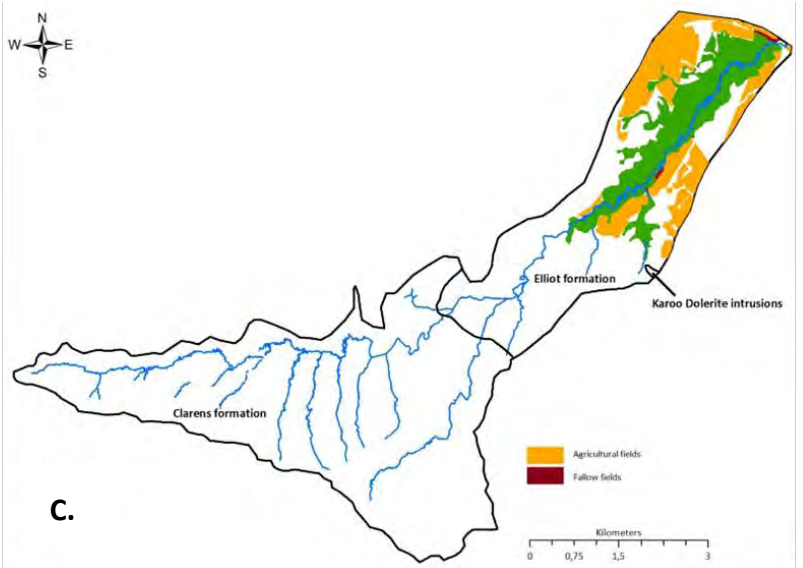
N
W
E
S
Elliot formation
Karoo Dolerite intrusions
Clarens formation
Agricultural fields
Fallow fields
Kilometers
0
0,75
1,5
3

C.

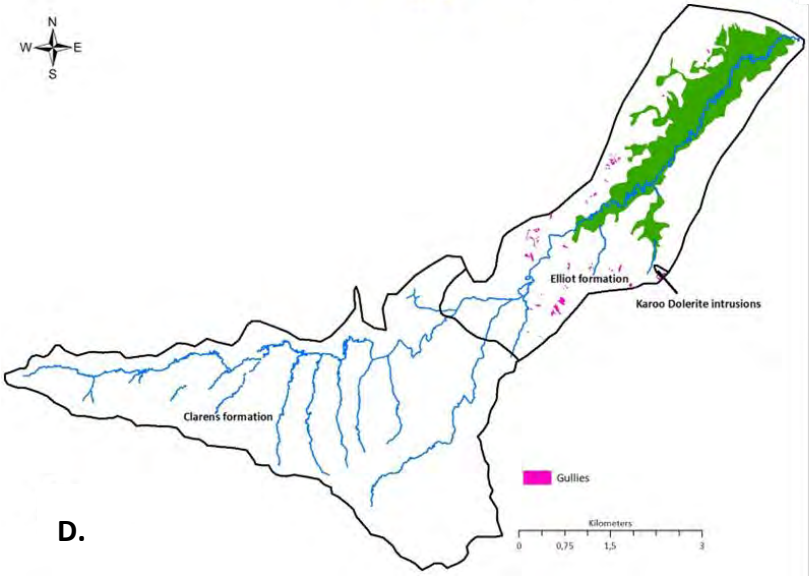
N
W
E
S
Elliot formation
Karoo Dolerite intrusions
Clarens formation
Gullies
Kilometers
0
0,75
1,5
3

D.

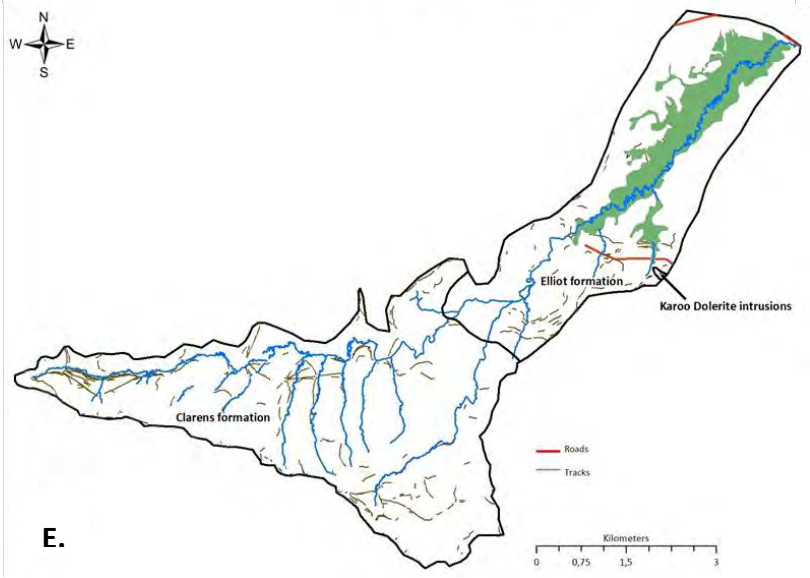
N
W
E
S
Elliot formation
Karoo Dolerite intrusions
Clarens formation
Roads
Tracks
Kilometers
0
0,75
1,5
3

E.

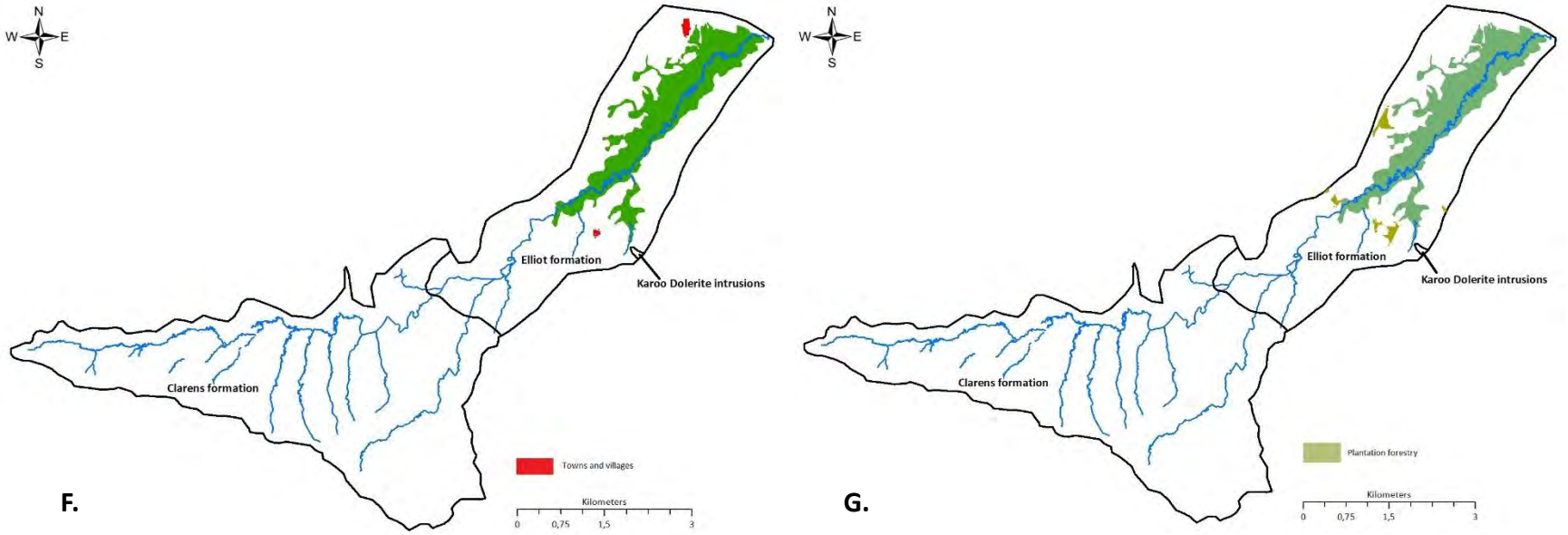

Figure 4.5 A) A slope map indicating gentle (< 5°), moderate (5-20°) and steep (> 20°) slopes for the Minnehaha River catchment. Also indicated are the geological provinces. The potential sediment and phosphorus source maps of the Minnehaha River catchment are displayed indicating B) North-facing slopes, C) Cultivated fields (currently and previously) and fallow land, D) Gullies, E) Roads, F) Towns and villages and G) Commercial forestry. All maps are included at a higher resolution in Appendix 1

4.3.2 TOPOGRAPHIC AND GEOLOGICAL CHARACTERISTICS OF POTENTIAL SEDIMENT AND PHOSPHORUS SOURCES IN THE TWO CATCHMENTS

4.3.2.1 CURRENT TOPOGRAPHIC AND GEOLOGICAL CHARACTERISTICS OF POTENTIAL SOURCE AREAS

In this section the current catchment characteristics of potential sediment sources for both floodplain system catchments are given. These include fields, fallow land, bare ground, gullies, roads and tracks, towns and villages, and commercial forestry (Figure 4.4 and Figure 4.5). The results are based on area calculations.

Cultivated fields (South African National Land Cover (SANLC) dataset 2020 and confirmed with 2022 Google images) in both catchments are shown in Table 4.2. In the Gatberg River catchment cultivated fields covered less 15 % of the total catchment area. A marginally higher number of fields were identified within the Elliot Formation (7 %) than the 5 % within the Molteno Formation (Figure 4.4C and Table 4.2). However, based on the area calculations for each geological province, slightly more fields (13 %) occurred within the Molteno Formation compared to 11 % within the Elliot Formation. Almost all the current cultivated fields were directly connected to the drainage network, with the proportion of fields connected being the highest (90 %) on the Elliot Formation. The fields were mainly (> 95 %) located on gentle slopes, with a small proportion (< 5 %) identified on moderate and steep slopes. Twenty per cent of the current cultivated fields were found on north-facing slopes, with the greatest proportion (65 %) on the Elliot Formation. In the Minnehaha River catchment current cultivated fields cover 7 % of the total catchment area (Figure 4.5C and Table 4.2). No fields were identified on the Clarens Formation. Based on the area calculations for the geological provinces, 12 % of the cultivated fields were identified in the Elliot Formation. Almost a quarter (19 %) of the current cultivated fields were connected to the drainage networks within the catchment. The fields were mainly (85 %) located on gentle slopes, with 2 % found on moderate slopes and none found on steep slopes. Less than 15 % of current cultivated fields were identified on north-facing slopes.

Table 4.2 Summary statistics for the characteristics of the cultivated fields for the Gatberg and Minnehaha River catchments

Catchment	Formation	Cultivated fields		Connected	% of cultivated fields on slope categories			Aspect
		km²	%	% of area	% gentle	% moderate	% steep	% north-facing
Gatberg River	Catchment area (206 km²)	23	11	85	97	3	0.3	20
	Elliot (126 km²)	13	10	90	98	2	0	65
	Molteno (80 km²)	10	13	77	96	4	0.7	36
Minnehaha River	Catchment area (40 km²)	3	7	19	85	2	0	12
	Clarens (18 km²)	0	0	0	0	0	0	0
	Elliot (22 km²)	3	12	19	85	2	0	12

Fallow land, previously cultivated fields and the bare ground covered 1 % of the total Gatberg Catchment area, with an equal area found within both geological formations (Figure 4.4C and Table 4.3). More than half were connected to the drainage network within the catchment, and the proportion of connected areas was the highest in the Molteno Formation. Most of the fallow land, previously cultivated fields, and bare ground were identified on gentle slopes (between 82 and 95 %) and a small proportion (less than 20 %) on moderate slopes. Within the Minnehaha River catchment fallow land, previously cultivated fields and bare ground accounted for 5 % of the catchment (Figure 4.5C and Table 4.3), and slightly more (8 %) occurred within the Clarens Formation compared to the 2 % coverage of the Elliot Formation based on the area calculations for each of the geological provinces. Less than 25 % of the area was identified on north-facing slopes.

Table 4.3 Statistics regarding the location of fallow land, previously cultivated fields, and bare ground in terms of geology, connectivity, and slope for the Gatberg and Minnehaha River catchments

Catchment	Formation	Fallow land, previously cultivated fields, and bare ground		Connected	% of fallow land, previously cultivated fields, and bare ground on slope categories			Aspect
		km²	% of area	% of area	% gentle	% moderate	% steep	% north-facing
Gatberg River	Catchment area	2	1	61	87	13	0	11
	Elliot	1	1	40	95	5	0	31
	Molteno	1	1	66	82	18	0.1	69
Minnehaha River	Catchment area	2	5	28	44	44	11	17
	Clarens	1.6	8	7	29	57	14	21
	Elliot	0.4	2	75	100	0	0	5

Gullies, with an average depth of > 2m, covered less than 1 % of the total Gatberg and Minnehaha River catchment areas, slightly more in both catchments (0.2 and 0.5 % respectively) identified in the Elliot Formation (Figure 4.4D, Figure 4.5D, and Table 4.4) and a slightly smaller proportion in the Molteno Formation (0.1 % for the Gatberg) and none were identified in the Clarens Formation. Within the Gatberg River catchment, less than 50 % of the gully area was structurally connected to the drainage network, with an increase in connectivity for the Elliot Formation. Within the Minnehaha River catchment, 91 % of the gully area was structurally connected to the drainage network. Gullies were only identified in the Elliot Formation within the Minnehaha River catchment. Gullies (catchment-wide) were infrequently (< 1 %) identified on currently cultivated fields and less than 5 % on fallow land, previously cultivated fields, and bare ground, for both catchments. Gullies were identified mainly (67 and 91 % for the Gatberg and Minnehaha respectively) on moderate slopes, with an increasing proportion identified on the Elliot

Formations (75 and 91 % respectively) for both catchments. Less than 50 % of the identified gullies are on north-facing slopes for both catchments.

Table 4.4 Statistics regarding the location of gullies in terms of geology, connectivity, and slope for the Gatberg and Minnehaha River catchments

Catchment	Formation	Gullies		Connected	On fields	On fallow land	% of gullies on slope categories			Aspect
		km²	%	% of area	% of area	% of area	% gentle	% moderate	% steep	% north-facing
Gatberg River	Catchment area	0.3	0.1	33	0.02	0.02	33	67	0	23
	Elliot	0.2	0.2	50	0.03	0.04	25	75	0	30
	Molteno	0.1	0.1	30	0	0	50	50	0	10
Minnehaha River	Catchment area	0.1	0.3	91	0.05	1	9	91	0	18
	Clarens	0	0	0	0	0	0	0	0	0
	Elliot	0.1	0.5	91	0.05	3	9	91	0	18

Table 4.5 shows the coverage of roads and livestock tracks within the Gatberg and Minnehaha River catchments. Roads and tracks covered < 1 % of the Gatberg catchment area The 90 km length had an average width of ca. 4.04 m (Figure 4.4E). Within the Minnehaha River catchment, roads covered less than 1 % with a total length of 2.6 km and an average width of ca. 4.04 m (Figure 4.5E), the livestock tracks covered < 1 % with a total length of 51 km with an average width of 0.07 m. It was estimated that more than half of these roads and tracks in both catchments discharged directly into the drainage networks. All the roads and livestock tracks were identified on gentle and moderate slopes.

Table 4.5 Statistics regarding the location of roads and livestock tracks in terms of geology, connectivity, and slope for the Gatberg and Minnehaha River catchments

Catchment	Formation	Roads and tracks		Connected	% of roads and tracks on slope categories			Aspect
		km²	%	% of area	% gentle	% moderate	% steep	% north-facing
Gatberg River	Catchment area	0.36	0.2	69	81	19	0	14
	Elliot	0.22	0.2	73	77	23	0	14
	Molteno	0.14	0.1	86	86	14	0	14
Minnehaha River	Catchment area	0.05	0.1	40	48	52	0	26
	Clarens	0.03	0.02	20	33	33	0	17
	Elliot	0.02	0.09	50	35	60	0	40

Table 4.6, Figure 4.4F, and Figure 4.5F identify the towns, villages, and residential areas for both catchments. For both catchments' towns, villages and residential areas are mostly found on gentle and moderate slopes. Within the Gatberg River catchment, less than a quarter of the towns, villages, and residential areas were connected to the drainage network. None were identified as connected to the drainage network within the Minnehaha River catchment.

Table 4.6 Statistics regarding the location of towns, villages, and residential areas in terms of geology, connectivity, and slope for the Gatberg and Minnehaha River catchments

Catchment	Formation	Towns and villages		Connected	% of towns, villages, and residential area on slope categories			Aspect
		km²	%	% of area	% gentle	% moderate	% steep	% north-facing
Gatberg River	Catchment area	0.4	0.2	24	76	23	0.5	25
	Elliot	0.2	0.2	25	74	25	0.9	40
	Molteno	0.2	0.3	21	79	20	0	60
Minnehaha River	Catchment area	0.05	0.1	0	80	20	0	20
	Clarens	0	0	0	0	0	0	0
	Elliot	0.05	0.2	0	80	20	0	20

Commercial forestry covered almost a quarter of the total Gatberg River catchment (Figure 4.4G and Table 4.7). Based on the area calculations for each geological province, slightly more commercial forestry (24 %) occurred within the Molteno Formation compared to 23 % within the Elliot Formation. Almost all the area of the commercial forestry was connected to the drainage network, with the proportion of commercial forestry connected being the highest (96 %) in the Elliot Formation. Commercial forestry was identified mainly on gentle (> 60 %) and moderate (> 30 %) slopes, with a small proportion (< 1 %) identified on steep slopes. Thirty per cent of the commercial forestry was found on north-facing slopes, with the greatest proportion (64 %) facing north on the Elliot Formation. There were very few (< 1 %) commercial forestry within the Minnehaha River catchment (Figure 4.5G and Table 4.7).

Table 4.7 Statistics regarding the location of commercial forestry in terms of geology, connectivity, and slope for the Gatberg and Minnehaha River catchments

Catchment	Formation	Commercial forestry		Connected	% of commercial forestry on slope categories			Aspect
		km²	%	% of area	% gentle	% moderate	% steep	% north-facing
Gatberg River	Catchment area	48	23	94	67	33	0.4	31
	Elliot	29	23	96	70	30	0.4	64
	Molteno	19	24	91	63	37	0.4	36
Minnehaha River	Catchment area	0.2	0.4	0	73	27	0	13
	Clarens	0	0	0	0	0	0	0
	Elliot	0.2	0.7	0	73	27	0	13

The Elliot Formation was the most impacted in terms of density of sediment source features, erosion, and connectivity (Table 4.8). This is likely to be a function of the erodible nature of the soils and ongoing anthropogenic activity, and pressures found within this geological province.

Table 4.8 A summary table for all the mapped potential source features for both catchments

Catchment	Feature	% cover of the total catchment	Formation with the highest density	Dominant slope	% of the area connected
Gatberg River	Currently cultivated fields	11	Molteno	Gentle	85
	Fallow land, previously cultivated fields, and bare ground	1	Elliot and Molteno	Gentle	61
	Gullies	0.1	Elliot	Moderate	33
	Roads and tracks	0.2	Elliot	Gentle	69
	Towns, villages, and residential areas	0.2	Molteno	Gentle	24
	Commercial forestry	23	Elliot and Molteno	Gentle	94
Minnehaha River	Currently cultivated fields	7	Elliot	Gentle	19
	Fallow land, previously cultivated fields, and bare ground	5	Clarens	Gentle and moderate	28
	Gullies	0.3	Elliot	Moderate	91
	Roads and tracks	0.1	Elliot	Moderate	40
	Towns, villages, and residential areas	0.1	Elliot	Gentle	0
	Commercial forestry	0.4	Elliot	Gentle	0

4.3.2.2 TOPOGRAPHIC AND GEOLOGICAL CHARACTERISTICS OF DRAINAGE FEATURES- EFFECTIVE DENSITIES

Gullies, roads, and livestock tracks contribute significantly to the connectivity and drainage density within the two catchments (Table 4.9). Within the Gatberg River catchment, gullies contributed approximately 11 % to the natural drainage network density, slightly more within the Elliot Formation geological province compared to the Molteno Formation (ca. 10 and 6 %, respectively). Within the Minnehaha River catchment gullies were only observed within the Elliot Formation geological province and contributed ca. 23 % to the overall natural drainage network density and 67 % within the Elliot Formation. Gullies were observed to be effective conduits, especially in the wet season because these features were orientated down-slope and mostly connected directly to the drainage system.

The roads and livestock tracks were found to be orientated mostly across the slope. Within the Gatberg River catchment, roads and livestock tracks added ca. 21 % to the density of the drainage network. The roads and livestock tracks within the geological province of the Molteno Formation contributed more to the density of the drainage network (24 %) than those found within the geological province of the Elliot Formation (19 %). Within the Minnehaha River catchment roads and livestock tracks contributed significantly (~100 %) to the density of the drainage network. Roads and livestock tracks contributed over 110 % in the Clarens Formation and 78 % within the Elliot Formation. Roads and livestock paths often follow the contour (gently sloping) or are along ridges, although, they regularly intersect down-slope orientated drainage features, allowing hillslope runoff to accumulate and be routed towards the drainage network during storm events.

Table 4.9 Densities of the drainage features for the two catchments and the various geological provinces

Catchment	Feature	Unit	Catchment	Molteno Formation	Elliot Formation	Clarens Formation
Gatberg River	Area	km²	206	80	126	
	% of total	%		39	61	
	Natural drainage	Length (km)	397	135	262	
		Density (km km⁻²)	2	2	2	
	Gullies	Length (km)	31	9	21	
		Density (km km⁻²)	0.2	0.1	0.2	
		% of drainage	11	6	10	
	Roads and livestock tracks	Length (km)	90	35	55	
		Density (km km⁻²)	0.4	0.4	0.4	
		% of drainage	21	24	19	
Minnehaha River	Area	km²	40		22	18
	% of total	%			55	45
	Natural drainage	Length (km)	54		19	35
		Density (km km⁻²)	1		1	2
	Gullies	Length (km)	12		12	0
		Density (km km⁻²)	0.3		0.6	
		% of drainage	23		67	
	Roads and livestock tracks	Length (km)	55		15	38
		Density (km km⁻²)	1		1	2
		% of drainage	100		78	111

4.3.3 TOPOGRAPHIC AND GEOLOGICAL CHARACTERISTICS OF POTENTIAL SEDIMENT AND PHOSPHORUS BUFFERS AND BARRIERS IN THE TWO CATCHMENTS

Current catchment characteristics of potential sediment buffers and barriers (Fryirs et al. 2007), e.g., natural vegetation (grasslands and forests), herbaceous wetlands, natural and artificial impoundments (dams or lakes), and anti-erosional structures are given in this section. Results are based on area calculations.

Within the Gatberg River catchment buffers account for 36 % of the total catchment area (Table 4.10). According to the SANLC (2020) dataset, most of the catchment is covered in natural grasslands with several herbaceous wetlands found along the length of the drainage network. Within the Minnehaha River catchment, the buffers cover 36 % of the total catchment area (Table 4.10). Two large floodplains are located within the catchment covering 10 % of its area. Like the Gatberg River catchment, the Minnehaha River catchment is predominantly covered by natural grassland vegetation.

Table 4.10 Statistics regarding the location of buffers in terms of geology for the Gatberg and Minnehaha River catchments

Catchment	Formation	Natural grasslands		Natural forests		Herbaceous wetlands	
		km²	%	km²	%	km²	%
Gatberg River	Catchment area	62	30	2	1	10	5
	Elliot	38	30	1	1	6	5
	Molteno	24	30	1	1	4	5
Minnehaha River	Catchment area	10	25	0.3	0.8	4	10
	Clarens	6	33	0	0	1	6
	Elliot	4	18	0.3	1	3	14

Within the Gatberg River catchment barriers such as artificial and natural impoundments cover an area of 0.9 km² or 0.4 % of its total area (Figure 4.6). Several (40) rehabilitation structures (anti-erosional structures) have been built along the Gatberg River as part of the Working for Wetlands Gatberg River rehabilitation program to preserve the numerous floodplain systems and other types of wetlands occurring along the river (Table 4.11). Within the Minnehaha River catchment, there were fewer impoundments and anti-erosional structures. Natural and artificial impoundments made up 0.03 % of the catchment and only occurred in the Elliot Formation.

Table 4.11 Statistics regarding the location of barriers in terms of geology for the Gatberg and Minnehaha River catchments

Catchment	Formation	Natural and artificial impoundments		Anti-erosional structures	
		km²	%	km	number
Gatberg River	Catchment area	0.9	0.4	4	40
	Elliot	0.4	0.3	2.5	25
	Molteno	0.5	0.6	1.5	15
Minnehaha River	Catchment area	0.01	0.03	0.2	3
	Clarens	0	0	0	0
	Elliot	0.01	0.05	0.2	3

Figure 4.6 An example of a typical farm impoundment found in the two catchments

4.3.4 POTENTIAL SEDIMENT AND PHOSPHORUS SOURCES AND STORAGE WITHIN THE FLOODPLAIN SYSTEMS

In Figure 4.7, the potential sources of sediment and nutrients for the Gatberg River floodplain system were identified. These sources were pinpointed through visual observations made during field trips. The potential upstream contributing areas have already been mapped, including both sediment and phosphorus, in the preceding section. The primary sources of sediment and phosphorus entering the Gatberg floodplain system probably stem from various land uses in the upstream catchment area. However, there are additional potential sources within the floodplain and the land adjacent to it. These include the commercial forestry surrounding one side of the floodplain, an unsealed gravel road, livestock grazing within the floodplain, disturbances caused by biological activity, bank erosion, bank collapse due to livestock activities (Figure 4.8), and erosional gullies that feed into the floodplain system.

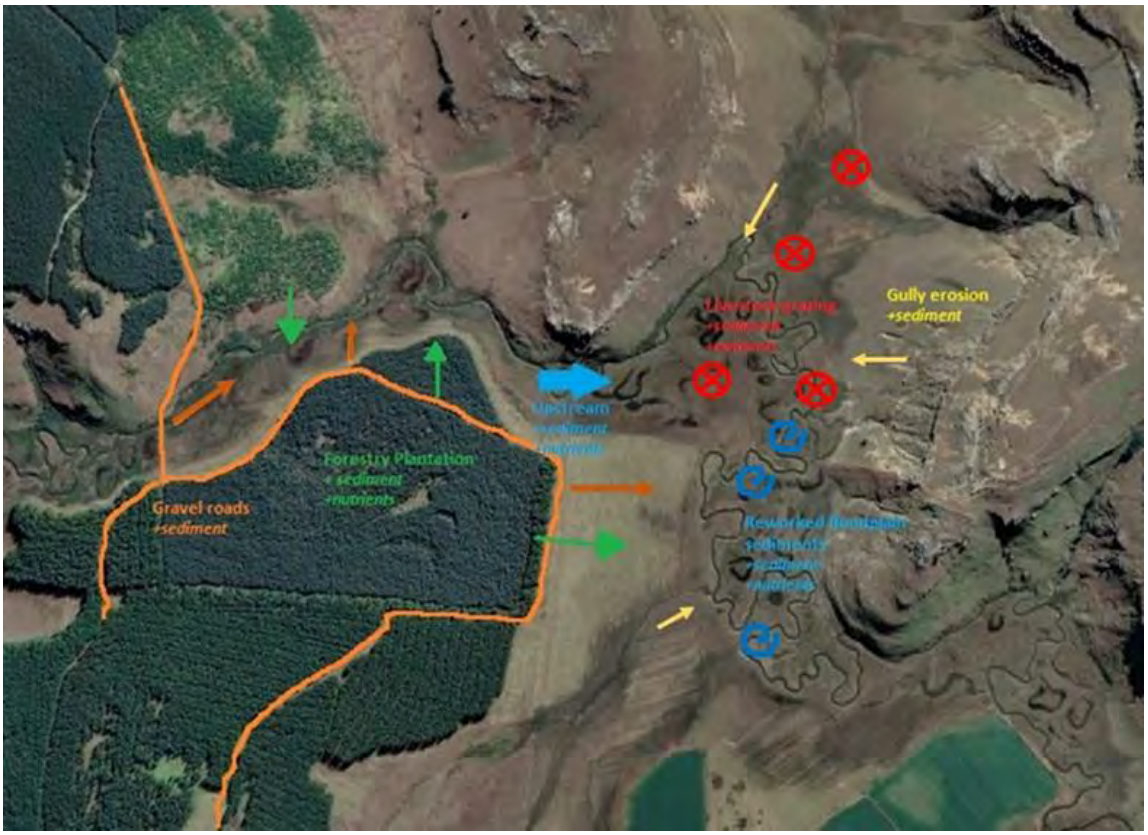

Figure 4.7 Potential sediment and phosphorus sources identified adjacent and within the Gatberg River floodplain system

Figure 4.8 A typical cattle crossing path through the Gatberg River

In Figure 4.9, the possible origins of sediment and nutrients for the Minnehaha River floodplain system were identified. Potential sources from upstream were previously delineated. The area upstream of the floodplain system maintains its natural state largely, with the land primarily used for livestock grazing. However, there are several potential contributors of increased sediment delivery to the system from within and adjacent to the floodplain. These include multiple cultivated agricultural fields that surround the system, an unsealed gravel road, livestock grazing within the floodplain, disturbances caused by biological activity, collapse of riverbanks due to livestock, livestock pens and silage pits, erosional gullies feeding into the floodplain, and residential structures associated with farms.

Figure 4.9 Potential sediment and phosphorus sources identified adjacent and within the Minnehaha River floodplain system

4.3.5 POTENTIAL TOTAL PHOSPHORUS SOURCES IN THE CATCHMENTS

Total phosphorus has been identified to be strongly correlated with the fine sediment particle size fraction (Allan 1986; Horowitz 1991; Moustakidis et al. 2019). Therefore, understanding the source, transport, and deposition of sediment is paramount to understanding the source, transport, and deposition of phosphorus. However, total phosphorus has its own set of distinct sources, point sources and non-point sources in a river's catchment.

Potential phosphorus sources in the Gatberg and Minnehaha River catchments are point sources such as sewage and industrial effluents from towns, villages and residential areas, fertiliser production, feedlots, meat processing and packaging and milk processing. Diffuse sources in the catchments comprise urban run-off, run-off from cultivated land or previously cultivated land, commercial forestry, the atmosphere, and the natural background levels.

4.4 DISCUSSION

4.4.1 INTRODUCTION

This section discusses the mapping results presented in Section 4.3. General topographic characteristics for the catchment and identified sources, barriers and buffers are discussed. Furthermore, linkages and their influence on water and sediment transport are discussed.

4.4.2 LONGITUDINAL PROFILES AND CATCHMENT CHARACTERISTICS

Rivers are the principal conveyors of water, sediment, and dissolved constituents through the landscape to the oceans. The transport of material is carried out under the influence of gravity from high-elevation areas to low-elevation areas. Rivers naturally move sediment with minimal energy expenditure, aiming to maintain a balanced slope that accommodates both the discharge and the amount of sediment present (Schumm 1977). This equilibrium slope is achieved by adjusting the river's transport capacity, primarily determined by discharge, to match the supply of available sediment. Hence, the longitudinal profile is critical to maintaining the movement of water and the transport of sediment within river systems. Longitudinal profiles of both rivers and wetlands have been measured due to the well-known concept of a "graded stream profile" being in a stable equilibrium state (Goldrick and Bishop 1995; Ellery et al. 2009), which means that the river has a logarithmic shape (Schumm 1977; Goldrick and Bishop 1995; Ellery et al. 2009). Any deviation from this 'equilibrium' condition and logarithmic shape is generally attributed to one or more variables, such as a change in geology, tectonics, climate, and tributary influence (Goldrick and Bishop 1995; Brierley and Fryirs 1999; MacGregor et al. 2000; Partridge and Maud 2000; Crosby and Whipple 2006; McCarthy et al. 2011). Several researchers (King 1963; Partridge and Maud 2000; McCarthy and Rubidge 2005) have observed marked variations in longitudinal slope along South African rivers that have been attributed to one or more of these factors. Wetlands usually form along the longitudinal profile where there are local decreases in slope, and widening of valleys which increase accommodation space, where resistant lithology or intrusions inhibit downward incision thereby increasing lateral erosion. Because floodplain wetlands are linked to river systems in South Africa, the study of fluvial geomorphology has become essential to understanding the formation, behaviour, storage, and vulnerability of floodplain wetlands (Jain et al. 2008).

The Gatberg catchment is a typical representation of the steep headwater areas of the Drakensberg Escarpment with steep slopes dominating the upper catchment and tier edges of the lower parts of the catchment (De Decker 1981; Mucina et al. 2006). The Gatberg River has an abrupt step which separates the upper distinctly logarithmic longitudinal profile from a lower relatively uniformly sloping reach, where the research floodplain system is located. The step-like feature is related to harder more resistant layers (Seidl et al. 1994; Tooth et al. 2004) as can be seen in the Elliot Formation, where softer layers are removed by erosion, leaving the harder layers to form steep near vertical cliffs (Moon and Selby 1983). Landscape relief is somewhat gentler at lower altitudes. Small 'beads' of floodplain systems occur along the length of the Gatberg River, either associated with local wider valley widths or lithological changes such as

dolerite intrusions creating features of more erosional resistance. In comparison, the Minnehaha has a distinctly gentler uniform longitudinal profile disrupted by a large step feature at the junction between the Clarens and Elliot geological formations. The Minnehaha River has two very large floodplain systems, one in the upper section and one in the lower section (the research site). The floodplain system on the lower section seems to have formed due to the abrupt valley widening below the waterfall as well as the relationship between the tributary (Minnehaha River) and the trunk system, Little Pot River (McCarthy et al. 2011).

The impact of a resistant geological outcrop, such as a dolerite outcrop, or an abrupt change in accommodation space, or the relationship between a tributary and trunk stream has on the geomorphology or a river or floodplain and the geomorphological processes occurring within, in South Africa, are relatively well documented (Tooth et al. 2002, 2004, 2007; McCarthy et al. 2010; Ellery et al. 2012; Job 2014). Both the Gatberg and Minnehaha River floodplain systems are meandering systems with low levees and alluvial ridges situated in wide valleys, like the other South African systems, occurring due to the interactions mentioned above. Both floodplain systems owe their origins to resistant dolerite outcrops. The Gatberg River floodplain system has a dolerite dyke crossing the system and the Minnehaha has a dolerite control close to the confluence with the trunk of the Little Pot River.

4.4.3 POTENTIAL SOURCE AREAS IN THE TWO CATCHMENTS

In many parts of Africa, soil erosion is an important problem, which is evident from high sediment yields and poor and turbid river quality (Rowntree et al. 2008; Le Roux and Sumner 2012). In river catchments, sediment sources are linked to land use (agricultural fields, fallow land, and commercial forestry), poor management, road networks, livestock tracks and gully erosion.

In the Gatberg floodplain systems catchment, agricultural fields (livestock feed crops and commercial maize), previously cultivated and fallow lands mainly occurred on the edges of plantations and wetland systems utilising the gentler slopes, makeup 11 and 1 %, respectively, of the total catchment. Most (85 %) of the currently cultivated fields and 60 % of previously cultivated fields, fallow lands and bare ground are connected to the drainage network allowing sediment and phosphorus to be freely exported from these features into the river system. Based on the area calculations for each geological province, slightly more currently cultivated fields occurred within the Molteno Formation. In the Minnehaha floodplain system catchment, the agricultural fields (predominantly used for fodder crops) and previously cultivated fields, fallow land and bare ground were in the lower catchment on the edges of the floodplain system along the alluvial terrace (7 and 5 %, respectively, of the total catchment). Nineteen per cent of the currently

cultivated fields and 28 % of the previously cultivated, fallow land and bare ground are connected to the drainage network. Most of the previously cultivated fields occurred in the Clarens Formation, however, all the fields that are currently cultivated occur in the Elliot Formation. This is likely due to a change in farming practices. The probable reasons for the location of the fields are mainly practical; the use of gentle slopes that had deeper soils and were less prone to erosion would be more favourable for agriculture. Kroese et al. (2020) in a study in Kenya found that out of the four main sediment sources in a montane catchment (agricultural land, unpaved tracks, gullies, and channel banks) agricultural land accounted for 75 % of the total sediment in the river. Similarly, in the Root River catchment, in south-eastern Minnesota, Kuehner et al. (2016) estimated that 44 % of the annual sediment load was derived from agricultural fields in the catchment. Agricultural fields also introduce extra nutrients into the river system such as Phosphorus from fertilizers.

Based on a comprehensive review of research, Stott and Mount (2004) found that mean sediment yields increase in rivers with substantial commercial forestry activities in their catchments. Sediment yields increase at the initial ground disturbance and clearing phase, recover as the forest matures, and increase again more significantly at the timber harvesting phase. This is supported by two of the longest-running forest hydrology studies in the UK found that suspended sediment concentration increased from < 4 mg L^{-1} to 30 mg L^{-1} during ploughing in dry periods and 150 mg L^{-1} during wet periods (Robinson et al. 1998). The authors also found that phosphate levels increased from background concentrations of < l mg L^{-1} to 2.1 mg L^{-1} after ploughing, this was mainly due to soil preparation and the addition of fertilisers before ploughing operations. Similarly, in two catchments in Llanbrynmair Wales, Francis and Taylor (1989) found that the total sediment loads increased from 37 to 90 kg ha^{-1} yr^{-1} after ploughing, in one, and the other from 7 to 31 kg ha^{-1} yr^{-1}. Commercial forest harvesting activities increase the delivery of fine sediment to streams due to intensified erosion or mass wasting from hillslopes, roads, and stream channels. In the Gatberg floodplain system catchment, commercial forestry represented the largest potential sediment source of anthropogenic land uses (23 %). Ninety-five per cent of the plantations are connected to the drainage system and are mainly on gentle (> 60 %) and moderate (> 30 %) slopes near the drainage networks, with a small proportion (< 1 %) identified on steep slopes. In the Minnehaha floodplain system catchment, commercial forestry accounted for a relatively small area (< 1 %). Research has shown that wood harvesting operations in river catchments regularly resulted in increased suspended sediment concentrations and yields in river systems (Beschta 1978; Reid and Dunne 1984; Grayson et al. 1993). Plantation road networks are the primary sources of sediment delivery to rivers (Luce 2002; Wemple and Jones 2003; Brown et al. 2013); however, the use of heavy machinery, such as harvesters, during wood

harvesting operations can also compact soils (Motha et al. 2003; Litschert and MacDonald 2009). Soil disturbance and compaction and its associated changes in soil physical properties (Bilby et al. 1989; Megahan et al. 2001; Lane and Sheridan 2002; Sidle et al. 2004) can lead to lower infiltration rates and increased erosion from harvested slopes (Croke et al. 1999). Secondary activities associated with wood harvesting, such as slash burning and disposal, can also expose soils and increase rates of erosion (Beschta 1978; Robichaud and Waldrop 1994). Furthermore, the removal of trees and the ensuing alteration of the hydrologic regime (increased runoff and peak flows), may increase riverbank erosion and remobilisation of stored sediment on floodplains or within the channel (Jones and Grant 1996; Basher et al. 2011; Birkinshaw et al. 2011).

The footprint of roads and livestock tracks was small in both catchments (< 1 % of the catchment), but their relatively good connectivity suggests that they could contribute and route a significant amount of sediment regularly. Most roads in the catchments are gravel roads. Several studies (Minella et al. 2008; Ramos-Scharrón and LaFevor 2016) have highlighted the effect of unpaved roads and tracks on routing water and sediment to the river network.

Gully erosion, like roads and tracks, increases drainage density and are effective link for transporting runoff, sediment, and sediment-associated nutrients within the catchment, as well as directly contributing as a sediment source in catchments (Poesen et al. 2003; Valentin et al. 2005; Haregeweyn et al. 2006; Vanmaercke et al. 2011). Within the Gatberg River catchment, less than 50 % of the gully area was connected, with an increase in connectedness for the Elliot Formation. Within the Minnehaha River catchment, 91 % of the gully area was connected to the drainage network. The gullies were only identified on the Elliot Formation within the Minnehaha River catchment. Although, gully erosion contributed a small area in both catchments (< 1 %) research has shown that gully erosion has the potential to be a large contributor to sediment and phosphorus inputs to river systems. Research has shown that gully erosion worldwide can contribute from 30 % to 83 % of total soil erosion in catchments (Foster 1986; Bogen and Berg 1994; Poesen et al. 2011; Daggupati et al. 2014). It is especially important to manage erosion in areas that experience high-intensity rainfall events such as the Gatberg and Minnehaha catchments. Van der Waal (2015) calculated that the total soil loss for all erosion features was approximately 13 t ha^{-1} y^{-1} in the nearby Vuvu River catchment, which was higher than the global average, calculated by Yang et al. (2003) of ca. 10 t ha^{-1} y^{-1}. Erosion, especially of previously cultivated fields, may be an important source of phosphorus to river systems. In North Queensland in Australia, over 85 % of the sediment-bound phosphorus is derived from hillslope erosion of surface soils (Croke and Nanson 2002). In general, gullies

were found on moderate slopes (more than 50 %) for both catchments. Vetter (2007) and van der Waal (2015) had similar results. Researchers have postulated that this is the case because there is sufficient energy and runoff and sufficient depth of material to initiate gully formation (Schumm 1979; Brierley and Murn 1997; Hoffman and Todd 2000; Kakembo 2000; Kheir et al. 2007; Grenfell and Ellery 2009). Gullies in both the Gatberg and Minnehaha River catchments occur predominantly in the Elliot Formation. This could be because soils that make up the Elliot Formation are highly susceptible to chemical erosion and do not need a high-energy environment to initiate erosion (Vetter 2009).

Towns, villages and residential areas were relatively small in both catchments (< 0.5 % of the catchment), however, research has shown that urban and residential areas decrease the vegetation cover, increase impervious surfaces and as a result increase surface runoff which can increase the sediment and sediment-associated nutrients transport capacity, increase the potential for erosion and increase connectivity in the catchment (Booth 1991; Walsh et al. 2012, 2016; Wohl et al. 2015; Vietz et al. 2016; Russell et al. 2017; 2018).

4.4.3.1 Effective densities

In the Gatberg River catchment, down-slope features, for example, gullies, contributed an 11 % increase in the overall drainage density of the catchment and the across-slope features, for example, roads and livestock tracks, contributed a 21 % increase. In the Minnehaha River catchment, down-slope features contributed 23 % and the across-slope features contributed 100 % to the overall drainage density. This increase in the drainage density of both catchments' is substantially greater than the 10 % calculated by Croke and Hairsine (2006), but comparable to the results found by van der Waal (2015) in the neighbouring Vuvu River catchment. This highlights the highly connected nature and increased drainage in both the Gatberg and Minnehaha River catchments. Gullies were the major pathways as they directly linked the adjacent slopes to the river network and transported and delivered sediment under wet conditions synchronously with the flow of the river networks (Croke and Hairsine 2006). Gullies arise primarily in the upper regions of the natural drainage network that would be vegetated in the absence of the influence of the gullies. The removal of vegetation and the entrenchment of natural drainage features changes the hydrological and sedimentological behaviour of the catchment, allowing water and sediment to be transported more efficiently down the catchment (Brierley and Murn 1997; Cammeraat 2002; Vanacker et al. 2005; Rommens et al. 2006; Grenfell and Ellery 2009). Although livestock tracks and roads are not as efficient as downslope gullies as water and sediment conduits, they concentrate overland and upper subsurface flow. Huchzermeyer (2014) discovered that livestock tracks and roads increased

hillslope-channel connectivity on the Elliot Formation in the Vuvu River catchment, particularly on gentler slopes. Roads and livestock tracks regularly intersect downslope drainage features, increasing the drainage density significantly (Hoffman and Todd 2000; Croke and Hairsine 2006; Huchzermeyer 2014; van der Waal 2015).

4.4.4 POTENTIAL BARRIERS AND BUFFERS IN THE TWO CATCHMENTS

Sediment conveyance through a river catchment may be buffered by different features (e.g., wetland systems, floodplain systems and vegetation cover). The configuration of these features and the nature of connectivity within and between catchment features affect the transport, deposition, and storage of sediment through the catchment. According to Fryirs et al. (2007), buffering features are features that limit sediment transport and delivery to channels (Brunsden and Thornes 1979; Meade 1982; Phillips 1992; Harvey 2002; Michaelides and Wainwright 2002; Hooke 2003). Sediment barriers inhibit the movement of sediment within the channel (Fryirs et al. 2007), such as vegetation, impoundments, bedrock outcrops and anti-erosion structures. In the Gatberg and Minnehaha floodplain system catchments, sediment buffering, and barrier features identified were the natural grassland vegetation, herbaceous wetlands, artificial and natural waterbodies (including impoundments) and anti-erosional structures. The natural vegetation accounted for 31 % of the land cover in the Gatberg catchment and 81 % of the Minnehaha catchment. Natural vegetation stabilises the soil, decreases the rainfall intensity on the earth's surface, and increases the infiltration rate which in turn decreases runoff. Wetlands (including the research sites) accounted for an area of 5 % and 10 % in the Gatberg and Minnehaha catchment respectively. Riparian wetlands are natural traps for fine sediments, organic matter, and phosphorus, because of their low gradient and the resultant low transport energy. Phillips and Slattery (2007) analysed fluvial sediment budget studies and showed that in ten study basins of various sizes, an estimated 14 to 58 % of the total upland sediment production was stored in alluvial wetlands.

In both catchments, natural and artificial waterbodies accounted for less than 1 % of the total area. Impoundments regulate river systems resulting in an altered flow regime, a sediment deficit downstream, and coarsening of the sediment downstream (Williams and Wolman 1984; Kondolf 1997; Grams and Wilcock 2007; Yang et al. 2014) and channel morphological changes. Wolf et al. (2022) in a study of the Rur dam in Germany, found that the impoundments had changed the flow regime, created a deficit in sediment supply downstream, and increased the mean sediment particle size downstream. Sediment-associated nutrients and contaminants can also be trapped and potentially stored within impoundments (Ziegler and Nisbet 1995; Palanques et al. 2014).

4.4.5 POTENTIAL SOURCE AREAS WITHIN THE FLOODPLAIN SYSTEMS

The Gatberg River floodplain system is surrounded by commercial forestry on one side which ranges from 50 to 200 meters away from the outer extent of the floodplain. There is an unsealed gravel road that crosses the Gatberg River just upstream of the floodplain system and continues to run along the edge of the commercial forestry. This road is used by the local farm owner and commercial forestry personnel. Within the floodplain system itself, livestock (cattle and goats) graze and cause bioturbation and bank collapse that could introduce both sediment and phosphorus to the system. According to Alexander et al. (2008), 37 % of the phosphorus transported to the Gulf of Mexico came from animal manure on pasture and rangeland. Similarly, Iowa-based research found that catchments with more grazed pastureland had higher sediment and phosphorus levels in surface water than agricultural catchments (Downing et al. 2001). However, the sources of the sediment and phosphorus were not identified by Downing et al. (2001).

The active channel is highly sinuous and regularly switches from the left to right side of the valley margin throughout the floodplain system. In the wet season, after heavy rains, flood waters covered most of the floodplain surface and filled the oxbow features (observed in December 2019, February 2020, and November 2020). Freshly deposited sediment was evident on the lower flood benches, channel banks and levees, and further away from the channel on the floodplain surface during wet season field surveys. This indicated that this floodplain system was still active in transporting and storing sediment on its surface. Bank collapse was observed along the outer bend on some of the channels' meander bends, reworking sediment stored in the banks and levees.

A gully had formed along a drainage line coming off the steep mountainside on the left bank at the top of the floodplain system. This introduced sediment from the hillside to the main channel. In the middle of the floodplain system, a small valley bottom wetland entered the system from the right bank. The sediment carried by the water that flows through this system was deposited where the water's carrying capacity is reduced by the change in slope as it spills onto the relatively flat floodplain surface. A small channel was cutting through the valley bottom wetland from the Gatberg active channel, reworking stored sediment and making the valley bottom wetland less efficient at storing sediment and introducing more sediment to the Gatberg active channel during the wet season. There were a few gully stems on the mountainsides creating sediment pathways to the system, especially during intensive rainfall events.

The Minnehaha River floodplain system falls within two private farm boundaries. Both these farms use the floodplain system for livestock grazing (cattle and sheep) causing tracks, bioturbation, increased

nutrient levels and riverbank collapse. Several cultivated fields are mostly used for growing livestock fodder. Fertilisers and crop harvesting increase nutrients and sediments in the floodplain system. Livestock feed is also stored in silage pits adjacent to the floodplain system that leak nutrients. There is a residential and farm building on a hilltop adjacent to the floodplain system that has the potential to introduce nutrients and sediment.

The active channel is sinuous and has a straight and narrow meander belt through the floodplain system. In the wet season, after heavy rains, flood waters covered most of the floodplain surface and filled the oxbows and backswamp (observed in December 2019, February 2020, and November 2020). Freshly deposited sediment was evident on the lower flood benches, channel banks and levees and further away on the floodplain surface during wet season field surveys, indicating that this floodplain system was still active in transporting and storing sediment on its surface. Bank collapse was observed along the outer bend on some of the channels' meander bends, reworking sediment stored in the banks and levees. The livestock crossing points through the river were areas of erosion, sediment mobilisation and transport, and reworking sediment stored in the channel, banks, and levees. The floodplain system is bounded on both sides by a gently sloping alluvial terrace. Some valley-bottom wetlands enter the floodplain system from either bank, introducing water and nutrients from the surrounding area.

4.5 CONCLUSION

In conclusion, the discussion presented in this section sheds light on the intricate interplay between various factors influencing the transport of water and sediments within the Gatberg and Minnehaha catchments. Through an examination of longitudinal profiles, catchment characteristics, potential source areas, effective densities, barriers, and buffers, a comprehensive understanding of the geomorphological processes at play emerges.

The desktop analysis using a mixture of GIS, different datasets and field observations proved to be useful in identifying the potential sediment and phosphorus sources and buffers in the Gatberg and Minnehaha River catchment and the two research floodplain systems, as well as identifying potential pathways and connectivity between the different sources and the river network.

The longitudinal profiles of both rivers exemplify the equilibrium that river systems seek, with deviations attributed to geological, tectonic, and anthropogenic influences. The identification of potential source areas reveals the possible significant impact of land use practices, such as agriculture and commercial forestry, on hydrology, sediment yield and nutrient transport. In addition, the effective densities of the

drainage features underscore the increased connectivity within these catchments, particularly emphasising the potential for these to have a role in sediment transport.

Importantly, the discussion also highlights the presence of barriers and buffers within the catchments, including natural features such as wetlands and vegetation, as well as anthropogenic impoundments and structures such as dams. These features play crucial roles in modulating sediment transport and deposition, offering insights into potential strategies for sediment management and conservation.

Overall, the findings presented underscore the complex dynamics governing water and sediment transport within river catchments, emphasizing the need for holistic approaches to land and water management that consider both natural and anthropogenic factors as well as the different spatial scales. By understanding and mitigating the impacts of various land use practices, it becomes possible to protect the integrity of river systems and the ecosystems they support for future generations.

CHAPTER 5 : INVESTIGATING SEDIMENT CHARACTERISTIC VARIABLES IN MEANDERING RIVER AND FLOODPLAIN SURFACE SEDIMENT: IMPLICATIONS FOR SEDIMENT AND PHOSPHORUS DEPOSITION

5.1 INTRODUCTION

Increased suspended sediment loads in rivers are recognised as a pollutant that has many detrimental effects on the geomorphology and ecology of riverscapes (Owens et al. 2005). Wetlands and floodplains have been established to be one of the most crucial natural buffers occurring along a river system in terms of sediment movement and are recognised as important sinks for storing suspended sediment and sediment-associated contaminants from their catchments (Walling et al. 1996; Fryirs et al. 2013). As such, recognition of the crucial role that floodplains play in the landscape has increased interest in their dynamics.

Overbank deposition, lateral migration and channel avulsions are the primary floodplain processes (Rhoads 2020) responsible for sediment and sediment-associated contaminants and nutrients storage, cycling, and reintroduction into river systems (e.g., Middelkoop and Asselman 1998; Walling 1999; Thoms et al. 2000; Croke and Nanson 2002; Walling and Owens 2003). Due to these processes, floodplains are effective buffers along the river corridor and are important for regulating flood waters, storing sediment, nutrients, and pollutants, and are self-maintaining under the right hydro-morphological conditions.

Due to the dynamic nature of sediment mobilisation, transport, and deposition; both the suspended sediment transported by a river and the ensuing overbank floodplain deposits display significant spatial variation in sediment particle size composition (Marriott 1992; Walling 1996; Walling et al. 1996). Since many nutrients and contaminants are associated with fine-grained sediment (< 63 µm; Allan 1986; Horowitz 1991), investigation of the spatial variability of floodplain sediment particle size composition is a vital prerequisite for understanding the cycling and fate of nutrients and contaminants in fluvial systems.

There is insufficient data on the function of floodplains in semi-arid regions of South Africa and their capacity to trap sediment and phosphorus, which hampers the effective prioritisation and evaluation of restoration projects. Most research on the variability of overbank deposition has focused on the northern more humid regions (Walling et al. 1996; He and Walling 1997; Simm and Walling 1998; Thonon et al. 2007; Swanson et al. 2008), on historical floodplain deposits (Lecce and Pavlowsky 1997, 2004) or has used modelling to predict overbank deposition (Nicholas and Walling 1997; Sweet et al. 2003; van der Lee

et al. 2004). Against this background, there is a need for information concerning the spatial variability of sediment characteristics of overbank floodplain deposits.

Variability in the overbank deposition of sediment and associated nutrients, between river sections and rivers, is determined by several factors including channel morphology, floodplain width, sediment load, and discharge regime (Lecce 1997; Foster et al. 2002; Sweet et al. 2003; Lecce and Pavlowsky 2004). Variations in hydraulic patterns of overbank flow, local topography, and vegetation form the key source of variability in deposition within and between floodplains (Lambert and Walling 1987; Nicholas and Walling 1997; Lecce and Pavlowsky 2004).

From field observations, it was observed that recent sediment was deposited on the floodplain surfaces of both the Gatberg and Minnehaha River floodplain systems during the two wet seasons that were monitored. The overall purpose of this chapter is to investigate spatial variability of sediment and phosphorus composition of the riverbeds and banks and recently deposited sediment on the floodplain surfaces, and to explore the relationship of these factors with the geomorphological characteristics of the two floodplain systems. The focus objectives are as follows:

1. To investigate and describe the channel and floodplain morphometrics.
2. To determine the channel sediment and total phosphorus dynamics and the relationships between sediment spatial variability and composition with the morphological and geomorphological characteristics of the two river-floodplain systems.
3. To establish the dynamics of recently deposited sediment and associated phosphorus on the floodplain surfaces and investigate the relationships between sediment spatial variability and composition with the morphological and geomorphological characteristics of the two river-floodplain systems.

5.2 METHODS

5.2.1 FIELD DATA COLLECTION

Samples of sediment deposited on the floodplain surface were collected using a 30 mm diameter hand-held corer during the dry season (see Figure 5.1 for sample locations). A composite sample (5 samples of the top 5 cm of sediment in a 1-meter radius, representing sediment that has been recently deposited) was taken at each sample site. Samples were collected following a stratified sampling approach along five transects oriented perpendicular to the river's thalweg. Between 8 and 15 surface sediment samples were collected along each cross-section according to changes in topography, geomorphic units, and vegetation.

A total of 42 samples from the five cross-sectional surveys in the Gatberg floodplain system and a total of 71 samples from the five cross-sectional surveys in the Minnehaha floodplain system were collected for analysis. This method was chosen to enhance the spatial detail in documenting the selectivity of deposition, although it comes at the expense of temporal detail, as samples collected from surface samples represent amalgamations of multiple flood occurrences. Nonetheless, they offer valuable insights into spatial deposition dynamics.

The suspended sediment from the rivers was sampled at the inlet and outlet of the two floodplain systems using time-integrated pipe-suspended sediment samplers, installed at a height above the bed equal to 0.4 bank-full flow depth (Phillips et al. 2000). These samplers provide information on suspended sediment characteristics; however, they do not provide suspended sediment concentrations. They provide a measure of the relative differences in suspended sediment characteristics that enter and exit the systems, and thus a measure of what type of sediment is being retained within and released from the systems. The suspended samplers were installed before the wet season (the wet season is from October to May) and collected when the river water levels had dropped sufficiently for the samplers to be collected safely.

Cross-sectional surveys were measured across the Gatberg and Minnehaha River floodplain systems using a Differential Global Positioning System (DGPS). The cross-sectional surveys describe the topography of the channel and the floodplain surface. Complex micro-topography of floodplain surfaces creates a dynamic mosaic that affects hydrology, vegetation communities, and transport and deposition of sediment and adsorbed phosphate (Fryirs et al. 2007).

The flooding frequency (Chapter 3) was calculated using Solinst level loggers. Solinst level loggers are water level dataloggers that use an absolute pressure sensor to detect the depth (or pressure) of water above the logger. Loggers were installed in the two channels (Gatberg and Minnehaha Rivers) in winter 2019 along one of the cross-sectional surveys. Loggers were placed into a protective cover that was attached to a metal stake. This was installed as close to the channel bed as possible, either by inserting the stake into the channel bed or banks. The logger height was measured using a DGPS to calibrate the sensor data. A barometric compensation was carried out on the level logger data using a Solinst Barologger which was installed in the catchment proximal to the level loggers. These loggers measured the continuous flow variation over the research period. The loggers were used to measure inundation water level changes throughout the two years. The number of flood events over bankfull was calculated from this data set.

Vegetation parameters (vegetation density, stem height and diameter) in one-meter plots were measured along floodplain cross-sectional surveys at the same location as surface sediment samples. Vegetation in floodplain systems is one of the most important factors influencing the hydrodynamics of overbank floodwaters, which affects sediment transport and deposition (Nehal et al. 2012; Curran and Hession 2013).

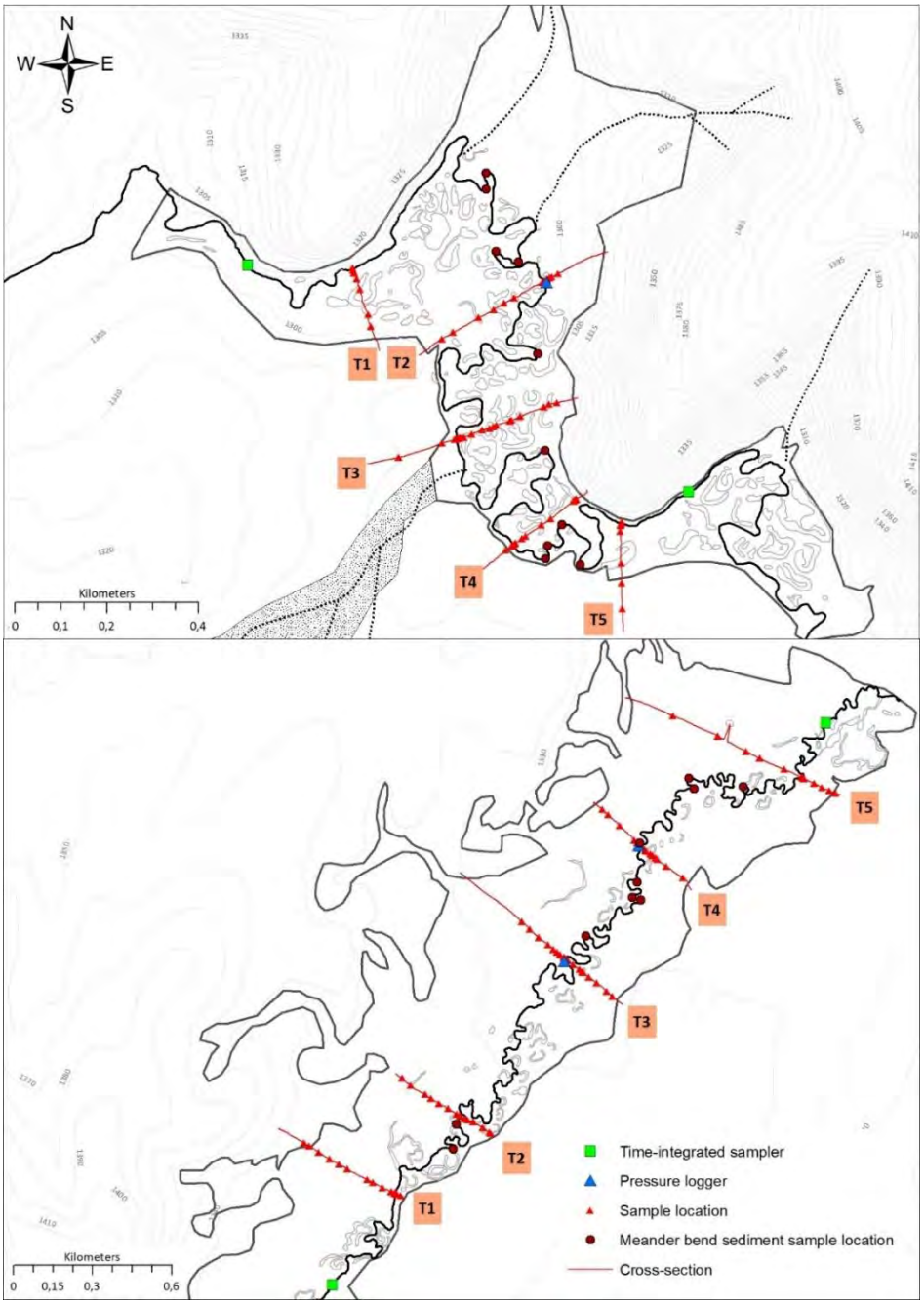

Figure 5.1 Map of the Gatberg and Minnehaha River floodplain systems showing the location of cross-sectional surveys and the location of sediment samples, pressure loggers and time-integrated samplers

5.2.2 LABORATORY ANALYSIS

The sediment samples were analysed in the Geography Department Laboratory at Rhodes University. All sediment samples collected were oven-dried at 50°C, gently disaggregated, weighed, and passed through a 2 mm mesh sieve to remove gravel and macro-organics. After homogenising the sediment samples, the samples were sub-sampled (~5 g) to determine the organic matter content by the loss-on-ignition method at 450°C in a muffle furnace (Donkin 1991; Leonard et al. 2002). Samples were removed after 4 hours and placed in a glass desiccator for an hour to avoid moisture re-absorption while they cooled (Leonard et al. 2002). Once the crucibles and samples had cooled, they were reweighed, and the mass recorded. Loss in mass after the ignition was used as a representation of the organic matter content in each sample, expressed as a percentage of the original dry mass of the sample. After the organic matter was removed, the same sub-samples were dispersed using a sodium hexametaphosphate solution and then separated into the absolute grain size distributions by laser diffraction using a Malvern Mastersizer 2000 (measuring range from 0.01 to 3500 μm). The particle size distribution is reported as median grain size (D_{50}), percentage by mass for the sediment classes, using Wentworth (1922) grain size classification scale, as well as the 16th and 84th percentile particle sizes by mass.

These measures of sediment particle size and distribution were chosen to present the composition of the sediment samples as well as to sufficiently characterise trends in the spatial distribution of particle sizes on the floodplain. Evaluating the particle size distribution of the surface sediment is an important characterisation of the two-dimensional floodplain surface. It can offer an understanding of the transport dynamics across the floodplain, characterising the sediment delivered to the floodplain from the channel, the overall composition of accumulated sediment stored in the different sections of the floodplain and what parts of the floodplain are 'activated' for possible sediment deposition.

The original homogenised sample was further sub-sampled (~35 g) and sent to BEMLAB (Somerset West, South Africa), an independent accredited analytical agricultural laboratory, to analyse the soil samples for total phosphate (TP), organic phosphate (OP) by the Bray II method, aluminium (Al), iron (Fe), magnesium (Mg) and calcium (Ca). TP in soil samples was determined using a method adapted from Sommers and Nelson (1972). Phosphate was extracted by acid digestion using a 1:1 mixture of nitric acid and hydrochloric acid at 80°C for 30 minutes. The phosphate concentration in the extract was then determined with a Varian ICP-OES (Inductively coupled plasma-optical emission spectrometer). Total extractable cations (Al, Mg and Ca) were extracted using 0.2 M ammonium acetate. Micronutrient (Fe) was extracted with diammonium salt of ethylenediaminetetraacetic acid (0.02 M) and boron (B) using a 1:2 hot water

ratio (The Non-affiliated Soil Analyses Work Committee 1990) and measured using an ICP-OES. The organic phosphate concentration in the samples was determined by the Bray II method, which is a method for measuring organic phosphorus in soils that involves sequential extractions using concentrated hydrochloric acid (HCl) and 0.5 N sodium hydroxide (NaOH) at room temperature, followed by 0.5 N NaOH at 90°C. The amount of organic phosphorus in the soil is determined by subtracting the inorganic phosphorus content from the total phosphorus content in the combined extracts.

5.2.3 DESKTOP DATA ANALYSIS

All desktop analyses were performed to determine the morphometrics of the channel and floodplain for the two research sites, as well as to perform a spatial analysis of the sediment and phosphorus dynamics using ArcMap 10.8.2. The morphometrics of channels, floodplains, and the associated hydraulic patterns of overbank flow play a crucial role in determining the quantity and distribution of sediment deposition in these areas.

This section describes the methods used to evaluate the longitudinal and cross-sectional profiles of the channel and floodplain of the Gatberg and Minnehaha River floodplain systems to determine the morphometrics that influence the spatial variability in sediment and total phosphorus dynamics. The methods were based on field investigations using a DGPS (sub-centimetre accuracy in the x, y, and z fields) imported into ArcMap 10.8.2. The channel morphometrics measured were the longitudinal slope of the channel bed and banks, the sinuosity, the channel width, depth, area, and the depth/width ratio. The floodplain morphometrics measured were longitudinal slope, perpendicular slope, width, and local relief.

5.2.4 DATA ANALYSIS

In total, 113 surface sediment samples were analysed. Excel, R statistical software and ArcGIS 10.8.2 were used to analyse and visualise that data. To identify the factors driving variability in sediment characteristics, partial correlation analysis was applied followed by stepwise multiple linear regression analysis.

The relationships between sediment properties followed by the relationship between the wetland variables and the sediment properties were studied using partial correlation analysis based on the Spearman rank correlation coefficient, which indicates the degree of association between the variables, controlling for effects from all other variables after a test for normality was conducted. For the variables, an ANOVA, or the non-parametric Kruskal-Wallis test with a pairwise post-hoc Dunn test, depending on whether the samples showed a normal or non-normal distribution, was applied to test for differences

within all the variables. Based on the result of the partial correlation analysis and the Kruskal-Wallis tests, variables were selected for a multiple linear regression model using the bidirectional approach to examine spatial and temporal change and interrelationships between sediment parameters and amounts of total phosphorus and controlling factors (e.g., morphometric parameters of the channel and floodplain). All analyses were carried out using the R software package (RCore Team 2022).

The explanatory variables, which are tested for significance, were selected based on a logical relationship between sediment properties and then those properties with wetland characteristics. It is assumed that local deposition is a function of both supply and the local transport capacity, which is related to sediment size, discharge, and the channel slope. The average longitudinal (downstream) and perpendicular (away from the channel) floodplain slope was introduced as a variable, as it will be the slope of the floodplain rather than the slope of the channel that influences the floodplain deposition (Notebaert et al. 2010). This was measured using the DGPS coordinates of the floodplain cross-sections. The other wetland characteristic variables were chosen because research has shown that these variables play a role in sediment and sediment-associated phosphorus deposition.

5.3 RESULTS

5.3.1 RIVER SEDIMENT AND PHOSPHORUS DYNAMICS

5.3.1.1 CHANNEL AND FLOODPLAIN MORPHOLOGY

5.3.1.1.1 Longitudinal floodplain channel profile

Figure 5.2A shows the longitudinal channel profile of the sections of the Gatberg River within the floodplain system. The Gatberg River section is a mixed-bed meandering river characterised by pools, riffles, and runs. Pools occur within the many meander bends and are characterised by lower elevations. Riffles and runs occur in the straight sections between the meander bends and are characterised by steeper gradients and higher elevations (Figure 5.2A). The mean longitudinal floodplain channel bed slope is 0.04 % and the sinuosity index is 3.8. The average height of the left bank from the thalweg is 1.9 m and the range is 1.2 to 2.9 m. The average height of the right bank from the thalweg is 2 m, and the range is 1.3 to 3.5 m. The slope of the left bank from the head to the toe of the floodplain system is 0.06 % while the slope for the right bank is 0.05 %. Two tributaries enter the Gatberg River marked by blue arrows in Figure 5.2A.

Figure 5. 2B shows the longitudinal channel profile of the sections of the Minnehaha River within the floodplain system. The Minnehaha is a mixed-bed meandering river characterised by pools, riffles and

runs. The mean longitudinal floodplain channel bed slope is 0.15 % and the sinuosity index is 2.4 (Figure 5.2B). The average height of the left bank from the thalweg is 1.5 m and the range is 0.6 to 2.6 m. The average height of the right bank from the thalweg is 1.4 m, and the range is 0.7 to 2.5 m. The slope of the left and right bank from the head to the toe of the floodplain system is 0.14 %.

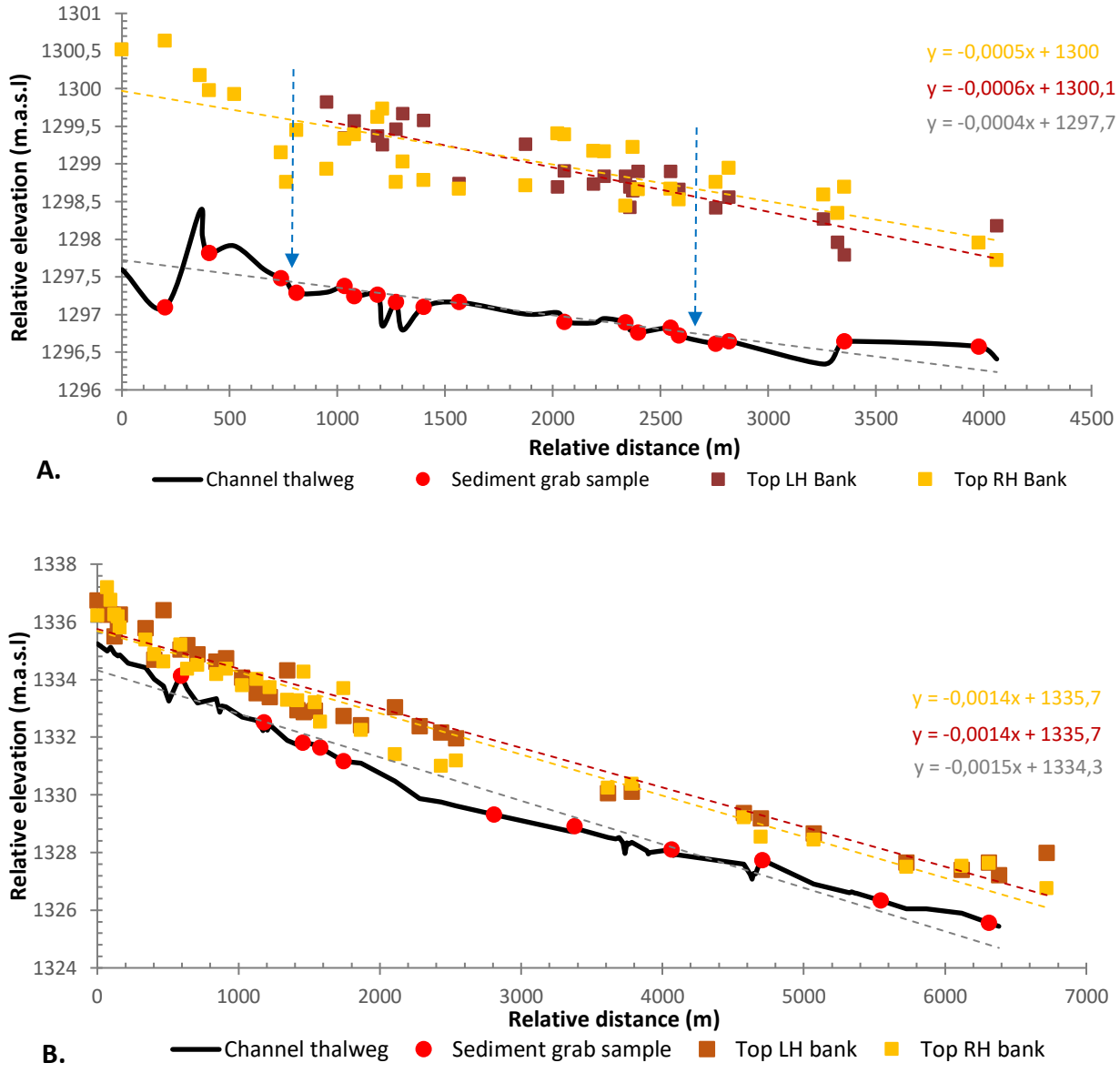

Figure 5.2 A) Gatberg River section longitudinal profile along the thalweg, top of the left (LH) and right (RH) bank down the river section, location of bed sediment grab samples and the location of the two tributaries entering the river section. B) Minnehaha River section longitudinal profile along the thalweg, top of the left and right bank down the river section, and location of bed sediment grab samples

5.3.1.1.2 Channel and floodplain cross-sectional morphology

Table 5.1 shows the summary statistics of the morphometric variables of the research river reach of the Gatberg and Minnehaha River floodplain systems. Thirty-five channel cross-sections were conducted down the length of the Gatberg River research reach. The Gatberg River reach had an average bankfull width of 8.3 m (mode = 7.4 m) with a minimum of 5.2 m and a maximum of 12.3 m. The bankfull channel widths do not show any pattern of either increasing or decreasing with distance downstream. The Gatberg channel within the floodplain has a mean bankfull channel depth of 2.0 m (mode of 2.1 m, maximum of 3 m and minimum of 1.3 m), while the channel mean bankfull width to depth ratio is 4.2. The width-to-depth ratio increases slightly with distance downstream. The bankfull channel area decreases downstream (mean = 11 m^2, mode 25 m^2, minimum = 1.5 m^2 and maximum= 25 m^2). The channel moves from the left to the right margin of the valley. The mean slope of the channel bed was 0.3 % and has a range of between 0.002 and 1.3 %.

Twenty-five channel cross-sections were conducted along the length of the Minnehaha River research reach. Bankfull channel widths had an average of 5.6 m (mode = 5.3 m) with a minimum of 3.5 m and a maximum of 13.4 m. The bankfull channel widths decreased with the distance downstream (r^2= 0.4 log) and increased with increasing elevation (r^2= 0.4). The Minnehaha channel within the floodplain has a mean bankfull channel depth of 1.6 m (mode of 2.2 m, maximum of 2.5 m, and a minimum of 0.7 m), while the channel mean bankfull width to depth ratio is 3.8. The width-to-depth ratio increases slightly with distance downstream. The channel meanders slightly through a narrow meander belt in the middle of the valley. The mean channel bed slope was 0.4 % and ranges of between 0.03 and 2.5 %.

Table 5.2 shows the summaries of the floodplain morphometric of the Gatberg and Minnehaha River floodplain systems. Figure 5.3 and Figure 5.4 show the floodplain cross-section morphology, geomorphic features, and floodplain surface sediment sample locations across the two research floodplain systems. The morphology of the Gatberg River floodplain system was examined to investigate the topography, sediment, and phosphorus dynamics of the study areas. The width of the floodplain was variable along its length, with the surveyed cross-sections 2 and 3 representing broader sections of the floodplain system (Table 5.2 and Figure 5.3). In the broad zones, widths ranged between 300 m and 370 m. In the narrower zones, the floodplain widths range between 150 m to 230 m (floodplain cross-sections 1, 4 and 5). The basin is bounded on the left bank by a steep mountain and on the right bank by a gently sloped hill. On the left side, the transition is more abrupt, and the gradient increases rapidly from the valley bottom to the mountain. The valley floor, which is covered primarily by the floodplain, has an average local relief of

0.4 m (minimum 0.07 m and maximum 1 m) over 250 m. For floodplain cross-sections 1, 2, 4 and 5 the floodplain surface slopes predominantly towards the floodplain margin from the top of the channel levee or bank (average slope of 0.23 %). The floodplain surface, in floodplain cross-section 3, slopes towards the channel from the floodplain margin (slope of 0.04 % from the left margin and 1.8 % from the right margin). A total of 106 oxbows are found on the floodplain surface that vary in size, depth, and distance from the channel.

The width of the Minnehaha River floodplain was variable along its length, and the surveyed cross-sections 3 and 5 represent broader sections of the floodplain system (Table 5.2 and Figure 5.4). In the broad zones, the widths were 690 and 820 m, respectively. In the narrower zones, the floodplain widths range between 415 m to 435 m (floodplain cross-sections 1, 2, and 4). The basin is bound on both sides by a gentle sloping alluvial terrace that separates the floodplain from the other wetlands running parallel to the research site. The valley floor, which is covered primarily by the floodplain, has an average local relief of 0.5 m (minimum 0.2 m and maximum 0.7 m) over more than 290 m. For floodplain cross-sections 1, 2, 3, and 4 the floodplain surface slopes predominantly towards the floodplain margin from the top of the channel levee or bank (average slope of 0.48 %). The floodplain surface at floodplain cross-section 5 slopes towards the channel from the floodplain margin (slope of 0.3 % from the left margin and 0.8 % from the right margin). A total of 50 oxbows are found within a narrow (50 m) band within the floodplain system, varying in size, depth, and distance from the channel.

Table 5.1 Summary statistics of channel morphometrics for the Gatberg and Minnehaha River floodplain system

Floodplain river system	Summary statistics	Mean depth (m)	Bankfull depth (m)	Bankfull width (m)	Bankfull cross-sectional area (m^2)	Width/depth ratio	Slope (%)
Gatberg River floodplain	Mean	1.4	2.0	8.3	11.0	4.2	0.3
	Median	1.4	2.1	8.4	9.6	4.1	0.2
	Mode	1.3	2.1	7.4	25.0	3.5	0.2
	Standard Deviation	0.3	0.4	1.5	6.8	1.0	0.3
	Range	1.1	1.7	7.1	23.5	5.2	1.3
	Minimum	0.9	1.3	5.2	1.5	2.6	0.0
	Maximum	2.0	3.0	12.3	25.0	7.8	1.3
	Standard Error	0.0	0.1	0.2	1.2	0.2	0.1
Minnehaha River floodplain	Mean	1.0	1.6	5.6	4.9	3.8	0.4
	Median	0.8	1.5	5.2	5.0	3.2	0.2
	Mode	1.5	2.2	5.3	4.9	2.4	0.4
	Standard Deviation	0.4	0.5	2.1	2.5	2.2	0.5
	Range	1.5	1.8	9.9	10.4	10.8	2.4
	Minimum	0.5	0.7	3.5	0.3	2.1	0.0
	Maximum	2.0	2.5	13.4	10.6	13.0	2.5
	Standard Error	0.1	0.1	0.4	0.5	0.4	0.1

Table 5.2 Floodplain surface morphometrics by cross-section for the Gatberg and Minnehaha River floodplain system

Floodplain river system	Cross-section number	Floodplain cross-sectional morphometrics				
		Floodplain width, Left bank (m)	Floodplain width, Right bank (m)	Mean floodplain surface slope, Left bank (%)	Mean floodplain surface slope, Right bank (%)	Average local relief (m)
Gatberg River floodplain	1	1.0	139.5	-	0.2	1.0
	2	32.0	269.5	0.5	0.2	0.3
	3	212.6	124.7	0.0	1.8	0.5
	4	169.9	24.9	0.3	0.5	0.3
	5	0.0	173.1	-	0.1	0.3
Minnehaha River floodplain	1	303.3	8.6	0.3	0.8	0.2
	2	300.9	109.8	0.1	0.4	0.4
	3	443.2	243.7	0.1	0.6	0.6
	4	203.1	224.2	0.3	0.6	0.7
	5	111.7	686.9	0.1	0.3	0.6

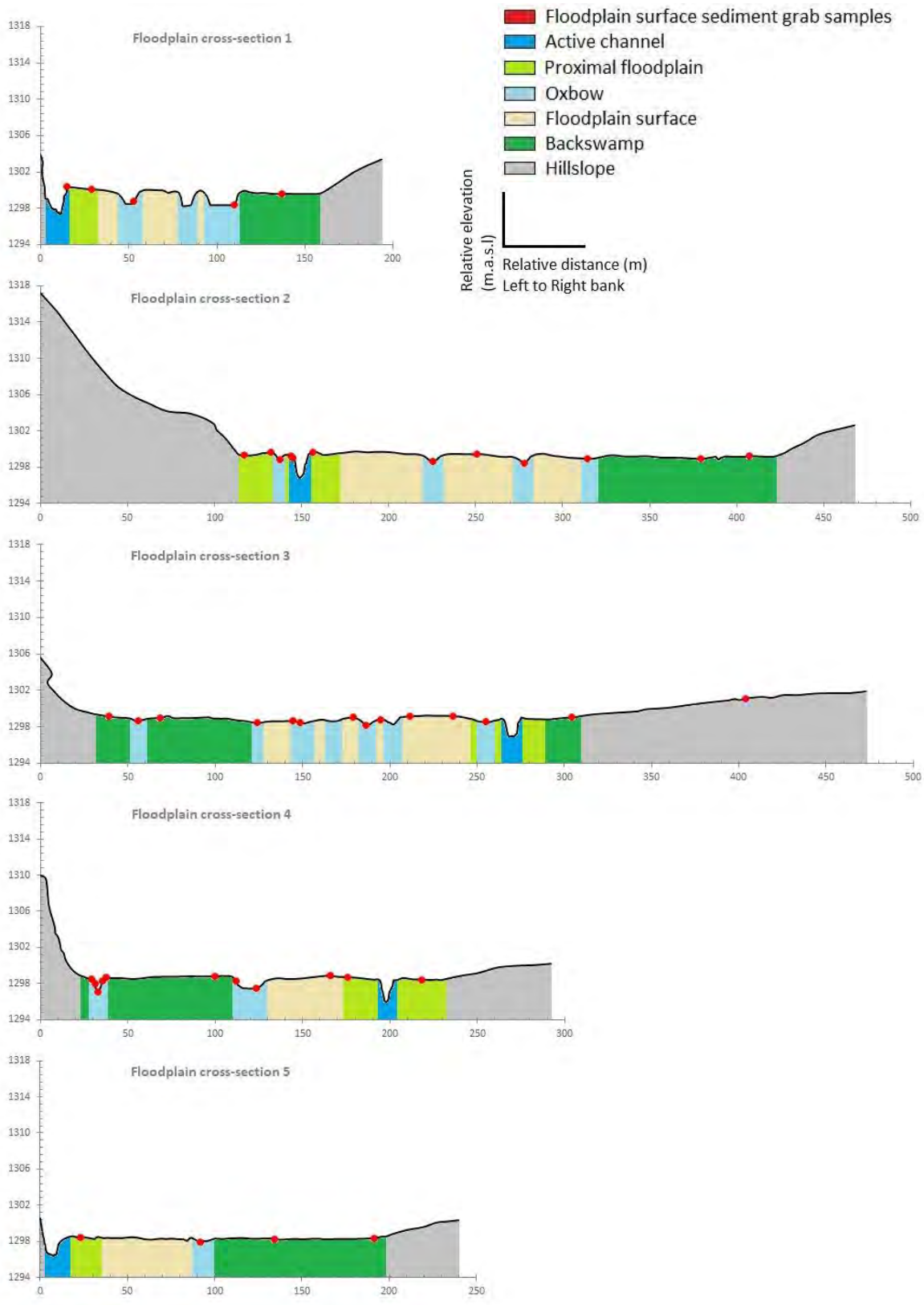

Figure 5.3 Gatberg River floodplain cross-section morphology, geomorphic features, and floodplain surface sediment sample locations

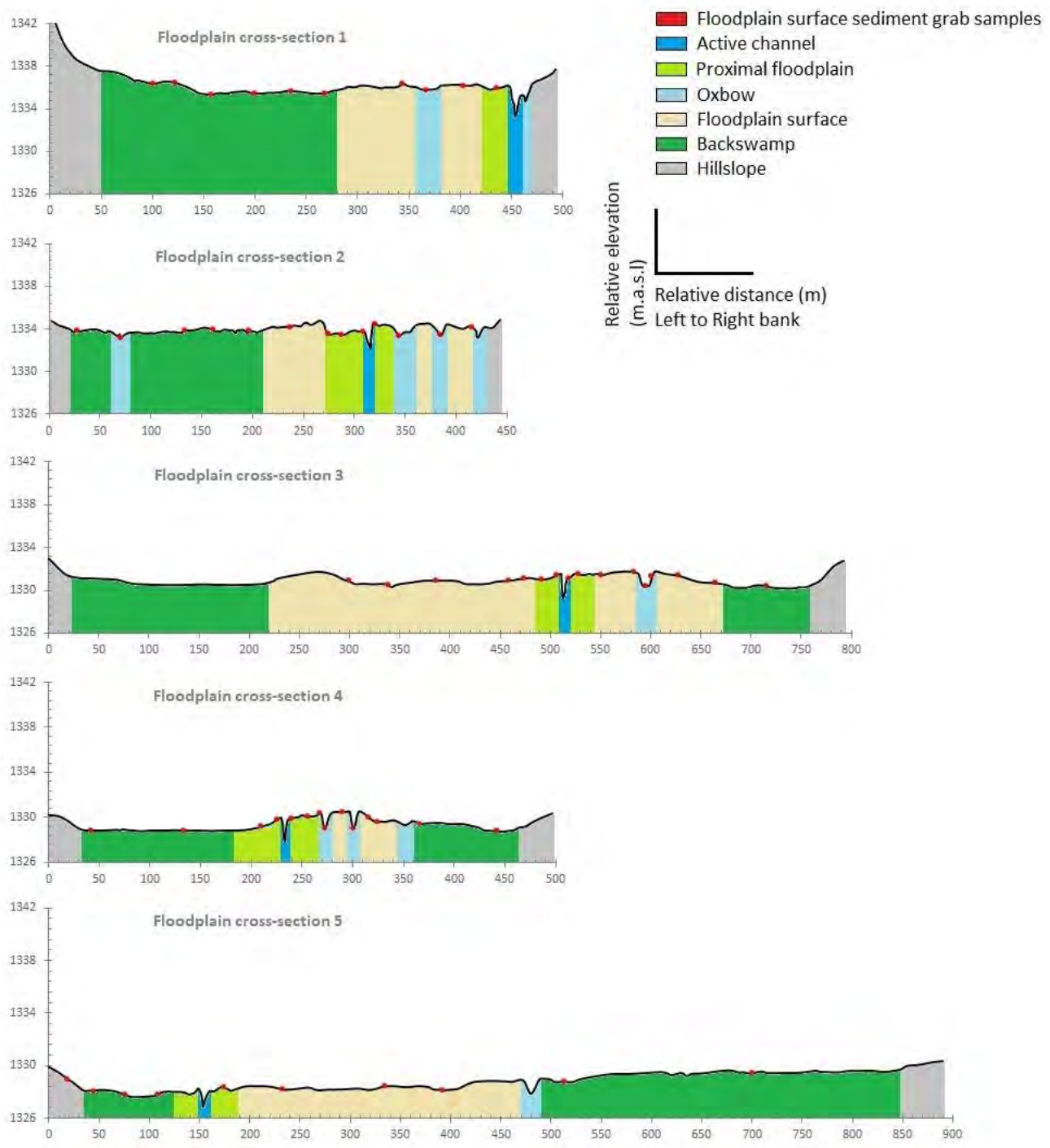

Figure 5.4 Minnehaha River floodplain cross-section morphology, geomorphic features, and floodplain surface sediment sample locations

5.3.1.2 CHANNEL SEDIMENT AND PHOSPHORUS DYNAMICS

5.3.1.2.1 Incoming and outgoing sediment characteristics

The results of the analysis of the deployed time-integrated samplers at the head and toe of the meandering channel of the Gatberg and Minnehaha floodplain and the two tributaries that enter the Gatberg River within the research area are presented in Table 5.3.

Within the Gatberg River, the total mass of sediment collected by the time-integrated samplers at the head of the study site was 250 g with a mean sediment particle size of 24 µm (medium silt). The total phosphorus concentration in the incoming suspended sediment collected was 0.14 g kg^{-1}. The total sediment collected by the time-integrated samplers at the toe of the study site was 156 g with a mean sediment particle size of 17 µm. The total phosphorus concentration of the outgoing suspended sediment collected was the same as the incoming concentration. The percentage of the organic matter content increased by one per cent from 8 to 9 % (incoming to outgoing). The geochemical concentrations of the suspended sediment increased a small fraction from the incoming to outgoing collected suspended sediment, except for iron which remained the same. The total sediment mass from the left bank tributary entering the Gatberg River system close to the head of the system was 45 g with a mean sediment particle size of 25 µm. An extra 0.10 g kg^{-1} sediment-associated phosphorus concentration entered the Gatberg River system from this tributary. The percentage of the organic matter content was 10 % and the geochemical concentrations were iron 4.53 g kg^{-1}, aluminium 3.75 g kg^{-1}, magnesium 0.78 g kg^{-1} and calcium 1.3 g kg^{-1}. The total sediment mass from the second tributary with a valley bottom wetland entered the Gatberg River approximately halfway through the study site from the right bank was 62 g with a mean sediment particle size of 17 µm. The associated total phosphorus concentration from this tributary was 0.15 g kg^{-1}. The per cent organic matter content was 11 % and the geochemical concentrations were iron 5.76 g kg^{-1}, aluminium 3.2 g kg^{-1}, magnesium 0.31 g kg^{-1} and calcium 0.44 g kg^{-1}.

Within the Minnehaha River, the total sediment mass collected by the time-integrated samplers at the head of the study site was 578 g with a mean sediment particle size of 20 µm. The total phosphorus concentration in the incoming suspended sediment collected was 0.08 g kg^{-1}. The total mass of sediment collected by the time-integrated samplers at the toe of the study site was 309 g with a mean sediment particle size of 15 µm. The total phosphorus concentration attached to the outgoing suspended sediment collected was the same as the incoming concentration. The percentage of organic matter content was 7 % for the sediment collected at the head and toe of the system. The geochemical concentrations associated with the incoming suspended sediment were iron 5.76 g kg^{-1}, aluminium 3.73 g kg^{-1},

magnesium 0.17 g kg^{-1}, and calcium 0.44 g kg^{-1}. The geochemical concentrations associated with the outgoing suspended sediment remained the same for aluminium (3.84 g kg^{-1}) and calcium (0.5 g kg^{-1}); iron decreased to 5.04 g kg^{-1} and magnesium increased to 0.26 g kg^{-1}.

Table 5.3 Results of the deployed time-integrated sediment samplers for both floodplain systems

Floodplain system	Property	Head of the system Mean	Toe of the system Mean
Gatberg floodplain system	Total sediment mass (g) over first wet season	250	156
	Sediment (µm)	24	17
	Total phosphorus (g kg^{-1})	0.14	0.14
	Organic matter content (%)	8.2	8.5
	Iron (g kg^{-1})	8.02	7.89
	Aluminium (g kg^{-1})	3.11	3.91
	Magnesium (g kg^{-1})	0.43	0.59
	Calcium (g kg^{-1})	0.72	0.98
Left bank tributary	Total sediment mass (g) over first wet season	45	
	Sediment (µm)	25	
	Total phosphorus (g kg^{-1})	0.09	
	Organic matter content (%)	10.0	
	Iron (g kg^{-1})	4.53	
	Aluminium (g kg^{-1})	3.75	
	Magnesium (g kg^{-1})	0.78	
	Calcium (g kg^{-1})	1.30	
Right bank tributary with valley bottom wetland	Total sediment mass (g) over first wet season	62	
	Sediment (µm)	17	
	Total phosphorus (g kg^{-1})	0.15	
	Organic matter content (%)	11.4	
	Iron (g kg^{-1})	5.76	
	Aluminium (g kg^{-1})	3.20	
	Magnesium (g kg^{-1})	0.31	
	Calcium (g kg^{-1})	0.41	
Minnehaha floodplain system	Total sediment mass (g) over first wet season	578	309
	Sediment (µm)	20	15
	Total phosphorus (g kg^{-1})	0.08	0.07
	Organic matter content (%)	5.9	7.4
	Iron (g kg^{-1})	5.76	5.04
	Aluminium (g kg^{-1})	3.73	3.84
	Magnesium (g kg^{-1})	0.17	0.26
	Calcium (g kg^{-1})	0.44	0.50

5.3.1.2.2 Characterising channel-bed sediments, channel-bank (cut bank) and point bar material

I. Bed material

The distribution of D_{50} particle size of the bed material along the Gatberg River during the study period ranged from medium silt to coarse sand (25 to 870 µm), with an average of 435 µm. Most of the particle size distributions were unimodal. The D_{84} particle sizes ranged from 57 to 5622 (coarse silt to pebbles), with an average D_{84} bedload particle size being 1504 µm in diameter. The D_{16} particle sizes ranged from 4 to 387 (very fine silt to medium sand), with an average of 143 µm (Figure 5.5).

Figure 5.6 shows that the sand fraction dominated the samples taken along the bed of the Gatberg River down the system. The percentage of the sediment size fractions does not display a smooth downstream decline in sediment size but is characterised by several coarse sediment spikes associated with riffles within the alluvial valley where the research floodplain occurs. A small increase in the percentage of gravel appears to occur just downstream of both tributaries.

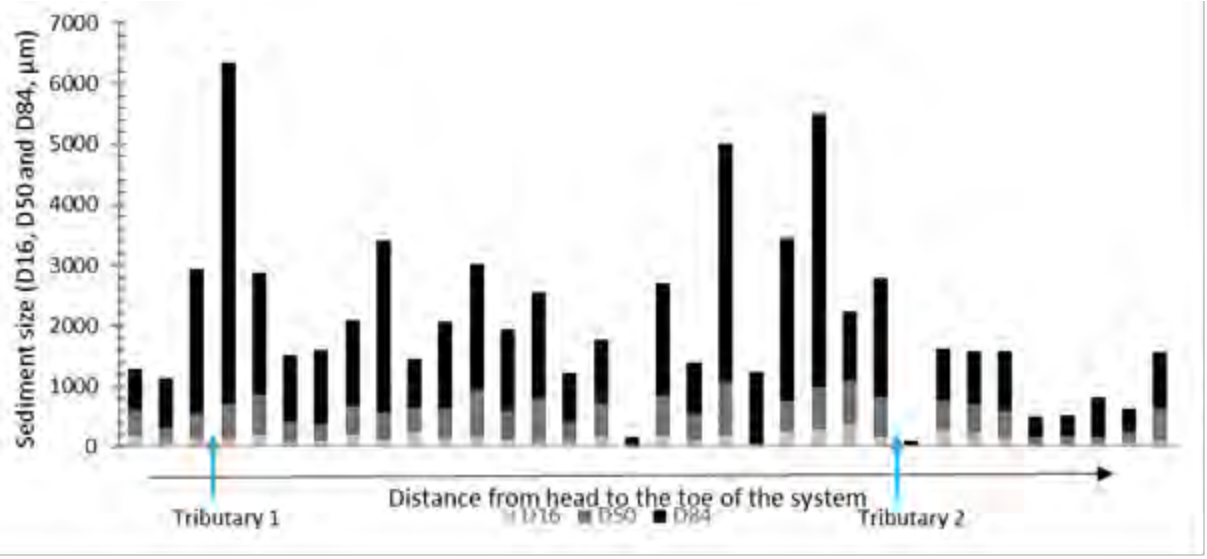

Figure 5.5 Gatberg Riverbed material sediment size (D_{16}, D_{50} and D_{84}) distributions. The locations of the two tributaries indicated

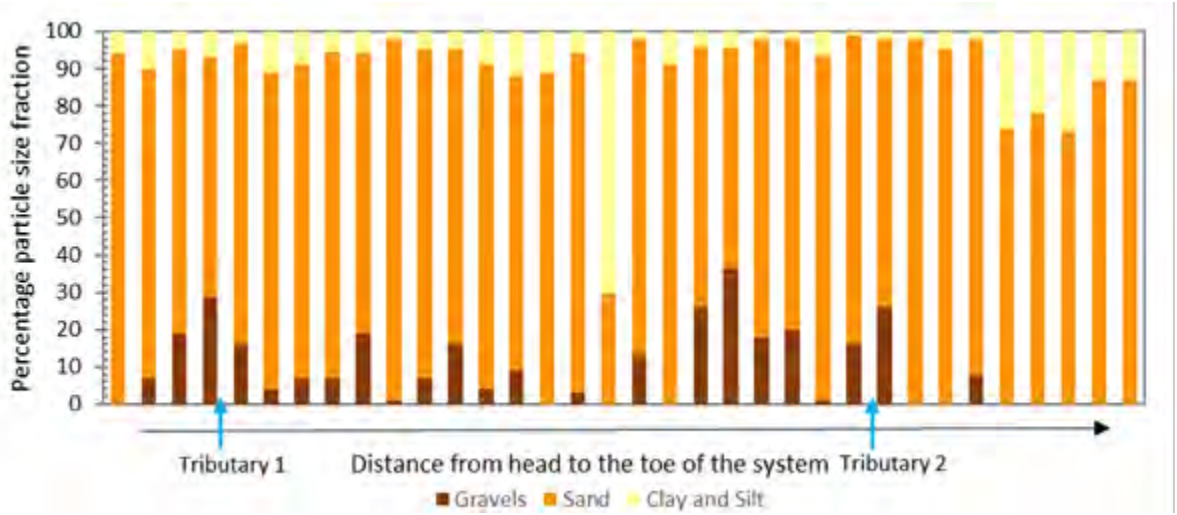

Figure 5.6 Gatberg Riverbed percentage sediment size fractions (Gravel, sand, clay, and silt) distributions with the locations of the two tributaries indicated

The percentage of organic matter content was low (below 6 %) for all the bed sediment samples (Figure 5.7). The average percentage of organic matter was 1.9 % (mode of 3.3 %). There was no trend between the percentage of organic matter and the distance downstream ($P > 0.05$).

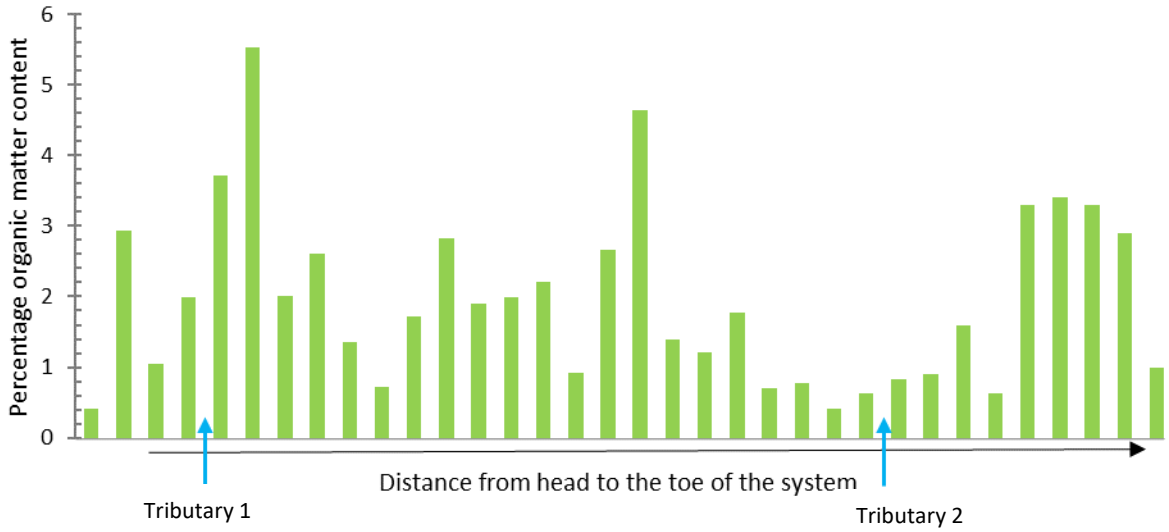

Figure 5.7 Gatberg Riverbed percentage organic matter content distributions with the locations of the two tributaries indicated

The total phosphorus concentration was low (below 1 g kg^{-1}) for all the bed sediment samples (Figure 5.8). The average total phosphorus concentration was 0.05 g kg^{-1}. There was no trend between total phosphorus concentration and distance downstream ($P > 0.05$). Several peaks can be seen downstream.

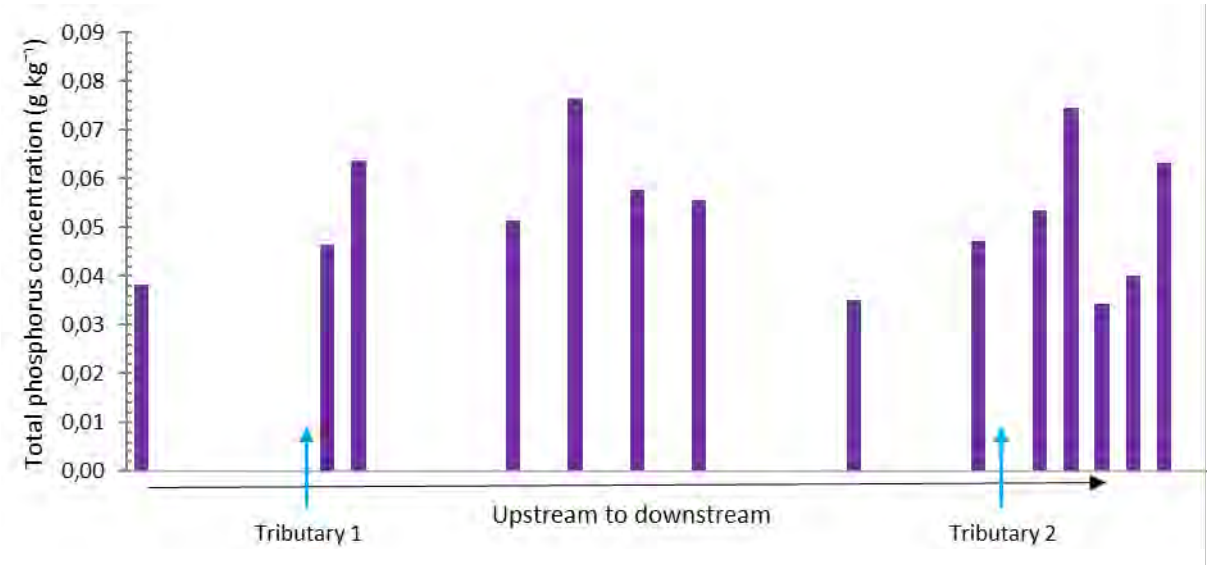

Figure 5.8 Gatberg Riverbed total phosphorus concentration distributions with the locations of the two tributaries indicated

In Table 5.4, the geochemical concentrations in the sediment samples ranged from 0.1 to 0.7 g kg^{-1} for iron, 0.5 to 4.3 g kg^{-1} for aluminium, 0.1 - 0.2 g kg^{-1} for magnesium, and 0.2 - 0.6 g kg^{-1} for calcium. The highest geochemical concentrations in the bed sediments were recorded for aluminium with a mean concentration of 2.6 g kg^{-1} followed by calcium and iron with mean concentrations of 0.4 and 0.2 g kg^{-1}, respectively. The lowest geochemical concentrations were recorded in the bed sediments for magnesium with a mean concentration of 0.1 g kg^{-1}. The CV values for all the major chemical element constituents measured were low with values below 1, indicating that the data do not deviate much from the mean.

Figure 5.9 shows the various concentrations for each geochemical measured in the bed sediments that were sampled downstream. The geochemical concentrations fluctuate downstream. The data shows that the tributaries had very little influence on the geochemical concentrations.

Table 5.4 Descriptive statistics of the geochemical concentrations in the Gatberg Riverbed sediment samples

Geochemical	N	Minimum	Maximum	Mean	Standard deviation	CV
Iron (g kg^{-1})	13	0.1	0.7	0.2	0.2	0.7
Aluminium (g kg^{-1})	13	0.5	4.3	2.6	1.1	0.4
Magnesium (g kg^{-1})	13	0.1	0.2	0.1	0.05	0.3
Calcium (g kg^{-1})	10	0.2	0.6	0.4	0.1	0.3

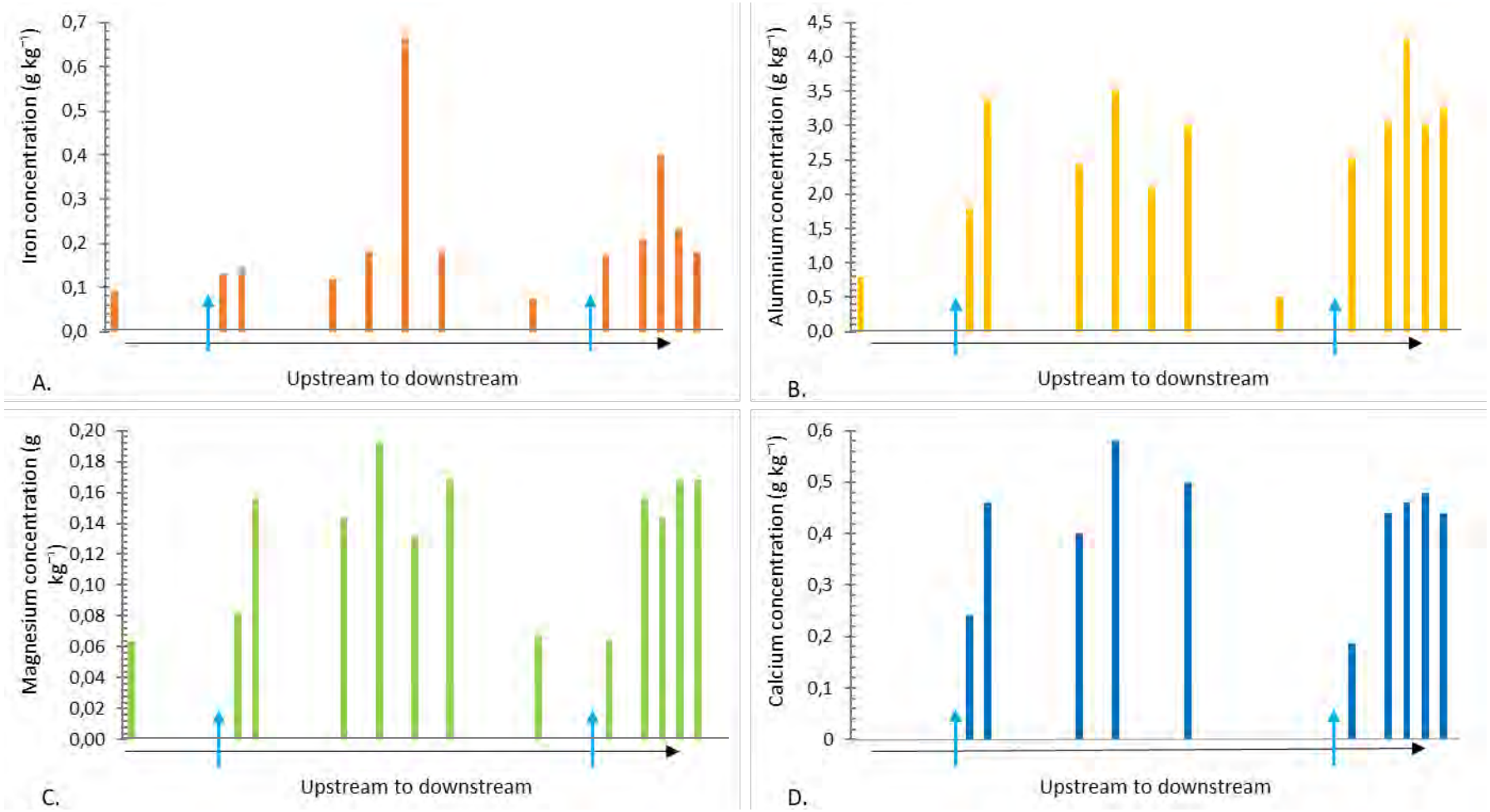

Figure 5.9 Gatberg Riverbed geochemical concentration distributions. A) Iron concentration, B) Aluminium concentration, C) Magnesium concentration, and D) Calcium concentration. Locations of the two tributaries indicated by blue arrows

Figure 5.10 shows the percentage of the sediment size fractions (gravel, sand, clay, and silt) for all the samples classified by the morphological units in which the samples were taken. As was previously shown sand dominated all the samples. The run morphological unit had the highest mean and the lowest variation in percentage sand. Riffles had the second-highest mean sand percentage and the highest variability. Riffles also had the highest mean gravel percentage and most variability in per cent gravels. Pools had the highest mean percentage of the finer sediment size fraction (clay and silt).

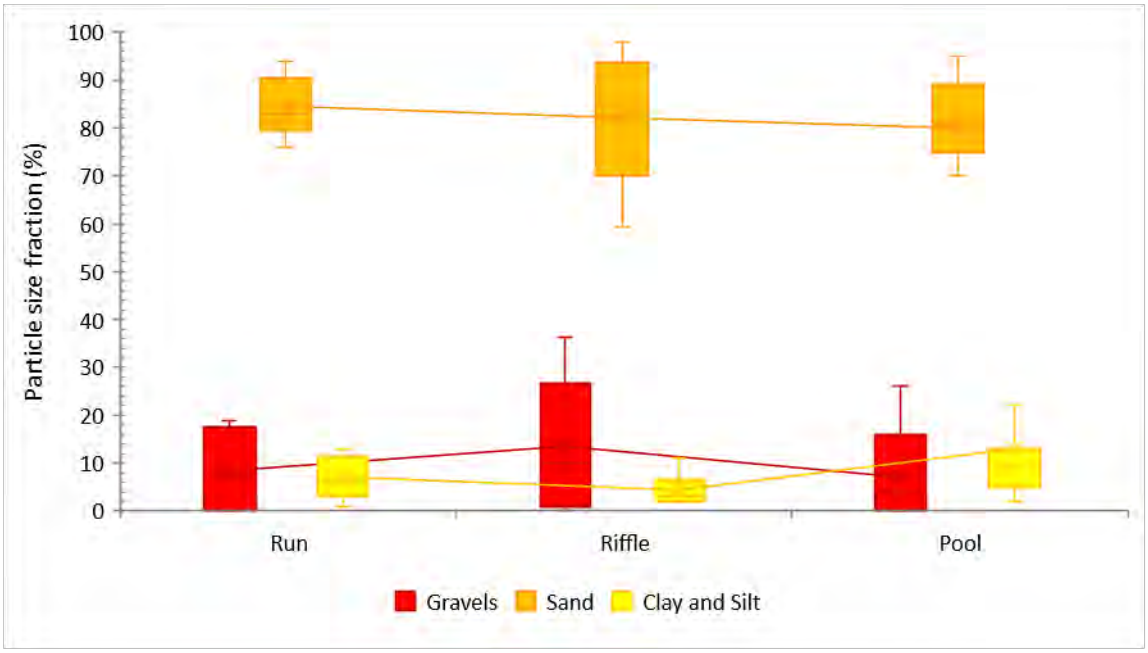

Figure 5.10 Gatberg Riverbed percentage sediment size fractions (gravel, sand, and clay and silt) categorised into alluvial channel morphological units (run, riffle, and pool)

Figure 5.11 shows the percentage of organic matter content for the samples categorised by the morphological units the samples were taken in. The pool morphological unit had the highest mean in percentage organic matter content. Riffles had the second-highest mean percentage of sand and the highest variability. Runs had the lowest mean percentage of organic matter content.

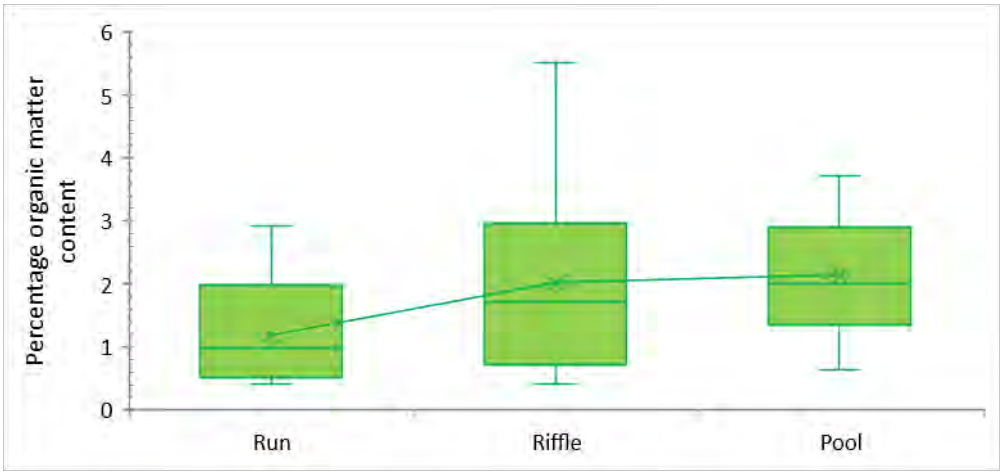

Figure 5.11 Gatberg Riverbed percentage organic matter content categorised into alluvial channel morphological units (run, riffle, and pool)

Figure 5.12 shows the total phosphorus concentration for the samples categorised by the morphological units the samples were taken in. The pool morphological unit had the highest mean (0.1 g kg^{-1}) and the highest variability. Unfortunately, only one sample was taken in the riffle morphological unit with a value of 0.04 g kg^{-1}. Runs had a slightly lower mean (0.05 g kg^{-1}) and less variability than the pool morphological unit.

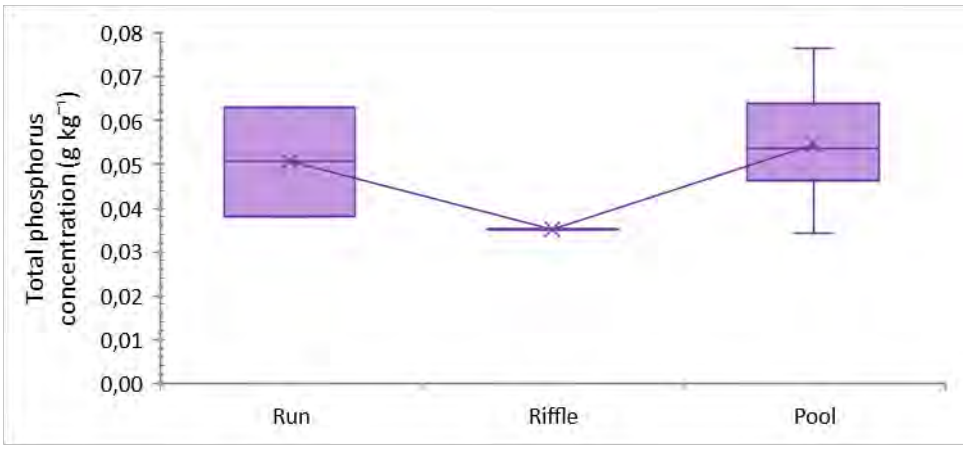

Figure 5.12 Gatberg Riverbed total phosphorus concentration categorised into alluvial channel morphological units (run, riffle, and pool)

The distribution of the D_{50} particle size of the bed material along the Minnehaha River during the period of study ranged from medium silt to very coarse sand (24 to 1237 µm), with an average particle size of 248 µm (fine sand). Most of the particle size distributions were unimodal. The D_{84} particle sizes ranged

from 55 to 6640 (coarse silt to pebbles), with an average particle size of 1397 µm (very coarse sand). The D_{16} particle sizes ranged from 5 to 217 (very fine silt to fine sand), with an average particle size of 65 µm (very fine sand; Figure 5.13A).

Figure 5.13B shows that the sand fraction dominated the samples taken along the bed of the Minnehaha River down the system. The percentage sediment size fractions do not display a smooth downstream decline in sediment size but were characterised by several coarse sediment spikes within the alluvial valley where the research floodplain occurs.

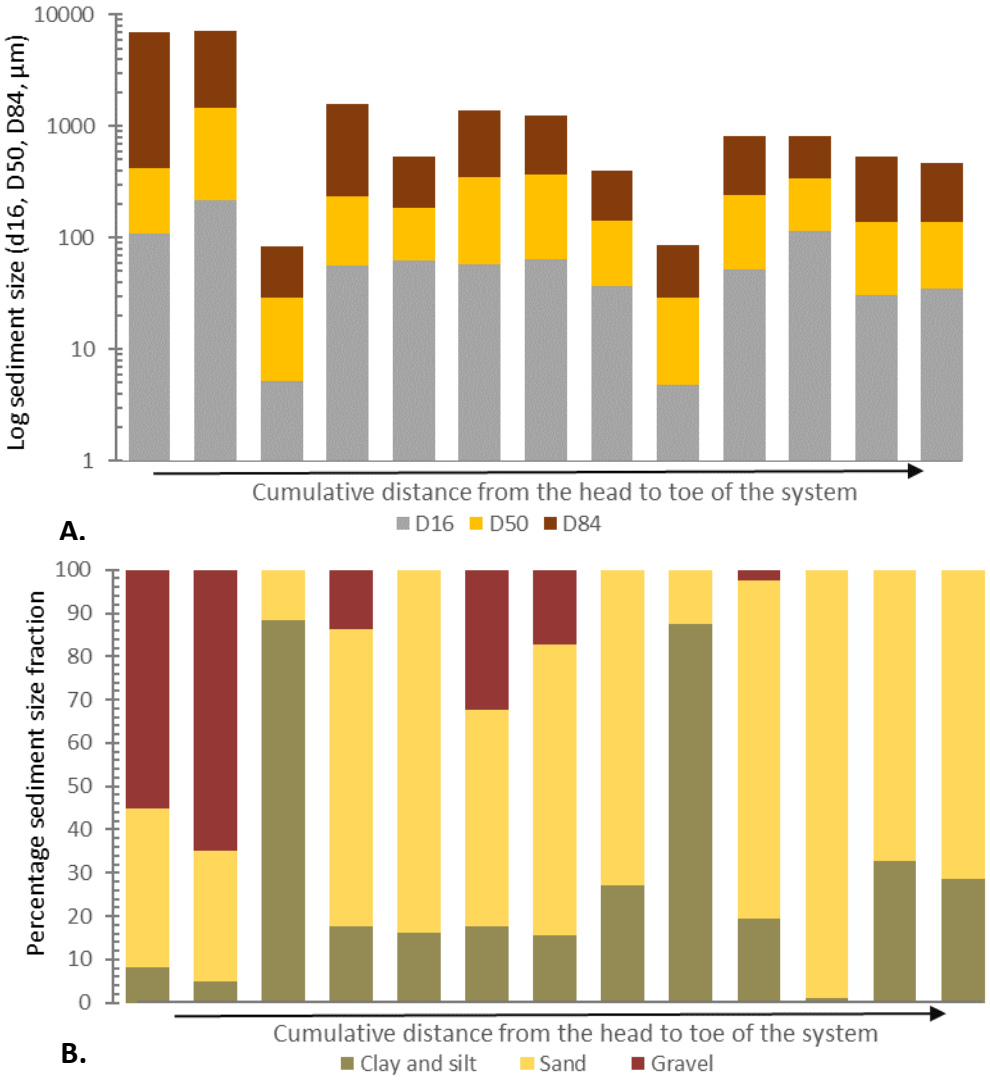

Figure 5.13 A) Minnehaha Riverbed sediment size (D16, D50 and D84) distributions. B) Minnehaha Riverbed percentage sediment size fractions (clay and silt, gravel, and sand) distributions

The percentage of organic matter content was low at a mean of 4 % for all the bed sediment samples (Figure 5.14). There was no trend between the percentage of organic matter and the distance downstream ($P > 0.05$).

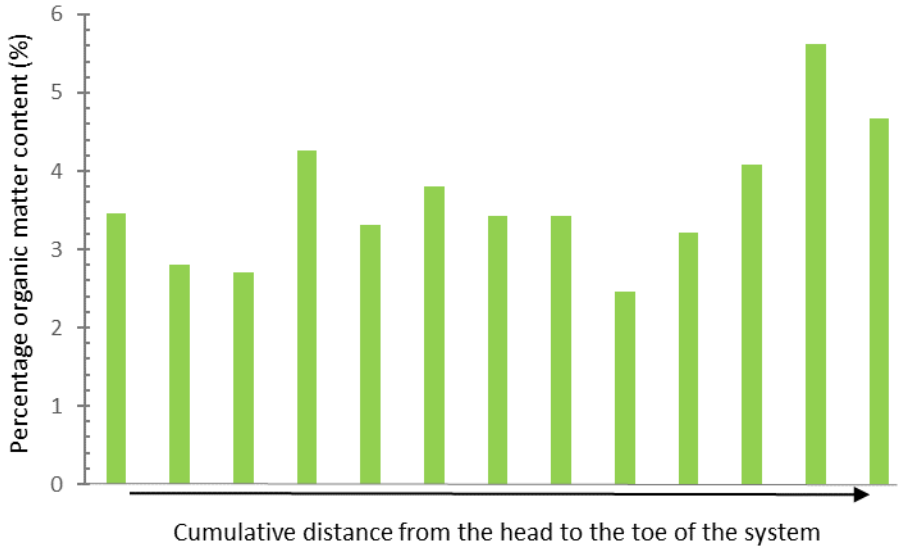

Figure 5.14 Minnehaha Riverbed percentage organic matter content distributions

The total phosphorus concentration was low (below 1 g kg^{-1}) for all the bed sediment samples (Figure 5.15). The average total phosphorus concentration was 0.07 g kg^{-1}. There was no trend between total phosphorus concentration and distance downstream. Several peaks can be seen downstream.

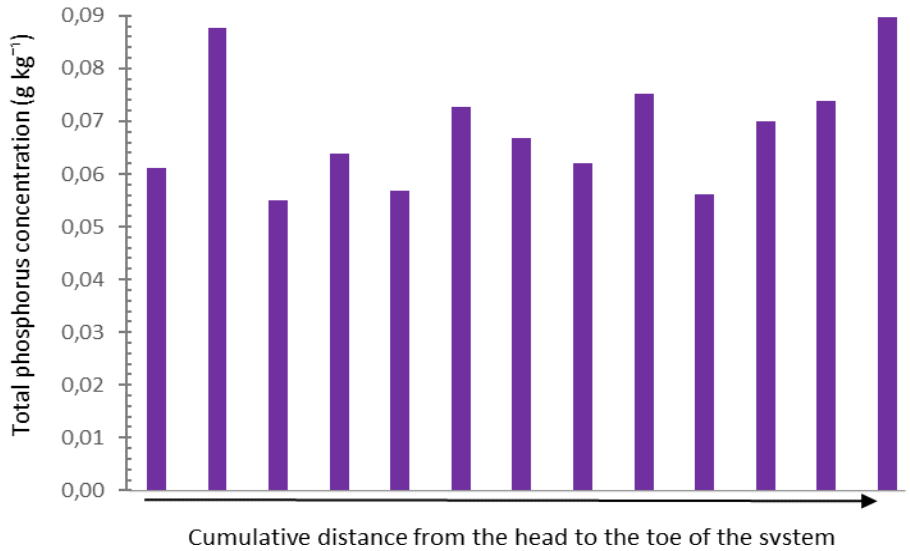

Figure 5.15 Minnehaha Riverbed total phosphorus concentration distributions

The geochemical concentrations in the sediment samples ranged from 0.05 - 10.5 g kg^{-1} for iron, 2.2 - 5.9 g kg^{-1} for aluminium, 0.1 - 0.2 g kg^{-1} for magnesium, and 0.3 - 0.9 g kg^{-1} for calcium (Table 5.5). The highest geochemical concentrations in the bed sediments were recorded for aluminium with a mean concentration of 4.1 g kg^{-1} followed by calcium with a mean concentration of 0.4 g kg^{-1}. The lowest geochemical concentration in the bed sediments were recorded for iron and magnesium with a mean concentration of 0.1 g kg^{-1}. CV values for all chemically measured were low with values below 1, indicating the data does not deviate much from the mean, except for iron concentration (CV value > 2.2). The geochemical concentrations fluctuate downstream.

Table 5.5 Descriptive statistics of the geochemical concentrations in the Minnehaha Riverbed sediment samples

Geochemical	N	Minimum	Maximum	Mean	Standard deviation	CV
Iron (g kg^{-1})	13	0.1	10.5	1.6	3.6	2.2
Aluminium (g kg^{-1})	13	2.2	5.9	4.2	1.0	0.2
Magnesium (g kg^{-1})	13	0.1	0.2	0.1	0.04	0.3
Calcium (g kg^{-1})	13	0.3	0.9	0.5	0.1	0.3

Relationships between sediment properties and channel morphometrics and geometry

Correlation analysis was used to identify the potential between the sediment properties of the channel bed samples and the channel morphometrics and geometry. The results of the statistical normality test indicated that most of the sediment and morphological data were not normally distributed, thus violating one of the assumptions of Pearson's correlation analysis. Consequently, Spearman rank correlation analyses were performed, along with trend analysis. The Spearman correlation matrix obtained is provided in Table 5.6.

The statistical relationship between sediment properties and channel morphometric variables was considered significant under specific criteria, including Spearman rank correlation coefficient values (r_s) between 0.4 and 1, p-values between less than 0.01 and 0.05, and trend analysis (r^2) values between 0.5 and 1.

In the context of the Gatberg River system, the Spearman correlation within the channel bed samples revealed several significant findings (Table 5.6):

Strong Spearman's coefficient and p-values were observed between the geochemical elements measured and a few of the channel morphometric variables e.g. Iron and aluminium concentration with relative elevation (r_s -0.7; p-values < 0.05; $r^2 > 0.5$) and calcium concentration with average channel depth (r_s -0.7; p-values < 0.05; $r^2 > 0.5$).

Table 5.6 Results of the Spearman's correlation matrix showing the Spearman's coefficient, p-value and R^2 values (from top to bottom), to explore the relationships between sediment properties and the morphological and geometrical properties of the Gatberg channel bed samples. Significant relationships are highlighted in grey.

Independent variable	Dependent variable										
	D_{16} (µm)	D_{50} (µm)	D_{84} (µm)	Sand fraction (%)	Clay and silt fraction (%)	OMC (%)	TP (g kg^{-1})	Fe (g kg^{-1})	Al (g kg^{-1})	Mg (g kg^{-1})	Ca (g kg^{-1})
Distance downstream (m)	0.0	0.0	-0.4	-0.1	0.0	-0.1	0.0	0.6	0.4	0.4	0.2
Relative elevation (m.a.s.l)	0.2	0.2	0.5	0.0	-0.2	-0.1	-0.2	-0.7	-0.7	-0.6	-0.1
Channel morphological unit	0.2	0.0	0.0	0.0	-0.3	-0.3	-0.2	-0.6	-0.6	-0.6	
Bankfull depth (m)	-0.1	-0.2	-0.1	0.1	0.3	0.2	0.0	-0.1	0.0	-0.2	-0.4
Average depth (m)	0.1	0.1	0.2	0.1	-0.1	-0.2	0.0	-0.6	-0.2	-0.4	-0.7
Channel slope (%)	0.0	0.1	0.0	0.1	0.3	0.1	-0.1	-0.2	0.1	-0.1	0.2
Channel width (m)	0.1	-0.1	-0.1	0.3	0.0	-0.3	0.0	-0.6	-0.1	-0.4	-0.1
Channel width/ depth ratio	0.2	0.1	0.0	0.2	-0.3	-0.3	0.1	-0.5	0.0	-0.2	0.2
Channel area (m^2)	-0.2	-0.4	-0.3	0.3	0.5	0.2	0.2	-0.2	0.3	-0.1	0.1

Distance downstream (m)	0.42	0.46	0.01	0.28	0.46	0.37	0.46	0.02	0.07	0.10	0.33
Relative elevation (m.a.s.l)	0.15	0.08	0.001	0.47	0.18	0.30	0.27	0.004	0.002	0.02	
Channel morphological unit	0.18	0.44	0.39	0.41	0.03	0.03	0.20	0.01	0.01	0.02	
Bankfull depth (m)	0.21	0.17	0.23	0.36	0.05	0.19	0.49	0.39	0.48	0.21	0.10
Average depth (m)	0.22	0.27	0.10	0.28	0.24	0.14	0.50	0.02	0.28	0.06	0.02
Channel slope (%)	0.42	0.28	0.49	0.31	0.06	0.33	0.42	0.28	0.42	0.32	0.31
Channel width (m)	0.30	0.37	0.21	0.03	0.47	0.06	0.45	0.02	0.32	0.12	0.38
Channel width/ depth ratio	0.11	0.27	0.41	0.12	0.03	0.04	0.35	0.05	0.48	0.27	
Channel area (m^2)	0.11	0.01	0.03	0.06	0.003	0.09	0.20	0.23	0.15	0.39	0.38

Distance downstream (m)	0.0	0.0	0.1	0.0	0.0	0.0	0.0	0.3	0.2	0.1	0.0
Relative elevation (m.a.s.l)	0.0	0.1	0.3	0.0	0.0	0.0	0.0	0.5	0.6	0.3	0.0
Channel morphological unit	0.0	0.0	0.0	0.0	0.1	0.1	0.1	0.4	0.4	0.3	
Bankfull depth (m)	0.0	0.0	0.0	0.0	0.1	0.0	0.0	0.0	0.0	0.1	0.2
Average depth (m)	0.0	0.0	0.0	0.0	0.0	0.0	0.0	0.3	0.0	0.2	0.5
Channel slope (%)	0.0	0.0	0.0	0.0	0.1	0.0	0.0	0.0	0.0	0.0	0.0
Channel width (m)	0.0	0.0	0.0	0.1	0.0	0.1	0.0	0.3	0.0	0.1	0.0
Channel width/ depth ratio	0.0	0.0	0.0	0.0	0.1	0.1	0.0	0.2	0.0	0.0	0.1
Channel area (m^2)	0.1	0.2	0.1	0.1	0.2	0.1	0.1	0.1	0.1	0.0	0.0

The Spearman correlation analysis conducted within the channel bed samples of the Minnehaha River system revealed several significant relationships between sediment properties and channel morphometric variables, indicating strong or moderate positive or negative correlations at a statistically significant level (Table 5.7).

Strong Spearman's coefficient and p-values were observed between percentage gravel fraction and relative distance downstream (r_s -0.8; p-values < 0.05; $r^2 > 0.5$) and relative elevation (r_s 0.7; p-values < 0.05; $r^2 > 0.5$). Several other combinations had moderate correlations with strong p-values, however, the trend analysis revealed that these relationships were below r^2 0.5 indicating a poor trend relationship.

The Spearman correlation analysis conducted within the pebble bar samples in the channel of the Minnehaha River system revealed significant relationships between sediment particle sizes and channel morphometric variables, indicating very strong positive or negative correlations at a statistically significant level (Table 5.8).

Very strong Spearman's coefficient and p-values were observed between the sediment particle size of D_{16}, D_{50}, and D_{84} with the relative elevation of the channel bed ($r_s > -0.9$; p-values < 0.05; $r^2 > 0.5$) and relative elevation ($r_s > 0.9$; p-values < 0.05; $r^2 > 0.5$). Several other combinations had moderate correlations with strong p-values, however, the trend analysis revealed that these relationships were below r^2 0.5 indicating a poor trend relationship.

Table 5.7 Results of the Spearman's correlation matrix showing the Spearman's coefficient, p-value and R^2 values (from top to bottom), to explore the relationships between sediment properties and the morphological and geometrical properties of the Minnehaha channel bed samples. Significant relationships are highlighted in grey.

	Dependent variable												
Independent variable	**D_{16} (µm)**	**D_{50} (µm)**	**D_{84} (µm)**	**OMC (%)**	**Clay and silt fraction (%)**	**Sand fraction (%)**	**Gravel fraction (%)**	**TP (g kg^{-1})**	**Bioavailable phosphorus (g kg^{-1})**	**Fe (g kg^{-1})**	**Al (g kg^{-1})**	**Mg (g kg^{-1})**	**Ca (g kg^{-1})**
Distance downstream (m)	-0.4	-0.4	-0.5	0.4	0.3	0.5	-0.8	0.4	0.5	0.6	0.6	0.4	0.5
Relative elevation (m.a.s.l)	0.4	0.5	0.5	-0.4	-0.3	-0.5	0.7	-0.4	-0.5	-0.6	-0.5	-0.3	-0.4
Channel slope (%)	0.3	0.3	0.3	0.3	-0.2	-0.1	0.6	0.0	0.4	-0.5	0.2	0.0	0.2
Channel width (m)	0.3	0.2	0.2	0.0	-0.3	-0.1	0.1	-0.2	-0.1	-0.1	-0.5	-0.4	-0.1
Bankfull depth (m)	-0.1	-0.3	-0.5	-0.1	0.1	-0.1	0.2	0.0	-0.1	0.2	-0.5	-0.5	-0.4
Average depth (m)	-0.3	-0.5	-0.6	-0.2	0.3	-0.1	-0.3	0.0	-0.2	0.4	-0.4	-0.2	-0.2
Channel width/ depth ratio	0.4	0.5	0.6	0.2	-0.4	0.1	-0.3	-0.2	0.1	-0.3	0.2	0.1	0.3
Channel area (m²)	0.2	0.2	0.3	0.3	-0.2	0.4	-0.6	-0.4	0.1	-0.1	0.2	-0.4	0.0
Distance downstream (m)	0.08	0.07	0.06	0.08	0.14	0.05	0.04	0.09	0.03	0.01	0.02	0.08	0.06
Relative elevation (m.a.s.l)	0.09	0.06	0.05	0.09	0.16	0.06	0.06	0.06	0.04	0.01	0.05	0.13	0.10
Channel slope (%)	0.16	0.12	0.19	0.14	0.21	0.41	0.10	0.45	0.10	0.05	0.26	0.47	0.27
Channel width (m)	0.20	0.24	0.24	0.46	0.18	0.38	0.39	0.24	0.34	0.36	0.04	0.08	0.37
Bankfull depth (m)	0.31	0.16	0.06	0.33	0.34	0.35	0.35	0.48	0.41	0.21	0.03	0.05	0.10
Average depth (m)	0.13	0.06	0.02	0.25	0.14	0.34	0.31	0.44	0.29	0.10	0.09	0.29	0.24
Channel width/ depth ratio	0.09	0.05	0.01	0.24	0.09	0.34	0.31	0.24	0.41	0.14	0.31	0.38	0.13
Channel area (m²)	0.30	0.31	0.20	0.16	0.26	0.07	0.10	0.07	0.35	0.35	0.21	0.08	0.44
Distance downstream (m)	0.2	0.2	0.2	0.2	0.1	0.2	0.6	0.2	0.3	0.4	0.3	0.2	0.2
Relative elevation (m.a.s.l)	0.2	0.2	0.2	0.2	0.1	0.2	0.5	0.2	0.3	0.4	0.2	0.1	0.1
Channel slope (%)	0.0	0.0	0.0	0.0	0.0	0.0	0.3	0.0	0.1	0.2	0.1	0.0	0.0
Channel width (m)	0.1	0.0	0.0	0.0	0.1	0.0	0.0	0.0	0.0	0.0	0.3	0.2	0.0
Bankfull depth (m)	0.0	0.1	0.2	0.0	0.0	0.0	0.0	0.0	0.0	0.1	0.3	0.2	0.1
Average depth (m)	0.1	0.2	0.3	0.0	0.1	0.0	0.1	0.0	0.0	0.1	0.2	0.0	0.0
Channel width/ depth ratio	0.2	0.2	0.4	0.0	0.2	0.0	0.1	0.0	0.0	0.1	0.0	0.0	0.1
Channel area (m²)	0.0	0.0	0.1	0.1	0.0	0.2	0.4	0.2	0.0	0.0	0.1	0.2	0.0

Table 5.8 Results of the Spearman's correlation matrix showing the Spearman's coefficient, p-value and R^2 values (from top to bottom), to explore the relationships between sediment properties and the morphological and geometrical properties of the Minnehaha pebble bar samples in the channel. Significant relationships are highlighted in grey.

Independent variable	Dependent variable			
	D_{16} (µm)	D_{50} (µm)	D_{84} (µm)	Gravel fraction (%)
Distance downstream (m)	-0.98	-0.96	-0.92	-0.52
Relative elevation (m.a.s.l)	0.98	0.96	0.92	0.52
Channel slope (%)	0.04	0.07	0.19	-0.06
Channel width (m)	0.41	0.41	0.44	0.06
Bankfull depth (m)	0.10	0.12	0.02	
Average depth (m)	0.02	0.07	-0.05	
Channel width/ depth ratio	0.29	0.19	0.31	
Channel area (m^2)	-0.64	-0.52	-0.50	
Distance downstream (m)	0.00	0.00	0.00	0.06
Relative elevation (m.a.s.l)	0.00	0.00	0.00	0.06
Channel slope (%)	0.45	0.43	0.30	0.44
Channel width (m)	0.12	0.12	0.10	0.44
Bankfull depth (m)	0.41	0.39	0.48	
Average depth (m)	0.48	0.43	0.46	
Channel width/ depth ratio	0.25	0.33	0.23	
Channel area (m^2)	0.04	0.09	0.10	
Distance downstream (m)	1.0	0.9	0.9	0.3
Relative elevation (m.a.s.l)	1.0	0.9	0.9	0.3
Channel slope (%)	0.0	0.0	0.0	0.0
Channel width (m)	0.2	0.2	0.2	0.0
Bankfull depth (m)	0.0	0.0	0.0	
Average depth (m)	0.0	0.0	0.0	
Channel width/ depth ratio	0.1	0.0	0.1	
Channel area (m^2)	0.4	0.3	0.3	

Relationships between sediment properties

Spearman's correlation analysis within the channel bed samples of the Gatberg River system revealed significant relationships between sediment properties, indicating strong or moderate positive or negative correlations at a statistically significant level (Table 5.9).

Strong Spearman's coefficient and p-values were observed between iron concentrations and all the independent variables (r_s > ±0.7 and < ± 0.8; p-values < 0.05; r^2 > 0.5) and between aluminium concentration and percentage organic matter content (r_s = 0.8; p-values < 0.05; r^2 > 0.5). Several other combinations had moderate correlations with strong p-values, however, the trend analysis revealed that these relationships were below r^2 0.5 indicating a poor trend relationship.

Table 5.9 Results of the Spearman's correlation matrix showing the Spearman's coefficient, p-value and R^2 values (from top to bottom), to explore the relationships between sediment properties of the Gatberg channel bed samples. Significant relationships are highlighted in grey.

Independent variable	Dependent variable					
	OMC (%)	TP (g kg^{-1})	Fe (g kg^{-1})	Al (g kg^{-1})	Mg (g kg^{-1})	Ca (g kg^{-1})
D_{16} (µm)	-0.4	-0.2	-0.8	-0.4	-0.4	-0.3
D_{50} (µm)			-0.8			
D_{84} (µm)	-0.1	-0.1	-0.8	-0.3	-0.2	-0.3
Sand fraction (%)	-0.3	-0.1	-0.7	-0.2	-0.3	-0.1
Clay and silt fraction (%)	0.5	0.2	0.8	0.3	0.5	0.4
OMC (%)		0.2	0.8	0.7	0.5	0.2
D_{16} (µm)	0.01	0.26	0.00	0.11	0.06	0.20
D_{50} (µm)	0.10	0.43	0.00	0.14	0.16	0.24
D_{84} (µm)	0.22	0.42	0.00	0.19	0.30	0.22
Sand fraction (%)	0.02	0.38	0.00	0.27	0.13	0.42
Clay and silt fraction (%)	0.00	0.25	0.00	0.12	0.04	0.13
OMC (%)		0.21	0.00	0.00	0.04	0.28
D_{16} (µm)			0.7		0.2	
D_{50} (µm)			0.7			
D_{84} (µm)	0.0	0.0	0.6	0.1	0.0	0.1
Sand fraction (%)	0.1	0.0	0.5	0.0	0.1	0.0
Clay and silt fraction (%)	0.2	0.0	0.7	0.1	0.3	0.2
OMC (%)		0.1	0.6	0.5	0.3	0.0

The Spearman correlation analysis within channel bed samples of the Minnehaha River system revealed significant relationships between sediment properties, indicating strong or moderate positive or negative correlations at a statistically significant level (Table 5.10).

Strong positive Spearman's coefficient and p-values were observed between bioavailable phosphorus and calcium concentration with percentage organic matter content (r_s = 8; p-values < 0.05; r^2 > 0.5); iron concentration with percentage clay and silt fractions (r_s = 0.8; p-values < 0.05; r^2 > 0.5); and between aluminium concentration with percentage organic matter content (r_s = 0.7; p-values < 0.05; r^2 > 0.5). Strong negative Spearman's coefficient and p-values were observed between iron concentration and D_{16},

D_{50}, D_{84} sediment particle size (r_s > -0.7 and < -0.8; p-values < 0.05; r^2 > 0.5). Several other combinations had moderate correlations with strong p-values, however, the trend analysis revealed that these relationships were below r^2 0.5 indicating a poor trend relationship.

Table 5.10 Results of the Spearman's correlation matrix showing the Spearman's coefficient, p-value and R^2 values (from top to bottom), to explore the relationships between sediment properties of the Minnehaha channel bed samples. Significant relationships are highlighted in grey.

Independent variable	Dependent variable						
	OMC (%)	TP (g kg^{-1})	Bioavailable phosphorus (g kg^{-1})	Fe (g kg^{-1})	Al (g kg^{-1})	Mg (g kg^{-1})	Ca (g kg^{-1})
D_{16} (µm)	0.1	0.0	0.1	-0.8	-0.1	-0.4	0.0
D_{50} (µm)	0.1	0.0	0.0	-0.8	-0.1	-0.2	0.2
D_{84} (µm)	0.3	0.1	0.0	-0.7	0.1	0.0	0.4
OMC (%)		0.3	0.8	0.0	0.7	0.1	0.7
Clay and silt fraction (%)	-0.1	0.0	-0.2	0.8	0.1	0.4	-0.1
Sand fraction (%)	-0.4	-0.2	0.6	-0.1	0.6	-0.2	0.2
D_{16} (µm)	0.39	0.49	0.34	0.00	0.35	0.07	0.46
D_{50} (µm)	0.38	0.47	0.46	0.00	0.40	0.30	0.21
D_{84} (µm)	0.20	0.39	0.46	0.00	0.42	0.46	0.09
OMC (%)		0.15	0.00	0.49	0.00	0.34	0.01
Clay and silt fraction (%)	0.35	0.44	0.30	0.00	0.35	0.09	0.43
Sand fraction (%)	0.12	0.29	0.01	0.34	0.02	0.21	0.28
D_{16} (µm)	0.0	0.0	0.0	0.7	0.0	0.2	0.0
D_{50} (µm)	0.0	0.0	0.0	0.7	0.0	0.0	0.1
D_{84} (µm)	0.1	0.0	0.0	0.5	0.0	0.0	0.2
OMC (%)		0.1	0.6	0.0	0.5	0.0	0.4
Clay and silt fraction (%)	0.0	0.0	0.0	0.6	0.0	0.2	0.0
Sand fraction (%)	0.1	0.0	0.4	0.0	0.4	0.1	0.0

Relationships between total phosphorus and geochemical properties

Spearman correlation analysis within the channel bed samples of the Gatberg River system revealed a significant relationship between total phosphorus concentration and aluminium concentration, indicating a strong positive correlation at a statistically significant level (r_s = 0.7; p-values < 0.05; r^2 > 0.5). Total phosphorus concentration had moderate Spearman's coefficients however, both the p-values (> 0.05) and the trend analysis revealed that these relationships were below r^2 0.5 indicating a poor trend relationship (Table 5.11).

Table 5.11 Results of the Spearman's correlation matrix showing the Spearman's coefficient, p-value and R^2 values (from top to bottom), to explore the relationships between total phosphorus content and the measured geochemical elements of the Gatberg channel bed samples. Significant relationships are highlighted in grey.

Independent variable	Dependent variable TP (g kg^{-1})
Fe (g kg^{-1})	0.5
Al (g kg^{-1})	0.7
Mg (g kg^{-1})	0.5
Ca (g kg^{-1})	-0.1
Fe (g kg^{-1})	0.07
Al (g kg^{-1})	0.01
Mg (g kg^{-1})	0.06
Ca (g kg^{-1})	0.41
Fe (g kg^{-1})	0.2
Al (g kg^{-1})	0.5
Mg (g kg^{-1})	0.2
Ca (g kg^{-1})	0.0

Spearman correlation analysis within the channel bed samples of the Minnehaha River system revealed a moderate positive correlation between total phosphorus concentration and magnesium concentration (r_s = 0.5), however, both the p-values (> 0.05) and the trend analysis revealed that these relationships were below r^2 0.5 indicating a poor trend relationship (Table 5.12).

Table 5.12 Results of the Spearman's correlation matrix showing the Spearman's coefficient, p-value and R^2 values (from top to bottom), to explore the relationships between total phosphorus content and the measured geochemical elements of the Minnehaha channel bed samples. Significant relationships are highlighted in grey.

Independent variable	Dependent variable TP (g kg^{-1})
Bioavailable phosphorus (g kg^{-1})	0.4
Fe (g kg^{-1})	0.2
Al (g kg^{-1})	0.1
Mg (g kg^{-1})	0.5
Ca (g kg^{-1})	0.4
Bioavailable phosphorus (g kg^{-1})	0.11
Fe (g kg^{-1})	0.31
Al (g kg^{-1})	0.35
Mg (g kg^{-1})	0.06
Ca (g kg^{-1})	0.10
Bioavailable phosphorus (g kg^{-1})	0.1
Fe (g kg^{-1})	0.0
Al (g kg^{-1})	0.0
Mg (g kg^{-1})	0.2
Ca (g kg^{-1})	0.1

II. Channel-bank (cut bank) material

During the study period along the Gatberg River, the distribution of the D_{50} particle size of the cut bank material ranged from medium silt to medium sand, spanning 16 to 309 µm, with an average of 135 µm. Most of the particle size distributions were unimodal. The D_{84} particle sizes ranged from coarse silt to coarse sand, varying between 45 to 727 µm, with an average of 397 µm. Similarly, the D_{16} particle sizes ranged from clay to fine sand, with diameters ranging from 2 to 128 µm, with an average of 38 µm.

The cut banks exhibited an average percentage of clay and silt fraction of 38 %, indicating a significant proportion of fine-grained sediment. Additionally, the cut bank material contained an average organic matter content of 4 % and a total phosphorus concentration of 0.06 g kg^{-1}.

The Spearman correlation analysis within the channel bank (cut-bank) samples of the Gatberg River system revealed significant relationships between sediment properties and channel morphometric variables, indicating strong positive correlations at a statistically significant level (Table 5.13).

Strong positive Spearman's coefficient and p-values were observed between D_{16} sediment particle size and channel bankfull area (r_s = 0.7; p-values < 0.05; r^2 > 0.5), and bioavailable phosphorus with average channel bed slope (r_s = 0.8; p-values < 0.05; r^2 > 0.5). Several other combinations had moderate correlations with strong p-values, however, the trend analysis revealed that these relationships were below r^2 0.5 indicating a poor trend relationship.

Table 5.13 Results of the Spearman's correlation matrix showing the Spearman's coefficient, p-value and R^2 values (from top to bottom), to explore the relationships between sediment properties and the morphological and geometrical properties of the Gatberg cut-bank samples. Significant relationships are highlighted in grey.

Independent variable	Dependent variable											
	D_{16} (µm)	D_{50} (µm)	D_{84} (µm)	OMC (%)	Sand fraction (%)	Clay and silt fraction (%)	TP (g kg^{-1})	Bioavailable phosphorus (g kg^{-1})	Fe (g kg^{-1})	Al (g kg^{-1})	Mg (g kg^{-1})	Ca (g kg^{-1})
Distance downstream (m)	-0.2	-0.1	-0.1	0.1	-0.1	0.1	-0.3	-0.4	-0.2	-0.3	0.2	-0.1
Relative elevation (m.a.s.l)	0.1	0.0	0.0	-0.1	0.1	-0.1	0.4	0.2	-0.1	0.4	-0.1	0.2
Bankfull depth (m)	0.5	0.3	0.2	0.0	0.4	-0.4	0.1	-0.7	0.0	0.3	-0.2	0.0
Average depth (m)	0.0	0.0	-0.1	0.0	0.1	-0.1	0.0	0.2	-0.3	0.0	-0.1	0.0
Channel slope (%)	0.2	0.3	0.3	0.0	0.1	-0.1	-0.2	0.8	-0.1	0.2	0.0	0.1
Channel width (m)	0.2	0.1	0.0	0.1	0.1	-0.1	0.1	0.2	0.1	0.0	-0.3	-0.1
Channel width/ depth ratio	-0.3	-0.3	-0.3	0.0	-0.3	0.3	0.1	0.6	0.2	-0.4	-0.4	-0.5
Channel area (m^2)	0.7	0.6	0.5	-0.2	0.6	-0.6	0.3	0.2	0.0	0.5	-0.3	-0.3
Distance downstream (m)	0.17	0.33	0.34	0.31	0.36	0.36	0.13	0.25	0.23	0.15	0.26	0.36
Relative elevation (m.a.s.l)	0.36	0.48	0.48	0.41	0.36	0.36	0.05	0.40	0.31	0.07	0.32	0.30
Bankfull depth (m)	0.02	0.08	0.21	0.42	0.05	0.05	0.32	0.11	0.45	0.11	0.21	0.48
Average depth (m)	0.45	0.47	0.39	0.49	0.37	0.37	0.45	0.40	0.17	0.49	0.32	0.48
Channel slope (%)	0.20	0.15	0.13	0.49	0.32	0.32	0.20	0.04	0.36	0.24	0.44	0.39
Channel width (m)	0.20	0.29	0.45	0.40	0.31	0.31	0.41	0.37	0.43	0.47	0.14	0.40
Channel width/ depth ratio	0.10	0.12	0.12	0.47	0.14	0.14	0.42	0.16	0.20	0.04	0.07	0.07
Channel area (m^2)	0.00	0.01	0.02	0.25	0.00	0.00	0.09	0.37	0.47	0.02	0.16	0.18
Distance downstream (m)	0.1	0.0	0.0	0.0	0.0	0.0	0.1	0.2	0.0	0.1	0.0	0.0
Relative elevation (m.a.s.l)	0.0	0.0	0.0	0.0	0.0	0.0	0.2	0.0	0.0	0.1	0.0	0.0
Bankfull depth (m)	0.2	0.1	0.0	0.0	0.2	0.2	0.0	0.4	0.0	0.1	0.1	0.0
Average depth (m)	0.0	0.0	0.0	0.0	0.0	0.0	0.0	0.0	0.1	0.0	0.0	0.0
Channel slope (%)	0.0	0.1	0.1	0.0	0.0	0.0	0.0	0.7	0.0	0.0	0.0	0.0
Channel width (m)	0.0	0.0	0.0	0.0	0.0	0.0	0.0	0.0	0.0	0.0	0.1	0.0
Channel width/ depth ratio	0.1	0.1	0.1	0.0	0.1	0.1	0.0	0.3	0.1	0.2	0.2	0.2
Channel area (m^2)	0.5	0.3	0.2	0.0	0.4	0.4	0.1	0.0	0.0	0.3	0.1	0.1

During the study period along the Minnehaha River, the distribution of the D_{50} particle size of the cut bank material ranged from medium silt to medium sand, spanning 18 to 271 µm, with an average of 115 µm. Most of the particle size distributions were unimodal. The D_{84} particle sizes ranged from coarse silt to very coarse sand, varying between 48 and 1504 µm, with an average of 448 µm. Similarly, the D_{16} particle sizes ranged from clay to very fine sand, with diameters ranging from 4 to 74 µm, with an average of 36 µm.

The cut banks exhibited an average percentage of clay and silt fraction of 42 %, indicating a significant proportion of fine-grained sediment. Additionally, the cut bank material contained an average organic matter content of 5 % and a total phosphorus concentration of 0.07 g kg^{-1}.

The Spearman correlation analysis within the channel bank (cut-bank) samples of the Minnehaha River system revealed significant relationships between sediment properties and channel morphometric variables, indicating strong negative, moderate positive, and moderate negative correlations at a statistically significant level (Table 5.14).

There was a strong negative Spearman's coefficient and p-values between D_{50} sediment particle size and both channel bankfull depth (r_s = -0.8; p-values < 0.05; r^2 > 0.5), and channel average depth (r_s = -0.7; p-values < 0.05; r^2 < 0.5); and both channel bankfull depth (r_s = -0.8; p-values < 0.05; r^2 > 0.5), and channel average depth (r_s = -0.7; p-values < 0.05; r^2 < 0.5). Several other combinations had moderate correlations with strong p-values, however, the trend analysis revealed that these relationships were below r^2 0.5 indicating a poor trend relationship.

However, the only variability within the sediment properties that the channel morphometrics could explain according to a trend analysis was between D_{50} and D_{84} sediment particle size and channel bankfull depth (r^2 > 0.5).

Table 5.14 Results of the Spearman's correlation matrix showing the Spearman's coefficient, p-value and R^2 values (from top to bottom), to explore the relationships between sediment properties and the morphological and geometrical properties of the Minnehaha cut-bank samples. Significant relationships are highlighted in grey.

Independent variable	Dependent variable											
	D_{16} (µm)	D_{50} (µm)	D_{84} (µm)	OMC (%)	Clay and silt fraction (%)	Sand fraction (%)	TP (g kg^{-1})	Bioavailable phosphorus (g kg^{-1})	Fe (g kg^{-1})	Al (g kg^{-1})	Mg (g kg^{-1})	Ca (g kg^{-1})
Distance downstream (m)	0.2	0.1	-0.1	0.3	-0.1	0.4	0.0	0.0	0.3	-0.2	0.3	0.3
Relative elevation (m.a.s.l)	-0.1	0.0	0.2	-0.3	0.1	-0.3	-0.1	0.0	-0.3	0.2	-0.2	-0.2
Channel slope (%)	-0.2	0.1	0.2	0.1	0.2	-0.2	0.3	0.1	0.0	0.2	0.1	0.5
Channel width (m)	-0.3	-0.4	-0.1	0.2	0.2	-0.2	0.4	0.5	0.2	0.0	-0.3	-0.2
Bankfull depth (m)	-0.6	-0.8	-0.8	0.2	0.6	-0.5	0.6	0.5	0.6	-0.4	0.0	-0.1
Average depth (m)	-0.5	-0.7	-0.7	0.0	0.4	-0.3	0.2	0.1	0.4	-0.4	0.1	-0.2
Channel width/ depth ratio	0.4	0.5	0.7	0.2	-0.4	0.4	-0.2	0.1	-0.5	0.5	-0.2	0.1
Channel area (m^2	0.3	0.2	0.2	0.1	-0.3	0.5	0.0	0.1	-0.3	0.5	-0.2	-0.1
Distance downstream (m)	0.26	0.43	0.33	0.17	0.32	0.11	0.47	0.45	0.17	0.31	0.18	0.18
Relative elevation (m.a.s.l)	0.32	0.46	0.25	0.20	0.38	0.16	0.40	0.48	0.14	0.22	0.22	0.22
Channel slope (%)	0.30	0.32	0.22	0.39	0.28	0.23	0.20	0.31	0.44	0.26	0.40	0.05
Channel width (m)	0.19	0.10	0.35	0.28	0.24	0.25	0.10	0.03	0.26	0.49	0.20	0.29
Bankfull depth (m)	0.01	0.00	0.00	0.30	0.02	0.05	0.02	0.05	0.01	0.07	0.48	0.36
Average depth (m)	0.05	0.01	0.01	0.44	0.08	0.19	0.24	0.34	0.09	0.11	0.31	0.22
Channel width/ depth ratio	0.09	0.05	0.01	0.31	0.08	0.11	0.23	0.37	0.06	0.06	0.29	0.42
Channel area (m^2	0.16	0.23	0.23	0.36	0.13	0.03	0.47	0.31	0.12	0.03	0.22	0.34
Distance downstream (m)	0.0	0.0	0.0	0.1	0.0	0.1	0.0	0.0	0.1	0.0	0.1	0.1
Relative elevation (m.a.s.l)	0.0	0.0	0.0	0.1	0.0	0.1	0.0	0.0	0.1	0.1	0.1	0.1
Channel slope (%)	0.0	0.0	0.1	0.0	0.0	0.1	0.1	0.0	0.0	0.0	0.0	0.2
Channel width (m)	0.1	0.1	0.0	0.0	0.0	0.0	0.1	0.3	0.0	0.0	0.1	0.0
Bankfull depth (m)	0.4	0.7	0.6	0.0	0.3	0.2	0.3	0.2	0.4	0.2	0.0	0.0
Average depth (m)	0.2	0.4	0.4	0.0	0.2	0.1	0.0	0.0	0.2	0.1	0.0	0.1
Channel width/ depth ratio	0.2	0.2	0.4	0.0	0.2	0.1	0.0	0.0	0.2	0.2	0.0	0.0
Channel area (m^2	0.1	0.1	0.0	0.0	0.1	0.3	0.0	0.0	0.1	0.3	0.1	0.0

Relationships between sediment properties

The Spearman correlation analysis within the channel bank (cut-bank) samples of the Gatberg River system revealed significant relationships between sediment properties, indicating strong positive, strong negative, moderate positive, and moderate negative correlations at a statistically significant level (Table 5.15).

There was a strong positive Spearman's coefficient and p-values between bioavailable phosphorus and D_{84} sediment particle size ($r_s = 0.7$; $r^2 = 0.5$); aluminium concentration and various sediment particle sizes, including D_{16}, D_{50}, and D_{84}, as well as the percentage sand fraction ($r_s > 0.7$ and < 0.8; p-values < 0.05; $r^2 > 0.5$), and between magnesium concentrations and percentage of organic matter content ($r_s > 0.7$ and < 0.8; p-values < 0.05; $r^2 < 0.5$). A strong negative correlation was observed between aluminium concentration and the percentage of clay and silt fraction ($r_s > -0.7$; p-values < 0.05; $r^2 > 0.5$).

However, the only variability within the sediment properties that the other sediment properties could explain according to a trend analysis was between bioavailable phosphorus and D_{84} sediment particle size ($r^2 = > 0.5$), and aluminium concentration with the various sediment particle sizes, as well as the percentage sand and clay and silt fraction ($r^2 = > 0.5$). This suggests that sediment particle size and composition characteristics play a significant role in determining aluminium concentration within the Gatberg River system.

Table 5.15 Results of the Spearman's correlation matrix showing the Spearman's coefficient, p-value and R^2 values (from top to bottom), to explore the relationships between sediment properties of the Gatberg cut-bank samples. Significant relationships are highlighted in grey.

	Dependent variable						
Independent variable	**OMC (%)**	**TP (g kg^{-1})**	**Bioavailable phosphorus (g kg^{-1})**	**Fe (g kg^{-1})**	**Al (g kg^{-1})**	**Mg (g kg^{-1})**	**Ca (g kg^{-1})**
D_{16} (µm)	0,0	0,0	0,6	-0,4	0,7	0,2	-0,1
D_{50} (µm)	0,0	-0,1	0,6	-0,4	0,8	0,3	0,0
D_{84} (µm)	0,0	-0,1	0,7	-0,5	0,8	0,4	0,1
Sand fraction (%)	-0,1	0,0	0,4	-0,4	0,7	0,1	-0,2
Clay and silt fraction (%)	0,1	0,0	-0,4	0,4	-0,7	-0,1	0,2
OMC (%)	-0,1		0,1	-0,3	0,2	0,7	0,6
D_{16} (µm)	0,47	0,45	0,16	0,11	0,00	0,29	0,38
D_{50} (µm)	0,48	0,39	0,16	0,08	0,00	0,16	0,50
D_{84} (µm)	0,50	0,28	0,09	0,05	0,00	0,07	0,37
Sand fraction (%)	0,31	0,44	0,26	0,10	0,00	0,34	0,26
Clay and silt fraction (%)	0,31	0,44	0,26	0,10	0,00	0,34	0,26
OMC (%)	0,32		0,47	0,14	0,20	0,00	0,04
D_{16} (µm)	0,0	0,0	0,3	0,1	0,6	0,0	0,0
D_{50} (µm)	0,0	0,0	0,3	0,2	0,6	0,1	0,0
D_{84} (µm)	0,0	0,0	0,5	0,2	0,6	0,2	0,0
Sand fraction (%)	0,0	0,0	0,2	0,1	0,5	0,0	0,1
Clay and silt fraction (%)	0,0	0,0	0,2	0,1	0,5	0,0	0,1
OMC (%)	0,0		0,0	0,1	0,0	0,4	0,3

The Spearman correlation analysis within the channel bank (cut-bank) samples of the Minnehaha River system revealed significant relationships between sediment properties, indicating strong positive, strong negative, moderate positive, and moderate negative correlations at a statistically significant level (Table 5.16).

There was a strong positive Spearman's coefficient and p-values between iron concentration and percentage clay and silt fractions (r_s = 0.7; p-values < 0.05; r^2 = 0.5); aluminium concentration with D_{84} sediment particle size (r_s = 0.8; p-values < 0.05; r^2 > 0.5), and between calcium concentration with percentage organic matter content (r_s = 0.7; p-values < 0.05; r^2 = 0.5). A strong negative correlation was observed between iron concentration and sediment particle sizes, including D_{16}, D_{50}, and D_{84} (r_s = -0.7; p-values < 0.05; r^2 = 0.5). Several other combinations showed moderate correlations with strong p-values, but the trend analysis indicated that these relationships had r^2 values below 0.5, suggesting a weak trend connection.

Table 5.16 Results of the Spearman's correlation matrix showing the Spearman's coefficient, p-value and R^2 values (from top to bottom), to explore the relationships between sediment properties of the Minnehaha cut-bank samples. Significant relationships are highlighted in grey.

	Dependent variable						
Independent variable	**OMC (%)**	**TP (g kg^{-1})**	**Bioavailable phosphorus (g kg^{-1})**	**Fe (g kg^{-1})**	**Al (g kg^{-1})**	**Mg (g kg^{-1})**	**Ca (g kg^{-1})**
D_{16} (µm)	-0.1	-0.4	-0.4	-0.7	0.4	-0.1	0.1
D_{50} (µm)	-0.1	-0.5	-0.5	-0.7	0.6	0.0	0.2
D_{84} (µm)	-0.1	-0.3	-0.2	-0.7	0.8	0.0	0.4
Clay and silt fraction (%)	0.1	0.4	0.4	0.7	-0.4	0.1	-0.1
Sand fraction (%)	0.2	-0.3	-0.3	-0.5	0.5	0.1	0.3
OMC (%)		0.3	0.5	0.4	0.0	0.6	0.7
D_{16} (µm)	0.39	0.07	0.08	0.00	0.08	0.37	0.31
D_{50} (µm)	0.36	0.06	0.06	0.00	0.01	0.44	0.22
D_{84} (µm)	0.40	0.18	0.23	0.00	0.00	0.49	0.11
Clay and silt fraction (%)	0.41	0.08	0.09	0.01	0.07	0.37	0.32
Sand fraction (%)	0.27	0.16	0.17	0.03	0.03	0.37	0.20
OMC (%)		0.18	0.04	0.08	0.46	0.02	0.00
D_{16} (µm)	0.0	0.2	0.2	0.5	0.2	0.0	0.0
D_{50} (µm)	0.0	0.2	0.2	0.5	0.4	0.0	0.1
D_{84} (µm)	0.0	0.1	0.1	0.5	0.6	0.0	0.1
Clay and silt fraction (%)	0.0	0.2	0.2	0.5	0.2	0.0	0.0
Sand fraction (%)	0.0	0.1	0.1	0.3	0.3	0.0	0.1
OMC (%)		0.1	0.3	0.2	0.0	0.4	0.5

Relationships between total phosphorus and geochemical properties

The Spearman correlation analysis within the channel bank (cut-bank) samples of the Gatberg River system revealed significant relationships between total phosphorus concentration and geochemical sediment properties, particularly with iron concentration.

A strong positive correlation existed between total phosphorus concentration and iron concentration (Spearman's $\rho = 0.7$, $p = 0.01$).

The results of the Spearman correlation within the channel bank (cut-bank) samples did not show correlations between the concentration of total phosphorus and the geochemical properties of the Minnehaha River system sediment.

III. Point bar material

During the study period along the Gatberg River, the point bar material exhibited a range of particle sizes, with associated distributions indicative of varying sediment compositions. D_{50} particle size ranged from fine silt to coarse sand, with sizes spanning 12 to 565 µm (average diameter= 184 µm). Most of the distributions were unimodal, suggesting a predominant size class within the sampled material. The size of the D_{84} particles ranged from coarse silt to very coarse sand, with sizes ranging from 51 to 1424 µm (average 429 µm). This further illustrates the variability in sediment size within the point bar material. The particle size of D_{16} ranged from clay to fine sand, with sizes varying from 2 to 227 µm (average 76 µm). This indicates the presence of finer sediment fractions in addition to coarser particles. The average percentage of clay and silt fraction was 33 %, suggesting a significant proportion of fine-grained material within the point bar samples. The organic matter content of the samples was 3 %. The total phosphorus concentration observed in the samples was 0.06 g kg^{-1}, reflecting the phosphorus level within the point bar material.

The Spearman correlation within the point bar (depositing bank) samples of the Gatberg River system revealed significant relationships between sediment properties and channel morphometrics (Table 5.17).

There was a very strong positive Spearman's coefficient and p-values between D_{16} and D_{84} sediment particle size with bankfull area ($r_s = 0.9$; p-values < 0.05; $r^2 > 0.5$); and organic matter content with average distance downstream ($r_s = 0.9$; p-values < 0.05; $r^2 > 0.5$). A very strong negative correlation was observed between organic matter content with bankfull area ($r_s = -0.9$; p-values < 0.05; $r^2 = 0.5$); and between iron concentration with average channel depth ($r_s = -0.9$; p-values < 0.05; $r^2 = 0.5$). A strong positive correlation was detected between D_{50} sediment particle sizes and the sand fraction with channel bankfull area ($r_s = 0.8$; p-values < 0.05; $r^2 = 0.5$); total phosphorus concentrations with relative distance downstream ($r_s = 0.8$; p-values < 0.05; $r^2 = 0.5$); and calcium concentrations with relative distance downstream ($r_s = 0.7$; p-values < 0.05; $r^2 = 0.5$). A strong negative correlation was detected between D_{16}, D_{84} sediment particle sizes and relative distance downstream ($r_s = -0.7$; p-values < 0.05; $r^2 = 0.5$); between the percentage organic matter content, total phosphorus, bioavailable phosphorus and calcium with relative elevation (r_s

between -0.7 and -0.8; p-values < 0.05; $r^2 = 0.5$); between clay and silt fraction, bioavailable phosphorus and iron concentrations with channel bankfull area ($r_s = -0.8$; p-values < 0.05; $r^2 = 0.5$); between iron concentrations with channel width and channel width/ depth ration ($r_s = -0.8$; p-values < 0.05; $r^2 = 0.5$); and calcium concentration with average channel depth ($r_s = -0.7$; p-values < 0.05; $r^2 = 0.5$). Several other combinations showed moderate correlations with strong p-values, but the trend analysis indicated that these relationships had r^2 values below 0.5, suggesting a weak trend connection.

Table 5.17 Results of the Spearman's correlation matrix showing the Spearman's coefficient, p-value and R^2 values (from top to bottom), to explore the relationships between sediment properties and the morphological and geometrical properties of the Gatberg point bar samples. Significant relationships are highlighted in grey.

Independent variable	Dependent variable											
	D_{16} (µm)	D_{50} (µm)	D_{84} (µm)	OMC (%)	Sand fraction (%)	Clay and silt fraction (%)	TP (g kg^{-1})	Bioavailable phosphorus (g kg^{-1})	Fe (g kg^{-1})	Al (g kg^{-1})	Mg (g kg^{-1})	Ca (g kg^{-1})
Distance downstream (m)	-0.7	-0.8	-0.7	0.9	-0.6	0.6	0.8	0.6	0.6	0.6	0.6	0.7
Relative elevation (m.a.s.l)	0.6	0.6	0.6	-0.8	0.6	-0.6	-0.8	-0.7	-0.3	-0.5	-0.4	-0.7
Bankfull depth (m)	0.4	0.3	0.3	-0.4	0.2	-0.2	-0.5	-0.1	-0.4	-0.3	-0.1	-0.1
Average depth (m)	0.4	0.3	0.4	-0.3	0.3	-0.3	-0.5	-0.5	-0.9	-0.4	-0.6	-0.7
Channel slope (%)	0.4	0.4	0.4	-0.2	0.6	-0.6	0.1	0.3	-0.6	0.1	-0.6	0.1
Channel width (m)	0.5	0.4	0.5	-0.4	0.5	-0.5	-0.4	-0.5	-0.8	-0.2	-0.5	-0.2
Channel width/ depth ratio	0.0	-0.1	0.2	0.0	0.1	-0.1	-0.1	-0.6	-0.8	0.0	-0.5	-0.4
Channel area (m^2)	0.9	0.8	0.9	-0.9	0.8	-0.8	-0.5	-0.8	-0.8	-0.2	-0.6	-0.4
Distance downstream (m)	0.00	0.00	0.00	0.00	0.00	0.00	0.00	0.03	0.03	0.01	0.02	0.01
Relative elevation (m.a.s.l)	0.01	0.00	0.01	0.00	0.01	0.01	0.00	0.02	0.19	0.02	0.06	0.02
Bankfull depth (m)	0.06	0.09	0.15	0.06	0.20	0.23	0.03	0.38	0.08	0.11	0.43	0.44
Average depth (m)	0.09	0.11	0.07	0.17	0.11	0.11	0.02	0.08	0.00	0.05	0.01	0.02
Channel slope (%)	0.04	0.05	0.05	0.24	0.01	0.01	0.32	0.18	0.02	0.37	0.02	0.43
Channel width (m)	0.03	0.07	0.02	0.07	0.04	0.04	0.05	0.11	0.00	0.25	0.06	0.26
Channel width/ depth ratio	0.47	0.42	0.24	0.45	0.33	0.32	0.33	0.05	0.00	0.48	0.04	0.15
Channel area (m^2)	0.00	0.00	0.00	0.00	0.00	0.00	0.02	0.01	0.00	0.21	0.02	0.14
Distance downstream (m)	0.5	0.6	0.5	0.8	0.4	0.4	0.7	0.4	0.3	0.3	0.3	0.5
Relative elevation (m.a.s.l)	0.4	0.4	0.4	0.6	0.3	0.3	0.6	0.5	0.1	0.3	0.2	0.5
Bankfull depth (m)	0.2	0.1	0.1	0.2	0.1	0.0	0.2	0.0	0.2	0.1	0.0	0.0
Average depth (m)	0.1	0.1	0.1	0.1	0.1	0.1	0.3	0.3	0.7	0.2	0.4	0.5
Channel slope (%)	0.2	0.2	0.2	0.0	0.3	0.3	0.0	0.1	0.3	0.0	0.3	0.0
Channel width (m)	0.2	0.1	0.3	0.1	0.2	0.2	0.2	0.2	0.7	0.0	0.2	0.1
Channel width/ depth ratio	0.0	0.0	0.0	0.0	0.0	0.0	0.0	0.3	0.6	0.0	0.2	0.2
Channel area (m^2)	0.7	0.7	0.8	0.7	0.7	0.7	0.3	0.6	0.7	0.0	0.3	0.2

The distribution of the D_{50} particle size of the point bar material along the Minnehaha River during the period of study ranged from medium silt to very coarse sand (27 to 1003 µm), with an average of 180 µm. Most of the particle size distributions were unimodal. The D_{84} particle sizes ranged from 61 to 6630 µm (coarse silt to pebbles), with an average of 784 µm. The D_{16} particle sizes ranged from 7 to 467 µm (very fine silt to medium sand), with an average of 70 µm. The point bars had an average percentage of clay and silt fraction of 39 %, a content of organic matter of 3 % and a total phosphorus concentration of 0.08 g kg^{-1}.

The Spearman correlation within the point bar (depositing bank) samples of the Minnehaha River system unveiled significant relationships between sediment properties and channel morphometrics (Table 5.18).

There was a strong positive Spearman's coefficient and p-values between iron concentration and percentage clay and silt fractions with average channel depth (r_s = 0.8; p-values < 0.05; r^2 = 0.5); and between aluminium concentration with channel width/ depth ratio (r_s = 0.7; p-values < 0.05; r^2 > 0.5). A strong negative correlation was observed between sediment particle sizes, including D_{16}, D_{50}, and D_{84} and average channel depth (r_s = -0.8; p-values < 0.05; r^2 = 0.5); and between aluminium concentrations and average channel depth (r_s = -0.7; p-values < 0.05; r^2 = 0.5). Several other combinations showed moderate correlations with strong p-values, but the trend analysis indicated that these relationships had r^2 values below 0.5, suggesting a weak trend connection.

Table 5.18 Results of the Spearman's correlation matrix showing the Spearman's coefficient, p-value and R^2 values (from top to bottom), to explore the relationships between sediment properties and the morphological and geometrical properties of the Minnehaha point bar samples. Significant relationships are highlighted in grey.

Independent variable	Dependent variable											
	D_{16} (μm)	D_{50} (μm)	D_{84} (μm)	OMC (%)	Clay and silt fraction (%)	Sand fraction (%)	TP (g kg^{-1})	Bioavailable phosphorus (g kg^{-1})	Fe (g kg^{-1})	Al (g kg^{-1})	Mg (g kg^{-1})	Ca (g kg^{-1})
Distance downstream (m)	-0.1	0.0	0.0	0.4	0.0	0.3	0.1	-0.3	0.1	0.2	0.2	0.4
Relative elevation (m.a.s.l)	0.1	0.0	0.0	-0.4	-0.1	-0.3	-0.1	0.3	-0.1	-0.1	-0.1	-0.3
Channel slope (%)	0.2	0.2	0.1	-0.5	-0.2	0.1	-0.3	0.3	-0.2	-0.3	-0.3	-0.3
Channel width (m)	-0.4	-0.3	-0.2	0.0	0.4	-0.6	-0.1	-0.3	0.3	-0.2	-0.1	-0.3
Bankfull depth (m)	-0.6	-0.6	-0.6	0.0	0.6	-0.5	-0.4	-0.3	0.5	-0.6	-0.4	-0.6
Average depth (m)	-0.8	-0.8	-0.8	0.1	0.8	-0.5	-0.3	-0.1	0.8	-0.7	-0.4	-0.6
Channel width/ depth ratio	0.2	0.4	0.4	0.1	-0.3	-0.1	0.6	0.2	-0.2	0.7	0.6	0.5
Channel area (m^2)	0.1	0.1	0.2	0.6	-0.1	0.2	-0.1	-0.1	-0.1	0.6	0.3	0.5
Distance downstream (m)	0.42	0.50	0.45	0.10	0.45	0.16	0.35	0.21	0.40	0.26	0.31	0.13
Relative elevation (m.a.s.l)	0.37	0.44	0.49	0.11	0.40	0.20	0.39	0.20	0.36	0.34	0.37	0.18
Channel slope (%)	0.25	0.28	0.36	0.05	0.23	0.44	0.17	0.20	0.27	0.17	0.19	0.18
Channel width (m)	0.12	0.17	0.26	0.48	0.13	0.01	0.33	0.14	0.13	0.28	0.43	0.18
Bankfull depth (m)	0.02	0.01	0.03	0.44	0.02	0.07	0.09	0.18	0.04	0.02	0.07	0.02
Average depth (m)	0.00	0.00	0.00	0.35	0.00	0.04	0.18	0.32	0.00	0.00	0.09	0.02
Channel width/ depth ratio	0.23	0.11	0.09	0.41	0.21	0.35	0.03	0.32	0.30	0.01	0.02	0.04
Channel area (m^2)	0.36	0.39	0.32	0.02	0.38	0.25	0.42	0.41	0.34	0.02	0.20	0.06
Distance downstream (m)	0.0	0.0	0.0	0.2	0.0	0.1	0.0	0.1	0.0	0.0	0.0	0.1
Relative elevation (m.a.s.l)	0.0	0.0	0.0	0.1	0.0	0.1	0.0	0.1	0.0	0.0	0.0	0.1
Channel slope (%)	0.0	0.0	0.0	0.3	0.1	0.0	0.1	0.1	0.0	0.1	0.1	0.1
Channel width (m)	0.1	0.1	0.0	0.0	0.1	0.4	0.0	0.1	0.1	0.0	0.0	0.1
Bankfull depth (m)	0.3	0.4	0.3	0.0	0.4	0.2	0.2	0.1	0.3	0.3	0.2	0.3
Average depth (m)	0.6	0.7	0.6	0.0	0.6	0.3	0.1	0.0	0.6	0.5	0.2	0.3
Channel width/ depth ratio	0.1	0.1	0.2	0.0	0.1	0.0	0.3	0.0	0.0	0.4	0.4	0.3
Channel area (m^2)	0.0	0.0	0.0	0.4	0.0	0.0	0.0	0.0	0.0	0.4	0.1	0.2

Relationships between sediment properties

The results of the Spearman correlation analysis within the point bar (depositing bank) samples of the Gatberg River system revealed significant relationships between the various sediment properties. These correlations shed light on the interplay between sediment characteristics (Table 5.19).

There was a very strong negative Spearman's coefficient and p-values between the percentage of organic matter and magnesium concentration with D_{50} sediment particle sizes (r_s = -0.9; p-values < 0.05; $r^2 > 0.5$); and iron and magnesium concentrations with D_{16} sediment particle sizes (r_s = 0.9; p-values < 0.05; $r^2 > 0.5$). A strong positive correlation was observed between organic matter content, iron and magnesium concentrations with clay and silt fractions (r_s = 0.7 between 0.8; p-values < 0.05; r^2 = 0.5); and between total phosphorus, bioavailable phosphorus, iron, magnesium and calcium concentrations with the percentage of organic matter content with average channel depth (r_s = 0.7 between 0.8; p-values < 0.05; r^2 = 0.5). A strong negative correlation was detected between the percentage organic matter content and calcium concentration with D_{16} sediment particle sizes (r_s = -0.8; p-values < 0.05; r^2 = 0.5); iron and calcium concentrations with D_{50} sediment particle sizes (r_s = -0.7 between -0.8; p-values < 0.05; r^2 = 0.5); iron and the percentage organic matter content with D_{84} sediment particle sizes (r_s = -0.8; p-values < 0.05; r^2 = 0.5). Several other combinations showed moderate correlations with strong p-values, but the trend analysis indicated that these relationships had r^2 values below 0.5, suggesting a weak trend connection.

Table 5.19 Results of the Spearman's correlation matrix showing the Spearman's coefficient, p-value and R^2 values (from top to bottom), to explore the relationships between sediment properties of the Gatberg point bar samples. Significant relationships are highlighted in grey.

Independent variable	Dependent variable: OMC (%)	TP (g kg^{-1})	Bioavailable phosphorus (g kg^{-1})	Fe (g kg^{-1})	Al (g kg^{-1})	Mg (g kg^{-1})	Ca (g kg^{-1})
D_{16} (µm)	-0.8	-0.4	-0.3	-0.9	-0.3	-0.9	-0.8
D_{50} (µm)	-0.9	-0.5	-0.4	-0.8	-0.3	-0.9	-0.7
D_{84} (µm)	-0.8	-0.4	-0.9	-0.8	-0.1	-0.6	-0.4
Sand fraction (%)	-0.8	-0.3	-0.2	-0.8	-0.2	-0.8	-0.6
Clay and silt fraction (%)	0.7	0.3	0.2	0.8	0.2	0.8	0.6
OMC (%)		0.7	0.8	0.7	0.4	0.7	0.8
D_{16} (µm)	0.00	0.06	0.26	0.00	0.15	0.00	0.01
D_{50} (µm)	0.00	0.04	0.16	0.00	0.13	0.00	0.01
D_{84} (µm)	0.00	0.07	0.00	0.00	0.36	0.01	0.14
Sand fraction (%)	0.00	0.12	0.33	0.00	0.27	0.00	0.04
Clay and silt fraction (%)	0.00	0.12	0.33	0.00	0.29	0.00	0.04
OMC (%)		0.00	0.00	0.01	0.09	0.00	0.01
D_{16} (µm)	0.7	0.2	0.1	0.7	0.1	0.8	0.6
D_{50} (µm)	0.8	0.2	0.1	0.6	0.1	0.8	0.5
D_{84} (µm)	0.7	0.2	0.7	0.6	0.0	0.4	0.2
Sand fraction (%)	0.6	0.1	0.0	0.7	0.0	0.7	0.4
Clay and silt fraction (%)	0.6	0.1	0.0	0.7	0.0	0.7	0.4
OMC (%)		0.5	0.7	0.4	0.1	0.5	0.6

The results of the Spearman correlation analysis within the point bar (depositing bank) samples of the Minnehaha River system revealed significant relationships between the various sediment properties. These correlations shed light on the interplay between the sediment characteristics (Table 5.20).

There was a very strong positive Spearman's coefficient and p-values between iron concentrations with clay and silt fraction (r_s = 0.9; p-values < 0.05; r^2 > 0.5). A very strong negative correlation between iron with D_{16}, D_{50} and D_{84} sediment particle sizes (r_s = -0.9; p-values < 0.05; r^2 > 0.5). Several other combinations showed moderate correlations with strong p-values, but the trend analysis indicated that these relationships had r^2 values below 0.5, suggesting a weak trend connection.

Table 5.20 Results of the Spearman's correlation matrix showing the Spearman's coefficient, p-value and R^2 values (from top to bottom), to explore the relationships between sediment properties of the Minnehaha point bar samples. Significant relationships are highlighted in grey.

	Dependent variable						
Independent variable	**OMC (%)**	**TP (g kg^{-1})**	**Bioavailable phosphorus (g kg^{-1})**	**Fe (g kg^{-1})**	**Al (g kg^{-1})**	**Mg (g kg^{-1})**	**Ca (g kg^{-1})**
D_{16} (µm)	-0.3	-0.2	-0.1	-1.0	0.5	0.2	0.4
D_{50} (µm)	-0.4	-0.1	-0.1	-0.9	0.6	0.2	0.4
D_{84} (µm)	-0.4	0.0	-0.2	-0.9	0.6	0.2	0.4
OMC (%)		0.2	0.1	0.3	0.2	0.5	0.5
Clay and silt fraction (%)	0.3	0.2	0.1	0.9	-0.5	-0.2	-0.4
Sand fraction (%)	0.1	0.1	0.3	-0.5	0.5	0.3	0.6
D_{16} (µm)	0.19	0.24	0.41	0.00	0.04	0.30	0.12
D_{50} (µm)	0.11	0.44	0.40	0.00	0.02	0.23	0.09
D_{84} (µm)	0.12	0.45	0.29	0.00	0.01	0.23	0.08
OMC (%)		0.30	0.41	0.17	0.24	0.07	0.07
Clay and silt fraction (%)	0.18	0.26	0.41	0.00	0.04	0.24	0.09
Sand fraction (%)	0.37	0.42	0.14	0.03	0.06	0.20	0.02
D_{16} (µm)	0.1	0.1	0.0	0.9	0.3	0.0	0.1
D_{50} (µm)	0.1	0.0	0.0	0.8	0.4	0.1	0.2
D_{84} (µm)	0.1	0.0	0.0	0.7	0.4	0.1	0.2
OMC (%)		0.0	0.0	0.1	0.1	0.2	0.2
Clay and silt fraction (%)	0.1	0.0	0.0	0.9	0.3	0.1	0.2
Sand fraction (%)	0.0	0.0	0.1	0.3	0.2	0.1	0.4

Relationships between total phosphorus and geochemical properties

The results of the Spearman correlation analysis within the point bar (depositing bank) samples of the Gatberg River system revealed significant relationships between total phosphorus concentration and the geochemical sediment properties. These correlations elucidate the interaction between the total phosphorus concentration and the geochemical properties (Table 5.21).

There was a very strong positive Spearman's coefficient and p-values between total phosphorus concentrations with calcium concentrations (r_s = 0.9; p-values < 0.05; r^2 > 0.5). A strong positive

correlation between total phosphorus concentration with bioavailable phosphorus and aluminium concentrations (r_s between 0.7 and 0.8; p-values < 0.05; $r^2 > 0.5$).

However, the only variability within the total phosphorus concentrations that the other geochemical properties could explain according to a trend analysis was between total phosphorus concentration and bioavailable phosphorus, aluminium, and calcium (r^2 = .5, .7, and .8, correspondingly).

Table 5.21 Results of the Spearman's correlation matrix showing the Spearman's coefficient, p-value and R^2 values (from top to bottom), to explore the relationships between total phosphorus content and the measured geochemical elements of the Gatberg point bar samples. Significant relationships are highlighted in grey.

Independent variable	Dependent variable TP (g kg^{-1})
Bioavailable phosphorus (g kg^{-1})	0.7
Fe (g kg^{-1})	0.6
Al (g kg^{-1})	0.8
Mg (g kg^{-1})	0.5
Ca (g kg^{-1})	0.9
Bioavailable phosphorus (g kg^{-1})	0.02
Fe (g kg^{-1})	0.06
Al (g kg^{-1})	0.00
Mg (g kg^{-1})	0.04
Ca (g kg^{-1})	0.00
Bioavailable phosphorus (g kg^{-1})	0.5
Fe (g kg^{-1})	0.3
Al (g kg^{-1})	0.7
Mg (g kg^{-1})	0.3
Ca (g kg^{-1})	0.8

The results of the Spearman correlation analysis within the point bar (depositing bank) samples of the Minnehaha River system revealed significant relationships between total phosphorus concentration and the geochemical sediment properties. There was a moderately strong correlation between total phosphorus concentration and bioavailable phosphorus, magnesium, and calcium concentrations (r_s = 0.5; p-values < 0.05; $r^2 < 0.5$).

However, only 30 % of the variability within total phosphorus concentrations could be explained by bioavailable phosphorus, magnesium, and calcium concentrations according to a trend analysis.

5.3.2 FLOODPLAIN SURFACE SEDIMENT AND PHOSPHORUS DYNAMICS

5.3.2.1 SPATIAL VARIABILITY OF SEDIMENT CHARACTERISTICS ACROSS THE FLOODPLAIN SURFACE

Figure 5.16 illustrates the distribution of the sediment particle size (µm), organic matter content (%), and the total phosphorus concentration (g kg^{-1}) among the surface sediment grab samples taken from the Gatberg floodplain.

During the study period, the D_{50} particle size distribution of sediment samples from the Gatberg River floodplain surface ranged from very fine silt to very fine sand (5 to 105 µm), with an average of 17 µm (mode 12 µm). Most distributions were unimodal. The D_{84} particle sizes ranged from 23 to 251 µm (medium silt to medium sand), averaging 56 µm. The D_{16} particle sizes ranged from 2 to 17 µm (clay to medium silt), with an average of 3 µm (mode 3 µm). The organic matter content varied from 2 to 30 %, averaging 12 %. Total phosphorus concentration in sediment samples ranged from 0.04 to 0.2 g kg^{-1}, with an average and mode of 0.1 g kg^{-1}.

Figure 5.17 shows the distribution of the D_{50} sediment particle size (µm), organic matter content (%), and total phosphorus concentration (g kg^{-1}) for the surface sediment grab samples for the Minnehaha floodplain surface.

The distribution of the D_{50} particle size of the floodplain surface sediment samples along the Minnehaha River during the period of study ranged from fine silt to coarse silt (9 to 36 µm), with an average of 22 µm (median 21 µm). Most of the particle size distributions were unimodal. The D_{84} particle sizes ranged from 26 to 71 (medium silt to very fine sand), with an average of 50 µm. The D_{16} particle sizes ranged from 2 to 11 (clay to fine silt), with an average of 5 µm. The per cent organic matter content ranged from 4 to 26 % with an average of 9 %. The distribution of the total phosphorus concentration of the sediment samples ranged from 0.04 to 0.4 g kg^{-1} (average 0.1 g kg^{-1}).

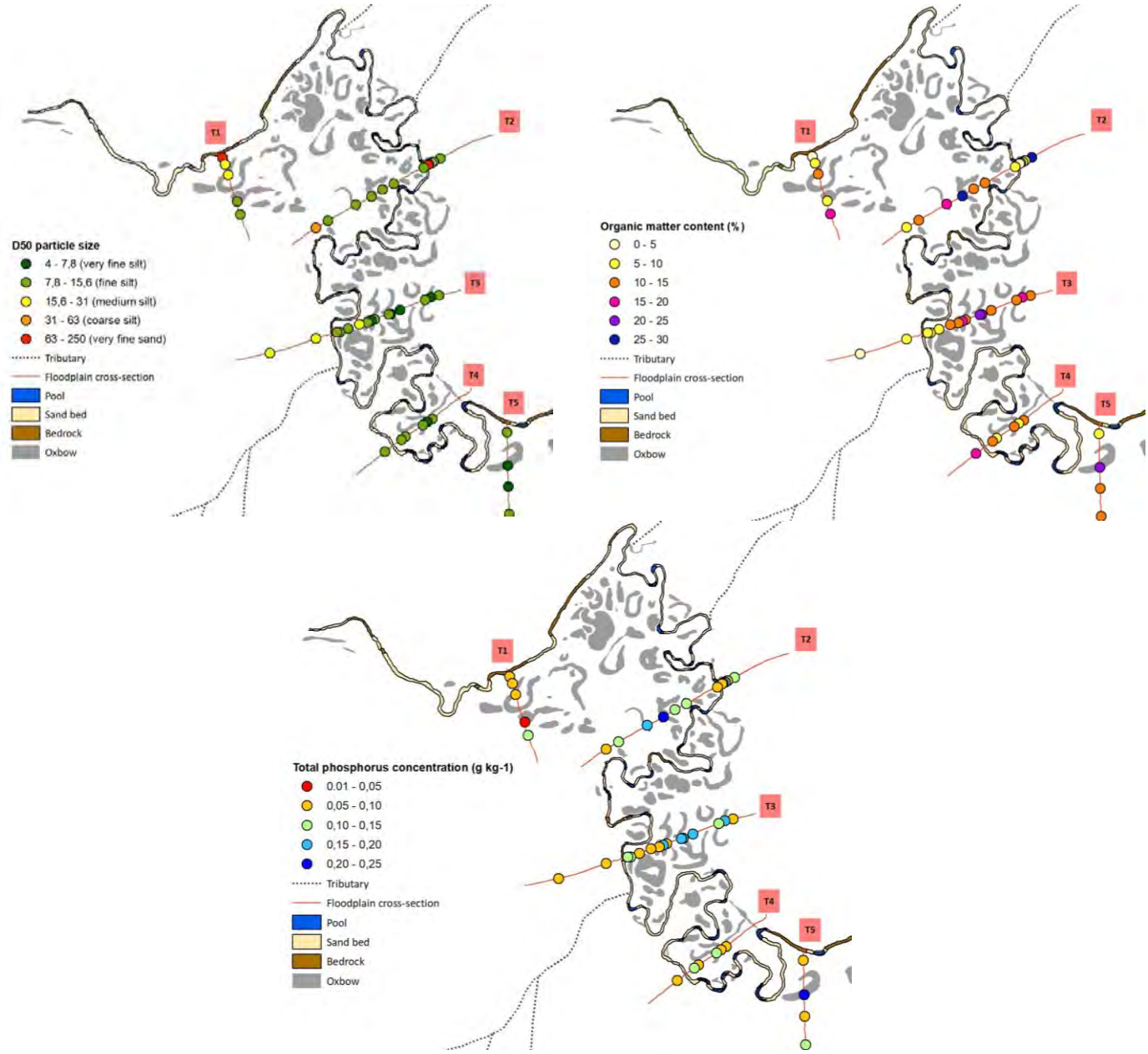

Figure 5.16 D_{50} particle size (µm), organic matter content (%), and total phosphorus concentration (g kg^{-1}) along each transect for the floodplain surface sediment grab samples in the Gatberg River floodplain system

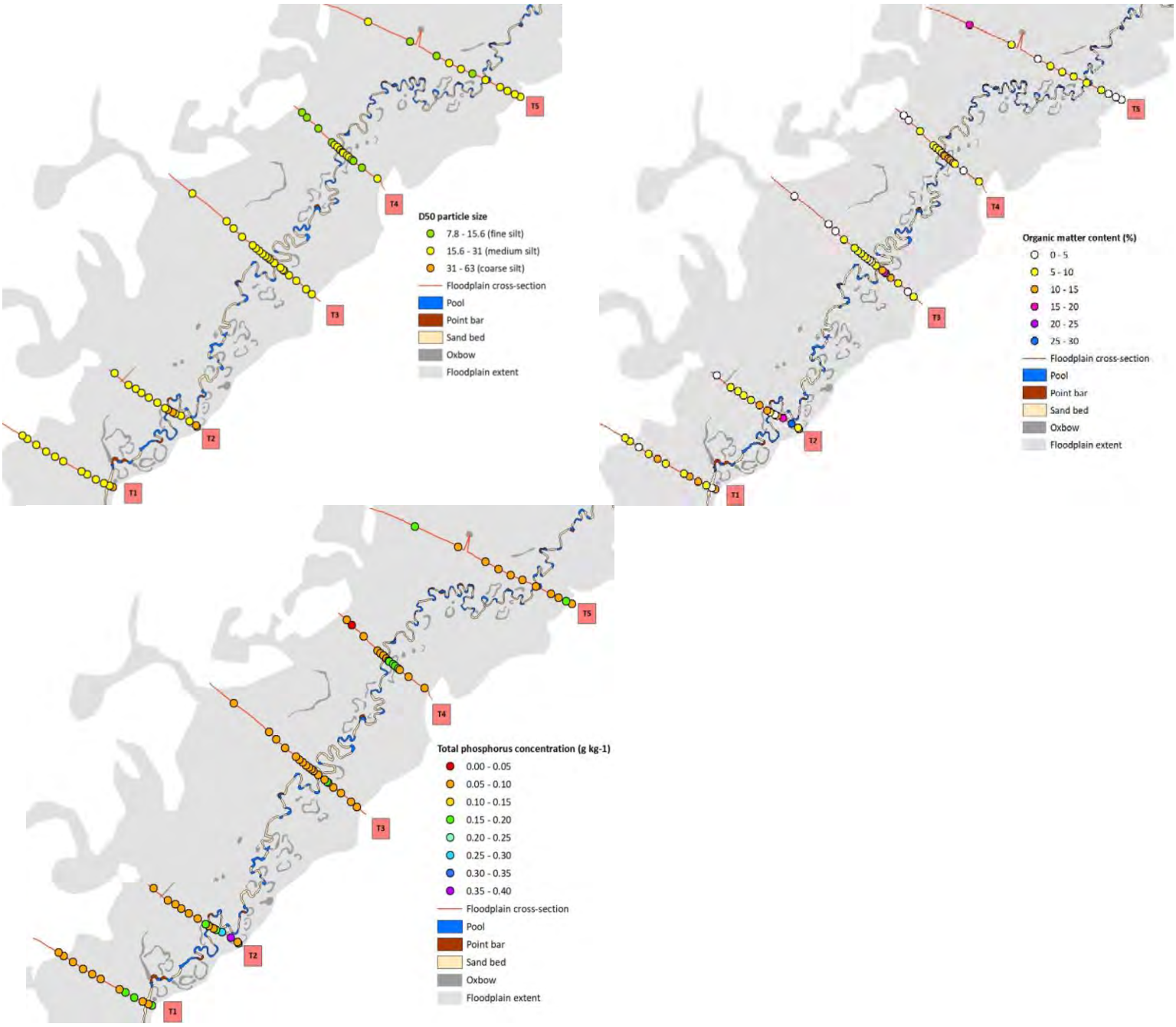

Figure 5.17 D_{50} particle size (µm), organic matter content (%), and total phosphorus concentration (g kg^{-1}) along each transect for the floodplain surface sediment grab samples in the Minnehaha River floodplain system

The Figure 5.18 shows the logarithmic trend of various percentages of sediment size fractions on the floodplain surface with distance from the channel (the sediment source). It highlights the prevalence of clay and silt fractions in samples collected along the Gatberg River floodplain. These fine sediment fractions accounted for 34 to 97 % of the floodplain deposits, with the remainder being sand, indicating the predominance of fine-grained suspended sediment transported by the river.

The distance from the channel, recognised as a crucial factor that influences the grain size composition of the deposited sediment, is evident in Figure 5.18. Here, the sand fraction (> 60 %) dominates the deposits near the channel (< 4 m), gradually decreasing across the floodplain. Conversely, the fine sediment fraction (clay and silt) generally increases with distance from the river channel in the overbank sediment deposits.

However, it is worth noting that the explanatory power of the logarithmic functions is relatively low overall ($R^2 < 0.35$).

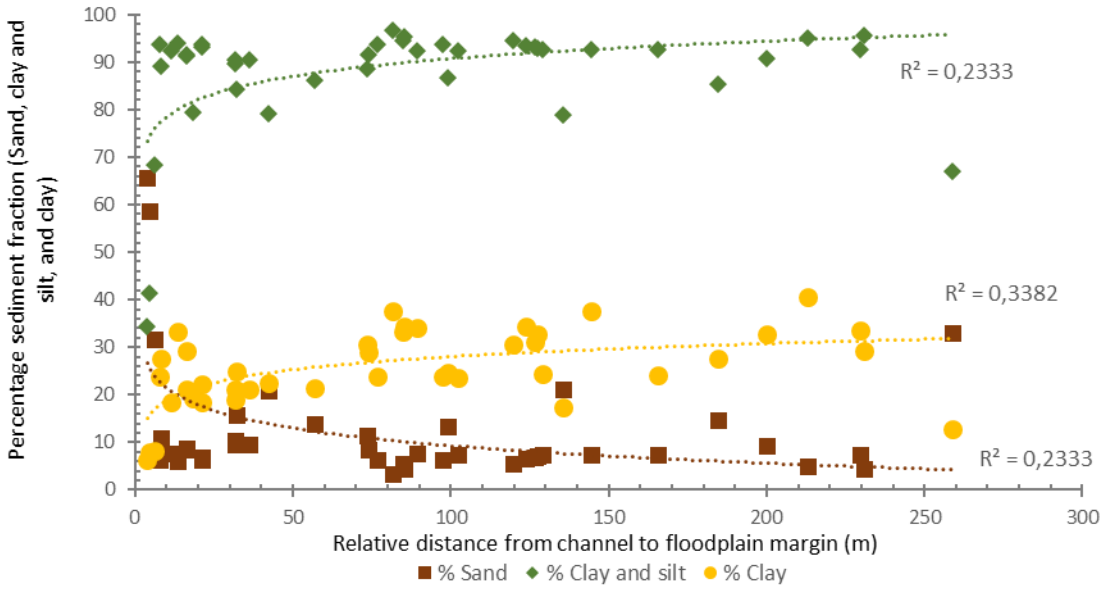

Figure 5.18 Gatberg River floodplain surface grab samples percentage sediment size fractions (sand, clay and silt, and clay) distributions

Figure 5.19 illustrates the logarithmic trend of various percentage sediment size fractions across the floodplain surface from the channel (the sediment source) in the Minnehaha River floodplain system. It reveals the predominance of clay and silt fractions in the samples, with the percentage of fine sediment (clay and silt) ranging from 78 % to 100 % of the floodplain deposits, while the remaining percentage constitutes sand. There's a slight decrease in the percentage of sand fraction from the channel towards the floodplain surface. However, the overall explanatory power of the logarithmic functions is relatively low ($R^2 < 0.22$).

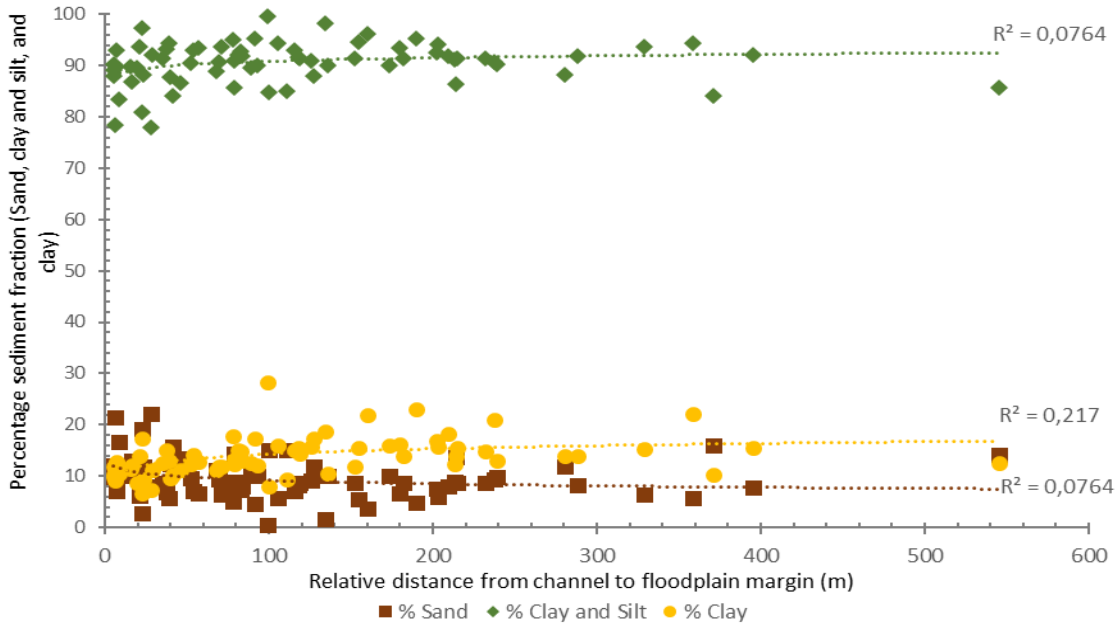

Figure 5.19 Minnehaha River floodplain surface grab samples percentage sediment size fractions (Sand, clay and silt, and clay) distributions

Organic matter content varied from 2 to 30 % across the Gatberg floodplain surface (Figure 5.20), with an average of 12 %. A slight increasing trend was observed between the percentage of organic matter and the distance from the channel across the floodplain surface. However, the overall explanatory power of the logarithmic functions remains relatively low ($R^2 < 0.2$).

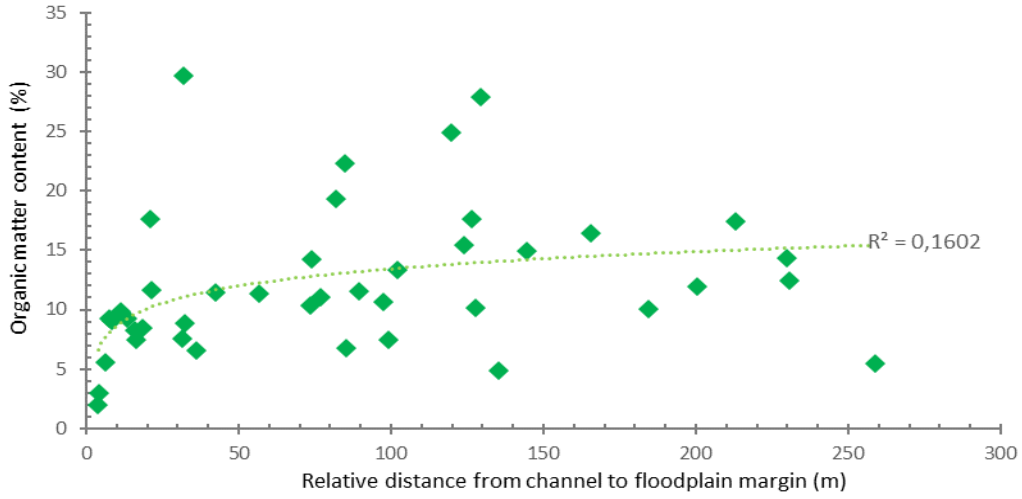

Figure 5.20 Gatberg River floodplain surface samples percentage organic matter content distributions

The percentage of organic matter content varied from 4 to 26 % across the Minnehaha River floodplain surface (Figure 5.21), with an average of 9 %. A slight decreasing trend was observed between the percentage of organic matter and the distance from the channel across the floodplain surface. However, the overall explanatory power of the linear functions remains relatively low ($R^2 < 0.1$).

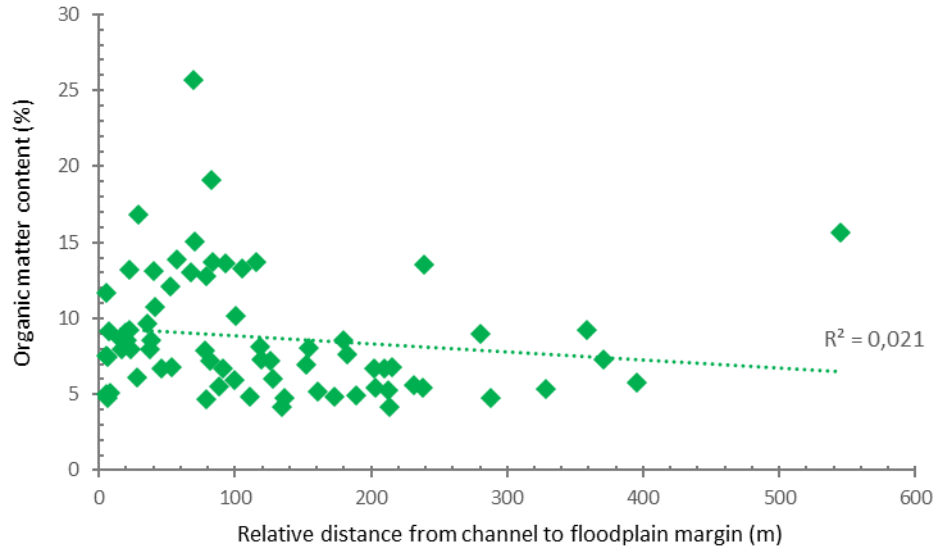

Figure 5.21 Minnehaha River floodplain surface percentage organic matter content distributions

The total phosphorus concentration was low (below 1 g kg^{-1}) across the Gatberg River floodplain surface (ranging from 0.04 to 0.2 g kg^{-1}; Figure 5.22). The average total phosphorus concentration was 0.1 g kg^{-1}. There was no trend between total phosphorus concentration and distance downstream.

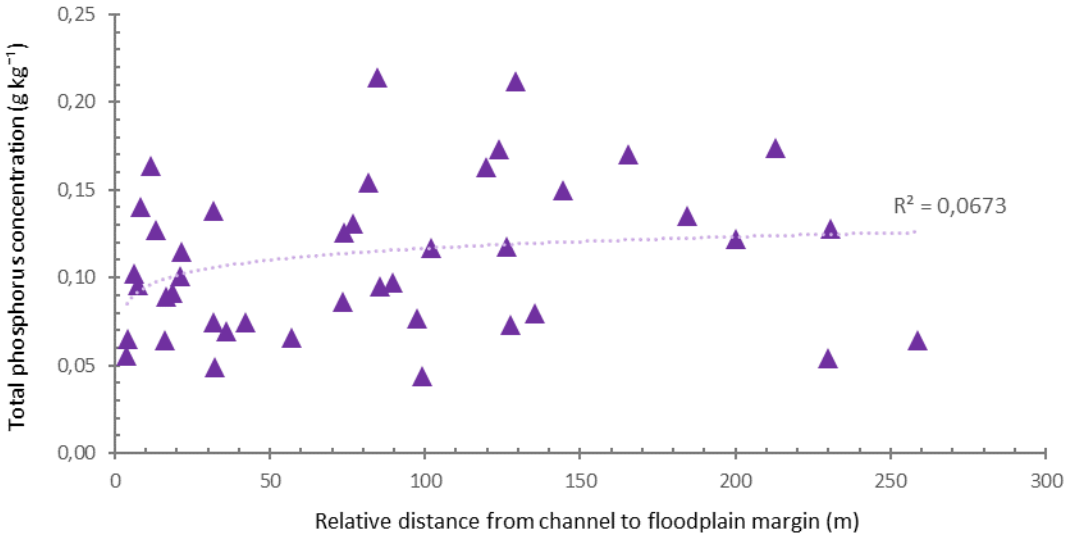

Figure 5.22 Gatberg River floodplain surface total phosphorus concentration distributions

The total phosphorus concentration was low (below 1 g kg^{-1}) across the Minnehaha River floodplain surface (ranging from 0.04 to 0.4 g kg^{-1}; Figure 5.23). The average total phosphorus concentration was 0.1 g kg^{-1}. There was a decreasing trend between total phosphorus concentration and distance downstream. Although overall, the degree of explanation provided by the logarithmic functions is relatively low (R^2 < 0.1).

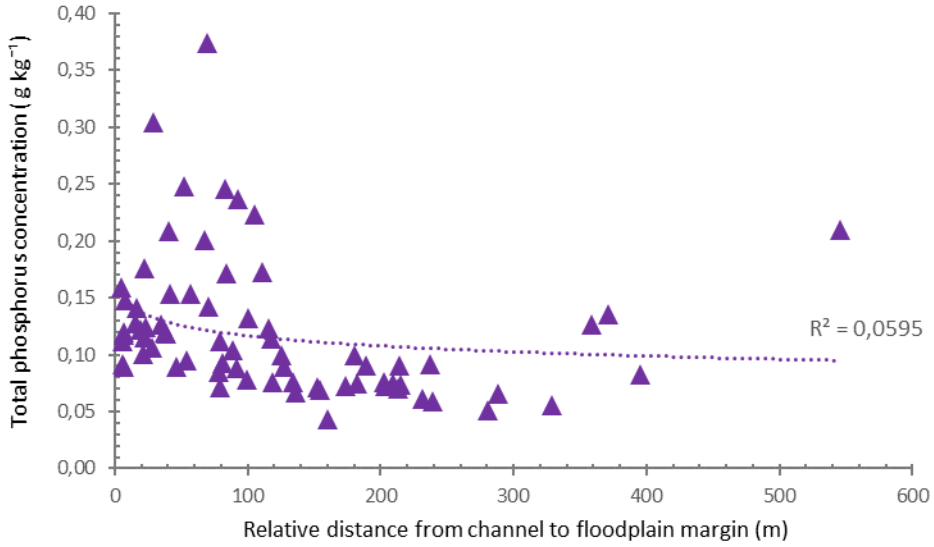

Figure 5.23 Minnehaha River floodplain surface total phosphorus concentration distributions

In Table 5.22, the geochemical concentrations of the sediment samples for the Gatberg floodplain ranged from 0.1 – 1.5 g kg^{-1} for iron, 2 – 5.7 g kg^{-1} for aluminium, and 0.1 – 0.4 g kg^{-1} for magnesium. The highest geochemical concentrations were recorded in the floodplain surface sediments for aluminium with a mean concentration of 3.3 g kg^{-1}. The lowest geochemical concentrations in the floodplain surface sediments were recorded for magnesium with a mean concentration of 0.2 g kg^{-1}. The CV values for all the chemical samples measured were low with values below 1, indicating the data does not deviate significantly from the mean.

Table 5.22 Descriptive statistics of the geochemical concentrations in the Gatberg River floodplain surface sediment samples

Geochemical	N	Minimum	Maximum	Mean	Standard deviation	CV
Iron (g kg^{-1})	34	0.1	1.5	0.5	0.4	0.7
Aluminium (g kg^{-1})	40	2.0	5.7	3.3	0.9	0.3
Magnesium (g kg^{-1})	38	0.1	0.4	0.2	0.1	0.3

In Table 5.23, the geochemical concentrations in the sediment samples in the Minnehaha River floodplain system ranged from 1.6 – 10.1 g kg^{-1} for iron, 1.1 – 5.4 g kg^{-1} for aluminium, 0.1 – 0.3 g kg^{-1} for magnesium,

and 0.2 – 0.7 g kg^{-1} for calcium. The highest geochemical concentrations in the floodplain surface sediments were recorded for iron with a mean concentration of 6 g kg^{-1}. The lowest geochemical concentrations in the floodplain surface sediments were recorded for magnesium with a mean concentration of 0.1 g kg^{-1}. The CV values for all the chemicals measured were low with values less than 0.5, indicating the data does not deviate significantly from the mean.

Table 5.23 Descriptive statistics of the geochemical concentrations in the Minnehaha River floodplain surface sediment samples

Geochemical	N	Minimum	Maximum	Mean	Standard deviation	CV
Iron (g kg^{-1})	71	1.6	10.1	6.0	2.1	0.3
Aluminium (g kg^{-1})	71	1.1	5.4	3.0	1.0	0.3
Magnesium (g kg^{-1})	71	0.1	0.3	0.1	0.1	0.4
Calcium (g kg^{-1})	71	0.2	0.7	0.4	0.1	0.3

Figure 5.24 shows the various concentrations of each major chemical element measured in the floodplain surface sediments that were sampled in the Gatberg River floodplain system. Iron and aluminium concentrations show a decreasing trend across the floodplain surface from the channel, magnesium concentrations increase slightly and then are almost stable across the floodplain surface. Aluminium concentration has a better relationship with distance across the floodplain surface. Although, in general, the degree of explanation provided by the logarithmic functions is relatively very low ($R^2 < 0.1$).

Figure 5.25 shows the various concentrations for each geochemical measured in the floodplain surface sediments that were sampled in the Minnehaha River floodplain system. All geochemical concentrations show a decreasing trend across the floodplain surface from the channel. Iron and calcium concentrations have a better logarithmic relationship with distance across the floodplain surface. Although, in general, the degree of explanation provided by the logarithmic functions is relatively low ($R^2 < 0.4$).

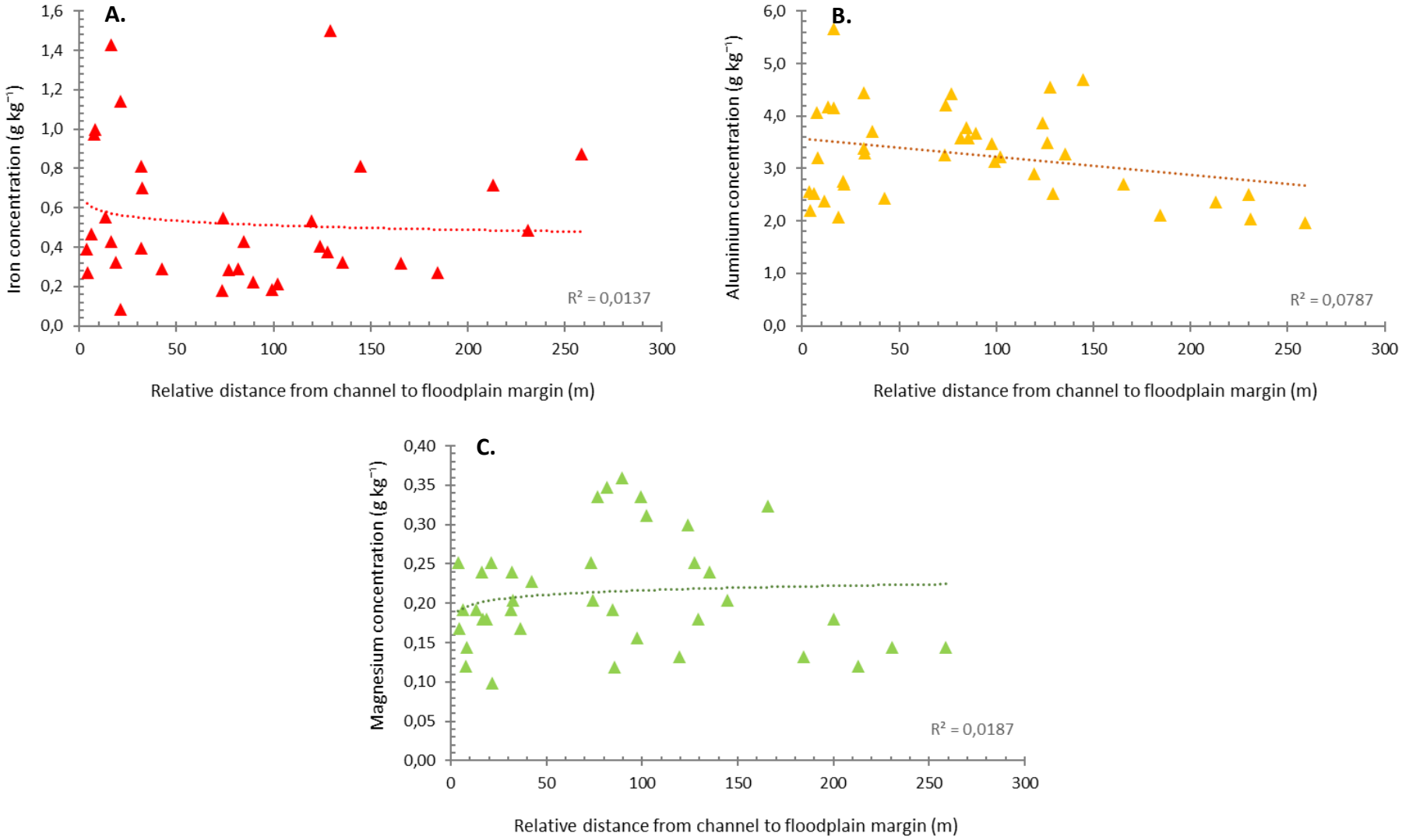

Figure 5.24 Gatberg River floodplain surface geochemical concentration distributions. A) Iron concentration, B) Aluminium concentration, C) Magnesium concentration

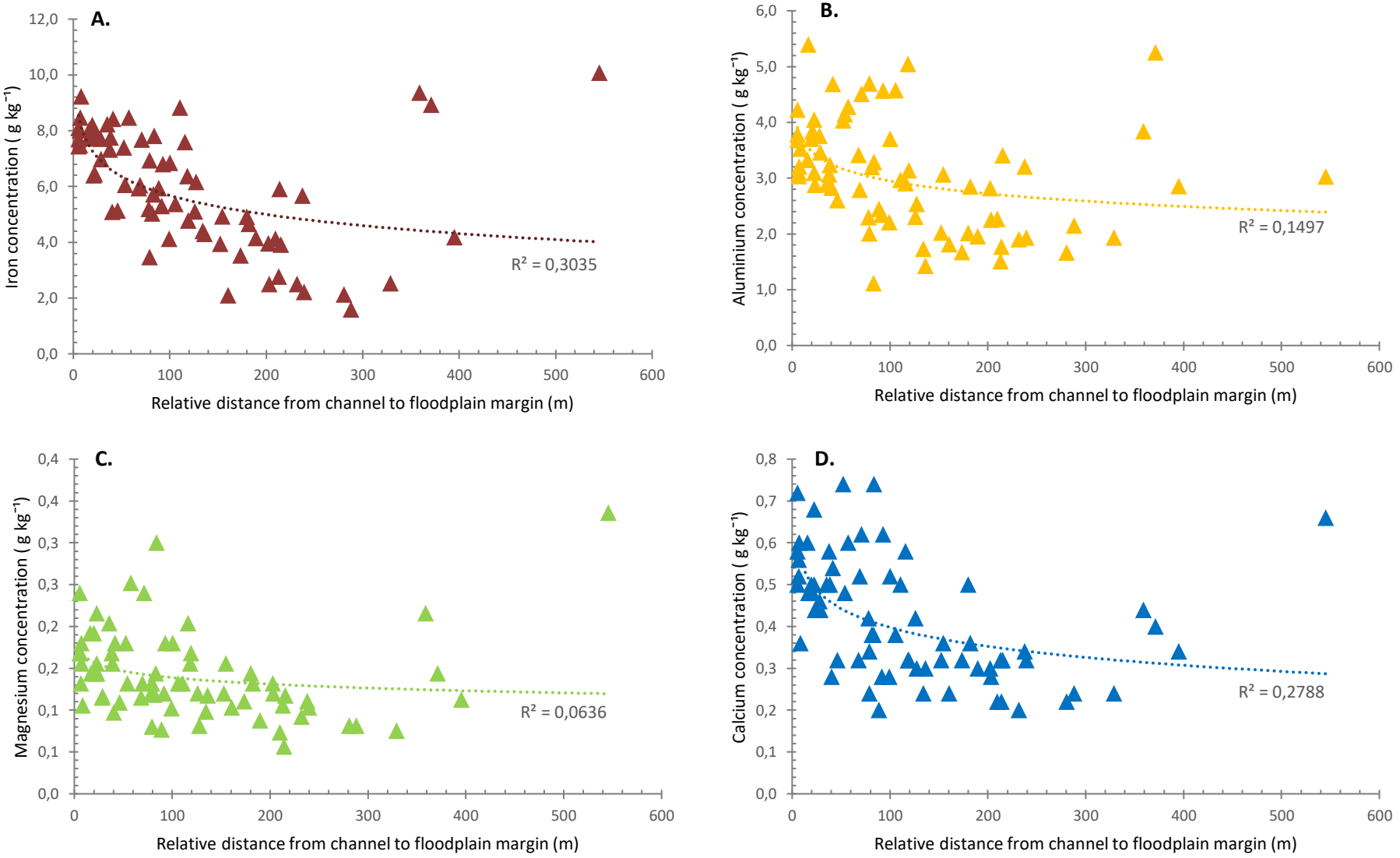

Figure 5.25 Minnehaha River floodplain surface geochemical concentration distributions. A) Iron concentration, B) Aluminium concentration, C) Magnesium concentration, and D) Calcium concentration

Relationships between floodplain surface sediment properties and floodplain morphometrics and geometry

A normality test conducted on sediment and morphological data revealed that most of the data did not follow a normal distribution, thereby violating one of the assumptions for Pearson correlation analysis. Consequently, Spearman rank correlation analyses were conducted, along with trend analysis, to explore relationships between sediment properties, floodplain, and channel morphological characteristics. Only statistically significant relationships (with p-values between 0.01 and 0.05) are presented here; detailed analyses are available in Appendix 2.

For a correlation between sediment properties and channel morphometric variables to be considered significant, the following criteria were applied (for either negative or positive correlations):

i. When the Spearman rank correlation coefficient values (r_s) were between 0.4 and 1.
ii. The p-values were between less than 0.01 and 0.05.
iii. and the trend analysis (r^2) values were between 0.5 and 1.

The results of the Spearman correlation analysis between the floodplain surface sediment samples and the floodplain and channel morphometrics of the Gatberg River floodplain system revealed moderate significant relationships (Table 5.24). However, none of the variability within the surface sediment properties of the floodplain could be explained by the morphometrics of the floodplain and the channel according to a trend analysis (r^2 = or > .5).

Table 5.24 Results of the Spearman's correlation matrix showing the Spearman's coefficient, p-value and R^2 values (from top to bottom), to explore the relationships between sediment properties and the morphological and geometrical properties of the Gatberg floodplain surface samples. Significant relationships are highlighted in grey.

Independent variable	Dependent variable										
	D_{16} (µm)	D_{50} (µm)	D_{84} (µm)	OMC (%)	Sand fraction (%)	Clay and silt fraction (%)	Clay fraction (%)	TP (g kg^{-1})	Fe (g kg^{-1})	Al (g kg^{-1})	Mg (g kg^{-1})
Distance from channel (m)	-0.4	-0.5	-0.4	0.4	-0.3	0.3	0.5	0.1	0.2	0.4	-0.2
Distance downstream (m)	-0.4	-0.4	-0.3	0.1	-0.3	0.3	0.4	0.1	-0.2	0.3	0.1
Relative elevation (m.a.s.l)	0.5	0.6	0.5	-0.4	0.5	-0.5	-0.6	-0.4	-0.4	-0.4	0.1
Floodplain perpendicular slope (%)	0.4	0.6	0.5	-0.5	0.4	-0.4	-0.5	-0.4	-0.4	-0.3	0.1
Floodplain downstream slope (%)	0.5	0.5	0.4	-0.2	0.3	-0.3	-0.5	-0.1	0.1	-0.4	-0.1
Floodplain width (m)	-0.3	-0.2	-0.2	0.1	-0.1	0.1	0.3	0.2	0.0	0.4	0.1
Floodplain width/ Channel width ratio	-0.3	-0.2	-0.2	0.1	-0.1	0.1	0.3	0.2	0.0	0.4	0.1
Channel slope (%)	-0.1	0.0	0.1	-0.1	0.1	-0.1	0.1	-0.3	0.0	-0.1	-0.2
Sinuosity	0.0	0.2	0.2	0.0	0.2	-0.2	-0.1	0.1	0.2	-0.1	-0.1
Distance from channel (m)	0.00	0.00	0.01	0.01	0.05	0.05	0.00	0.27	0.14	0.02	0.13
Distance downstream (m)	0.01	0.00	0.02	0.24	0.04	0.04	0.01	0.36	0.21	0.04	0.30
Relative elevation (m.a.s.l)	0.00	0.00	0.00	0.01	0.00	0.00	0.00	0.01	0.02	0.01	0.32
Floodplain perpendicular slope (%)	0.01	0.00	0.00	0.00	0.01	0.01	0.00	0.01	0.03	0.03	0.30
Floodplain downstream slope (%)	0.00	0.00	0.02	0.17	0.04	0.04	0.00	0.29	0.28	0.01	0.31
Floodplain width (m)	0.03	0.12	0.16	0.20	0.23	0.23	0.04	0.12	0.43	0.01	0.32
Floodplain width/ Channel width ratio	0.03	0.12	0.16	0.20	0.23	0.23	0.04	0.12	0.43	0.01	0.32
Channel slope (%)	0.38	0.47	0.36	0.31	0.29	0.29	0.34	0.05	0.50	0.28	0.17
Sinuosity	0.42	0.12	0.15	0.47	0.12	0.12	0.35	0.37	0.16	0.38	0.33
Distance from channel (m)	0.2	0.3	0.2	0.2	0.1	0.1	0.2	0.0	0.0	0.1	0.0
Distance downstream (m)	0.1	0.2	0.1	0.0	0.1	0.1	0.2	0.0	0.0	0.1	0.0
Relative elevation (m.a.s.l)	0.3	0.3	0.3	0.1	0.2	0.2	0.3	0.1	0.2	0.1	0.0
Floodplain perpendicular slope (%)	0.2	0.3	0.3	0.3	0.2	0.2	0.2	0.1	0.1	0.1	0.0
Floodplain downstream slope (%)	0.2	0.2	0.1	0.0	0.1	0.1	0.2	0.0	0.0	0.2	0.0
Floodplain width (m)	0.1	0.0	0.0	0.0	0.0	0.0	0.1	0.0	0.0	0.2	0.0
Floodplain width/ Channel width ratio	0.1	0.0	0.0	0.0	0.0	0.0	0.1	0.0	0.0	0.2	0.0
Channel slope (%)	0.0	0.0	0.0	0.0	0.0	0.0	0.0	0.1	0.0	0.0	0.0
Sinuosity	0.0	0.0	0.0	0.0	0.0	0.0	0.0	0.0	0.0	0.0	0.0

The results of the Spearman correlation analysis between the floodplain surface sediment samples and the floodplain and channel morphometrics of the Minnehaha River floodplain system revealed moderate significant relationships (Table 5.25). However, none of the variability within the surface sediment properties of the floodplain could be explained by the morphometrics of the floodplain and the channel according to a trend analysis (r^2 = or > .5).

Table 5.25 Results of the Spearman's correlation matrix showing the Spearman's coefficient, p-value and R^2 values (from top to bottom), to explore the relationships between sediment properties and the morphological and geometrical properties of the Minnehaha floodplain surface samples. Significant relationships are highlighted in grey.

Independent variable	Dependent variable												
	D_{16} (µm)	D_{50} (µm)	D_{84} (µm)	OMC (%)	Sand fraction (%)	Clay and silt fraction (%)	Clay fraction (%)	TP (g kg^{-1})	Bioavailable phosphorus (g kg^{-1})	Ca (g kg^{-1})	Fe (g kg^{-1})	Al (g kg^{-1})	Mg (g kg^{-1})
Distance from channel (m)	-0.5	-0.4	-0.3	-0.3	-0.2	0.2	0.5	-0.5	-0.1	-0.6	-0.6	-0.5	-0.4
Distance downstream (m)	-0.1	-0.1	-0.1	-0.2	-0.1	0.1	0.1	-0.1	-0.3	0.0	0.0	-0.3	0.0
Relative elevation (m.a.s.l)	0.3	0.3	0.2	0.2	0.2	-0.2	-0.3	0.1	0.3	0.2	0.1	0.4	0.2
Floodplain perpendicular slope (%)	-0.1	-0.1	-0.1	0.0	-0.1	0.1	0.1	0.0	0.2	-0.1	0.0	0.0	-0.1
Floodplain downstream slope (%)	-0.1	0.0	0.0	0.0	0.0	0.0	0.1	0.0	0.1	0.0	0.0	0.0	0.0
Floodplain width (m)	0.0	0.1	0.1	-0.2	0.2	-0.2	0.0	-0.1	-0.2	0.0	0.0	-0.1	-0.1
Floodplain width/ Channel width ratio	-0.1	-0.1	0.0	-0.2	0.0	0.0	0.1	-0.1	-0.3	0.0	0.0	-0.3	0.0
Channel slope (%)	0.2	0.3	0.3	0.1	0.3	-0.3	-0.2	0.0	0.0	0.1	0.0	0.2	0.1
Sinuosity	-0.2	-0.2	-0.2	-0.2	-0.2	0.2	0.2	0.0	-0.3	-0.1	0.1	-0.3	-0.1
Distance from channel (m)	0.00	0.01	0.06	0.06	0.10	0.10	0.00	0.00	0.30	0.00	0.00	0.00	0.01
Distance downstream (m)	0.23	0.20	0.23	0.13	0.30	0.30	0.21	0.30	0.04	0.46	0.45	0.04	0.47
Relative elevation (m.a.s.l)	0.07	0.06	0.11	0.10	0.15	0.15	0.06	0.29	0.04	0.13	0.36	0.01	0.12
Floodplain perpendicular slope (%)	0.30	0.32	0.28	0.41	0.26	0.26	0.31	0.43	0.18	0.33	0.44	0.48	0.38
Floodplain downstream slope (%)	0.38	0.46	0.49	0.48	0.47	0.47	0.37	0.49	0.32	0.47	0.47	0.49	0.49
Floodplain width (m)	0.49	0.35	0.23	0.19	0.16	0.16	0.43	0.35	0.16	0.40	0.41	0.22	0.38
Floodplain width/ Channel width ratio	0.27	0.31	0.39	0.11	0.48	0.48	0.23	0.28	0.06	0.42	0.46	0.05	0.41
Channel slope (%)	0.08	0.04	0.02	0.35	0.02	0.02	0.09	0.44	0.42	0.27	0.41	0.08	0.36
Sinuosity	0.11	0.11	0.15	0.17	0.19	0.19	0.10	0.41	0.04	0.32	0.35	0.03	0.36
Distance from channel (m)	0.3	0.2	0.1	0.1	0.0	0.0	0.3	0.3	0.0	0.3	0.3	0.2	0.2
Distance downstream (m)	0.0	0.0	0.0	0.0	0.0	0.0	0.0	0.0	0.1	0.0	0.0	0.1	0.0
Relative elevation (m.a.s.l)	0.1	0.1	0.0	0.1	0.0	0.0	0.1	0.0	0.1	0.0	0.0	0.2	0.0
Floodplain perpendicular slope (%)	0.0	0.0	0.0	0.0	0.0	0.0	0.0	0.0	0.0	0.0	0.0	0.0	0.0
Floodplain downstream slope (%)	0.0	0.0	0.0	0.0	0.0	0.0	0.0	0.0	0.0	0.0	0.0	0.0	0.0
Floodplain width (m)	0.0	0.0	0.0	0.0	0.0	0.0	0.0	0.0	0.0	0.0	0.0	0.0	0.0
Floodplain width/ Channel width ratio	0.0	0.0	0.0	0.0	0.0	0.0	0.0	0.0	0.1	0.0	0.0	0.1	0.0
Channel slope (%)	0.1	0.1	0.1	0.0	0.1	0.1	0.1	0.0	0.0	0.0	0.0	0.1	0.0
Sinuosity	0.0	0.0	0.0	0.0	0.0	0.0	0.1	0.0	0.1	0.0	0.0	0.1	0.0

Relationships between sediment properties

The results of the Spearman correlation within the floodplain surface sediment samples between the sediment properties of the Gatberg River system indicated significant statistical correlations (Table 5.26).

A strong positive correlation was detected between total phosphorus and iron concentrations with percentage organic matter content (r_s = 0.7; p-values < 0.05; r^2 = 0.5). A strong negative correlation was detected between the percentage organic matter content with D_{50} and D_{84} sediment particle sizes (r_s = -0.7; p-values < 0.05). Several other combinations showed moderate correlations with strong p-values, but the trend analysis indicated that these relationships had r^2 values below 0.5, suggesting a weak trend connection.

However, the only variability within the sediment properties that could be explained by the other sediment properties according to a trend analysis was between total phosphorus, iron concentration, percentage organic matter content and D_{84} sediment particle size, (r^2 = .5).

Table 5.26 Results of the Spearman's correlation matrix showing the Spearman's coefficient, p-value and R^2 values (from top to bottom), to explore the relationships between sediment properties of the Gatberg floodplain surface samples. Significant relationships are highlighted in grey.

Independent variable	Dependent variable				
	OMC (%)	TP (g kg^{-1})	Fe (g kg^{-1})	Al (g kg^{-1})	Mg (g kg^{-1})
D_{16} (µm)	-0.5	-0.4	-0.3	-0.5	-0.2
D_{50} (µm)	-0.7	-0.5	-0.4	-0.5	-0.1
D_{84} (µm)	-0.7	-0.6	-0.3	-0.6	-0.3
OMC (%)		0.7	0.7	0.5	0.1
Sand fraction (%)	-0.6	-0.6	-0.2	-0.6	-0.3
Clay and silt fraction (%)	0.6	0.6	0.2	0.6	0.3
Clay fraction (%)	0.5	0.4	0.3	0.5	0.1
D_{16} (µm)	0.00	0.02	0.06	0.00	0.19
D_{50} (µm)	0.00	0.00	0.02	0.00	0.26
D_{84} (µm)	0.00	0.00	0.06	0.00	0.10
OMC (%)		0.00	0.00	0.00	0.25
Sand fraction (%)	0.00	0.00	0.11	0.00	0.08
Clay and silt fraction (%)	0.00	0.00	0.11	0.00	0.08
Clay fraction (%)	0.00	0.01	0.04	0.00	0.24
D_{16} (µm)	0.2	0.1	0.1	0.2	0.0
D_{50} (µm)	0.4	0.3	0.2	0.3	0.0
D_{84} (µm)	0.5	0.3	0.1	0.4	0.1
OMC (%)		0.5	0.5	0.3	0.0
Sand fraction (%)	0.4	0.3	0.1	0.4	0.1
Clay and silt fraction (%)	0.4	0.3	0.1	0.4	0.1
Clay fraction (%)	0.3	0.1	0.1	0.2	0.0

The results of the Spearman correlation within the floodplain surface sediment samples between the sediment properties of the Minnehaha River system indicated significant statistical correlations (Table 5.27).

A strong positive correlation was detected between total phosphorus and percentage organic matter content (r_s = 0.7; p-values < 0.05; r^2 = 0.5). Several other combinations showed moderate correlations with strong p-values, but the trend analysis indicated that these relationships had r^2 values below 0.5, suggesting a weak trend connection.

However, the only variability within the sediment properties that could be explained by the other sediment properties according to a trend analysis was between total phosphorus and percentage organic matter content (r^2 = .5).

Table 5.27 Results of the Spearman's correlation matrix showing the Spearman's coefficient, p-value and R^2 values (from top to bottom), to explore the relationships between sediment properties of the Minnehaha floodplain surface samples. Significant relationships are highlighted in grey.

Independent variable	Dependent variable						
	OMC (%)	TP (g kg^{-1})	Bioavailable phosphorus (g kg^{-1})	Ca (g kg^{-1})	Fe (g kg^{-1})	Al (g kg^{-1})	Mg (g kg^{-1})
D_{16} (µm)	0.2	0.4	0.2	0.4	0.5	0.4	0.3
D_{50} (µm)	0.1	0.3	0.2	0.3	0.4	0.3	0.2
D_{84} (µm)	0.0	0.3	0.2	0.2	0.4	0.2	0.0
OMC (%)		0.7	0.4	0.6	0.4	0.5	0.6
Sand fraction (%)	-0.1	0.2	0.1	0.1	0.3	0.2	0.0
Clay and silt fraction (%)	0.1	-0.2	-0.1	-0.1	-0.3	-0.2	0.0
Clay fraction (%)	-0.2	-0.5	-0.2	-0.4	-0.5	-0.4	-0.3
D_{16} (µm)	0.13	0.01	0.09	0.01	0.00	0.02	0.05
D_{50} (µm)	0.31	0.02	0.13	0.04	0.00	0.05	0.16
D_{84} (µm)	0.50	0.05	0.18	0.16	0.01	0.11	0.41
OMC (%)		0.00	0.02	0.00	0.00	0.00	0.00
Sand fraction (%)	0.37	0.08	0.21	0.20	0.02	0.13	0.49
Clay and silt fraction (%)	0.37	0.08	0.21	0.20	0.02	0.13	0.49
Clay fraction (%)	0.10	0.00	0.08	0.00	0.00	0.01	0.04
D_{16} (µm)	0.0	0.2	0.1	0.2	0.2	0.1	0.1
D_{50} (µm)	0.0	0.1	0.0	0.1	0.2	0.1	0.0
D_{84} (µm)	0.0	0.1	0.0	0.0	0.1	0.0	0.0
OMC (%)		0.5	0.1	0.4	0.2	0.2	0.4
Sand fraction (%)	0.0	0.1	0.0	0.0	0.1	0.0	0.0
Clay and silt fraction (%)	0.0	0.1	0.0	0.0	0.1	0.0	0.0
Clay fraction (%)	0.0	0.2	0.1	0.2	0.3	0.1	0.1

Relationships between total phosphorus and geochemical properties

The results of the Spearman correlation within the floodplain surface sediment samples between total phosphorus concentration and the geochemical sediment properties of the Gatberg River system indicated moderately significant relationships.

However, only 30 % of the variability within the total phosphorus data set could be explained by the aluminium concentration data set (r^2 = .3).

The results of the Spearman correlation within the floodplain surface sediment samples between total phosphorus concentration and the geochemical sediment properties of the Minnehaha River system indicated that there were significant relationships between total phosphorus concentrations and the percentage of organic matter content, calcium and iron concentrations (r_s between 0.7 and 0.8; p-values < 0.05; $r^2 = 0.5$).

5.3.2.2 FLOODPLAIN GEOMORPHIC STORAGE UNITS

5.3.2.2.1 Description of floodplain potential storage units

In the Gatberg and Minnehaha River floodplain systems, sediment deposition predominantly occurred on various sections of the floodplain surface, including the proximal floodplain, oxbows, and backswamp regions. Figure 5.26 provides a conceptual representation of these distinct geomorphic units, while Table 5.28 offers detailed descriptions of the identified storage units. Overall, within both floodplain systems, the features were relatively well-defined.

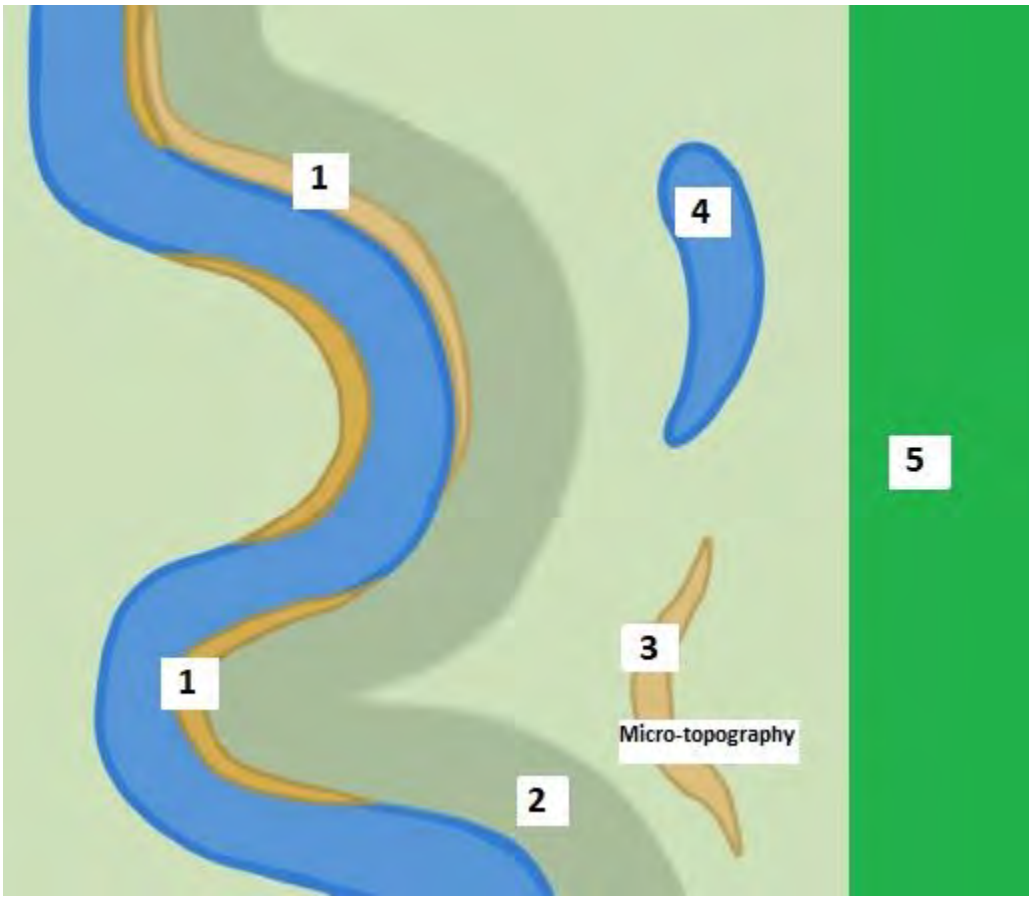

Figure 5.26 Conceptual River floodplain diagram of floodplain geomorphic unit classification system created for this study (adapted from Triantafillou (2021). 1. Bank and levee; 2. Proximal floodplain; 3. Floodplain surface; 4. Oxbow; and 5. Backswamp

Table 5.28 Description of terminology of floodplain storage units identified in this chapter

Floodplain geomorphic unit	Description	Expected flow velocities	Expected sediment properties	Expected vegetation cover	Expected sedimentation
Active floodplain	The floodplain refers to the expansive, generally flat alluvial region situated alongside the river channel, formed by the current river within its current course. Essentially acting as a reservoir or repository, the floodplain plays a crucial role in regulating sediment movement within a river's drainage basin over varying timescales, spanning from years to millennia. It also dictates the extent to which the river channel can naturally shift its position. Periodic inundation of the floodplain, accompanied by the deposition of fine sediment and associated nutrients, is a common occurrence, typically happening once every one to two years				
Proximal floodplain	The proximal floodplain, as studied here, denotes the immediate floodplain surface adjoining the river channel, encompassing levees and the lower elevated floodplain area extending less than 6 meters beyond the levee. Meanders, which are sinuous curves in a river channel, give rise to features such as point bars, also known as meander bars. These bars form gradually through the accumulation of sediment on the inner bank of a meander as the channel migrates towards its outer bank, a process termed lateral accretion. Typically composed of sand, gravel, or a mixture of both, point bars are submerged during high water or floods, allowing helical flows to transport sediment onto them. While the inner bend of a meander is often lower in elevation compared to the outer bend, the outer bend, being concave, cuts into the floodplain surface. Although typically associated with sediment erosion and re-working, in significant floods, water can breach the banks, depositing sediment in this area. Thus, the proximal floodplain serves as a zone for potential sediment exchange, influenced by the dynamics of meander formation and flood events.	Medium to fast	Fine to coarse sediment	Medium-density. medium cover	High sedimentation rates
Oxbow features	Oxbows are natural features commonly found on undisturbed floodplains, resulting from the natural process of river meandering. As a river meanders, its channel gradually curves, leading to the formation of a narrow neck within the meander. Eventually, the river cuts through this narrow neck, creating a cutoff meander. Subsequently, sediment-laden river water flows into the cutoff meander, depositing sediment and gradually blocking both ends, thus forming an oxbow. Once formed, an oxbow becomes isolated from the main flow of the river. During flood events, fine-grained sediment is deposited into the oxbow, leading to the gradual accumulation of organic-rich sediments over time. Consequently, oxbows tend to become filled in with these sediments, highlighting their role as dynamic features shaped by both fluvial processes and periodic flooding.	Slow	Very fine sediment (clay and silt)	High-density. high cover	Low to high sedimentation rates. depending on the distance to the channel and flood frequency
Backswamp	A low-lying area lies between the valley margin and the proximal floodplain and is usually inundated less frequently than the proximal floodplain.	Slow	Very fine sediment (clay and silt)	High-density. high cover	Low to high sedimentation rates. depending on the distance to the channel and flood frequency

Figure 5.27 A and B are two oblique photographs depicting the arrangement of floodplain features in the floodplain systems of the Gatberg (A) and Minnehaha (B) Rivers.

Areas close to the main channel (proximal floodplain) mainly store sediment that has been transported downriver. However, there may be differences between those areas close to the channel but on the outer bend compared to those areas that are close to the channel on the inner bend (Figure 5.28A). This is because the inner bend is usually lower in elevation than the outer bend and the flow characteristics that transport sediment are different along the inner and outer bends.

Oxbows are typically a crescent-shaped geomorphic feature on a floodplain surface formed from a single meander loop that was cut off from a meandering stream. In the Gatberg River floodplain system, oxbows were identified across the whole valley and varied in shape, depth, and distance from the channel. In the Minnehaha River floodplain system, oxbows were identified within a narrow band along the current active channel (Figure 5.27B). Some of the oxbows were permanently wet within the research period and some had hardy *Typha capensis* stands. This suggests that the Gatberg River moved extensively and actively within the valley margins compared to the Minnehaha River.

Backswamps are the lower, poorly drained areas of a floodplain that retain water, usually extending to the floodplain margin (Figure 5.28B). Depending on floodplain topography, vegetation, and planform of the channel and floodplain the backswamp and those features farther away from the main channel may no longer receive input through overbank flooding but rather from the adjacent hillslopes. However, from field observations during the two wet seasons both the Gatberg and Minnehaha floodplain backswamp regions are connected to the active channel and are flooded yearly by the overbank floodwaters.

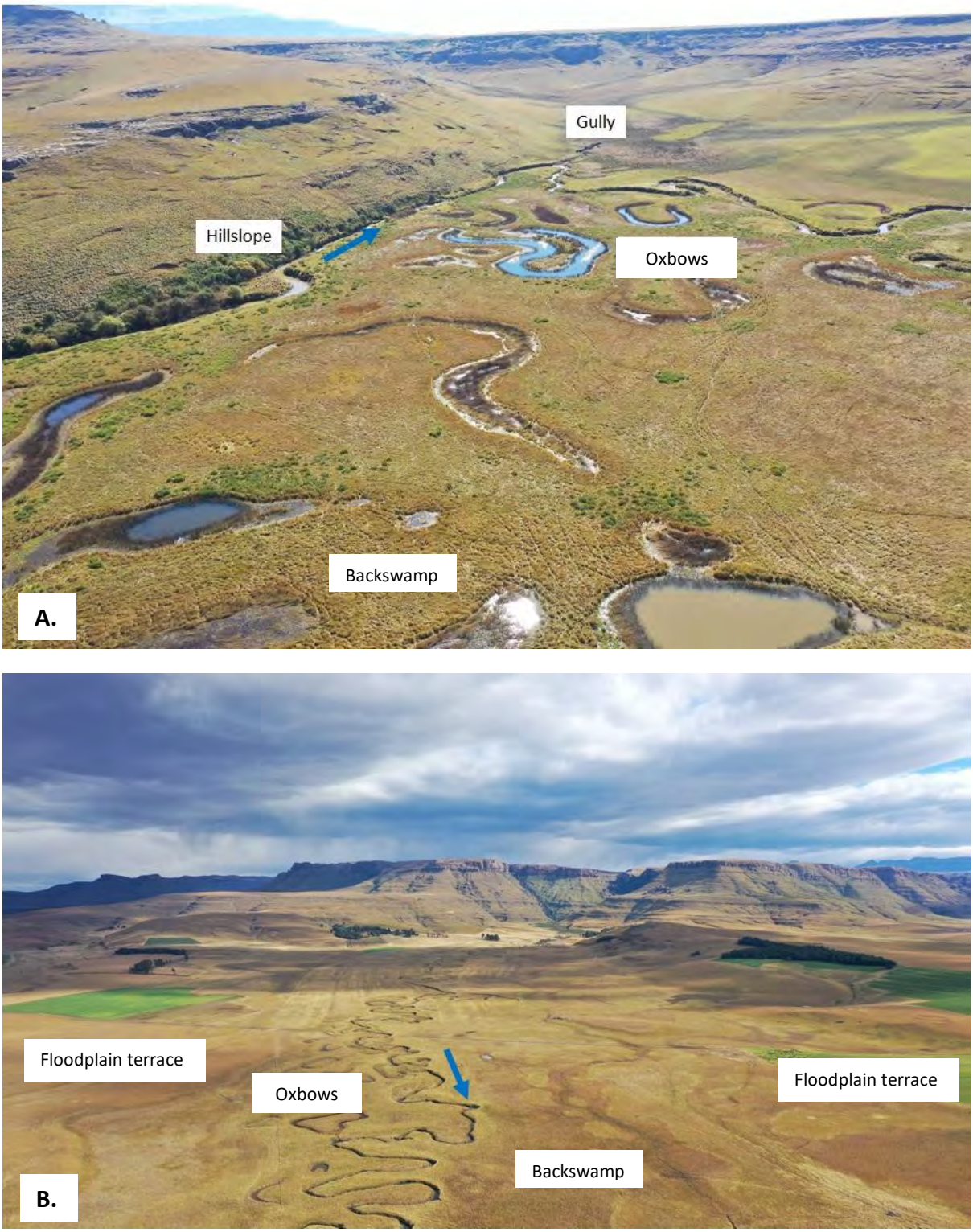

Figure 5.27 Oblique photograph showing the arrangement of the different geomorphic features found within the A. Gatberg River floodplain system and B. Minnehaha River floodplain system. Blue arrow depicts flow direction in active channel

Figure 5.28 A) A photo showing a typical meander bend within the Minnehaha River floodplain system. Note the cobble and gravel bar on the lower inner bend and the steep outer bend experiencing some bank collapse. B) Backswamp region of the Minnehaha River floodplain system in the wet season

5.3.2.2.2 Sediment and phosphorus characteristics of geomorphic storage units

Figure 5.29 shows two box-and-whisker plots depicting the D_{50} sediment particle size on the different geomorphic units identified across the floodplain surface on the A) Gatberg River and B) the Minnehaha River floodplain systems.

In the box and whisker plot depicting the Gatberg River floodplain system, the geomorphic unit of the bank and levee exhibited the largest D_{50} particle sizes, ranging from 39 to 105 µm (coarse silt to very fine sand), with a mean of 75 µm (very fine sand). The D_{50} sediment particle size rapidly decreases from the bank and levee geomorphic unit to approximately 35 m, identified as the proximal floodplain. The D_{50} particle size for the proximal floodplain ranged from 10 to 29 µm (fine to medium silt) with a mean of 17 µm (medium silt). Moving further away from the channel (35 to 230 m), the floodplain surface showed a mean D_{50} particle size of 10 µm, ranging from 8 to 12 µm (fine silt). Oxbows distributed throughout the floodplain surface (from 13 to 90 m) displayed a mean D_{50} particle size of 10 µm, varying from 5 to 16 µm (very fine silt to medium silt). In the geomorphic unit of the backswamp, the D_{50} particle size ranged from 8 to 35 µm (fine silt to coarse silt), with a mean of 14 µm (fine silt).

The box and whisker plot for the Minnehaha River floodplain system shows that the bank and levee geomorphic unit was dominated by medium and coarse silt (20 to 34 µm) with a mean of 25 µm. The proximal floodplain had the largest D_{50} particle sizes with the largest range from 14 to 36 µm (fine silt to coarse silt) with a mean of 28 µm (medium silt). The rest of the floodplain surface (30 to 200 m from the channel) had a mean D_{50} particle size of 22 µm and range from 17 to 32 µm (medium silt). Oxbows that were identified in a narrow band around the active channel from 8 to 110 m, had a mean D_{50} particle size of 23 µm and ranged from 18 to 28 µm (medium silt). The backswamp geomorphic unit had a D_{50} particle size range from 9 to 31 µm (fine silt to medium silt) with a mean of 19 µm (medium silt).

In the Gatberg River floodplain, silt-sized sediments were most common, and most sample medians were identified as fine silt, except for the bank and levee geomorphic unit, where the median was very fine sand. Conversely, in the Minnehaha River floodplain, although silt-sized sediments were dominant, all the various geomorphic units exhibited a more uniform nature, with medians characterised as medium silt.

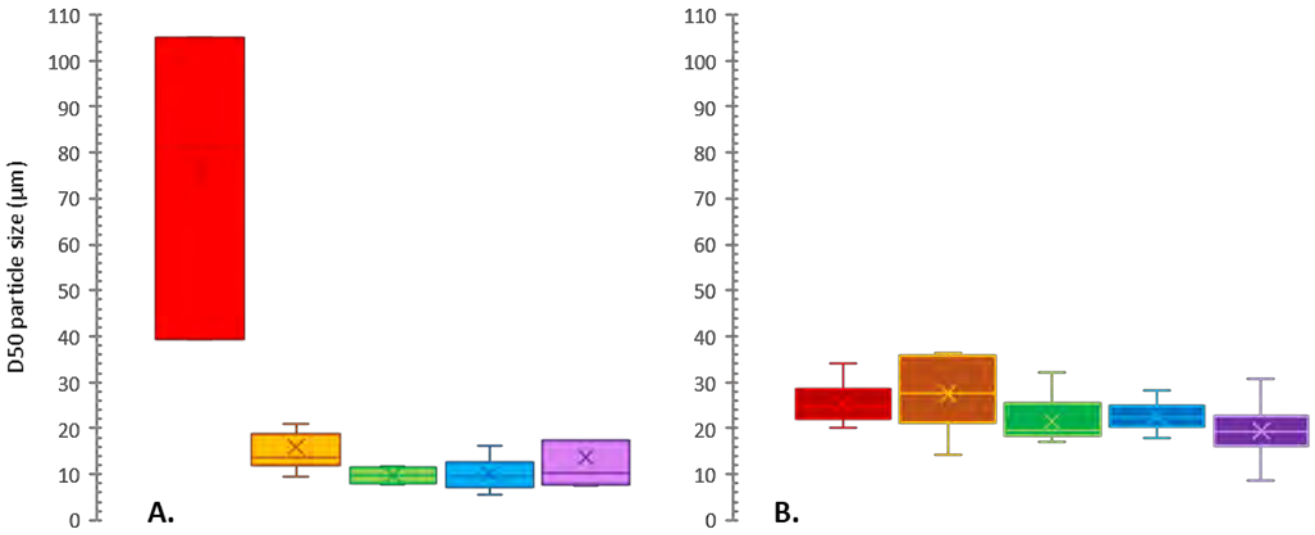

Figure 5.29 Box and whisker diagrams showing D_{50} sediment particle size for the different floodplain geomorphic units identified (Red- Bank and levee, Orange- Proximal floodplain, Green- Floodplain surface, Blue- Oxbow, and Purple- Backswamp) in the A) Gatberg River and B) the Minnehaha River floodplain systems

Figure 5.30 shows two box and whisker plots for each floodplain system depicting the percentage sand and clay fractions across the different geomorphic units identified across the floodplain surface of the Gatberg River (A) and the Minnehaha River floodplain systems (B).

The figure for the Gatberg River floodplain system shows that the bank and levee geomorphic unit was dominated by the sand sediment fraction (mean 52 % and median 59 %) and the clay fraction only comprised 8 % of the samples. The sand fraction rapidly decreased from the geomorphic unit of the bank and levee to the proximal floodplain. The median sand fraction for the proximal floodplain was 9 %, with a mean of 11 %. The clay fraction increased to 21 % (median). The rest of the floodplain surface had a median sand fraction of 7 % a mean of 8% and a median and mean clay fraction of 28 %. Oxbows had the highest clay fraction, a median of 31 % and a mean of 29 %. The backswamp geomorphic unit had a slightly higher sand fraction than the floodplain surface and oxbows with a median of 7 % and a mean of 12 %. The clay fraction made up slightly more than a quarter of the samples in this geomorphic unit.

The figure for the Minnehaha River floodplain system shows that the bank and levee geomorphic unit was dominated by silt fraction. The proximal floodplain samples had the highest amount of sand, median and mean 28 % (max 36 %) with a median clay fraction of 11 %. The rest of the floodplain surface had a mean sand fraction of 22 % and a median of 20 %; and a mean and median clay fraction of 9 and 8 %. The oxbows had a median sand and clay fraction of 22 and 10 %, respectively. The backswamp geomorphic unit had a median sand clay fraction of 19 and 9 %, respectively.

The floodplain of the Gatberg River was dominated by a greater percentage of the clay particle size fraction, with most sample medians being characterised with less than 10 % sand and more than 20 % clay, except for the bank and levee geomorphic unit where the samples were dominated by the sand fraction (> 50 %). In comparison, the Minnehaha River floodplain samples were dominated by a higher percentage of the sand particle size fraction, with all the different geomorphic units' medians at more than 19 % and the clay fraction medians at 11 % and less.

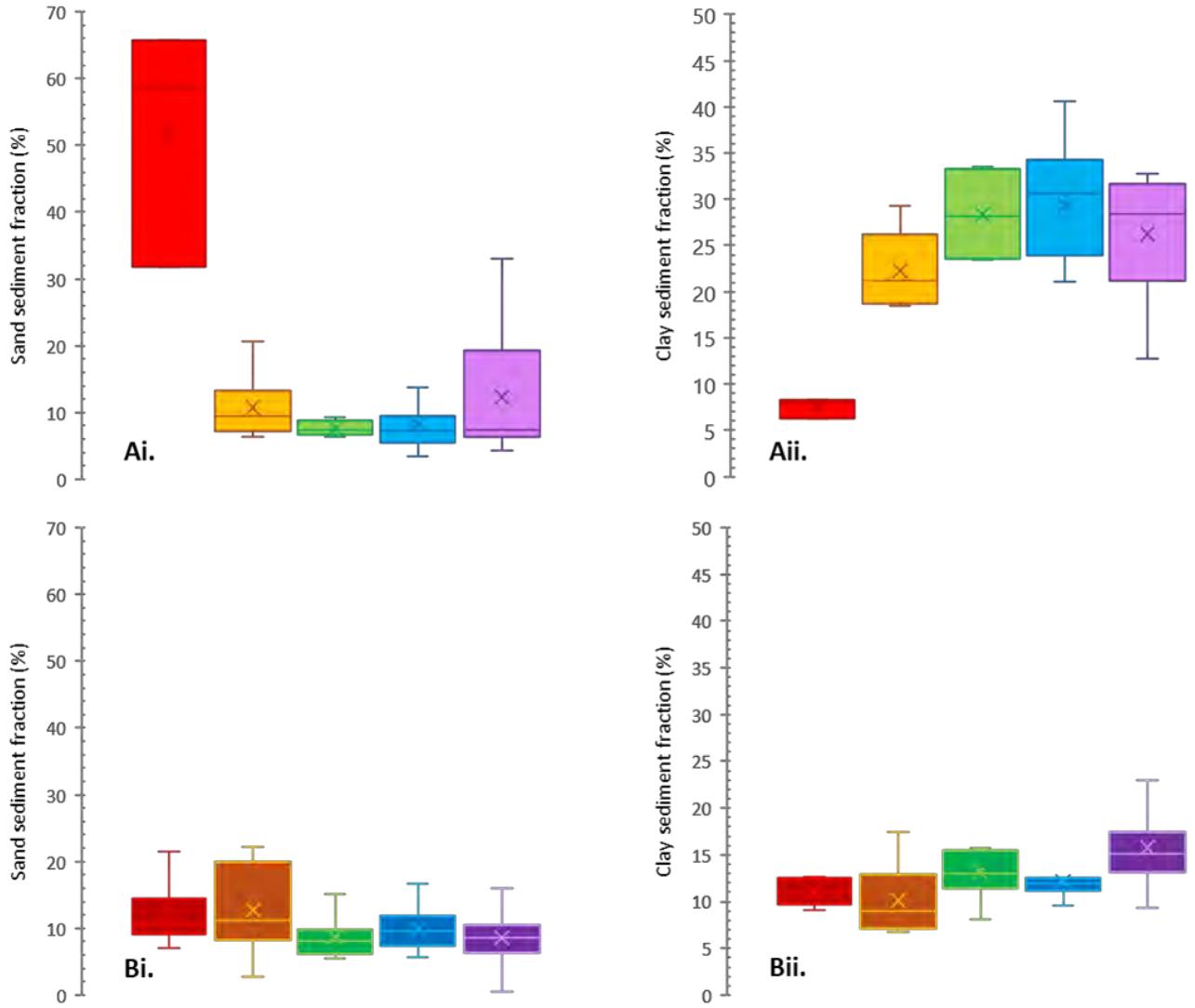

Figure 5.30 Box and whisker diagrams showing percentage sand fraction (Ai and Bi) and percentage clay fraction (Aii and Bii) for the different floodplain geomorphic units identified (Red- Bank and levee, Orange- Proximal floodplain, Green- Floodplain surface, Blue- Oxbow, and Purple- Backswamp) in the A) Gatberg River and B) the Minnehaha River floodplain systems

Figure 5.31 shows two box and whisker plots depicting the percentage organic matter content for the different geomorphic units identified across the floodplain surface of A) Gatberg River and B) Minnehaha River floodplain systems.

The figure for the Gatberg River floodplain system shows that the bank and levee geomorphic unit had the lowest organic matter content, with a mean of 3.5 % and a median of 3.0 % for all the samples. The organic matter content more than doubled from the bank and levee geomorphic unit to the proximal floodplain. The median organic matter content for the proximal floodplain was 8.7 %, with a mean of 10.0 %. The rest of the floodplain surface had a median and mean organic matter content of 13 %. Oxbows had the greatest organic matter content, with a median of 11.5 % and a mean of 14.8 % (range between 7 and 30 %). The backswamp geomorphic unit had a median of 11.3 % and a mean of 12.0 %.

The figure for the Minnehaha River floodplain system shows that the bank and levee geomorphic unit had the second lowest organic matter content, with a median and mean of 7.6 %. The proximal floodplain samples had a median and mean of 9.0 % organic matter content. The rest of the floodplain surface had a mean organic matter content of 9.0 % and a median of 8.1 %. Oxbows had the highest organic matter content, median, and mean of 13.2 %. The backswamp geomorphic unit had the lowest organic matter content, with a median of 6.7 and a mean of 7.2 %.

The Gatberg River floodplain had a greater percentage of organic matter content, with most sample medians being characterised with above 10 %, except for the bank and levee and the proximal floodplain geomorphic units where the samples were less than 10 %. In comparison, the Minnehaha River floodplain samples were dominated by a percentage of organic matter content less than 10 %, except for the oxbow geomorphic unit which was dominated by values greater than 10 %.

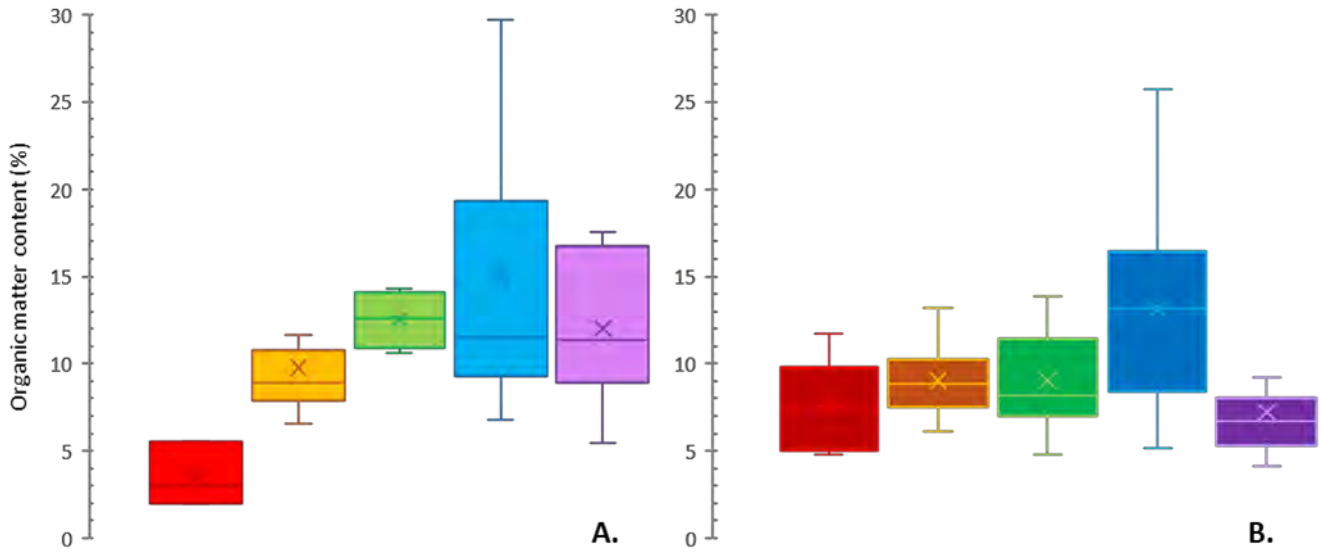

Figure 5.31 Box and whisker diagrams showing percentage organic matter content for the different floodplain geomorphic units identified (Red- Bank and levee, Orange- Proximal floodplain, Green- Floodplain surface, Blue- Oxbow, and Purple- Backswamp) in the A) Gatberg River and B) the Minnehaha River floodplain systems

Figure 5.32 shows two box and whisker plots depicting the total phosphorus concentration for the different geomorphic units identified across the floodplain surface of the Gatberg River (A) and Minnehaha River (B) floodplain systems.

The figure for the Gatberg River floodplain system shows that the bank and levee geomorphic unit had the lowest total phosphorus concentration, with a mean and a median of 0.07 g kg^{-1}. The total phosphorus concentration increased slightly from the bank and levee geomorphic unit to the proximal floodplain. The median total phosphorus concentration for the proximal floodplain was 0.09 g kg^{-1}, with a mean of 0.10 g kg^{-1}. The rest of the floodplain surface had a median and mean total phosphorus concentration of 0.10 and 0.09 g kg^{-1}, respectively. Oxbows had the highest total phosphorus concentration, median and mean 0.13 g kg^{-1} (range between 0.04 and 0.21 g kg^{-1}). The backswamp geomorphic unit had the second-highest total phosphorus concentration, with a median of 0.12 g kg^{-1} and a mean of 0.11 g kg^{-1}.

The bank and levee geomorphic unit in the Minnehaha River floodplain system had the second lowest total phosphorus concentration, with a median and mean of 0.11 g kg^{-1}. The proximal floodplain samples had a median of 0.12 g kg^{-1} and a mean of 0.13 g kg^{-1} total phosphorus concentration. The rest of the floodplain surface had a mean and median total phosphorus concentration of 0.12 g kg^{-1}. Oxbows had the highest total phosphorus concentration, median and mean of 0.21 and 0.20 g kg^{-1}, respectively (range

between 0.10 and 0.37 g kg^{-1}). The backswamp geomorphic unit had the lowest total phosphorus concentration, with a median and mean of 0.08 and 0.09 g kg^{-1}, respectively.

The Minnehaha River floodplain was dominated by a higher overall total phosphorus concentration, except for the backswamp geomorphic unit compared to the Gatberg River floodplain samples.

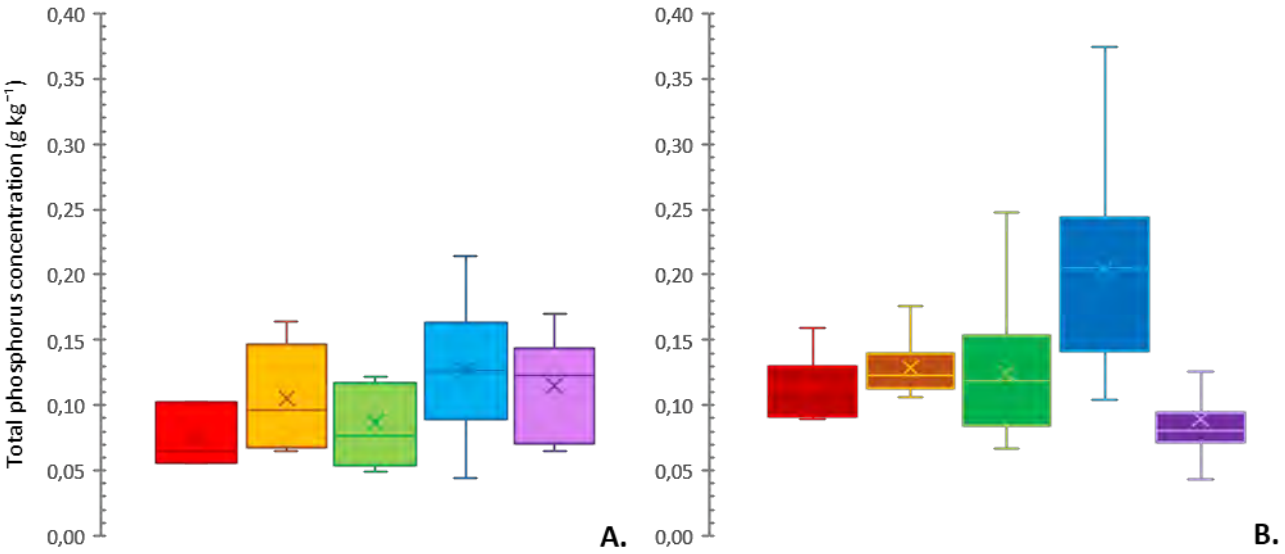

Figure 5.32 Box and whisker diagrams showing total phosphorus concentration for the different floodplain geomorphic units identified (Red- Bank and levee, Orange- Proximal floodplain, Green- Floodplain surface, Blue- Oxbow, and Purple- Backswamp) in the A) Gatberg River and B) the Minnehaha River floodplain systems

Figure 5.33 shows six box and whisker plots depicting the total iron, aluminium, and magnesium concentrations for the different geomorphic units identified across the floodplain surface of the A) Gatberg River and B) Minnehaha River floodplain systems.

The figure for the Gatberg River floodplain system shows that the median and mean iron concentration in all the samples taken across all the geomorphic units was between 0.3 and 0.7 g kg^{-1}. The bank and levee geomorphic unit had the lowest total iron concentration, with a mean and a median of 0.3 g kg^{-1}. Oxbows had the highest total iron concentration, median and mean 0.6 and 0.7 g kg^{-1}, respectively (range between 0.2 and 1.5 g kg^{-1}). The backswamp geomorphic unit had the second-highest total iron concentrations, with a median and mean of 0.5 g kg^{-1}. Figure 5.33Aii shows that the median and mean aluminium concentration in all the samples taken across all the geomorphic units was the highest out of all the geochemical measurements (iron, aluminium, and magnesium). All the median and mean aluminium concentration values ranged between 2.2 and 3.7 g kg^{-1}. The bank and levee geomorphic unit had the lowest total aluminium concentration, with a mean and a median of 2.2 g kg^{-1}. The floodplain

surface geomorphic unit had the greatest total aluminium concentration, median and mean 3.7 g kg^{-1} (range between 3.5 and 3.9 g kg^{-1}). The oxbow geomorphic unit had the second highest total aluminium concentrations, with a median and mean of 3.3 and 3.5 g kg^{-1}, respectively. However, the oxbow geomorphic unit had the largest range, between 2.0 and 5.7 g kg^{-1}. Figure 5.33Aiii shows that the median and mean magnesium concentration in the samples taken across all the geomorphic units was the lowest among all geochemical measurements (iron, aluminium, and magnesium). All median and mean magnesium concentration values ranged from 0.2 to 0.3 g kg^{-1}. The backswamp geomorphic unit had the lowest total magnesium concentration, with a mean of 0.2 and a median of 0.1 g kg^{-1}. The floodplain surface geomorphic unit had the greatest total magnesium concentration, a mean of 0.3 and a median of 0.2 g kg^{-1} (range between 0.2 and 0.4 g kg^{-1}).

The figure for the Minnehaha River floodplain system shows that the median and mean iron concentration in all the samples taken across all the geomorphic units was the highest out of all the geochemical measurements (iron, aluminium, and magnesium). All the median and mean iron concentration values ranged from 4.5 to 7.9 g kg^{-1}. The bank and levee geomorphic unit had the highest mean and median value, 7.9 g kg^{-1}. The backswamp geomorphic unit had the lowest total iron concentrations, with a median and mean of 4.5 and 4.9 g kg^{-1}, respectively. However, the backswamp geomorphic unit had the greatest range of values, from 1.6 to 10.1 g kg^{-1}. Figure 5.33Bii shows that the median and mean aluminium concentration in all the samples taken across all the geomorphic units ranged between 2.3 and 3.5 g kg^{-1}. The bank and levee, the proximal floodplain and the oxbow geomorphic units all had the highest total aluminium concentration, with a mean of 3.4 and a median of 3.5 g kg^{-1}. However, the oxbow geomorphic unit had the largest range, between 1.1 and 5.4 g kg^{-1}. The backswamp geomorphic unit had the lowest total aluminium concentrations, with a mean of 2.6 and a median of 2.6 g kg^{-1}. Figure 5.33Biii shows that the median and mean magnesium concentration in all the samples taken across all the geomorphic units was the lowest of all the geochemical measurements (iron, aluminium, and magnesium). All median and mean magnesium concentration values ranged between 0.06 and 0.34 g kg^{-1}. The backswamp geomorphic unit had the lowest total magnesium concentration, with a mean and a median of 0.12 and 0.11 g kg^{-1}, correspondingly. The bank and levee and the proximal floodplain geomorphic units had the highest total magnesium concentration, median and mean 0.17 g kg^{-1}.

The Minnehaha River floodplain was dominated by a greater overall total iron concentration compared to the Gatberg River floodplain samples. In the Minnehaha system, iron concentrations were highest in the bank and levee geomorphic and lowest in the backswamp geomorphic unit, whereas in the Gatberg

system, the greatest concentration was in the oxbow geomorphic unit and the lowest in the bank and levee geomorphic unit. Aluminium concentrations were similar in both floodplain systems. The highest aluminium concentrations were found in the floodplain surface geomorphic unit in the Gatberg system and in the bank and levee and proximal floodplain in the Minnehaha River system. For both floodplain systems, total magnesium concentrations were the lowest of the measured geochemical variables. Magnesium concentrations were slightly higher in the Gatberg River system across the geomorphic units. For the Gatberg River floodplain system, the proximal floodplain and the floodplain surface had the highest magnesium values. For the Minnehaha River floodplain system, the bank and levee and proximal floodplain had the highest magnesium values. For both systems, the lowest magnesium concentration occurred in the backswamp geomorphic unit.

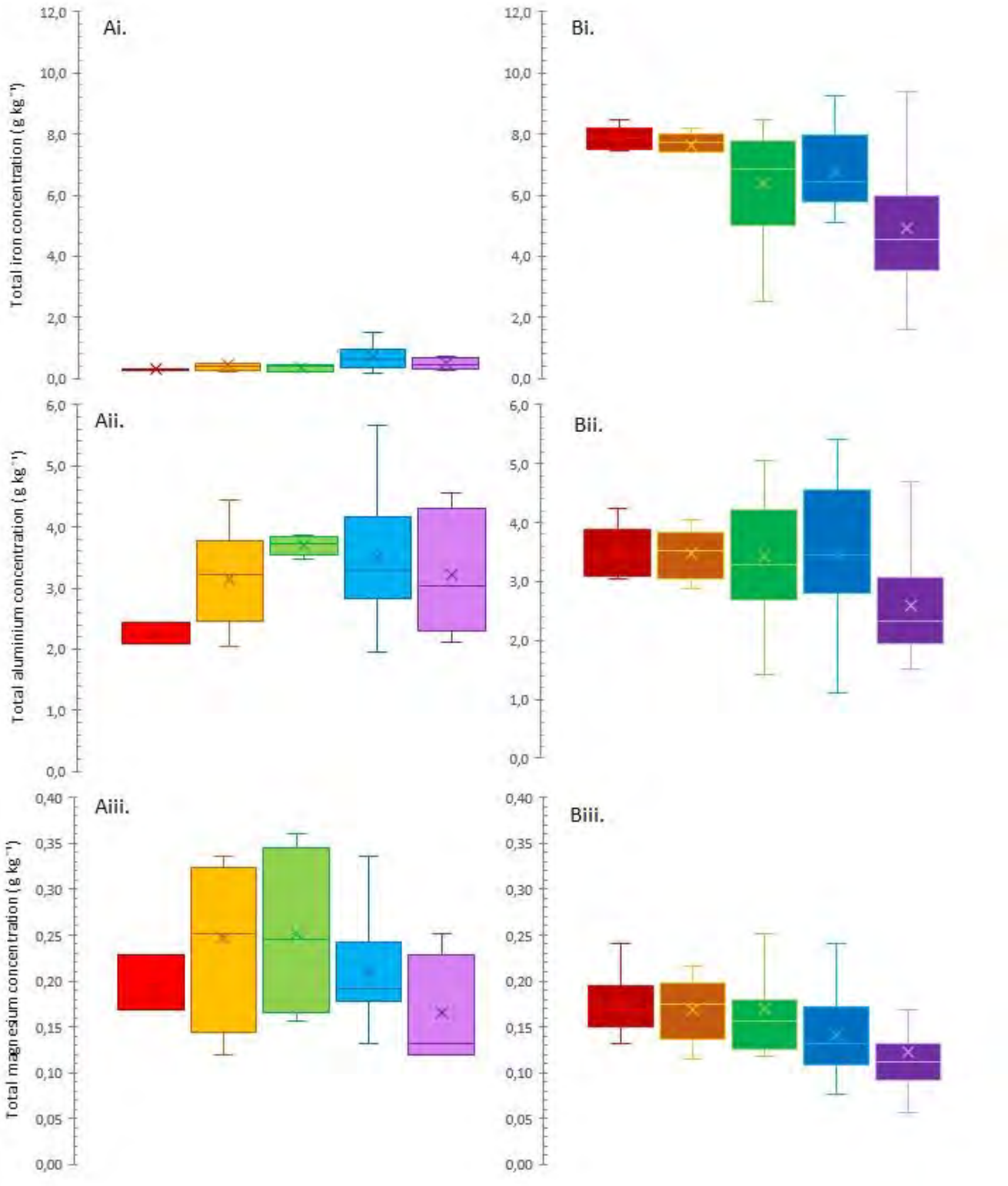

Figure 5.33 Box and whisker diagrams showing iron concentration (Ai and Bi), aluminum concentration (Aii and Bii), and magnesium concentration (Aiii and Biii) for the different floodplain geomorphic units identified (Red- Bank and levee, Orange- Proximal floodplain, Green- Floodplain surface, Blue- Oxbow, and Purple- Backswamp) in the A) Gatberg River and B) the Minnehaha River floodplain systems

5.4 DISCUSSION

5.4.1 INTRODUCTION

This section discusses the river and floodplain surface sediment and phosphorus results presented in Section 5.3. General river and floodplain characteristics, relationships, and trends are discussed.

5.4.2 CHANNEL AND FLOODPLAIN MORPHOLOGY

Rivers transport water, sediment, and dissolved elements from higher to lower elevations and eventually to the oceans. Under the action of gravity, this net flow of material travels downward. Both the Gatberg River and Minnehaha River reaches were characterised as mixed-bed meandering rivers with pools, riffles, and runs occurring down the system. Pools arise among the many meander bends and have lower elevations and slopes, whereas riffles and runs occur in the straight sections between the meander bends and have steeper slopes and higher elevations. Pools, riffles, and runs play an important role in sediment entrainment, transport, and deposition. According to the velocity-reversal concept (Keller 1971; Thompson 2011), near-bed velocities are stronger in riffles at low water levels and then increase in pools at the bank-full stage. At high-flow events, sediments are transported from pools and deposited in riffles, whereas the opposite is true during low-flow events, where sediments are transported from riffles and deposited in pools. Sediment at higher flows is deflected from the thalweg to the concave section of the bend due to helical flow depositing on point bars. The Gatberg River reach has a lower bed and floodplain surface longitudinal slope (0.04 and 0.06 %, respectively) compared to the Minnehaha River reach (0.15 and 0.14 %, respectively). Research has shown that vertical accretion is the dominant process along various low-gradient single-thread channels (Beckinsale and Richardson 1964; Schumm 1968; Ritter et al. 1975; Rose et al. 1980; Nanson and Young 1981; Burrin and Scaife 1984; Burrin 1985).

Floodplain morphology and the hydraulic patterns of the overbank flow constitute a major control over the amounts, calibre, and patterns of sediment deposition on floodplains. In general, variability in overbank sediment particle size deposition is driven by processes that work at two scales: the river branch and the individual floodplain section. Much of the variability in floodplain particle size deposition between river branches is determined by channel morphology, floodplain width, sediment load, and flow regime (Lecce 1997; Foster et al. 2002; Sweet et al. 2003; Lecce and Pavlowsky 2004). The primary explanation for the diversity of deposition within and between floodplains was the variation in hydraulic patterns of overbank flow and local topography (Lambert and Walling 1987; Nicholas and Walling 1997; Lecce and Pavlowsky 2004).

The Gatberg River floodplain research site is a relatively small floodplain "bead" (~0.3 km²) within a relatively large catchment (~135 km²), whereas the Minnehaha River floodplain research site is a comparatively large (~1.5 km²) floodplain within its catchment (~40 km²). Both floodplains varied in width downstream, the Gatberg floodplain was widest in the middle of the system (cross-sections 2 and 3), whereas in the Minnehaha floodplain system, the widest cross-sections were found at cross-sections 3 and 5. The floodplain/ channel width ratios in the Minnehaha system were over 3 times greater than those of the Gatberg system. The mechanisms of exchanging water and fine sediments between the main channel and floodplains in a meandering floodplain system govern geomorphological evolution and are critical for the preservation of floodplain ecosystem services. Juez et al (2019) found that these hydrodynamic and morphodynamic processes are influenced by variables such as the flow-depth ratio between the main channel and the floodplain, the width ratio between the main channel and the floodplain, and the floodplain land cover as defined by the type of roughness.

Both systems were characterised by typical floodplain features such as levees, oxbows, undulating micro-topography and backswamps. The Gatberg River crossed from one side of its floodplain to the other multiple times downstream, while the Minnehaha River generally meandered in the middle of its floodplain. The Gatberg River valley floor, which is primarily covered by the floodplain, has an average local relief of 0.4 m (minimum 0.07 m and maximum 1 m) over more than 250 m. The Minnehaha floodplain has an average local relief of 0.5 m (minimum 0.2 m and maximum 0.7 m) over more than 290 m. The ability of floodplains, like the Gatberg and Minnehaha floodplain systems, to provide multiple ecosystem functions is supported by a mosaic of environmental conditions, such as overbank floods and groundwater fluxes, which are shaped by floodplain topography, i.e. elevation, distance to the river, or roughness (Doble et al. 2006; Thonon et al. 2007), as well as the presence of floodplain geomorphic units, such as oxbows, scroll bars, secondary channels, and other undulating features (Jung et al. 2004; Acreman and Holden 2013). Elevation's influence on flooding parameters has ramifications for the functioning of floodplain ecosystems, such as sedimentation (Asselman and Middelkoop 1995; McMillan and Noe 2017). The hydrological distance reflects a water flow path from the channel to the floodplain and is related to floodplain connectivity (Heiler et al. 1995; Bracken and Croke 2007).

5.4.3 RIVER SEDIMENT AND PHOSPHORUS DYNAMICS

The Gatberg River floodplain and the Minnehaha River floodplain occur within the same climatic zone (warm temperate), geological setting (Stormberg Group, Karoo Supergroup) and the land use within both

floodplains is livestock grazing. Both rivers are mixed-bed meandering rivers. However, they show distinct differences in spatial variability of sediment characteristics and total phosphorus.

Fine material is conveyed in suspension in river systems, referred to as the suspended sediment load (Owens et al. 2005). The fine fraction contains organic and mineral particles (for example, sand and silt) with diameters greater than 0.45 µm and less than 2000 µm. Most of the material eroded from the surrounding landscape and transported by rivers comprises particles in this size range (Meade et al. 1990). Elevated suspended sediment loads in rivers are currently a global environmental problem that has intensified in recent decades (Woodward and Foster 1997). Suspended sediment may be temporarily stored in the channel during low to medium flows (below bankfull) and resuspended and transported during high discharge events. Meandering channels that typically characterise floodplain systems, like the Gatberg and Minnehaha River floodplain systems, store sediment in the channel along the inside bend of meander bends as point bars (Page et al. 2003; Rhoads 2020) and along the channel bed. Moody (2018) found that point bars were twice as efficient at trapping sediment than floodplains in the Powder River in the USA. This deposition is balanced by sites of erosion along the outer banks of meander bends (cut-banks) as the river migrates (Sundborg 1956; Wolman and Leopold 1957; Ritter et al. 1975; Jackson 1976; Nanson 1980).

5.4.3.1 INCOMING AND OUTGOING SEDIMENT AND PHOSPHORUS

Overbank sedimentation during flood occurrences is a critical component of floodplain development, maintenance, and structure. Overbank deposition of fine sediment, in addition to its relevance for floodplain development, frequently results in decreases of the suspended sediment load conveyed through a river system to the catchment outflow (Frickel et al. 1975; Trimble 1981; Walling 1983). Although deposition rates are typically low, and in some cases, nearly undetectable, significant volumes of sediment may be deposited due to the huge areas involved.

In the Gatberg and Minnehaha River floodplain reaches, over one wet season (multiple overbank events), the conveyance loss through the systems was approximately 44 % and 54 %, respectively, suggesting a decrease in sediment load. This most likely includes channel and floodplain deposition. Similarly, Middelkoop and Asselman (1995), for example, calculated that overbank deposition reduced the suspended sediment load transported by the River Waal in the Netherlands during a major (40-year) flood that occurred between December 1993 and January 1994 by approximately 19 %. However, it must be noted that a sediment budget approach generalises the site-specific variations which may be important. Furthermore, this approach assumes that deposition is uniform across the whole of the system.

It is critical to assess whether the material involved is just a fraction of the load entering the reach or if selective deposition occurs. The latter circumstance may be significant where sediment-associated nutrients were related to a certain fraction of the load. Nutrients, such as phosphorus, and many contaminants, such as heavy metals and pesticides, are well known to be transported in association with fine sediment (Allan 1986), and these sediment-associated contaminants are also deposited on river floodplains during overbank flows (Hudson-Edwards et al. 1999; Walling et al. 2000).

A preliminary analysis of sediment particle size characteristics upstream and downstream within the Gatberg and Minnehaha study reaches revealed intriguing patterns. Although both systems predominantly transported fine sediment, there was a discernible downstream fining trend, with suspended sediment at the system's head being coarser (24 µm for the Gatberg River and 20 µm for the Minnehaha River) than at its toe (17 µm and 15 µm, respectively). This suggests possible variations in sediment supply and transport dynamics along the river reaches.

Several factors may contribute to these variations. Differences in the sources of eroded material from the different land uses in the upper catchments of the floodplain systems e.g., sediment eroded from agricultural fields might be finer in composition than soils eroded from recently felled forestry plantation. Additionally, differences in river slope and tributary contributions between the Gatberg and Minnehaha systems may further influence sediment transport capacity and particle size distribution.

In conclusion, both the Gatberg and Minnehaha River floodplain systems retained sediment. The coarser fractions of the suspended sediment were reduced and deposited within the system over the wet season, suggesting these systems are probably storing sediment both in the river (short-term) and on the floodplain surface (short to long-term storage). Understanding the complexities of river sedimentation and its implications for sediment transport dynamics and pollutant deposition is crucial for effective river management and floodplain conservation efforts.

5.4.3.2 CHARACTERISING IN-CHANNEL SEDIMENT AND TOTAL PHOSPHORUS (BED AND BANKS)

During the study period, the D_{50} particle size distribution of the bed material along the Gatberg River ranged from medium silt to coarse sand (25 to 870 µm), with an average of 435 µm, which was slightly coarser than those found in the channel bed along the Minnehaha River, although the range was greater (range = 24 to 1237 µm, average = 248 µm). The deposits of the channel bed in the Gatberg River were dominated by the sand fraction (average = 79 %) with only 9 % average clay and silt fraction. Although the samples taken along the bed of the Minnehaha River were also dominated by the sand fraction (average = 58 %) they were lower than those found along the Gatberg River, and the clay and silt fraction was

greater along the channel bed of the Minnehaha River (average = 28 %). This probably reflects the finer sediment of the surrounding catchment on the Minnehaha River. Additionally, the coarser components could be trapped by the large wetland upstream and gentle slopes surrounding the Minnehaha floodplain. The tributaries that join the Gatberg River reach, especially the left bank tributary which is being eroded introducing some larger sediment into the reach.

Research has shown that the particle size of bed sediment usually decreases with distance downstream, i.e., from boulders and cobbles to sand, especially in large river systems (Surian 2002; Frings 2008). However, the D_{50} particle size in the Gatberg River does not decrease with distance downstream but rather shows two generalised characteristics: the channel bed shows a nonuniform trend in particle size with distance downstream, as well as the occurrence of sediment zonation, with riffles and runs sites having coarser material and pools and bars having finer material. Pools also had a higher percentage of the clay and silt fraction, whereas riffles had the highest percentage of gravel and sand fractions and the highest variability in sediment particle size fractions. This can be attributed to river sedimentological processes such as the dominance of selective transport mechanisms in the channel bed, variability in flow frequency, flood size, and tributary effect (Surian 2002; Frings 2008; Wang et al. 2009). High flow velocities in riffles promote turbulent mixing in pools, resulting in energy and velocity dissipation and finer sediment deposition (Surian 2002; Gordon et al. 2004; Brierley and Fryirs 2005; Wang et al. 2009; Brierley et al. 2013). High-flow energy turbulences create coarser particle sizes in riffles, which increases roughness during high flows.

5.4.4 FLOODPLAIN SURFACE SEDIMENT AND PHOSPHORUS DYNAMICS

5.4.4.1 SPATIAL VARIABILITY OF SEDIMENT CHARACTERISTICS

For floodplains such as those represented by the detailed study sites, variability in the particle size composition and sediment properties (such as organic matter content and total phosphorus concentration) of the sediment deposits will be controlled by the suspended sediment properties and the hydraulics of the local floodplain flow, which will in turn be influenced by river discharge as well as the local floodplain geometry and topography. The Gatberg River floodplain is a small system in a large catchment with many other floodplain systems, impoundments (e.g. artificial dams), tributaries, and land uses upstream, which affects the sediment supply and flows to this floodplain. In contrast, the Minnehaha River floodplain is a relatively large floodplain within a small catchment. There is another floodplain system upstream of the Minnehaha research site and a steep waterfall.

In general, deposits in the Gatberg River floodplain (mean = 17 µm, fine to medium silt) are finer than those in the Minnehaha River floodplain (mean = 22 µm, medium silt). However, the difference is minor and within the error margins of the particle size analysis methods. Floodplains and flood basins are typically composed of suspended loads when overbank deposition is a primary mechanism for the accretion and storage of sediment in the floodplain (Bridge 2003). There are two potential explanations for this variation. Firstly, the suspended sediment supplied to the floodplains will be different due to the slightly different geology and the occurrence of more 'storage units' upstream of the Gatberg system. In addition, the two tributaries entering the Gatberg system may introduce more suspended sediment than the Minnehaha system. The Minnehaha River has a steeper slope (3 %) compared to the 1 % slope of the Gatberg River, which increases the flow energy and consequently the capacity of the river to carry larger particle sizes. There could also be a geological influence; the Clarens Formation in the Minnehaha River catchment could bring in more coarse-grained material.

The Gatberg River floodplain deposits were dominated by clay and silt and only a small fraction of the floodplain was composed of sand. Floodplain sediment deposits also fined with increasing distance from the channel (D_{50} was 75 µm <10 m from the channel to <11 µm beyond 20 m), as expected based on the differential settling velocities of particles of the different diameters being transported away from the channel and the loss of flow energy and consequently the carrying capacity (Allen 1965; Pizzuto 1987; Asselman and Middelkoop 1995; Battin et al. 2008; Thonon 2006; Dunne and Aalto 2013; Swanson 2013).

Most of the sand fraction (52 %) was deposited in the first 10 m from the channel. The rapid reduction in the greater particle size (medium to fine sand) content in the sediment with increasing distance from the channel in the area close to the channel suggests that the fine fractions of the suspended sediment are transported onto the floodplain from the channel primarily through diffusive processes because the energy associated with overbank floodplain flow is generally relatively low. This is consistent with the diffusive model proposed by James (1985).

Fining of overbank sediment deposits has been documented on the Mississippi River, Powder River, and other rivers (see e.g., Moody et al. 1999; Autin and Aslan 2001). Moody et al. (1999) discovered that the Powder River's (a gravel-sand bed river) narrow floodplain bench fined with increasing distance from the channel. Even though sand made up around 18 % of the Powder River's suspended load and clay made up 47 %, sand made up 55 % of the sediment closest to the channel bank on the floodplain and only about 10 % in the floodplain trough. The floodplain crest, on the other hand, was made up of 10 % clay and the trough of 40 % (Moody et al. 1999). However, some outliers exist in the Gatberg system, and this may be

due to preferential flow paths, such as livestock tracks, increasing local slopes and flow velocities or/ and sediment inputs from the surrounding hillslopes.

The distance from the channel exerts an important influence, as the sediment is generally coarser in areas near the channel and finer in areas near the floodplain's outer margins. The degree of lateral advection and turbulence in the shear layer between the floodplain and channel most likely limited the distance sand travelled (Swanson 2013). The D_{50} particle diameter decreased rapidly (explained mostly by a logarithmic trend) with increasing distance from the channel; this was similarly observed on floodplains by Walling and He (1998) and in levee deposits by Adams et al. (2004). Adams et al. (2004) observed that the D_{50} of surface sediment decreased exponentially over the width of the Saskatchewan River levees. Walling and He (1998) noted a decrease in particle size with distance from the channel in surface sediments on small rivers in the UK, but distinguished two distinct deposition processes: an exponential decrease in coarse sediment deposition with distance from the channel and a layer of fine sediment deposited in proportion to the depth of the overlying flood water in the distal floodplain, most likely due to clay settling from the flood waters trapped in the floodplain.

On the other hand, the floodplain deposits of the Minnehaha River, although also dominated by the clay and silt fraction, were coarser than the Gatberg system. Although, the sand fraction did decrease (12 % <10 m from the channel to 9 % >60 m, and the finer sediment fraction did increase (11 % <10 m from the channel to 15.6 % >100 m) with distance on the Minnehaha floodplain it was much more subtle than the Gatberg system. The particle size of floodplain sediments was markedly constant as a function of distance from the channel for the Minnehaha system, suggesting that sediment transport is primarily associated with convective overbank flow, and this implies that the concentrations of fine sediment particles in the overlying floodwater will be relatively uniform across the floodplain surface. Therefore, rates of deposition of the sediment will be mostly governed by floodwater depth and consequently the local floodplain topography, with higher rates of deposition occurring in depression areas.

There could be topographical and morphological reasons for this difference between the two systems. Firstly, the Minnehaha floodplain is a much wider system with a less distinct slope towards the floodplain margin compared to the Gatberg floodplain. This could explain why the trend is weaker for the Minnehaha system due to the longer distances that sediment-laden flood water must travel. Second, the Minnehaha River has a lower sinuosity than the strongly meandering Gatberg River (sinuosity index of 2.4 and 3.75 respectively). Bathurst et al. (2002) found that transfer of sandy sediment (in their experiment having a D_{50} of 100 μm) only takes place in a confined strip along a straight channel, whereas it was deposited

further away on the floodplain in the case of a meandering channel because of stronger convective flow over the floodplain. Similarly, Hudson and Heitmuller (2003) found that the distance of sediment transfer onto the floodplain was greater for more pronounced meanders due to increased flow competence. In short, because of the more pronounced meandering of the Gatberg River, the stronger the relationship that particle size has with distance.

In the case of the Gatberg River floodplain, the sediment particle size parameters exhibit appreciable variation between the floodplain variables (relative distance downstream, relative channel elevation, channel bankfull width, channel depth, average channel depth etc.). There were statistically significant relationships with moderate trend analysis values between particle size parameters and distance downstream, relative floodplain surface elevation, and floodplain surface perpendicular slope (%); see Section 5.3.2.1. This result shows that there is significant fining from the sediment source (channel) which indicates perpendicular exhaustion of coarser suspended matter. This has been observed in other research (Walling and Moorehead 1989; Middelkoop and Asselman 1998; Walling and He 1998; Thonon et al. 2007; Kaase and Kupfer 2016). Although downstream variation in the particle size composition of suspended sediment will frequently exist and will influence the particle size composition of the floodplain deposits (Walling and Moorehead 1989; He and Walling 1997), local flow patterns, vegetation density and structure, and microtopography on the floodplains will also exert an important influence on the mean sediment particle size composition for each cross-section. For example, in the Gatberg floodplain, transect 2 is located downstream from a tributary and the D_{50} particle size is significantly higher than that associated with the D_{50} particle size from the other transects. On the other hand, the relatively high mean clay content in the sediment from transects 3 and 5 may reflect the relatively flat and broad nature of these transects. In the Gatberg floodplain system, the mean clay and silt content of the transects increases downstream, whereas the mean sand content decreases, with transect 1 having the lowest clay content and highest sand content. To a certain degree, this trend reflects a downstream fining of the suspended sediment transported and deposited through this reach. This has been observed in other research (Walling and Moorehead 1989; He and Walling 1997).

In the Minnehaha River floodplain system, within the sediment size parameters only D_{16}, D_{50} and percent clay fraction show a statistically significant relationship with distance downstream, although there were no significant trend analysis values associated with the relationship. Both the mean clay and silt and sand fraction contents exhibit some variation between the transects, where the percentage of clay and silt fraction increases with the distance downstream and the percentage of the sand fraction decreases with

the downstream distance. Although the coefficient determination is quite weak for both, see section 5.3.2.1, the D_{50} particle size (which falls within the medium silt fraction (15.6 - 31 µm) for all the transects) decreases downstream. To a certain degree, this trend reflects a downstream fining of the suspended sediment transported and deposited through this reach. In summary, sediment size parameters in the Minnehaha River floodplain system show little to no relationship with the floodplain or river variables measured, suggesting that other variables, such as flood water inundation extent, depth and residence time, or flow paths and velocities on the floodplain surface etc., are responsible for the variation in sediment particle size parameters.

Floodplains serve a variety of physical and ecological roles, which are intricately linked. The primary physical purpose of floodplains is to attenuate water flows, as well as dissolved material, sediment, and organic matter conveyed by floodwaters (Wohl 2021). Floodplain systems also play an important role in the global carbon cycle, owing to their ability to store soil organic carbon (Cole et al. 2007; Battin et al. 2009). In general, the organic matter content in the floodplain deposits on the Gatberg River system was slightly higher than that found in the Minnehaha River floodplain. In the Gatberg system, like the sediment particle size parameters, the percentage of organic matter content exhibits a statistically moderate relationship with distance from the channel (positive correlation), relative floodplain surface elevation and floodplain perpendicular slope (both had a negative correlation). However, the only association with organic matter content that was seen in the trend analysis was with the floodplain surface perpendicular slope. In comparison, the Minnehaha system's, percentage of organic matter content had no relationship with any of the physical floodplain and channel variables measured.

The soil organic matter content is associated with many soil properties, such as sediment particle size, sediment texture, nutrient content, and pH (Heger et al. 2021). Heger et al. (2021) found that the fine texture of sediment stored in floodplain forests was one of the strongest predictors of soil carbon stocks ($r^2 = 0.6$). Similar conclusions were drawn by other researchers (Pinay et al. 1992; Wigginton et al. 2000; Hoffmann et al. 2009; Graf-Rosenfellner et al. 2016; Hennings et al. 2021). In the surface floodplain samples of the Gatberg River, the percentage of organic matter content has a significant statistical relationship with the D_{16}, D_{50}, and D_{84} sediment sizes parameters, the percentage of sand, clay and silt, and clay fractions. However, the only significant trend analysis association was with the D_{84} sediment size. In comparison, the organic matter content in the Minnehaha floodplain system had no statistical relationship with the sediment size parameters. This could partly be explained by the longer high groundwater levels which will slow decomposition of soil carbon.

Phosphorus is one of two of the most studied solutes, the other being nitrogen. This is partially because they constitute a paradox. Although these elements are required by most living organisms, human activities have introduced large quantities of phosphorus and nitrogen into rivers the excess now causes severe environmental problems such as eutrophication, or a decrease in dissolved oxygen in the water that causes fish die-offs. Total phosphorus is the sum of all phosphorus compounds found in soils or a watercourse. Although in soils, phosphorus exists primarily as particulate (i.e., sediment-bound) phosphorus, with dissolved phosphorus accounting for less than 0.1 % of total phosphorus (Magette and Carton 1996). Within the Gatberg River floodplain system, the total phosphorus concentration in soils was found to be less than 0.25 g kg^{-1}. Within the Minnehaha River floodplain system, total phosphorus concentration in soils was found to be less than 0.40 g kg^{-1}. These soil total phosphorus content levels are far lower than those commonly reported in the literature. The United States national average total phosphorus concentration in soil, for example, is around 0.6 g kg^{-1} (Stevenson 1986; Abrams and Jarrell 1995) and for Africa is estimated to be 0.4 g kg^{-1} (He et al. 2021). However, most of the literature findings on soil total phosphorus concentrations come from croplands or pastures where fertiliser would enhance phosphorus inputs.

Within the Gatberg floodplain system, total phosphorus concentration had a moderate negative statistical relationship with the relative floodplain elevation and the perpendicular slope of the floodplain; however, only 10 % of the variation within the total phosphorus concentrations could be explained by the floodplain variables according to the trend analysis. Within the Minnehaha floodplain system, on the other hand, total phosphorus had a moderate negative significant relationship with distance from the channel and 30 % of the variation in the total phosphorus concentrations could be linked to this floodplain variable.

The Spearman's statistical analysis found significant relationships between total phosphorus concentration and the sediment particle size parameters within the Gatberg system. However, only 30 % of the variation in total phosphorus could be explained by the sediment particle size parameters. Total phosphorus concentrations in this system had the highest statistically significant positive relationship with organic matter content and the trend analysis found that the relationship between total phosphorus concentration and the percentage of organic matter content could be satisfactorily described by a simple linear regression line. In the surface samples of the Gatberg floodplain, total phosphorus had a moderate statistical relationship with iron and aluminium, although only 30 % of the variability of the total phosphorus concentrations could be explained by the variability of the geochemical variables.

Comparatively, in the Minnehaha system, Spearman's statistical analysis found significant relationships between total phosphorus concentration and the D_{16} particle size (positive relationship) and percentage of clay (negative relationship). However, only 20 % of the variation in total phosphorus could be explained by the fine sediment particle size content. Like the Gatberg system, total phosphorus concentrations in the Minnehaha system had the highest statistically significant relationship with organic matter content (positive relationship). This indicates that the relationship between the total phosphorus concentration and the percentage of organic matter content could be satisfactorily described by a simple linear regression line. In the surface samples of the Minnehaha floodplain, total phosphorus had a moderate statistical relationship with aluminium and magnesium, although the trend analysis found that only 40 % of the variability could be explained by these two geochemical variables. There was a strong statistical relationship between total phosphorus concentration with iron and calcium, and the trend analysis found that only 50 % of the variability could be explained by these two geochemical variables.

The relationship between fine particle content and total phosphorus concentration in soils is a well-established aspect of phosphorus geochemistry. Phosphorus sorption mechanisms play a crucial role in governing the availability and mobility of phosphorus in soil environments, such as floodplains.

Phosphorus sorption occurs primarily through the interaction of negatively charged phosphate ions (for example, $H_2PO_4^-$ and HPO_4^{2-}) with various soil constituents, including iron, aluminium, magnesium, calcium, and organic carbon. This process, documented by numerous studies (Williams and Saunders 1956; Tiessen et al. 1983; O'Halloran et al. 1985, 1987; Roberts and Strobel 1985; Day et al. 1987; Steegen et al. 2001; Six et al. 2002; Young et al. 2012), involves strong interactions between phosphate anions and soil particle surfaces, leading to tight binding of phosphorus.

Large specific surface areas of fine soil particles further enhance phosphorus absorption capacity, as highlighted in studies by Agbenin and Tiessen (1995) and Newman (1995), among others. This increased surface area facilitates greater contact between phosphate ions and soil particles, enhancing phosphorus retention.

The fixation of phosphorus is influenced by soil pH, with different mechanisms operating in acidic and alkaline soils. In acid soils rich in aluminium and iron oxides, both crystalline and amorphous forms, phosphorus solubility is reduced through fixation on positively charged surfaces and the formation of insoluble aluminium and iron precipitates. On the contrary, in alkaline soils, phosphorus readily interacts with calcium to form sparingly soluble calcium phosphates. Studies, such as that by Johan et al. (2021) in Malaysia, have illustrated the pH-dependent nature of phosphorus fixation. In acidic soils, phosphorus

becomes bound by sesquioxide, particularly iron and aluminium, resulting in reduced phosphorus availability. On the contrary, Johan et al. (2021), showed that under alkaline conditions, phosphorus precipitation occurs with calcium, limiting its availability. They discovered that phosphorus precipitates to both iron and aluminium when the soil pH is below 5.5 and calcium when the pH is above 7. Both the Gatberg and Minnehaha floodplain surface sediment had a pH of 5.5 and 5.6 respectively. Iron oxide minerals dissolve and release their adsorbed elements into the water column, such as phosphorus, when conditions become anoxic such as when floodplain surfaces are covered in flood waters (Dellwig et al., 2018; Häusler et al., 2018). These metals then become more readily bioavailable (Rogan Šmuc et al., 2018) or more easily transported back to the channel when the flood waters retreat.

5.4.4.2 FLOODPLAIN GEOMORPHIC UNITS

Meandering river floodplains are often made up of a variety of geomorphic units due to their nature and history (Schumm and Winkley 1994; Bridge 2003). A geomorphic unit is a landform constructed and reshaped by a specific set of earth surface processes. Every geomorphic unit has its own morphology and sediment characteristics (Minar and Evans 2008). Geomorphic unit assemblages and patterns represent the available energy at any given location in the landscape (Downs and Gregory 2014). The combination and balance of erosional and depositional processes in river systems create diverse patterns of geomorphic units at the reach scale. Given that geomorphic units make up all sections of all valley bottoms, the geomorphic unit analysis presents an applicable resource for doing systematic geomorphic research on river and floodplain systems (Brierley et al. 2013; Fryirs and Brierley 2013). Floodplain topography, a mosaic of geomorphic units, has a large impact on the spatial distribution of sediment that is eventually deposited along meandering alluvial floodplains during overbank flooding (Asselman and Middelkoop 1995; Nicholas and Walling 1997; Walling and He 1998).

The hydraulic connectivity of the meandering alluvial floodplains is determined by the interaction of the floodplain geomorphic units and the surrounding topography with the overbank flow. Given the topography of different floodplain geomorphic units, their distance from the channel, and their relative elevation, this interconnectivity is typically complex and dynamic (Cabezas et al. 2010). This implies that, regardless of type, each of these units may have a unique hydraulic connectivity to the river channel during overbank inundation. The hydraulic connectivity of a floodplain geomorphic unit can vary with flood magnitude since floodplain geomorphic units are typically more easily accessed by overbank flow as overbank height increases. Furthermore, because overbank inundation is a mechanism of conveying suspended sediment, the geographical patterns of overbank deposition may be comparable. The

floodplain geomorphic units identified in the Gatberg and Minnehaha River floodplain systems were: 1.) bank and levee, 2.) proximal floodplain, 3.) floodplain surface, 4.) oxbows, and 5.) backswamp (see Section 5.3.2.2).

At the reach scale, within the Gatberg floodplain system, the banks and levee geomorphic unit had the highest mean D_{50} particle size and percentage sand fraction, the lowest percentage clay fraction, organic matter content, and total phosphorus concentration. Oxbows had the lowest mean D_{50} particle size and percentage sand fraction, the highest percentage clay fraction, organic matter content, and total phosphorus concentration. Within the Gatberg floodplain system the biggest difference in the D_{50} particle size, the fine particle size fractions, and the organic matter content occurred between the oxbow geomorphic unit and the proximal floodplain. This result can be explained both morphologically and topographically. Firstly, the bank and levee geomorphic unit is the closest floodplain geomorphic feature to the channel and has a higher elevation compared to the rest of the floodplain surface; this area is more likely to receive more of the larger particle sizes as turbulent water carrying sand and finer particles spill onto the floodplain. The settling velocities of the coarser particles promote rapid deposition, with finer suspended sediment flowing onto the remainder of the floodplain. Whereas the oxbows are found across the floodplain at various distances from the channel and are characterised by lower elevations (depression-like features). Floodwaters are more likely to be stored in these depressions, allowing the finer particles and the associated adsorbed particles (organic matter content) to settle out of suspension. Similar results were found by Simm 1993; Swanson 2013; Thomas et al. (2022), and others. Interestingly, in the Gatberg floodplain system, the backswamp geomorphic unit had a secondary input of coarser sediment, probably from the surrounding hillslope and the unsealed gravel road.

Like the Gatberg system, within the Minnehaha floodplain system, the area closest to the channel had the highest D_{50} particle size and percentage sand fraction, and the lowest percentage clay fraction, organic matter content, and total phosphorus concentration. The lowest D_{50} particle size and the highest percentage clay fraction were found within the backswamp unit. The highest organic matter content and total phosphorus concentration were found within the oxbow geomorphic unit. Compared to the Gatberg system, in the Minnehaha River floodplain, the biggest difference between the sediment particle size fractions and the organic matter content occurred between the backswamp and almost all the other geomorphic units. This could be explained by the morphology of the floodplain system. The Minnehaha is a larger system with widths that extend much further away from the channel. In addition, all the old features occur relatively close to the channel in a narrow band.

5.5 CONCLUSION

The results presented above demonstrate that the particle size composition and properties (organic matter content and total phosphorus concentration) of the overbank floodplain deposits exhibit significant spatial variability. Cross-valley, downstream, elevation, and geomorphic feature variations in the grain size composition and properties of surface sediments representative of contemporary floodplain deposits have been documented within the study reaches. This spatial variability reflects the interaction between overbank floodplain flows and suspended sediment transport and deposition at these sites, which is in turn influenced by the local river planform and floodplain topography.

Within both the Gatberg and Minnehaha River floodplain systems, it was possible to relate differences in spatial variations of sediment particle sizes and sediment properties to geomorphological and hydrological variables such as floodplain width, sinuosity, distance from sediment source, microtopography, and catchment characteristics. Several trends were verified for the floodplain systems on the Gatberg and Minnehaha Rivers that have been reported in the literature. In general, sediment particle size decreases with increasing distance to the river. Total phosphorus concentrations increase with increasing fine particle size fractions (clay and silt) and organic matter content. However, exceptions to these trends show that they do not suffice to describe the pattern in more complex situations. For example, there may be secondary sources of sediment besides the river channel itself complex hydrodynamic patterns at the beginning of the flood inundation or the catchment characteristics that need to be considered.

CHAPTER 6 : FLOODPLAIN SEDIMENTATION RATES, SOIL PROPERTIES AND SEDIMENT-ASSOCIATED PHOSPHORUS ACCUMULATION RATES FOR TWO FLOODPLAIN SYSTEMS

6.1 INTRODUCTION

Floodplain systems are dynamic and important ecosystems along river corridors. Floodplains are vital buffers between the river and the surrounding land, attenuating floods, creating ecological 'hot spots' and transporting and storing overbank channel sediment and the associated nutrients and contaminants attached to that sediment. As floodplain systems are dynamic, sediment deposited on floodplains may be reworked in the future and may thus also become a source of nutrients and contaminants and become a problem for future river management (Conner and Day 1982; Brinson et al. 1984; Elder 1985; Leenaers and Schouten 1989; Stoeckel and Miller-Goodman 2001). Against this background, an improved understanding of the regulatory ecosystem services that floodplains provide, such as sediment trapping and phosphate assimilation, as well as the reworking of these systems, is needed. This is especially true for data-scarce dryland regions, like South Africa.

When considering the role of floodplain systems as sediment and nutrient sinks, attention commonly focuses either on the coarse channel deposits and the interaction between channel migration and floodplain construction and destruction (Wolman and Leopold 1957; Howard 1992) or on the fine over bank deposits which usually make up the large areas of most floodplains resulting in vertical accretion of the floodplain surface (Ottesen et al. 1989; Alexander and Marriott 1999; Gomez et al. 1999; Moody and Troutman 2000; Swanson et al. 2008). To better comprehend the role that storage plays in the supply of ecosystem services in floodplain systems, more information on the magnitude and spatial variability of overbank sedimentation rates is required both to quantify the processes involved and to provide a basis for model development (Pizzuto 1987; Nicholas and Walling 1996, 1997).

Methods for estimating overbank sedimentation rates on floodplain systems include the use of sedimentation traps (e.g., Gretener and Strömquist 1987; Lambert and Walling 1987; Asselmann and Middelkoop 1995), topographical surveys before and after events (e.g., Brown 1983; Marriot 1992; Walling et al. 1996), and dating sediment layers (e.g., Costa 1975; Trimble 1983; Lewin and Macklin 1987; Hupp 1988). However, each of these techniques has in-built assumptions and challenges. For example, sediment traps have representativeness problems and practical constraints on sampling density and potentially losing data if they get washed away. Topographical surveys rely on overbank deposits to be

measurable, previous data, and to be able to recognise the interface between the 'new' deposited sediment and the original floodplain surface. The use of sediment dating techniques will provide longer-term average values which will amalgamate inter-event variability.

The application of environmental radionuclides, specifically the fallout radionuclide caesium-137 (^{137}Cs) and unsupported lead-210 (^{210}Pb), has been widely used in documenting rates and patterns of floodplain sedimentation. Where down-profile variations in the concentrations of these radionuclides can provide a basis for establishing the recent chronology of overbank sediment deposition, and measurements of total radionuclide inventories can be used to estimate average sedimentation rates (e.g., Walling and He 1992, 1994, 1996 a, b, 1997; Walling et al. 1996; Terry et al. 2002, 2011; Ritchie et al. 2004; Hughes et al. 2009; Locas et al. 2010; Golosov and Walling 2014). There are many advantages over other methods for estimating overbank floodplain sedimentation, for example, the general applicability to a range of environments and locations, the medium-term timescales involved (i.e., 60 years for ^{137}Cs and 100 years for unsupported ^{210}Pb), the relatively low cost, and the potential for gathering data for many points on a floodplain and the potential to estimate the spatial variability of deposition rates and the patterns involved.

6.1.1 Sedimentation Rates: the use of Radioisotopes

Radioisotopes have now been recognised as the most used and reliable method to calculate sediment deposition and accumulation rates in estuarine, fluvial, and lacustrine environments (Robbins and Edgington 1975; DeLaune et al. 1978; Benoit and Rozan 2001; Kim et al 2003). This is generally achieved using a combination of ^{210}Pb and ^{137}Cs radioisotope dating procedures.

6.1.1.1 Lead-210 technique

Lead-210 (^{210}Pb) is a naturally occurring radionuclide and a product of the Uranium-238 decay series with a half-life of 22.2 years. Its presence in the atmosphere is due to the dispersion of Radon-222 (daughter of Radium-226) from the earth's crust into the atmosphere. The existence of ^{210}Pb in the atmosphere is short-lived, approximately 5 to 10 days (Krishnaswami et al. 1978). ^{210}Pb is then deposited on the earth's surface as atmospheric fallout, where it rapidly gets adsorbed to fine-grained sediment, iron-oxides, and organic matter. Approximately 90 % of all ^{210}Pb fallout is derived through precipitation, and consequently, ^{210}Pb fluxes are strongly linked to rainfall patterns (Binford 1993). However, deposition rates are thought to be constant and spatially uniform within a limited geographic area (DeLaune et al. 1989). ^{210}Pb is useful for determining the age of recent sediment because, provided that the atmospheric flux is constant, the

decay profile relates directly to the sedimentation rate. Hence, ^{210}Pb is useful for dating sediments up to a century old.

Not all Radon-222 escapes the earth's surface before it decays, and a portion of the ^{210}Pb present in the soil is formed in situ by the decay of Radium-226. A distinction is made between ^{210}Pb derived from the atmosphere (excess ^{210}Pb) and that derived from sediment (supported ^{210}Pb). The excess ^{210}Pb component of total ^{210}Pb activity is used in sediment dating. The total activity of ^{210}Pb shows an exponential decay with depth, assuming a uniform sedimentation rate over 100-150 years. However, due to anthropogenic and environmental effects, this is not often the case (Appleby and Oldfield 1978). Several models for ^{210}Pb analysis have been developed, depending on environmental conditions and sediment processes.

The Constant Rate of Supply (CRS) model is the most widely accepted and used model to determine ^{210}Pb-derived sedimentation rates. The model assumes that no post-depositional mixing or sediment disturbance has occurred. Assuming a constant fallout of ^{210}Pb, the CRS model can be used to determine the age of a given depth (z) by:

$$^{210}\mathbf{Pbxs(z)} = {}^{210}\mathbf{Pbxs(0)}e\text{-}\lambda t$$

Where ^{210}Pbxs(0) represents the excess activity of ^{210}Pb on the sediment surface, λ is the radioactive decay constant for ^{210}Pb (0.0311), and t is the deposition time. When ln^{210}Pbxs(z) is plotted against depth, the resulting profile is linear, and the accumulation rate can then be determined from the slope of this line.

The use of ^{210}Pb in sediment geochronology was pioneered by Goldberg (1964), Krishnaswami et al. (1971) and Ritchie et al. (1973). Nowadays it is applied in many fields of research in wetlands (Wang et al. 2004; Fávaro et al. 2007), estuaries (Weis et al. 2001; Pfister et al. 2004) and floodplains (Saxena et al. 2002; Aalto and Dietrich 2005) to estimate sediment accumulation rates over the last 100 - 150 years. Generally, an accumulation rate of 1 mm yr^{-1} or more is considered sufficient for ^{210}Pb dating (Oldfield and Appleby 1984). Accumulation rates below 1 mm yr^{-1} may still permit ^{210}Pb dating, however, they can introduce uncertainties and potential biases due to reduced signal strength, greater sediment mixing, and decreased dating precision. The accuracy of ^{210}Pb sediment age dating can be affected by post-depositional processes, such as compaction, bioturbation, and erosion, that disturb the sediment column. Therefore, an independent tracer is usually used in combination with ^{210}Pb to validate calculations derived from ^{210}Pb activity (Smith 2001). Typically, ^{137}Cesium is used as an independent time-stratigraphic marker to test the accuracy and validity of ^{210}Pb derived geochronology.

6.1.1.2 CAESIUM-137 TECHNIQUE

Caesium-137 (^{137}Cs) has a half-life of 30 years and is an artificial radionuclide that was introduced into the environment by nuclear weapons testing during the late 1950s and 1960s (Ritchie and McHenry 1990). ^{137}Cs was released into the atmosphere and was dispersed globally and subsequently deposited as fallout on the earth's surface.

Significant levels of ^{137}Cs fallout first appeared in 1954, with peak quantities detected in 1963. Since then, due to a global weapon testing ban, global atmospheric ^{137}Cs deposition has decreased steadily. Cambray et al. (1985) reported in 1983/1984 that fallout deposition rates of ^{137}Cs were below the limits of detection. The fallout of ^{137}Cs resulting from the Chernobyl explosion in 1986 was confined to Europe, with minimal effect on global fallout rates and patterns (Ritchie and McHenry 1990).

Like ^{210}Pb, once deposited, ^{137}Cs is adsorbed onto fine sediment particles. As such, it is a useful marker in soils. Although ^{137}Cs deposition occurred primarily through rainfall, fine sediment containing ^{137}Cs can be transported downstream during flood events and deposited in floodplains, wetlands, lakes, and oceans. The 1963 peak is used as a marker layer in sediment accumulation studies, thus offering an average sedimentation rate since then (Ritchie and McHenry 1990). When used in combination with measurements of ^{210}Pb fallout, ^{137}Cs is recognised as a useful tool for the calculation of sediment accumulation rates and the history of sediment-associated nutrients and contaminants in a variety of environments.

6.1.1.3 LIMITATIONS IN THE SOUTHERN HEMISPHERE

Although studies have successfully used both ^{210}Pb and ^{137}Cs for sediment dating, most of this research was conducted in the northern hemisphere (see, Walling and He 1997; Goodbred and Kuehl 1998; Owens and Walling 2002; Pavlovic et al. 2005). Very limited radioisotope research has been carried out in the southern hemisphere due to difficulties in obtaining ^{210}Pb concentration data that are above the detection limit of analysis (Owens and Walling 1996; Bonotto and de Lima 2006; Hughes et al. 2009). The annual supply of ^{210}Pb from the atmosphere can be eight times lower in the southern hemisphere compared to European and North American countries (Humphries 2008). ^{210}Pb fallout also declines with increasing latitude due to decreasing precipitation rates (Outridge et al. 2002).

The Southern Hemisphere similarly received approximately 10 times less ^{137}Cs fallout than the northern hemisphere (Figure 6.1; McCallan et al. 1980; Longmore et al. 1983). However, in the Southern

Hemisphere an initial rise in ^{137}Cs activity has been dated at ca. 1958 (Longmore 1982; Foster et al. 2005, 2007), even though the weapons fallout peak in 1965 is difficult to distinguish.

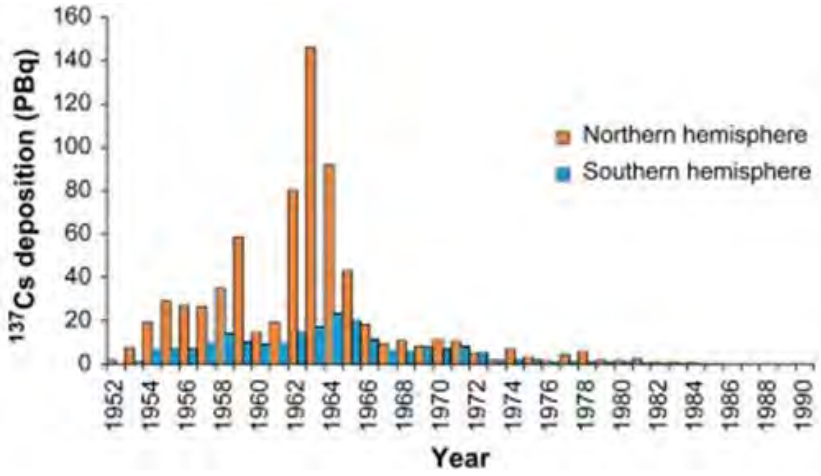

Figure 6.1 Comparison of ^{137}Cs deposition amounts from 1952 to 1990 for the Northern and Southern Hemisphere (McCallen et al. 1980; Longmore et al. 1983)

6.1.2 NUTRIENT ACCUMULATION RATES

Floodplain systems are generally known to be important material and energy sinks, sources, and transformations in landscapes (Johnston 1991; Mitsch and Gosselink 1993). Floodplains are biogeochemical "hotspots" because they are located between both terrestrial and aquatic systems allowing the transport and transfer of material and energy (McClain et al. 2003). Nutrient dynamics is an important part of the biogeochemical ecosystem service of floodplains because floodplains are areas of high productivity and decomposition, elevated nutrient loading rates, and dynamic nutrient processing at the oxidation-reduction boundary. In addition, floodplain vegetation reduces water velocity, making floodplains crucial areas for the deposition of suspended sediment and its associated nutrients and contaminants (Gurnell 1997).

Floodplains provide opportunities for nutrient uptake, transport, and storage during flooding when nutrient loading is at its most in rivers (Pinay et al. 1992). Floodplains can be sinks for inorganic, organic, dissolved, and particulate fractions of both nitrogen and phosphorus during overbank flooding (Yarbro et al. 1983; Hamilton and Lewis 1987; Tockner and Stanford 2002), but they can also be a source or transformer of some nutrient fractions (Conner and Day 1982; Brinson et al. 1983; Elder 1985; Stoeckel and Miller-Goodman 2001) during periods of re-suspension or erosion. In contrast, rivers have low

nutrient retention rates, with most of their nutrient load transported downstream (Alexander et al. 2000). Consequently, floodplains are important limiting zones within the conveyance of nutrients through a river catchment, or they may export less-bioavailable nutrient fractions, from rivers to downstream ecosystems.

Understanding and quantifying floodplain nutrient accumulation rates will help clarify their function in fluvial systems and identify the potential benefits of floodplain restoration and management.

6.1.3 TRENDS AND PATTERNS OF SEDIMENT AND PHOSPHORUS DEPOSITION AND ACCUMULATION ON FLOODPLAINS

Trends that have come out of research done on sedimentation rates show that sediment deposition decreases with increasing distance from the river. This trend was observed by He and Walling (1998); Middelkoop and Asselman (1998); Swanson 2013 and others. Fine particle sedimentation has been recorded to remain relatively constant with distance from the channel (Middlekoop and Asselman 1998). Sedimentation is greatest in floodplain features where flood flows (transport energy) rapidly decrease, such as levees, sloughs, edges of accessory channels, oxbows, and other depression-like floodplain features (Asselman and Middlekoop 1995; Bridge 2009; Pizzuto 2016). Conversely, areas with lower deposition rates tend to be farther from the channel and on elevated surfaces within the floodplain.

Vertical phosphorus distribution patterns are strongly related to silt and clay fraction contents within the sediment profile (Williams and Saunders 1956; Tiessen et al. 1983; O'Halloran et al. 1985, 1987; Roberts and Strobel 1985; Day et al. 1987; Six et al. 2002; Young et al. 2012). In their research, O'Halloran et al. (1985, 1987) concluded that soil texture variability resulted in soil total phosphorus variability. They found that changes in the sand fraction content produced the highest soil total-phosphorus variability, due to the strong negative correlation that phosphorus has to the sand fraction. In other words, the soil total phosphorus distributions follow similar trends to the fine sediment particles' vertical distributions regardless of the spatial location. Comparable results have also been described by other researchers (see Schilling et al. 2009; Ishee et al. 2015). In addition to these studies, the main parameters controlling the rates of phosphorus release and deposition in floodplain sediments are the phosphorus content of the parent material, the phosphorus supply, the topography, and the depth profile of the floodplain soil (Walker and Adams 1958, 1959; Walker 1965; Walker and Syers 1976; Roberts and Strobel 1985).

Floodplains are widely recognised for the sediment and nutrient storage and processing services they provide to society (Opperman et al. 2009). However, the overall magnitude by which floodplains store and process nutrients such as phosphorus is not well understood, especially in sub-humid, data-scarce

areas such as the Eastern Cape in South Africa. Understanding the role floodplains play in sediment and nutrient storage and processing is critical information needed to develop policy and management actions to address environmental problems such as eutrophication and climate change (Battin et al. 2008; Sutfin et al. 2016; Fabre et al. 2020).

Investigating sedimentation patterns and phosphorus assimilation within two floodplain systems in the Eastern Cape will significantly improve our understanding of the sediment and nutrient retention functions that these vital floodplains offer to a society which currently lacks comprehensive data. The focus objectives for this research are as follows:

1. Quantify historical sedimentation rates within the selected floodplain systems through sediment core analysis and ^{210}Pb and ^{137}Cs dating techniques.
2. Determine historical phosphorus storage rates within floodplain sediments by analysing phosphorus concentrations and distribution profiles.
3. Assess trapping efficiencies of sediment and phosphorus within the floodplain systems.
4. Investigate the influence of geomorphological factors on sedimentation patterns and phosphorus assimilation.

These specific objectives aim to address the broader goal of improving our understanding of sediment and nutrient retention functions in floodplains, with a focus on the Eastern Cape region, and to contribute valuable insights for informed decision-making and management strategies.

6.2 METHODS

6.2.1 FIELD DATA COLLECTION

Fieldwork was carried out between August 2019 and October 2021. Six sediment cores, between 50 and 120 cm deep, were taken at each study site (Gatberg and Minnehaha River floodplain systems; Figure 6.2). Samples from each core were sectioned at vertical intervals of between 2 and 5 cm. A small or large diameter gouge corer was used to core into the floodplain sediment depending on the consistency of the sediment found at each site, sectioned, and stored in sealed polyethylene bags. Coring sites were chosen to represent different geomorphic units found within the floodplain systems (e.g., the proximal floodplain -inner meander bend, outer meander bend, oxbows and backswamp). Each core was described according to its stratigraphy. Topographic elevation and core location sites were recorded using a differential GPS with a remote base station (accurate to 1 cm in the x, y, and z fields).

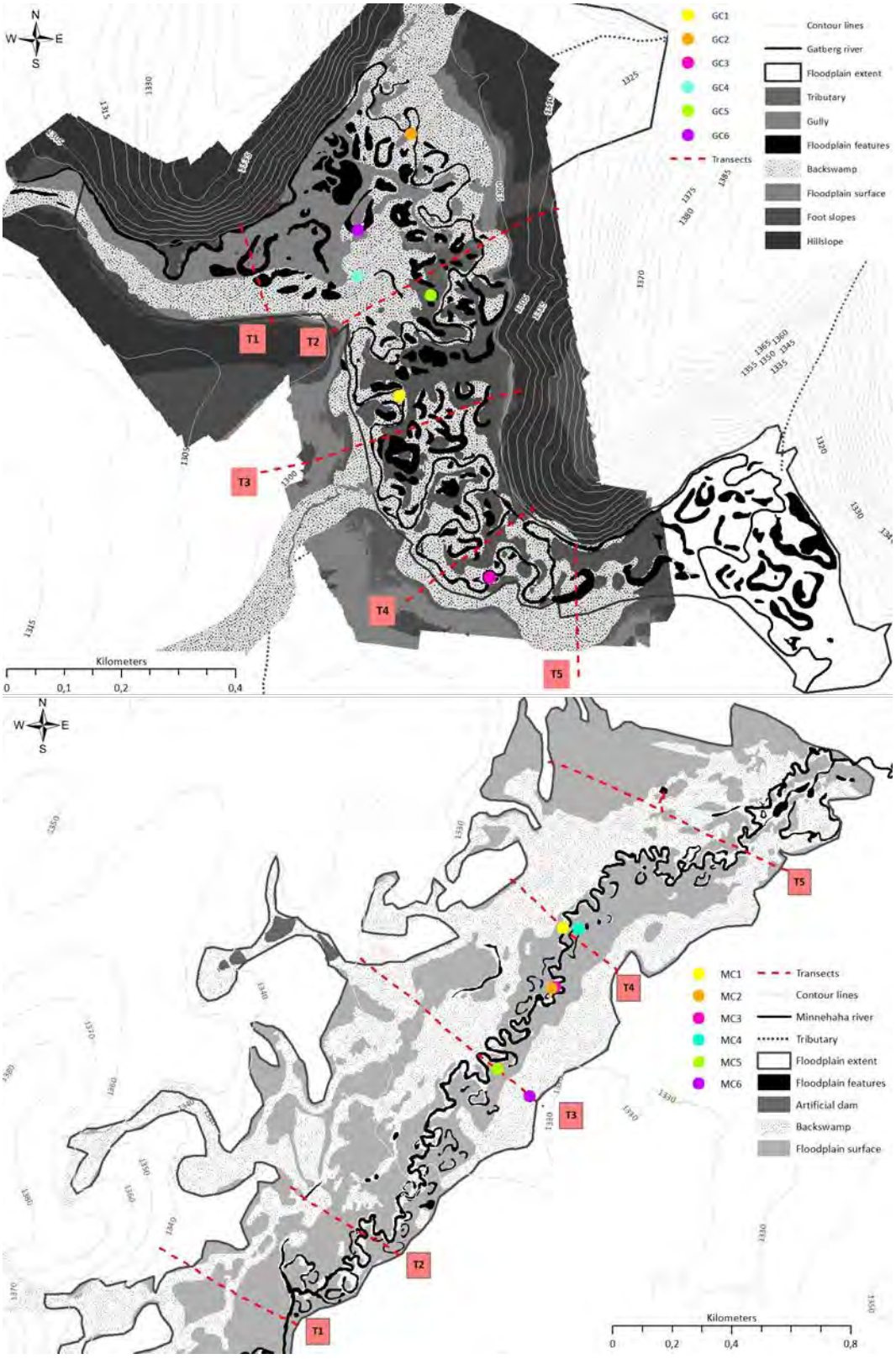

Figure 6.2 Core locations on the Gatberg River floodplain (top) and the Minnehaha River floodplain (bottom)

6.2.2 LABORATORY ANALYSIS

6.2.2.1 SEDIMENT ANALYSIS

All subsampled sediment samples (vertical increments) from the collected cores were oven-dried at 50°C, gently disaggregated, weighed, and passed through a 2 mm mesh sieve. Subsequently, the bulk density deposition amounts were calculated (g m^{-3}). After homogenising the sediment samples, the samples were subsampled (~5 g) to determine the organic matter content by the loss on ignition method at 450°C (Ball 1964) and presented as a percentage by mass. Samples were removed after 4 hours and placed in a glass desiccator for an hour to avoid moisture re-absorption while they cooled (Leonard et al. 2002). Once the crucibles and samples had cooled, they were reweighed, and the weight was recorded. The loss in mass following ignition was used as a representation of the organic matter content in each sample, expressed as a percentage of the original dry mass of the sample. After the organic matter was removed the same sub-samples were then separated into the absolute grain size distributions by laser diffraction using a Malvern Mastersizer 2000 (measuring range from 0.01 to 3500 µm). The particle size distribution is reported as median grain size (D_{50}), percentage by mass for sediment classes, using Wentworth's (1922) grain size classification scale, clay (0 - 4 µm), very fine silt (4 - 7.8 µm), fine silt (7.8 - 15.6 µm), medium silt (15.6 - 31 µm), coarse silt (31 - 63 µm), very fine sand (63 - 125 µm), fine sand (125 - 250 µm), medium sand (250 - 500 µm), coarse sand (500 - 1000 µm), and very coarse sand (1000 - 2000 µm), as well as the 16th, 50th and 84th percentage particle sizes by mass. These measures of sediment particle size and distribution were chosen to present the composition of the sediment samples as well as to sufficiently characterise trends in the vertical distribution of particle sizes within the cores on the floodplain.

The original homogenised sample was likewise subsampled (~35 g) and sent to an independent accredited analytical agricultural laboratory to analyse the soil samples for total phosphorus (TP), bioavailable phosphorus (OP) by the Bray II method, aluminium (Al), iron (Fe), magnesium (Mg) and calcium (Ca). These elements were chosen for their known effect on soil phosphorus adsorption. Total phosphorus in the soil samples was determined by a method adapted from Sommers and Nelson (1972). Phosphorus was extracted through acid digestion using a 1:1 mixture of nitric acid and hydrochloric acid at 80°C for 30 minutes. The phosphorus concentration in the extract was then determined with a Varian ICP-OES (Inductively coupled plasma-optical emission spectrometer). Organic phosphorus concentration in the samples was determined by the Bray II method, based on the reaction with 95 % Ammonium fluoride and 32 % Hydrochloric acid. Total extractable cations (Al, Mg and Ca) were extracted using 0.2 M ammonium

acetate. The micronutrient Fe was extracted with Di-ammonium EDTA (0.02 M) and boron (B) using a 1:2 hot water ratio (The Non-affiliated Soil Analyses Work Committee 1990).

In total, 6 cores for each floodplain wetland were divided into 160 core sections of 5 cm. A total of 69 samples were analysed for the Gatberg floodplain system and 91 samples for the Minnehaha floodplain system.

The spatial distribution of overbank deposition is variable, but the study of this variability is limited by the number of samples that can be analysed with the available time and funding.

6.2.2.2 ^{210}Pb and ^{137}Cs Geochronology

Sediment subsamples from each core were potted and then processed at the Environmental Sciences Laboratory at the University of Northampton, UK. Cores were tested for their inventories of ^{210}Pb and ^{137}Cs by gamma spectrometry, to derive estimates of the medium-term sedimentation rates at each of the sampling points for the two floodplain systems. All sediment samples for radioisotope analysis were air-dried, gently disaggregated and sieved to 63 µm. ^{137}Cs and ^{210}Pb measurements were made by gamma-ray spectrometry performed at the University of Northampton, using a low-energy Ge (Germanium detector) gamma spectrometer. A total of 160 samples were analysed. All activities were determined using a program called HYPERMET and all errors were determined from counting statistics and the error associated with the HYPERMET curve fitting routine (Phillips and Marlow 1976). The total ^{210}Pb was measured by its emission at 46.5 KeV and supported ^{210}Pb by the weighted average decays of ^{226}Ra daughters at 295, 351, and 609 KeV. Excess ^{210}Pb was calculated as the difference between the measured total ^{210}Pb at 46.5 KeV and the estimate of the supported ^{210}Pb activity (*^{210}Pbex = ^{210}Pbtot – ^{226}Ra derived supported Pb*). ^{137}Cs was determined using its gamma emission photopeak at 661 KeV. Samples were sealed for 21 days before analysis to allow for equilibrium between ^{226}Ra and ^{222}Rn (^{210}Pb is derived from the decay of gaseous ^{222}Rn, the daughter of ^{226}Ra (Joshi 1987)). Count times were typically in the range of 165 000 to 620 000 seconds, giving a measurement precision between ca. ±5 % and ±10 % at the 95 % confidence level. The distribution of excess ^{210}Pb with depth was used to calculate vertical accretion rates using the Constant Rate of Supply (CRS) model (Appleby and Oldfield 1978). All results were corrected for salt content and porosity.

The average overbank sedimentation rates of the two floodplain systems were determined for two different periods. The depth distribution of ^{137}Cs was used to estimate the average sedimentation rate since 1958. The approach is described in detail in Longmore (1982); Walling and He (1997); and Foster et al. (2005, 2007). It is based on the known temporal pattern of atmospheric fallout of nuclear weapon-

derived ^{137}Cs, which first peaked in 1958 in the southern hemisphere and the assumption that the peak ^{137}Cs concentration in the floodplain sediment profile can be equated with the 1958 fallout peak. The second approach is to use the excess ^{210}Pb using the CRS model to determine the sedimentation rates over the last 100 years. Unlike ^{137}Cs, it can be assumed that the fallout of unsupported ^{210}Pb is effectively constant over time. Due to radioactive decay, accumulating overbank sediments tend to exhibit an exponential decrease in the content of unsupported ^{210}Pb with depth, and the rate of decrease allows the average sediment accumulation rate to be estimated over the last ~100 years (i.e., five times the 22.2 years half-life of ^{210}Pb).

6.2.3 DATA ANALYSIS

Sediment accumulation rates were calculated using ^{210}Pb and ^{137}Cs derived sediment ages and the averaged dry bulk density (DBD) of each dated sediment profile (Eq. (1)). The rate of phosphorus accumulation was calculated using sediment accumulation rates and averaged total phosphorus concentrations in the surface depth increments of the dated sediment profiles (Eq. (2)):

$$\textit{(Eq. (1)) Sediment accumulation rate (g m}^{-2}\textit{ yr}^{-1}\textit{) = accretion (m yr}^{-1}\textit{) x DBD (g m}^{-3}\textit{)}$$

$$\textit{(Eq. (2)) Total phosphorus accumulation rate (g m}^{-2}\textit{ yr}^{-1}\textit{) = sediment accumulation rate (g m}^{-2}\textit{ yr}^{-1}\textit{) x total phosphorus concentration (g g}^{-1}\textit{)}$$

To place the estimates of floodplain storage of sediment for each floodplain storage unit within the broader context of the sediment budgets for the study catchments, it is useful to compare them with estimates of the suspended sediment yields. As there were no measured, estimated, or modelled suspended sediment yields for the two study sites, scaled estimates from a neighbouring catchment (Pot River Catchment, 47-79 t km^{-2} yr^{-1}), were used (see Bannatyne et al. (2022) for sediment yield estimates). This was chosen to represent the closest suspended sediment yield values that could occur within the Gatberg and Minnehaha River catchments, due to its similar geology, climate, and land cover and use.

The potential sediment trapped and exchanged per geomorphic feature was calculated to estimate sediment and trapping efficiencies. This was done by using the average sedimentation and phosphorus accumulation for each geomorphic unit and multiplying it by the area of each geomorphic unit. The area of the units was estimated by mapping each unit as polygons in ArcMap 10.8.2.

6.3 RESULTS

6.3.1 SEDIMENTATION RATES USING PB-210 AND CS-137 GEOCHRONOLOGY

The cores were positioned to target the main geomorphic units found in the floodplain systems. For each system, two inner bends, an outer bend, two oxbows, and a core within the backswamp zone were taken (Figure 6.3). Field evidence (e.g., debris and fine sand deposits) was observed at the locations of the cores on the inner and outer bends confirming that these levels were still active and were inundated frequently. The oxbows were located further away from the channel; however, observations in the field suggest that these are still connected to the channel and experience inundation as well as deposition. The backswamp areas were observed to be inundated throughout the wet season (2019-2021). This suggests that all geomorphic units are still active and are frequently inundated during overbank flood flows.

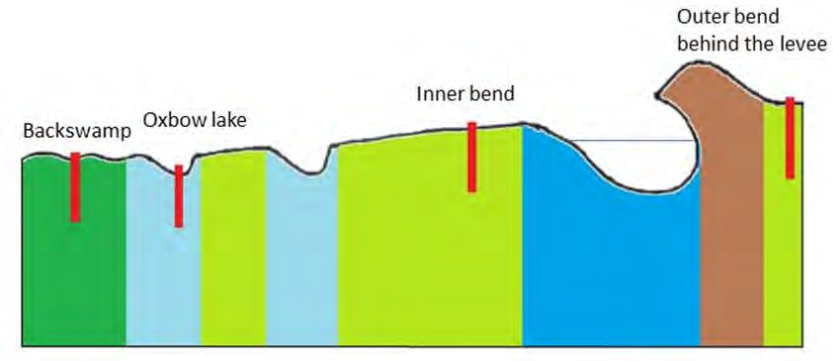

Figure 6.3 Schematic showing the core locations in each floodplain geomorphic unit

6.3.1.1 TEMPORAL VARIATION IN SEDIMENTATION RATES OF THE GATBERG AND MINNEHAHA RIVER FLOODPLAINS SYSTEMS

Figure 6.4 and Figure 6.5 illustrate the contrasting depth distributions of ^{137}Cs and unsupported ^{210}Pb in floodplain cores collected from sites characterised by different sedimentation rates in the Gatberg and Minnehaha River floodplain systems, respectively.

In the Gatberg River floodplain system, ^{137}Cs activities for the cores ranged between 0 and 9.54 mBq g^{-1} and unsupported ^{210}Pb values for the cores ranging from 0 to 392.45 Bq g^{-1}, with multiple peaks or detectible activities along each core. All cores showed a clear zero ^{137}Cs section at the bottom of each core. The first occurrence of ^{137}Cs can thus be used as the 1958 marker (first peak in Cs fallout in the southern hemisphere) with confidence. Generally, unsupported ^{210}Pb increased towards the surface for the cores, with the biggest increase for the two oxbows cores 5 and 6). This showed that sediment has

been accumulating steadily at these sites. The dates produced for the cores estimated the initiation of accumulation as pre-1936; except for core 6, the dates showed an initiation of accumulation pre-1950.

In the case of cores 1 and 3 which were collected on inner bends, the 1958 ^{137}Cs peak is located at ca. 50 and 40 cm depth (4.33 and 0.9 mBq g^{-1}), respectively, while the peak for the core collected from core 2 which was collected on the outside bend, is located at ca. 30 cm depth (2.2 mBq g^{-1}). Core 4's peak was at ca. 45 cm (1.77 mBq g^{-1}), located in the backswamp. Cores 5 and 6, both located in oxbows, the ^{137}Cs peaks occurred at depths of 45 and 40 cm (1.76 and 1.75 mBq g^{-1}).

In the Minnehaha River floodplain system, the ^{137}Cs activities for the cores had a slightly higher range of 0 to 14.31 mBq g^{-1}, with multiple peaks or detectable activities along each core, except for core 6 which had a single peak. All cores except core 5 showed a clear zero ^{137}Cs section at the bottom of each core. Although the results from core 5 are comparable to the other sedimentation rates and fall within an acceptable range for sedimentation rates in oxbows (Wren et al. 2019; Davidson et al. 2004; Lo et al. 2022), there is a low certainty attached to the results. Core 5 might have a higher average sedimentation rate compared to core 4, the other oxbow tested, because core 5 is upstream and may receive more flood waters with more sediment. Unsupported ^{210}Pb values for the cores ranged from 0.63 to 733.53 Bq g^{-1}, with multiple peaks along each core. Generally, unsupported ^{210}Pb increased towards the surface for the cores, with the biggest increase for the two oxbows (cores 4 and 5). The dates produced for the cores estimated the initiation of accumulation as pre-1940, except for core 3, the dates showed an initiation of accumulation before 1921.

In the case of cores 1 and 3 which were collected on inner bends, the 1958 ^{137}Cs peak is located at ca. 100 and 70 cm depth (0.68 and 1.56 mBq g^{-1}), respectively, while the 1958 ^{137}Cs peak for the core collected from the outside bend, core 2, is located at depth of approximately 40 cm (0.45 mBq g^{-1}). Cores 4 and 5, both located in oxbows, the ^{137}Cs peaks occurred at depths of 32 and 60 cm (0.65 and 0.38 mBq g^{-1}). Core 6's 1958 ^{137}Cs peak was at ca. 15 cm (2.14 mBq g^{-1}), located in the backswamp.

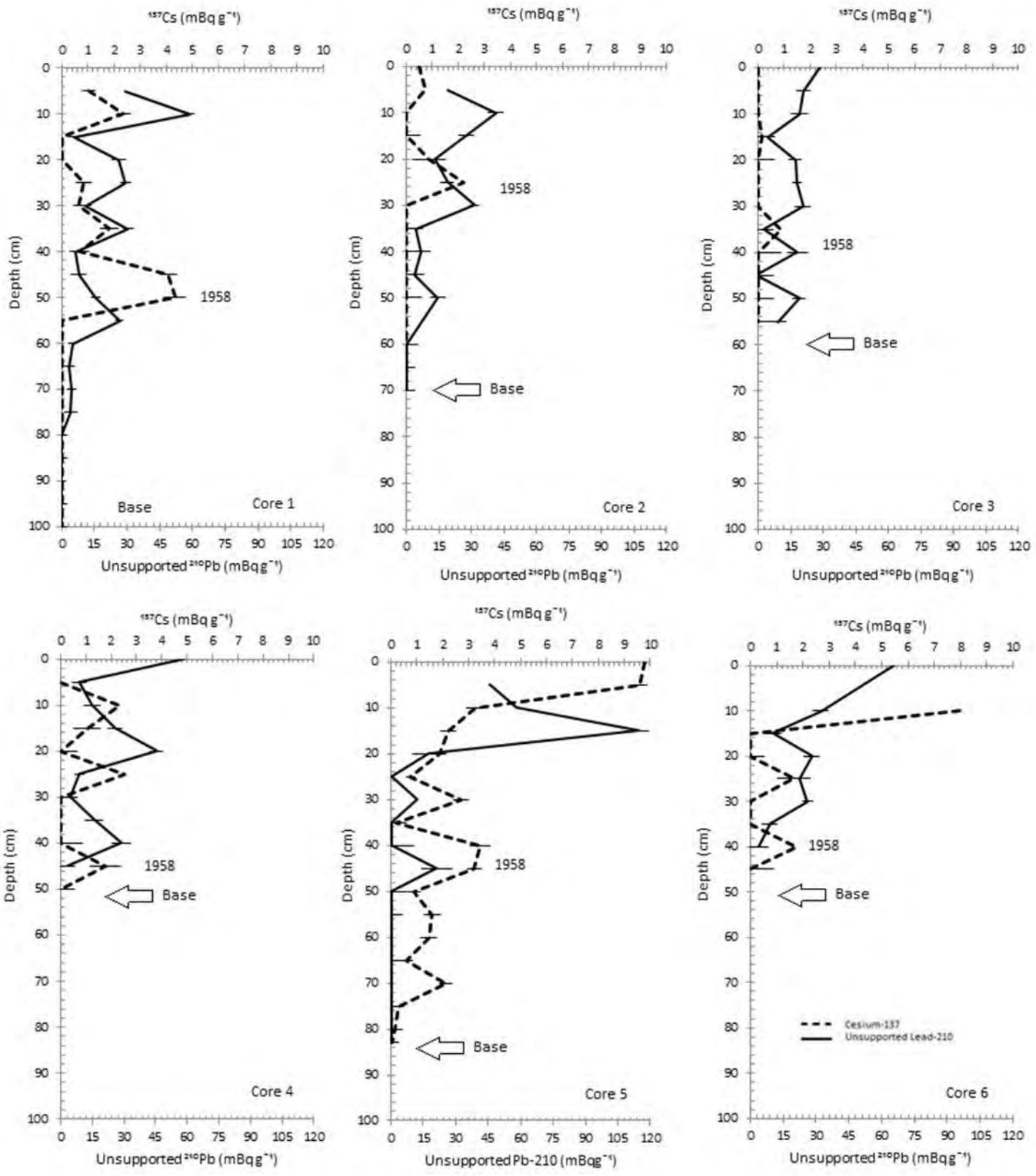

Figure 6.4 ^{137}Cs and unsupported ^{210}Pb data for cores: Core 1. Inner bend, Core 2. Outer bend, Core 3. Inner bend, Core 4. Backswamp, Core 5. Oxbow, Core 6. Oxbow in the Gatberg River floodplain system. Measurement error given by horizontal lines

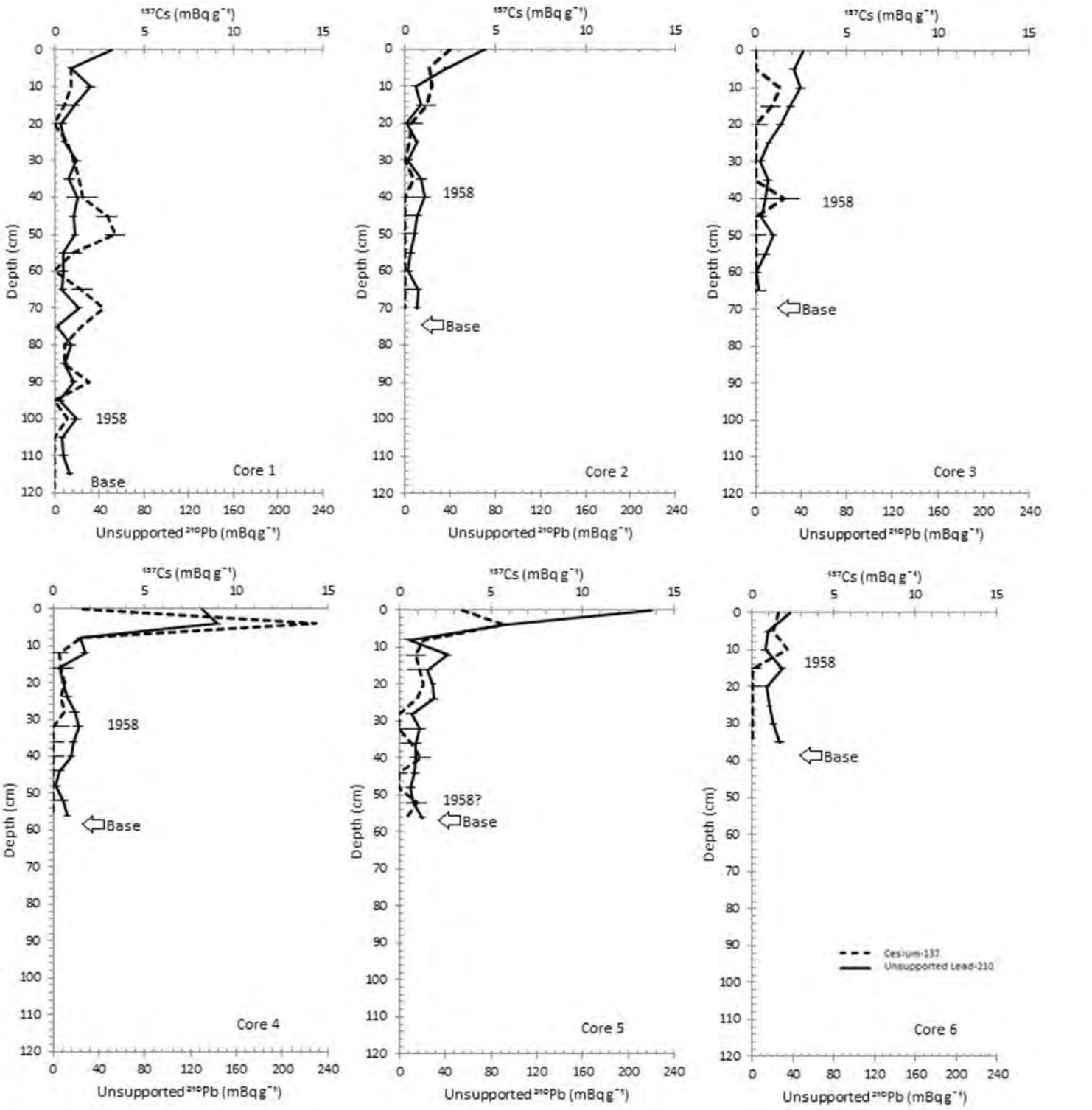

Figure 6.5 ^{137}Cs and unsupported ^{210}Pb data for cores: Core 1. Inner bend, Core 2. Outer bend, Core 3. Inner bend, Core 4. Oxbow, Core 5. Oxbow, Core 6. Backswamp in the Minnehaha River floodplain system. Measurement error given by horizontal lines

Table 6.1 presents estimates of the average sedimentation rate over the last ca. 30 and 100 years for each of the twelve cores on both floodplain systems. The average sediment accumulation rates for the Gatberg and Minnehaha floodplain systems show considerable variation between the core sites and range from 0.2 to 2.6 g cm^{-2} yr^{-1}.

When the average sedimentation rates estimated for the two different periods for each core are compared, they are in some cases, i.e., cores 4 and 5 in the Gatberg system and cores 3, 5 and 6 in the Minnehaha system, almost the same. In other cases, i.e., core 6 in the Gatberg system and cores 2 and 4 in the Minnehaha system, there is evidence to suggest that average sedimentation rates over the last ca. 30 years were less than those for the last ca. 100 years, while for cores 1, 2 and 3 in the Gatberg system and core 1 in the Minnehaha system, sedimentation rates appear to have increased in recent times. For most of the core sites, the sedimentation rates estimated for the last ca. 30 years are within 30 % of the average for the last ca. 100 years, and thus rates of overbank deposition can be seen as being quite variable over the entire period. There are a few major exceptions to this, core 4 in the Gatberg system and cores 5 and 6 of the Minnehaha system where the average sedimentation rates for the last ca. 30 years are within 10 % of the average for the last ca. 100 years, and thus rates of overbank deposition for these cores can be seen as being essentially constant over the entire period.

Table 6.1 The average sedimentation rate over the last ca. 30 and 100 years and the dates at which sedimentation rates peak for each of the cores on both floodplain systems

Floodplain system	Core number	Description	Distance from the channel (m)	Average sedimentation rate for each core, ca. 100 years (g cm^{-2} yr^{-1})	Average sedimentation rate for each core, ca. 30 years (g cm^{-2} yr^{-1})	2011-2021	2001-2010	1991-2000	1981-1990	1971-1980	1961-1970	1951-1960	1941-1950	1931-1940
Gatberg River floodplain system	1	Inner bend	4.5	1.1	1.4	2017	2007	1991		1973				
	2	Outer bend	6	0.7	0.9	2021		1995						
	3	Inner bend	5	0.9	1.2	2011	2001					1957		*1937
	4	Backswamp	150	1.3	1.4	2011			1985					
	5	Oxbow	25	0.5	0.4				1987		1969	1953		1933
	6	Oxbow	122	1.1	0.4				1981	1973		*1953		
Minnehaha River floodplain system	1	Inner bend	5.6	2	2.6	2015	2007; 2001	1993	1985; 1981	1975	1969	1957	1945	
	2	Outer bend	3	0.7	0.2					1979; 1971	1963			
	3	Inner bend	3	0.5	0.6						1967	1953		
	4	Oxbow	34	0.7	0.4				1989	1977				
	5	Oxbow	34	1.2	1.2			1995	1989	1979; 1975	1965			
	6	Backswamp	166	0.2	0.2	Uniform sedimentation rates								

Red highlight- same dates occurring between cores in the Gatberg River floodplain system;
Green highlight- same dates occurring between cores in the Minnehaha River floodplain system;
Orange highlight- same dates occurring between cores in both Gatberg and Minnehaha River floodplain system;
Blue highlight- same dates occurring between cores within the Gatberg River floodplain system and between both systems.
*- depicts the dates where the sedimentation rates indicate another peak, however, the whole peak is not shown

6.3.1.2 Variations in sedimentation rates between geomorphic units for the Gatberg and Minnehaha River floodplains systems

The average sediment accumulation rates for each core in the Gatberg River floodplain system varied between 0.3 and 1.4 g cm^{-2} yr^{-1} with an average of 0.9 g cm^{-2} yr^{-1} for all the cores (Table 6.1 and Figure 6.6). The highest rate was observed for core 4 (backswamp). There were three peaks in sedimentation rates through the core in 2011, 1985 and 1937. The lowest sedimentation rate was recorded for core 3 (inner bend). There were three peaks in sedimentation rates through the core, the first in 2011, the second in 2001 and the last in 1957. However, core 1 (inner bend, upstream of core 3) had the second highest sedimentation rate, the highest median particle sizes, and the lowest per cent clay fraction (Table 6.2). There were several peaks in sedimentation rates through the core in 2017, 2007, 1991 and 1973. Cores 5 and 6, were located on oxbows on the floodplain surface. Core 6 had a slightly higher average sedimentation rate of 0.9 g cm^{-2} yr^{-1} compared to core 5 at 0.5 g cm^{-2} yr^{-1}. Core 5 is further away from the channel and has a slightly lower median particle size and per cent of clay particle size fraction. This could indicate that distance from the channel has a role to play along this floodplain system. Core 5 had several peaks of sedimentation rates in 1987, 1969, 1953 and 1933. The peaks have been higher in recent years.

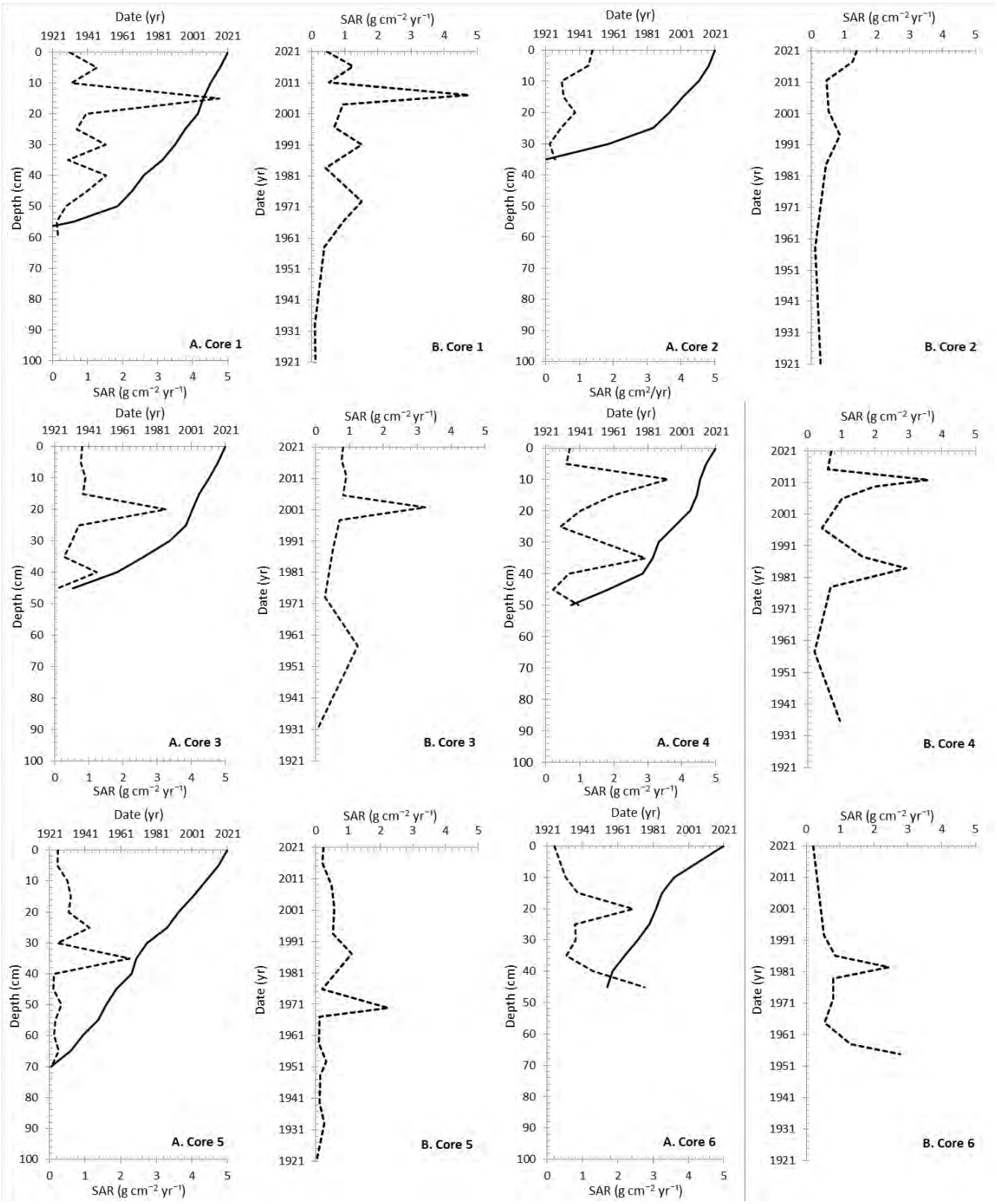

Figure 6.6 A) CRS dates and sedimentation rates with depth, B) Sedimentation rates with years for each core within the Gatberg River floodplain system

The average sediment accumulation rates for each core in the Minnehaha River floodplain system varied between 0.2 and 2 g cm^{-2} yr^{-1} with an average of 1.2 g cm^{-2} yr^{-1} for all the cores (Table 6.1 and Figure 6.7). The lowest rate was observed for Core 6 (backswamp). The highest sedimentation rate was recorded for core 1 (inner bend). Core 1 also had the highest median particle sizes and the lowest percentage clay fraction (Table 6.2). Core 1 had several sedimentation peaks in 2015, 2007, 2001, 1993, 1985, 1981, 1975, 1969, 1957 and 1945. Cores 2 and 3, were located on the same meander bend, on the outer and inner bend, respectively. Core 2 had a slightly higher average sedimentation rate of 0.7 g cm^{-2} yr^{-1} compared to core 3 at 0.5 g cm^{-2} yr^{-1}. Core 2 has a slightly higher percentage of clay particle size fraction. This could indicate oblique accretion has a role to play along this floodplain system. Core 2 had three sedimentation peaks down the core length in 1979, 1971 and 1963. Core 3 had two peaks in 1967 and 1953.

The peaks in sediment accumulation rates for both floodplain systems have some correspondences between the cores within each system and between the two systems (Table 6.1).

Above-average rainfall years for Maclear (SAWS- South African Weather Services) and peak flow years recorded for the Tsitsa River at Xonkonxa and the Mooi River at Maclear matched the recorded peak sedimentation years in the two floodplain systems by almost 40 %. This indicates that although rainfall is very localised, some large weather patterns could result in large peak flows that can be seen in the sediment records of the two systems.

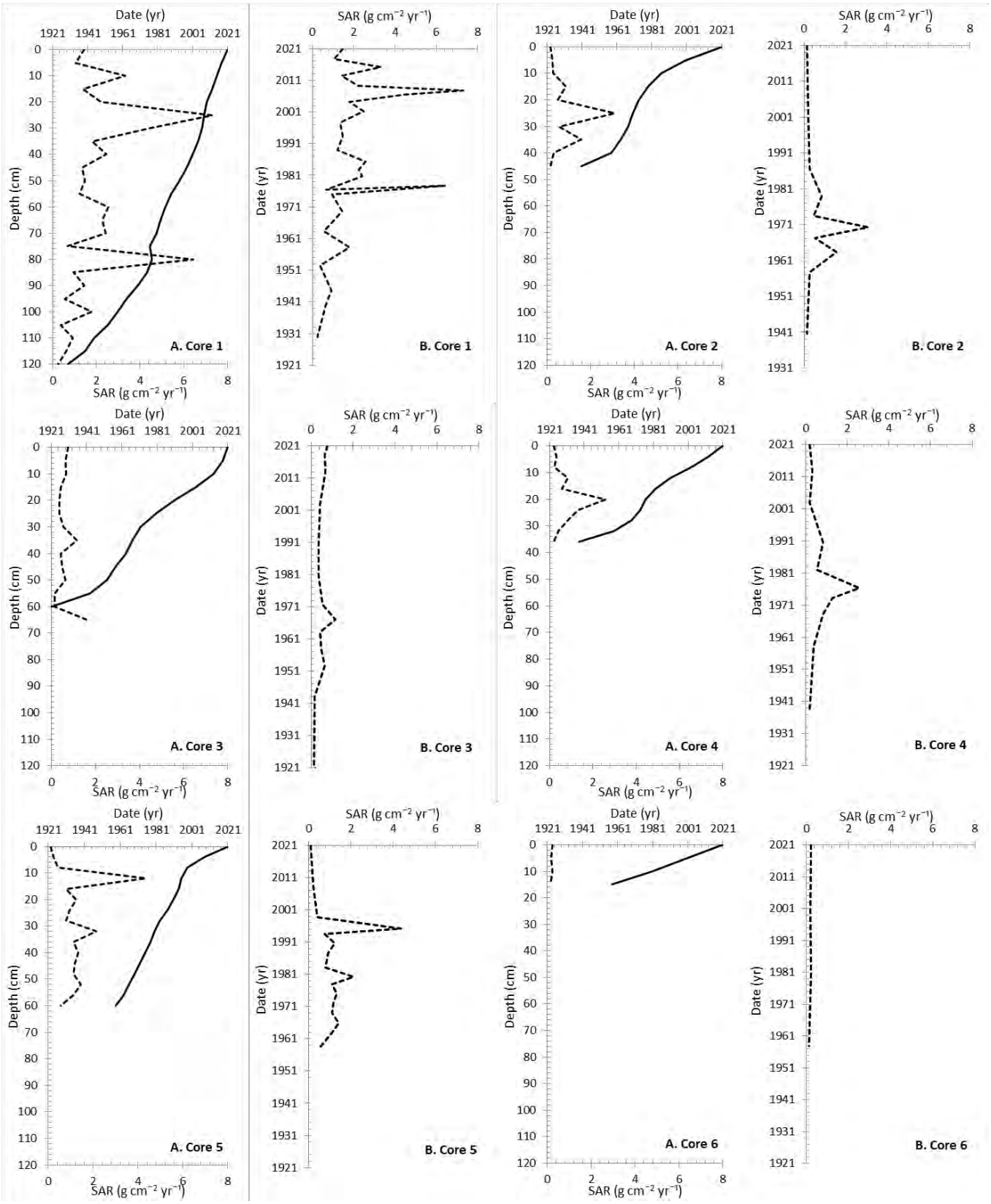

Figure 6.7 A) CRS dates and sedimentation rates with depth, B) Sedimentation rates with years for each core within the Minnehaha River floodplain system

Table 6.2 Average sediment properties for each core in the Gatberg and Minnehaha River floodplain systems

Floodplain system	Core number	Description	Average sedimentation rate (g cm² yr⁻¹)	D_{50} sediment particle size (µm)	Average clay fraction (%)	Average sand fraction (%)	Average organic matter content (%)
Gatberg floodplain system	1	Inner bend	1.1	29.7	13.6	17.7	4.5
	2	Outer bend	0.7	26.9	60.1	14.1	5.3
	3	Inner bend	0.9	21.7	14.9	12.7	5.7
	4	Backswamp	1.3	19.1	15.9	8.3	5.5
	5	Oxbow	0.5	17.5	15.9	7.7	8.3
	6	Oxbow	1.1	17.5	17.0	10.1	10.9
Minnehaha floodplain system	1	Inner bend	2.0	44.8	8.7	53.8	3.0
	2	Outer bend	0.7	22.8	12.3	14.7	7.6
	3	Inner bend	0.5	24.7	13.0	20.3	6.2
	4	Oxbow	0.7	20.9	14.8	18.4	6.0
	5	Oxbow	1.2	14.8	18.8	6.0	7.5
	6	Backswamp	0.2	12.3	24.1	10.9	4.4

6.3.2 SEDIMENT TRAPPING EFFICIENCIES FOR THE FLOODPLAIN GEOMORPHIC UNITS

Table 6.3 shows the estimated suspended sediment yields (SSY) from direct measurements for the Tsitsa, Inxu, Gqukunqa and Pot River catchments from 2015 to 2019 (Nyamela 2018; Bannatyne et al. 2022) and modelled estimates for the Tsitsa, lower Tsitsa, Inxu and Pot River catchments using a variety of model software (Figure 6.8; Le Roux et al. 2015; Pretorius et al. 2016; Gwapedza 2020; Theron et al. 2021; Gwapedza et al. 2021). It is evident from the modelled values for the Tsitsa River catchment summarised in Table 6.3 that the modelling approaches affect the SSY estimates and show large variability. Direct measurements, in general, were well below the modelled estimates. Bannatyne et al. (2022) found that land use and land management, geology, catchment size, and hydrological regime (especially flashiness) influenced the SSY values to some degree. No suspended sediment yield estimates were conducted for the study sites in this research (Gatberg and Minnehaha Rivers). As such, direct measurements (not modelled) for the Pot River catchment (Bannatyne et al. 2022) were chosen to represent the closest values that could potentially occur within the Gatberg and Minnehaha River catchments, due to their similar geology, climate, and land cover/ use (Figure 6.8).

Table 6.3 A comparison of estimated and modelled SSY in the Tsitsa, lower Tsitsa, Inxu, Gqunkunqa, and Pot River catchments

Approach	Suspended yield (t km^{-2} yr^{-1})					Reference
	Tsitsa River	Lower Tsitsa River	Inxu River	Gqukunqa River	Pot River	
Direct measurements	93-222 (a.)		236-1443 (a. & b.)	58-146 (a.)	47-79 (a.)	a. Bannatyne et al. (2022) b. Nyamela (2018)
Modelled using the soil and water assessment tool (SWAT) with GIS	500 (average)	100-2500	100-2500		200-599	Le Roux et al. (2015)
Modelled using SWAT and remote sensing/ object-based image analysis (OBIA)	1050					Pretorius et al. (2016)
Modelled using the Water Quality and Sediment Model (WQSED)	153					Gwapedza, 2020
Modelled using SWAT (average 2015–2035)	1-30					Theron et al. (2021)
Modelled using the modified USLE			5000			Gwapedza et al. (2021)

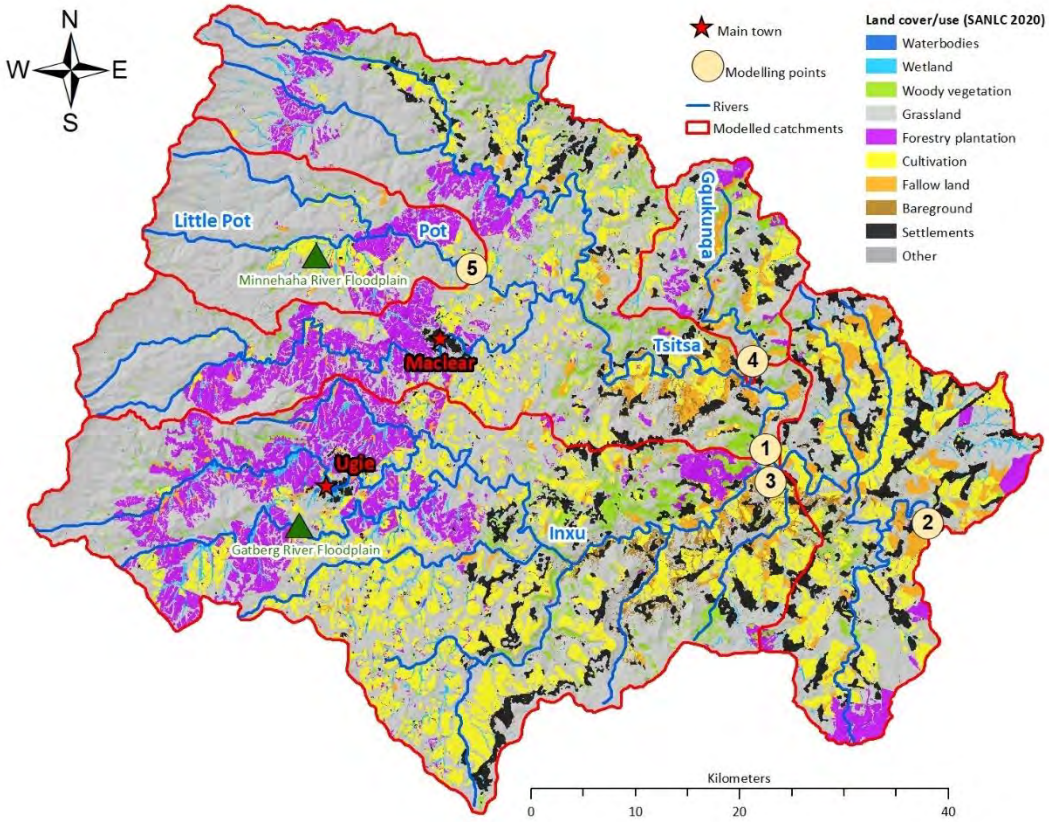

Figure 6.8 Land cover and use of the Tsitsa River Catchment. Modelled sub-catchments shown (1- Tsitsa River, 2 - Lower Tsitsa River, 3 - Inxu River, 4 - Gqukunqa River) and direct measurement sub-catchment (3 - Inxu River, 4 - Gqukunqa River, and 5 - Pot River) in relation to study sites

Table 6.4 shows the potential sediment trapped and exchanged per geomorphic feature (proximal floodplain and sediment sinks (oxbows and backswamp)) and the potential per cent proportion of the sediment accumulated of the total suspended sediment yield the Gatberg and Minnehaha River catchments.

In the Gatberg River floodplain system, the potential sediment exchange flux areas, i.e., the sediment that is temporarily stored in lateral and overbank accretion deposits within the proximal floodplain (inner and outer bend) covered an area of 0.04 km² for the mapped valley fill. Using a median sedimentation rate of 0.6 g cm^{-2} yr^{-1} this equated to a mean total of 247 t yr^{-1} of sediment that is potentially accumulated and exchanged in these features per year. Using the minimum, mean and maximum observed sediment yield values (6345, 8235 and 10665 t yr^{-1}) for the Pot River catchment adjusted for the Gatberg River floodplain; 4, 3 and 2 % (respectively) proportion of the total suspended sediment yield can be accumulated and has the potential to be exchanged by the proximal floodplain zone (Table 6.4).

The oxbows covered an area of 0.05 km² for the mapped floodplain system. A depth of 1.38 m (based on the average depth from the bottom of oxbows to the current thalweg depth) was used as the average depth of fine sediment in the oxbows and equated to 69 000 m³ of sediment that has been stored. The dating of oxbows would suggest that these were active sinks over the last 100+ years. The median sedimentation rate calculated from the cores is 0.4 g cm^{-2} yr^{-1} which equates to a mean of 247 t yr^{-1} of the sediment that is potentially trapped, stored, and exchanged in these floodplain geomorphic units per year. Using the same sediment yield values as above the percent of the sediment that is trapped by oxbows are 4, 3 and 2 % of the minimum, mean, and maximum annual SSY values.

The backswamp zone covered an area of approximately 0.09 km² for the mapped floodplain system. A depth of 1.9 m (based on the average depth from the bottom of the backswamp to the current thalweg depth) was used as the average depth of fine sediment in the backswamp and equated to 171 000 m³ of sediment that has been stored. The dating of the backswamp would suggest that these were active sinks over the last 100+ years. The median sedimentation rate calculated from the cores is 0.9 g cm^{-2} yr^{-1} which equates to a mean of 823.5 t yr^{-1} of sediment is potentially accumulated and exchanged in this floodplain geomorphic unit per year. Using the same sediment yield values as above, the percentage of the sediment that is potentially trapped by the backswamp zone was 13, 10 and 8 % of the total minimum, mean, and maximum of the Pot River suspended sediment yield values.

In the Minnehaha River floodplain system, the potential sediment exchange flux areas (proximal floodplain- inner and outer bends) covered an approximate area of 0.05 km² for the mapped valley fill.

Using a median sedimentation rate of 0.8 g cm^{-2} yr^{-1} which equates to a mean of 390.4 t yr^{-1} of sediment is potentially accumulated and exchanged in these features per year. Using the minimum, mean and maximum observed sediment yield values (1880, 2440 and 3160 t yr^{-1}) for the Pot River catchment adjusted for the Minnehaha River floodplain; 21, 16 and 13 % (respectively) proportion of the total suspended sediment yield can be accumulated and has the potential to be exchanged by the proximal floodplain zone.

Oxbows covered an area of approximately 0.06 km^2 for the mapped floodplain system. A depth of 1.28 m (based on the average depth from the bottom of the oxbows to the current thalweg depth) was used as the average depth of fine sediment in the oxbows and equated to 76 800 m^3 of sediment that has been stored. The dating of oxbows would suggest that these were active sinks over the last 100+ years. The median sedimentation rate calculated from the cores is 0.8 g cm^{-2} yr^{-1} which equates to a mean of 488 t yr^{-1} of sediment is trapped, stored, and exchanged in these geomorphic units per year. Using the same sediment yield values as above the percentage of the sediment that is trapped by oxbows are 15, 20 and 26 % of the minimum, mean and maximum of the adjusted annual SSY values.

The backswamp zone covered an area of approximately 0.1 km^2 for the mapped floodplain system. A depth of 1.73 m (based on the average depth from the bottom of the backswamp to the current thalweg depth) was used as the average depth of fine sediment in the backswamp and equated to 173 000 m^3 of sediment that has been stored. The dating of the backswamp would suggest that these were active sinks over the last 100+ years. The median sedimentation rate calculated from the cores is 0.2 g cm^{-2} yr^{-1} which equates to a mean of 195.2 t yr^{-1} of sediment is trapped and exchanged in this geomorphic unit per year. Using the same sediment yield values as above the percent of the sediment that is potentially accumulated from the total suspended sediment yield by backswamp geomorphic unit ranged from 6 to 11 %.

Table 6.4 The potential sediment trapped and exchange per geomorphic feature (proximal floodplain and sediment sinks) and the potential percentage proportion of the sediment accumulated of the total suspended sediment yield adjusted from the SSY values of the Pot River catchment for the Gatberg and Minnehaha River catchments. The mean proportion values (%) are highlighted

		Gatberg River floodplain system			Minnehaha River floodplain system		
		Minimum	**Mean**	**Maximum**	**Minimum**	**Mean**	**Maximum**
Annual sediment yield of the floodplain system catchment (tonnes yr^{-1})		6345	8235	10665	1880	2440	3160
Sediment exchange flux (i.e., proximal floodplain zone)	Mean potential sediment exchange flux (i.e., sediment temporarily stored in lateral accretion deposits within the proximal floodplain zone, tonnes yr^{-1})	253.8	247.1	213.3	394.8	390.4	410.8
	Mean proportion of total suspended sediment yields (%)	4	3	2	21	16	13
	Minimum potential sediment trapped (tonnes yr^{-1})	190.4	164.7	213.3	244.4	244.0	252.8
	Minimum proportion of total suspended sediment yields (%)	3	2	2	13	10	8
	Maximum potential sediment trapped (tonnes yr^{-1})	317.3	329.4	320	752.0	756.4	758.4
	Maximum proportion of total suspended sediment yields (%)	5	4	3	40	31	24
Sediment sinks (i.e., oxbows and backswamp units)	Mean sediment sinks (i.e., sediment stored in the oxbow and backswamp geomorphic units, tonnes yr^{-1})	1078.7	1070.6	1066.5	676.8	683.2	695.2
	Mean proportion of total suspended sediment yields (%)	17	13	10	36	28	22
	Minimum potential sediment trapped (tonnes yr^{-1})	888.3	905.9	959.9	507.6	488.0	505.6
	Minimum proportion of total suspended sediment yields (%)	14	11	9	27	20	16
	Maximum potential sediment trapped (tonnes yr^{-1})	1205.6	1235.3	1173.2	808.4	805.2	790.0
	Maximum proportion of total suspended sediment yields (%)	19	15	11	43	33	25
Combined sediment exchange flux and sediment sinks	Mean total annual potential sediment sink (oxbow and backswamp units) and exchange flux (proximal floodplain zone, tonnes yr^{-1})	1269.0	1317.6	1279.8	1071.6	1073.6	1074.4
	Mean proportion of total suspended sediment yields (%)	20	16	12	57	44	34
	Minimum potential sediment trapped (tonnes yr^{-1})	1078.7	1070.6	1066.5	752.0	756.4	758.4
	Minimum proportion of total suspended sediment yields (%)	17	13	10	40	31	24
	Maximum potential sediment trapped (tonnes yr^{-1})	1522.8	1564.7	1493.1	1541.6	1561.6	1548.4
	Maximum proportion of total suspended sediment yields (%)	24	19	14	82	64	49

6.3.3 TOTAL PHOSPHORUS ACCUMULATION RATES

6.3.3.1 TEMPORAL VARIATION IN TOTAL PHOSPHORUS ACCUMULATION RATES OF THE GATBERG AND MINNEHAHA RIVER FLOODPLAINS SYSTEMS

Total phosphorus accumulation rates for the cores in the Gatberg River floodplain system ranged from 0.04 to 5.9 g m^{-2} yr^{-1}, with multiple peaks along each core (Figure 6.9). Figure 6.10 shows the relationship between total phosphorus accumulation rates, phosphorus concentrations, organic matter content, clay fraction, and D_{50} particle size with years for each core. Regression analysis showed there was no significant relationship between distance from the channel, total phosphorus concentration and total phosphorus accumulation rate ($r_s < 0.4$; p-values > 0.05; $r^2 < 0.5$). There was a significant positive relationship between sedimentation rate, D_{50} particle size, and depth with total phosphorus accumulation rates, ($r_s < 0.4$; p-values < 0.05; $r^2 < 0.5$). There was a significant negative relationship between the percentage of clay particle size, the percentage of the organic matter content, and depth with total phosphorus accumulation rates ($r_s < 0.4$; p-values < 0.05; $r^2 < 0.5$).

The average total phosphorus accumulation rates for each core for the past ca. 100 years in the Gatberg River floodplain system, ranged from 0.5 to 1.1 g m^{-2} yr^{-1} with an average of 0.8 g m^{-2} yr^{-1} and a median of 0.6 g m^{-2} yr^{-1} (Table 6.5). The average accumulation rates for the past ca. 30 years ranged from 0.6 to 1.4 g m^{-2} yr^{-1}. The average total phosphorus accumulation rates were consistently higher for the past ca. 30 years, except core 6 (oxbow).

In the case of core 1 which was collected on an inner bend within the proximal floodplain, the peaks in total phosphorus accumulation occurred at 5 cm (dated 2016, 1 g m^{-2} yr^{-1}), 15 cm (dated 2007, 4.7 g m^{-2} yr^{-1}), 30 cm (1991, 1.6 g m^{-2} yr^{-1}) and 50 cm (1973, 1.5 g m^{-2} yr^{-1}). Core 3, located on another inner bend, had only one major peak at 20 cm (dated 2002, 4 g m^{-2} yr^{-1}). Core 2, located on an outer bend, had 3 peaks, at 0, 5 and 20 cm (dated 2021, 1.7; 2017, 1.5; and 1994 0.7 g m^{-2} yr^{-1}, respectively). Core 5 and 6, were both collected on oxbows. Core 5 had four peaks, at 10, 15, 25 and 35 cm (2009, 0.7; 2002, 0.7; 1987, 1.1 and 1970, 2 g m^{-2} yr^{-1}). Core 6, located upstream but further away from the channel compared to core 5 had three peaks, at 15, 20 and 45 cm (dated 1986, 1.1; 1983, 2.2 and 1955, 1.1 g m^{-2} yr^{-1}). Core 4 had three peaks, at ca. 10, 15 and 35 cm (dated 2012, 3.5; 2010, 1.3 and 1984, 1.2 g m^{-2} yr^{-1}), located in the backswamp.

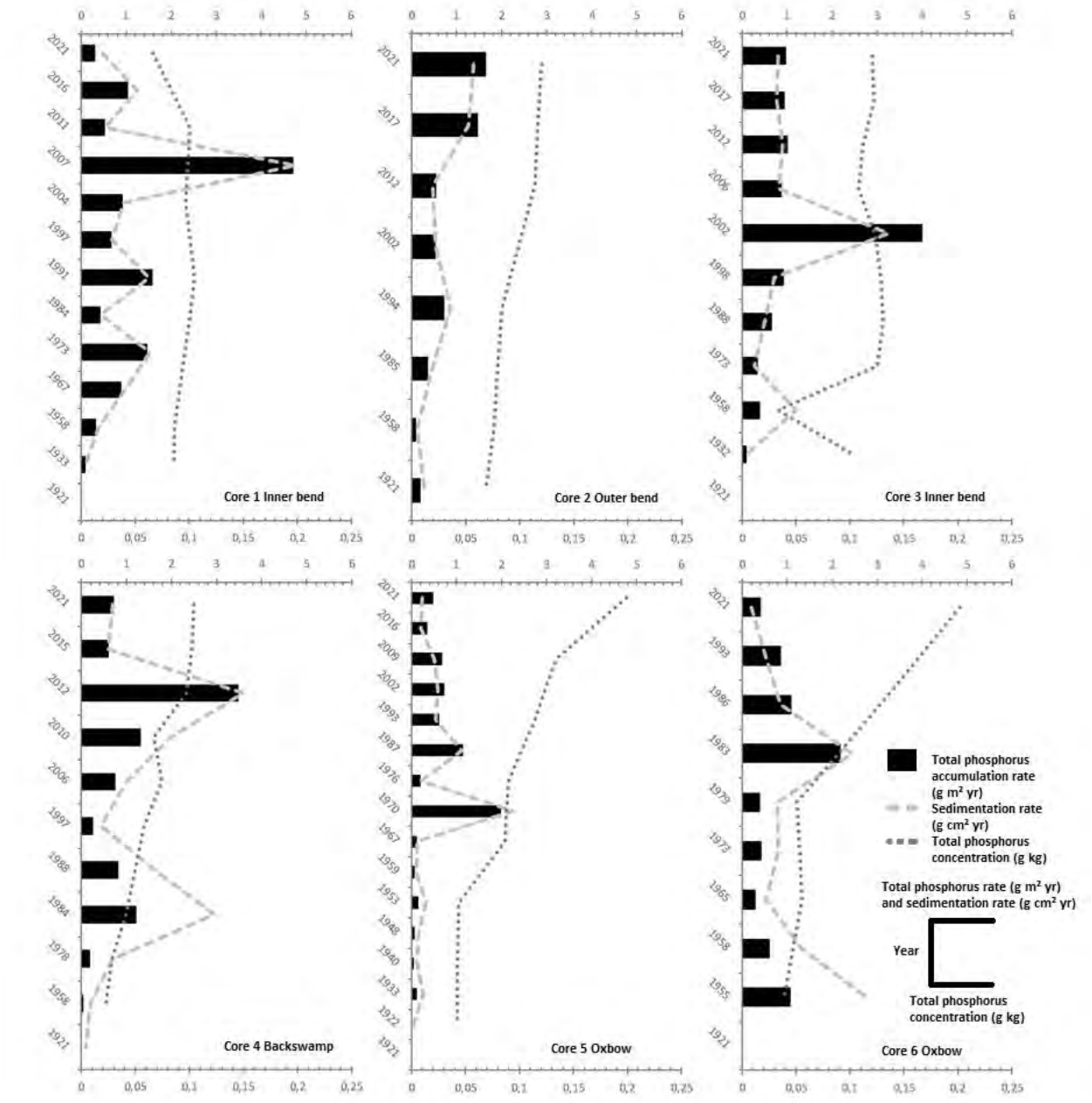

Figure 6.9 Total phosphorus accumulation rates, sedimentation rates, and phosphorus concentrations with years for each core within the Gatberg River floodplain system

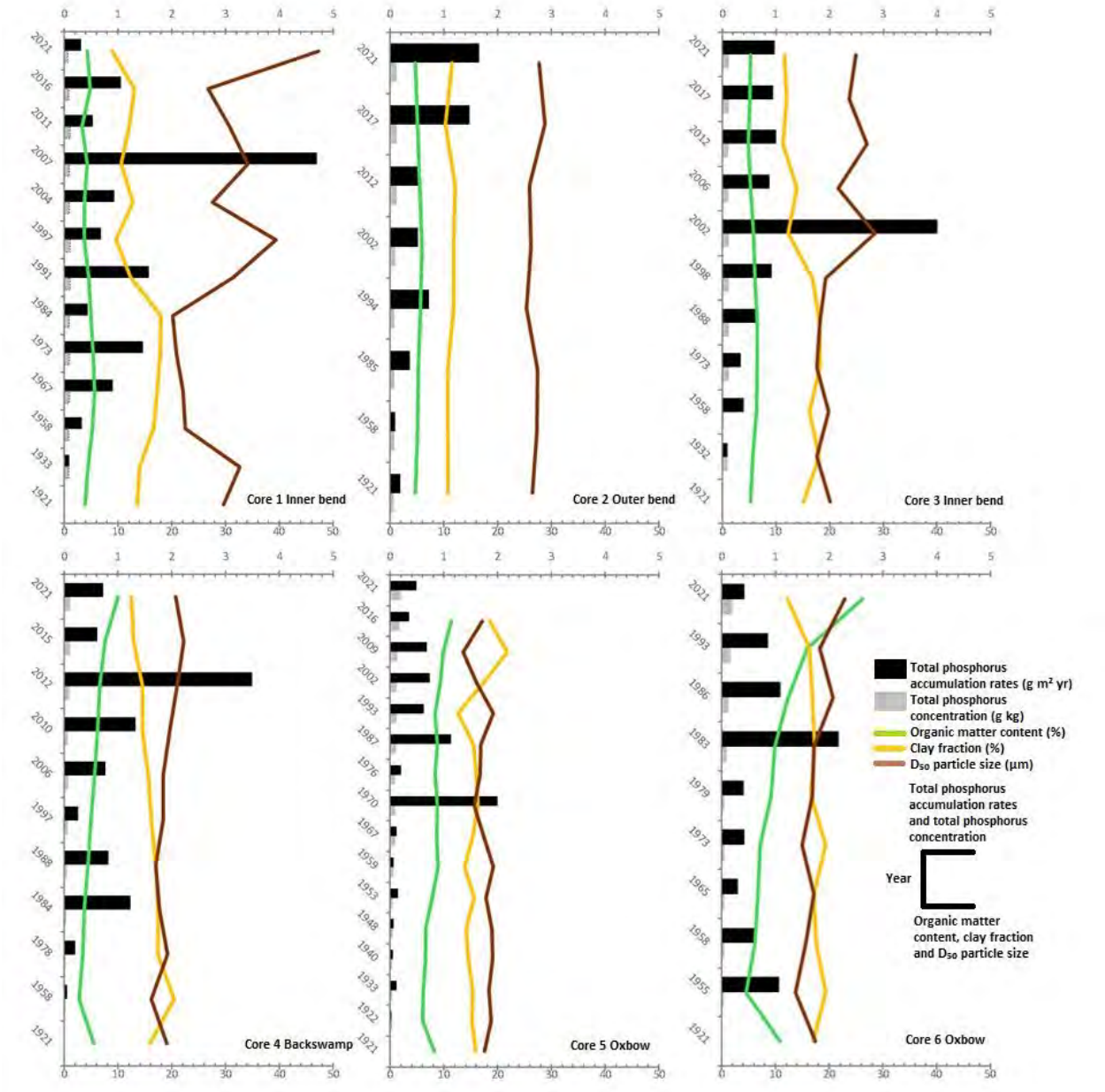

Figure 6.10 Total phosphorus accumulation rates, phosphorus concentrations, organic matter content, clay fraction, and D_{50} particle size with years for each core within the Gatberg River floodplain system

Table 6.5 The average total phosphorus accumulation rates over the last ca. 30 and 100 years and the dates at which accumulation rates peak for each of the cores on both floodplain systems

Floodplain system	Core number	Description	Distance from the channel (m)	Average total phosphorus accumulation rate for each core, ca. 100 years (g m^{-2} yr^{-1})	Average TP accumulation rate for each core, ca. 30 years (g m^{-2} yr^{-1})	2011-2021	2001-2010	1991-2000	1981-1990	1971-1980	1961-1970	1951-1960
Gatberg River floodplain system	1	Inner bend	4.5	1.1	1.4	2016	2007	1991		1973		
	2	Outer bend	6	0.7	1	2017; *2021		1994				
	3	Inner bend	5	1	1.5		2002					
	4	Backswamp	150	0.9	1.2	2012	2010		1984			
	5	Oxbow	25	0.5	0.6		2002; 2009		1987		1970	
	6	Oxbow	122	0.8	0.6				1983; 1986			1955
Minnehaha River floodplain system	1	Inner bend	5.6	1.4	1.8	2012; 2015; *2021	2001; 2004 2007; 2008; 2009		1981; 1983; 1985	1978		1958
	2	Outer bend	3	0.6	0.3					1979	1963; 1970	
	3	Inner bend	3	0.5	0.6	2013; 2018; *2021					1967	1953
	4	Oxbow	34	0.8	0.5	2013; *2021		1991		1973; 1976	1968	
	5	Oxbow	34	1.4	1.5			1991; 1994; 1995	1983; 1987	1972; 1975; 1978; 1980	1966; 1969	
	6	Backswamp	166	0.09	0.1	Uniform total phosphorus accumulation rates						

Red highlight- same dates occurring between cores in the Gatberg River floodplain system;
Green highlight- same dates occurring between cores in the Minnehaha River floodplain system;
Orange highlight- same dates occurring between cores in both Gatberg and Minnehaha River floodplain systems;
Blue highlight- same dates occurring between cores within each of the floodplain systems and between both systems.
**- depicts the dates where the sedimentation rates indicate another peak, however, the whole peak is not shown*

Total phosphorus accumulation rates for the cores in the Minnehaha River floodplain system ranged between 0.05 and 5.3 g m^2 yr^{-1}, with multiple peaks along each core (Figure 6.11). Figure 6.12 shows the relationship between total phosphorus accumulation rates, phosphorus concentrations, organic matter content, clay fraction, and D_{50} particle size with years for each core. A regression analysis showed that there was no significant relationship between D_{50} particle size, per cent clay fraction, per cent of organic matter content, total phosphorus concentration, and distance from the channel with the total phosphorus accumulation rate ($r_s < 0.4$; p-values > 0.05; $r^2 < 0.5$). There was a significant positive relationship between sedimentation rate and depth with the total phosphorus accumulation rates ($r_s > 0.4$; p-values < 0.05; $r^2 > 0.5$).

For the Minnehaha River floodplain system, the average total phosphorus accumulation rates for each core for the last ca. 100 years ranged from 0.09 to 1.4 g m^{-2} yr^{-1} with an average of 1 g m^{-2} yr^{-1}, median 0.7 g m^{-2} yr^{-1} (Table 6.5). The average accumulation rates for the past ca. 30 years ranged from 0.1 to 1.8 g m^{-2} yr^{-1}. The average accumulation rates were consistently higher for the past ca. 30 years, except for core 2 (the outer bend on the proximal floodplain) and core 4 (oxbow).

In the case of core 1 which was collected on an inner bend within the proximal floodplain, it had the most peaks in total phosphorus accumulation rates (13 peaks greater than 1 g m^{-2} yr^{-1}, Figure 6.11). Core 3, which is located on another inner bend, had five major peaks; however, these were below 1 g m^{-2} yr^{-1}. Core 2, located on an outer bend, had 3 peaks, at 15, 25 and 35 cm (dated 1979, 0.8; 1970, 2.5; and 1963 1.1 g m^{-2} yr^{-1}, respectively). Core 4 and 5, both were collected in oxbows. Core 4 had six peaks, at 0, 4, 12, 20, 24, and 28 cm (2021, 0.6; 2013, 0.5; 1991, 0.7; 1976, 2.3; 1973, 1.2; and 1968, 1 g m^{-2} yr^{-1}). Core 5, located upstream of core 4, had 11 above 1 g m^{-2} yr^{-1}. Core 6, located on the backswamp, had no peaks in total phosphorus accumulation rates.

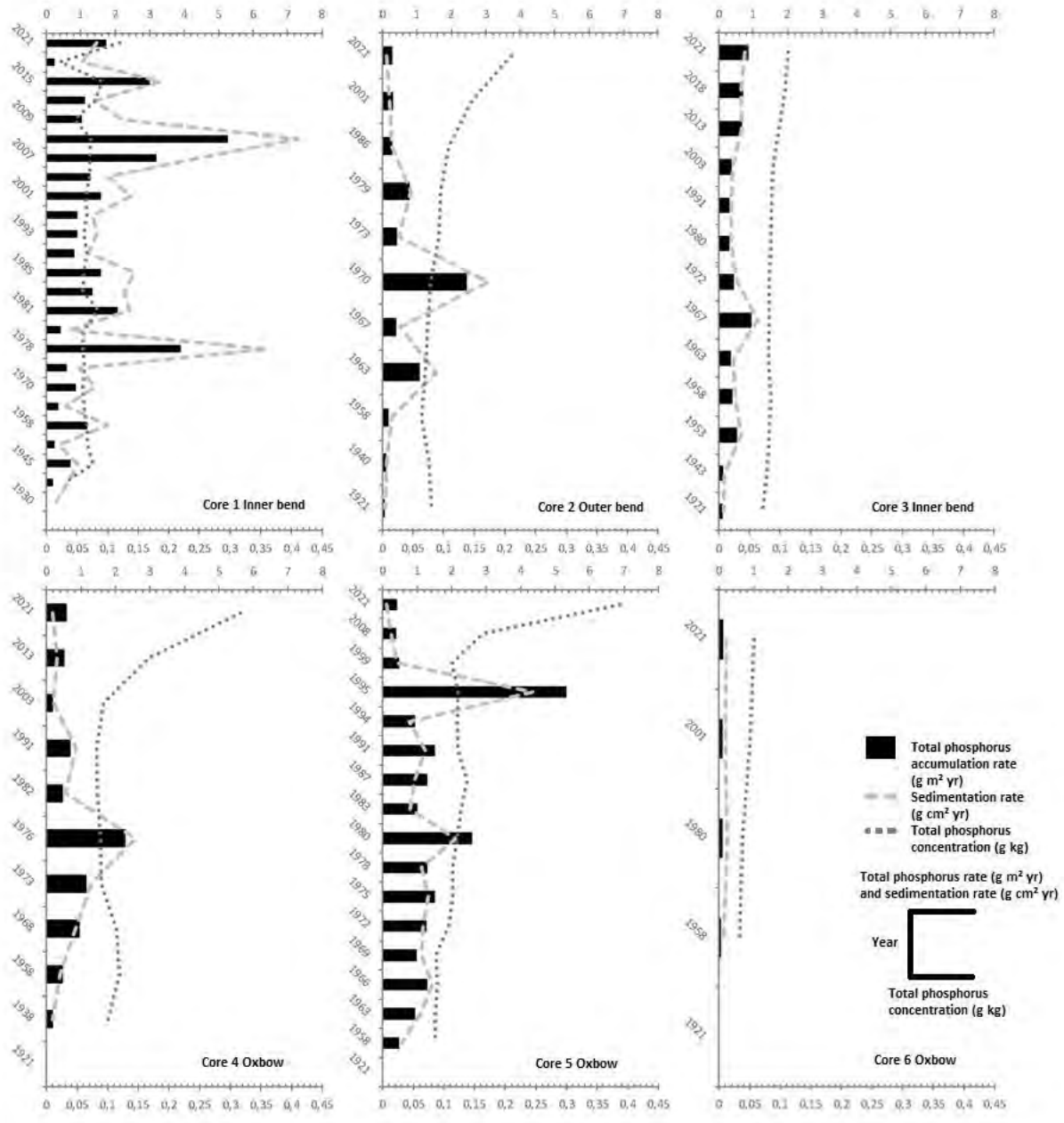

Figure 6.11 Total phosphorus accumulation rates, sedimentation rates, and total phosphorus concentration with years for each core within the Minnehaha River floodplain system

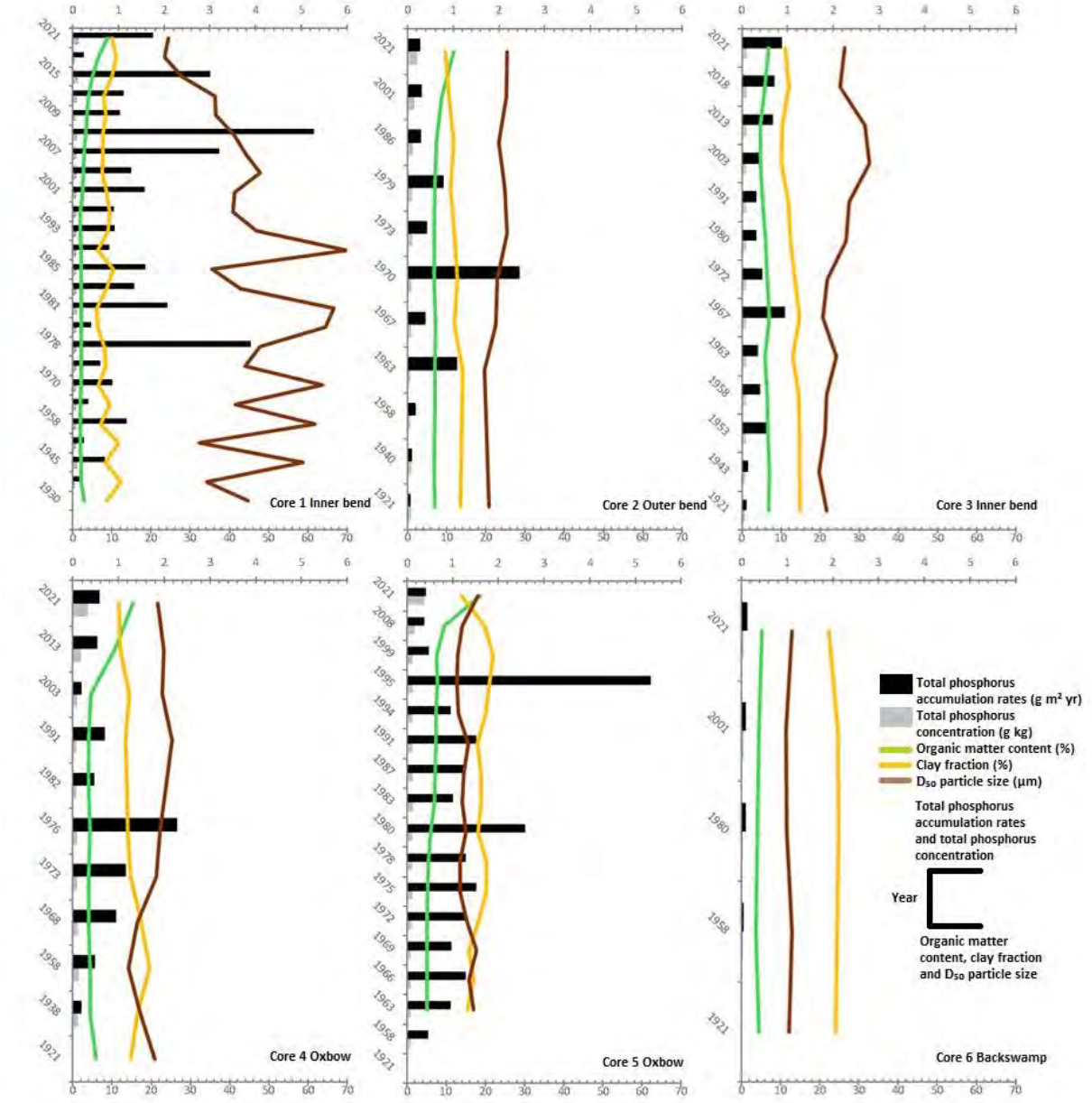

Figure 6.12 Total phosphorus accumulation rates, phosphorus concentrations, organic matter content, clay fraction, and D_{50} particle size with years for each core within the Minnehaha River floodplain system

6.3.3.2 Variations in total phosphorus accumulation rates between geomorphic units for the Gatberg and Minnehaha River floodplain systems

The accumulation rates for the cores were grouped by geomorphic unit (proximal floodplain- inner and outer bend, oxbows and backswamp) and are shown in Table 6.6.

In the Gatberg River floodplain system, the lowest total phosphorus accumulation rates were observed for the oxbows with an average of 0.6 g m^{-2} yr^{-1} (median 0. 4 g m^{-2} yr^{-1}). This geomorphic unit also had the lowest average sedimentation rate and median particle size, the highest percentage clay particle size fraction and organic matter content. The highest phosphorus accumulation rates were recorded for the inner bends within the proximal floodplain (average 1.1 and median 0. 9 g m^{-2} yr^{-1}), this zone had the second highest sedimentation average rate. Outer bends within the proximal floodplain had slightly lower total phosphorus accumulation rates than the inner bends (average 0.7 and median 0.5 g m^{-2} yr^{-1}). The outer bends had the highest median particle size and the lowest percentage clay particle size fraction. The backswamp geomorphic zone had the second-highest total phosphorus accumulation rate (average 0.9 and median 0.7 g m^{-2} yr^{-1}), the highest average sedimentation rate and the lowest total phosphorus concentrations and median particle size.

In the Minnehaha River floodplain system, the backswamp geomorphic zone had the lowest total phosphorus accumulation rates out of all geomorphic zones for both floodplain systems (average 0.1 and median 0.01 g m^{-2} yr^{-1}). The backswamp had the lowest average sedimentation rate, total phosphorus concentrations, median particle size and the highest percentage clay particle size fraction. The highest average total phosphorus accumulation rates were recorded for the oxbows (average 1.1 and median 1 g m^{-2} yr^{-1}) and the inner bends within the proximal floodplain (average 1.1 and median 0.8 g m^{-2} yr^{-1}). The oxbows had the highest total phosphorus concentrations. The inner bends had the highest average sedimentation rates and the lowest percentage of organic matter content.

Although the average total phosphorus accumulation rates for both systems are similar (0.8 g m^{-2} yr^{-1} for the Gatberg system and 1 g m^{-2} yr^{-1} for the Minnehaha system) different geomorphic zones within each floodplain system are more active as phosphorus stores (Table 6.6).

Table 6.6 Sedimentation rate, total phosphorus accumulation rate, total phosphorus concentration and sediment properties for the Gatberg and Minnehaha River floodplain geomorphic units

Floodplain system	Geomorphic units		SAR (g cm^{-2} yr^{-1})		TP accumulation rate (g m^{-2} yr^{-1})		TP concentration (g kg^{-1})		D_{50} particle size (μm)		Clay fraction (%)		Organic matter content (%)	
			average	median	average	median	average	median	average	median	average	median	average	median
Gatberg River floodplain system	Proximal floodplain	Inner bend	1.0	0.8	1.1	0.9	0.10	0.10	26.1	24.3	14.2	13.5	5.1	5.2
		Outer bend	0.7	0.5	0.7	0.5	0.10	0.09	26.9	26.9	11.3	11.2	5.3	5.2
		Both	0.9	0.7	1.0	0.7	0.10	0.10	26.3	26.3	13.4	12.3	5.2	5.2
	Oxbows		0.7	0.5	0.6	0.4	0.09	0.10	17.5	17.2	16.3	16.4	9.3	8.7
	Backswamp		1.3	1.0	0.9	0.7	0.07	0.06	19.1	18.8	15.9	15.9	5.5	5.3
Minnehaha River floodplain system	Proximal floodplain	Inner bend	1.6	1.1	1.1	0.8	0.07	0.07	37.7	35.6	10.2	10.0	4.1	3.4
		Outer bend	0.7	0.3	0.6	0.3	0.10	0.08	22.8	22.9	12.3	12.0	7.6	7.0
		Both	1.4	0.8	1.0	0.7	0.08	0.08	34.3	27.6	10.7	10.5	4.9	5.2
	Oxbows		1.0	0.8	1.1	1.0	0.13	0.12	17.3	16.2	17.0	17.2	6.8	5.2
	Backswamp		0.2	0.2	0.1	0.1	0.05	0.05	12.3	12.3	24.1	24.6	4.4	4.3

6.3.4 TOTAL PHOSPHORUS TRAPPING EFFICIENCIES FOR THE FLOODPLAIN GEOMORPHIC UNITS

Using the same direct measurements of the suspended sediment yield values for the Pot River catchment as in the previous section (Table 6.3) adjusted using the total phosphorus yield for each of the floodplain system's catchments, the potential total phosphorus accumulation for each floodplain geomorphic zone is calculated (Table 6.7).

In the Gatberg River floodplain system the potential sediment exchange flux areas, i.e., the proportion of total phosphorus that is temporarily stored in the lateral and overbank accretion deposits within the proximal floodplain (inner and outer bend) covered an approximate area of 0.04 km² for the mapped valley fill. Using the average total phosphorus concentration of 100.8 mg kg^{-1} which equated to a total of 0.023 t yr^{-1} of total phosphorus that is potentially accumulated and exchanged in these features per year. Using the minimum, mean and maximum observed total phosphorus yield values (0.89, 1.16 and 1.50 t yr^{-1}) for the Pot River catchment adjusted for the Gatberg River floodplain; 3, 2 and 2 % (respectively) proportion of the total phosphorus yield that is potentially accumulated and has the potential to be exchanged by the proximal floodplain zone.

Oxbows covered an area of approximately 0.05 km² for the mapped floodplain system. The average total phosphorus concentration calculated from the cores is 87.4 mg kg^{-1} which means that 0.023 t yr^{-1} of total phosphorus is potentially trapped and exchanged in these floodplain geomorphic units. Using the same total phosphorus yield values as above the percentage of the total phosphorus that is trapped by oxbows are 2, 2 and 1 % of the minimum, mean and maximum total phosphorus yield values.

The backswamp zone covered an area of approximately 0.09 km² for the mapped floodplain system. The average total phosphorus concentration calculated from the cores is 62.5 mg kg^{-1} which means that 0.046 t yr^{-1} of total phosphorus is potentially accumulated and exchanged in this floodplain geomorphic unit. Using the same total phosphorus yield values as above the percent of the total phosphorus that is potentially trapped by the backswamp zone was 6, 4 and 3 % of the minimum, mean, and maximum total phosphorus yield values.

In the Minnehaha River floodplain system, the potential total phosphorus exchange flux (proximal floodplain- inner and outer bends) areas, covered an approximate area of 0.05 km² for the mapped valley fill. Using the average total phosphorus concentration of 76.6 mg kg^{-1} which equates to 0.032 t yr^{-1} of total phosphorus that is potentially accumulated and exchanged in these features per year. Using the minimum, mean and maximum adjusted total phosphorus yield values (0.15, 0.20 and 0.25 t yr^{-1}) for the Minnehaha River floodplain; 21, 16 and 12 % (respectively) proportion of the total

phosphorus yield is potentially accumulated and has the potential to be exchanged by the proximal floodplain zone.

Oxbows covered an area of approximately 0.06 km² for the mapped floodplain system. The average total phosphorus accumulation calculated from the cores is 116.1 mg kg^{-1} which means that potentially 0.058 t yr^{-1} total phosphorus is potentially trapped and exchanged in these geomorphic units per year. Using the same total phosphorus yield values as above the percentage of the total phosphorus that is trapped by oxbows are 37, 29 and 22 % of the minimum, mean and maximum of the adjusted total phosphorus yield values.

The backswamp zone covered an area of approximately 0.1 km² for the mapped floodplain system. The average total phosphorus concentration calculated from the cores is 45.1 mg kg^{-1} which means that 0.008 t yr^{-1} of total phosphorus could be accumulated and exchanged in this geomorphic floodplain unit. Using the same total phosphorus yield values as above the percentage of the total phosphorus that is potentially accumulated of the total phosphorus yield by backswamp geomorphic unit ranged from 4 to 6 %.

Table 6.7 The potential total phosphorus trapped and exchanged per geomorphic feature (proximal floodplain and sediment sinks) and the potential percentage proportion of the total phosphorus accumulated of the total phosphorus yield adjusted from the SSY values of the Pot River catchment for the Gatberg and Minnehaha River catchments. The mean proportion values (%) are highlighted

		Gatberg River floodplain system			Minnehaha River floodplain system		
		Minimum	**Mean**	**Maximum**	**Minimum**	**Mean**	**Maximum**
Annual adjusted total phosphorus yield (tonnes yr^{-1})		0.89	1.16	1.50	0.15	0.20	0.25
Total phosphorus exchange flux (i.e., proximal floodplain zone)	Mean potential total phosphorus exchange flux (i.e., total phosphorus temporarily stored in lateral accretion deposits within the proximal floodplain zone, tonnes yr^{-1})	0.027	0.023	0.030	0.030	0.032	0.030
	Mean proportion of total phosphorus yields (%)	3	2	2	20	16	12
	Minimum potential total phosphorus trapped (tonnes yr^{-1})	0.018	0.023	0.015	0.021	0.022	0.020
	Minimum proportion of total phosphorus yields (%)	2	2	1	14	11	8
	Maximum potential total phosphorus trapped (tonnes yr^{-1})	0.027	0.035	0.030	0.048	0.050	0.048
	Maximum proportion of total phosphorus yields (%)	3	3	2	32	25	19
Total phosphorus sinks (i.e., oxbows and backswamp units)	Mean total phosphorus sinks (i.e., total phosphorus stored in the oxbows and backswamp geomorphic units, tonnes yr^{-1})	0.071	0.070	0.075	0.065	0.066	0.065
	Mean proportion of total phosphorus yields (%)	8	6	5	43	33	26
	Minimum potential total phosphorus trapped (tonnes yr^{-1})	0.062	0.058	0.060	0.038	0.038	0.038
	Minimum proportion of total phosphorus yields (%)	7	5	4	25	19	15
	Maximum potential total phosphorus trapped (tonnes yr^{-1})	0.071	0.070	0.075	0.081	0.082	0.080
	Maximum proportion of total phosphorus yields (%)	8	6	5	54	41	32
Combined Total phosphorus exchange flux and sediment sinks	Mean total annual potential phosphorus sinks (oxbows and backswamp units) and exchange flux (proximal floodplain zone, tonnes yr^{-1})	0.098	0.093	0.090	0.095	0.098	0.095
	Mean proportion of total phosphorus yields (%)	11	8	6	63	49	38
	Minimum potential total phosphorus trapped (tonnes yr^{-1})	0.080	0.081	0.075	0.059	0.060	0.058
	Minimum proportion of total phosphorus yields (%)	9	7	5	39	30	23
	Maximum potential total phosphorus trapped (tonnes yr^{-1})	0.107	0.104	0.105	0.129	0.132	0.128
	Maximum proportion of total phosphorus yields (%)	12	9	7	86	66	51

6.4 DISCUSSION

6.4.1 INTRODUCTION

This section discusses the results for sedimentation rates, total phosphorus accumulation rates, and trapping efficiencies presented in Section 6.3: Results.

6.4.2 SEDIMENTATION RATES

6.4.2.1 SUITABILITY OF THE CRS MODEL FOR DATING THE FLOODPLAIN STORAGE UNITS

The composite CRS model produced dates and sediment accumulation rates that showed variability as would be expected for floodplain geomorphic storage units with varying degrees of connectivity over time. A combination of ^{137}Cs and ^{210}Pb was used to calculate the age of the floodplain geomorphic storage units. As expected, in the Southern Hemisphere, ^{137}Cs activity was relatively low and a date of 1958 was used for the first detection of ^{137}Cs (Foster et al. 2007). All cores except core 5 on the Minnehaha River floodplain system ran out of detectable ^{137}Cs before the end of the core. The sedimentation rates given by the CRS model for core 5 align with the other core results and are comparable to other sedimentation rates in oxbows, although there is a low certainty attached to the results (see Davidson et al. 2004; Wren et al. 2019; Thomas et al. 2021).

Unsupported ^{210}Pb concentrations for the cores in both the Gatberg and Minnehaha River floodplain systems generally increased toward the top of the sequence as was expected for undisturbed sediment chronologies that accrued steadily during the accumulation phase. The higher fluctuation in unsupported ^{210}Pb values for the cores closest to the active channels shows the rapid accumulation of sediment as was expected due to more frequent connectivity between the active channel and these areas and the coarser nature of the sediment. Most of the cores could be extrapolated to 1921 with moderate certainty.

The low inventory of ^{137}Cs is consistent with other measured inventories for southern Africa reported by Collins et al. (2001), Owens and Walling (1996), and Foster et al. (2005). Low ^{137}Cs levels are due to historical fallout being significantly lower in the Southern Hemisphere than in the Northern Hemisphere (Walling and He 1999; Alvarez-Iglesias et al. 2007). The unsupported ^{210}Pb profiles for the six cores exhibit a reduction in concentration with depth, which is mainly a function of the radioactive decay of unsupported ^{210}Pb in the deposited sediment, with differences in the shape of the profiles from the six sites mainly reflecting differences in sedimentation rates. The relatively uniform trend of the decrease in unsupported ^{210}Pb with depth in the six cores indicates that the overbank sedimentation was generally continuous. Fluctuations of unsupported ^{210}Pb concentrations throughout the core could suggest variations in the unsupported ^{210}Pb content of deposited sediment

(which may be due to different sediment sources or the particle size composition of the deposited sediment), variations in the depth of sedimentation associated with individual overbank floods and in the frequency and magnitude of those floods, or uncertainties and errors linked with analytical methods. The differences in the ^{137}Cs and unsupported ^{210}Pb concentrations evident between the study sites reflect several factors including differences in the radionuclide fallout flux and consequently precipitation, in the radionuclide content of the deposited sediment, and the sedimentation rate, between the sites.

6.4.2.2 Temporal and spatial variation in sedimentation rates of the Gatberg and Minnehaha River floodplains systems

Information on sedimentation rates and patterns of contemporary sedimentation along the Gatberg River and Minnehaha River floodplain systems has emphasised their importance as sediment sinks and sediment storage units along the river systems, as well as their importance as a component of the sediment budget of the two catchments.

The average sedimentation rate for both floodplain systems was very similar, an average of 0.9 g cm^{-2} yr^{-1} for the Gatberg River floodplain and 1.2 g cm^{-2} yr^{-1} for the Minnehaha floodplain system. The accumulation rates for the Gatberg River floodplain system for the proximal floodplain (inner and outer bends) showed the second highest accumulation rates that reflected the coarser nature of the sediment and the frequent connectivity to the channel. This suggests that rapid accumulation is linked to a larger particle size and inundation frequency, which was deposited more readily along the inner bend of meander bends close to the channel. A slight increase in sedimentation rates was observed in this floodplain geomorphic zone for the last ca. 30 years compared to the average for the last ca. 100 years. Similarly, the proximal floodplain zone, except the outer bend, in the Minnehaha River floodplain system showed the highest accumulation rates, reflecting the coarse nature of the sediment and its connectivity to the active channel. There was also an increase in sedimentation rates for the last ca. 30 years. This increase in sedimentation rates could be the result of increased stormflow over the last ca. 30 years, higher sediment concentrations during overbank floods or the model being sensitive to coarser sediment layers, which may have skewed the results. The outer bend within the proximal floodplain zone of the Minnehaha River system showed a decrease in sedimentation rates in the last ca. 30 years, this could reflect a decrease in connectivity (less frequent flooding) of this geomorphic zone. This could be due to the outer bend being built up vertically decreasing the frequency of connectivity with the active channel.

Sedimentation trends for the oxbows for both floodplain systems showed a slight decrease or were stable for the last 30 years compared to the last 100 years. This could reflect the historical

configuration of the active channel relative to the locations of the oxbows. The decrease in sedimentation rates could be a result of the movement of the current channel from the historical location where it would have been closer to the oxbows.

Interestingly, the backswamp zone within the Gatberg River floodplain system had the same sedimentation rate as the proximal floodplain zone (highest sedimentation rate). The sedimentation rate has also increased very slightly in the last 30 years. This reflects that the backswamp areas in this system potentially: 1) were connected to the main river and inundated frequently, 2) accumulated sediment during times when sediment deposition was more, or 3) were connected when fine sediment concentrations were quite high in the flood waters during overbank flooding, or 4) receive additional sediment from the surrounding hill slope or localised bioturbation. On the other hand, the backswamp zone within the Minnehaha River floodplain system had the lowest sedimentation rates, which is what is expected for the zone furthest away from the channel. This may be due to the lower sediment concentrations and the fine nature of the sediment fraction in the floodwaters. This agrees with the results of other empirical studies (e.g. Kesel et al. 1974; Walling and He 1997, 1998; Ross et al. 2004; Piégay et al. 2008; Swanson 2013) and is consistent with the diffusion effect documented by other researchers (James 1985; Pizzuto 1987).

The sediment accumulation rates amongst the individual cores did not match up well temporally. This mismatch could be due to dating inaccuracies and the variance in connectivity and conditions that were optimal for sediment deposition. However, there were some years where peaks in sedimentation rates matched between the two floodplain systems. This could be due to either wetter years where large tropical systems bring above-average rainfall events (see Stone and Walling 1997; Aalto et al. 2003; Turner et al. 2006; Nanayama et al. 2007; Grenfell et al. 2009; Boldt et al. 2010; Schuerch et al. 2012; Tweel and Turner 2012) or dry periods where erosion increases due a decrease in vegetation cover, exposing soils to erosive rainfall events (López-Bermúdez et al. 1998; van der Waal et al. 2015).

The variability of the sedimentation rates for the cores within each of the floodplain systems, as well as the variability between the two systems, reflects the local variations in the nature and geometry of the channel and floodplain surface (which affect the degree, frequency, and distance of overbank flooding), vegetation cover, microtopography, and roughness of the floodplain surface (which affect rates of sedimentation), as well as local suspended sediment inputs (which will influence the suspended sediment concentrations associated with the floodwaters).

The years of peaks in sediment accumulation rates for both floodplain systems have some correspondences between the cores within each system and between the two systems. The

differences recorded between cores within an individual system as well as the differences that occur between these two systems could be due to three main reasons: 1) sediment accumulated at different times at the different core sites suggesting topography plays an important role in the transport and deposition of sediment, or 2) it was difficult to produce accurate sediment accumulation rates using the composite CRS model, or 3) localised rainfall plays an important role in the hydrological and sediment regimes of these two systems.

6.4.3.3 Comparison of the sedimentation rates of the Gatberg and Minnehaha River floodplains with other floodplains

The Gatberg and Minnehaha River floodplains have similar sedimentation rates ranging from 0.2 to 2.6 g cm^{-2} yr^{-1}, for ca. 100 years. Both the Gatberg and Minnehaha Rivers are typical of rivers on the eastern seaboard of South Africa. Similar values were reported for the Vuvu River (0.2 to 3.3 g cm^{-2} yr^{-1}) for higher flood benches along a relatively steep river along the nearby Escarpment foothills (van der Waal 2015) and for the Mkuze River floodplain (0.2 to 0.4 g cm^{-2} yr^{-1}; Humphries et al. 2010). The values for the Gatberg and Minnehaha Rivers span the upper end of the range that occurs in dryland regions and the lower end of the range that occurs in more humid regions. Dryland (Aridity index < 0.65) sedimentation rates range from 0.01 g cm^{-2} yr^{-1} (for the Nyl River, South Africa; McCarthy et al. 2011) to 1.2 g cm^{-2} yr^{-1} (for the lower Tana River, Kenya; Omengo et al. 2016). Humid (Aridity Index > 0.65) sedimentation ranges from 0.2 to 2 g cm^{-2} yr^{-1} (in the upper Mississippi River; Knox 2006), to 2.5 to 5.9 g cm^{-2} yr^{-1} (in the Yamuna River in India; Saxena et al. 2002) and 0.1 to 1 g cm^{-2} yr^{-1} (for Rivers in the UK; He and Walling 1996; Walling et al. 1996; Owens et al. 1999).

The overall mean values for the Gatberg and Minnehaha River floodplain systems (1.1 and 1.2 g cm^{-2} yr^{-1}) were lower than the documented rates for floodplains in catchments disturbed by increased human activity (e.g., Trimble 1983; Knox 1987; Marron 1992). This is expected for these relatively undisturbed catchments (no large urban centres, etc.).

6.4.3 Sediment trapping efficiencies for the floodplain geomorphic units

Floodplain systems have been demonstrated to be important sediment sinks along the sediment conveyance system trapping a significant proportion of the suspended sediment flux transported through a river system during overbank flood events and thus represent an important component of the catchment sediment budget (e.g., Walling and Quine 1993; Middelkoop and Asselman 1995; Walling et al. 1998).

The results presented in the previous section highlight the significance that the data for the Gatberg and Minnehaha River floodplain systems contribute to our knowledge of trapping efficiencies of floodplain systems in drylands. The results indicated that the deposition on the Gatberg River

floodplain accounts for between 12 and 20 % of the suspended sediment yield values, and between 34 and 57 % for the Minnehaha River floodplain. These results are similar to the lower end of the sediment trapping efficiencies estimated around the world, e.g., sediment trapping efficiencies ranged between 10 and 95 % within floodplain systems in central and eastern USA (Kleiss 1996; Gellis et al. 2015, 2017; Hopkins et al. 2018; Pizzuto et al. 2018) and in the UK and eastern USA, values ranged from 30 to 50 % (Walling et al. 1998, 1999).

Sediment storage elements in the floodplain landscape are the medium through which sediment transport and deposition processes act, and therefore their quantification is of great importance in understanding the sediment trapping efficiency of floodplain systems.

Within the Gatberg River floodplain system, the three floodplain storage zones' mean proportion of the total sediment yield was 3 % for the proximal floodplain zone, 3 % for the oxbows and 10 % for the backswamp storage zone. This amounted to a total mean annual potential proportion of the sediment yield that is stored of 16 % or 1317.5 tonnes yr^{-1}. Within the Minnehaha River floodplain system, the three floodplain storage zones were 16 % for the proximal floodplain zone, 20 % for the oxbows and 8 % for the backswamp storage zone. This amounted to a total mean annual potential proportion of the sediment yield that is stored of 44 % or 1073.6 tonnes yr^{-1}. The greater relative proportion of sediment stored on the Minnehaha River floodplain system (44 %) compared to the Gatberg River floodplain system (16 %) partly reflects the much lower estimated annual sediment yield of the Minnehaha River (approximately 2440 tonnes yr^{-1}) compared to the Gatberg River (approximately 8235 tonnes yr^{-1}), most importantly the relative size of the floodplain system compared to its catchment (Minnehaha floodplain is 4 % of its catchment compared to the Gatberg floodplain which is 0.2 % of its catchment) as well as the estimated sedimentation rates for each of the features and extrapolated areas for those features. There were two assumptions made to calculate the storage efficiencies for each of the features that should be considered when assessing the accuracy of these results. First, there were only six floodplain sampling sites for each system, and extrapolation of the sedimentation rate results to the entire estimated area for each floodplain storage unit could result in an overestimation of floodplain storage. Second, there are some reaches where the floodplain is protected from overbank flooding by vegetation, microtopography, and distance from the channel, although these areas are most likely reached during larger flood events. As such the extrapolated estimates of floodplain storage produced for the floodplain storage units may be overestimated. Although the trapping efficiencies of the different floodplain storage units may be overestimated, the values presented for the study rivers compare well with the values documented for other floodplain systems and show that these two systems are important sediment buffers along the river sediment conveyance system. This research findings have important implications for

floodplain restoration management e.g. restoring overbank flows that reach all areas of the floodplain surface, especially oxbows and the backswamp area to trap and store the most sediment or removing blockades or drains on the floodplain surface that may inhibit or channel sediment-laden flows from these two zones.

6.4.4 TOTAL PHOSPHORUS ACCUMULATION RATES

When the importance of floodplain systems as sediment sinks and storage zones is coupled with the recognition of the fine fraction of sediment in the transport of nutrients and contaminants through river systems (Allan 1986), then floodplains may also represent important sinks and storage zones for sediment-associated nutrients and contaminants (Marron 1992; Walling and Quine 1993; Macklin et al. 1997; Hudson-Edwards et al. 1999; Walling et al. 2000). As with sediment deposition, nutrient deposition has two important implications. First, it can result in the accumulation of nutrients in floodplain systems. This may create a problem by increasing levels of contamination in the floodplain system, as well as the potential for future remobilisation back into the river system (Leece and Pavlowsky 1997). Secondly, it can decrease the amount of nutrients that reach downstream. This has benefits for downstream uses as the water quality would have improved. However, this also could result in an underestimation of the total mass of the nutrients transported through the catchment measured at the catchment outlet. There have been few attempts, in drylands, such as in South Africa, to extend studies to include the role of floodplain overbank sedimentation in catchment sediment budgets and to include corresponding investigations related to sediment-associated nutrient budgets.

6.4.4.1 TEMPORAL AND SPATIAL VARIATION IN TOTAL PHOSPHORUS ACCUMULATION RATES OF THE GATBERG AND MINNEHAHA RIVER FLOODPLAINS SYSTEMS

Information on the total phosphorus accumulation rates and patterns of contemporary total phosphorus accumulation along the Gatberg River and Minnehaha River floodplain systems have emphasised their importance as total phosphorus sinks and storage units along the river systems, as well as their importance as a component of the phosphorus budget of the two catchments.

The average total phosphorus accumulation rate for both floodplain systems was very similar, an average of 0.8 g m^{-2} yr^{-1} for the Gatberg River floodplain and 1 g m^{-2} yr^{-1} for the Minnehaha floodplain system. The accumulation rates for the Gatberg River floodplain system for the proximal floodplain (inner and outer bends) showed the highest total phosphorus accumulation rates that reflected the addition of total phosphorus from overbank floodwaters and the frequent connectivity to the channel. A slight increase in sedimentation rates was observed in this floodplain geomorphic zone for the last ca. 30 years compared to the average for the last ca. 100 years. For the Minnehaha River floodplain system, the proximal floodplain zone had the second-highest accumulation rates. There was also an

increase in total phosphorus accumulation rates for the last ca. 30 years. This increase in sedimentation rates could be the result of increased stormflow over the last ca. 30 years, higher sediment-associated phosphorus concentrations during overbank floods, a change in total phosphorus input from the upstream catchment, or the model being sensitive to coarser sediment layers, which may have skewed the results. The outer bend within the proximal floodplain zone of the Minnehaha River system showed a decrease in total phosphorus accumulation rates in the last ca. 30 years. This could reflect a decrease in connectivity (less frequent flooding) or the nature of the sediment being deposited. This could be due to the outer bend being built up vertically decreasing the frequency of connectivity with the active channel.

The sedimentation trends for the oxbows for both floodplain systems showed a slight increase or were stable for the last 30 years compared to the last 100 years. This could reflect the historical configuration of the active channel relative to the locations of the oxbows.

The variability of the total phosphorus accumulation rates for the cores within each of the floodplain systems as well as the variability between the two systems reflects the local variations in the nature and geometry of the channel and floodplain surface (which affect the degree, frequency and distance of overbank flooding (Wissmar and Bisson 2003; Drouin et al. 2011), vegetation cover, microtopography and roughness of the floodplain surface (which affect rates of sedimentation; Swanson et al. 1988; Mitasova et al. 1997; Kneller et al. 1999; Van Oost et al. 2000; Jeffries et al. 2003; Zheng 2006), as well as local suspended sediment-associated phosphorus inputs, such as land use, which will influence the suspended sediment-associated phosphorus concentrations associated with the floodwaters (Hupp et al. 1993; Langland and Cronin 2003; Ross et al. 2004).

6.4.5 TOTAL PHOSPHORUS TRAPPING EFFICIENCIES FOR THE FLOODPLAIN GEOMORPHIC UNITS

The results presented in the previous section indicated that the Gatberg River floodplain's total phosphorus deposition accounts for between 6 and 11 % of the suspended sediment-associated total phosphorus yield values, and between 38 and 63 % for the Minnehaha River floodplain. These results fall within the global sediment-associated total phosphorus trapping efficiencies that ranged from 5 to 80 % (Brunet and Astin 1997, 2000; Walling and Owens 2003; van der Lee et al. 2004; Kronvang et al. 2007; Noe and Hupp 2009; Gillespie et al. 2018) for all types of wetlands in humid climates. In the Gatberg and Minnehaha River floodplain systems, the estimated mean sediment-associated total phosphorus trapped amounts to 0.093 and 0.098 t yr^{-1}, respectively. The results presented in the previous section highlight the significance of the Gatberg and Minnehaha River floodplain systems in contributing to our knowledge of total phosphorus trapping efficiencies of floodplain systems in drylands.

Sediment storage elements, also known as geomorphic units, within the floodplain landscape, serve as the conduit for sediment and phosphorus transport and deposition processes. Quantifying these elements is crucial to understanding the overall efficiency of phosphorus trapping within floodplain systems.

Within the Gatberg River floodplain system, the three floodplain storage zones' mean proportion of the total sediment-associated phosphorus yield was 2 % for the proximal floodplain zone, 2 % for the oxbows and 4 % for the backswamp storage zone. This amounted to a total mean annual potential proportion of the phosphorus yield that is stored of 8 % or 0.093 t yr^{-1}. Within the Minnehaha River floodplain system, the three floodplain storage zones were 16 % for the proximal floodplain zone, 29 % for the oxbows, and 4 % for the backswamp storage zone. This amounted to a total mean annual potential proportion of the sediment yield that is stored of 49 % or 0.098 t yr^{-1}.

Due to the relationship between phosphorus dynamics and suspended sediment dynamics, the same two assumptions made for the sediment trapping efficiencies of each floodplain storage unit on each floodplain need to be considered when assessing the accuracy of these results. As such, the extrapolated estimates of floodplain total phosphorus storage produced for the floodplain storage units may be overestimated. Although the total phosphorus trapping efficiencies of the different floodplain storage units may be overestimated, the values presented for the study rivers compare well with values documented for other floodplain systems and show that these two systems are important total phosphorus buffers along the river sediment conveyance system.

Total phosphorus accumulated faster in the floodplain storage units that were capturing more sediment. Sediment total phosphorus concentrations did not correlate with sediment accumulation rates in the Gatberg system; rather, the total phosphorus accumulation rates correlated to the increased amount of sediment that was deposited. Within the Minnehaha floodplain system, there was a better correlation between total phosphorus accumulation rates, total phosphorus concentrations, and sedimentation rates. Other researchers have found similar correlations in floodplain systems (Cooper and Gilliam 1987; Johnston et al. 2001; Stoeckel and Miller-Goodman 2001; Noe and Hupp 2005). Connectivity between the channel and floodplain is a limiting factor in determining how much of an effect a floodplain system has on the nutrient budget of a river system. Depending on how well the floodplain is connected to the river system will determine the potential nutrient (total phosphorus) accumulation rates and trapping efficiencies. This is also true for the different storage units into which the floodplain systems were divided. Such that those areas that are well connected have the highest sedimentation and total phosphorus accumulation rates. In the Gatberg River floodplain system, these were the proximal floodplain, followed by the backswamp zone. In the Minnehaha River floodplain system, these were the oxbows followed by the proximal

floodplain. Within the Gatberg River system, total phosphorus trapping efficiencies showed a slight discrepancy with these results due to the estimated area that made up the different floodplain storage units. For example, even though the proximal floodplain had the highest total phosphorus accumulation rate, it had a low trapping efficiency due to the small area that the proximal floodplain made up out of the total floodplain extent.

Both the Gatberg and Minnehaha River floodplain systems contribute to a reduction in the total phosphorus loading of the rivers. However, these systems are likely to release phosphorus back into the system due to re-suspension, movement in solution by throughflow, and erosional process (see Chapter 7). According to the trapping efficiencies of the two systems, Minnehaha has the potential to trap the largest proportion of its total phosphorus yield. However, the Gatberg River floodplain system traps the most sediment as tonnes per year. These findings indicate that floodplains function as an important nutrient sink in these fluvial landscapes.

6.5 CONCLUSION

A comprehensive analysis of sedimentation rates and patterns, as well as total phosphorus accumulation rates and trapping efficiencies, within the Gatberg and Minnehaha River floodplain systems and their different geomorphic units, provides valuable insight into the dynamics of these systems within their respective catchments.

Results from this work suggest that during floods, the Gatberg River floodplain experienced average sediment deposition rates for the last 100 years between 0.5 and 1.3 g cm^{-2} yr^{-1}. The Minnehaha River floodplain had sedimentation rates of between 0.2 and 2 g cm^{-2} yr^{-1}. Both floodplain systems' sedimentation rates increased slightly in the last 30 years. Flood-derived sediment captured in the cores during this study in the Gatberg and Minnehaha River floodplain systems had an average total phosphorus concentration of 99 mg kg^{-1} and 94.5 mg kg^{-1}, respectively. As a result, the Gatberg River floodplain may capture as much as 1.1 g TP m^{-2} yr^{-1}, or as little as 0.5 g TP m^{-2} yr^{-1} (average for the last 100 years for all the cores). The Minnehaha River floodplain may capture between 0.09 and 1.4 g TP m^{-2} yr^{-1} (average for the last 100 years for all the cores). The variability in sediment and sediment-associated phosphorus floodplain deposition may be governed, in part, by a floodplain's topography, flood magnitude and duration, suspended sediment concentrations, the grain size distribution of the suspended sediment, the relative importance of various transporting mechanisms and, over a longer timescale, inundation frequency.

Sedimentation rates exhibited variability in the different geomorphic zones of the floodplains, reflecting local geomorphic characteristics and hydrological processes. While some areas showed rapid sediment accumulation due to frequent connectivity to the active channel and coarser sediment,

others exhibited lower rates, indicating reduced connectivity or finer sediment deposition further from the channel. The highest sediment and sediment-associated phosphorus deposition rates in the Gatberg floodplain were associated with the backswamp and the proximal floodplain geomorphic units. Within the Minnehaha floodplain, the highest sedimentation rates were found in the proximal floodplain and oxbow geomorphic units. The highest total phosphorus accumulation rate occurred in the oxbow geomorphic unit. These findings underscore the complex interplay of factors influencing sediment dynamics within floodplain environments.

Moreover, the assessment of total phosphorus accumulation rates and trapping efficiencies highlights the role of floodplains as significant sinks for sediment-associated nutrients. The results indicate that both floodplain systems effectively trap sediment-associated total phosphorus, thus contributing to a reduction in total phosphorus loading in the rivers.

The comparison of sedimentation rates and total phosphorus trapping efficiencies between the Gatberg and Minnehaha River floodplains, as well as with other floodplain systems globally, emphasises the contextual variability in floodplain functioning. Despite similarities in sedimentation rates, differences in trapping efficiencies suggest that variations in floodplain size to catchment extent, suspended sediment quantity, floodplain morphology, hydrology, connectivity, and sediment dynamics play a crucial role in trapping efficiencies between the two systems.

Overall, this study underscores the importance of floodplains as integral components of riverine landscapes, playing critical roles in sediment storage, nutrient cycling, and overall ecosystem function. The findings contribute valuable information to understanding fluvial geomorphology and have implications for land and water management strategies aimed at preserving and enhancing the ecological integrity of rivers and their floodplains.

CHAPTER 7 : EROSION AND RECYCLING

7.1 INTRODUCTION

Floodplains are formed due to alluvium accumulation and once developed these fluvial landforms can be altered by erosional processes. The most common erosional processes (Rhoads 2020) are 1.) stripping of floodplain surfaces, 2.) lateral movement of cut banks and related shaving of floodplains; 3.) carving of minor channels into floodplain surfaces; and 4.) avulsive incision of a new main river channel. The effectiveness of erosional processes, like depositional processes, varies spatially and with the river type. For example, floodplains of rivers with high stream power that carry coarse bed material are more prone to erosional change than floodplains of rivers with moderate stream power that transport primarily suspended sediment loads that form cohesive deposits. This chapter focuses on channel change and erosion in the Minnehaha and Gatberg study areas.

Channel bank erosion processes contribute to sediment in river catchments and have been found to account for a large portion of a catchment's sediment budget (Collins et al. 1997; Walling et al. 1999, 2008; Owens et al. 2001; De Rose et al. 2005; Walling and Collins 2005; Walling 2005; Wilkinson et al. 2005; Collins et al. 2012; Kronvang et al. 2013; Lu et al. 2015; Neal and Andera 2015). Bank erosion can release and transport fine-grained sediments laden with contaminants (e.g., phosphorus and heavy metals). Furthermore, increased sediment mobilisation and delivery can have negative biological and ecological impacts on river systems. Numerous factors influence channel-bank erosion rates, including bank material composition (Hooke 1980; Bull 1997; Couper 2003; Julian and Torres 2006), bank geometry (Micheli and Kirchner 2002; Laubel et al. 2003; Walling 2005; Walling et al. 2006), discharge magnitude (Knighton 1973; Gautier et al. 2007; Hooke 2008), and riparian vegetation (Micheli and Kirchner 2002; Simon and Collison 2002; Laubel et al. 2003; Mattia et al. 2005).

Several studies (see Hickin and Nanson 1975; Thorne 1991; Hudson and Kesel 2000; Hooke 2003) noted the influence of variations in channel radius of curvature on bank erosion rates due to changes in flow geometry within the channel. High-velocity flow is directed towards the outer channel bank when the radius of curvature decreases, increasing bank erosion rates. Below this influence, bank erosion rates decrease as the radius of curvature is further reduced because of the creation of secondary cells, protecting the channel bank (Hey and Thorne 1975; Bathurst et al. 1977). Knighton (1998) also observed a change in shear stress distribution within the low radius of curvature channels, which resulted in increased downstream migration. In very sinuous channels, the location of the maximum flow velocity (and thus the maximum shear stress) is downstream of the bend apex. The channel curvature ratio (the radius of curvature divided by the channel width) is inversely related to the channel sinuosity up to sinuosity of ~1.5 (Janes et al. 2017). Above this value, the channel

curvature ratio decreases with increasing sinuosity (Julien 2002). Bank erosion and channel sinuosity have also been linked (Abam 1993; Janes et al. 2017; Schilling et al. 2023). Valley boundaries may also limit channel-bank erosion (and thus lateral migration). Lewin and Brindle (1977) described three degrees of confinement based on the decreasing valley width relative to the channel width: (1) wide-floored valleys with infrequent contact with valley walls, (2) floodplains narrower than the amplitude of meander bends, and (3) well-developed meandering restricting further meander development. Channel sinuosity and confinement have been linked for example, low sinuosity is associated with confined reaches (Milne 1983; Tooth et al. 2002; Nicoll and Hickin 2010).

Previous empirical studies have used a variety of field techniques (Collins and Walling 2004) to observe bank erosion rates over timescales ranging from months to years, such as erosion pin monitoring (Lawler 1993; Ashbridge 1995), repeated cross-channel surveys (Hickin and Nanson 1975), and aerial imagery (Hooke 1980; Micheli and Kirchner 2002). Total channel-bank erosion and deposition can be measured using consecutive cross-channel surveys (Lawler 1993; Julian and Torres 2006). Although labour-intensive, these approaches can assess bank erosion at relatively modest spatial scales (ranging from a few kilometres to single channels). Planimetric alterations have also been observed using aerial photogrammetry (Kondolf et al. 2002; Michalková et al. 2011) in conjunction with LIDAR data (De Rose and Basher 2011). However, these approaches are constrained by the availability and temporal coverage of the photogrammetric and LIDAR data.

The Gatberg and Minnehaha Rivers are categorised as mixed-bed single-thread meandering rivers with banks predominantly consisting of very fine to fine sand. Field observations showed that bank erosion, collapse, and slumping occurred in both river systems during the wet seasons. The overall purpose of this chapter is to estimate and describe the contemporary channel erosion and deposition, explore the historical channel change, estimate lateral migration rates, and investigate the channel's potential for future change and how this affects sediment and phosphorus patterns and dynamics in the two floodplains. The objectives of this study are as follows:

1. To determine the contemporary erosion and deposition cross-sectional areal extent using repeat cross-sectional surveys over two wet seasons for 10 meander bends within both floodplain systems.
2. To estimate the volumes of erosion, as well as the sand, clay and silt, organic matter, and the total phosphorus volumes of the eroded material.
3. Examine the local scale planform channel change events, namely meander bend cutoffs, using historical images from 1958, 1993 and 2020 for the Gatberg River reach and 1958, 1966 and 2015 for the Minnehaha River reach.

4. Estimate lateral migration rates from ^{14}Carbon dates of two oxbows in a nested sequence on the Gatberg River floodplain system (de Villiers 2022).
5. Investigate channel geometry change using the geometry measurements of the oxbows (historical channel), 1958 channel dimensions, and either the 2020 (Gatberg River) or 2015 (Minnehaha River) images for the contemporary channel dimensions.
6. Examine the future potential channel changes using the chute and neck meander bend stability ratios.

7.2 METHODS

7.2.1 FIELD DATA COLLECTION AND LABORATORY ANALYSIS

A total of 38 and 34 topographical cross-sections were measured down the Gatberg and Minnehaha River reaches respectively. The first survey was in December 2019 and the re-survey was in May 2021. The channel banks were surveyed using a Differential Global Positioning System (DGPS) with a remote base station (accuracy of ± 1 cm in the x, y, and z fields). Clear breaks in slope, channel features and erosional features were noted. A fence dropper was used to mark the start and end of the transects as benchmarks for the repeat surveys to eliminate positional errors.

The estimated ages of the oxbows were calculated by de Villiers (2022). The following is a summary of de Villiers (2022) methods. In November of the same year, four oxbows located on the Gatberg River floodplain were carefully chosen for coring. These selections aimed to establish a lateral sequence, varying in distance from the main channel to gauge lateral erosion and accretion rates. Using a gouge corer and bucket auger, four cores were extracted from the middle of each selected oxbow, ranging in depth from 1.85 m to 2.5 m. The precise location and elevation of each core were recorded using a DGPS. Subsequently, four samples, one from each core, were dispatched to Direct Accelerator Mass Spectrometry in the USA for age determination using Accelerator Mass Spectrometry (AMS) radiocarbon methods. AMS is a dating technique that is most often used to determine the concentration of ^{14}Carbon (^{14}C) for radiocarbon dating. Compared to other radiocarbon dating methods AMS requires smaller sample sizes while yielding highly precise chronologies. AMS enables the measurement of the number of ^{14}C atoms present in the sample. To ensure accurate results, especially in samples with low organic material content, the lowermost sample, typically rich in clay, was selected from each core. Thus, the burial age (the time when this clay-rich layer was deposited and then buried by subsequent sediment deposits) of the basal (lowermost) sediments in the oxbows of the nested sequence was measured. Unfortunately, this meant that the layer above refusal could not be measured. However, for the analysis in this chapter, only two of the cores were found to be in chronological sequence. Thus, only these two cores were used. For a detailed

methodology, refer to de Villiers (2022). Particle size analysis, organic matter content and total phosphorus analysis were also conducted by de Villiers (2022).

7.2.2 DESKTOP AND DATA ANALYSIS

Volumetric estimates of sediment loss from meander migration were made for each of the rivers. To calculate the eroded volumes, a subset of the meander bend cross-sectional data was created. The cross-sections that showed erosional channel area changes from the 2019 surveys to the 2021 surveys were extracted. From this subset, the median and maximum values of eroded channel change were calculated. To estimate the approximate volumes these median and maximum values were multiplied by the average length of the meander bends. The volume contributed was converted to mass using a bulk density of 1.55 g cm^{-3} (Flemming and Hay 1984; Brady and Weil 2008; van der Waal 2015). These values were divided by two years to get a value of tonnes per year. The total volumes of eroded material per year were then scaled for the number of meander bends that experienced erosion in each river reach (in the Gatberg the volume was multiplied by 0.47 (29 out of 62 meander bends experienced erosion) and in the Minnehaha, the volume was multiplied by 0.42 (81 out of the 192 meander bends experienced erosion)). This allowed for extrapolation of individual measurements to the system scale. To calculate volumetric estimates of the sediment eroded, which was sand, clay and silt, organic matter, and total phosphorus data from Chapter 5 (cut banks) were used (summarised in Table 7.1).

Table 7.1 A table summarising the percentage constituents of the cut bank sediment samples

	Sand fraction (%)		Clay and silt fraction (%)		Organic matter content (%)		Total phosphorus (%)	
	Median	Max	Median	Max	Median	Max	Median	Max
Gatberg River (cut banks)	82	98	18	27	3	8	0.05	0.09
Minnehaha River (cut banks	76	82	21	40	4	8	0.06	0.09

To assess the evolution of the floodplain reaches of the Gatberg and Minnehaha Rivers, three aerial images (at a scale of 1:30 000), from 1958, 1993, and 2020 (for the Gatberg); and 1958, 1966 and 2015 (for the Minnehaha) were used. The aerial images were obtained from the CDNGI Geospatial Portal, a database containing a wide range of geospatial information for South Africa (CDNGI Geospatial Portal, accessed 2023.03.15). The 1958 aerial images were used as they were of reasonable definition and were the oldest date available for the study sites. The 1958 photos had to be georeferenced as described below.

Historical aerial photos were georeferenced using the adjusted transformation in ArcInfo. Large boulders, rocky outcrops, houses, and gravel roads were used as georeferencing control points, as

they were easily identifiable. Care was taken to use as many control points as possible. Approximately 50 control points were used per image, minimising the root mean square error to below 0.01.

A morphometric investigation of the floodplain features of active channels, oxbows, and meanders was carried out for both the floodplain systems of the Gatberg and Minnehaha Rivers. Using aerial images, shapefiles of the oxbows, meander bends, and active channels were produced in ArcGIS. Each oxbow's area, length, diversion angle, and radius of curvature were computed. For meander bends, the wavelength (m), the bend length (m), the bend amplitude (m), the radius of curvature (m), the mean channel bankfull width (m), and the tightness of the bend (m) were captured. Following the methods of Dieras et al. (2013), the length was measured by digitising a line through the centre of the feature. The bankfull width was measured, using the measuring tool in ArcMap 10.8.2, for 5 to 10 cross-sections across the identified oxbows and averaging the calculated widths. The diversion angle, defined as the angle between the main channel and the point where the former meander merged, was calculated by digitising centrelines in both the active and abandoned channels (Figure 7.1) (Dieras et al. 2013). A best-fit circle was digitised on each of the identified oxbows and meander bends to determine the radius of curvature. The best-fit circle has the closest circumference to the meander bend or oxbow centreline (Billi et al. 2017). Sinuosity was measured using the ArcMap 10.8.2 measurement tool and calculated by dividing the length of the channel centreline by the length of the valley.

Potential neck cutoff events were examined using the neck cutoff stability by applying the rule of one channel width (Lewis and Lewin 1983). The basis for this rule is that neck cutoff occurs when the separation between two sections of a meander bend is less than one channel width (Lewis and Lewin 1983). Meander bends with neck lengths equal to one channel width in the floodplain systems of the Minnehaha and Gatberg Rivers were identified. To evaluate the potential for meander chute cutoff events the chute cutoff stability ratio was used (Joglekar 1971). To calculate the chute cutoff ratio, the length of the channel bend is divided by the length of the potential cutoff channel.

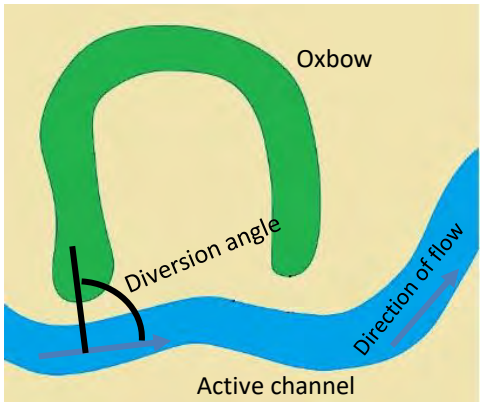

Figure 7.1 Schematic of the calculation of the diversion angle (adapted from Constantine et al. 2010; Dieras et al. 2013)

7.3 RESULTS

7.3.1 CHANNEL CHANGE FROM REPEAT SURVEYS

Figure 7.2 shows the locations of the channel cross-sections in the Gatberg (A) and Minnehaha (B) River floodplain reaches used in the repeat survey calculations. Ten meander bends were chosen in each system and cross-sections are numbered from upstream to downstream. Figure 7.3 shows an example of a meander bend (A) showing erosion of the cut bank and deposition on the point bar and (B) an example of bank slump and collapse along the outer bend (cut bank) of a meander bend. Figure 7.4 shows two examples of the cross-sections from 2019 and 2020 superimposed on each other. The change in channel shape can be seen.

Results are presented for all the cross-section survey locations for both the Gatberg and Minnehaha Rivers collected during the two survey seasons (2019 and 2021). The results are summarised by main-channel bankfull cross-sectional areas (Table 7.2), changes in bankfull channel widths, changes in maximum bankfull depth, and changes in average bankfull depth (Figure 7.5 and Figure 7.6).

In the Gatberg River floodplain system, Table 7.2 indicates there was a reduction in cross-sectional area between survey years for select cross-sections; however, this is largely a combination of deposition along channel banks (which increases channel capacity and was still accompanied by an increase in channel depth caused by channel bed scouring- Figure 7.5). Table 7.2 indicates that 18 of the 38 cross-sections experienced an increase in cross-sectional area. Of these, eight changes in the cross-sectional area were accompanied by an increase in bankfull width and depth (both bank erosion and channel bed scour); six changes in the area were accompanied by an increase in depth only; 1 with an increase in width only and 3 that were accompanied by changes in neither width nor depth. A total of 76 % of the cross-sections experienced varying magnitudes of scouring along the channel beds, indicating a general absence of sediment aggradation within the main channel bed. Only 9 % of the cross-sections indicated varying amounts of bank erosion (not accompanied by scouring of the channel bed). Approximately 8 m^2 of the cumulative cross-sectional area was eroded and 12 m^2 was deposited. The maximum change in the cross-sectional area was 1.14 m^2 and occurred in cross-section 6. There was no change calculated for cross-section 29. The largest change of the channel bed occurred at cross-section 37 with 0.83 m of deposition. The largest erosional change in the channel bed occurred at cross-section 34, with 0.62 m of sediment being scoured from the bed between the two survey seasons. The largest channel bank change occurred at cross-section 19, with 3.56 m of sediment being eroded.

In the Minnehaha River floodplain system, Table 7.2 indicates a reduction in cross-sectional area between survey years for select cross-sections; however, this is largely a combination of erosion along

channel banks accompanied by an increase in channel depth caused by channel bed scouring (Figure 7.6). The table indicates that 14 of the 33 cross-sections experienced an increase in cross-sectional area. Of these, 9 changes in the cross-sectional area were accompanied by an increase in bankfull width and depth (both bank erosion and channel bed scour); 1 area change was accompanied by an increase in depth only; 2 with an increase in width only and 2 that were accompanied by changes in neither width nor depth. 73 % of the cross-sections experienced varying magnitudes of scouring along the channel beds indicating a general absence of sediment aggradation within the main channel bed. A total of 11 % of all the cross-sections indicated varying amounts of bank erosion (not accompanied by scouring of the channel bed). Approximately 4 m^2 of the cumulative cross-sectional area was eroded and 17 m^2 was deposited. The maximum cross-sectional area change was 1.23 m^2 and occurred at cross-section 12. The largest channel bed erosional change occurred in cross-section 14 with 0.77 m^2 of sediment being scoured from the bed between the two survey seasons. The largest channel bank change occurred at cross-section 14 with 2.94 m^2 of sediment being eroded.

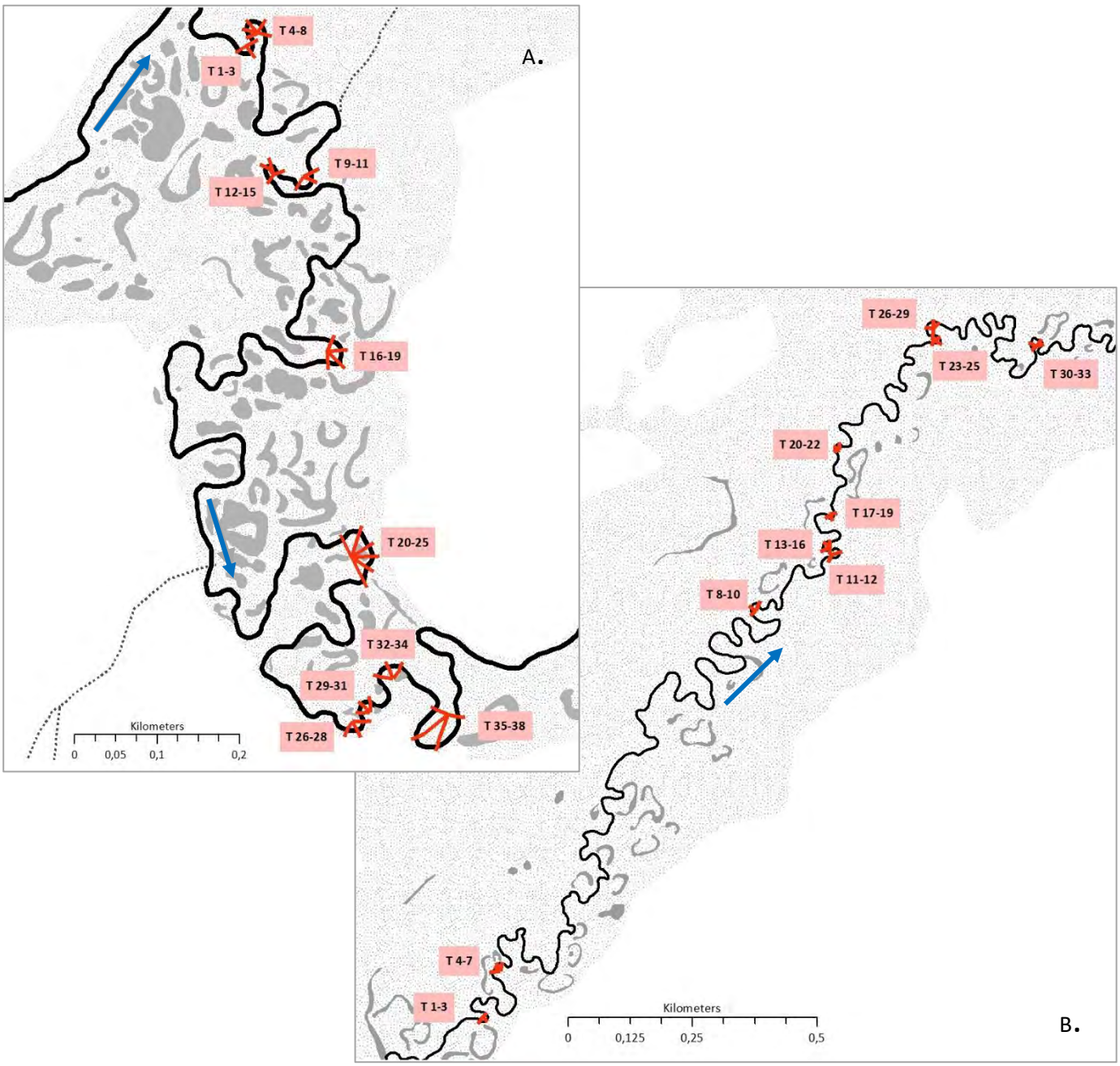

Figure 7.2 Channel cross-section locations in A) Gatberg and B) Minnehaha River floodplain reaches. Transects are numbered from upstream to downstream across 10 meander bends

Figure 7.3 An example of a meander bend showing the cut bank erosion and deposition on the point bar (A). An example of bank slumping and collapse along the outer bend (cut bank) of a meander bend (B)

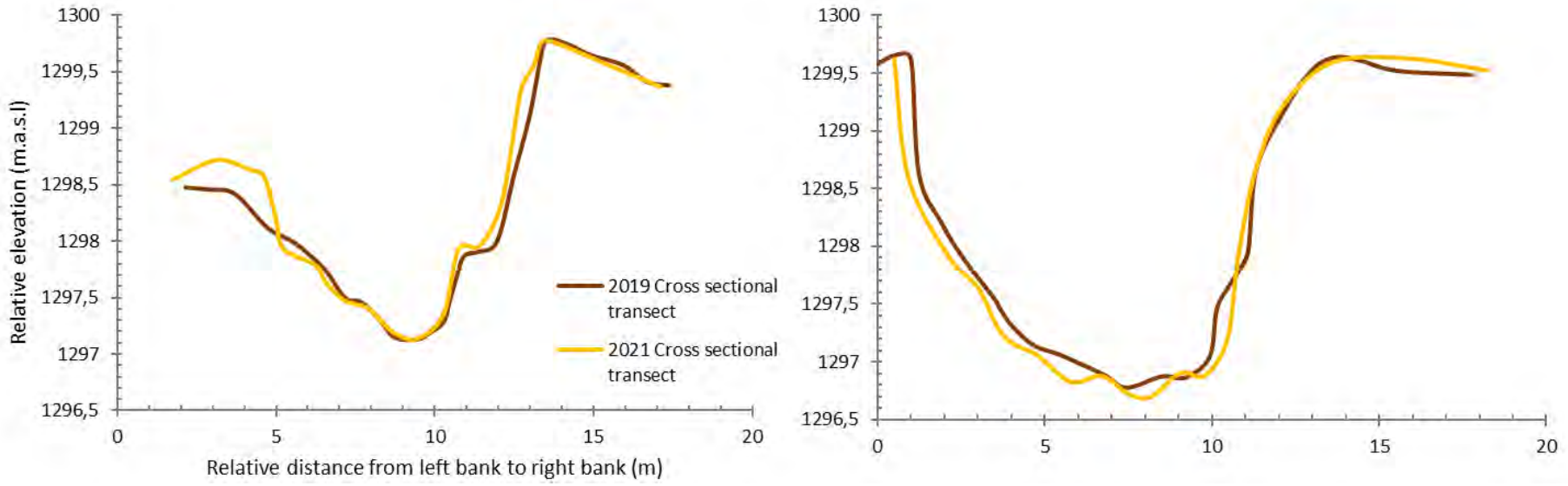

Figure 7.4 Two examples of the cross-sectional data from the re-surveys (2019 and 2021) showing areas of deposition and erosion

Table 7.2 Changes in cross-sectional area between 2019 and 2021 surveys within the Gatberg and Minnehaha River floodplain reaches (cross-sections that were dominated by erosion are highlighted in grey)

	Gatberg River floodplain reach				Minnehaha River floodplain reach			
Cross-section number	**Cumulative distance (m)**	**Channel area 2019 (m²)**	**Channel area 2021 (m²)**	**Channel change (%)**	**Cumulative distance (m)**	**Channel area 2019 (m²)**	**Channel area 2021 (m²)**	**Channel change (%)**
1	963	9.4	9.9	5.3	855	0.6	0.9	32.2
2	980	17.3	17.7	2.4	871	5.5	5.6	1.2
3	992	11.1	11.1	0.4	886	5.5	6.0	9.2
4	1000	6.7	6.2	-7.6	1158	8.1	6.1	-33.4
5	1009	20.5	21.0	2.3	1172	4.5	4.8	7.6
6	1018	23.0	24.1	4.7	1180	7.0	6.1	-14.7
7	1036	20.1	19.9	-0.9	1190	4.1	3.8	-9.0
8	1048	10.8	10.1	-7.1	3398	5.6	5.2	-6.7
9	1384	13.7	12.8	-6.7	3411	10.6	8.6	-23.5
10	1392	13.7	13.2	-3.5	3429	6.5	6.9	6.4
11	1417	9.8	9.9	1.5	3715	4.1	4.8	14.0
12	1447	12.0	12.1	0.8	3741	5.0	6.3	19.6
13	1460	20.7	20.7	-0.1	3766	4.9	3.9	-25.5
14	1466	19.1	18.5	-3.1	3779	6.3	6.6	4.8
15	1482	11.6	12.0	3.2	3791	5.0	4.2	-19.1
16	1590	10.0	10.6	5.0	3802	4.4	4.6	3.7
17	1607	12.2	12.6	3.3	3937	9.3	9.1	-1.9
18	1622	15.4	15.5	0.4	3947	7.4	6.6	-11.1
19	1636	12.2	11.9	-2.7	3958	4.6	4.7	1.7
20	2708	8.6	9.1	5.7	4111	3.7	3.9	5.1
21	2731	17.9	18.2	2.1	4121	6.8	6.5	-5.6
22	2751	10.2	10.3	0.6	4128	3.0	3.6	15.6
23	2764	9.5	8.9	-7.1	4667	5.5	5.4	-2.8
24	2780	12.1	10.8	-11.9	4681	7.3	5.9	-23.4
25	2797	19.0	19.6	2.9	4690	4.8	3.7	-27.3
26	2897	12.5	12.7	2.0	4705	5.3	3.9	-36.0
27	2910	9.3	9.9	5.6	4710	4.4	5.3	16.9
28	2923	10.5	10.3	-1.6	4734	5.5	5.8	5.2
29	2935	5.8	5.8	0.0	4754	5.6	5.6	-1.1
30	2946	18.6	17.5	-5.9	4766	4.6	4.5	-0.2
31	2957	15.8	15.0	-5.5	5390	2.8	2.6	-5.7
32	3019	17.0	15.7	-8.2	5403	10.3	5.9	-73.6
33	3036	11.0	10.9	-0.6	5431	6.6	6.3	-4.6
34	3052	13.2	12.6	-5.2	5441	8.3	7.2	-15.0
35	3126	9.6	9.2	-4.9				
36	3168	15.1	13.3	-13.2				
37	3200	13.5	14.6	7.7				
38	3246	9.8	9.6	-2.0				

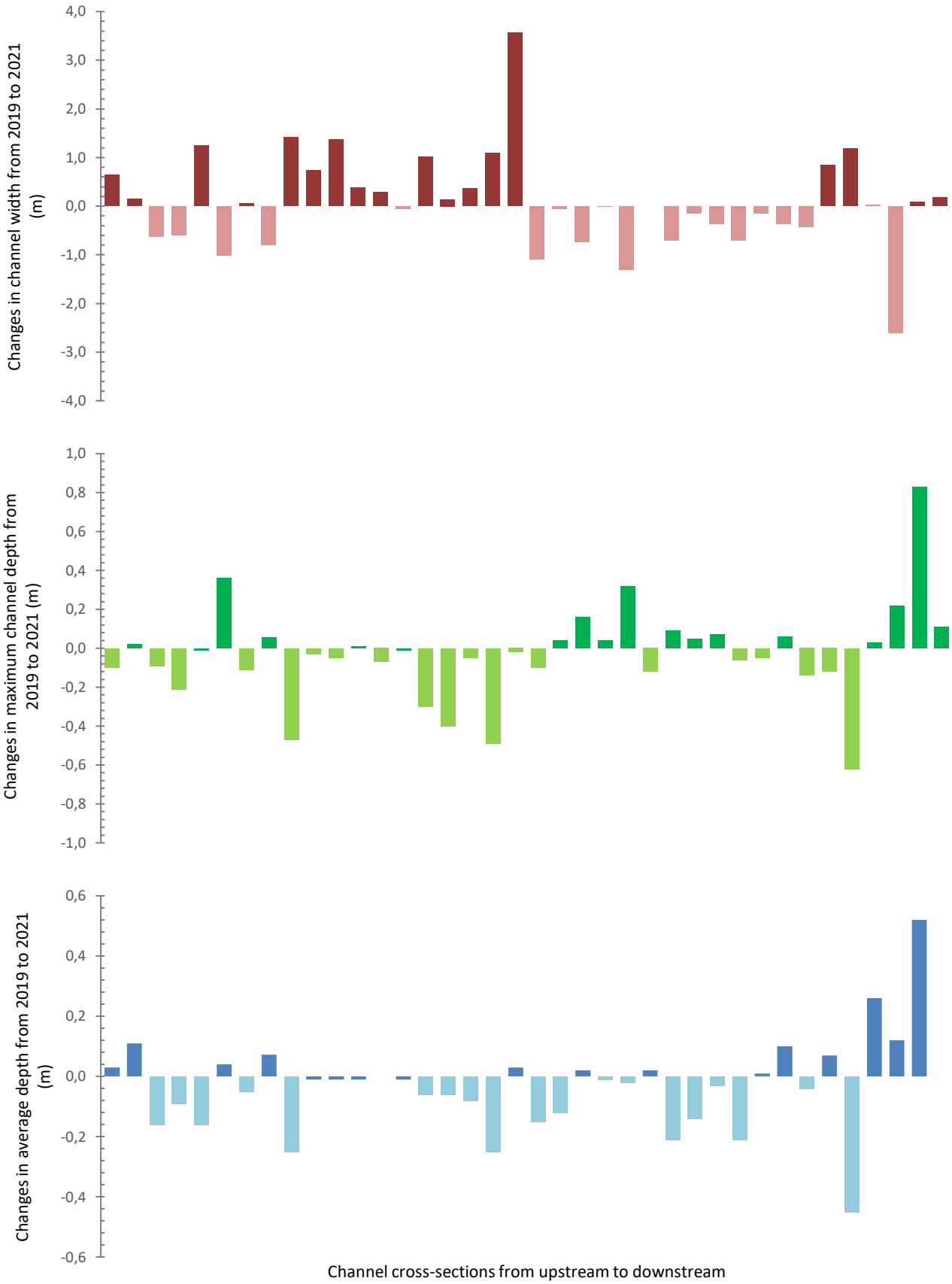

Figure 7.5 Changes in channel width, maximum channel depth, and average depth between 2019 and 2021 surveys within the Gatberg River floodplain reaches

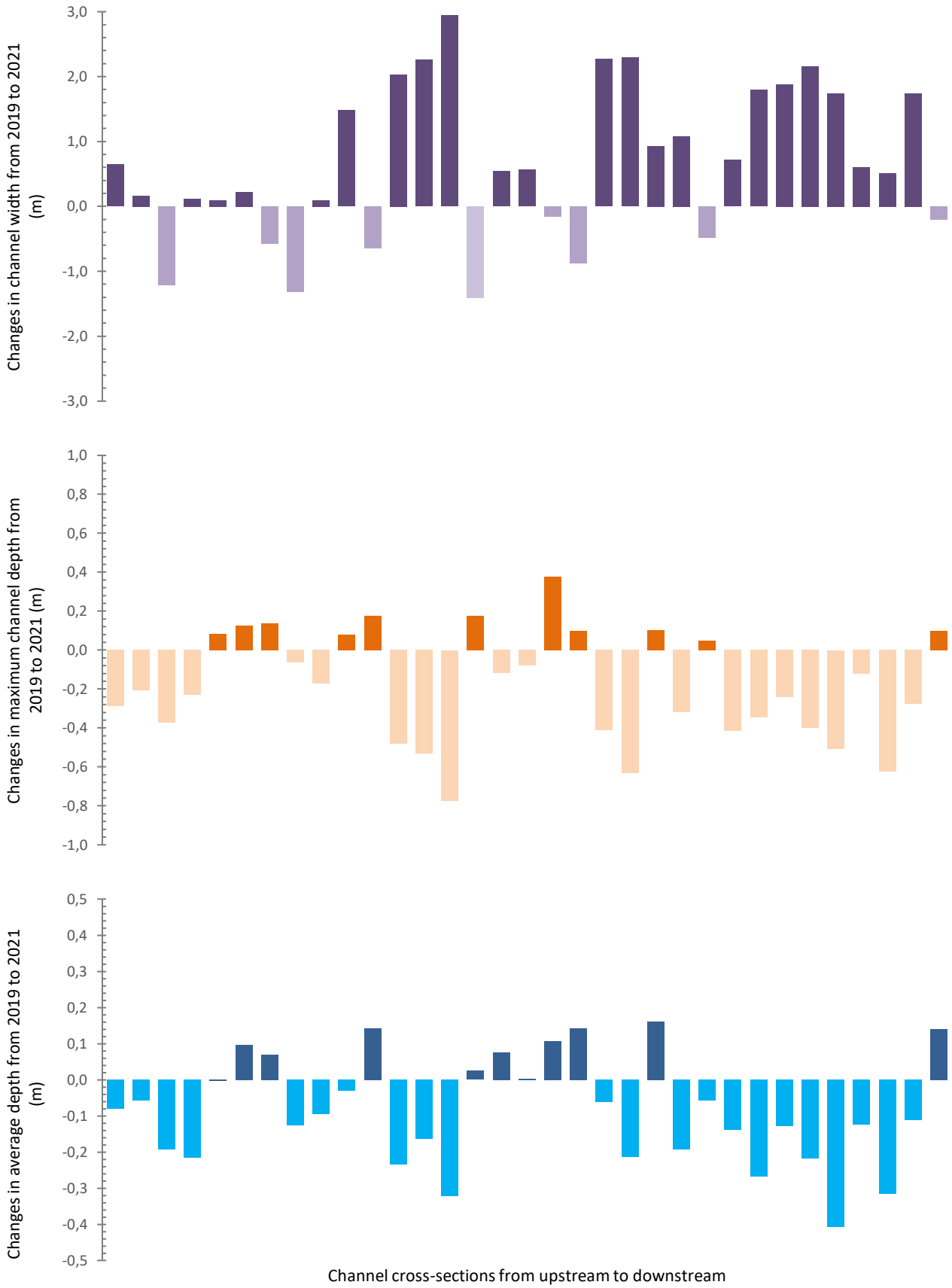

Figure 7.6 Changes in channel width, maximum channel depth, and average depth between 2019 and 2021 surveys within the Minnehaha River floodplain reaches

7.3.1.1 CHANNEL EROSION VOLUMES AND CHARACTERISTICS

The volumetric estimates of the eroded material for the Gatberg and Minnehaha River reaches are shown in Table 7.3. Table 7.3 also shows the estimated volumes of the sediment variables (sand fraction, clay and silt, organic matter, and total phosphorus) that were eroded from the two channels.

In the Gatberg River, the median meander bend length was 34 m, and the median and maximum cross-sectional area change over one wet season was 0.1 and 0.3 m^2 respectively. The estimated median volume of eroded material from the measured meander bends was 3.4 m^3 (maximum 9.1 m^3). For the whole floodplain river reach the median volume was estimated to be 520.1 t yr^{-1} (maximum 1411.8 t yr^{-1}). The median volume of sand that is eroded from the channel was approximately 427 t yr^{-1} and the clay and silt fraction was 93.1 t yr^{-1}. The estimated median amount of eroded and transported organic matter was 15.6 t yr^{-1} and the total phosphorus was 0.3 t yr^{-1}.

In the Minnehaha River, the median meander bend length was slightly less than the Gatberg at 32 m. The Minnehaha River experienced the same change in cross-sectional area of 0.1 and 0.3 m^2 during one wet season. The estimated volumes extrapolated for the whole research site were less than the Gatberg (median 359.4 and maximum 1281.2 t yr^{-1}). The median volume of sand that is eroded from the channel was approximately 273.1 t yr^{-1} and the clay and silt fraction was 14.4 t yr^{-1}. The estimated median organic matter eroded and transported was 14.4 t yr^{-1} and total phosphorus was 0.2 t yr^{-1}.

Table 7.3 Volumetric estimates for the eroded material from the Gatberg and Minnehaha channels. Sediment characteristics (sand fraction, clay and silt fraction, organic matter content and total phosphorus) volumetric contributions were estimated

	Gatberg River		Minnehaha River	
	Median	**Maximum**	**Median**	**Maximum**
Meander bend length (m)	34		32	
Channel cross-sectional area change (m^2)	0.1	0.3	0.1	0.3
Volume of eroded material (m^3)	3.4	9.1	2.3	8.3
Volume (t yr^{-1})	520.1	1411.8	359.4	1281.2
Sand fraction (t yr^{-1})	427.0	1376.5	273.1	1050.6
Clay and silt fraction (t yr^{-1})	93.1	381.2	75.5	512.5
Organic matter (t yr^{-1})	15.6	112.9	14.4	102.5
Total phosphorus (t yr^{-1})	0.3	1.3	0.2	1.1

7.3.2 CHANNEL REACH CHANGES USING HISTORICAL IMAGES

The historical aerial image analysis showing the river channel changes for the Gatberg River floodplain system is shown in Figure 7.7 and for the Minnehaha River floodplain system is shown in Figure 7.10. A time sequence of the aerial images of the identified changes is shown in Figure 7.8 and Figure 7.9, for the Gatberg River and Figure 7.11, Figure 7.12, and Figure 7.13 for the Minnehaha River floodplain system.

Results for the time sequence analysis for the Gatberg River floodplain system show that there have been three meander bend cutoff events between the years 1958 and 1993. Unfortunately, the intervening years could not be analysed either because there were no aerial images or because the images were not clear enough to trace the river path. Figure 7.8 (1) shows the cutoff event of the most upstream meander bend. In the year 1958, the meander bend was elongated, asymmetrically upstream skewed, and had a narrow neck; by 1993, the meander bend had been cut off at the narrow neck and followed the path that the river channel currently has. Figure 7.8 (2) shows the next cutoff event from the meander bend found in a zone where the river abruptly changes direction. Similarly, this meander bend has a narrow neck, elongated, but this meander bend is asymmetrical downstream skewed. Figure 7.8 (3) shows the last historical river change. In the year 1958 there was an elongated, narrow neck, asymmetrical upstream skewed meander bend just downstream of another abrupt channel direction change. Likewise, the bend has been completely cut off by 1993. Figure 7.9 shows a meander bend that is in the process of being cut off. Observations in the field noted that a tortuous, elongated meander bend was close to being cut off through a thin meander bend neck.

The results of the time sequence analysis for the Minnehaha River floodplain system show that there have been four changes along the river course between the years 1958, 1966 and 2015 (Figure 7.10). Unfortunately, the intervening years could not be analysed either because there were no aerial images or because the images were not clear enough to trace the river path. Figure 7.11 (1) shows the most upstream channel course change zone. In the 2015 aerial image, a few meander bends have 'grown' in amplitude, elongated, created a compound bend shape, or skewed downstream from the aerial image of 1958. In the 1966 aerial image, the same changes in the river course can be seen. From field observations in this section of the river, the channel bed and banks are comprised of coarse (sand, gravel, and pebbles) materials, and the banks are lower compared to downstream. This section is approximately 1 km downstream of the waterfall. In the 1958 aerial image in Figure 7.11 (2), there was a large complex compound (mushroom-shaped) meander bend comprising a few meander bend loops within, by the 1966 aerial image this complex bend has been cut off at the neck of the 'mushroom'. In the 2015 aerial image, the meander bend that was created when the first complex bend was cut off is beginning to elongate and has its own narrow meander bend neck that may be cut off in the future. In Figure 7.12 the meander bend in the 1958 aerial image has already started the process of being cut off. Although, in 1958 river flow was still being diverted into the meander bend complex. The next few meander bends downstream of the meander bend complex, have extended, rotated, or changed into compound loops. In Figure 7.13 the river reach went through two separate changes. In the 1958 aerial image, the meander bend is being cut off by a chute cutoff. In 1966 another chute cutoff occurred in the next upstream meander bend and flowed in both the previous channel

course and down the older meander bend that was being cut off in 1958. In the 2015 aerial image channel reach is once again following the course created just after the 1958 event.

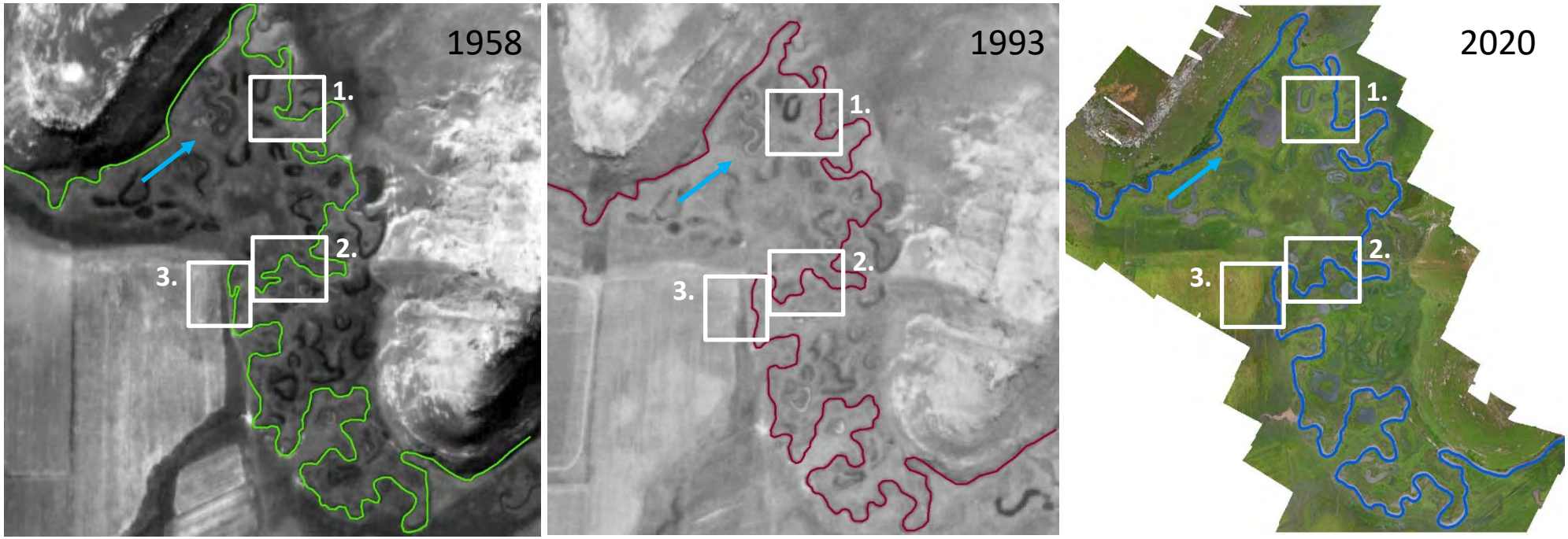

Figure 7.7 Aerial images of 1958, 1993, and 2020 show 3 changes in the Gatberg channel marked by white boxes. The blue arrow indicates flow direction

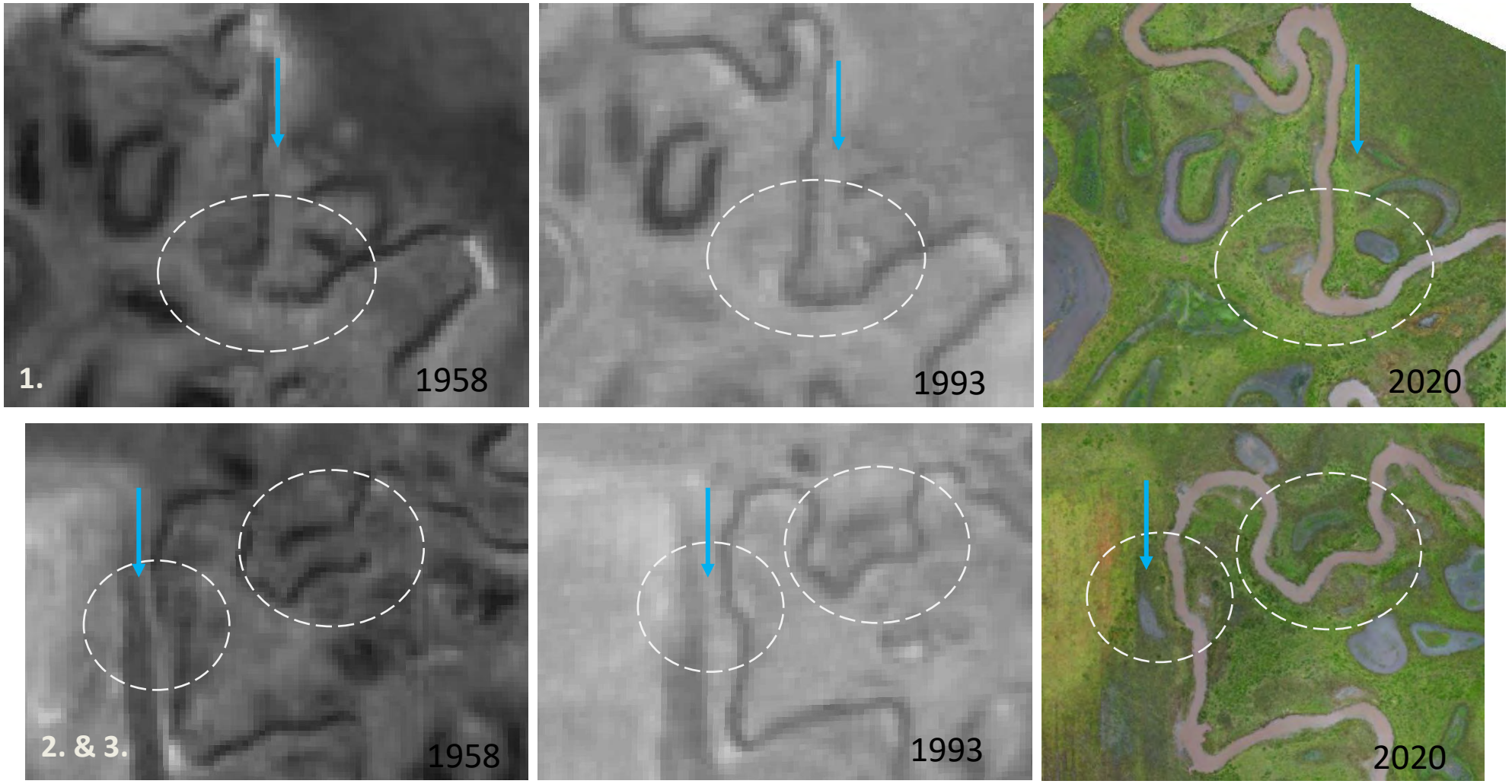

Figure 7.8 Identified meander bend changes. Numbered changes correspond to Figure 7.7

Figure 7.9 Meander bend cut off event occurring over the study period

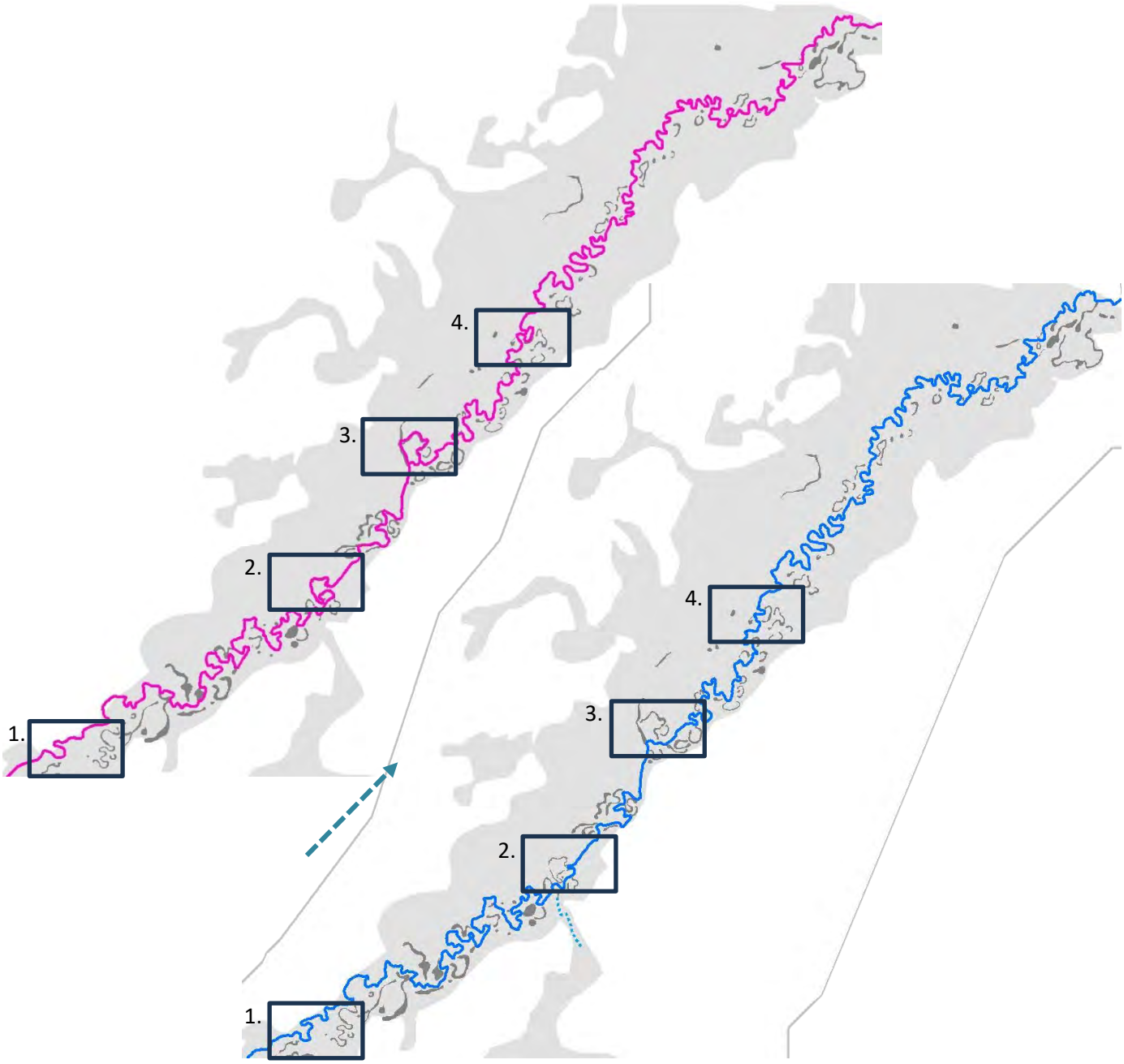

Figure 7.10 Aerial images of 1958 (Pink channel line) and 2015 (Blue channel line) showing 4 changes in the Minnehaha channel marked by black boxes. Blue dashed arrow indicates flow direction

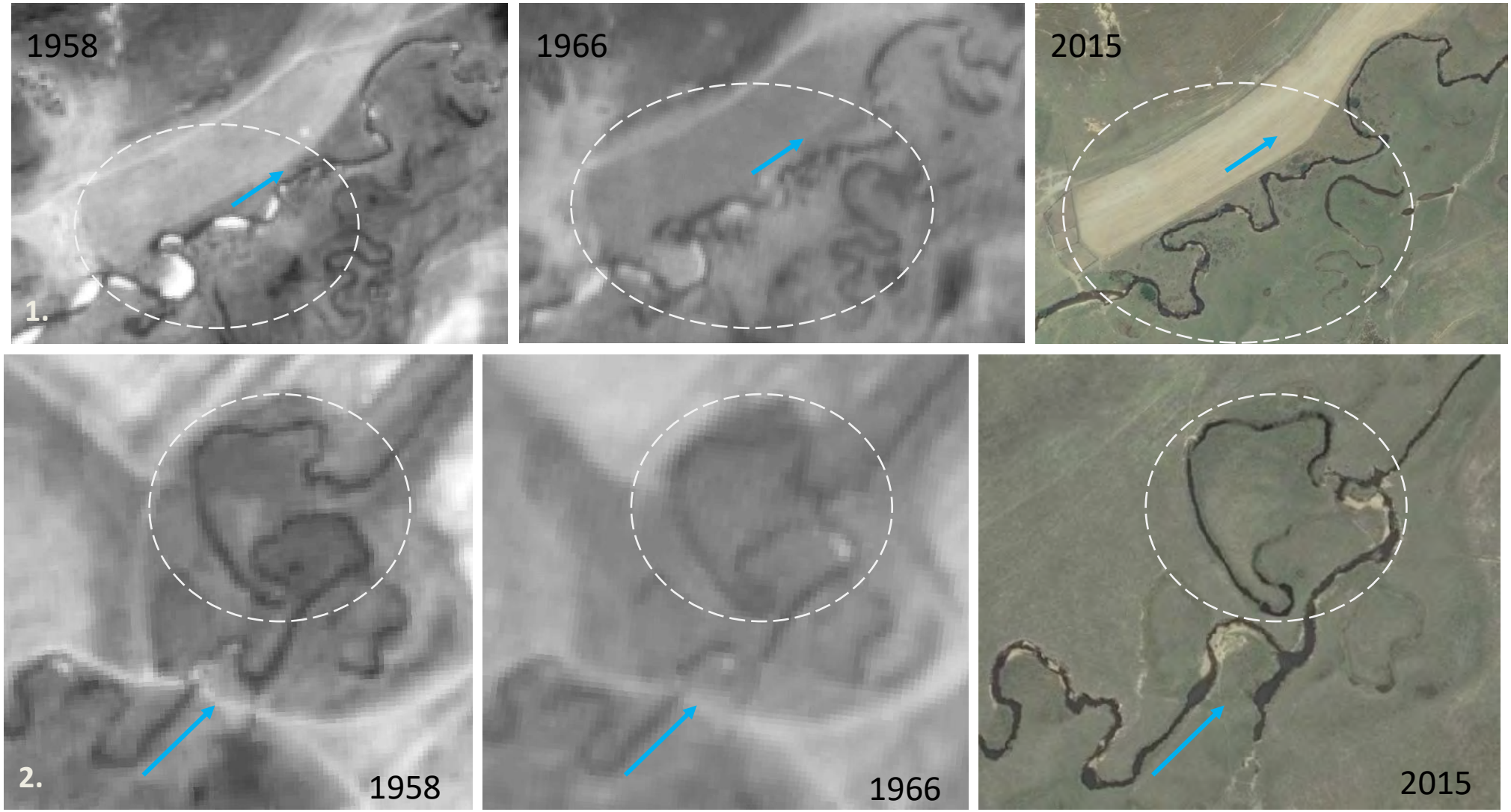

Figure 7.11 Identified first two meander bend changes. Numbered changes correspond to Figure 7.10

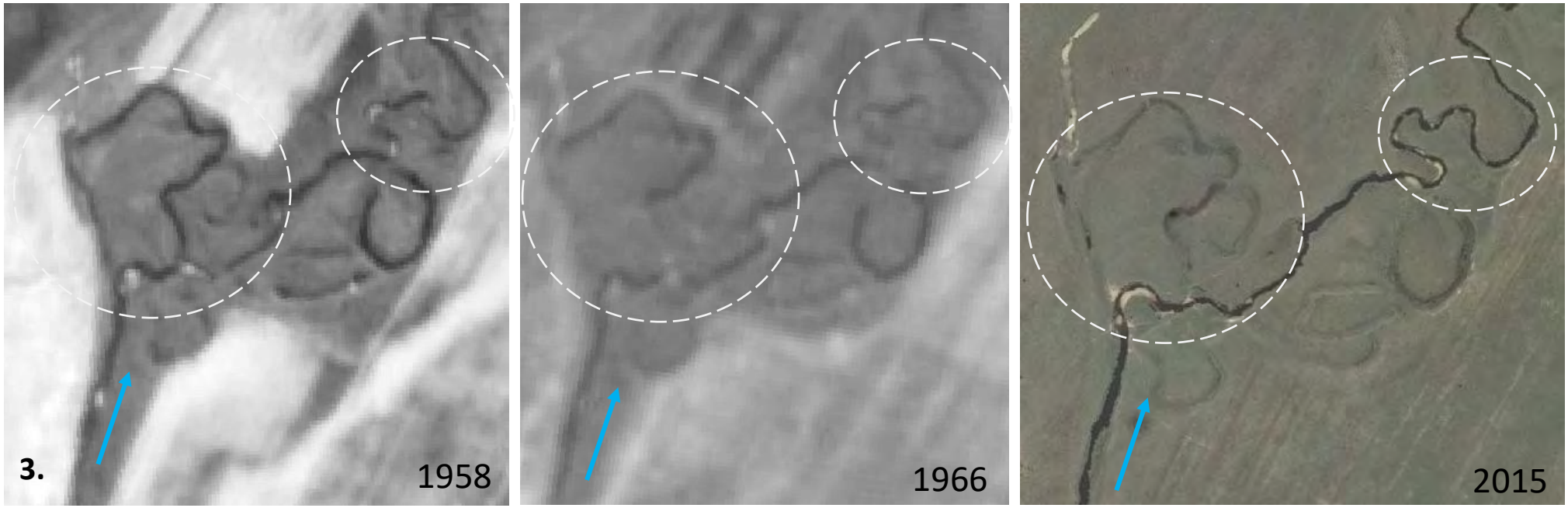

Figure 7.12 Identified third meander bend changes. Numbered changes correspond to Figure 7.10

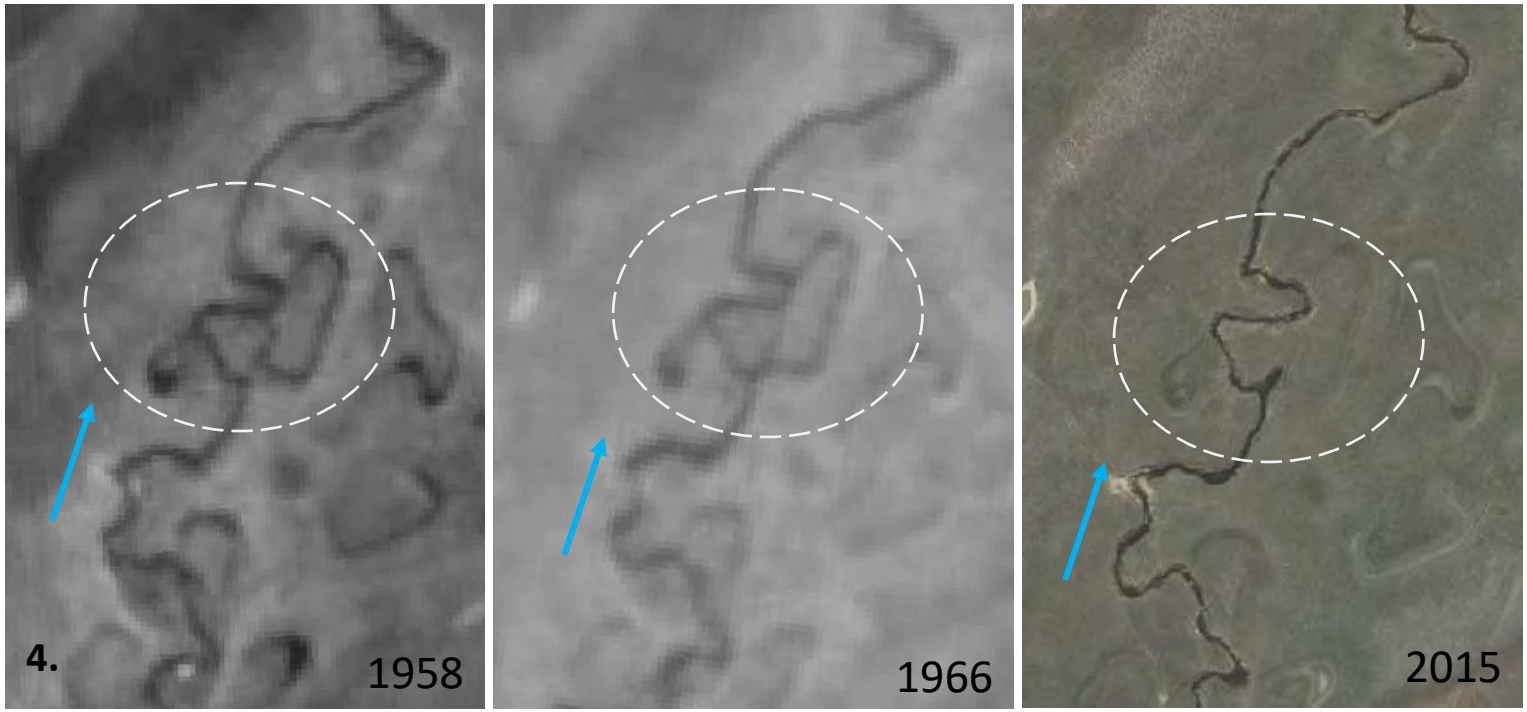

Figure 7.13 Identified fourth meander bend changes. Numbered changes correspond to Figure 7.10

Figure 7.14 and Figure 7.15 show the floodplain systems of the Gatberg and Minnehaha Rivers divided into four zones. Table 7.4 shows the calculated river lengths, valley lengths, and sinuosity indexes for the different zones of the two floodplain systems.

In the Gatberg River floodplain system, the floodplain was divided into four zones. Zone 1 represents the upper zone where the river flows along the hillslope in a north-easterly direction. This zone is relatively straight. In the 1958 aerial image, the river had a length of just over 560 m with a valley length of just under 430 m giving this zone a sinuosity index of 1.31. For the same zone in 2020, the river length is ~600 m giving this zone a calculated sinuosity index of 1.40. Zone 2 represents the next section of the river. This zone is a good example of a meandering river reach along the Gatberg River. This river reach flows along the left-hand margin of the valley in a southerly direction. In 1958 the length of the river for this zone was ~1111 m with a valley length of ~404 m and a sinuosity index of 2.75. In 2020 the same zone had a river length of 1100 m and a sinuosity index of 2.72. This zone includes the meander bend cutoff event 1 from the previous section and the meander bend that was about to be cutoff. In zone 3 the river abruptly changes direction (westerly) and flows across the valley to the right-hand valley margin. This zone includes the meander bend cutoff event 2 from the previous section. In 1958, the length of the river was 396 m, the valley length ~123 m and a sinuosity index of 3.23. In 2020, the length of the river was ~343 m and had a sinuosity index of 2.80. In the last zone, zone 4, the river flows along the right-hand floodplain margin until a tributary joins from the right bank. After the tributary, the river crosses the valley several times. This zone includes the meander bend cutoff 3 from the previous section. In 1958, the river had a length of ~1902 m, the valley length was ~576 m and the river reach had a sinuosity index of 3.30. In 2020, the length of the river length was ~1857 m, and the sinuosity index was 3.23 for the reach. The average sinuosity index for the Gatberg River floodplain system for 1958 was 2.65 and for 2020 was 2.54.

In the Minnehaha River floodplain system, the floodplain was divided into four zones. Zone 1 represents the upper zone where the river flows in a north-easterly direction. This zone is relatively straight. In the aerial image of 1958, the river had a length of ~1860 m with a valley length of ~1486 m, giving this zone a sinuosity index of 1.25. For the same zone in 2015, the river length was slightly longer ~1879 m giving this zone a calculated sinuosity index of 1.26. This zone includes the meander bend cutoff event 1 from the previous section. Zone 2 represents the next section of the river. In 1958 the river length for this zone was ~4087 m with a valley length of ~1750 m and a sinuosity index of 2.34. In 2015 the same zone had a river length of ~3994 m and a sinuosity index of 2.28. This zone includes the meander bend cutoff event 2 from the previous section. In zone 3 in the 1958 aerial image, the river length was ~5050 m, the valley length ~2021 m and a sinuosity index of 2.50. In 2015, the length of the river was ~4828 m and had a sinuosity index of 2.39. This zone included the meander

bend cutoff events 3 and 4 from the previous section. In the last zone, zone 4, the river length in 1958 was ~1631 m, valley length of ~850 m and had a sinuosity index of 1.92. In 2015 the river length was ~1744 m, and the sinuosity index was 2.05. The average sinuosity index for the Minnehaha River floodplain system for 1958 and 2015 remained at 2.00.

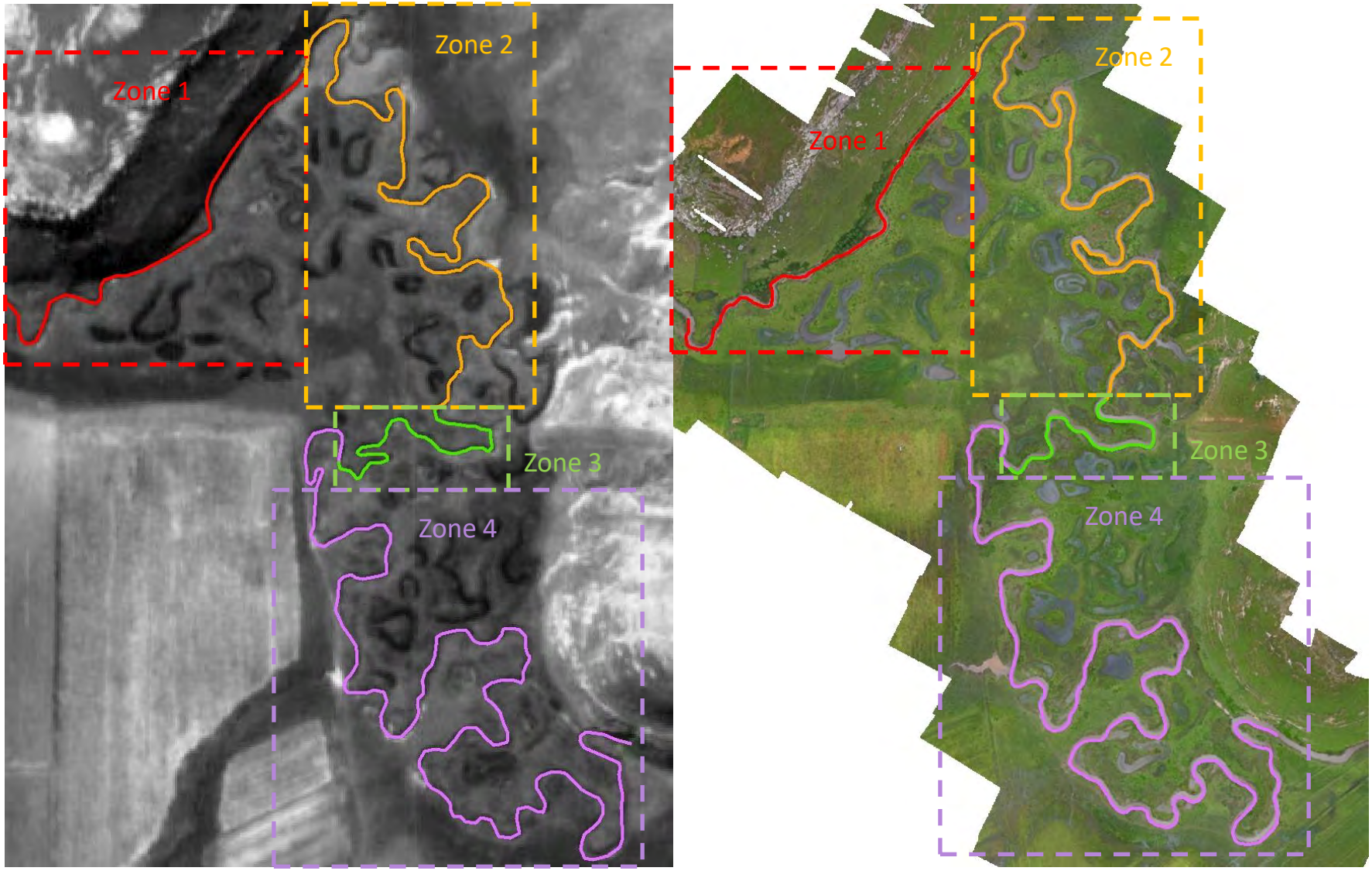

Figure 7.14 The different zones used to calculate the change in sinuosity from 1958 to 2020 in the Gatberg River floodplain system

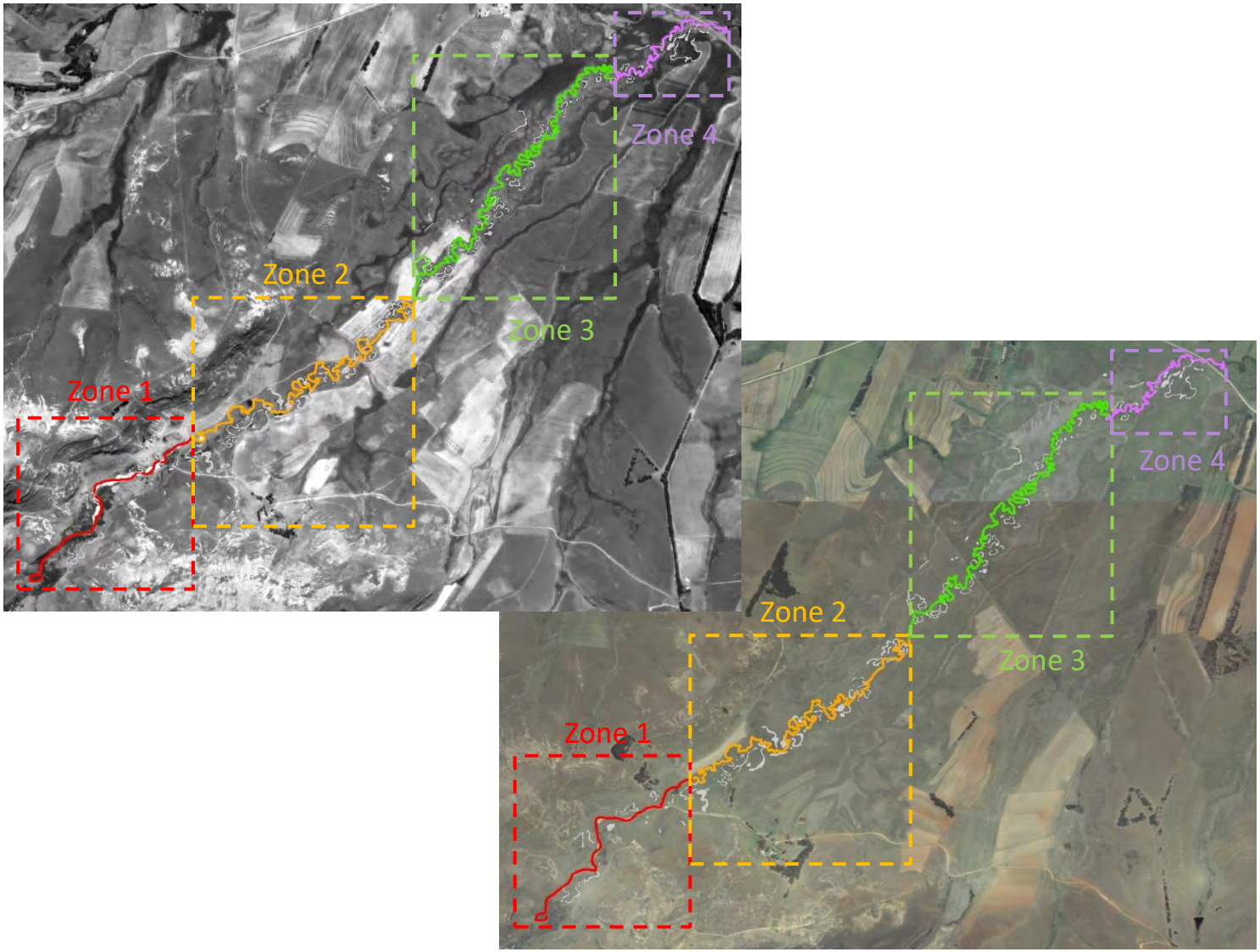

Figure 7.15 The different zones used to calculate the change in sinuosity from 1958 to 2015 in the Minnehaha River floodplain system

Table 7.4 Change in river length, valley length and sinuosity index for the different zones from the aerial images in the Gatberg and Minnehaha River floodplain systems

Floodplain system	Section	Year	River length	Valley length	Sinuosity Index
Gatberg River floodplain system	1	1958	563.8	428.9	1.3
		2020	600.3		1.4
	2	1958	1111.2	404.0	2.8
		2020	1100.0		2.7
	3	1958	396.0	122.7	3.2
		2020	343.1		2.8
	4	1958	1901.8	575.5	3.3
		2020	1856.8		3.2
Minnehaha River floodplain system	1	1958	1859.2	1485.8	1.3
		2015	1878.5		1.2
	2	1958	4087.0	1749.4	2.3
		2015	3993.7		2.3
	3	1958	5054.6	2021.3	2.5
		2015	4827.8		2.4
	4	1958	1630.7	849.6	1.9
		2015	1743.5		2.1

7.3.3 LATERAL MIGRATION RATES ESTIMATED BY OXBOW ^{14}C DATES

The sample from the oxbow 1 (OX 4, de Villiers 2022) has an age of 2830 ± 25 years (before measurement date, i.e., 2021; see Figure 7.16 and Table 7.5). As expected, this sample is slightly younger than the cutoff event itself because the sample that was used for the ^{14}C dating was at a depth between 0.6 and 0.75 m whereas the depth to refusal (bed load associated with initial cutoff filling) was at 1.9 m. The sample of oxbow 2 (OX 3, de Villiers 2022) has an estimated age of 3627 ± 23 years. This sample would also be younger than the cutoff event itself, because the sample used for ^{14}C dating was between 1.5 and 1.75 m, while the depth of refusal was at 2.4 m. These two oxbow samples were chosen because the central values of the ages fall in the correct chronological order for the depositional sequence (Figure 7.16). Oxbow 1 had a sediment fill depth of 1.7 m with a D_{50} sediment particle size range of 111 to 1130 µm, as expected, the lowest section of the core has the highest D_{50} sediment size. Oxbow 1 had a mean organic matter content of 1 % and decreased with depth. The average rate of sediment accumulation was 0.03 cm yr^{-1}. Oxbow 2 had a sediment fill depth of 2 m with a D_{50} sediment particle size range of 133 to 672 µm, as expected, the lowest section of the core has the highest D_{50} sediment size. Oxbow 2 had a mean organic matter content of 1.4 % which decreased with depth. The average rate of sediment accumulation was 0.05 cm yr^{-1}. Using the distance

between the two oxbows, the results indicate that the meander bend migrated ~24 m over ~800 years, giving an average lateral migration rate of 0.03 m yr^{1}.

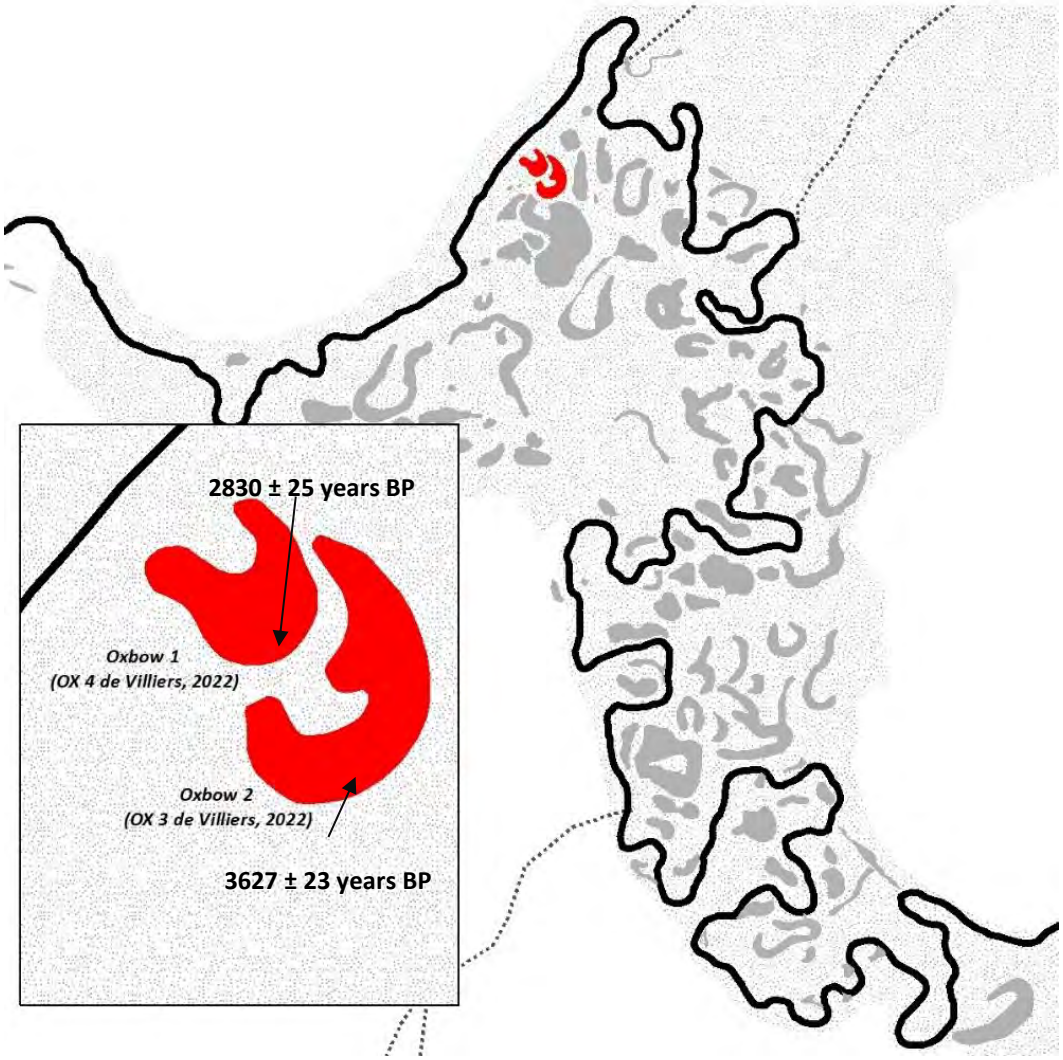

Figure 7.16 Map illustrating the location of two of the oxbows that were used investigated by de Villiers (2022). The inset map shows the dates calculated using ^{14}Carbon

Table 7.5 Description and age (BP) of the two oxbows investigated

Sample	Oxbow 1 (OX 4, de Villiers 2022)	Oxbow 2 (OX 3, de Villiers 2022)
Depth of sediment infill (m)	1.7	2.0
Depth to refusal (m)	1.9	2.4
Depth of dated sample (m)	0.6 - 0.75	1.5 – 1.75
D_{50} sediment size range (µm)	111 - 1130	133 - 672
Mean organic matter (%)	1.0	1.4
Mean total phosphorus (g kg^{-1})	0.05	0.08
Age (years before present 2021)	2830 ± 25	3627 ± 23
Age (years BP, ± 1σ)	834 - 784	1629 - 1583
Mean accretion rate (cm yr^{-1})	0.03	0.05
Mean migration rate (m yr^{-1})	0.03	

7.3.4 Evidence of channel change (Number of oxbows, meander bend evolution, the radius of curvature, diversion angle, the ratio of curvature and width)

There were 42 oxbows identified in the Gatberg River floodplain system (Figure 7.17). Oxbows were observed across the whole floodplain surface on both sides of the river. A morphometric study revealed that the distance between the identified oxbows and the present channel course ranged from 13 to 145 m (Table 7.6). Morphometric research found that the oxbows were between 20 and 189 m long, with a mean length of 74 m. The oxbows ranged in size from 128 to 3291 m², with a mean of 788 m². The oxbow diversion angles ranged from 60° to 105°, with a mean diversion angle of 85°. The radius of curvature ranged from 6 to 32 m, with an average of 15 m. The ratio of the radius of curvature to width, which evaluates the tightness of the bend, varied between 1 and 5 for the oxbows, with a mean of 2.

There were 62 meander bends identified along the current (year 2020) Gatberg River reach (Figure 7.18). Of the meander bends identified, 19 % were compound bends and the rest were simple bends (Table 7.7). Within the simple bends 22 % were downstream skewed and 31 % were upstream skewed. 1 of the 62-meander bends was identified as a multiple-loop bend. A morphometric analysis found that for 2020 the meander bend lengths ranged between 18 and 100 m with an average of 46 m. Bend lengths calculated for 1958 were similar and meander bend lengths ranged from 20 to 95 m (average 46 m). In 2020 the bend amplitudes ranged from 8 to 84 m (average 25 m). The bend amplitude was slightly less in 1958, and amplitudes ranged from 8 to 80 m (average 23 m). In 2020 the meander bend radius of curvature ranged from 5 to 19 m, with an average of 12 m. In 1958 the meander bend radius of curvature was less than 2020, ranging from 3 to 19 m (average 11 m). In 2020 the ratio of the radius of curvature to width varied between 1 and 4 for the meander bends, with a mean of 2. In 1958 the ratio of the radius of curvature to bankfull width varied between 1 and 5 with an average of 2; Table 7.8). In the Gatberg River extension and rotation was the most common mode of meander bend change, identified from the 2020 aerial image, which accounted for 37 % of the bends (Table 7.9).

A total of 72 oxbows were identified in the Minnehaha River floodplain system (Figure 7.17). Oxbows were discovered on both sides of the existing river. A morphometric analysis revealed that the distance between the identified oxbows and the present channel course ranged from 5 to 199 m (Table 7.6). The oxbows were between 24 and 443 m long, with a mean length of 124 m. The oxbows ranged in size from 107 to 10279 m², with a mean of 1704 m². The oxbow diversion angles ranged from 45° to 120°, with a mean diversion angle of 88°. The radius of curvature ranged from 6 to 57 m, with an average of 21 meters. The ratio of the radius of curvature to width, varied between 1 and 7 for the oxbows, with a mean of 3.

In the 2015 aerial imagery, 192 meander bends were identified along the current Minnehaha River reach (Figure 7.18). Of the meander bends identified, 25 % were compound bends and the rest were simple bends (Table 7.7). Within the simple bends 22 % were downstream skewed and 18 % were upstream skewed. Fifteen of the 192 meander bends were part of multiple loop bends. A morphometric analysis found that the meander bend lengths in 2015 ranged between 11 and 153 m with an average of 39 m; in 1958 the range was 15 to 335 m (average 47 m). The bend amplitudes ranged from 4 to 98 m (average 22 m) on the 2015 imagery; on the 1958 imagery, the range was 4 to 125 m (average 26 m). In the 2015 images, the meander bend radius of curvature ranged from 4 to 53 m, with an average of 10 m; in 1958 the range was 5 to 50 m (average 11 m). The ratio of the radius of curvature to width varied between 1 and 13 for the meander bends, with an average of 3; and on the 1958 imagery it varied between 1 and 7, with an average of 2 (Table 7.8). In the Minnehaha River extension and rotation were the most common modes of meander bend change, identified from the 2015 aerial image, which accounted for 34 % of the bends (Table 7.9).

Table 7.6 Descriptive statistics for the different morphological variables of the oxbows found in the Gatberg and Minnehaha River floodplain systems

Floodplain system	Descriptive statistics	Distance from channel (m)	Area (m^2)	Length (m)	Average bankfull width (m)	Diversion angle (^{o})	Radius of curvature ($r = \sqrt{(A / \pi)}$) (m)	Tightness of meander bend (Rc/Width) (m)
Gatberg River floodplain system oxbows (42)	Average	52	788	74	8	85	15	2
	Minimum	13	128	20	5	60	6	1
	Maximum	145	3291	189	13	105	32	5
	Median	47	550	62	8	85	13	2
	STDEV	26	696	45	2	9	6	1
Minnehaha River floodplain system oxbows (72)	Average	30	1704	124	7	88	21	3
	Minimum	5	107	24	4	45	6	1
	Maximum	199	10279	443	13	120	57	7
	Median	22	1052	100	7	90	18	3
	STDEV	29	1796	87	2	14	10	1

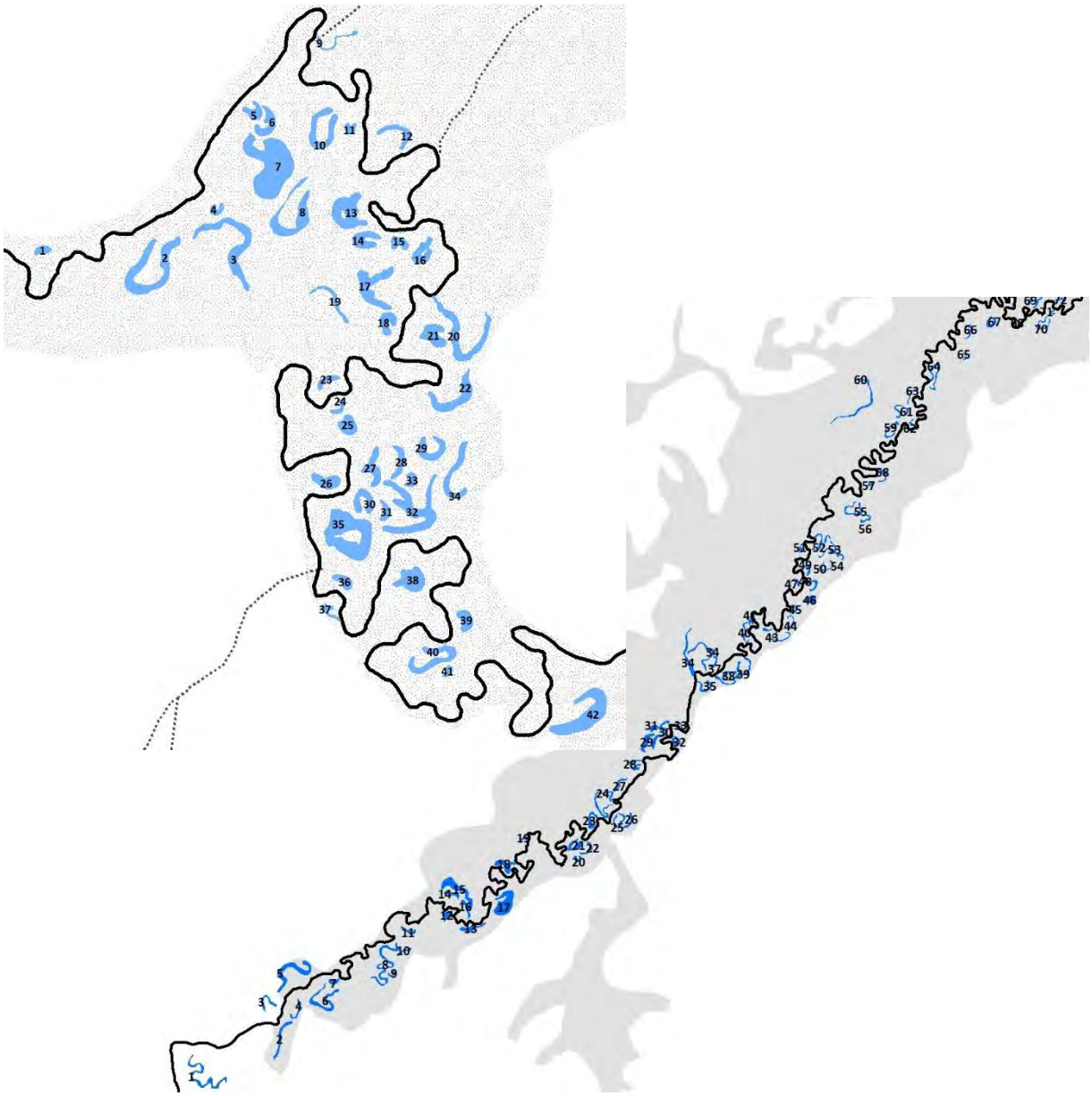

Figure 7.17 Maps showing the location of the identified and numbered oxbows in the Gatberg (top) and Minnehaha (bottom) River floodplain systems

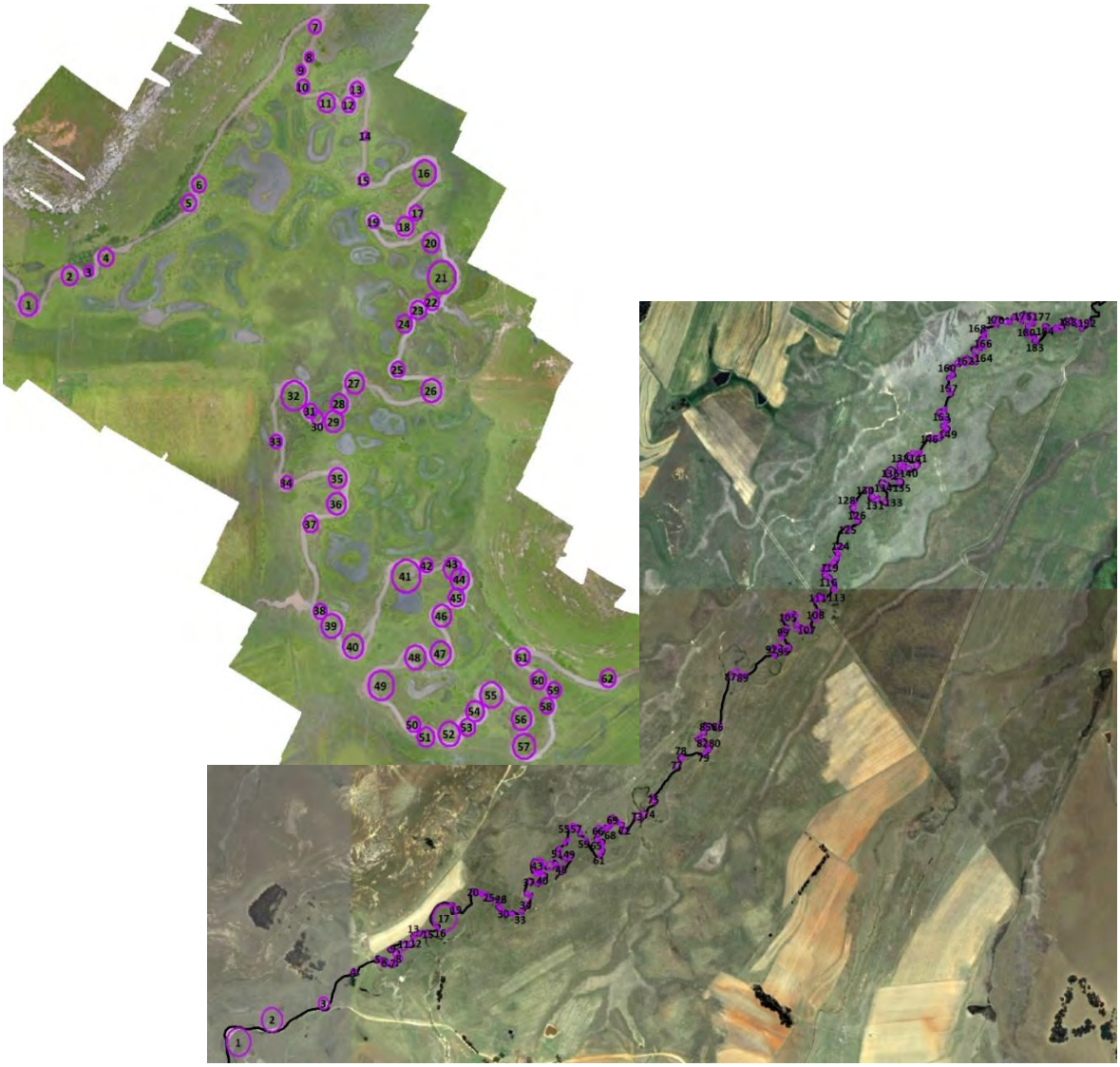

Figure 7.18 Maps showing the meander bend locations and best-fit circles (shown in purple) used to calculate the radius of curvature in the Gatberg and Minnehaha River floodplain systems

Table 7.7 Type of meander bends found in the Gatberg and Minnehaha River floodplain systems (after Hooke 1977)

Types of meander bends		Gatberg River reach Number of bends	Minnehaha River reach Number of bends
Total		62	192
Multiple loops		1	15
Compound		12	48
Simple	**Symmetrical**	24	87
	Downstream skewed	11	31
	Upstream skewed	16	26

Table 7.8 Descriptive statistics for the different morphological variables of the meander bends identified in the Gatberg and Minnehaha River floodplain systems

Floodplain system	Descriptive statistics	Wavelength (m)		Bend length (m)		Amplitude (m)		Radius of curvature (m)		Mean bankfull width (m)		Tightness of bend (m)	
		2020	1958	2020	1958	2020	1958	2020	1958	2020	1958	2020	1958
Gatberg River floodplain system meander bends (62)	Average	103	109	46	46	25	23	12	11	7	5	2	2
	Minimum	45	44	18	20	8	8	5	3	2	2	1	1
	Maximum	215	236	100	95	84	80	19	19	10	7	4	5
	Median	96	102	41	40	21	19	11	11	7	5	2	2
	STDEV	39	43	19	19	17	16	3	3	1	1	1	1
Minnehaha River floodplain system meander bends (192)	Average	100	105	39	47	22	26	10	11	4	5	3	2
	Minimum	27	45	11	15	4	4	4	5	2	3	1	1
	Maximum	450	453	153	335	98	125	53	50	17	20	13	7
	Median	85	88	34	38	20	22	9	9	4	5	2	2
	STDEV	55	63	20	41	12	18	6	7	2	2	1	1

Table 7.9 Type of meander bend change in the Gatberg and Minnehaha floodplain systems (after Hooke 1977)

Type of bend change	Gatberg River reach Number of bends	Minnehaha River reach Number of bends
Total	62	192
Extension	6	42
Expansion	-	3
Rotation	8	-
Extension and expansion	4	22
Extension and rotation	23	66
Extension, expansion, and rotation	3	8
No evidence of change	18	51

7.3.4 POTENTIAL FOR FUTURE CHANNEL CHANGE

7.3.4.1 NECK CUTOFF STABILITY

Visual evaluation of the meander bends of the Gatberg River identified two meander bends to analyse the neck cutoff stability. The results show that, based on the one channel width rule, there is only one meander bend with a high neck cutoff potential (< 1, Figure 7.19A). This was followed by another bend with a neck length/ channel width ratio of 1.6 (Figure 7.19B). The others have stability values > 2 indicating that these bends are less likely to experience neck cutoffs in the near future.

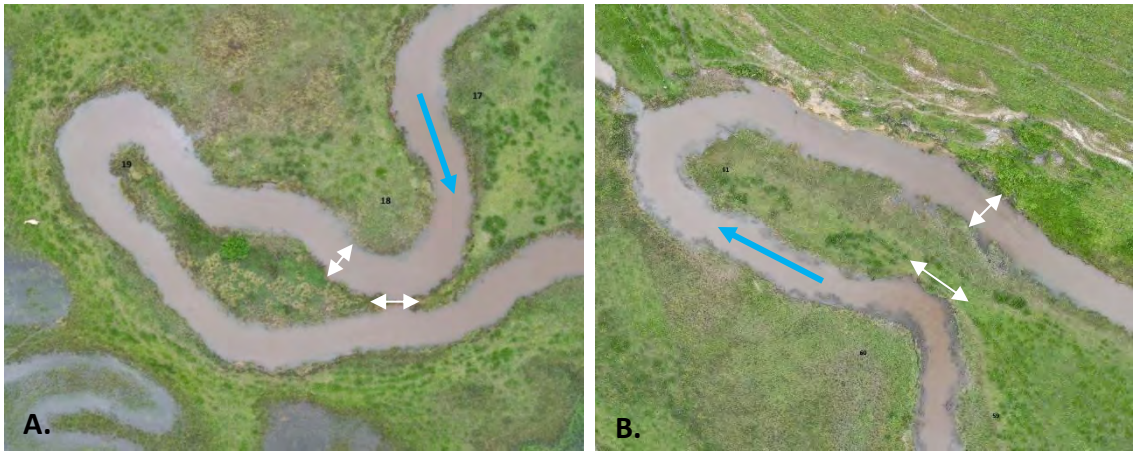

Figure 7.19 The two-meander bends identified in the Gatberg River floodplain system that may experience a meander bend neck cutoff event in the future based on the one channel width rule

Visual evaluation of the Minnehaha River meander bends identified three meander bends to analyse the neck cutoff stability. The results show that, based on one channel width rule, there were no meander bends with a high neck cutoff potential (< 1). There were 3 meander bends identified with a neck length/ channel width ratio of < 2 (Figure 7.20). The others have stability values of > 2 indicating that these bends are less likely to experience neck cutoffs in the future.

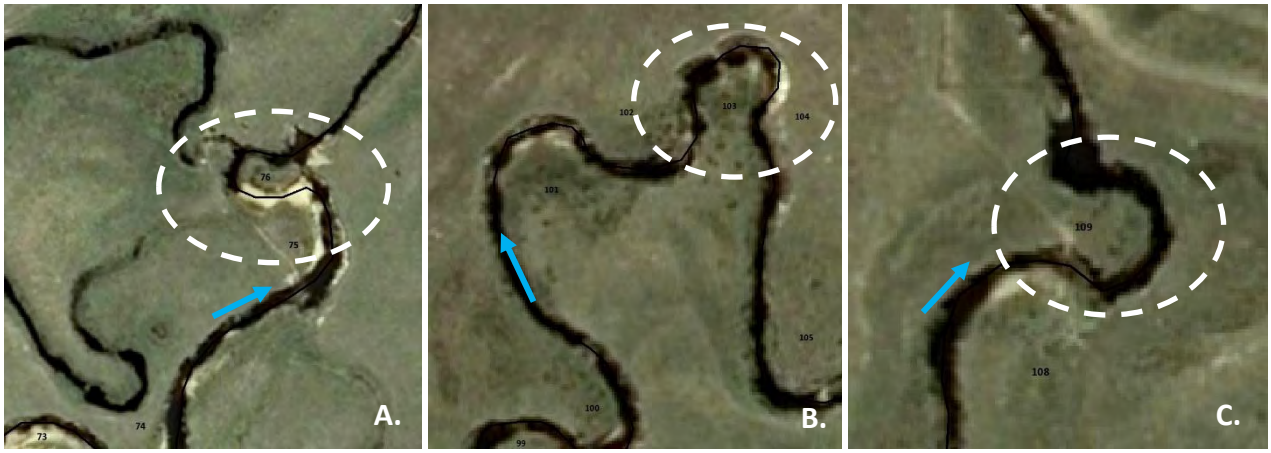

Figure 7.20 The three-meander bends identified in the Minnehaha River floodplain system that may experience a meander bend neck cutoff event in the future based on the one channel width rule

7.3.4.2 CHUTE CUTOFF STABILITY

Similarly, the visual evaluation identified 5 meander bends that satisfy the chute cutoff stability criteria in the Gatberg River reach (Table 7.10). Among these, 2 meander bends had a stability ratio of 4 and three had a stability ratio of 3. The rest of the meander bends had a stability ratio of < 3.

Visual evaluation of meander bends in the Minnehaha River resulted in a higher amount of bends for the chute cutoff potential than for the neck cutoff potential (Table 7.10). A total of 20 meander bends

with a chute stability ratio of ≤ 3. One meander bend had a stability ratio of 10, 4 meander bends had a ratio of 4, and 15 meander bends had a stability ratio of 3.

Table 7.10 Chute cut off stability meander bends identified in the Gatberg and Minnehaha River floodplain systems

Floodplain system	Meander bend number	Bend length (m)	Neck length (m)	Bend length/ neck length ratio
Gatberg River floodplain system	13	74	21	4
	57	126	35	4
	19	99	33	3
	26	82	28	3
	61	102	31	3
Minnehaha River floodplain system	184	69	7	10
	47	47	12	4
	134	110	30	4
	150	54	15	4
	174	64	16	4
	49	54	18	3
	72	60	19	3
	76	32	10	3
	83	55	21	3
	91	40	14	3
	92	54	19	3
	103	34	12	3
	124	66	19	3
	136	104	31	3
	137	43	16	3
	152	57	20	3
	163	80	30	3
	165	38	13	3
	169	38	14	3
	176	31	12	3

7.4 DISCUSSION

7.4.1 INTRODUCTION

This section discusses the historical and potential river change, as presented in the results in Section 7.3, in the Gatberg and Minnehaha River floodplain systems.

7.4.2 CHANNEL CHANGE AND CHANNEL EROSION VOLUMES

Although floodplains are primarily depositional features and form through the build-up of alluvium, they are frequently shaped and modified by erosional processes (Rhoads 2020). Channel erosion is a natural dynamic process and forms one of the principal processes of meandering river migration. Channel erosion can occur when the water's erosive strength exceeds the resistance of the bed and bank materials due to an increase in slope or depth of flow. It also has an important impact on sediment and sediment-associated nutrients and contaminates budgets due to the movement, sorting, and dispersion of sediment and organic materials. There may be several changes made to the channel when bed (scour and incision) or bank (undercutting and slumping) erosion commences.

Both the Gatberg and Minnehaha River floodplain reaches experienced deposition and erosion down the study area. From the measured cross-sections, the Gatberg River reach experienced slightly higher cross-sectional area erosion (47 %) compared to 42 % in the Minnehaha River reach. For both systems, channel bed scouring occurred in > 70 % of the cross-sections, indicating a general absence of sediment aggradation within the main channel bed. From the re-surveys over two wet- seasons both the Gatberg and Minnehaha River floodplain reaches experienced minor erosion (median of 0.4 m^2 for both), while the median amount of deposited material was estimated to be 0.5 and 0.7 m^2, correspondingly. Whether channel banks erode is mostly determined by how resistant the channel boundary materials are to the shear stress and stream power applied. Boundary resistance is a result of the type and density of riparian vegetation and the size and cohesiveness of inorganic bank materials (e.g., clay, sand, gravel, and cobbles). According to the Hjulstrom curve, lower critical erosion velocities are needed to entrain and transport sand particles compared to the clay and silt fraction or larger gravels (Hjulstrom 1935). This is due to the nature of fine particles to form tight particle bonds and clump together, resulting in higher resistance to entrainment and transport. Numerous researchers have established the significance of clay concentration with streambank failure (Vanoni 1977; Thorne 1982; Julian and Torres 2006). Hanson and Simon (2001) discovered that in addition to soil texture, soil structure, organic content, and clay mineralogy were important factors for streambank stability. These results support the finding in Chapter 5 where the D_{50} channel bed material sampled for the Gatberg was 435 µm (medium sand) and 248 µm (fine sand) for the Minnehaha system. The channel bed had a 9 % (Gatberg River) and 18 % (Minnehaha River) clay and silt sediment particle size fraction. The riverbanks of the Gatberg reach had a D_{50} particle size of fine sand with > 30 % clay and silt sediment particle size fraction and < 5 % organic matter content. The riverbanks of the Minnehaha reach had a D_{50} particle size of very fine sand with ~40 % clay and silt sediment particle size fraction and < 5 % organic matter content.

In the Gatberg River, the estimated median volume of eroded material is 3.4 m^3, with a maximum of 9.1 m^3. Extrapolating these values to the entire study site, the median volume of eroded material is estimated to be 520.1 t yr^{-1}, with a maximum of 1411.8 t yr^{-1}. In comparison, the Minnehaha River shows a slightly lower median volume of eroded material of 2.3 m^3 and a maximum of 8.3 m^3. Extrapolating to the entire study site, the median volume is estimated to be 359 t yr^{-1}, with a maximum of 1281 t yr^{-1}. The comparison between the Gatberg and Minnehaha Rivers reveals differences in the magnitude of sediment erosion and transport between the two systems. While both rivers exhibit similar patterns in terms of the composition of eroded material, with sand being the dominant fraction followed by clay and silt, there are notable variations in the median volume of eroded material. Both these estimates are within an order of magnitude for the floodplain deposition estimates (see Chapter

6). These differences suggest variations in sediment transport dynamics between the two river systems, which could be attributed to factors such as differences in catchment characteristics, land use patterns, and hydraulic properties of the rivers. Although the representativeness of this database is debatable, it provides a limited, nevertheless valuable, perspective considering the data scarcity in South Africa.

The results obtained from the analysis of sediment erosion and deposition in the Gatberg and Minnehaha Rivers show that both systems are active. The deposition values obscured the erosion values, as a result the erosion volumes are likely an underestimation. However, the values provide valuable insights into the dynamics of sediment transport in these river systems. The estimated median volume of eroded material and associated components highlight the significant role of these rivers in sediment mobilisation and downstream transport processes.

7.4.3 HISTORICAL CHANNEL CHANGES

One of the most dynamic earth-surface systems is a meandering river. They are crucial to the dynamics of riverine ecosystems, the evolution of landscapes, and terrestrial-sediment fluxes. Because of the fascinating intricacy of meander morphodynamics, researchers from a wide variety of disciplines have been interested in meandering rivers. Additional interest comes from socioeconomic concerns due to river dangers caused by bank erosion, channel shifts and flooding, as well as the responses of meandering rivers to changes in the environment brought on by humans and climate change. To explore how meandering river–floodplain systems respond to environmental changes, a thorough, process-based knowledge of these systems' dynamics is essential.

In the Gatberg River floodplain system, between 1958 and 1993, there were three meander bend cutoff events. The inferred channel change is ~1 event in 9 years. Field observations in 2022 showed one meander bend in the process of being cut off. In the Minnehaha River floodplain system, 4 meander bend cutoff events were identified between 1958 and 2015, approximately 1 event in 7 years. In the Gatberg River floodplain, the 3 meander bend cutoff events and the meander bend in the process of being cut off all occurred between the two tributaries entering the system. The 4 events identified in the Minnehaha River floodplain occurred along the length of the system. However, numerous meander bend cutoffs have occurred in the pre-1958 period, which is seen in the form of traces of oxbows on both floodplain systems. The result of meander bend cutoff events is a decreased channel length, increased channel slope and a corresponding increase in sediment conveyance, especially of the bedload. The resultant abandoned section of the channel increases floodplain sediment storage capacity by increasing the floodplain volume (if the floodplain elevation stays the

same). These processes are important to consider in the sediment and nutrient continuity through a sediment cascade.

The Gatberg River floodplain system was compartmentalised into four zones to calculate changes in river section lengths and sinuosity between 1958 and 2022 aerial images. In zone 2, 3, and 4 the river length was shortened and there was a subsequent decrease in sinuosity due to the meander bend cutoff events that occurred. In zone 1 (uppermost zone) the river length and sinuosity increased due to meander bend 'growth'. The Minnehaha River floodplain system was also divided into four zones. Zones 1 and 4 experienced an increase in channel length from 1958 to 2015. Sinuosity in zone 1 decreased, whereas sinuosity increased in zone 4. Zone 1 experienced a meander bend cutoff event; however, the increase in length may be due to meander bend 'growth'. Zone 4 did not experience a cutoff event. Zones 2 and 3 both experienced meander bend cutoff events during the intervening years, which resulted in decreasing river lengths and sinuosity indices. Ferguson (1987) linked channel straightening and steepening to an increase in either the discharge responsible for shaping the channel or the quantity and/or size of the sediment load. Meander bend cutoff events in both the Gatberg and Minnehaha River floodplain systems are relatively compared to systems with highly mobile channel beds and banks, however, the changes precipitated by cutoff events to the sediment budget, transport and storage are significant. Zinger et al (2011) found that two cutoff events on the Wabash River in Midwestern USA mobilised approximately 5.5 million m^3 of floodplain sediment.

Meander cutoffs decrease river sinuosity, increase local channel slope, increase sediment conveyance downstream (increasing bedload transport capacity), and decrease overbank floodwater access to the floodplain, all of which are important aspects of river morphodynamics. Cutoffs are episodic, eliminating small to large sections of a river over brief periods, in contrast to channel modifications of width, depth, and length, which are often spatially and temporally continuous. Cutoffs may affect meander migration rates over extended periods by forming oxbows, which increase floodplain resistance heterogeneity (Schwenk and Foufoula-Georgiou 2016). Through the consolidation of silt, clay, and organic matter, oxbows create "plugs" that hinder or constrain meander flow and boost local resistance to erosion (Fisk et al. 1949; Hudson and Kesel 2000). Cutoffs function as "shot" perturbations (Camporeale et al. 2008) to river morphodynamics over shorter time scales by injecting downstream pulses of sediment and sediment-associated nutrients and contaminants excavated from the floodplain during chute channel formation (Fuller et al. 2003; Zinger et al. 2011). This increases the bed slope and stream power both upstream and downstream (Biedenharn et al. 2000; Hooke 2004; Jugaru Tiron et al. 2009), and significantly changes the local channel planform and hydrodynamics (Hooke 2004; Zinger et al. 2013).

The instability of river channels can be derived from two sets of factors: those related to the catchment and those related to the channel itself (Baker 1977). These factors jointly shape the form and dynamics of the channel over space and time. The stability of a river's morphology is influenced by the volume of water flow and sediment it carries, which are outcomes of catchment processes, as indicated by studies like those by Schumm (1969) and Lewin et al. (1988). For instance, Schumm's model illustrates how changes in discharge and sediment yield can affect the sinuosity, gradient, and form ratio of a channel. Any modifications to the hydrology of the catchment or the sediment supply are likely to lead to instability in the channel.

A change in rainfall patterns (climatic oscillations) has also been linked to alterations in river channels, potentially causing instability (see Warner 1987; Eybergen and Imeson 1989; Harvey 1991). Warner (1987) observed changes in the MacDonald River in Australia, attributing them to shifts in sediment and hydraulic patterns influenced by climate alongside changes in land use. Research in Australia by Erskine and Warner (1988) also highlighted the occurrence of periodic shifts between drought- and flood-dominated conditions, leading to fluctuations in channel processes between erosion and deposition. The eastern seaboard of South Africa is affected by tropical cyclones which can bring large amounts of rain and flooding such as Tropical Storm Domoina in 1984, which caused large areas to experience 100-year floods and caused many rivers to alter their courses.

Additionally, changes in land use have been identified as influential factors affecting both hydrological processes and sediment yield, potentially leading to channel instability (Smith 1982; Higgs 1987; Lewin et al. 1988; Prosser 1991; Thorne 1991; Dollar and Rowntree 1995). Knighton (1989) exemplifies how increased sedimentation from tin mining can drastically alter the morphology of the river in Tasmania. In addition, channel instability may arise from increased sediment loads due to accelerated erosion in the catchment, often linked to inadequate land management practices. Debano and Schmidt (1989) highlight the intricate connection between the hydrology of the catchment, soil erosion, and the general condition of the catchment, influenced by factors such as grazing management, land use, and climate. The Tsitsa River Catchment is characterised by veld degradation and in many areas increased erosion (Huchzermeyer et al. 2019)

7.4.4 LATERAL MIGRATION RATES

The depositional age of sediments from a pair of nested oxbows with a distinct relative age sequence (see de Villiers 2022) was determined to estimate the historical lateral migration rate of the Gatberg River. The two oxbows are in the upper section of the floodplain system. The innermost (youngest) oxbow is situated nearer the modern channel, whereas the outermost (oldest) oxbow is situated farther away from the active channel. The radiocarbon ages from the oxbows fall in the expected

chronological order, given their spatial arrangement. The oldest oxbow was abandoned following a meander bend cutoff at ~3627 BP and later a meander bend occurred at ~2830 BP. The sequence of meander bend cutoffs has resulted in episodic channel migration with an average lateral channel migration rate of ~0.03 m yr^{-1}. While the accuracy of this data may be subject to debate, it offers a restricted yet significant value, particularly given the scarcity of data in South Africa.

The floodplain reworking rates of the Gatberg River floodplain are very low when compared to other systems in humid regions around the world (Black et al. 2010; Giardino and Lee 2011; Jarriel et al. 2021). The Gatberg system does compare well with migration rates of rivers in dryland regions (Owens 1998; Ellery et al. 2003; Grenfell 2007; Keen-Zebert et al. 2011; Tooth et al. 2014; Larkin et al. 2017). A comparison of migration rates with other meandering rivers in South Africa showed that the Gatberg River (~0.03 m yr^{-1}) falls within the migration rates calculated for other dryland rivers. Examples of lateral migration rates in drylands include; the lower Tshwane River which experiences lateral migration rates of approximately > 0.2 m y^{-1}; the upper Klip River at a relatively slow rate of < 0.2 m y^{-1}; the Blood River experiences lateral migration downstream of the flood-out at rates between 0.0 and 0.2 m y^{-1} over the past 100 years (Tooth 2018); and the lateral migration rates in the Okavango Delta Panhandle in Botswana of < 0.5 m y^{-1} (Tooth and McCarthy 2004). According to Lauer and Parker (2008), channel migration can gradually remove over-bank deposits over the floodplain's entire width. The eastern region of South Africa has had remarkable stability in fluvial processes and morphologies despite late Quaternary climate shifts (Keen-Zebert et al. 2011). This contrasts with many rivers around the world where the balance between sediment supply and discharge has been altered to such an extent by climate change that rivers have seen major changes in channel dimensions or have transitioned from braided to meandering. The stability of the Gatberg River floodplain system could be due to a combination of very low slope, low stream power, low sediment supply, and cohesive channel banks. These results provided new insights into the development of theories for explaining and predicting bend migration and meander evolution.

7.4.5 Evidence of channel change

In alluvial streams, the channel is created by the flow of water across boundary materials that the stream has deposited and can erode and transport. In alluvial streams, bank migration due to erosion and accretion is the norm rather than the exception, and over time, floodplains, islands, and side channels will change (Lagasse et al. 2004). This is especially true of actively meandering streams, which are constantly changing their positions and forms due to hydraulic pressures and fluvial processes acting on their beds and banks (Nanson and Croke 1992). These modifications might be system-wide or local; incremental or episodic, gradual, or abrupt (Lawler 1993; Bierman and Montgomery 2014).

Although meanders naturally develop and migrate, human activity may hasten this process or bring about brand-new modifications brought on by morphological responses and feedback in the fluvial system.

The primary cause of channel migration in meandering streams is the propensity of meander bends to amplify and migrate downstream over time. On the other hand, meander growth means that a bend could grow so extended and tightly curled that a chute or neck cutoff event occurs. Therefore, channel migration is a progressive process that occasionally experiences dramatic shifts in channel alignment and location due to cutoffs. Given that channel migration has important impacts on downstream users in terms of sediment and sediment-associated nutrients and contaminants, a practical methodology is required to assess the potential for bend movement. This aids in defining the rates and direction of historic channel shifts, helps to estimate future channel migration and can be used to evaluate the risk posed by channel migration. It is necessary to consider both system-wide and local parameters when predicting channel migration. The water and sediment flow from upstream have a significant influence on the morphology and behaviour of a particular downstream river reach. The rate of lateral movement in dynamically regulated systems increases as the supply of water and sediment increases. Variations in sediment and runoff yield due to human activity or natural processes will cause variations in channel migration rates and patterns.

Locally, channel behaviour will be governed by the distribution of shear stress and velocity as well as the properties of the bed and bank materials (Fisk 1944, 1947). Consequently, the local morphology of the channel will reflect the upstream controls and provide information on the direction and rate of channel migration. These characteristics include width, depth, meander wavelength (Leopold and Wolman 1957, 1960; Schumm 1968), and amplitude; pattern, which includes sinuosity and bend radius of curvature (Hickin and Nanson 1975, 1984); shape, which includes width/depth ratio (Markham and Thorne 1992); and bend geometry, which includes radius of curvature/ width ratio (Bagnold 1960; Hickin and Nanson 1975, 1984; Thorne 1992, 1997).

In the Gatberg, results indicate that the radii of curvature for the oxbows had a higher average (15 m) than both the river meander bend radii of curvature for 1958 (11 m) and for the current channel (12 m). In the Minnehaha system, the radii of curvature for the oxbows were double (21 m) the average of both the radii of curvature for the river meanders in 1958 (11 m) and 2015 (10 m). This suggests that for both floodplain systems at the time of the cutoff event, the historical meander bends (current oxbows) had wider bends compared to the current river. Additionally, from 1958 to 2020 the bends are gradually getting wider in the Gatberg system, although this is a slow process. The opposite is occurring within the Minnehaha system.

Bagnold (1960) demonstrated that energy losses resulting from the flow's curvature at the bend were reduced for radius-of-curvature and channel width ratio values between 2 and 3. The most efficient bends for eroding their bed and banks are those with a channel width ratio of 2 to 3. As the channels migrate over the floodplain, many bends in nature develop and maintain a channel width ratio of 2 to 3. This might be explained by the bends' adherence to the most effective hydraulic shape, which also maximises their geomorphic efficacy (Thorne 1997). Furthermore, Crosato (2009) states that the values of the channel width ratio influence channel migration, with a maximum amount of channel migration occurring at specific channel width ratio values. Channel migration rates are highest in systems with channel width ratio values between 2 and 3, and migration decreased both below and above these values, according to Hickin and Nanson (1975, 1984) and Nanson and Hickin (1986); further substantiated by Hooke (1987), Biedenharn et al (1989) and Hudson and Kesel (2000). This is because of the energy loss that occurs while water flows through a meander bend. In extremely tight bends (channel width ratio < 2), deposition may even occur along the outer bank of the meander bend. In the Gatberg system, the mean channel width ratio values for the oxbows were 2, while for the channel in 1958, the mean channel width ratio value was 2.1, and the current channel (2020) had a mean channel width ratio value of 1.8. Accordingly, it can be demonstrated that channel migration on the Gatberg River floodplain happens slowly since the channel width ratio ratios of the oxbows, the old channel in 1958, and the present channel in 2020 are below or near the values reported by Hudson and Kesel (2000). The cohesive channel banks that enhance resistance or the comparatively low stream power, or maybe a mix of both, are potentially the reasons for the Gatberg River's slow channel migration rate. Meanwhile, in the Minnehaha system, the mean channel width ratio value for the oxbows was 3, for the meander bends in 1958 the mean channel width ratio value was 2.2 and 2.6 for the meander bends in 2015. These values fall within the values mentioned by Hudson and Kesel (2000). This suggests that the Minnehaha River floodplain system migrates more often than the Gatberg floodplain system.

7.4.6 POTENTIAL FOR FUTURE CHANNEL CHANGE

A meander bend cutoff is a natural form of river adjustment and can be seen as a form of local avulsion that creates a new river course. Meander bend cutoffs are a direct result of gradual bend migration. They occur as natural and regular responses to lengthening of the channel and decreasing channel slope resulting from river migration (Allen 1965; Hickin and Nanson 1975; Bridge et al. 1986; Erskine et al. 1992; Hooke 1995). Meander bend cutoffs are spatially and temporally common in actively migrating meandering rivers. Brierley (1996) distinguishes two types of avulsions: neck cutoffs and chute cutoffs. Meander bend cutoffs can occur when an extended bend gradually migrates upon itself to generate a neck cutoff or when a new channel erodes over the bend's neck to form a chute cutoff

and are a result of more mobile meander bends (Lewis and Lewin 1983). Chute cutoffs typically occur in relatively stable channels, where a new channel develops across the floodplain, bypassing the old channel. The meander bends gradually grow and extend due to erosion of the channel bank on the outside of the bend, simultaneously lateral deposition of sediment occurs on the inside of the meander bend. Therefore, channel migration is controlled by stream flow and the erodibility of soils on the outside meander cutbanks (Nanson and Croke 1992). As such, bank erosion rates typically increase with increasing discharge, velocity, and the duration of flows exceeding a threshold condition (Konrad 2012). Because meander cutoffs are rare and there is a wide variety of hydro-geomorphic variables influencing the patterns and processes of meandering-river floodplains, there is a lack of understanding regarding the physical mechanisms leading to their development (Hooke 1995; 2004). However, research has shown that meander bends lengthen, increases their amplitude, and become more sinuous as they migrate.

To measure the potential for future channel change in the Gatberg and Minnehaha River floodplain systems, two processes were evaluated by measuring the channel dimensions of the current channel courses. The first was to evaluate the potential of meander neck cutoff events. The meander bend neck was measured with the channel width. Cutoff events may potentially occur when the meander neck is shorter than one channel width. In the Gatberg floodplain system, there is only one meander bend with a high neck cutoff potential (< 1) and in the Minnehaha floodplain there were no meander bends with a high neck cutoff potential. The second was to evaluate the potential for meander chute cutoff events. As the ratio value rises and other environmental factors like vegetation, flood discharge, bed slope, and bed material are favourable, a cutoff will become more likely (Joglekar 1971). Rivers differ in the typical chute cutoff ratios at which cutoffs occur; bigger rivers, like the Mississippi River, where neck cutoffs predominate, have values between 8 and 10, whereas chute cutoff ratios for smaller rivers where chute cutoffs are occasional have a range of ratios between 1 and 3. A visual evaluation identified 5 meander bends that meet the chute cutoff stability criteria in the Gatberg River reach and 20 meander bends in the Minnehaha River floodplain system. Given that the visual evaluation of the meander bends in both the Gatberg and Minnehaha systems had chute cutoff stability ratios of < 3, a chute cutoff stability ratio of ≤ 3 was chosen as the potential chute cutoff value.

Both the current channels in the Gatberg and Minnehaha River floodplain systems have a low potential for neck cutoff events, this is likely due to the high clay content within the channel banks, relatively low sediment supply, and bank protection from vegetation which means that the bank erosion rates are low, which decreases the potential for neck cutoff events.

The Minnehaha River floodplain system had the greatest potential for chute cutoff events using the chute cutoff ratio compared to the neck cutoff potential and compared to the Gatberg floodplain

system. This could be attributed to the steeper slope of the Minnehaha River which would increase the stream power and shear stress. This is supported by observations from Tower (1904), Lewis and Lewin (1983), and Kleinhaus and van den Berg (2011). An increase in the valley and river slope is likely to increase the sinuosity index, and entrance angle, and lower the values of curvature; thereby initiating chute cutoff events (Lewis and Lewin 1983; Howard 1996; Micheli and Larsen 2010). According to Micheli and Larsen (2010), bend geometry dictates whether a bend is set up for a cutoff event, but the timing of chute cutoff events is mostly determined by the type and frequency of large floods (following Hooke 2008).

7.5 CONCLUSION

The continual and intricate interactions between river channels and their surrounding floodplains, particularly during periods of high overbank flows, foster the development of meandering and hydraulically intricate rivers (Zinger et al. 2013; Gualtieri et al. 2020). The diverse landscapes associated with meandering rivers, including the features of the floodplain surfaces such as oxbows, scroll bars and levees (Sabo et al. 2005), signify that these rivers and their floodplains serve as biodiversity hotspots and play a crucial role in sustaining a growing human population by providing essential ecosystem services and resources (Hamilton et al. 2007; Heckenberger et al. 2007; de Moel et al. 2011; Junk et al. 2012; Leauthaud et al. 2013; Pastor et al. 2022). However, because meandering rivers migrate laterally, erosion may threaten nearby riverine settlements and jeopardise infrastructure, as well as reintroduce sediment and associated nutrients and contaminants that were previously stored on the floodplain surface (Donovan et al. 2015; Basnayaka et al. 2022; Lelpi and Lapôtre 2022; Nagel et al. 2022). Therefore, studies on meandering rivers and floodplains are essential to gain a better understanding of how to maximise biodiversity and ecosystem services supplied by floodplain systems while safeguarding nearby populations and the infrastructure they depend on. This is especially true for developing areas such as South Africa and key water source areas such as the Gatberg and Minnehaha River systems.

In this chapter, an attempt was made to measure contemporary channel erosion and deposition, historical channel changes, lateral migration rates, changes in channel geometry, and the potential for future channel changes. The objectives required the collection, analysis, and interpretation of multiple datasets. The techniques used provide a useful dataset for river channel changes in the sub-humid rivers of the southeastern Drakensberg. The information about the dynamics, historical, and present status of fluvial erosion and accretion of these two meandering rivers may be used to compare with other meandering rivers of the same size and contribute to knowledge on dryland floodplain systems.

The results revealed that during the two wet seasons, both the Gatberg and Minnehaha River floodplain reaches experienced both deposition and erosion in the study reaches. The Gatberg River reach experienced slightly higher cross-sectional area erosion compared to the Minnehaha River reach. For both systems channel bed scouring occurred in most of the cross-sections, indicating a general absence of sediment aggradation within the main channel bed. From the re-surveys over two wet seasons both the Gatberg and Minnehaha River floodplain reaches experienced more deposition than erosion. Estimated eroded sediment volumes were 520 t yr^{-1} for the Gatberg reach and 360 t yr^{-1} for the Minnehaha reach. Although both rivers display comparable trends regarding the makeup of eroded material, where sand is the primary constituent followed by clay and silt, significant differences arise in the median volume of eroded material. Both estimates fall within a similar range as for the floodplain deposition estimates outlined in Chapter 6. These distinctions indicate diverse sediment transport dynamics between the two river systems, likely influenced by factors such as variations in watershed characteristics, land usage, and hydraulic properties of the rivers.

The outcome of the time sequence analysis for the Gatberg River floodplain system shows that there have been three meander bend cutoff events between the years 1958 and 1993. The analysis of the Minnehaha River floodplain system indicated that there have been four changes along the river course between 1958, 1966 and 2015. Both floodplain systems were divided into four zones to map and calculate changes in river length and sinuosity indices from the historical river course (1958) and the current river course (2020 for the Gatberg River and 2015 for the Minnehaha River). For both floodplain systems, most of the zones decreased in sinuosity from the historical river course to the current course. This reflects the few meander bend cutoff events that occurred within each of the zones. Meander cutoffs play a vital role in river morphodynamics by increasing the local channel slope, decreasing river sinuosity, and reducing floodplain access. They also have a substantial effect on sediment and phosphorus flux for that period by injecting a significant amount of sediment back into the river system. The likely drivers of channel change in the Gatberg floodplain system would have been changes in land use. The channel straightened to accommodate an increase in sediment loads, bed loads and an increase in hillslope-channel connectivity likely to have occurred because of an increase in road density (unsealed gravel roads in commercial forestry), erosion, changes in natural vegetation cover etc. The likely drivers of channel changes in the Minnehaha floodplain system would have been an increase in sediment loads from adjacent land due to agricultural practices and an increase in the hillslope-channel connectivity due to livestock tracks.

The results from the geochronology of two nested oxbows in sequences were used to estimate the lateral migration rates for the Gatberg River reach. Ages indicate stepwise lateral channel migration through the meander cutoff. The floodplain reworking rates of the Gatberg River floodplain are very

low compared to other systems in humid regions around the world, although the Gatberg system compares well with migration rates of rivers in dryland regions.

In conclusion, the comprehensive analysis of channel change and historical channel dynamics in the Gatberg and Minnehaha River floodplain systems provides valuable insights into the intricate processes shaping these riverine environments. Examining channel erosion volumes highlights the significant role of these rivers in sediment mobilisation and downstream transport processes, emphasising variations in sediment dynamics between the two systems.

Historical channel change analysis reveals the dynamic nature of meandering rivers, characterised by frequent meander bend cutoff events and subsequent changes in channel morphology and sinuosity. The examination of lateral migration rates indicates migration rates for the Gatberg floodplain as comparable to other systems in drylands, with implications for sediment transport and floodplain dynamics.

Furthermore, the evaluation of potential future channel change highlights the importance of considering both system-wide and local parameters in predicting river behaviour. While both systems exhibit low potential for neck cutoff events due to factors such as high clay content and slow bank erosion rates, the Minnehaha River floodplain system demonstrates a higher potential for chute cutoff events, influenced by factors such as slope and stream power.

Overall, this research enhances our understanding of the complex interactions driving channel change in meandering river systems, providing insights for informed management and conservation strategies in these dynamic environments. Information on the historical and current trends of channel change is crucial to creating baselines of river behaviour and ecosystem service provision of these systems. These baselines provide insights into long-term shifts and provide early warning systems of ecosystem decline or tipping points. More studies are warranted that integrate hydrological, geomorphological, and ecological perspectives are warranted to comprehensively address the challenges posed by future channel dynamics and environmental change in dryland floodplain systems.

CHAPTER 8 : SYNTHESIS AND WIDER IMPLICATIONS OF THIS RESEARCH

8.1 INTRODUCTION

This chapter synthesises the findings of the research aim and objectives. This research provides a greater understanding and quantification of sediment and associated phosphorus trapping efficiency in two meandering floodplain wetlands in the Eastern Cape of South Africa, namely the Gatberg and Minnehaha River floodplains. This synthesis touches on the wider implications of this research in supporting ecosystem service assessment methods (e.g. the South African WET-Ecosystem Services and WET-Health rapid assessment tools) and wetland management and rehabilitation prioritisation. This is achieved through the investigation of the fundamental biophysical factors controlling sediment and phosphorus dynamics in these two floodplain wetlands. The most relevant results of each chapter of this research are integrated into this synthesis to form a broader perspective of the temporal and spatial variability of sediment and phosphorus dynamics of meandering river floodplain systems in South Africa, followed by some suggestions of potential areas for future research.

Up to 40 % of all ecosystem services worldwide are provided by wetlands, which offer a wide range of benefits to downstream ecosystems and society (MEA 2005). The three main categories of ecosystem services that wetlands provide are provisioning (such as water, fibre, and food), regulating (such as flood mitigation, water quality improvements, sediment, and nutrient retention), and cultural services (such as tourism and recreational activities; MEA 2005). De Groot et al. (2012) estimate that the yearly value of ecosystem services provided by a single hectare of palustrine wetland exceeds US$ 25 600. Even though laws on the management and protection of wetlands, such as the Ramsar Convention, have been developed with the help of the economic valuation of wetlands, a clear deficiency remains in the empirical knowledge of important wetland processes and the connection of these processes with ecosystem service provision. This is particularly evident in South Africa due to its relatively young history of research into ecosystem service provision, unmonitored systems, and data scarcity. This has probably contributed to the exploitation and rapid degradation of South Africa's wetlands (Ellery et al. 2009; Maltby and Acreman 2011; Maila et al. 2017). Due to projected water constraints, population expansion, and increased reliance on dryland water supplies, this trajectory is probably going to become worse. The range of data collection methodologies applied during this research helped to address this gap in empirical knowledge. The findings of this research can aid in supporting the methods of assessing floodplain wetland ecosystem service provision and management decisions by providing a deeper level of detail and quantification of ecosystem processes in floodplain systems in South Africa.

Using field observations, field measurements, desktop analysis, satellite imagery and geochronology, this study investigated and described the nature and controls of sediment and associated phosphorus patterns and dynamics for two case study floodplain wetlands in the Eastern Cape of South Africa. The study also quantified, both temporally and spatially, the sediment and phosphorus trapping efficiencies of the meandering floodplain systems.

The research was focused on floodplain wetlands because i) floodplains in drylands are hotspots of ecosystem service delivery in these climatically variable environments (Scoones 1991; Silvius et al. 2000; Tooth et al. 2015); ii) there is a lack of empirical data and quantification of sediment and phosphorus trapping efficiencies of floodplain systems in South Africa; iii) they are vulnerable to climatic and anthropogenic changes; iv) effective management and prioritisation cannot happen due to the lack of empirical data; v) there is a lack of data for validation and calibration of sediment processes in numerical models and sediment budgets.

8.2 THE IMPORTANCE OF LAND USE ON SEDIMENT CONNECTIVITY AT THE CATCHMENT SCALE

A river's physical attributes and functionality are primarily influenced by the flow of water and sediment through its catchment (Rosgen 1994). The amount of material accessible and the pathways or linkages needed to carry the material to the river define the amount of sediment input from the catchment (Owens 2005). The basis for this sediment routing is connectivity. "Connectivity" can be used to describe the flow of water, sediment, and other materials (or species) through a landscape (Wohl et al. 2018). At the catchment scale, the main active geomorphic connectivity zones are hillslopes and channels, and the main fluxes are inside and between these two components (Bracken et al. 2015; Heckmann et al 2018). Connectivity is offset by storage units, such as buffers, barriers, and blankets, within the catchment that allows sediment and water to be retained or stored within the system (Fryirs et al. 2007a). The role of sediment and associated phosphorus sources and connectivity both within the broader catchment and a floodplain system is vital when trying to understand the sediment and nutrient dynamics within a floodplain system, to identify the potential risks associated with land use changes, and to prioritise management or rehabilitation programs.

The Gatberg and Minnehaha River catchments both have a well-developed drainage network given their regional setting in high relief headwaters draining the Drakensberg Escarpment. It would be expected in this setting that the sediment connectivity is high due to the steep topography with high drainage densities and hillslope-channel connectivity. From field observations, it was noted that the Gatberg and Minnehaha River catchments were characterised by high sediment concentrations during rainfall events (chocolate-brown river water). Through the combination of field research and the mapping, analysis and classification of high-resolution aerial images, potential sediment and

phosphorus sources were identified. Drainage pathways (connectivity) were assessed and allowed for the differentiation between features that are directly linked to the drainage network from those where sediment transfer is hindered by buffers or barriers.

In the Gatberg River catchment, commercial forestry emerges as the primary potential source of sediment, constituting 23 % of the land use. Ninety-five per cent of the commercial forestry plantations are connected to the drainage system, primarily situated on gentle and moderate slopes, with only a small proportion identified on steep slopes. This has likely increased sediment-laden runoff, especially in the initial clearing and ploughing stages and again in the harvesting stage of the plantations. Contrastingly, in the Minnehaha River catchment, commercial forestry plays a relatively minor role, accounting for less than 1 % of the total catchment area. Current agricultural activities, in the Gatberg River catchment and previously cultivated fields are primarily concentrated on the edges of plantations and wetland systems, accounting for 12 % of the total area. A significant proportion (> 60 %) of these are connected to the drainage network, leading to the potential unrestricted export of sediment and phosphorus into the river system especially during harvesting and preparation of the fields for planting (burning, ploughing, tilling and the addition of fertilisers). Within the Minnehaha River catchment, agricultural fields, and previously cultivated fields occurred in the lower catchment along the alluvial terrace, comprising < 15 % of the total catchment area. Less than 50 % of these are connected to the drainage network. Although roads, livestock tracks, and gully erosional features accounted for a small percentage of the catchment areas (< 1 % in both catchments) all these features were well connected to the river network and increased the drainage density significantly. These results allude to the importance of understating the spatial configuration of land-use units and their connection to the drainage network. In conclusion, both catchments have been modified by changes in land use. These changes are usually well connected to the drainage network suggesting that any sediment or phosphorus may be easily transported to the drainage network and reach the floodplain systems.

Sediment conveyance through a river catchment may be buffered by different features, both natural or anthropogenic (e.g., wetland systems, vegetation cover, artificial impoundments (dams), and anti-erosional structures). The configuration of these features and the nature of connectivity within and between catchment features affect the transport, deposition, and storage of sediment through the catchment. In both river catchments, natural vegetation was identified as the primary buffer and accounted for 31 % of the land cover in the Gatberg catchment and 81 % of the Minnehaha catchment. Wetlands (including the research sites) accounted for 5 % and 10 % of the total area in the Gatberg and Minnehaha catchment respectively. Less than 1 % of each of the catchment areas was covered by artificial impoundments.

The Eastern Cape presently has the third most extensive commercial forestry plantations in South Africa with approximately 1200 km² currently established. Additionally, the province has been identified as the most suitable location for expanding plantations, with the government actively promoting the establishment of another 1000 km² (Department of Forestry, Fisheries, and the Environment 2007). The Tsitsa River catchment, in which the Gatberg and Minnehaha River floodplain wetlands are situated, is one of the poorest and least developed regions of South Africa and is earmarked for future development projects and programs (Calmeyer and Muruven 2015).

As shown by the literature and key findings of this research as discussed in Chapter 4, catchment configuration and connectivity within and between landscape compartments affect the transport, delivery and buffering of sediment and associated phosphorus. To show the wider implications of this research for management and ecosystem services assessments, the effects of land use units and buffer configuration are explored in a few scenarios (Figure 8.1). The effects of climate change, specific land uses, and land use changes on river flows and sediment regimes have been widely studied in the literature. Here an attempt is made to link potential changes in catchment configuration scenarios to the potential sediment and phosphorus trapping efficiencies based on the findings of the research described in the chapters of this thesis.

Figure 8.1A shows a scenario in which the catchment is undisturbed. The grey-shaded area depicts a meandering floodplain system. The blue arrows show the relative quantity of flow through the catchment. Flow increases in the trunk stream as tributaries join. Overbank floods will spill across the floodplain, sediment would be deposited on the surface of the floodplain and as point bars within the channel. This process would be balanced by erosion of the banks and some remobilisation of material on the surface of the floodplain during very large events.

Figure 8.1B shows an increase in commercial forestry plantations with a forestry gravel road joining the plantations along one of the tributaries. The plantations are situated close to the tributary on gentle and moderate slopes (as shown by the current plantation locations in the Gatberg River catchment, see Chapter 4) which would increase the effective connectivity between the land use and the river. The intensification of the road networks between the different plantation blocks would increase the routing of runoff flows predominantly in an across-slope direction (as shown by the research results in Chapter 4) until the water meets a drain which will channelise and increase flow velocities towards the drainage network. The red arrows coming off the plantations and the roads indicate the increase in sediment-laden runoff. An increase in the tributaries (due to the plantations) contributions to sediment-laden flow is depicted by a wider arrow. This increases the flow and sediment concentration in the trunk stream. An increase in flow and sediment concentration increases overbank flood frequencies (see Chapter 3 for inundation frequencies of the two floodplain systems)

and thus the potential of the floodplain to trap and store sediment as well as phosphorus (used as a fertiliser in the plantations) would also increase. This potential is also influenced by the size of the floodplain system compared to its catchment, inundation frequency and magnitude, floodplain microtopography and the different geomorphic units (see Chapter 5). Because both the Gatberg and Minnehaha River floodplain systems are grassland-dominated systems it was found in this research that vegetation did not play a crucial role in sediment and phosphorus floodplain deposition (see Chapter 4 and Appendix 2). Channel bank erosion on the outer meander bend would also increase due to higher velocity flows, shown by a thicker yellow arrow. Mobilisation of floodplain surface sediments might occur where flood flows are channelised along livestock tracks, abandoned channels or artificial drains and furrows, depicted by the thicker red arrows, and be reintroduced to the channel downstream. The effects of this scenario on floodplain dynamics would probably return to Figure 8.1A due to the disturbance being relatively small in a large catchment. The effects of the disturbance are likely to be further diluted given that the position of the disturbance is on a tributary upstream of the floodplain system.

Figure 8.1C shows an exponential increase in commercial forestry plantation along the tributaries, the trunk stream and along the edge of the floodplain system, as well as an increase in the road network. This will result in an exponential increase in sediment-laden flood flows and initially, this would increase the potential effectiveness of the floodplain to trap and store sediment and phosphorus. However, larger, higher-velocity flows also increase the chance of erosion and remobilisation of this stored sediment by increasing stream power and the river's ability to do geomorphic work on the beds and banks. This leads to scouring of the bed material, exposing the channel bed to erosion and thus faster rates of channel incision. Channel incision will lead to a decrease in overbank floods and some extreme cases a complete disconnect between river and floodplain. The effects of this scenario would likely be much larger than Figure 8.1B due to the extent of the disturbance across the catchment and the proximity of the disturbance to the floodplain system.

Figure 8.1D shows the potential effect of a buffer. In this scenario, the buffer is a large impoundment (artificial dam) upstream of the floodplain system and a tributary. Sediment-laden flows from the commercial forestry plantation will be trapped behind the dam wall, decreasing flows and sediment concentration downstream, except for large flood events. Flow and sediment starvation below the impoundment may change the river's planform, initiate incision, and cause riverbed armouring. In this scenario the effectiveness of the floodplain to trap and store sediment and phosphorus will be decreased as medium floods, flood seasonality and fine sediment will be trapped by the impoundment. In this scenario, the effects of the impoundment are mitigated by the tributary downstream of the impoundment which would still supply the floodplain with flow and sediment.

Figure 8.1E shows the potential negative effects of a buffer. In this scenario, the buffer is a large dam upstream of the floodplain system. There is no tributary joining the trunk stream below the impoundment. Like the previous example, sediment-laden flows from the commercial forestry plantation will be trapped behind the dam wall, decreasing flows and sediment concentration downstream, except for large flood events. Flow and sediment starvation below the impoundment may change the river's planform, initiate incision, and cause riverbed armouring. In this scenario the effectiveness of the floodplain to trap and store sediment and phosphorus will be decreased as medium floods, flood seasonality and fine sediment will be trapped by the impoundment. Sediment concentration in the trunk stream would be less compared to the same scenario without the impoundment. The potential for this floodplain system to trap sediment and phosphorus would be significantly less.

In conclusion, these scenarios demonstrate the significance of landscape unit configuration and crucial connectivity factors in the floodplain system's capacity to offer sediment and phosphorus-trapping ecosystem services. Mapping changes in the landscape structure (i.e., the arrangement of land cover and land use in a catchment), as well as the configuration of land use units and connectivity, are essential elements that can inform effective integrated management and help predict changes in the floodplain systems' ability to provide ecosystem services. In South Africa, there is a need for better catchment-integrated planning and management. An increase in developments, such as commercial forestry plantations and impoundments (artificial dams), need to be done in a way that allows the natural systems to cope, mitigate and still be able to continue to function and provide ecosystem services, i.e. developments should not overload or starve the system.

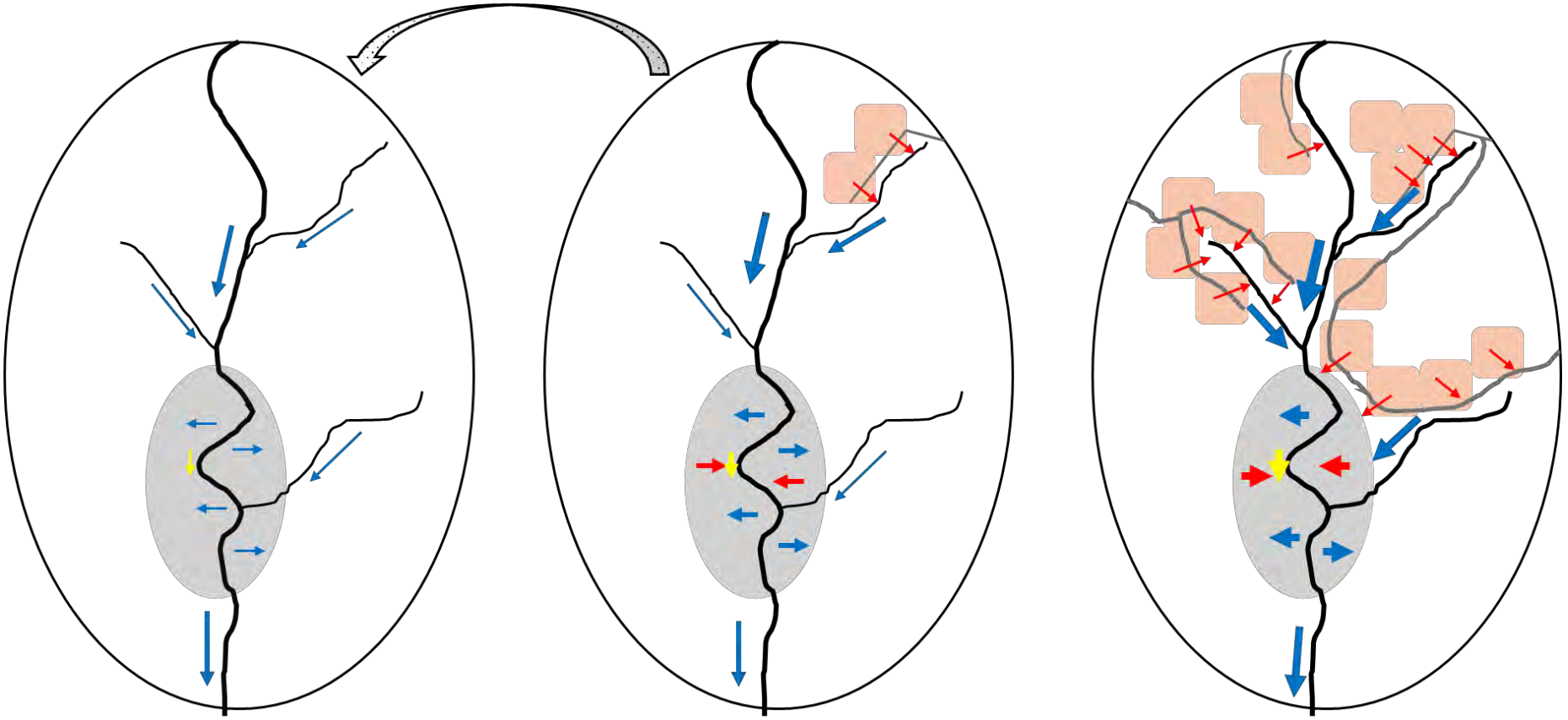

A.

Balanced conditions

Input (Low) +/- Δ Storage (Balanced)
Overland transport (Low) Bank erosion (Low)
Upstream transport (Low) Floodplain deposition (Low)
= Output (Low)
Downstream transport (Low)

B.

Modified conditions

Input (Medium) +/- Δ Storage (Depositional)
Overland transport (Medium) Bank erosion (Medium)
Upstream transport (Medium) Floodplain deposition (Medium)
= Output (Medium)
Downstream transport (Medium)

C.

Highly modified conditions

Input (High) +/- Δ Storage (Depositional/ erosional)
Overland transport (High) Bank erosion (High)
Upstream transport (High) Floodplain deposition (High/ low)
= Output (High)
Downstream transport (High)

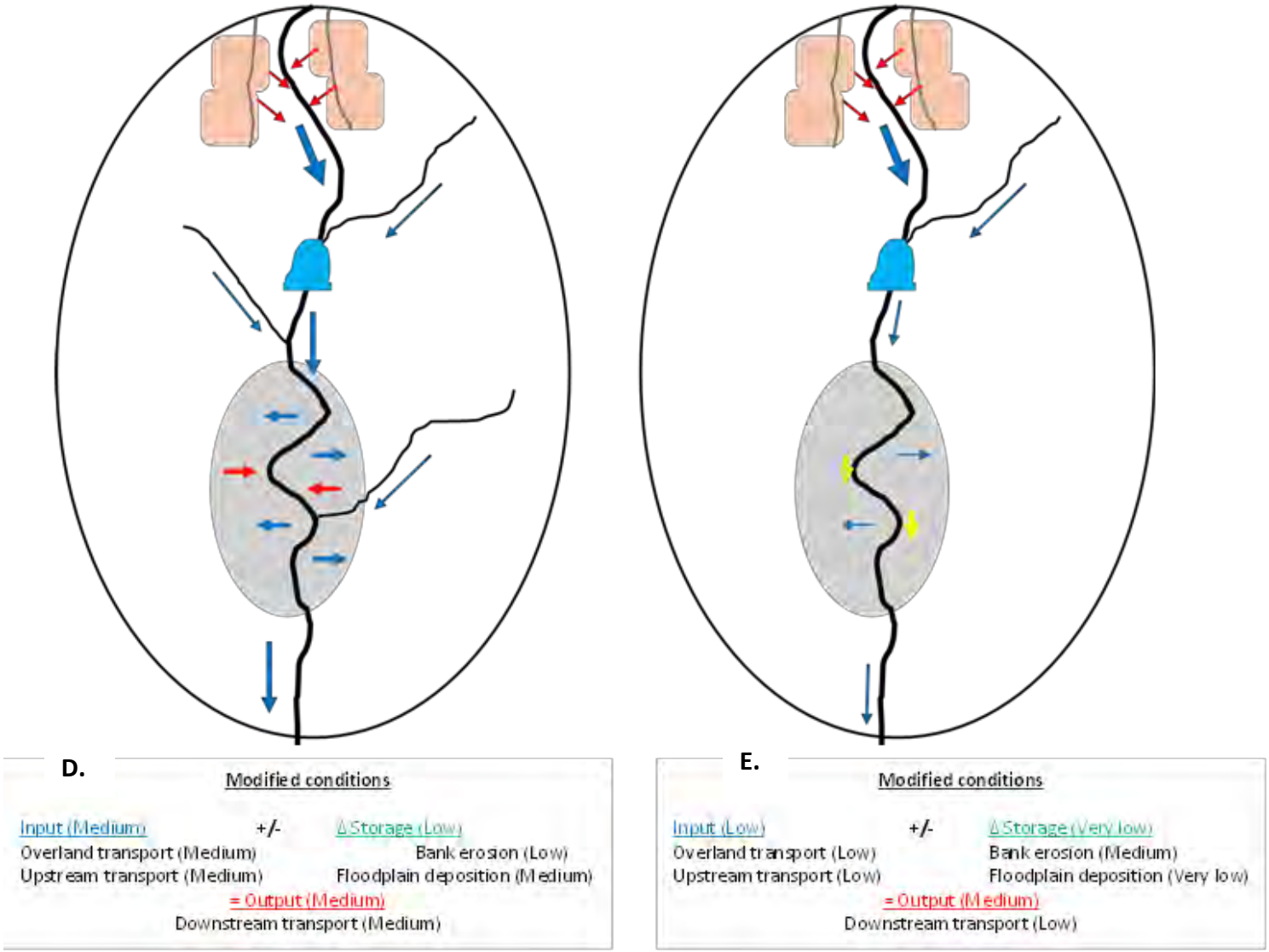

Figure 8.1 Showing the inferred relative rates of water, sediment and phosphorus inputs, storage, and export in different catchment conditions. A) Natural catchment; B) Slightly modified catchment with forestry plantations and roads; C) Highly modified catchment with forestry plantations and roads; D) Modified catchment with forestry plantations, roads, and an artificial dam; E) Modified catchment with forestry plantations, roads, and an artificial dam

8.3 THE SPATIAL SELECTIVITY OF SEDIMENT PROPERTIES WITHIN THE CHANNEL AND OVERBANK ON THE FLOODPLAIN SURFACE

As set out in Objective 2, the study investigated the spatial variability of the sediment particle size, organic matter content and total phosphorus composition of contemporary overbank floodplain deposits through the analysis of surface sediment samples collected from floodplain sites on the two meandering floodplain systems. Using a combination of field data, laboratory, desktop and statistical analysis, the results obtained from the study demonstrate that significant spatial variability in the particle size, organic matter content and total phosphorus composition of the sediment deposits exists at these sites. An attempt has been made to interpret this spatial variability in terms of local channel and floodplain geometry and topography (Chapter 5). The relationships between organic matter, total phosphorus, and sediment particle composition were also explored.

The particle size of the channel bed sediments in both river channels was larger, with a greater percentage of sand, compared to the channel banks (see Chapter 5 for more details). The Gatberg River had a slightly coarser particle size distribution than the Minnehaha River, which is likely due to the differences in the underlying geology of the catchments and where sediment is being delivered from (land use type, slope etc., see Chapter 4). In terms of the channel banks, the cut banks had a slightly higher percentage of clay, silt, and organic matter content compared to the point bar deposits for both channels. According to the statistical analysis, the distribution, and dynamics of phosphorus concentrations in the channel and channel banks were linked to and driven by the dynamics of the organic matter content.

The sediment particles found in both floodplain systems were significantly smaller in size compared to the samples taken from the channel bed and banks (see Chapter 5 for more details). The patterns in sediment and total phosphorus accumulation were used to analyse the relative importance of different processes, floodplain characteristics and sediment characteristics in controlling sedimentation and total phosphorus rates. In both systems, the D_{50} and highest sand fraction were found deposited within the proximal floodplain. The flow velocities are too low to transport the sand fraction further across the floodplain surface. In the Gatberg system, the rapid reduction in the greater particle size (medium to fine sand) content in the deposited sediment with increasing distance from the channel suggests that the fine fractions of the suspended sediment are transported onto the floodplain from the channel primarily through diffusive processes (see Chapter 5; James (1985)). However, some outliers exist in the Gatberg system, and this may be due to preferential flow paths, such as livestock tracks, increasing local slopes and flow velocities and/or sediment inputs from the surrounding hillslopes. In the Minnehaha system, the effects of distance on particle size composition

were more subtle than in the Gatberg system. The particle size of floodplain sediments was markedly constant as a function of distance from the channel for the Minnehaha system, suggesting that sediment transport is primarily associated with convective overbank flow. There could also be topographical and morphological reasons for this difference between the two systems. Firstly, the Minnehaha floodplain is a much wider system with a less distinct slope towards the floodplain margin compared to the Gatberg floodplain. This could explain why the trend is weaker for the Minnehaha system due to the longer distances that sediment-laden flood water must travel. Secondly, the Minnehaha River has a lower sinuosity than the strongly meandering Gatberg River. Beyond the levee, across-floodplain trends display a moderate to low decrease in mean particle size with distance from the channel potentially because of the calibre of the sediment load- clay and silt accounted for over 85 % of the samples. The floodplain samples also exhibited a higher percentage of organic matter content and total phosphorus concentration compared to those taken from the channel. The distribution dynamics of phosphorus were mainly influenced by the organic matter content, such that in general areas with higher organic matter content also have higher total phosphorus concentrations.

The patterns and trends of surface sediment characteristics were more pronounced when the floodplain was divided into geomorphic units. The analysis of floodplain geomorphic units revealed that both floodplain systems had the highest D_{50} particle size and percentage of the sand fraction in the bank and levee, as well as in the proximal floodplain units. These units also had the lowest per cent clay fraction, organic matter content, and total phosphorus concentrations. These geomorphic units form the potential exchange zone and where channel processes have the greatest effect. In the Minnehaha River floodplain system, the oxbows and backswamp units had the lowest D_{50} particle sizes and per cent sand fractions. These units had the highest per cent clay fraction, organic matter content, and total phosphorus concentrations. This suggests that these features experience lower flow velocities and are therefore less at risk from erosion and are likely to store sediment for longer periods. In the Gatberg River floodplain system, like the Minnehaha system, the oxbow geomorphic unit had the lowest D_{50} particle size and percentage sand fractions, as well as the highest clay fraction, organic matter content, and total phosphorus concentrations. This alludes to the importance of oxbows in trapping fine sediment, phosphorus, and organic carbon. However, the backswamp unit had the second-highest percentage sand fraction, which may indicate a secondary input of sand from the surrounding hillslopes. The relationships between geomorphic unit type, hydraulic conditions, processes within the unit, sediment size characteristics, organic matter content, and phosphorus concentrations found in this study are highlighted in Table 8.1.

Field observations in both the Gatberg and Minnehaha River floodplain systems revealed that both oxbows and backswamps were frequently flooded during the wet season. This suggests a strong

connection between these systems and their channels, with multiple occurrences of overbank floodwaters throughout the wet season.

Therefore, the evidence of selective deposition strongly suggests that particle size is the main factor that determines sediment-characteristic deposition. The distribution of particle sizes is influenced by various factors, such as the type of geomorphic unit, the distance from the channel, the frequency, depth and velocity of floodwater, and the length of time the particles spend in the area (residence time). By comparing the hydraulic conditions that occur in specific geomorphic units with the observed size distribution of particles in over-bank deposits, the different modes of deposition can be inferred.

The wider implication of preferential deposition is its significant impact on the fate of contaminants. Although fines can be easily washed on and off the floodplain, a considerable portion of fines can settle and be deposited during ponding where floodwaters are retained. Consequently, contaminants like heavy metals and nutrients such as phosphorus, which readily bind to fines, may become concentrated in the floodplain environment. This study sheds light on the preferential accumulation of fine sediment in floodplain environments, such as oxbows, emphasizing its environmental implications for water quality and floodplain pollution. The accumulation of heavy metals on floodplains may have adverse effects on environmental health, particularly for livestock grazing in polluted areas. Additionally, this study provides empirical data to complement numerical models of sediment transport and deposition. Lastly, the study highlights that morphological units and hydrological conditions, play a significant role in the functioning of these systems.

Table 8.1 The general characteristics, processes, and relationships identified for the different geomorphic unit types used in this study

Geomorphic unit	Hydraulic conditions	Processes operating	Sediment particle size characteristics	Organic matter content	Total phosphorus concentration	Gatberg floodplain median values	Minnehaha floodplain median values
Bank and levee	Overbank floodwaters; high energy; turbulent conditions; shallow water depths; low residence time; rough vegetation; channel-floodplain interactions	Advective transfer of sediment; preferential deposition of coarser sediment fractions; potential bank erosion (lateral migration)	Higher D_{50} particle size; higher proportion sand fraction; Low clay and silt fraction	Low organic matter content (OMC)	Low total phosphorus concentration (TP)	D_{50}= 81µm; Sand= 59%; Clay and silt= 41%; OMC= 3%; TP= 0.07 g kg	D_{50}= 25µm; Sand= 10%; Clay and silt= 90%; OMC= 8%; TP= 0.11 g kg
Proximal floodplain	Overbank floodwaters; high energy; turbulent conditions; slightly deeper water depths (especially in the lower elevation area behind the levee; low residence time; vegetation changes (shrubs to a mixture of shrubs and grass)	Advective transfer of sediment; sediment may be remobilised in subsequent floods; potential high zone of sediment exchange (deposition and erosion)	Exponentially finer than above	Slightly higher organic matter content than above	Slightly higher total phosphorus concentration than above	D_{50}= 15µm; Sand= 9%; Clay and silt= 91%; OMC= 9%; TP= 0.10 g kg	D_{50}= 28µm; Sand= 11%; Clay and silt= 89%; OMC= 9%; TP= 0.12 g kg
Floodplain surface	Variable energy regime dependent upon discharge magnitude; water depths deeper than above; variable residence times dependent on microtopography (higher areas will only be inundated in very large floods); vegetation is grass	Deposition and remobilisation of sediment; livestock tracks may play a role in the movement and deposition of sediment; some perpendicular flow was observed; most of the floodplain surface was covered in water for the whole of the wet season	Slightly finer than above; a lower proportion of sand; a higher proportion of clay and silt	Very slightly higher organic matter content than above	Minimal change in total phosphorus concentrations from above	D_{50}= 12µm; Sand= 8%; Clay and silt= 92%; OMC= 12%; TP= 0.08 g kg	D_{50}= 20µm; Sand= 8%; Clay and silt= 92%; OMC= 8%; TP= 0.12 g kg
Oxbow	Stilling of floodwaters; low energy; moderate to high water depths; longer residence times (some oxbows contained water all year round); some were covered in reeds	Retention ponding; sediment settles out in situ; in these two floodplains distance did not play a role because the whole floodplain was inundated in the wet season	Very fine sediment; lowest proportion of sand; high proportion of clay and silt fraction	High organic matter content	High total phosphorus concentration	D_{50}= 9µm; Sand= 7%; Clay and silt= 93%; OMC= 12%; TP= 0.13 g kg	D_{50}= 22µm; Sand= 10%; Clay and silt= 90%; OMC= 13%; TP= 0.21 g kg
Backswamp	Shallower water depth; sheet flow; perpendicular flow along the floodplain margin was observed; livestock tracks may play a role in routing flow to this area from the higher floodplain surface geomorphic unit; moderate energy; remobilisation of sediment; vegetation is grass	Deposition and remobilisation of sediment; livestock tracks may play a role in the movement and deposition of sediment; some perpendicular flow was observed; most of the backswamp was covered in water for the whole of the wet season; adjacent hillslopes and the unpaved road played a role in introducing sand to the backswamp geomorphic zone in the Gatberg floodplain system	Same as above, except for the input of sand from the adjacent hillslopes in the Gatberg floodplain system	Slightly lower organic matter content than above	Slightly lower total phosphorus concentration than above	D_{50}= 10µm; Sand= 7%; Clay and silt= 93%; OMC= 11%; TP= 0.12 g kg	D_{50}= 19µm; Sand= 9%; Clay and silt= 91%; OMC= 7%; TP= 0.08 g kg

8.4 TEMPORAL AND SPATIAL PATTERNS OF SEDIMENT AND PHOSPHORUS DEPOSITION

Floodplains provide valuable social and ecological functions and understanding the rates and patterns of overbank sedimentation is critical for river catchment management and rehabilitation. The accumulation of alluvium typically represents a long-term aggrading environment (Chapter 6). However, it has been documented that overbank deposition is not uniform across the floodplain but is often associated with local preferentially aggrading sites. Thus, floodplains are composed of segments of different ages and sedimentological character (Brown and Keough 1992; Simm 1993; Thonon 2006; Swanson 2013). To gain a more comprehensive understanding of the role of storage in providing ecosystem services in floodplain systems, it is crucial to acquire additional information on the extent and spatial variations in overbank sedimentation rates. This is necessary for quantifying the involved processes, developing effective policies and management actions, and establishing a foundation for the development and calibration of models, as emphasised by Pizzuto (1987) and Nicholas and Walling (1996, 1997).

The information on sedimentation rates and patterns of contemporary sedimentation along the Gatberg River and Minnehaha River floodplain systems (Objective 3; Chapter 6) has emphasised their importance as sediment sinks and sediment storage units along the river systems, as well as their importance as component of the sediment budget of the two catchments.

The results of this study suggest that the Gatberg and Minnehaha floodplain systems store a significant amount of sediment and associated phosphorus (see Chapter 6). Geochronology cores were positioned to target the main geomorphic units found in the floodplain systems (identified in Chapter 5). Field evidence (e.g., debris and fine sand deposits) was observed at the locations of the cores on the meander bends which confirmed that these levels were still active and were inundated frequently. The oxbows were located further away from the channel, however, observations in the field suggest that these were still connected to the channel during flooding and experienced inundation as well as deposition. The backswamp areas were observed to be inundated throughout the wet season (2019-2021). This suggests that all geomorphic units remained active and frequently inundated during overbank flood flows.

The average amount of sediment deposited on the Gatberg River floodplain was 1.1 g cm^{-2} yr^{-1}. The sedimentation in the Minnehaha River floodplain system was slightly more, on average 1.2 g $cm^{-2}yr^{-1}$. The sediment accumulation across the different geomorphic units showed clear patterns, related to the distance from the main channel, sediment particle size, inundation frequency, and local relief. In both systems, accumulations of larger sediment D_{50} particle sizes and the sand fraction with low organic matter content occurred in the proximal floodplain geomorphic zone (Table 8.2). Oxbows in

both systems were found to have a high clay fraction and organic matter content with lower sedimentation rates. The backswamp in the Minnehaha system had the lowest sedimentation rates and the highest clay fraction. There was one unexpected outlier in the Gatberg floodplain system: the backswamp had one of the highest sedimentation rates. This was thought to be related to additional inputs from the surrounding hillslope and connectivity to the adjacent uncapped gravel road. Total phosphorus accumulation rates followed a similar pattern as the sedimentation rates. This study found that sedimentation rates were difficult to separate using the aridity index (a numerical measure of how dry the climate is at a specific location). The ranges of sedimentation rates were wide and varied a large amount across the climatic zones when categorised by the aridity index. The study found that specific hydrological, morphological, and physiological factors were more important in predicting sedimentation rates.

To place the estimates of floodplain storage of both sediment and sediment-associated total phosphorus within the broader context of the sediment and total phosphorus budgets for the two research catchments, it is useful to compare them with estimates of the estimated annual suspended sediment and sediment-associated phosphorus yield for their respective catchments (Chapter 6). The results summarised in Table 8.2 indicated that the Gatberg floodplain deposition accounts for an average of 16 % of the mean estimated suspended sediment input. The Minnehaha floodplain deposition accounts for an average of 44 % of the mean estimated suspended sediment input, and 8 % and 49 % (respectively) of the equivalent sediment-associated total phosphorus flux (Table 8.2). This was further divided into geomorphic units to estimate the relative importance of each unit to the sediment and total phosphorus budget. For the Gatberg floodplain system, the greatest potential proportion of sediment stored on the floodplain surface of the total sediment yield was for the backswamp zone. The proximal floodplain zone and the oxbows had the same mean proportion (Figure 8.2). For the Minnehaha floodplain system, the greatest potential proportion of sediment stored on the floodplain surface of the total sediment yield was for the oxbow geomorphic unit, followed by the proximal floodplain zone and the least proportion was estimated for the backswamp zone (Figure 8.3).

To compare the Gatberg and the Minnehaha floodplain systems' ability to trap sediment and phosphorus the total sediment and phosphorus trapped by each floodplain can be normalised by dividing the total values of sediment and phosphorus (t km^2 yr^{-1}) by the catchment extent. The normalised sediment and phosphorus trapped by the Gatberg floodplain system were 9.76 and 0.0007 t km^2 yr^{-1}, respectively. For the Minnehaha floodplain system, the normalised sediment and phosphorus trapped were 26.84 and 0.003 t km^2 yr^{-1}, respectively. These results suggest that the Minnehaha floodplain system has a greater influence on the sediment and phosphorus fluxes by

trapping significantly more sediment and phosphorus. These results show the importance of the relative size of the floodplain system to the catchment extent.

The storage of sediment and sediment-associated total phosphorus represents an important component of the suspended sediment and phosphorus budgets of the study catchments. Floodplain storage has important implications for both the routing of sediment through fluvial systems and the determination and interpretation of downstream sediment fluxes. The dynamic nature of sediment storage and remobilisation adds to the complexity of this issue. Additionally, sediment storage on floodplains also has important implications for the fate of nutrients, such as phosphorus, and contaminants associated with fine-grained sediment. Further research which uses field measurements is needed to quantify the storage (both alluvial and colluvial) and routing of sediment in a wider range of river catchments. Such studies should be carried out at a variety of different spatial scales since many geomorphological processes have scale dependencies, which means that the fraction of sediment in storage is likely to be proportional to the catchment size.

Table 8.2 Comparison of the general characteristics, sediment and phosphorus accumulation rates, and the mean proportion of sediment and phosphorus trapped by each geomorphic unit within each floodplain system

	Proximal floodplain		Oxbows		Backswamp	
	Gatberg floodplain	Minnehaha floodplain	Gatberg floodplain	Minnehaha floodplain	Gatberg floodplain	Minnehaha floodplain
D_{50} (μm)	25.4	32.8	18.0	17.8	19.1	12.8
Sand fraction (%)	15.0	21.2	8.4	8.1	7.8	8.8
Clay fraction (%)	13.6	10.7	16.3	16.8	15.9	4.4
Organic matter content (%)	5.2	4.9	9.3	6.9	5.5	4.4
Total phosphorus concentration (mg kg^{-1})	99.3	79.8	92.3	129.2	64.5	45.3
Sedimentation rate (g cm^{-2} yr^{-1})	1.0	1.4	0.7	1.0	1.4	0.2
Total phosphorus accumulation rate (g m^{-2} yr^{-1})	1.0	1.0	0.6	1.1	0.9	0.1
Mean proportion of total suspended sediment yields trapped by each geomorphic unit (%)	3	16	3	20	10	8
Mean proportion of total phosphorus yields trapped by each geomorphic unit (%)	3	16	2	29	4	4

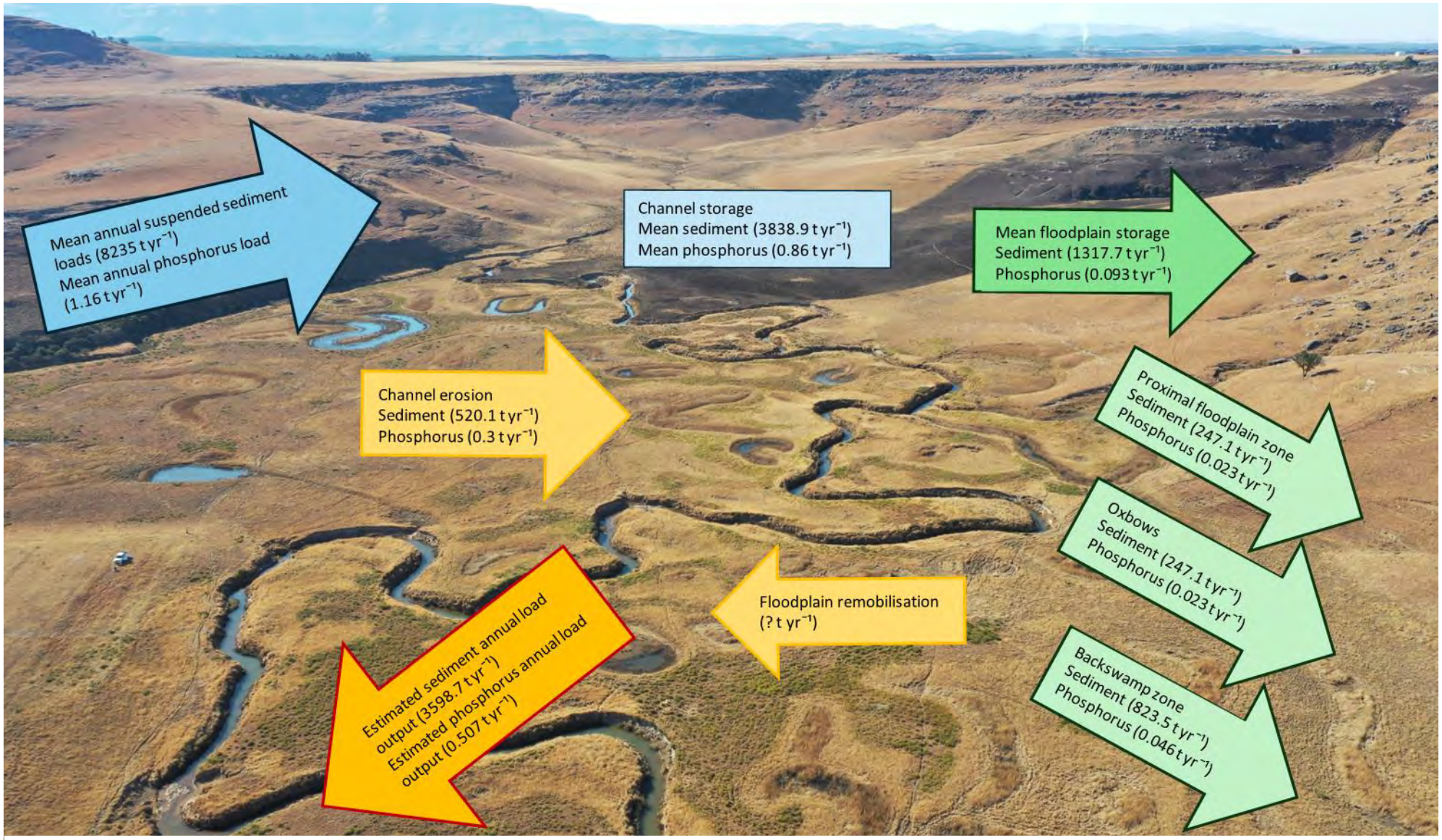

Figure 8.2 Sediment and total phosphorus mass balance estimates for the Gatberg River floodplain

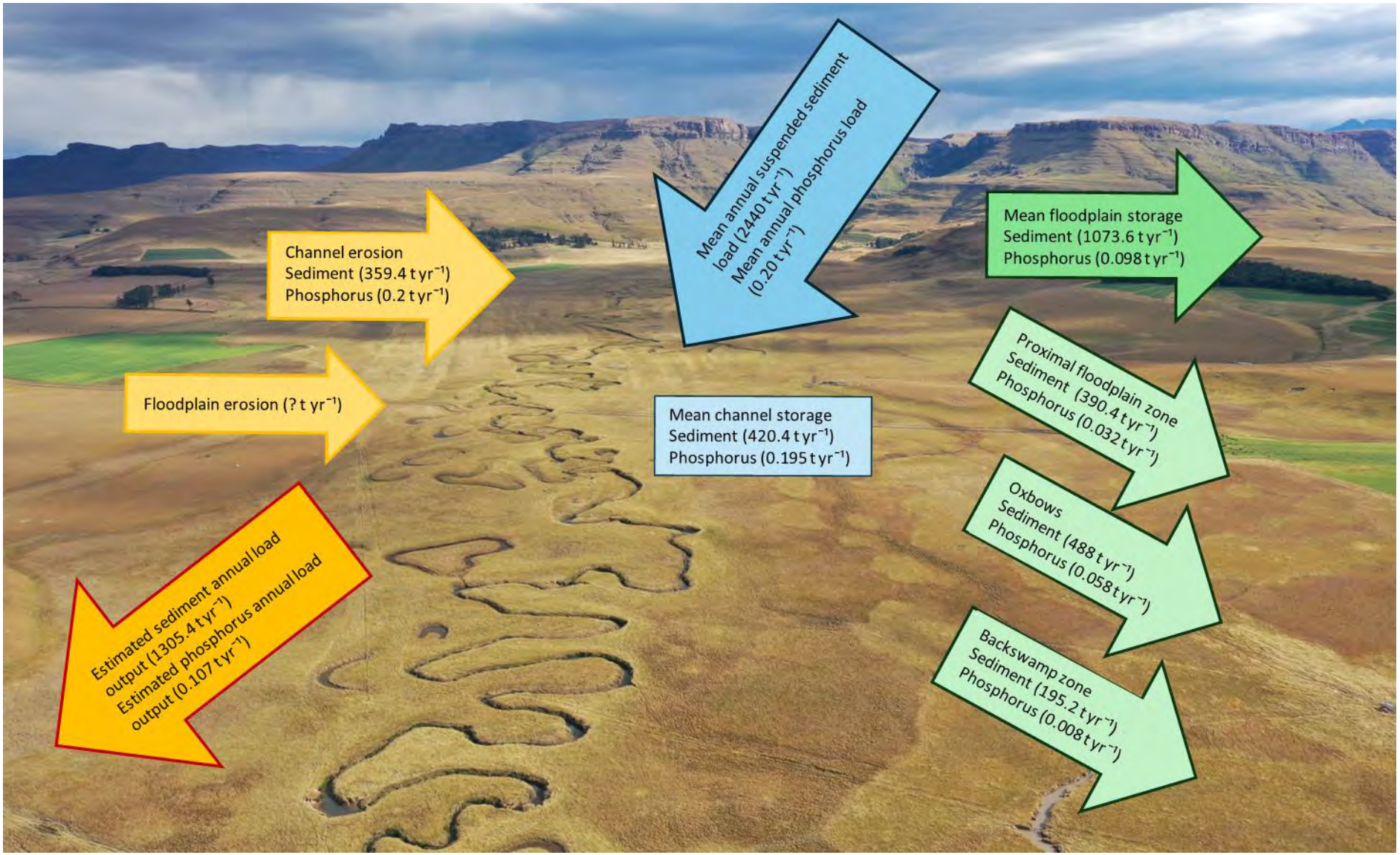

Figure 8.3 Sediment and total phosphorus mass balance estimates for the Minnehaha River floodplain

8.5 EROSION AND RECYCLING

While floodplains are predominantly formed through the accumulation of alluvial deposits, they are often subject to erosional forces that shape and modify their surface (Rhoads 2020). Channel erosion, although a natural and dynamic process integral to the migration of meandering rivers, significantly influences the sediment and sediment-associated nutrients and contaminants budget. River meander migration plays a key role in the unsteady "conveyor belt" of sediment redistribution from source to sink areas. This impact stems from the movement, sorting, and dispersion of sediment and sediment-associated nutrients, contaminants, and organic materials caused by channel and floodplain surface erosion. Like depositional processes, the efficiency of erosional processes varies spatially and depends on the type of river. Erosional processes have the potential to re-work deposited material on floodplain surfaces, thereby transforming it into a source of sediment, nutrients, and contaminants. Therefore, estimating floodplain sediment and nutrient retention should consider the net flux of both depositional and erosive processes.

The Gatberg and Minnehaha Rivers are both categorised as mixed-bed single-thread meandering rivers with the channel beds mostly consisting of the sand fraction and banks predominantly comprised of very fine to fine sand. Both channel beds and banks in both systems had < 10 % organic matter content (see Chapter 5). Field observations showed that bank erosion, collapse, and slumping occurred in both river systems during the wet seasons. Chapter 7 (objective 4) evaluated contemporary channel bank erosion and deposition, historical channel alterations, lateral migration rates, changes in channel geometry, and the potential for future channel adjustments using a combination of aerial and historical image analysis, fieldwork, and ArcGIS software.

The median volume of eroded material from the meander bends measured over the study period was low (3.4 m^3 for the Gatberg floodplain system and 2.3 m^3 for the Minnehaha floodplain system). These median values were extrapolated to the whole floodplain (520 t yr^{-1} for the Gatberg and 359 t yr^{-1} for the Minnehaha- see Chapter 7; Figure 8.2 and Figure 8.3). The greatest proportion of the eroded material was sand for both systems, suggesting that the eroded material comes from the channel banks and point bars. The median extrapolated volumetric estimates of total phosphorus were 0.3 t yr^{-1} for the Gatberg and 0.2 t yr^{-1} for the Minnehaha.

Historical satellite imagery was utilised to conduct a temporal analysis for both the Gatberg and Minnehaha River floodplain systems. The analysis of historical images for the Gatberg River floodplain system revealed three instances of meander bend cutoff events between 1958 and 1993, suggesting an inferred frequency of one event every nine years. Field observations conducted in 2022 identified one

meander bend in the process of being cut off. All three-meander bend cutoff events, along with the meander bend currently undergoing the process, took place between the two tributaries entering the system. Within the Minnehaha River floodplain system, a total of four meander bend cutoff events were identified along the length of the system between images from 1958 and 2015, indicating an average frequency of approximately one event per seven years. However, numerous meander bend cutoffs have occurred in the pre-1958 period, which is seen in the form of traces of oxbows on both floodplain systems. Meander bend cutoff events can have significant implications for sediment transport and storage within river systems: 1) meander cutoffs can create oxbows, which are often characterised by slower water velocities compared to the main river channel. As a result, sediment carried by the river water tends to settle out and accumulate within these abandoned channels, leading to sediment trapping; 2) after a meander cutoff event, the river's energy is concentrated in the new, shorter, and straighter channel. This increased energy can lead to greater erosion along the new channel's banks and bed, as well as downstream. Consequently, sediment that was previously stored in the abandoned meanders is re-mobilised and transported downstream, contributing to sediment recycling within the river system. Both floodplain systems were partitioned into four zones to delineate and compute alterations in river length and sinuosity indices between the historical river course and the present river course. In both floodplain systems, most zones exhibited a decrease in sinuosity from the historical river course to the current course, reflecting the occurrence of the few identified meander bend cutoff events within each zone. Meander cutoffs play a crucial role in river morphodynamics by elevating the local channel slope, reducing river sinuosity, and limiting floodplain access. They also significantly influence the sediment and phosphorus flux during the respective periods by reintroducing a substantial amount of sediment back into the river system.

The lateral migration rates were estimated by ^{14}Carbon geochronology from a nested oxbow sequence on the Gatberg River floodplain system. This data was supplied by de Villiers (2022). The two oxbows were in the upper section of the floodplain system. The abandonment of the oldest oxbow followed a meander bend cutoff approximately 3627 years before the present (BP), succeeded by another meander bend occurrence around 2830 BP. These meanders bend cutoff events have led to episodic channel migration, with an average lateral migration rate of approximately 0.03 meters per year. The rates of floodplain reworking in the Gatberg River floodplain, akin to other wetlands in South Africa, are notably lower than those in humid regions worldwide (Black et al. 2010; Keen-Zebert et al. 2011). Nevertheless, the Gatberg system compares well with migration rates observed in rivers within dryland regions (Owens 1998; Ellery et al. 2003; Grenfell 2007; Tooth et al. 2014; Larkin et al. 2017). The low estimated lateral migration rates

of the Gatberg River floodplain system could be due to a combination of very low slope, low stream power, low sediment supply and cohesive channel banks.

The river and oxbow morphological analysis revealed that the mean ratio of curvature to bankfull width values decreased from 2 for the oxbows, 2.1 for the channel in 1958, to 1.8 for the current channel in the Gatberg system. All the curvature to bankfull width ratios were below or close to the curvature to bankfull width values (between 2 and 3) that coincide with peak migration values as supported by many studies (e.g., Finotello et al. 2018; Hudson and Kesel 2000; Hooke 2003; Güneralp and Rhoads 2008; Nicoll and Hickin 2010), further indicating that channel migration on the Gatberg River floodplain occurs slowly. In contrast, the mean curvature to bankfull width ratios in the Minnehaha system was 3 for the oxbows, 2.2 for the meander bends in 1958, and 2.6 for the meander bends in 2015. These figures indicate a higher frequency of migration for the Minnehaha River floodplain system compared to the Gatberg floodplain system.

To assess the likelihood of future channel alterations within the Gatberg and Minnehaha River floodplain systems, two processes were examined by analysing the dimensions of the existing channel courses (see Chapter 7). Within the Gatberg floodplain systems, only one meander bend exhibited a high potential for future neck cutoff (< 1), whereas in the Minnehaha floodplain, no meander bends were identified with a high potential for neck cutoff. Visual evaluations identified 5 meander bends meeting chute cutoff stability criteria in the Gatberg floodplain and 20 in the Minnehaha floodplain.

Measuring river change is crucial for effective river management for several reasons: 1) to understand natural processes. Rivers are dynamic systems that undergo continuous changes in response to natural processes such as erosion, sediment transport, and channel migration. Measuring river change helps managers understand these natural processes and their impacts on river morphology, hydrology, and ecosystems; 2) to evaluate environmental impacts. River change can have significant environmental impacts, affecting aquatic habitats, biodiversity, water quality, and ecosystem services. Monitoring and measuring river change allow managers to assess these impacts and identify areas of concern where intervention may be necessary to mitigate negative effects on the environment; 3) assess floodplain inundation and flood risk. Changes in river morphology, such as channel widening, meander migration, or sediment accumulation, can affect the flow capacity of rivers and alter floodplain inundation frequency and flood risk levels. By monitoring river change, managers can assess changes in flood risk and implement appropriate measures to mitigate flood hazards; 4) optimise water resource management. Rivers are vital sources of freshwater for various human activities, including agriculture, industry, and municipal water

supply. Understanding river change is essential for optimising water resource management, including water allocation and hydropower generation. Measuring changes in river flow, sediment transport, and water quality provides valuable data for decision-making in water resource planning and management; 5) effective river management is crucial for promoting sustainable development that balances socio-economic development with environmental conservation. Measuring river processes helps ensure that development activities along rivers are conducted in a sustainable manner that minimises negative impacts on the environment while maximising socio-economic benefits.

Overall, understanding river and floodplain processes is fundamental for informed decision-making in river management, enabling managers to maintain the ecological integrity of river systems, reduce risks to human communities, and sustainably utilise water resources for the benefit of present and future generations.

8.6 CONCLUSION

Floodplains play a crucial role in providing essential ecosystem services to both local communities and those downstream by effectively retaining floodwaters, sediments, and associated nutrients. These areas exhibit a dynamic nature in which they can accumulate sediment and nutrients through deposition, while simultaneously exporting materials downstream through erosion. The provision of these ecosystem services is vulnerable through the loss of floodplain functioning brought on by land use change, climate change and degradation. By the assessment, quantification, and valuation of floodplain dynamics, we can start to predict the importance of functional floodplain systems on human well-being and provide information on trade-offs between development pressures and conservation goals to improve management and rehabilitation priorities.

Floodplain wetlands in dryland settings, including South Africa, are widespread and dynamic environments found along drainage lines. Floodplain wetlands are hot spots for ecosystem service provision and form critical areas of resilience and buffers against climate and anthropogenic changes. Globally and in South Africa there has been widespread wetland deterioration and exploitation, and this has driven large-scale investment into the conservation and rehabilitation of these systems (Ellery et al., 2009; Kotze et al., 2009; Dini and Bahadur 2018). In South Africa, this amounted to approximately R826.6 million from 2004 for the rehabilitation of about 1000 wetlands across the country (DFFE: Working for Wetlands Program n.d.). However, there is a lack of empirical data on how these systems naturally function, to what extent they provide ecosystem services, and whether season, climate, geomorphology, and humans affect these processes and to what extent. Current management and rehabilitation protocols

in South Africa for wetlands are mostly focused on surface hydrological and ecological principles based on the hydrogeomorphic classification system, with very little focus on process-based geomorphology evaluations, such as sediment dynamics (McCarthy et al. 2010; Grenfell et al. 2019; Grenfell et al. 2020). Understanding and quantifying the spatial and temporal variability, availability and composition of suspended sediment mass fluxes, phosphorus fluxes, and floodplain storage has significant implications for future management and rehabilitation programs for floodplain systems as well as supplying data for calibration of sediment and scenario models. This research, using two case studies, has generated a baseline knowledge and provides quantification and insights into the efficacy of the two floodplain systems in regulating downstream fluxes of suspended sediment and associated total phosphorus concentrations. The research has provided sedimentation and phosphorus accumulation rates for different floodplain geomorphic units, highlighting the spatial diversity and complexity of sediment and phosphorus storage within these systems.

Although sediment is a natural component of aquatic ecosystems, excess fine-grained sediment can cause many negative impacts on the health of these environments and impact local and downstream users. Understanding the potential catchment source assemblages and their relative connectivity to the river system is critical to understanding catchment use and impairment and where to target potential water quality improvement management practices (Novotny and Chesters 1989; Gellis et al. 2016). A complete understanding of sediment sources, movement, fate, and delivery, to tailor management measures in a way that would minimise downstream loading of sediment and its detrimental effects is required. Landscape connectivity in both the Gatberg and Minnehaha River catchments are naturally high due to the generally steep landscape, however, this has been increased due to anthropogenic land use changes. This means that the sediment and associated phosphorus that is mobilised throughout the catchments are more likely to be transported to the river, especially during high-intensity summer rainfall events that are a natural occurrence in this environment.

The results of the study make it clear that sediment and associated phosphorus dynamics in floodplain systems are complex and can change over both spatial and temporal scales. Floodplain system research requires the use of both desktop analysis and field observations and measurements to understand the processes that underpin the sediment dynamics and storage of these systems.

8.7 LIMITATIONS AND SOURCES OF ERROR

- COVID-19 lockdown and movement restriction had a huge effect on field investigations and the thesis in general. Field equipment could not be downloaded, checked and re-installed. Laboratory work could not be conducted.
- Time-integrated samplers were intended to be collected every month during the wet season; however, high flow conditions made it unsafe to do so and could have led to sediment loss during removal, potentially misrepresenting and underestimating data such as trapping efficiencies. Additionally, it was found that astroturf mats and small PVC samplers installed on the floodplain surface were unsuitable for sediment capturing in these systems as the PVC samplers captured little to no sediment and the astroturf mats were either eaten by livestock or burnt, limiting the representation of seasonal or monthly variations in sediment accumulation. Consequently, the study used sediment cores for a longer-term investigation into the sediment dynamics of these systems.
- The study field investigations were limited to two years, research over a longer period would give key trends and potentially a better indication of the natural range of variability.
- Due to time and funding constraints limited the number of cores investigated. Increasing the number of cores in each of the floodplains would increase the spatial resolution and give a better indication of the sedimentation and phosphorus rates of the different geomorphic features.
- Using sediment yield data from another catchment that is a different size, with a slightly different land use configuration (although scaled by area to my research sites) might introduce inaccuracies and uncertainties in the trapping efficiency values estimated for the study sites, especially as the method was sensitive to the input yield values.
- Erosion from the channel banks on straight sections was not conducted this may have introduced uncertainties in the estimation of the contributions of sediment and phosphorus from the channel bank. Time and funding constraints limited the assessment of the channel erosion to visual observations and desktop analysis rather than direct measurement.
- Maps and aerial photographs serve as representations of reality and are affected by factors such as scale, geometric transformations, and projections. Inaccuracies from photo and map representations and digitising could be significant.
- Rainfall measurement is only representative of the area measured by the rain gauge, thus upscaling a single point measurement to the catchment scale will introduce error.

- Sediment chronology introduced significant errors. The measurement error of laboratory equipment was in the range of 2-10 %. Using the data in models introduced a further error of 10-30 %. Dating-related errors could thus be high, which excludes the representativeness of the actual field sampling.

8.8 DIRECTION FOR FUTURE RESEARCH

Further research should focus on quantifying sediment and phosphorus storage in floodplain systems in other climatic zones as well as investigations in other types of wetlands in South Africa this would create a robust baseline database in which management and rehabilitation practices could make informed and nuanced policies and implementation strategies. Hydrological and vegetation monitoring in the two study sites would provide more in-depth knowledge of the spatial dynamics of sediment and phosphorus across the floodplain surface. Future research could attempt to establish the relationship between rainfall variability and sediment trapping over longer periods. Attempts to include the different forms of phosphorus (e.g. metal-bound phosphorus and organic phosphorus) would add valuable insights. This research only examined two of the water-quality improvement ecosystem services outlined by the MEA (2005), and further research could investigate a wider range of water-quality improvement scenarios to create a more holistic view of the ecosystem services that these floodplains provide. A larger number of geochronological cores will provide a better temporal and spatial resolution of the sediment dynamics in these systems. Long-term monitoring should be conducted to validate the conclusions that were drawn from this study.

CHAPTER 9 : REFERENCES

2022 Google images (© Maxar Technologies, Google Earth, 2021)

Aalto R, Dietrich WE. 2005. Sediment accumulation determined with Pb210 geochronology for Strickland River floodplains, Papua New Guinea. Sediment Budgets 1 (Proceedings of symposium S1 held during the Seventh IAHS Scientific Assembly at Foz do Iguaçu, Brazil, April 2005). IAHS Publ. 291

Aalto R, Lauer JW, Dietrich WE .2008. Spatial and temporal dynamics of sediment accumulation and exchange along Strickland River floodplains (Papua New Guinea) over decadal-to-centennial timescales. Journal Geophysical Research Earth Surfuce, 113 (1), 1–22. https:// doi. org/ 10. 1029/ 2006JF0006 27

Aalto R, Maurice-Bourgoin L, Dunne T, Montgomery DR, Nittrouer CA, Guyot JL. 2003. Episodic sediment accumulation on Amazonian floodplains influenced by El Niño/Southern Oscillation. Nature, 425, 493-497

Abam TKS. 1993. Bank Erosion and Protection in the Niger Delta. Hydrological Science Journal, 38, 231-241. https://doi.org/10.1080/02626669309492665

Abrams MM, Jarrell WM. 1995. Soil Phosphorus as a Potential Nonpoint Source for Elevated Stream Phosphorus Levels. Journal of Environmental Quality, 24 (1), 132-138. https://doi.org/10.2134/jeq1995.00472425002400010019x

Acreman M, Holden J. 2013. How Wetlands Affect Floods. Wetlands, 33, 773-786. https://doi.org/10.1007/s13157-013-0473-2

Agbenin JO, Tiessen H. 1995. Phosphorus Sorption at Field Capacity and Soil Ionic Strength: Kinetics and Transformation. Soil Science Society of America Journal, 59 (4), 998-1005. https://doi.org/10.2136/sssaj1995.03615995005900040006x

Agrometeorology Staff. 1984-2008. ARC-ISCW Agrometeorology Weather Station Network Data for South Africa, Unpublished. ARC-Institute for Soil, Climate and Water: Pretoria, South Africa

Airbus, USGS, NGA, NASA, CGIAR, NLS, OS, NMA Geodatastyrelsen, GSA, GSI and the GIS user community. Received on 19 July 2022

Alexander RB, Smith RA, Schwarz GE, et al. 2008. Differences in Phosphorus and Nitrogen Delivery to The Gulf of Mexico from the Mississippi River Basin. Environmental Science and Technology, 42 (3), 822-830. DOI: 10.1021/es0716103

Alexander RB, Smith RA, Schwarz GE. 2000. Effect of stream channel size on the delivery of nitrogen to the Gulf of Mexico. Nature, 403, 758-761. 10.1038/35001562

Allan RJ. 1986. The role of particulate matter in the fate of contaminants in aquatic ecosystems. Environment Canada, Inland Waters Directorate. Burlington,142

Allen JRL. 1965. A review of the origin and characteristics of recent alluvial sediments, Sedimentology, 5 (2), 89–191

Allison R, Walker TA, Chiew F, O'Neill I, McMahon T .1998. From roads to rivers: gross pollutant removal from urban waterways. Cooperative Research Centre for Catchment Hydrology, Clayton

Alvarez-Iglesias P, Quintana B, Rubio B, Perez-Arlucia M. 2007. Sedimentation rates and trace metal input history in intertidal sediments from San Simon Bay (Rıa de Vigo, NW Spain) derived from 210Pb and 137Cs chronology. Journal of Environmental Radioactivity, 98, 229-250. doi:10.1016/j.jenvrad.2007.05.001

Amoros C, Bornette G. 2002. Connectivity and Biocomplexity in Waterbodies of Riverine Floodplains. Freshwater Biology. 47 (4). 10.1046/j.1365-2427.2002.00905.x

Appleby, PG, Oldfield, F. 1978. The Calculation of Lead-210 Dates Assuming a Constant Rate of Supply of Unsupported 210Pb to the Sediment. Catena, 5, 1-8. https://doi.org/10.1016/S0341-8162(78)80002-2

Ashbridge D. 1995. Processes of river bank erosion and their contribution to the suspended sediment load of the River Culm, Devon. I. Foster, A. Gurnell, B. Webb (Eds.), Sediment and Water Quality in River Catchments, John Wiley and Sons, Chichester, 229-245

Asselmann NEM and Middelkoop H. 1995. Floodplain sedimentation. Quantities, patterns and processes. Earth Surface Processes and Landforms, 20, 481-489

Axt JR and Walbridge MR. 1999. Phosphate Removal Capacity of Palustrine Forested Wetlands and Adjacent Uplands in Virginia. Soil Science of America Journal, 63 (4), 1019-1031. https://doi.org/10.2136/sssaj1999.6341019x

Bagnold RA. 1960. Some Aspects of the Shape of River Meanders, U.S. Geological Survey Professional Paper 282-E

Baker VR. 1977. Stream channel response to floods, with examples from central Texas, Geological Society of America Bulletin, 88, 1057-1071

Ball DF. 1964. Loss-on-ignition as an estimate of organic matter and organic carbon in non-calcareous soils. European Journal of Soil Science, 15 (1), 84-92. https://doi.org/10.1111/j.1365-2389.1964.tb00247.x

Bannatyne LJ, Foster IDL, Rowntree KM, van der Waal BW. 2022. Suspended sediment load estimation in a severely eroded and data poor catchment. Hydrological processes, 36 (11), 1-19. https://doi.org/10.1002/hyp.14730

Barry WJ, Garlo AS, Wood CA. Duplicating the Mound-and-Pool Microtopography of Forested Wetlands. Ecological Restoration, June 1996, 14 (1), 15-21; DOI: https://doi.org/10.3368/er.14.1.15

Base F, Helmschrot H, Flugel. 2007. The impact of land use change on the hydrological dynamic of the semi-arid Tsitsa catchment in South Africa. Global Change Issues in Developing and Emerging Countries. Proceedings of the 2nd göttingen GIS and remote sensing days 2006, 4th to 6th October, Göttingen, Germany, 4, 257

Basher LR, Hicks DM, Clapp B, Hewitt T. 2011. Sediment yield response to large storm events and forest harvesting, Motueka River, New Zealand. New Zealand Journal of Marine and Freshwater Research, 45, 333-356. https://doi.org/10.1080/00288330.2011.570350

Bates HW .1962. The naturalist on the river Amazons. University of California Press, Berkeley

Bathurst JC, Sheffield J, Vicente C, White SM, Romano N. 2002. Modelling large basin hydrology and sediment yield with sparse data: the Agri basin, southern Italy. In Mediterranean Desertification: A Mosaic of Processes and Responses, Geeson NA, Brandt, CJ, Thornes JB (eds.), Wiley, Chichester, UK, 397-415

Bathurst JC, Thorne CR, Hey RD. 1977. Direct measurement of secondary currents. Nature, 269 (5628), 504-505

Batson J, Noe GB, Hupp CR, Krauss KW, Rybicki NB, Schenk ER. 2015. Soil greenhouse gas emissions and carbon budgeting in a short-hydroperiod floodplain wetland. Journal of Geophysical Research: Biogeosciences, 120 (1), 77-95

Battin TJ, Luyssaert S, Kaplan LA, et al. 2009. The boundless carbon cycle. Nature Geoscience, 2, 598-600. DOI: 10.1038/ngeo618

Beck H, Zimmermann N, McVicar T et al. 2018. Present and future Köppen-Geiger climate classification maps at 1-km resolution. Science Data 5, 180214. https://doi.org/10.1038/sdata.2018.214

Beckinsale RP, Richardson L. 1964. Recent findings on the physical development of the lower Severn valley. Geographical Journal, 130, 87-105

Bellmore JR, Baxter CV. 2014. Effects of geomorphic process domains on river ecosystems: a comparison of floodplain and confine valley segments. River research and applications, 30 (5), 617-630. https://doi.org/10.1002/rra.2672

Benjankar R and Yager EM. 2012. The impact of different sediment concentrations and sediment transport formulas on the simulated floodplain processes. Journal of Hydrology, 450, 230-243.

Benoit G and Rozan TF. 2001. 210Pb and 137Cs dating methods in lakes: A retrospective study. Journal of Paleolimnology, 25, 455–465. https://doi.org/10.1023/A:1011179318352

Beschta RL. 1978. Long-term patterns of sediment production following road construction and logging in the Oregon Coast Range. Water resources research, 14 (6), 1011-1016. https://doi.org/10.1029/WR014i006p01011

Biedenharn DS, Combs PG, Hill GJ, Pinkard CF, and Pinkston CB. 1989. Relationship Between Channel Migration and Radius of Curvature on the Red River. In Wang SY (ed.), Sediment Transport Modeling: Proceedings of the International Symposium, American Society of Civil Engineers, New York, 536–541

Biedenharn DS, Thorne CR, Watson CC. 2000. Recent morphological evolution of the Lower Mississippi River, Geomorphology, 34, 227–249, doi:10.1016/S0169-555X(00)00011-8

Bierman PR and Montgomery DR. 2014. Key Concepts in Geomorphology. New York: W.H. Freeman

Bilby RE, Sullivan K, Duncan SH. 1989. The generation and fate of road-surface sediment in forested watersheds in southeastern Washington. Forest Science, 35 (2), 453-468

Billen G, Lancelot C, Meybeck M .1991. N, P, and Si retention along the aquatic continuum from land to ocean. In: Mantoura RFC, Martin J-M, Wollast R (eds) Ocean margin processes in global change. Wiley, Chichester

Billi P, Fazzini M. 2017. Global change and river flow in Italy. Global and Planetary Change, 155, 234-246

Bilotta GS and Brazier RE. 2008. Understanding the influence of suspended solids on water quality and aquatic biota. Water Research, 42 (12), 2849–2861. Available from: https://doi.org/10.1016/j.watres.2008.03.018

Binford MW. 1993. Interpretation of 210Pb profiles and verification of the CRS dating model in PIRLA project lake sediment cores. Journal of Paleolimnology, 9, 275-296

Birkinshaw SJ, Bathurst JC, Iroume A, Palacios H. 2011. The effect of forest cover on peak flow and sediment discharge—An integrated field and modelling study in Central-Southern Chile. Hydrological Processes, 25 (8), 1284-1297. DOI: 10.1002/hyp.7900

Black EE, Renshaw C, Magilligan FJ et al. 2010. Determining lateral migration rates of meandering rivers using fallout radionuclides. Geomorphology, 123 (3-4), 364-396

Blackwell MS, Hogan DV, Maltby E .2002. Wetlands as regulators of pollutant transport. In: Haygarth PM, Jarvis SC (eds) Agriculture, hydrology, and water quality. CAB International, New York, 321–339

Bledsoe BP, Shear TH. 2000. Vegetation along hydrologic and edaphic gradients in a north Carolina coastal plain Creek Bootom and implications for restoration. Wetlands, 20 (1), 126-1447

Blignaut JN, Mander M, Schulze R, et al. 2010. Restoring and managing natural capital towards fostering economic development: Evidence from the Drakensberg, South Africa. Ecological Economics, 69 (6), 1313–1323

Bogen BP, Berg TH. 1994. Vegetation along hydrologic and edaphic gradients in a north Carolina coastal plain Creek Bootom and implications for restoration. Wetlands, 19 (1), 126-1447

Boldt KV, Lane P, Woodruff JD, Donnelly JP. 2010. Calibrating a sedimentary record of overwash from Southeastern New England using modeled historic hurricane surges. Marine Geology, 275, 127-139. doi:10.1016/j.margeo.2010.05.002

Booth DB. 1991. Urbanization and the natural drainage system–impacts, solutions, and prognoses. Northwest Environmental Journal, 7, 93-118. http://hdl.handle.net/1773/17032

Bordy EM, Hancox PJ, Rubidge BS. 2004. Fluvial style variations in the Late Triassic–Early Jurassic Elliot Formation, main Karoo Basin, South Africa. Journal of African Earth Sciences, 38, 383–400

Botha GA, Singh R. 2012. Geology, geohydrology and development potential zonation of the uThukela district municipality; specialist contribution towards the environmental management framework. Council for Geo-Science: Pietermaritzburg

Bowie AJ. 1982. Investigations of vegetation for stabilizing eroding streambanks. Transactions of American Society of Agricultural Engineers, 25, 1601-1606 and 1611

Bracken LJ, Croke J. 2007. The concept of hydrological connectivity and its contribution to understanding runoff-dominated geomorphic systems. Hydrological Processes, 21 (13), 1749-1763. https://doi.org/10.1002/hyp.6313

Bracken LJ, Turnbull L, Wainwright J, Bogaart P. 2015. Sediment connectivity: a framework for understanding sediment transfer at multiple scales Earth Surface Processes. Landforms, 40, 177-188. 10.1002/esp.3635

Bradley DN and Tucker GE. 2013. The storage time, age, and erosion hazard of laterally accreted sediment on the floodplain of a simulated meandering river. KGR Earth Surface, 118 (3), 1308-1319. https://doi.org/10.1002/jgrf.20083

Bridge JS and Jarvis J. 1976. Flow and sedimentary processes in the meandering river South Esk, Glen Clova, Scotland. Earth Surface Processes., 1, 303–336

Bridge JS, Alexander J, Collier REL, Cawthorpe RL, Jarvis J. 1995. Ground penetrating radar and coring used to study the large-scale structure of point bar deposits in 3 dimensions. Sedimentology, 42, 839–852

Bridge JS, Smith ND, Trent F, Gabel SL, Bernstein P. 1986. Sedimentology and morphology of a low-sinuosity river: Calamus River, Nebraska Sand Hills. Sedimentology, 33, 851–870

Bridge JS. 2003. Alluvial Rivers and Floodplains. Blackwell.

Bridge JS. 2003. Rivers and floodplains: forms, processes, and sedimentary record. John Wiley & Sons, Blackwell Science, Oxford

Bridge JS. 2009. Rivers and Floodplains: forms, processes, and sedimentary record. John Wiley & Sons. 1444311263, 9781444311266

Bridgham SD, Johnston CA, Schubauer-Berigan JP, Weishampel P .2001. Phosphorus sorption dynamics in soils and coupling with surface and pore water in riverine wetlands. Soil Science Society American Journal, 65, 577–588. https:// doi. org/10. 2136/ sssaj 2001. 65257 7x

Brierley GJ, Fryirs K, Cullum C, Tadaki M, Huang H Q, Blue B. 2013. Reading the landscape: Integrating the theory and practice of geomorphology to develop place-based understandings of river systems. Progress in Physical Geography: Earth and Environment, 37 (5), 601-621. https://doi.org/10.1177/0309133313490007

Brierley GJ, Fryirs K, Jain V. 2006. Landscape connectivity: the geographic basis of geomorphic applications. Area 38 (2), 165–174

Brierley GJ, Fryirs K. 1999. Tributary–trunk stream relations in a cut-and-fill landscape: a case study from Wolumla catchment, N.S.W., Australia. Geomorphology, 28, 61–73

Brierley GJ, Fryirs K. 2005. Geomorphology and River Management: Applications of the River Styles Framework. Blackwell Publishing: Oxford

Brierley GJ, Murn CP. 1997. European impacts on downstream sediment transfer and bank erosion in Cobargo catchment, New South Wales, Australia. Catena, 31(1-2), 119-136. https://doi.org/10.1016/S0341-8162(97)00025-8

Brierley GJ. 1996. Channel morphology and element assemblages: a constructivist approach to facies modelling. In Advances in fluvial dynamics and stratigraphy. Carling PA, Dawson MR (Eds.). Wiley Interscience, Chichester, 263-298

Brinson MM, Bradshaw HD, Kane ES. 1984. Nutrient Assimilative Capacity of an Alluvial Floodplain Swamp. Journal of Applied Ecology, 21(3), 1041–1057. https://doi.org/10.2307/2405066

Brinson MM, Hauer FR, Lee LC, Nutter WL, Rheinhardt RD, Smith RD, Whigham D (1995) Guidebook for application of hydrogeomorphic assessments to riverine wetlands. Technical Report TR-WRP-DE-11, Waterways Experiment Station, Army Corps of Engineers, Vicksburg

Brown AG, Toms P, Carey C, Rhodes E. 2013. Geomorphology of the Anthropocene: time-trangressive discontinuities of human-induced alluviation. Anthropocene, 1, 3–13

Brown AG. 1983. An analysis of overbank deposits of a flood at Blandford-Forum, Dorset, England. Revue de Geomorphologie Dynamique, 32, 95-99

Bruland GL, Richardson CJ. 2004. A spatially explicit investigation of phosphorus sorption and related soil properties in two riparian wetlands. Journal Environmental Quality, 33 (2), 785–794. https:// doi. org/ 10. 2134/ jeq20 04. 7850

Brunet RC and Astin KB. 2000. A 12-month sediment and nutrient budget in a floodplain reach of the River Adour, southwest France. Regulated Rivers: Research & Management, 16 (3), 267–277. Available from: https://doi.org/ 10.1002/(SICI)1099-1646(200005/06)16:3<267::AID-RRR584>3.0.CO;2-4

Brunet RC, and Astin KB. 1997. Spatio-temporal variations in sediment nutrient levels: the River Adour. Landscape Ecology, 12, 171–184

Brunet RC, Pinay G, Gazelle F, Roques L. 1994. Role of the floodplain and riparian zone in suspended matter and nitrogen retention in the Adour River, South-West France. Regulated Rivers: Research & Management, 9, 55–63

Brunsden D, Thornes JB. 1979. Landscape Sensitivity and Change. Transactions of the Institute of British Geographers, 4 (4), 463–484. https://doi.org/10.2307/622210

Bull LJ. 1997. Magnitude and variation in the contribution of bank erosion to the suspended sediment load of the River Severn, UK. Earth Surface Processes Landforms, 22, 1109–1123

Burkham DE. 1972. Channel changes of the Gila River in Safford Valley, Arizona 1846–1970 U.S. Geological Surveyor Professional Papers, 655-G, 24

Burrin PJ, Scaife RG. 1984. Aspects of Holocene valley sedimentation in Southern England. Proceedings of the Geologists' Association, 95, 81-96

Burrin PJ. 1985. Holocene alluviation in southeast England and some implications for palaeohydrological studies. Earth Surface Processes Landforms, 10, 257-271

Cabezas A, Angulo-Martinez M, González-Sanchis M, Jiménez JJ, Comin FA .2010. Spatial variability in floodplain sedimentation: the use of generalized linear mixed-effects models. Hydrology and Earth System Sciences, 7 (8), 1589–1619. https:// doi. org/ 10. 5194/ hess- 14- 1655- 2010,2010

Calmeyer T, Muruven L. 2015. Environmental impact assessment for the Imzimvubu water project. Department of Water and Sanitation

Cambray RS, Playford K, Lewis GNJ. 1985. Radioactive fallout in air and rain: results to the end of 1984. Atomic Energy Research Establishment Report No. AERE-R 11915

Cammeraat LH. 2002. A review of two strongly contrasting geomorphological systems within the context of scale. Earth surface processes and landforms. Special Issue: Process geomorphology commemorating the work of Professor PD Jungerius, 27 (11), 1201-1222. https://doi.org/10.1002/esp.421

Campo SH, Desloges JR .1994. Sediment yield conditioned by glaciation in a rural agricultural basin of southern Ontario, Canada. Physical Geography, 15, 495–515. https:// doi.org/ 10. 1080/ 02723 646. 1994. 10642 531

Camporeale C, Perucca E, Ridolfi L. 2008. Significance of cutoff in meandering river dynamics, Journal of Geophysical Research: Earth Surface, 113, F01001, doi:10.1029/2006JF000694

Carey WC. 1969. Formation of floodplain lands. Journal of Hydraulic Division America Association Civil Engineering, 95 (HY3), 981-994

Carling PA, Cao Z, Holland MJ, Ervine DA and Babaeyan-Koopaei K. 2002. Turbulent flow across a natural compound channel. Water resources research, 38(12), 6-1.

CDNGI Geospatial Portal. Accessed via http://www.cdngiportal.co.za/CDNGIPortal/

Citterio A, Piegay H. 2009. Overbank sedimentation rates in former channel lakes: characterization and control factors. Sedimentology: The journal of international association of sedimentologists, 56 (2), 461-482. https://doi.org/10.1111/j.1365-3091.2008.00979.x

Climatology Staff. 1978-2012. ARC-ISCW Agrometeorology Weather Station Network Data for South Africa, Unpublished. ARC-Institute for Soil, Climate and Water: Pretoria, South Africa

Cole JJ, Prairie YT, Caraco NF, et al. 2007. Plumbing the Global Carbon Cycle: Integrating Inland Waters into the Terrestrial Carbon Budget. Ecosystems, 10, 172–185. https://doi.org/10.1007/s10021-006-9013-8

Coleman JM. 1969. Brahmaputra River: channel processes and sedimentation. Sedimentary geology, 3 (2), 139–239. https:// doi. org/10. 1016/ 0037- 0738(69) 90010-4

Collins AL, Naden PS, Sear DA, Jones JI, Morrow FIDL, K. 2011. Sediment targets for informing river catchment management: international experience and prospects. Hydrological Processes, 25, 2112–2129. https:// doi. org/ 10. 1002/hyp. 7965

Collins AL, Walling DE, Leeks GJL. 1997. Source type ascription for fluvial suspended sediment based on a quantitative composite fingerprinting technique. Catena, 29, 1-27

Collins AL, Walling DE. 2004. Documenting catchment suspended sediment sources: problems, approaches and prospects. Progress in Physical Geography, 28, 159–196

Collins AL, Walling DE. 2007. Sources of Fine Sediment Recovered From the Channel Bed of Lowland Groundwater Fed Catchments in the UK. Geomorphology, 88 (1-2), 120-138. 10.1016/j.geomorph.2006.10.018

Collins AL, Zhang Y, McChesney D, Walling DE, Haley SM, Smith P. 2012. Sediment source tracing in a lowland agricultural catchment in southern England using a modified procedure combining statistical analysis and numerical modelling. Science of the Total Environment, 414, 301-317. 10.1016/j.scitotenv.2011.10.062

Collins MG, Steiner FR, Rushman MJ. 2001. Land-use suitability analysis in the United States: historical development and promising technological achievements. Environmental Management, 28 (5), 611-621

Conner WH and Day JW. 1982. The ecology of forested wetlands in the southeastern United States. In Wetlands: Ecology and Management, eds. B. Gopal, et al. (Jaipur, India: National Institute of Ecology and International Scientific Publications), 69–87

Constantine JA, McLean SR, Dunne T. 2010. A mechanism of chute cutoff along large meandering rivers with uniform floodplain topography. Geological Society of America Bulletin, 122 (5-6), 855-869.

Cooper JR, Gilliam JW. 1987. Phosphorus Redistribution from Cultivated Fields into Riparian Areas. Soil Science Society of America Journal, 51 (6), 1600-1604. https://doi.org/10.2136/sssaj1987.03615995005100060035x

Costa JE. 1975. Effects of agriculture on erosion and sedimentation in the Piedmont Province, Maryland. Geological Society of America Bulletin, 86, 1281-1286

Costanza R, D'Arge R, De Groot R, Farber S, Grasso M, Hannon B, Limburg K, Naeem S, O'Neill RV, Paruelo J, Raskin RG, Suttom P, van den Belt M. 1997. The value of the world's ecosystem services and natural capital. Nature, 387, 253–260. https:// doi. org/ 10. 1038/ 38725 3a0

Council of Geoscience. 2019. South Africa 1:50 000 Geological Maps. Available from https://maps.geoscience.org.za/portal/apps/sites/#3. Accessed in 2021

Couper P, Stott TIM, Maddock IAN. 2002. Insights into river bank erosion processes derived from analysis of negative erosion-pin recordings: observations from three recent UK studies. Earth surface processes and landforms: the journal of the British Geomorphological Research Group, 79, 59–79

Couper P. 2003. Effects of silt–clay content on the susceptibility of river banks to subaerial erosion. Geomorphology, 56, 95–108

Courtwright J, Findley S. 2011. Effects of Microtopography on Hydrology, Physicochemistry, and Vegetation in a Tidal Swamp of the Hudson River. Wetlands, 31, 239-249

Craft CB, Casey WP. 2000. Sediment and nutrient accumulation in floodplain and depressional freshwater wetlands of Georgia, USA. Wetlands, 20, 323–332. https:// doi. org/10. 1672/ 0277- 5212(2000) 020[0323: SANAIF] 2.0. CO;2

Craft CB, Vymazal J, Kröpfelová L. 2017. Carbon sequestration and nutrient accumulation in floodplain and depressional wetlands. Ecological Engineering, 114, 137–145. https:// doi. org/10. 1016/j. ecole ng. 2017. 06. 034

Croke JC, Hairsine P, Fogarty P. 1999. Runoff generation and re-distribution in logged eucalyptus forests, south-eastern Australia. Journal of Hydrology, 216 (1-2), 56-77. https://doi.org/10.1016/S0022-1694(98)00288-1

Croke JC, Hairsine PB. 2006. Sediment delivery in managed forests: a review. Environmental Reviews, 14, 59–87

Croke JC, Nanson GC. 2002. Emerging issues in floodplain research. The Structure, Function and Management Implications of Fluvial Sedimentary Systems (Proceedings of an international symposium held al Alice Springs. Australia. September 2002). IAHS Publ. no. 276

Crosato A. 2009. Physical explanations of variations in river meander migration rates from model comparison. Earth Surface Processes and Landforms, 34 (15), 2078-2086

Crosby BT, Whipple KX. 2006. Knickpoint initiation and distribution within fluvial networks: 236 waterfalls in the Waipaoa River, North Island, New Zealand. Geomorphology, 82 (1-2), 16-38. https://doi.org/10.1016/j.geomorph.2005.08.023

Dada R, Kotze D, Ellery W, Uys M. 2007. WET-RoadMap: A guide to the Wetland. Management Series. WRC report TT321/07. Pretoria, South Africa

Daggupati P, Sheshukov AY, Douglas-Mankin KR. 2014. Evaluating ephemeral gullies with a process-based topographic index model Catena, 113, 177-186

Daly ER, Fox GA, Al-Madhhachi AST. Storm DE. 2015. Variability of fluvial erodibility parameters for streambanks on a watershed scale. Geomorphology, 231, 281-291

Daly ER, Fox GA, Enlow HK, Storm DE, Hunt SL. 2015. Site-scale variability of streambank fluvial erodibility parameters as measured with a jet erosion test. Hydrological processes, 29 (26), 5451-5464

Davidson GR, Carnley M, Lange T, Galicki SJ, Douglas A. 2004. Changes in sediment accumulation rate in an oxbow lake following late 19th century clearing of land for agricultural use: A 210 Pb, 137 Cs, AND 14 C study in Mississippi, USA. Proceedings of the 18th International Radiocarbon Conference, edited by N Beavan Athfield and R J Sparks. RADIOCARBON, 46 (2), 755–764

Day G, Dietrich WE, Rowland JC, Marshall A. 2008. The depositional web on the floodplain of the Fly River, Papua New Guinea. Journal of Geophysical Research: Earth Surface, 113, 1–19. https:// doi.org/ 10. 1029/ 2006J F0006 22

Day LD, Collins ME, Washer NE. 1987. Landscape position and particle-size effects on soil phosphorus distributions. Soil Science Society of America Journal, 51, 1547-155

De Decker R. 1981. Geology of the Kokstad area (sheet 3028), Geological survey, Government Printer, Pretoria

De Groot R, Brander L, Van Der Ploeg S, Constanza R, Bernard F, Braat L, Christie M, Crossman N, Ghermandi A, Hein L, Hussain S, Kumar P, McVittie A, Portela R, Rodriguez LC, Ten Brink P, van Beukering P. 2012. Global estimates of the value of ecosystems and their services in monetary units. Ecosystem services, 1, 50–61. https://doi. org/ 10. 1016/j. ecoser. 2012. 07. 005

Dellwig O, Schnetger B, Meyer D, Pollehne F, Häusler K and Arz HW. 2018. Impact of the major Baltic inflow in 2014 on manganese cycling in the Gotland Deep (Baltic Sea). Frontiers in Marine Science, 5, 248

De Rose RC, Basher LR. 2011. Measurement of river bank and cliff erosion from sequential LIDAR and historical aerial photography. Geomorphology, 126, 132–147

De Rose RC, Wilson DJ, Bartley R, Wilkinson SN. 2005. Riverbank erosion and its importance to uncertainties in large scale sediment budgets. In: Walling DE, Horowitz JA (eds) Proceedings of the international symposium on sediment budgets (S1) held during the seventh scientific assembly of the IAHS at Foz do Iguacu, Brazil, 3–9 April 2005, Sediment Budgets 1, IAHS Publ., 291, IAHS Press, 85–92

de Villiers S, Thiart C. 2007. The nutrient status of South African rivers: concentrations, trends and fluxes from the 1970s to 2005. South African Journal of Science, 103 (7–8), 343–349

de Villiers ZO. 2022. Vertical accretion and sediment storage in oxbows and meander cut-offs on the Gatberg River Floodplain, Eastern Cape, South Africa. MA thesis, Geography and Environmental Studies in the Faculty of Arts and Social Sciences at Stellenbosch University

Debano LF, Schmidt LJ. 1989. Interrelationship between watershed condition and health of riparian areas in south-western United States, In Creswell, R.E., Barton, B.A. and Kershner, J.L. (eds), Practical Approaches to Riparian Resource Management: An Educational Workshop, Billings, Montana, 45-52

DeLaune RD, Patrick W, Buresh R. 1978. Sedimentation rates determined by 137Cs dating in a rapidly accreting salt marsh. Nature, 275, 532–533. https://doi.org/10.1038/275532a0

DeLaune RD, Whitcomb JH, Patrick WH, Pardue JH, Pezeshki SR. 1989. Accretion and Canal Impacts in a Rapidly Subsiding Wetland. I. 137 Cs and 210 Pb Techniques. Estuaries, 12 (4), 247–259. https://doi.org/10.2307/1351904

Department of Agriculture, Forestry and Fisheries. Forestry 2030 Roadmap: Forestry Strategy 2009-2030)

Department of Forestry, Fisheries and the Environment. 2007. Eastern Cape Forestry Sector Profile. Available at https://www.dffe.gov.za/sites/default/files/reports/easterncape_forestrysectorprofile.pdf

Department of Water and Sanitation: Verified flow data website. Available at https://www.dws.gov.za/Hydrology/Verified/hymain.aspx. Accessed 2021

DFFE. 2020. South Africa National Land Cover. Available from https://egis.environment.gov.za/data_egis/data_download/current. Accessed on 2021

Dieras PL, Constantine JA, Hales TC, Piegay H, Riguier J. 2013. The role of oxbow lakes in the off-channel storage of bed material along the Ain River, France. Geomorphology, 188, 110-119. https://doi.org/10.1016/j.geomorph.2012.12.024

Dietrich WE and Smith JD. 1983. Influence of the point bar on flow through curved channels. Water Resources Research, 19, 1173–1192

Dietrich WE and Smith JD. 1984. Bed Load Transport in a River Meander. Water Resources Research, 20, 1355–1380

Dijkshoorn JA, van Engelen VWP and Huting JRM 2008. Soil and landform properties for LADA partner countries (Argentina, China, Cuba, Senegal and The Gambia, South Africa and Tunisia). ISRIC report 2008/06 and GLADA report 2008/03, ISRIC – World Soil Information and FAO, Wageningen

Dini JA, and Bahadur U. 2018. South Africa's National Wetland Rehabilitation Programme: Working for Wetlands. In: Finlayson CM, Everard M, Irvine K, McInnes R, Middleton B, van Dam A, and Davidson NC (Eds.) The Wetland Book. Dordrecht: Springer, 691–697 https://doi.org/10.1007/978-90-481-9659-3_145

Doble R, Simmons C, Jolly I, Walker G. 2006. Spatial relationships between vegetation cover and irrigation-induced groundwater discharge on a semi-arid floodplain, Australia. Journal of Hydrology, 329, 75-97. doi:10.1016/j.jhydrol.2006.02.007

Dollar ESJ, Rowntree KM. 1995. Hydroclimatic trends, sediment sources and geomorphic response in the Bell River Catchment, Eastern Cape, Drakensberg, South Africa

Donkin M.J. 1991. Loss-on-ignition as an estimator of soil organic carbon in A-horizons of forestry soils. Communications in Soil Science and Plant Analysis, 22, 233–241

Downing JA, Polasky S, Olmstead SM and Newbold SC. 2021. Protecting local water quality has global benefits. Nature communications, 12(1), 2709., 2709. https://doi.org/10.1038/s41467-021-22836-3

Downs P, Gregory K. 2014. River Channel Management: Towards Sustainable Catchment Hydrosystems. Routledge. 113817341X, 9781138173415

Drago EC. 1990. Geomorphology of large alluvial rivers: Lower Paraguay and Middle Paraná. Interciencia 15, 378-387

Driver A., Sink, K.J., Nel, J.N., Holness, S., Van Niekerk, L., Daniels, F., Jonas, Z., Majiedt, P.A., Harris, L. & Maze, K. 2012. National Biodiversity Assessment 2011: An assessment of South Africa's biodiversity and ecosystems. Synthesis Report. South African National Biodiversity Institute and Department of Environmental Affairs, Pretoria.

Drouin A, Saint-Laurent D, Lavoie L, Ouellet C. 2011. High-precision elevation model to evaluate the spatial distribution of soil organic carbon in active floodplains. Wetlands, 31 (6), 1151-1164

Dunne T, Aalto RE. 2013. 9.32 Large River Floodplains. In Treatise on Geomorphology. UC Santa Barbara. http://dx.doi.org/10.1016/b978-0-12-374739-6.00258-x Retrieved from https://escholarship.org/uc/item/0jq4h4ww

Elder JF. 1985. Nitrogen and phosphorus speciation and flux in a large Florida river-wetland system. Water Resource Research, 21, 724–732

Ellery WN, Dahlberg AC, Strydom R, Neal MJ, Jackson J. 2003. Diversion of water flow from a floodplain wetland stream: an analysis of geomorphological setting and hydrological and ecological consequences. Journal of Environmental Management, 68, 51-71

Ellery WN, Grenfell MC, Grenfell S, Kotze D, McCarthy TS, Tooth S, et al. 2009. WET-origins: controls on the distribution and dynamics of wetlands in South Africa. Rep TT 334/09. Pretoria: Water Research Commission.

Ellery WN, Grenfell SE, Grenfell MC, Humphries MS, Barnes K, Dahlberg A, et al. 2012. Peat formation in the context of the development of the Mkuze floodplain on the coastal plain of Maputaland, South Africa. Geomorphology, 141, 11–20. doi: 10.1016/j.geomorph.2011.11.009

Ellery WN, Grenfell SE, Grenfell MC, Powell R, Kotze D, Marren P, Knight J. 2016. Wetlands in southern Africa, in: Knight, J., Grab, S. (Eds.), Quaternary Environmental Change in Southern Africa: Physical and Human Dimensions. Cambridge University Press, Cambridge, 188–202.

Engstrom DR, Almendinger JE, Wolin JA. 2009. Historical changes in sediment and phosphorus loading to the upper Mississippi River: mass-balance reconstructions from the sediments of Lake Pepin. Journal of Paleolimnology, 41, 563–588. https://doi.org/10.1007/s10933-008-9292-5

Environment and Rural Solutions (ERS). 2011. Umzimvubu Catchment Overview. Matatiele: Environment and Rural Solutions

Erskine W, McFadden C, Bishop, P. 1992. Alluvial cutoffs as indicators of former channel conditions. Earth Surface Processes & Landforms, 17 (1), 23-37

Erskine WD, Livingstone EA. 1999. In-channel benches: the role of floods in their formation and destruction on bedrock-confined rivers. In: Varieties of Fluvial Forms (ed. by A. Miller & A. Gupta), 445–475. Wiley, Chichester, UK

Erskine WD, Warner RF. 1988. Geomorphic effects of alternating flood- and drought-dominated regimes on N.S.W. coastal rivers. In: R.F. Warner (Ed), Fluvial Geomorphology of Australia. Academic Press, Sydney, 223-242

Evans DJA, Phillips ER, Hiemstra JF, et al. 2006. Subglacial till: Formation, sedimentary characteristics and classification. Earth-Science Reviews, 78, 115–176

Eybergen FA, !meson AC. 1989. Geomorphological processes and climatic change, Catena, 16, 307-319

Fabricius KE, Logan M, Weeks SJ, Lewis SE, Brodie J. 2016. Changes in water clarity in response to river discharges on the Great Barrier Reef continental shelf: 2002–2013. Estuarine, Coastal and Shelf Science, 173, 1-15. https://doi.org/10.1016/j.ecss.2016.03.001

Farraj A, Harvey AM. 2010. Influence of hillslope-to-channel and tributary-junction coupling on channel morphology and sediments: Bowderdale Beck, Howgill Fells, NW England. Zeitschrift für Geomorphologie, 54 (2), 203-224. 10.1127/0372-8854/2010/0054-0018

Fávaro DIT, Damatto SR, Moreira EG, Mazzilli BP, Campagnoli F. 2007. Chemical characterization and recent sedimentation rates in sediment cores from Rio Grande reservoir, SP, Brazil. Journal of Radioanalytical and Nuclear Chemistry, 273 (2), 451–463. 10.1007/s10967-007-6855-2

Ferguson R. 1987. Hydraulic and sedimentary controls of channel pattern, in Richards, K. (Ed.), River Channels, Environment and Process, Basil Blackwell, Oxford, 129-158

Fey M. 2010. Soils of South Africa. Cambridge University Press, Cape Town, South Africa. ISBN 978-1-107-00050-6

Finotello A, Lanzoni S, Ghinassi M, Marani M, Rinaldo A, D'Alpaos A. 2018. Field migration rates of tidal meanders recapitulate fluvial morphodynamics. Proceedings of the National Academy of Sciences, 115 (7), 1463–1468. https://doi.org/10.1073/pnas.1711330115

Fisher J and Acreman MC. 2004. Wetland nutrient removal: a review of the evidence. Hydrology and Earth System Sciences, 8 (4), 673–685. Available from: https://doi.org/10.5194/hess-8-673-2004

Fisk HN, Mabrey PR, Steinriede JWB, Osanik A, Turnbull WJ. 1949. Geological Investigation of Mississippi River Acitivity: Memphis, Tennessee, to Mouth of Arkansas River, U.S. Army Corp of Engineers Technical Memorandum (USACE), Vickburg, Miss

Fisk HN. 1944. Geological Investigation of the Alluvial Valley of the Lower Mississippi River, U.S. Army Corps of Engineers, Mississippi River Commission, Vicksburg, Mississippi

Fisk HN. 1947. Fine Grained Alluvial Deposits and Their Effects on the Mississippi River Activity, U.S. Army Corps of Engineers Waterways Experiment Station, Vicksburg, Mississippi

Foster IDL, Boardman J, Keay-Bright J, Meadows ME. 2005. Land degradation and sediment dynamics in the South African Karoo. Sediment Budgets 2 (Proceedings of symposium S1 held during the Seventh IAHS Scientific Assembly at Foz do Iguaçu, Brazil, April 2005). IAHS Publ., 292

Foster IDL, Lees JA, Jones AR, Chapman AS, Turner SE, Hodgkinson RM. 2002. The possible role of agricultural land drains in sediment delivery to a small reservoir, Worcestershire. U.K.: a multiparameter fingerprint study. IAHS Publication (Proceedings of the Alice Springs Symposium. Sept. 2002) 276, 433–442

Foster IDL. 1986. Rivers: Form and Process. Geological Association, 71 (1), 89-90

Foster IDL; Boardman J; Keay-Bright J. 2007. Sediment tracing and environmental history for two small catchments, Karoo Uplands, South Africa. Geomorphology, 90 (1-2), 126-143

Fox GA, Purvis RA, Penn CJ. 2016. Streambanks: A net source of sediment and phosphorus to streams and rivers. Journal of environmental management, 181, 602-614

Fox GA, Wilson GV, Periketi RK, Cullum RF. 2006. Sediment Transport Model for Seepage Erosion of Streambank Sediment. Publications from USDA-ARS / UNL Faculty. 475. https://digitalcommons.unl.edu/usdaarsfacpub/475

Fox GA, Wilson GV. 2010. The role of subsurface flow in hillslope and streambank erosion: A review. Soil Science Society of America Journal, 74 (3), 717-733

Fraser LH, Bradford ME, Steer DN. 2003. Global supply of freshwater: the role of treatment wetlands. International Journal of Environment and Sustainable Development, 2 (2), 174-183

Frickel DG, Shown LM, Patton PC. 1975. An evaluation of hillslope and channel erosion related to oil-shale development in the Piceance basin, northwestern Colorado (No. 30). Department of Natural Resources

Frings RM. 2008. Downstream fining in large sand-bed rivers. Earth-Science Reviews, 87 (1-2), 39-60

Froehlich W, Walling DE. 2006. The use of 137Cs and 210Pbex to investigate sediment sources and overbank sedimentation rates in the Teesta River basin, Sikkim Himalaya, India. Sediment Dynamics and the Hydromorphology of Fluvial Systems (Proceedings of a symposium held in Dundee, UK, July 2006). IAHS Publ., 306, 380–388

Fryirs K, Brierley GJ, Preston NJ, Kasai M. 2007. Buffers, barriers and blankets: the (dis)connectivity of catchment-scale sediment cascades. Catena, 70 (1), 49–67

Fryirs K, Brierley GJ, Preston NJ. Spencer J. 2007. Catchmentscale (dis) connectivity in sediment flux in the upper Hunter catchment, New South Wales Australia. Geomorphology, 84 (3–4), 297–316. Available from: https://doi.org/10.1016/j.geomorph.2006.01.044

Fryirs K, Brierley GJ. 1999. Slope–channel decoupling in Wolumla catchment, New South Wales, Australia: the changing nature of sediment sources following European settlement. Catena, 35 (1), 41-63

Fryirs K, Brierley GJ. 2013. Geomorphic Analysis of River Systems: An approach to reading the landscape. 1st ed. Fryirs KA and Brierley GJ (eds). Blackwell Publishing Ltd: United Kingdom

Fryirs K, Gore D. 2013. Sediment tracing in the upper Hunter catchment using elemental and mineralogical compositions: Implications for catchment-scale suspended sediment (dis) connectivity and management. Geomorphology, 193, 112-121

Fuller IC, Large ARG, Milan DJ. 2003. Quantifying channel development and sediment transfer following chute cutoff in a wandering gravel-bed river, Geomorphology, 54, 307–323. doi:10.1016/S0169-555X(02)00374-4

Gabler RE, Petersen JF, Trapasso LM. 2007. Essentials of Physical Geography: Eighth Edition. Thomson Brooks/Cole, Canada, 491

Gautier E, Brunstein D, Vauchel P, Roulet M, Fuertes O, Guyot J, Darozzes J, Bourrel L. 2007. Temporal relations between meander deformation, water discharge and sediment fluxes in the floodplain of the Rio Beni (Bolivian Amazonia). Earth Surface Processes and Landforms, 32, 230–248

Gell P, Bulpin S, Wallbrink P, Hancock G, Bickford S. 2005. Tareena Billabong–a palaeolimnological history of an ever-changing wetland, Chowilla Floodplain, lower Murray–Darling Basin, Australia. Marine and Freshwater Research, 56 (4), 441-456

Gell P, Fluin J, Tibby J, Haynes D, Khanum S, Walsh B, Hancock G, Harrison J, Zawecki A, Little F. 2006. Changing fluxes of sediments and salts as recorded in lower River Murray wetlands, Australia. In: Rowan J, Duck R, Werrity A (eds) Proceedings of the IAHS conference, International Association of Hydrological Sciences, Dundee, UK, July 2006, 306, 416–424

Gell P, Little F. 2006. Water quality history of Murrumbidgee River floodplain wetlands. Wagga Wagga: Murrumbidgee Catchment Management Authority

Gellis AC, Fitzpatrick FA, and Schubauer-Berigan J. 2016. A manual to identify sources of fluvial sediment (EPA/600/R-16/210). Washington, DC: EPA. Retrieved from http://pubs.er.usgs.gov/publication/70182516.

Giardino JR, Lee AA. 2011. Rates of Channel Migration on the Brazos River. Final Report. Texas Water Development Board

Gillespie JL, Noe GB, Hupp CR, Gellis AC, Schenk ER. 2018. Floodplain trapping and cycling compared to streambank erosion of sediment and nutrients in an agricultural watershed. JAWRA, 54 (2), 565–582. https:// doi. org/ 10.1111/ 1752- 1688. 12624

Goldberg ED, Griffin JJ. 1964. Sedimentation rates and mineralogy in the South Atlantic. Journal of Geophysical Research, 69 (20), 4293-4309

Goldrick G, Bishop P. 1995. Differentiating the roles of lithology and uplift in the steepening of bedrock river long profiles: an example from southeastern Australia. The Journal of Geology, 103 (2), 227-231

Golosov V and Walling DE. 2014. Using fallout radionuclides to investigate recent overbank sedimentation rates on river floodplains: an overview. Proceedings of the International Association of Hydrological Sciences, 367, 228-234

Gomez B, Eden DN, Hicks DM, Trustrum NA, Peacock DH and Wilmshurst JM. 1999. Contribution of floodplain sequestration to the sediment budget of the Waipaoa River, New Zealand, Special Publication in Geological Society, London, 163, 69 – 88

Goodbred S, Kuehl S. 1998. Floodplain processes in the Bengal Basin and the storage of Ganges-Brahmaputra river sediment: an accretion study using 137Cs and 210Pb geochronology. Sedimentary Geology, 121 (3–4), 239–258. https:// doi. org/ 10. 1016/ S0037- 0738(98) 00082-7

Goodwell AE, Zhu Z, Dutta D, Greenberg JA, Kumar P, Garcia MH, Rhoads BL, Holmes RR, Parker G, Berretta DP, Jacobson RB. 2014. Assessment of floodplain vulnerability during extreme Mississippi River flood 2011. Environmental science & technology, 48 (5), 2619-2625

Gordon AK, Niedballa J, Palmer G. 2013. Sediment as a Physical Water Quality Stressor on Macro-invertebrates: A Contribution to the Development of a Water Quality Guideline for Suspended Solids. Water Research Commission Report no. 2040/1/13, Pretoria

Gordon ND, McMahon TA, Finlayson BL, Gippel CJ, Nathan RJ. 2004. Stream hydrology: an introduction for ecologists. John Wiley and Sons

Graf-Rosenfellner M, Cierjacks A, Kleinschmit B, Lang F. 2016. Soil formation and its implications for stabilization of soil organic matter in the riparian zone. Catena, 139, 9-18

Grams PE, Wilcock PR. 2007. Equilibrium entrainment of fine sediment over a coarse immobile bed. Water Resources Research, 43 (10)

Granger B, Laval B, Vagle S, Petticrew EL, Owens PN, Baldwin SA. 2022. Initial Distribution and Interannual Decrease of Suspended Sediment in a Two-Basin Lake Following a Massive Mine Tailings Spill: Quesnel Lake, BC, Canada. Water Resources Research, 58 (5). p.e2021WR030574

Grayson RB, Haydon SR, Jayasuriya MDA, Finlayson BL. 1993. Water quality in mountain ash forests—separating the impacts of roads from those of logging operations. Journal of hydrology, 150 (2-4), 459-480

Grenfell MC. 2007. The origin and evolution of two wetland systems in the KwaZulu-Natal Drakensberg foothills: implications for rehabilitation. MSc Thesis, University of KwaZulu-Natal, Durban

Grenfell SE, Ellery WN, Grenfell MC. 2009. Geomorphology and dynamics of the Mfolozi River floodplain, KwaZulu-Natal, South Africa. Geomorphology, 107 (3-4), 226-240

Grenfell SE, Ellery WN. 2009. Hydrology, sediment transport dynamics and geomorphology of a variable flow river: the Mfolozi River, South Africa. Water SA, 35 (3), 270-282

Grenfell SE, Ellery WN, Grenfell MC, Ramsay LF and Fluegel TJ. 2010. Sedimentary facies and geomorphic evolution of a blocked - valley lake: Lake Futululu, northern Kwazulu - Natal, South Africa. Sedimentology, 57(5), 1159-1174

Grenfell SE, Grenfell MC, Ellery WN, Job N, Walters D. 2019. A genetic geomorphic classification system for southern African palustrine wetlands: global implications for the management of wetlands in drylands. Frontiers in Environmental Science, 7

Grenfell SE, Grenfell MC, Tooth S, Mehl A, O'Gorman E, Ralph T, Ellery WN. 2022. Wetlands in drylands: diverse perspectives for dynamic landscapes. Wetlands Ecology and Management, 30, 607–622

Gretener B, Strömquist L. 1987. Overbank sedimentation rates of fine-grained sediments. A study of the recent deposition in the lower River Fyrisan. Geografiska Annaler: Series A, Physical Geography, 69A (1), 139-146

Grizzetti B, Bouraoui F, Billen G, van Grinsven H, Cardoso AC, Thieu V, Garnier J, Curtis C, Howarth RW, Johnes P. 2011. Nitrogen as a threat to European water quality

Güneralp İ, and Rhoads BL. 2008. Continuous characterization of the planform geometry and curvature of meandering rivers: Planform geometry and curvature of meandering rivers. Geographical Analysis, 40, 1–25. https://doi.org/10.1111/j.0016-7363.2007.00711.x

Gurnell AM. 1997. Channel change on the River Dee meanders, 1946–1992, from the analysis of air photographs. Regulated Rivers: Research & Management: An International Journal Devoted to River Research and Management, 13 (1), 13-26

Gwapedza D, Nyamela N, Hughes DA, Slaughter AR, Mantel SK, van der Waal B. 2021. Prediction of sediment yield of the Inxu River catchment (South Africa) using the MUSLE. International Soil and Water Conservation Research, 9 (1), 37-48

Gwapedza D. 2020. The further development, application and evaluation of a sediment yield model (WQSED) for catchment management in African catchments. PhD Thesis. Rhodes University, South Africa

Hamilton SK, Lewis Jr, WM. 1987. Causes of seasonality in the chemistry of a lake on the Orinoco River floodplain, Venezuela 1. Limnology and Oceanography, 32 (6), 1277-1290

Handbook of Standard Soil Testing Methods for Advisory Purposes, 1990. Non-Affiliated Soil Analysis Work Committee, Soil Science Society of South Africa

Hanson GJ, Simon A. 2001. Erodibility of cohesive streambeds in the loess area of the midwestern USA. Hydrologic Processes, 15, 23-38

Haregeweyn N, Poesen J, Nyssen J, De Wit J, Haile M, Govers G, Deckers S. 2006. Reservoirs in Tigray (Northern Ethiopia): characteristics and sediment deposition problems. Land degradation & development, 17 (2), 211-230

Harmel RD, Haan CT, Dutnell RC. 1999. Evaluation of Rosgen's streambank erosion potential assessment in Northeast Oklahoma. JAWRA Journal of the American Water Resources Association, 35 (1), 113-121

Harvey AM. 1991. The influence of sediment supply on the channel morphology of upland streams, Howgill Fells, Northwest England, Earth Surface Processes and Landforms, 6, 675-684

Harvey AM. 1997. Fluvial geomorphology of north-west England. In Fluvial Geomorphology of Great Britain. Dordrecht: Springer Netherlands, 173-200

Harvey AM. 2002. Effective timescales of coupling within fluvial systems. Geomorphology, 44 (3–4), 175–201. Available from: https://doi. org/10.1016/S0169-555X(01)00174-X

Harvey J, Gooseff M. 2015. River corridor science: Hydrologic exchange and ecological consequences from bedforms to basins. Water Resources Research, 51 (9), 6893-6922

Hauer C, Habersack H. 2009. Morphodynamics of a 1000-year flood in the Kamp River, Austria, and impacts on floodplain morphology. Earth Surface Processes and Landforms, 34 (5), 654-682 https://doi.org/10.1002/esp.1763

Häusler K, Dellwig O, Schnetger B, Feldens P, Leipe T, Moros M, Pollehne F, Schönke M, Wegwerth A and Arz HW. 2018. Massive Mn carbonate formation in the Landsort Deep (Baltic Sea): Hydrographic conditions, temporal succession, and Mn budget calculations. Marine Geology, 395, 260-270

He Q, Walling DE. 1996. Use of fallout Pb-210 measurements to investigate longer-term rates and patterns of overbank sediment deposition on the floodplains of lowland rivers. Catena, 29 (3–4), 263–282. https:// doi. org/ 10. 1016/S0341- 8162(96) 00072-0

He Q, Walling DE. 1997. The distribution of fallout 137Cs and 210Pb in undisturbed and cultivated soils. Applied radiation and isotopes, 48 (5), 677-690

He Q, Walling DE. 1998. An investigation of the spatial variability of the grain size composition of floodplain sediments. Hydrological Processes, 12/7, 1079–1094

He X, Augusto L, Goll DS, Ringeval B, Wang Y, Helfenstein J, Huang Y, Yu K, Wang Z, Yang Y, Hou E. 2021. Global patterns and drivers of soil total phosphorus concentration. Earth System Science Data Discussions, 1-21

Heger A, Becker JN, Navas LKV, Eschenbach A. 2021. Factors controlling soil organic carbon stocks in hardwood floodplain forests of the lower middle Elbe River. Geoderma., 404

Heiler G, Hein T, Schiemer F, Bornette G. 1995. Hydrological connectivity and flood pulses as the central aspects for the integrity of a river-floodplain system. Regulated Rivers: Research & Management, 11 (3-4), 351-361

Hennings N, Becker JN, Guillaume T, Damris M, Dippold MA, Kuzyakov Y. 2021. Riparian wetland properties counter the effect of land-use change on soil carbon stocks after rainforest conversion to plantations. Catena, 196

Herndon WL. 1853. Exploration of the valley of the Amazon: U.S. 32nd Congress, 2nd Session, Senate Executive Document, no. 36, Part 1, 414

Hession WC, Curran JC. 2013. The Impacts of Vegetation on Roughness in Fluvial Systems. In: Shroder JF (Editor-in-chief), Butler DR, Hupp CR (Volume Editors). Treatise on Geomorphology, Ecogeomorphology, San Diego: Academic Press, 12, 75-93

Hey RD, Thorne CR. 1975. Secondary flow in river channels. Area, 7 (3), 191–19

Hickin EJ. 1979. Concave-bank benches on the Squamish River, British Columbia, Canada. Canadian Journal of Earth Sciences, 16, 200-203

Hickin EJ. and Nanson GC. 1975. The Character of Channel Migration on the Beaton River, Northeast British Columbia, Canada. Geological Society of America Bulletin, 86, 487–494

Hickin EJ. and Nanson GC. 1984. Lateral Migration Rates of River Bends. American Society of Civil Engineers, Journal of Hydraulic Engineering, 110, 1557–1567

Higgs G. 1987. Environmental change and hydrological response: flooding in the upper Severn catchment, in K.J. Gregory (ed.) Palaeohydrology in Practice, John Wiley & Sons, Chichester

Hjulstrum F. 1935. Studies of the morphological activities of rivers as illustrated by the River Fyris. Bulletin Geology Institute, University Uppsala, 25, 221-527

Hobo N, Makaske B, Middelkoop H, Wallinga J. 2010. Reconstruction of floodplain sedimentation rates: a combination of methods to optimize estimates. Earth Surface Processes and Landforms, 35 (13), 1499–1515. https:// doi. org/ 10. 1002/ esp. 1986

Hoffman TM, Todd S. 2000. A National Review of Land Degradation in South Africa: The Influence of Biophysical and Socio-Economic Factors. Journal of South African Studies, 26, 743-758. http://dx.doi.org/10.1080/713683611

Hoffmann CC, Kjaergaard C, Uusi-Kämppä J, Hansen HC, Kronvang B. 2009. Phosphorus retention in riparian buffers: review of their efficiency. Journal of Environmental Quality, 38 (5), 1942–1955. Available from: https://doi.org/10.2134/jeq2008.0087

Hooke J. 1980. Magnitude and distribution of rate of river bank erosion. Earth Surface Processes and Landforms, 5, 143–15

Hooke J. 2003. River meander behavior and instability: A framework for analysis: River meander behavior and instability. Transactions of the Institute of British Geographers, 28, 238–253. https://doi.org/10.1111/1475-5661.00089

Hooke JM. 1987. Changes in Meander Morphology, in Gardiner V (ed.), International Geomorphology, 1986: Proceedings of the First International Conference on Geomorphology, John Wiley & Sons, Chichester, UK, 591–609

Hooke JM. 1995. River channel adjustment to meander cutoffs on the River Bollin and River Dane, northwest England. Geomorphology, 14 (3), 235-253

Hooke JM. 2004. Cutoffs galore!: Occurrence and causes of multiple cutoffs on a meandering river, Geomorphology, 61, 225–238, doi:10.1016/j.geomorph.2003.12.006

Hooke JM. 2008. Temporal variations in fluvial processes on an active meandering river over a 20-year period. Geomorphology, 100, 3–13

Hooke RLB. 1975. Distribution of Sediment Transport and Shear Stress in a Meander Bend. The Journal of geology, 83, 543–565

Horowitz AJ, Elrick KA. 1987. The relation of stream sediment surface area, grain size and composition to trace element chemistry. Applied Geochemistry, 2, 437–451. https://doi. org/ 10. 1016/ 0883- 2927(87) 90027-8

Horowitz AJ. 1991. A primer on sediment-trace element chemistry, 2nd edition. Chelsea, Michigan: Lewis Publishers

Howard AD. 1992. Modelling channel migration and floodplain sedimentation in meandering streams: in Lowland Floodplain Rivers: Geomorphological Perspectives, eds. Carling PA and Petts GE, Wiley, Chichester, 1-41

Howard AD. 1996. Modelling channel evolution and floodplain morphology. In Floodplain Processes, Anderson MG, Walling DE, Bates PD (eds). John Wiley: Hoboken, NJ; 15–62 (15) (PDF) Chute channel dynamics in large, sand-bed meandering rivers. Available from: https://www.researchgate.net/publication/230545993_Chute_channel_dynamics_in_large_sand-bed_meandering_rivers [accessed Jan 26 2024]

Huchzermeyer N, Schlegel P, van der Waal, B. 2019. Biophysical monitoring methods in the Upper Tsitsa River Catchment (T35A-E). Ecosystem report, Tsitsa Project, Rhodes University

Huchzermeyer N. 2014. Investigating the connectivity of gully sediment sources and pathways in the Vuvu catchment (Honours Thesis). Rhodes University, Grahamstown, Eastern Cape, South Africa

Hudson PF and Kesel RH. 2000. Channel migration and meander-bend curvature in the lower Mississippi River prior to major human modification. Geology, 28 (6), 531-534

Hudson PF, Heitmuller, FT. 2003. Local and watershed-scale controls on the spatial variability of natural levee deposits in a large fine-grained floodplain: Lower Panuco basin, Mexico. Geomorphology 56, 255-269

Hudson-Edwards KA, Schell C, Macklin MG. 1999. Mineralogy and geochemistry of alluvium contaminated by metal mining in the Rio Tinto area, southwest Spain. Applied Geochemistry, 14, 1015-1030

Hughes AO, Olley JM, Croke JC and Webster IT. 2009. Determining floodplain sedimentation rates using 137Cs in a low fallout environment dominated by channel- and cultivation-derived sediment inputs, central Queensland, Australia. Journal Environmental Radioactivity, 100, 858–865

Humphries M. 2008. PhD thesis. Sedimentation and chemical processes on the Lower Mkuze floodplain: implications for wetland structure and function. University KwaZulu- Natal

Humphries MS, Kindness A, Ellery WN, Hughes JC, Benitez-Nelson CR. 2010. 137Cs and 210Pb derived sediment accumulation rates and their role in the long-term development of the Mkuze River floodplain. South Africa Geomorphology, 119 (1–2), 88–96. https:// doi. org/ 10.1016/j.geomorph. 2010. 03. 003

Hupp CR, Noe GB, Schenk ER, Benthem AJ. 2013. Recent and historic sediment dynamics along Difficult Run, a suburban Virginia Piedmont stream. Geomorphology, 180, 156–169. https:// doi. org/ 10. 1016/j. geomorph. 2012.10. 007

Hupp CR, Pierce AR, Noe GB. 2009. Floodplain geomorphic processes and environmental impacts of human alteration along Coastal Plain Rivers, USA. Wetlands, 29 (2), 413–429. https:// doi. org/ 10. 1672/ 08-169.1

Hupp CR, Woodside MD and Yanosky TM. 1993. Sediment and trace element trapping in a forested wetland, Chickahominy River, Virginia. Wetlands, 13 (2), 95–104. Available from: https://doi.org/10.1007/BF03160869

Hupp CR. 1988. Plant ecological aspects of flood geomorphology and palaeoflood history: in Baker VR, Kochel RC and Patton P C (Eds), Flood Geomorphology, Wiley-Interscience, New York, 335-356

Hupp CR. 2000. Geomorphology, sedimentation, and vegetation of coastal plain rivers in southeastern United States. Hydrological Processes

Hutton D and Haque CE. 2004. Human vulnerability, dislocation and resettlement: adaptation processes of river-bank erosion-induced displaces in Bangladesh. Disasters, 28 (1), 41–62

Ishee ER, Ross DS, Garvey KM, Bourgault RR, Ford CR. 2015. Phosphorus characterization and contribution from eroding streambank soils of Vermont's Lake Champlain Basin. Journal of Environmental Quality, 44 (6), 1745-1753

Ishii Y, Hori K. 2016. Formation and infilling of oxbow lakes in the Ishikari lowland, northern Japan. Quaternary International, 397, 136–146. https:// doi. org/ 10. 1016/j. quaint. 2015. 06.16

Jackson RG. 1976. Depositional model of point bars in the Lower Wabash River. Journal of Sedimentary Research, 46, 579-594

Jain V, Fryirs K and Brierley G .2008. Where do floodplains begin? The role of total stream power and longitudinal profile form on floodplain initiation processes. GSA Bulletin, 120 (1/2), 127–141. doi: 10.1130/B26092.1

James CS. 1985. Sediment transfer to overbank sections. Journal of Hydraulic Research, 23/5, 435–452

Janes VJJ, Holman I, Birkinshaw S, O'Donnell G, Kilsby C. 2018. Improving bank erosion modelling at catchment scale by incorporating temporal and spatial variability. Earth Surface Processes and Landforms 43, 124–133.

Janes VJJ, Nicholas AP, Collins AL, Quine TA. 2017. Analysis of fundamental physical factors influencing channel bank erosion: results for contrasting catchments in England and Wales. Environmental Earth Sciences, 76, 307. https://doi.org/10.1007/s12665-017-6593-x

Jarriel T, Swartz J, Passalacqua, P. 2021. Global rates and patterns of channel migration in river deltas. PNAS, 118 (46), 1-8. https://doi.org/10.1073/pnas.2103178118

Jeffries R, Darby SE, Sear DA. 2003. The influence of vegetation and organic debris on flood-plain sediment dynamics: a case study of a low-order stream in the New Forest, England. Geomorphology, 51, 61-80

Job N. 2014. MSc thesis. Geomorphic origin and dynamics of deep, peat-filled, valley bottom wetlands dominated by palmiet (Prionium serratum): a case study based on the Goukou Wetland, Western Cape. Rhodes University

Joglekar DV. 1971. Manual on river behaviour, control and training, Central Board of Irrigation and Power, New Delhi, India

Johan PD, Ahmed OH, Omar L, Hasbullah NA. 2021. Phosphorus Transformation in Soils Following Co-Application of Charcoal and Wood Ash. Agronomy, 11 (10). https://doi.org/10.3390/agronomy11102010

Johnston CA, Bridgham SD, Schubauer-Berigan JP. 2001. Nutrient dynamics in relation to geomorphology of riverine wetlands. Soil Science Society of America Journal, 65 (2), 557–577. https://doi. org/ 10. 2136/ sssaj 2001. 65255 7x

Johnston CA, Bubenzer GD, Lee GB, Madison FW, Mc Henry JR. 1984. Nutrient trapping by sediment deposition in a seasonally flooded lakeside wetland. American Society of Agronomy, Crop Science Society of America, and Soil Science Society of America, 13 (2), 283–290. https:// doi.org/ 10. 2134/ jeq19 84. 00472 42500 13000 20022x

Johnston CA. 1991. Sediment and nutrient retention by freshwater wetlands: effects on surface water quality. Critical Reviews in Environmental Science and Technology, 21 (5–6), 491–565

Jones JA and Grant GE. 1996. Peak flow responses to clear-cutting and roads in small and large basins, western Cascades, Oregon. Water resources research, 32 (4), 959-974

Joshi SR. 1987. Non-destructive determination of Lead-210 and Radium-226 in sediments by direct photon analysis. Journal of Radioanalytical and Nuclear Chemistry, 116, 169-18

Juez C, Schärer C, Jenny H, Schleiss AJ, Franca MJ. 2019. Floodplain Land Cover and Flow Hydrodynamic Control of Overbank Sedimentation in Compound Channel Flows. Water Resources Research, 55 (11), 9072-9091. https://doi.org/10.1029/2019WR024989

Jugaru TL, Le Coz J, Provansal M, Panin N, Raccasi G, Dramais G, Dussouillez P. 2009. Flow and sediment processes in a cutoff meander of the Danube Delta during episodic flooding, Geomorphology, 106, 186–197, doi:10.1016/j.geomorph.2008.10.016

Julian JP, Torres R. 2006. Hydraulic erosion of cohesive riverbanks. Geomorphology, 76, 193-206

Julien PY. 2002. River mechanic. Cambridge University Press, Cambridge

Jung KT, Jin JY, Kang H, Lee HJ. 2004. An analytical solution for the local suspended sediment concentration profile in tidal sea region. Estuarine, Coastal and Shelf Science, 61 (4), 657-667. https://doi.org/10.1016/j.ecss.2004.07.007

Junk W, Bayley P, Sparks R. 1989. The flood pulse concept in river–floodplain systems. Canadian Journal of Fisheries and Aquatic Sciences Special Publication, 106, 110–127

Kaase CT and Kupfer JA. 2016. Sedimentation patterns across a Coastal Plain floodplain: The importance of hydrogeomorphic influences and cross-floodplain connectivity. Geomorphology, 269, 43-55. https://doi.org/10.1016/j.geomorph.2016.06.020

Kakembo V and Rowntree KM. 2003. The relationship between land use and soil erosion in the communal lands near Peddie Town, Eastern Cape, South Africa. Land Degradation and Development, 14 (1), 39 - 49. DOI:10.1002/ldr.509

Kakembo V. 2000. Artificial drainage induced erosion: The case of railway culverts on the Kwezana Ridge, near Alice, Eastern Cape. South African Geographical Journal, 82 (3), 149-153. DOI:10.1080/03736245.2000.9713707

Keen-Zebert A, Tooth S, Rodnight H, Duller GAT, Robert HM, Grenfell M. 2013. Late Quaternary floodplain reworking and the preservation of alluvial sedimentary archives in unconfined and confined river valleys in the eastern interior of South Africa. Geomorphology, 185, 54–66. https://doi. org/ 10. 1016/j. geomorph. 2012. 12. 004

Keen-Zebert AK, Tooth S, Grenfell M. 2011. Floodplain Chronology of the Stillerust Vlei, Mooi River Floodplain Wetland, in Western KwaZulu-Natal, South Africa, In Key Concepts in Geomorphology, Vignettes, Science Education Resource Center, Carleton College: Northfield, MN

Keller EA. 1971. Areal sorting of bed-load material: the hypothesis of velocity reversal. Geological Society of America Bulletin, 82 (3), 753-756

Kesel RH, Dunne KC, McDonald RC, Allison KR, Spicer BE. 1974. Lateral erosion and overbank deposition on the Mississippi River in Louisiana caused by 1973 flooding. Geology, 2, 461–464. https:// doi. org/ 10. 1130/ 0091-7613(1974)2% 3c461: LEAODO% 3e2.0. CO;2

Kheir RB, Wilson J, Deng Y. 2007. Use of terrain variables for mapping gully erosion susceptibility in Lebanon. Earth Surface Processes and Landforms, 32, 1770-1782. DOI: 10.1002/esp.1501

Kim L-H, Choi E, Stenstrom MK. 2003. Sediment characteristics, phosphorus types and phosphorus release rates between river and lake sediments. Chemosphere 50, 53–61. PII: S 0 0 4 5 - 6 5 3 5 (0 2) 0 0 3 1 0 – 7

King LC. 1963. South African Scenery. Oliver and Boyd, Edinburgh, 308.

Kleinhans MG, van den Berg JH. 2011. River channel and bar patterns explained and predicted by an empirical and a physics-based method. Earth Surface Processes and Landforms, 36, 721–738. DOI:10.1002/esp.2090 (15) (PDF) Chute channel dynamics in large, sand-bed meandering rivers. Available from: https://www.researchgate.net/publication/230545993_Chute_channel_dynamics_in_large_sand-bed_meandering_rivers [accessed Jan 26 2024]

Kleiss BA. 1996. Sediment retention in a bottomland hardwood wetland in eastern Arkansas. Wetlands, 16 (3), 321–333. Available from: https://doi.org/10.1007/BF03161323

Kneller BC, Bennett SJ, McCaffrey WD. 1999, Velocity structure, turbulence, and fluid stresses in experimental gravity currents. Journal of Geophysical research, 104 (C3), 5381-5391

Knight DW and Shiono K. 1990. Turbulence measurements in a shear layer region of a compound channel. Journal of hydraulic research, 28(2), 175-196.

Knighton AD. 1973. Riverbank erosion in relation to streamflow conditions, river Bollin-Dean, Cheshire. East Midland Geographer, 5, 416–426

Knighton AD. 1989. River adjustment to changes in sediment load: the effects of tin mining on the Ringarooma River, Tasmania, 1875-1984, Earth Surface Processes and Landforms, !4, 333-359

Knighton D. 1998. Fluvial forms and processes: a new Perspective. Routledge, Oxford UK

Knox JC. 1987, Historical Valley Floor Sedimentation in the Upper Mississippi Valley. Annals of the Association of American Geographers, 77 (2), 224-244, https://doi.org/10.1111/j.1467-8306.1987.tb00155.x

Knox JC. 2006. Floodplain sedimentation in the Upper Mississippi Valley: Natural versus human accelerated. Geomorphology, 79 (3-4), 286-310

Kondolf G, Piégay H, Landon N. 2002. Channel response to increased and decreased bedload supply from land use change: contrasts between two catchments. Geomorphology, 45, 35–51

Kondolf GM. 1997. PROFILE: Hungry Water: Effects of Dams and Gravel Mining on River Channels. Environmental management, 21 (4), 533-51. doi: 10.1007/s002679900048. PMID: 9175542.

Konrad CP. 2012. Reoccupation of floodplains by rivers and its relation to the age structure of floodplain vegetation: Journal of Geophysical Research, 117, doi: 10.1029/2011JG001906

Kotze DC, Marneweck GC, Batchelor AL, Lindley DS, Collins NB. 2009. WET-EcoServices: a technique for rapidly assessing ecosystem services supplied by wetlands. WRC Report No TT 339/09. Water Research Commission

Koulouri M and Giourga C. 2007. Land abandonment and slope gradient as key factors of soil erosion in Mediterranean terraced lands. Catena, 69 (3), 274-281. https://doi.org/10.1016/j.catena.2006.07.001

Krishnaswami S and Lal D. 1978. Radionuclide limnochronology. In A. Lerman (ed.), Lakes: Chemistry, Geology, Physics. Springer-Verlag, N.Y, 153–177

Krishnaswami S, Lal D, Martin JM, Meybeck M. 1971. Geochronology of lake sediments. Earth and Planetary Science Letters, 11 (1-5), 407-414. https://doi.org/10.1016/0012-821X(71)90202-0

Kroening SE and Andrews WJ. 1997. Water-quality assessment of part of the Upper Mississippi River Basin, Minnesota and Wisconsin Nitrogen and phosphorus in streams, streambed sediment, and ground water, 1971-94, U.S. Geological Survey Water Resources Investigations Report, 97-4107, 67

Kroese JS, Batista PVG, Jacobs SR, Breuer L, Quinton JN, Rufino MC. 2020. Agricultural land is the main source of stream sediments after the conversion of an African montane forest. Scientific reports, 10, 14827. https://doi.org/10.1038/s41598-020-71924-9

Kronvang B, Andersen HE, Larsen SE, Audet J. 2013. Importance of bank erosion for sediment input, storages and export at the catchment scale'. Journal of Soils and Sediments, 13, 230–241

Kronvang B, Andersen IK, Hoffmann CC, Pedersen ML, Ovesen NB and Andersen HE. 2007. Water exchange and deposition of sediment and phosphorus during inundation of natural and restored lowland floodplains. Water, Air, and Soil Pollution, 181, 115–121.

Kronvang B, Svendsen LM, Brookes A, Fisher K, Møller B, Ottosen O, Newson M and Sear D. 1997. Restoration of the rivers Brede, Cole and Skerne: A joint Danish and British EU-LIFE demonstration project, III — Channel morphology, hydrodynamics and transport of sediment and nutrients. Aquatic Conservation: Marine and Freshwater Ecosystems, 8, 209–222

Kuehner KJ, Green JA, Wheeler BJ, Kasahara SM, Luhmann AJ, Alexander Jr EC. 2016, September. Water Tracing in the Crystal Creek Watershed in Minnesota. In Proceedings of the Geological Society of America Annual Meeting, Denver, CO, USA, 25-28

Lagasse PF, Spitz WJ, Zevenbergen LW, Zachmann DW. 2004. Handbook for Predicting Stream Meander Migration and Supporting Software. National Academies of Sciences, Engineering, and Medicine. Washington, DC: The National Academies Press. https://doi.org/10.17226/23346

Lambert CP and Walling DE. 1986. Suspended sediment storage in river channels: a case study of the River Exe, Devon, UK. In: Hadley RF (ed.): Drainage Basin Sediment Delivery. International Association of Hydrological Sciences Publication No. 159 (Proceedings of the Albuquerque Symposium), 263-276

Lambert CP, Walling DE. 1987. Floodplain sedimentation: a preliminary investigation of the contemporary deposition within the lower reaches of the River Culm, Devon, UK. Geografiska Annaler: Series A, Physical Geography 69A (3-4), 393-404

Land Type Survey Staff. 1972–2008. Land Types of South Africa: Digital Map (1:250 000 scale) and Soil Inventory Databases. ARC-Institute for Soil, Climate and Water: Pretoria.

Lane PNJ and Sheridan GJ. 2002. Impact of an Unsealed Forest Road Stream Crossing: Water Quality and Sediment Sources. Hydrological Processes, 16 (13), 2599 - 2612. DOI:10.1002/hyp.1050

Langland M and Cronin T. 2003. A summary report of sediment processes in Chesapeake Bay and watershed: U.S. Geological Survey Water-Resources Investigations Report, 2003–4123, 109. https://pubs.er.usgs.gov/publication/wri034123.

Larkin ZT, Tooth S, Ralph TJ, Duller GAT, McCarthy T, Keen-Zebert A, Humphries MS. 2017. Timescales, mechanisms, and controls of incisional avulsions in floodplain wetlands: insights from the Tshwane

River, semiarid South Africa. Geomorphology, 283, 158–172.https:// doi. org/ 10. 1016/j. geomorph. 2017. 01. 021

Laubel A, Kronvang B, Hald AB, Jensen C. 2003. Hydromorphological and biological factors influencing sediment and phosphorus loss via bank erosion in small lowland rural streams in Denmark. Hydrological processes, 17, 3443–3463

Lauer JW, Parker G. 2008. Net local removal of floodplain sediment by river meander migration. Geomorphology, 96,123–149. https:// doi. org/ 10. 1016/j. geomorph. 2007.08. 003

Lawler DM. 1993. The measurement of river bank erosion and lateral channel change: A review. Earth Surface Processes and Landforms, 18 (9), 777-821. doi:10.1002/esp.3290180905

Le Roux JJ, Barker CH, Weepener HL, van den Berg EC, Pretorius SN. 2015. Sediment Yield Modelling in the Mzimvubu River Catchment. WRC Report No. 2243/1/15. Water Research Commission, Pretoria

Le Roux JJ, Mashimbye ZE, Weepener HL, Newby TS, Pretorius DJ. 2008a. Erosion Status of Priority Tertiary Catchment Areas Identified by the Soil Protection Strategy of the Department of Agriculture, ISCW Report No. GW/A/2008/17. ARC-Institute for Soil, Climate and Water: Pretoria

Le Roux JJ, Morgenthal TL, Malherbe J, Sumner PD, Pretorius DJ. 2008b. Water erosion prediction at a national scale for South Africa. Water SA, 34, 305– 314

Le Roux JJ, Sumner PD. 2012. Factors controlling gully development: comparing continuous and discontinuous gullies. Land Degradation and Development, 23 (5), 440–449

Lecce SA, Pavlowsky RT. 1997. Storage of mining-related zinc in floodplain sediments, Blue River, Wisconsin. Physical Geography, 18, 424–439

Lecce SA, Pavlowsky RT. 2004. Spatial and temporal variations in the grain-size characteristics of historical flood plain deposits, Blue River, Wisconsin, USA. Geomorphology, 61, 361–371

Lecce SA. 1997. Spatial patterns of historical overbank sedimentation and floodplain evolution, Blue River, Wisconsin. Geomorphology, 18, 265–277

Leclerc RF, Hickin EJ. 1997. The internal structure of scrolled floodplain deposits based on ground-penetrating radar, North Thompson River, British Columbia. Geomorphology, 21 (1), 17–38

Leenaers H and Schouten CJ. 1989. Soil erosion and floodplain soil pollution: Related problems in the geographical context of a river basin: in Sediment and the Environment (Proceedings of the Baltimore Symposium), IASH Publication No. 184 75-83

Leonard LA, Wren PA, Beavers RL. 2002. Flow dynamics and sedimentation in Spartina Alterniflora and Phragmites Australis marshes of the Chesapeake Bay. Wetlands, 22 (2), 415–424

Leopold LB and Wolman MG. 1957. River Channel Patterns- Braided, Meandering, and Straight, U.S. Geological Survey Professional Paper, 282-B, 39–85

Leopold LB and Wolman MG. 1960. River Meanders. Geological Society of America Bulletin, 71

Lewin G and Brindle B. 1977. Confined meanders. In: Gregory K (ed) River channel changes. Wiley, Hoboken, 221–233

Lewin J and Macklin MG. 1987. Metal mining and floodplain sedimentation in Britain: in Gardiner V (Ed.), International Geomorphology, Part I, Wiley, Chichester, 1009-1027

Lewin J, Macklin MG, Newson MD. 1988. Regime theory and environmental change, irreconcilable concepts, In White, J.R. (ed), International Conference on River Regime, Hydraulics Research Institute, John Wiley and Sons, Chichester, 431-445

Lewin J. 1978. Floodplain geomorphology. Prog. Phys. Geogr., 2, 408-437

Lewin J. 1983. Changes of channel patterns and floodplains. In: KJ. Gregory (Editor), Background to Palaeohydrology: A Perspective. Wiley, Chichester, 161-175

Lewis GW and Lewin J. 1983. Alluvial cutoffs in Wales and the Borderlands. In Collinson and Lewin (1983), 145–154

Limaye ABS and Lamb MP. 2016. Numerical model predictions of autogenic fluvial terraces and comparison to climate change expectations. Journal of Geophysical Research: Earth Surface, 121 (3), 512-544

Litschert SE and MacDonald LH. 2009. Frequency and characteristics of sediment delivery pathways from forest harvest units to streams. Forest Ecology and Management, 259 (2), 143-150. https://doi.org/10.1016/j.foreco.2009.09.038

Liu C and Liu A. 2019. Estimation of river bend migration rate for a meandering river by using tree ring analysis. IAHR. https:// doi. org/ 10. 3850/ 38WC0 92019- 0248

Lo EL, Yeager KM, Bergier I, Domingos-Luz L, Silva A and McGlue MM. 2022. Sediment Infill of Tropical Floodplain Lakes: Rates, Controls, and Implications for Ecosystem Services. Frontiers in Earth Science, 10, 875919. doi: 10.3389/feart.2022.875919

Lokas E, Wachniew P, Ciszewski D, Owczarek P, Chau ND. 2010. Simultaneous use of trace metals, 210Pb and 137Cs in floodplain sediments of a lowland river as indicators of anthropogenic impacts. Water Air Soil Pollution, 207, 57–71

Longmore ME, O'leary BM, Rose CW, Chandica AL. 1983. Mapping soil erosion and accumulation with the fallout isotope caesium-137. Soil Research, 21 (4), 373-385

Longmore ME. 1982. The Caesium dating technique and associated applications in Australia. In: Archaeometry: an Australian Perspective (ed. by W. Ambrose & P. Duerden), 310–321. ANU Press, Canberra, Australia

López-Bermúdez F, Diaz AR, Martínez-Fernández J. 1998. Vegetation and soil erosion under a semi-arid Mediterranean climate: A case study from Murcia (Spain). Geomorphology, 24 (1), 51-58. 10.1016/S0169-555X(97)00100-1

López-Vicente M, Poesen J, Navas A, Gaspar L. 2013. Predicting runoff and sediment connectivity and soil erosion by water for different land use scenarios in the Spanish Pre-Pyrenees. Catena, 102, 62-73. 10.1016/j.catena.2011.01.001

Lu S, Kronvang B, Audet J, Trolle D, Andersen HE, Thodsen H, van Griensven A. 2015. Modelling sediment and total phosphorus export from a lowland catchment: comparing sediment routing methods. Hydrological processes, 29, 280–294

Luce C. 2002. Hydrological processes and pathways affected by forest roads: what do we still need to learn? Hydrological Processes, 16, 2901-2904

MacGregor KR, Anderson RS, Anderson SP, Waddington ED. 2000. Numerical simulations of glacial-valley longitudinal profile evolution. Geology, 28 (11), 1031-1034

Macklin MG, Hudson-Edwards KA, Dawson EJ. 1997. The significance of pollution from historic metal mining in the Pennine orefields on river sediment contaminant fluxes to the North Sea. The Science of the Total Environment, 194/195, 391-397

Magdaleno F, Fernández-Yuste JA. 2011. Meander dynamics in a changing river corridor. Geomorphology, 130 (3–4), 197–207. https:// doi. org/ 10. 1016/j. geomorph. 2011.03. 016

Magette W, Carton O. 1996. Agricultural Pollution. Environmental Engineering. McGraw-Hill, Berkshire, 420-434

Maila D, Mulders J, Naidoo N, Crafford J, Mitchell S, Harris K. 2017. An evidence-based approach to measure the costs and benefits of change in aquatic ecosystems. WRC Report No. TT 726/17, Pretoria

Makaske B, Weerts HJT. 2005. Muddy lateral accretion and low stream power in a sub-recent confined channel belt, Rhine-Meuse delta, central Netherlands. Sedimentology, 52, 651-668. doi: 10.1111/j.1365-3091.2005.00713.x

Malatesta LC, Prancevic JP, Avouac JP. 2017. Autogenic entrenchment patterns and terraces due to coupling with lateral erosion in incising alluvial channels: Journal of Geophysical Research: Earth Surface, 122, 335–355. https://doi.org/10.1002/2015JF003797

Maltby E, Acreman MC. 2011. Ecosystem services of wetlands: pathfinder for a new paradigm. Hydrological Sciences Journal, 56 (8), 1341–1359. https:// doi. org/ 10. 1080/ 02626 667.2011. 631014

Marcus WA, Meyer GA, Nimmo DR. 2001. Geomorphic control of persistent mine impacts in a Yellowstone Park stream and implications for the recovery of fluvial systems. Geology, 29 (4), 355–358. https:// doi. org/ 10.1130/ 0091- 7613(2001) 029% 3c0355: GCOPMI% 3e2.0.CO;2

Markham AJ. and Thorne CR. 1992. Geomorphology of Gravel-Bed River Bends, in Billie P, Hey RD, Thorne CR, and Tacconi P (eds.), Dynamics of Gravel-Bed Rivers, John Wiley & Sons, Chichester, UK, 433–450

Marriots B and Alexander J.1999. Floodplains: Interdisciplinary Approaches. Geological Society, London, Special Publications, 163, 1-13. Available from https://www.researchgate.net/publication/259074793

Marriott S. 1992. Textural analysis and modelling of a flood deposit: River Severn, U.K. Earth Surface Processes and Landforms 17, 687–697

Mattia C, Bischetti G, Gentile F. 2005. Biotechnical characteristics of root systems of typical Mediterranean species. Plant Soil, 278, 23–32

McCallan ME, O'Leary BM, Rose CW. 1980. Redistribution of caesium-137 by erosion and deposition on an Australian soil. Soil Research, 18, 119-128. https://doi.org/10.1071/SR9800119

McCarthy T and Rubidge B. 2005. The Story of Earth and Life—A South African Perspective on a 4.6 Billion Year Journey. Cape Town: Struik, 209-211, 262-264

McCarthy TS, Tooth S, Kotze DC, Collins NB, Wandrag G and Pike T. 2010. The role of geomorphology in evaluating remediation options for floodplain wetlands: the case of Ramsar-listed Seekoeivlei, eastern South Africa. Wetlands Ecology and Management, 18 (2), 119–134. Available from: https://doi.org/10.1007/s11273-009-9153-7

McClain M, Boyer E, Dent C. et al. 2003. Biogeochemical Hot Spots and Hot Moments at the Interface of Terrestrial and Aquatic Ecosystems. Ecosystems 6, 301–312. https://doi.org/10.1007/s10021-003-0161-9

McGlue MM, Silva A, Corradini FA, Zani H, Trees MA, Ellis GS, Parolin M, Swarzenski PW, Cohen AS, Assine ML. 2011. Limnogeology in Brazil's '"forgotten wilderness"': a synthesis from the large floodplain lakes of the Pantanal. Journal of Paleolimnology, 46, 273–289. https:// doi. org/ 10.1007/ s10933- 011- 9538-5

McMillan SK and Noe GB. 2017. Increasing floodplain connectivity through urban stream restoration increases nutrient and sediment retention. Ecological Engineering, 108, Part A, 284-295. https://doi.org/10.1016/j.ecoleng.2017.08.006

Meade RH, Weibezahn FH, Lewis Jr WM, Hernandez DP. 1990. Suspended-sediment budget for the Orinoco River. The Orinoco River as an ecosystem, 55-79

Meade RH. 1982. Sources, sinks and storage of river sediments in the Atlantic drainage of the USA. US Geological Survey, 90 (3)

Megahan WF, Wilson M, Monsen SB. 2001. Sediment production from granitic cutslopes on forest roads in Idaho, USA. Earth Surface Processes and Landforms, 26 (2), 153–163

Mertes LAK, Dunne T, Martinelli LA. 1996. Channel-floodplain geomorphology Solimões-Amazon River. Brazil Geological Society of America Bulletin, 108 (9), 1089–1107. https:// doi. org/10. 1130/ 0016- 7606(1996) 108% 3c1089: CFGATS%3e2.3. CO;2

Mertes LAK. 1994. Rates of flood-plain sedimentation on the central Amazon River. Geology, 22, 171–174. https:// doi. org/ 10. 1130/ 0091- 7613(1994) 022% 3c0171:ROFPSO% 3e2.3. CO;2

Mertes LAK. 1997. Documentation and significance of the perirheic zone on inundated floodplains. Water resources research, 33 (7), 1749-1762. https://doi.org/10.1029/97WR00658

Meyer JL and Likens GE. 1979. Transport and Transformation of Phosphorus in a Forest Stream Ecosystem. Ecology- Ecological Society of America, 60 (6), 1255-1269. https://doi.org/10.2307/1936971

Michaelides K and Wainwright J. 2002. Modelling the effects of hillslope–channel coupling on catchment hydrological response. Earth Surface Processes and Landforms, 27 (13), 1441–1457

Michalková M, Piégay H, Kondolf GM, Greco SE. 2011. Lateral erosion of the Sacramento River, California (1942–1999), and responses of channel and floodplain lake to human influences. Earth Surface Processes and Landforms, 36, 257–272

Micheli E and Kirchner J. 2002. Effects of wet meadow riparian vegetation on streambank erosion. 1. Remote sensing measurements of streambank migration and erodibility. Earth Surface Processes and Landforms, 27, 627–639

Micheli ER and Larsen EW. 2010. River channel cutoff dynamics, Sacramento River, California, USA. River Research and Applications. DOI: 10.1002/rra.1360

Middelkoop H and Asselman NEM. 1995. Floodplain sedimentation: quantities, patterns and processes. Earth surface processes and landforms, 20 (6), 481-499. https://doi.org/10.1002/esp.3290200602

Middelkoop H and Asselman NEM. 1998. Spatial variability of floodplain sedimentation at the event scale in the Rhine-Meuse delta, The Netherlands. Earth Surface Processes and Landforms, 23, 561–573

Middelkoop H and Van der Perk M. 1998. Modelling spatial patterns of overbank sedimentation on embanked floodplains. Geografiska Annaler: Series A, Physical Geography, 80A/2, 95–109

Midgley G, Cavana RY, Brocklesby J, Foote JL, Wood DRR, Ahuriri-Driscoll A. 2013. Towards a new framework for evaluating systemic problem structuring methods. European Journal of Operational Research, 229 (1), 143-154. https://doi.org/10.1016/j.ejor.2013.01.047

Midgley G, Marais S, Barnett M, Wågsæther K. 2012. Biodiversity, climate change and sustainable development - Harnessing Synergies and celebrating successes. South African National Biodiversity Institute (SANBI), Conservation South Africa (CSA), and Indigo Development and Change

Millennium Ecosystem Assessment. 2005. Ecosystems and Human Well-being: Synthesis. Island Press, Washington, DC.

Miller JD, Kim H, Kjeldsen TR, Packman J, Grebby S, Dearden R. 2014. Assessing the impact of urbanization on storm runoff in a peri-urban catchment using historical change in impervious cover. Journal of Hydrology, 515, 59-70. https://doi.org/10.1016/j.jhydrol.2014.04.011

Milne J. 1983. Patterns of confinement in some stream channels of upland Britain. Geografiska Annaler: Series A, Physical Geography, 65, 67–83

Minar J and Evans IS. 2008. Elementary forms for land surface segmentation: The theoretical basis of terrain analysis and geomorphological mapping. Geomorphology, 95 (3), 236-259. 10.1016/j.geomorph.2007.06.003

Minella JPG, Merten GH, Reichert JM, Clarke RT. 2008. Estimating suspended sediment concentrations from turbidity measurements and the calibration problem. Hydrological processes, 22, 1819-1830

Mitasove H, Hofierka J, Zlocha M, Iverson LR. 1997. Modeling topographic potential for erosion and deposition using GIS. International Journal of Geographical Information Science. 10.1080/02693799608902101

Mitsch WJ and Gosselink JG. 1993. Wetlands, 2nd ed. John Wiley, New York

Moody JA and Troutman BM. 2000. Quantitative model of the growth of floodplains by vertical accretion. Earth surface processes and landforms, 25 (2), 115-133, https://doi.org/10.1002/(SICI)1096-9837(200002)25:2<115::AID-ESP46>3.0.CO;2-Z

Moody JA. 2018. Sediment Deposition on Floodplains and Point Bars of Powder River in Southeastern Montana from 1979 through 2017. U.S. Geological Survey. https://doi.org/10.5066/P92G0ND0

Moody JA. 2019. Dynamic relations for the deposition of sediment on floodplains and point bars of a freely meandering river. Geomorphology, 327, 587–597.https:// doi. org/ 10. 1016/j. geomorph. 2018. 11. 032

Moon BP and Selby MJ. 1983. Rock mass strength and scarp forms in southern Africa. Geografiska Annaler, 65A, 135-145

Moore NJ. 2016. MSc thesis. The remote sensing of fires and their effects on soil properties in the uKhahlamba Drakensberg Park. Rhodes University

Morisawa M. 1985. Rivers: Form and Process. Geomorphology texts, 7. The University of Michigan

Motha JA, Wallbrink PJ, Hairsine PB, Grayson RB. 2003. Determining the sources of suspended sediment in a forested catchment in southeastern Australia. Water Resources Research, 39 (3). https://doi.org/10.1029/2001WR000794

Moustakidis IV, Schilling KE, Weber LJ. 2019. Soil total phosphorus deposition and variability patterns across the floodplains of an Iowa river. Catena, 174, 84–94. https:// doi. org/ 10. 1016/j. catena. 2018. 10. 019

Msadala V, Gibson L, Le Roux J, Rooseboom A, Basson GR. 2010. Sediment yield prediction for South Africa: 2010 Edition. WRC Report No. 1765/1/10. Water Research Commission, Pretoria.

Mucina L and Rutherford MC. 2006. The Vegetation of South Africa, Lesotho and Swaziland. South African National Biodiversity Institute: Pretoria.

Mucina L, Rutherford MC, Powrie W, Gerber J, Bezuidenhout H, Sieben EJJ, Cilliers SS, Preez PJ, Manning JC, Hoare B, Boucher C, Rebelo AG, George J, Siebert F. 2006. Inland Azonal Vegetation. In The vegetation of South Africa, Lesotho and Swaziland , Mucina L and Rutherford M (eds). Strelitzia: Pretoria, 618–652

Nakamura F and Kikuchi S-I. 1996. Some methodological developments in the analysis of sediment transport processes using age distribution of floodplain deposits. Geomorphology, 16, 139-145

Nanayama F, Furukawa R, Shigeno K, Makino A, Soeda Y, Igarashi Y. 2007.Unusually nine large tsunami deposits from the past 4000 years at Kiritappu marsh along the southern Kuril Trench, Sedimentary Geology, 200, 275-294

Nanson GC and Croke JC. 1992. A genetic classification of floodplains. Geomorphology, 4(6), 459-486

Nanson GC and Croke JC. 2002. Emerging issues in flood plain research. IAHS Publication, 276, 271–278

Nanson GC and Hickin EJ. 1986. A Statistical Analysis of Bank Erosion and Channel Migration in Western Canada. Geological Society of America Bulletin, 97, 497–504

Nanson GC and Young RW. 1981. Overbank deposition and floodplain formation on small coastal streams of New South Wales. Z. Geomorphology, 25, 332-347

Nanson GC. 1980. Point bar and floodplain development of the meandering Beatton River, northeastern British Columbia, Canada. Sedimentology, 27, 3-29

Nanson GC. 1986. Episodes of vertical accretion and catastrophic stripping: a mode of disequilibrium floodplain development. Geological Society of America Bulletin, 97, 1467-1475

Neal CWM and Andera AM. 2015. Suspended sediment supply dominated by bank erosion in a low-gradient agricultural watershed, Wildcat Slough, Fisher, Illinois, United States. Journal of Soil and Water Conservation, 70, 145–155

Nehal L, Yan ZM, Xia JH, Khaldi A. 2012. Flow through non-submerged vegetation: A flume experiment with artificial vegetation. In 6th International Water Technology Conference, Istanbul, Turkey

Newman MC. 1995. Quantitative methods in aquatic ecotoxicology. Lewis Publishers, Boca Raton, Florida

Nicholas AP and Walling DE. 1996. The significance of particle aggregation in the overbank deposition of suspended sediment on river floodplains. Journal of Hydrology, 186 (1-4), 275-293, https://doi.org/10.1016/S0022-1694(96)03023-5

Nicholas AP and Walling DE. 1997. Modelling flood hydraulics and overbank deposition on river floodplains. Earth surface processes and landforms, 22 (1), 59-77, https://doi.org/10.1002/(SICI)1096-9837(199701)22:1<59::AID-ESP652>3.0.CO;2-R

Nicholas AP and Walling DE. 1998. Numerical modelling of floodplain hydraulics and suspended sediment transport and deposition, Hydrol. Processes, 12, 1339–1355

Nicoll TJ and Hickin EJ. 2010. Planform geometry and channel migration of confined meandering rivers on the Canadian prairies. Geomorphology, 116, 37–47. https://doi.org/10.1016/j.geomorph.2009.10.0

Noe GB and Hupp CR. 2005. Carbon, nitrogen, and phosphorus accumulation in floodplains of Atlantic Coastal Plain rivers, USA. Ecological Applications, 15 (4), 1178–1190. Available from: https://doi.org/10. 1890/04-1677

Noe GB and Hupp CR. 2009. Retention of riverine sediment and nutrient loads by coastal plain floodplains. Ecosystems, 12 (5), 728–746. Available from: https://doi.org/10.1007/s10021-009-9253-5

Notebaert B, Verstraeten G, Govers G, Poesen J. 2010. Quantification of alluvial sediment storage in contrasting environments: Methodology and error estimation. Catena, 82 (3), 169-182. 10.1016/j.catena.2010.06.003

Novotny V and Chesters G. 1989. Delivery of sediment and pollutants from nonpoint sources: A water quality perspective. Journal of Soil and Water Conservation, 44 (6), 568–576 Retrieved from http://www.jswconline.org/content/44/6/568

Nyamela N. 2018. The suspended sediment yield of the Inxu catchment, Eastern Cape. MSc Thesis. Rhodes University

O'Halloran IP, Kachanoski RG, Stewart JWB. 1985. Spatial variability of soil phosphorus as influenced by soil texture and management. Canadian Journal of Soil Science, 65, 475-487

O'Halloran IP, Stewart JWB, De Jong E. 1987. Changes in P forms and availability as influenced by management practices. In: Van Diest, A. (eds) Plant and Soil Interfaces and Interactions. Developments in Plant and Soil Sciences, 28. Springer, Dordrecht. https://doi.org/10.1007/978-94-009-3627-0_8

Odgaard AJ. 1987. Streambank erosion along two rivers in Iowa. Water Resources Research, 23 (7), 1225-1236. https://doi.org/10.1029/WR023i007p01225

Odhiambo BK, Ricker MC, Le Blanc LM, Moxey KA. 2016. Effects of forested floodplain soil properties on phosphorous concentrations in two Chesapeake Bay sub-watersheds, Virginia, USA. Environmental Science and Pollution Research, 23 (16), 16056–16066. https:// doi. org/ 10. 1007/s11356- 016- 6668-3

Oestreicher JS, Lucotte M, Moingt M, Bélanger E, Rozon C, Davidson R, Mertens F, Romaña CA. 2016. Environmental and anthropogenic factors influencing mercury dynamics during the past century in floodplain lakes of the Tapajo's River Brazilian Amazon. Archives of environmental contamination and toxicology. https:// doi. org/ 10. 1007/s00244- 016- 0325-1

Olde Venterink H, Vermaat JE, Pronk M, Wiegman F, Van Der Lee GE, van den Hoorn MW, et al. 2006. Importance of sediment deposition and denitrification for nutrient retention in floodplain wetlands. Applied Vegetation Science, 9 (2), 163–174. Available from: https://doi.org/10.1111/j.1654-109X.2006.tb00665.x

Omengo FO, Alleman T, Geeraert N, Bouillon S, Govers G. 2016. Sediment deposition patterns in a tropical floodplain, Tana River, Kenya. Catena, 143, 57–69. https://doi. org/ 10. 1016/j. catena. 2016. 03. 024

Opperman JJ, Galloway GE, Fargione J, Mount JF, Richter BD, Secchi S. 2009. Sustainable Floodplains Through Large-Scale Reconnection to Rivers. Science, 326, 1487-1488. 10.1126/science.1178256

Ottesen RT, Bogen J, Bolviken B and Volden T.1989. Overbank sediment: a representative sample medium for regional geochemical mapping. Journal of geochemistry exploration, 32, 257-277

Outridge PM, Hermanson MH, Lockhart WL. 2002. Regional variations in atmospheric deposition and sources of anthropogenic lead in lake sediments across the Canadian Arctic. Geochimica et Cosmochimica Acta, 66 (20), 3521-3531. https://doi.org/10.1016/S0016-7037(02)00955-9

Owens JW. 1998. Late Quaternary evolution of fluvial and aeolian sediments in the upper Murrumbidgee valley: (unpublished MSc dissertation), Wagga Wagga, Australia, Charles Sturt University: in Floodplain Formation and Sediment Stratigraphy Resulting from Oblique Accretion on the Murrumbidgee River, Australia. https:// www. researchgate. net/ publication/250082670

Owens PN, Batalla RJ, Collins AJ, Gomez B, Hicks DM, Horowitz AJ, et al. 2005. Fine-grained sediment in river systems: environmental significance and management issues. River Research and Applications, 21 (7), 693–717. Available from: https://doi.org/10.1002/rra.878

Owens PN and Walling DE. 1996. Spatial variability of caesium-137 inventories at reference sites: an example from two contrasting sites in England and Zimbabwe. Applied Radiation and Isotopes, 47, 699–707

Owens PN and Walling DE. 2002. The phosphorus content of fluvial sediment in rural and industrialized river basins. Water Research, 36 (3), 685–701. Available from: https://doi.org/10.1016/S0043-1354(01)00247-0

Owens PN, Giles TR, Petticrew EL, Leggat MS, Moore RD, Eaton BC. 2013. Muted responses of streamflow and suspended sediment flux in a wildfire-affected watershed. Geomorphology, 202, 128-139. https://doi.org/10.1016/j.geomorph.2013.01.001

Owens PN, Walling DE, Carton J, Meharg AA, Wright J, Leeks GJL. 2001. Downstream changes in the transport and storage of sediment-associated contaminants (P, Cr and PCBs) in agricultural and industrialized drainage basins. The Science of the Total Environment, 266, 177–186

Owens PN, Walling DE, Leeks GJL. 1999. Use of floodplain sediment cores to investigate recent historical changes in overbank sedimentation rates and sediment sources in the catchment of the River Ouse, Yorkshire, UK. Catena, 36, 21–47. https:// doi. org/ 10. 1016/ S0341- 8162(99)00010-7

Owens PN. 2005. Conceptual models and budgets for sediment management at the river basin scale. Journal of Soils Sediments, 5, 201–212

Page KJ and Nanson GC. 1982. Concave bank benches and associated floodplain formation. Earth Surface Processes and Landforms, 7, 529-543

Page KL, Nanson GC, Frazier PS. 2003. Floodplain formation and sediment stratigraphy resulting from oblique accretion on the Murrumbidgee River, Australia. Journal of Sedimentary Research, 73 (1), 5–14. https:// doi. org/ 10. 1306/ 07010 27300 05

Palanques A, Grimalt J, Belzunces M, Estrada F, Puig P, Guillen J. 2014. Massive accumulation of highly polluted sedimentary deposits by river damming. Science of total environment, 497-498, 369-381. https://doi.org/10.1016/j.scitotenv.2014.07.091

Paola C, Mullin J, Ellis C, Mohrig DC, Swenson JB, Parker G, Hickson T, Heller PL, Pratson L, Syvitski J, Sheets B, Strong N. 2001. Experimental stratigraphy. GSA Today, 11 (7), 4–9

Papacostas NC, Bostick BC, Quicksall AN, Landis JD, Sampson M. 2008. Geomorphic controls on groundwater arsenic distribution in the Mekong River Delta, Cambodia. Geology, 36, 891–894. doi: 10.1130/G24791A.1.

Partridge TC amd Maud RR. 2000. The Cenozoic of southern Africa. Oxford University Press. ISBN0195125304, 9780195125306

Partridge TC and Maud RR. 1987. Geomorphic evolution of southern Africa since Mesozoic. South African Journal of Geology, 90 (2), 179–208

Partridge TC, Dollar ES., Moolman J, Dollar LH. 2010. The geomorphic provinces of South Africa, Lesotho and Swaziland: A physiographic subdivision for earth and environmental scientists. Transactions of the Royal Society of South Africa, 65, 1–47. DOI: 10.1080/00359191003652033

Pavlopoulos K, Evelpidou N, Vassilopoulos A. 2009. Mapping geomorphological environments. Springer Science & Business Media. ISBN3642019501, 9783642019500

Pavlovic G, Barisic D, Lovrencie I, Orescanin V, Prohic E. 2005. Use of fallout 137Cs for documenting the chronology of overbank sediments from the river Sava, Croatia, and interpreting their geochemical patterns. Environmental Geology, 47, 475-481. DOI 10.1007/s00254-004-1167-0

Peakall J, Ashworth PJ, Best JL. 2007. Meander-bend evolution, alluvial architecture, and the role of cohesion in sinuous river channels: a flume study. Journal of sedimentary research, 77, 197-212. DOI: 10.2110/jsr.2007.017

Pfister L, Kwadijk J, Musy A, Bronstert A, Hoffmann L. 2004. Climate change, land use change and runoff prediction in the Rhine-Meuse basins. River Research and Applications, 20/3, 229–241

Phillips GW, Marlow KW. 1976. Automatic analysis of gamma-ray spectra from germanium detectors. Nuclear instruments and methods, 137 (3), 525-536. https://doi.org/10.1016/0029-554X(76)90472-9

Phillips JD and Slattery MC. 2007. Downstream trends in discharge, slope, and stream power in a lower coastal plain river. Journal of Hydrology, 34, 290-303. DOI: 10.1016/j.jhydrol.2006.10 .018.

Phillips JD. 1989. Fluvial sediment storage in wetlands 1. JAWRA Journal of the American Water Resources Association, 25 (4), 867–873. Available from: https://doi.org/10.1111/j.1752-1688.1989.tb05402.x

Phillips JD. 1992. Nonlinear dynamical systems in geomorphology: revolution or evolution?. Geomorphology, 5, 219-229. 0169-555X/92/$05.00

Phillips JD. 2009. Changes, perturbations, and responses in geomorphic systems. Progress in physical geography: Earth and Environment, 33 (1), 17-30. https://doi.org/10.1177/0309133309103889

Pickup G and Warner RF. 1976. Effects of hydrologic regime on magnitude and frequency of dominant discharge. Journal of Hydrology, 29, 51-75

Piégay H, Alber A, Slater L, Bourdin L. 2009. Census and typology of braided rivers in the French Alps. Aquatic Sciences, 71, 371–388. DOI: 10.1007/s00027-009-9220-4

Pinay G, Fabre A, Vervier PH, Gazelle F. 1992. Control of C, N, P distribution in soils of riparian forests. Landscape Ecology, 6 (3), 121-132. 10.1007/BF00130025

Pizzuto JE. 1987. Sediment diffusion during overbank flows. Sedimentology, 34, 301-317

Pizzuto JE. 2016. Modelling fluvial morphodynamics. Tools in fluvial geomorphology. John Wiley and Sons Ltd, 442-455

Planet Team. 2017. Planet Application Program Interface: In Space for Life on Earth. San Francisco, CA. https://api.planet.com

Poesen J, Nachtergaele J, Verstraeten G, Valentin C. 2003. Gully erosion and environmental change: importance and research needs. Catena, 50 (2–4), 91–133

Poesen J, Torri D, Vanwalleghem T. 2011. Gully Erosion: Procedures to Adopt When Modelling Soil Erosion in Landscapes Affected by Gullying. In: Morgan R.P.C. & Nearing M.A. (eds.) Handbook of Erosion Modelling. Blackwell Publishing Ltd, Chichester, UK. Chapter 19, 360–386 + Plates 16–19

Pretorius SN, Weepener HL, le Roux JJ, Sumner PD. 2016. SWAT and OBIA based sediment yield analysis in the Tsitsa catchment of the Eastern Cape Province, South Africa. South African Geographers, 315, 315–323

Prosser IP. 1991. A comparison of past and present episodes of gully erosion at Wangrah creek, Southern Tablelands, NSW, Australian Geographic Studies, 29 (I), 137-154

Pulley S and Collins AL. 2024. Soil erosion, sediment sources, connectivity and suspended sediment yields in UK temperate agricultural catchments: Discrepancies and reconciliation of field-based measurements. Journal of Environmental Management, 351, 119810.

R Core Team. 2022. R: A Language and Environment for Statistical Computing. R Foundation for Statistical Computing, Vienna. https://www.R-project.org

Ramos-Scharrón CE and LaFevor MC. 2016. The role of unpaved roads as active source areas of precipitation excess in small watersheds drained by ephemeral streams in the Northeastern Caribbean. Journal of Hydrology, 533, 168–179. DOI:10.1016/j.hydrol.2015.11.051

Ramos-Scharrón CE and MacDonald LH. 2005. Measurement and prediction of sediment production from unpaved roads, St. John, US Virgin Islands. Earth Surface Processes and Landforms, 30, 1283–1304. DOI:10.1002/esp.1201

Rebelo AJ, Emsens WJ, Esler KJ, Meire P. 2018. Quantification of water purification in South African palmiet wetlands. Water Science and Technology, 78 (5), 1199–1207. https:// doi.org/ 10. 2166/ wst. 2018. 389

Reid LM and Dunne T. 1984. Sediment production from forest road surfaces. Water Resources Research, 20 (11), 1753-1761. https://doi.org/10.1029/WR020i011p01753

Rhoads BL. 2020. River dynamics: geomorphology to support management. Cambridge University Press, Cambridge. https:// doi. org/ 10. 1017/ 97811 08164 108. 014

Richardson CJ and Craft CB. 1993. Effective phosphorus retention in wetlands-fact or fiction? In: Moshiri CB (ed) Constructed wetlands for water quality improvement. Lewis Publishing Inc., Boca Raton

Riquier J, Piégay H, Lamouroux N, Vaudor L. 2017. Are restored side channels sustainable aquatic habitat features? Predicting the potential persistence of side channels as aquatic habitats based on their fine sedimentation dynamics. Geomorphology, 295, 507-528. 10.1016/j.geomorph.2017.08.001

Ritchie JC and McHenry JR. 1990. Application of Radioactive Fallout Cesium-137 for Measuring Soil Erosion and Sediment Accumulation Rates and Patterns: A Review. Journal of Environmental Quality, 19 (2), 215-233. https://doi.org/10.2134/jeq1990.00472425001900020006x

Ritchie JC, Finney VL, Oster KJ, and Ritchie CA. 2004. Sediment deposition in the flood plain of Stemple Creek Watershed, northern California. Geomorphology, 61, 347–360

Ritter DF.1975. Stratigraphical implications of coarse grained gravel deposited as overbank sediment, southern Illinois. The Journal of Geology, 83, 1515-1520

Robbins JA, Edgington D. 1975. Determination of Recent Sedimentation Rates in Lake Michigan Using Pb-210 and Cs-137. Geochimica et Cosmochimica Acta, 39, 285-304. http://dx.doi.org/10.1016/0016-7037(75)90198-2

Roberts MH and Strobel CJ. 1985. Evaluation of the toxicity of contaminated sediments in the James River, Virginia. Virginia Institute of Marine Science, William & Mary. https://scholarworks.wm.edu/reports/2611

Robichaud PR and Waldrop TA. 1994. A comparison of surface runoff and sediment yields from low and high severity site preparation burns. Water Resources Bulletin, 30 (1), 27-34

Rodnight H, Duller GAT, Tooth S, Wintle AG. 2005. Optical dating of a scroll-bar sequence on the Klip River, South Africa, to derive the lateral migration rate of a meander bend. The Holocene, 15 (6), 802–811. https:// doi. org/ 10.1191/ 09596 83605hl854ra

Rommens T, Verstraeten G, Bogman P, Peeters I, Poesen J, Govers G, van Rompaey A, Lang A. 2006. Holocene alluvial sediment storage in a small river catchment in the loess area of central Belgium. Geomorphology, 77, 187-201. doi:10.1016/j.geomorph.2006.01.028

Rondeau B, Cossa D, Gagnon P, Bilodeau L. 2000. Budget and sources of suspended sediment transported in the St. Lawrence River, Canada. Hydrological Processes, 14, 21-36. CCC 0885±6087/2000/010021±16$17.50

Rose J, Turner C, Coope GR, Byran MD.1980. Channel Change in a low-land river catchment over the past 13,000 years. In: R.A. Cullingford, D.A. Davidson, and J. Lewin (Editors), Timescales in Geography. Wiley, Chichester, 159-175

Roseboom DP. 1987. Case studies of stream and river restoration. in: Urbana-Champaign, U.o.I.a. (Ed.), Management of the Illinois River System: The 1990's and Beyond: Proceedings: a Governor's Conference on April 1–3, 1987 at Peoria, Illinois for Citizens, Organizations, Industry, and Government Representatives and Resources Management Professionals. Water Resources Center, University of Illinois, 184–194

Rosgen DL. 1994. A classification of natural rivers: Reply. Catena, 22, 169–199. DOI: 10.1016/0341-8162(94)90001-9

Ross KM, Hupp CR, Howard AD. 2004. Sedimentation in floodplains of selected tributaries of the Chesapeake Bay. Riparian Vegetation and Fluvial Geomorphology Water Science and Application, 187-208. doi:10.1029/008wsa14

Rowntree KM and Wadeson RA. 1999. A hierarchical geomorphological model for the classification of selected South African rivers. WRC Report No. 497/1/99

Russell KL, Vietz GJ, Fletcher TD. 2017. Global sediment yields from urban and urbanizing watersheds. Earth-Science Reviews, 168, 73-80. https://doi.org/10.1016/j.earscirev.2017.04.001

Russell KL, Vietz GJ, Fletcher TD. 2018. Urban catchment runoff increases bedload sediment yield and particle size in stream channels. Anthropocene, 23, 53-66. https://doi.org/10.1016/j.ancene.2018.09.001

Saint-Laurent D, Lavoie L, Drouin A, St-Laurent J, Ghaleb B. 2010. Floodplain sedimentation rates, soil properties and recent flood history in southern Québec. Global and planetary change, 70 (1-4), 76-91. https://doi.org/10.1016/j.gloplacha.2009.11.009

Samadi M, Germishuyse T, Van der Walt M. 2005. Understanding South African Soils. ARC-Institute for Soil, Climate and Water: Pretoria

Sambrook Smith GH, Best JL, Leroy JZ, Orfeo O. 2016. The alluvial architecture of a suspended sediment-dominated meandering river: the R ıo Bermejo, Argentina. Sedimentology, 63, 1187-1208. doi: 10.1111/sed.12256

Sánchez-Carrillo S, Álvarez-Cobelas M, Angeler DG. 2001. Sedimentation in the semi-arid freshwater wetland las tablas de Daimiel (Spain). Wetlands, 21, 112–124. https://doi. org/ 10. 1672/ 0277- 5212(2001) 021[0112: SITSAF] 2.0.CO;2

Saucier RT. 1994. Geomorphology and quaternary geologic history of the Lower Mississippi Valley. U.S. Army Engineers, Waterways Experiment Station, Vicksburg, MS.

Saxena DP, Joos P, Van Grieken R, Subramanian V. 2002. Sedimentation rate of the floodplain sediments of the Yamuna river basin (tributary of the river Ganges, India) by using 210Pb and 137Cs techniques. Journal of radioanalytical and nuclear chemistry, 251 (3). https:// doi. org/ 10. 1023/A: 10148 21906600

Schilling EB and Lockaby BG. 2005. Relationships between productivity and nutrient circulation within two contrasting southeastern U.S. floodplain forests. Wetlands, 26, 181-192. https://doi.org/10.1672/0277-5212(2006)26[181:RBPANC]2.0.CO;2

Schilling KE, Palmer JA, Bettis EA III, Jacobson P, Schultz RC, Isenhart TM. 2009. Vertical distribution of total carbon, nitrogen and phosphorus in riparian soils of Walnut Creek, southern Iowa. Catena, 77 (3), 266–273. https://doi. org/ 10. 1016/j. catena. 2009. 02. 006

Schilling KE, Wolter CF, Palmer JA, Beck WJ, Williams FF, Moore PL, Isenhart TM. 2023. An Assessment of Streambank Erosion Rates in Iowa. Environments, 10 (5)

Schlegel P, Huchzermeyer N, Van der Waal B. 2019. Biophysical Monitoring Plan of the Upper Tsitsa River Catchment (T35 A-E). Ecosystem report, Tsitsa Project, Rhodes University

Schnauder I and Sukhodolov A. 2012. Flow in tightly curving meander bend: Effects of seasonal changes in aquatic macrophyte cover, Earth Surface Processes and Landform, 37 (11), 1142-1157. https://doi.org/10.1002/esp.3234

Schuerch M, Rapaglia J, Liebetrau V, Vafeidis A, Reise K. 2012. Salt marsh accretion and storm tide variation: an example from a Barrier Island in the North Sea. Estuaries Coasts, 35, 486–500. doi: 10.1007/s12237-011-9461-z

Schumm SA and Lichty RW.1963. Channel widening and floodplain construction along Cimarron River in South Western Kansas. U.S. Geological Survey Professional Paper, 352-D, 71-78

Schumm SA and Winkley BR (eds).1994. The Variability of Large Alluvial Rivers. ASCE Press. New York, NY

Schumm SA. 1968. River Adjustment to Altered Hydrologic Regime—Murrumbidgee River and Paleochannels, Australia, U.S. Geological Survey Professional Paper 598

Schumm SA. 1969. River metamorphosis, Journal of the Hydraulics Division, Proceedings of the American Society of Civil Engineers, 6352, HYI

Schumm SA. 1977. The Fluvial System. Wiley, New York

Schumm SA. 1979. Geomorphic thresholds: the concept and its applications. Transactions of the Institute of British Geographers, 4 (4), 485–515.https:// doi. org/ 10. 2307/ 622211

Schwenk J and Foufoula-Georgiou E. 2016. Meander cutoffs nonlocally accelerate upstream and downstream migration and channel widening. Geophysical Research Letters, 43 (24), 12437-12445. https://doi.org/10.1002/2016GL071670

Seidl MA, Dietrich WE, Kirchner JW. 1994. Longitudinal profile development into bedrock: an analysis of Hawaiian channels. Journal of Geology, 102, 457-474

Sekely AC, Mulla DC, Bauer DW. 2002. Streambank slumping and its contribution to the phosphorus and suspended sediment loads of the Blue Earth River, Minnesota. Journal of Soil and Water Conservation, 57 (5), 243-250

Sherriff SC, Rowan JS, Melland AR, Jordan P, Fenton O, OhUallachain D. 2015. Identifying the controls of soil loss in agricultural catchments using ex-situ turbidity-based suspended sediment monitoring. Hydrology & Earth System Sciences Discussions., 12, 2707–2740. www.hydrol-earth-syst-sci-discuss.net/12/2707/2015/. doi:10.5194/hessd-12-2707-2015

Shields Jr FD, Cooper CM, Knight SS, Dabney SM. 2002. November. Little Topashaw Creek restoration project: context and overview. In Annual Water Resources Conference

Shields Jr FD, Simon A, Steffen LJ. 2000. Reservoir effects on downstream river channel migration. Environmental Conservation, 27 (1), 54-66. doi:10.1017/S0376892900000072

Shore M, Jordan P, Mellander PE, Kelly-Quinn M, Daly K, Sims JT, Wall DP, Melland AR. 2016. Characterisation of agricultural drainage ditch sediments along the phosphorus transfer continuum in two contrasting headwater catchments Journal of Soils and Sediments, 16 (5), 1643-1654

Sidle R, Ziegler AD, Negishi JN et al. 2006. Erosion processes in steep terrain—Truths, myths, and uncertainties related to forest management in Southeast Asia. Forest Ecology and Management, 224 (1), 199-225. 10.1016/j.foreco.2005.12.019

Simm DJ. 1995. The rates and patterns of overbank deposition on a lowland floodplain. In Foster IDL, Gumell AM, Webb BW (eds). Sediment and Water Quality in River Catchments Wiley. London, 247-264

Simon A and Collison AJC. 2002. Quantifying the Mechanical and Hydrologic Effects of Riparian Vegetation on Streambank Stability. Earth Surface Processes and Landforms, 27, 527-546. https://doi.org/10.1002/esp.325

Simon A and Darby SE. 1999. The nature and significance of incised river channels. Incised river channels: Processes, forms, engineering and management, S. E. Darby and A. Simon, eds, Wiley, New York

Simon A and Hupp CR. 1986. Channel evolution in modified Tennessee channels. Proceedings of the Fourth Interagency Sedimentation Conference, March 1986, vol. 2. Subcommittee on Sedimentation, Las Vegas, NV, 5, 71 – 5-82

Simon A and Thomas RE. 2002. Processes and forms of an unstable alluvial system with resistant, cohesive streambeds, Earth Surface Processes and Landforms, 27, 699–718

Simon A, Curini A, Darby SE, Langendoesn EJ. 1999. Streambank mechanics and the role of bank and near-bank processes in incised channels. In Darby SE and Simon A (eds.). Incised River Channels: Processes, forms, engineering and management, John Wiley and Sons, London, 123-152

Simon A, Dickerson W, Heins A. 2004. Suspended-sediment transport rates at the 1.5-year recurrence interval for ecoregions of the United States: transport conditions at the bankfull and effective discharge?. Geomorphology, 58, 243-262. 10.1016/j.geomorph.2003.07.003

Simon A, Kuhnle R, Dickerson W. 2002. Reference sediment-transport rates for Level III ecoregions for use in developing clean-sediment TMDLs. Proc. Water Resources Planning and Management, EWRI-ASCE, Roanoke, 10.

Six J, Conant RT, Paul EA, Paustian K. 2002. Stabilization mechanisms of soil organic matter: Implications for C-saturation of soils. Plant and Soil, 241, 155-176. 196.15.205.195

Slingerland R and Smith ND. 2004. River avulsions and their deposits. Annual Review of Earth and Planetary Sciences, 32, 257-285. https://doi.org/10.1146/annurev.earth.32.101802.120201

Smith BJ. 1982. Effects of climate and land-use change on gully development, an example from Northern Nigeria, Zietschrift fur Geomorphologie, 44, 33-51

Smith DG and Smith ND. 1980. Sedimentation in anastomosed river systems: examples from alluvial valleys near Banff, Alberta J. Sediment. Petrol., 50, 157-164

Smith DG. 1974. Aggradation of the Alexandra-North Saskatchewan River, Banff Park, Alberta. In: M. Morisawa (Editor), Fluvial Geomorphology. Binghampton, New York, 201-219

Smith DG. 2001. A Protocol for Standardizing Secchi Disk Measurements, Including Use of a Viewer Box. Journal of Lake and Reservoir Management, 17, 90–96

Smith HG, Sheridan GJ, Lane PNJ, Snyman P, Haydon S. 2011. Wildfire effects on water quality in forest catchments: a review with implications for water supply. Journal of Hydrology, 396 (1–2), 170–192. https:// doi. org/ 10. 1016/j.jhydr ol. 2010. 10. 043

Smith JS, Chandler J, Rose J. 2009. High spatial resolution data acquisition for the geosciences: kite aerial photography. Earth Surface Processes and Landforms, 34, 155–161. DOI: 10.1002/esp

Smith ND. 1971. Transverse bars and braiding in the lower Platte River, Nebraska. Geological Society of America Bulletin., 82, 3407- 3420

Šmuc NR, Dolenec M, Kramar S and Mladenović A. 2018. Heavy metal signature and environmental assessment of nearshore sediments: port of Koper (Northern Adriatic Sea). Geosciences, 8(11), 398

Snyman G. 2020. An investigation into the fire regimes of the upper Tsitsa River catchment. MSc Thesis. Rhodes University

Sommers LE and Nelson DW. 1972. Determination of Total Phosphorus in Soils: A Rapid Perchloric Acid Digestion Procedure. Soil Science Society of America Journal, 36 (6), 902-904. https://doi.org/10.2136/sssaj1972.03615995003600060020x

South African Department of Forestry, Fisheries and the Environment (DFFE). South African National Land Cover dataset. Available at https://egis.environment.gov.za/data_egis/data_download/current Accessed in December 2023.

South African Surveyor General. N.d. 1:10 000 orthophotographs. Available from https://ngi.dalrrd.gov.za/index.php/what-we-do/maps-and-geospatial-information/35-map-products/50-1-10-000-orthophoto-maps. Accessed on 2020

Steegen A, Govers G, Takken I, Nachtergaele J, Poesen J, Merckx R. 2001. Factors Controlling Sediment and Phosphorus Export from Two Belgian Agricultural Catchments. Journal of Environmental Quality, 30 (4), 1249-1258. https://doi.org/10.2134/jeq2001.3041249x

Stevenson FJ. 1986. Cycles of soil: Carbon, nitrogen, phosphorus, sulfur, micronutrients. John Wiley and Sons, New York

Stoeckel DM and Miller-Goodman MS. 2001. Seasonal Nutrient Dynamics of Forested Floodplain Soil Influenced by Microtopography and Depth. Soil Science Society of America Journal, 65 (3), 922-931

Stolt MH, Genthner MH, Daniels WL, Groover VA. 2001. Spatial Variability in Palustrine Wetlands. Soil Science Society of America Journal, 65 (2), 527-535. https://doi.org/10.2136/sssaj2001.652527x

Stone PM and Walling DE. 1997. Particle size selectivity considerations in suspended sediment budget investigations. Water, Air, and Soil Pollution, 99 (1), 63–70. Available from: https://doi.org/10.1007/BF02406845

Stott TA and Mount NJ. 2004. Plantation Forestry Impacts on Sediment and Channel Dynamics in the UK: A Review, Progress in Physical Geography, 28 (2), 197-240. 10.1191/0309133304pp410ra

Stouthamer E and Berendsen HJA. 2000. Factors Controlling the Holocene Avulsion History of the Rhine-Meuse Delta (The Netherlands). Journal of Sedimentary Research, 70 (5), 1051–1064. https://doi.org/10.1306/033000701051

Straub M, Sigman DM, Ren H, et al. 2013. Changes in North Atlantic nitrogen fixation controlled by ocean circulation. Nature, 501 (7466). 10.1038/nature12397

Sundborg A. 1956. The River Klaralven, a study of fluvial processes. Geografiska annaler, 38, 127-316

Surian N. 2002. Downstream variation in grain size along an Alpine river: Analysis of controls and processes. Geomorphology, 43, 137-149. 10.1016/S0169-555X(01)00127-1

Swanson FJ, Kratz TK, Caine N, Woodmansee RG. 1988. Landform Effects on Ecosystem Patterns and Processes. BioScience, 38 (2), 92-98

Swanson K. 2013. The rate and pattern of deposition on lowland river floodplains. PhD Thesis, University of California, Berkeley

Swanson KM, Watson E, Aalto R, Lauer LW, Bera MT, Marshall A, Taylor MP, Apte SC and Dietrich WE. 2008. Sediment load and floodplain deposition rates: Comparison of the Fly and Strickland Rivers, Papua New Guinea. Journal of Geophysical Research, 11, F01S03. https://doi. org/10.1029/2006JF000623

Sweet RJ, Nicholas AP, Walling DE, Fang X, .2003. Morphological controls on medium-term sedimentation rates on British lowland river floodplains. Hydrobiologia, 494, 177–183

Terry JP, Garimella S and Kostaschuk RA. 2002. Rates of floodplain accretion in a tropical island river system impacted by cyclones and large floods. Geomorphology, 42, 171–182

Terry JP, Lal R and Garimella S. 2011. Assessing the utility of 210Pb geochronology for estimating sediment accumulation rates on river floodplains in Fiji. Singapore. Journal Tropical Geography, 32, 102–114

Theron SN, Weepener HL, Le Roux JJ, Engelbrecht CJ. 2021. Modelling potential climate change impacts on sediment yield in the Tsitsa River catchment, South Africa. Water SA, 47 (1). http://dx.doi.org/10.17159/wsa/2021.v47.i1.9446

Thoma DP, Gupta SC, Bauer ME, Kirchoff CE. 2005. Airborne laser scanning for riverbank erosion assessment. Remote sensing of Environment, 95 (4), 493-501

Thomas G, Cojan I, Haurine Frédéric, Poirier Catherine, Marie-Anne Bruneaux. 2021. Demonstrating the influence of sediment source in dredged sediment recovery for brick and tile production. Resources, Conservation and Recycling. ff10.1016/j.resconrec.2021.105653ff. ffhal-03595683f

Thomas TS, Schlosser CA, Strzepek K, Robertson RD. 2022. Using a Large Climate Ensemble to Assess the Frequency and Intensity of Future Extreme Climate Events in Southern Africa. Font. Clim., 4. https://doi.org/10.3389/fclim.2022.787721

Thompson DM. 2011. The velocity-reversal hypothesis revisited. Progress in Physical Geography, 35 (1), 123-132

Thoms MC, Foster JM, Gawne B. 2000. Flood-plain sedimentation in a dryland river: the River Murry, Australia. IAHS Publication(International Association of Hydrological Sciences), 263, 227–236

Thoms MC, Hill SM, Spry MJ, Mount TJ, Chen XY, Sheldon F. 2004. The geomorphology of the Darling Basin. In The Barwon Darling Catchment. In The Darling, Breckwodth R, Boden R, Andrew J (eds). Murray Darling basin Commission: Canberra, 29–54

Thoms MC. 1998. Floodplain-wetlands: transient storage areas of sediment and pollutants. In: Williams WD (ed) Wetlands in a dry land: understanding for management. Environment Australia, Biodiversity Group, Canberra

Thoms MC. 2003. Floodplain–river ecosystems: lateral connections and the implications of human interference. Geomorphology, 56/3-4, 335–349

Thonon I, Middelkoop H, van der Perk M. 2007. The influence of floodplain morphology and river works on spatial patterns of overbank deposition. Netherlands Journal of Geosciences, 86 (1), 63-75

Thorne CR. 1981. Field measurements of rates of bank erosion and bank material strength. Erosion and Sediment Transport Measurement (Proceedings of the Florence Symposium, June 1981). IAHS Publ. no., 133, 503-512

Thorne CR. 1982. Processes and mechanisms of river bank erosion. Gravel-bed rivers, Hey RD, Bathurst JC, Thorne CR (eds). Wiley, Chichester, 227-259

Thorne CR. 1991. Analysis of channel instability due to catchment landuse change, In Peters, N.E., and Walling, D.E. (eds), Sediment and Stream Water Quality in a Changing Environment, IAHS 203, 111-122

Thorne CR. 1991. Bank erosion and meander migration of the Red and Mississippi rivers, USA. IAHS Wallingford, 301–313

Thorne CR. 1992. Bend Scour and Bank Erosion on the Meandering Red River, Louisiana, in Carling PA, and Petts GE (eds.), Lowland Floodplain Rivers- Geomorphological Perspectives, John Wiley & Sons, Chichester, UK, 95–115

Thorne CR. 1997. Channel Types and Morphological Classification (Chapter 7), in Thorne CR, Hey RD, and Newsom MD (eds.), Applied Fluvial Geomorphology for River Engineering and Management, John Wiley & Sons, Chichester, UK, 175–222

Tiessen H, Stewart JWB, Moir JO. 1983. Changes in organic and inorganic phosphorus composition of two grassland soils and their particle size fractions during 60–90 years of cultivation. European Journal of Soil Science, 34 (4), 815-823

Titus J. 1990. Responding to global warming along the U.S. coast. Changing Climate and the Coast Intergovernmental Panel on Climate Change, U.S. Environmental Protection Agency

Tockner K and Stanford JA. 2002. Riverine floodplains: present state and future trends. Environmental Conservation, 29, 308–330

Toonen WHJ, Kleinhans MG, Cohen KM. 2012. Sedimentary architecture of abandoned channel fills. Earth Surf Proc Land, 37, 459–472. https:// doi. org/ 10. 1002/ esp. 3189

Tooth S, Brandt D, Hancox PJ, McCarthy TS. 2004. Geological controls on alluvial river behaviour: a comparative study of three rivers on the South African Highveld. Journal of African Earth Sciences, 38, 79-97

Tooth S, Grenfell MC, Thomas A, Ellery WN. 2015. Wetlands in Drylands: "Hotspots" of Ecosystem Services in Marginal Environments (GSDR Science Brief)

Tooth S, McCarthy T, Rodnight H, Keen-Zebert A, Rowberry M, Brandt, D. 2014. Late Holocene development of a major fluvial discontinuity in floodplain wetlands of the Blood River, eastern South Africa. Geomorphology, 205, 128–141

Tooth S, McCarthy TS, Brandt D, Hancox PJ, Morris R. 2002. Geological controls on the formation of alluvial meanders and floodplain wetlands: the example of the Klip River, eastern Free State, South Africa. Earth Surface Processes and Landforms: The Journal of the British Geomorphological Research Group, 27 (8), 797–815. https:// doi. org/ 10. 1002/ esp. 353

Tooth S, Rodnight H, Duller GAT, McCarthy TS, Marren PM, Brandt D. 2007. Chronology and controls of avulsion along a mixed bedrock-alluvial river. GSA Bulletin, 119 (3–4), 452–461. https:// doi. org/ 10. 1130/ B26032.1

Torres A, Brandt J, Lear K, Liu J .2017. A looming tragedy of the sand commons. Science, (80-) 357, 970–971. https://doi.org/10.1126/science.aao0503

Tower WS. 1904. The development of cutoff meanders. Bulletin of the American Geographical Society of New York, 36, 589–599

Tranmer AW, Tonina D, Benjankar R, Tiedemann M, Goodwin P. 2015. Floodplain persistence and dynamic-equilibrium conditions in a canyon environment. Geomorphology, 250, 147-158

Triantafillou SP. 2021. The role of geomorphic variability on floodplain function: an analysis of sediment and phosphorus deposition. UVM College of Arts and Sciences College Honors Theses. 81. https://scholarworks.uvm.edu/castheses/81

Trimble SW. 1981. Changes in sediment storage in the Coon Creek basin, Driftless area, Wisconsin, 1953-1975. Science, 214, 181-183

Trimble SW. 1983. A sediment budget for Coon Creak basin in the Driftless Area, Wisconsin, 1853-1977. American Journal of Science, 283, 454-474

Tsitsa Project. N.d. Accessed from https://www.ru.ac.za/tsitsaproject/. Accessed in 2020

Turner RE, Baustian JJ, Swenson EM, Spicer JS. 2006. Wetland Sedimentation from Hurricanes Katrina and Rita. Science, 314

Tweel AW and Turner RE. 2012. Landscape-Scale Analysis Of Wetland Sediment Deposition From Four Tropical Cyclone Events. Plos One, 7 (11). https://doi.org/10.1371/journal.pone.0050528

U.S. Army Corps of Engineers. 1983. Chief's annual report; Annual report FY 83 of the Chief of Engineers on Civil Works activities. United States. Army. Corps of Engineers. Available at https://usace.contentdm.oclc.org/digital/collection/p16021coll6/id/652/

UNEP. 1997. World atlas of desertification. United Nations Environment Programme.

Uwimana A, van Dam AA, Gettel GM, Irvine K. 2018. Effects of agricultural land use on sediment and nutrient retention in valley-bottom wetlands of Migina catchment, southern Rwanda. Journal of Environmental Management, 219, 103–114. https:// doi. org/ 10. 1016/j. jenvm an. 2018. 04. 094

Valentin C, Poesen J, Yang L. 2005. Gully erosion: Impacts, factors and control. Catena, 63 (2-3), 132-153

van de Lageweg WI, van Dijk WM, Baar AW, Rutten J, Kleinhans MG. 2014. Bank pull or bar push: what drives scroll-bar formation in meandering rivers?, Geology, 42, 319–322. doi:10.1130/G35192.1

Van der Lee GEM, Olde Venterink H., Asselman NEM. 2004. Nutrient retention in floodplains of the Rhine distributaries in The Netherlands. River Research and Applications, 20, 315–325

van der Waal BW and Rowntree K. 2018. Landscape Connectivity in the Upper Mzimvubu River Catchment: An Assessment of Anthropogenic Influences on Sediment Connectivity. Land Degradation and Development, 29 (3), 713-723. https://doi.org/10.1002/ldr.2766

Van der Waal BW, Rowntree KM, Pulley S. 2015. Flood bench chronology and sediment source tracing in the upper Thina catchment, South Africa: The role of transformed landscape connectivity. Journal of Soils and Sediments, 15 (12), 2398–2411. https://doi.org/10.1007/s11368-015-1185-4

van der Waal BW. 2015. Sediment connectivity in the upper Thina Catchment, Eastern Cape, South Africa. PhD Thesis. Rhodes University

Van Oost K, Govers G, Desmet P. 2000. Evaluating the effects of changes in landscape structure on soil erosion by water and tillage. Landscape Ecology, 15 (6), 577-589

Vanacker V, Molina A, Govers G, Poesen J, Dercon G, Deckers S. 2005. River channel response to short-term human-induced change in landscape connectivity in Andean ecosystems. Geomorphology, 72 (1–4), 340-353

Vanmaercke M, Poesen J, Verstraeten G, de Vente J, Ocakoglu F. 2011. Sediment yield in Europe: spatial patterns and scale dependency. Geomorphology, 130, 142-161

Vanoni VA. 1977. Sedimentation Engineering. ASCE, New York, 745

Verhoeven JT, Arheimer B, Yin C, Hefting MM. 2006. Regional and global concerns over wetlands and water quality. Trends in ecology & evolution, 21 (2), 96–103. https:// doi. org/10. 1016/j. tree. 2005. 11. 015

Vetter S. 2007. Soil erosion in the Herschel district of South Africa: changes over time, physical correlates and land users' perceptions. African Journal of Range and Forage Science, 24 (2), 77-86

Vietz GJ, Walsh CJ, Fletcher TD. 2016. Urban hydrogeomorphology and the urban stream syndrome: Treating the symptoms and causes of geomorphic change. Progress in Physical Geography: Earth and Environment, 40 (3), 480-492. https://doi.org/10.1177/0309133315605048

Vivian-Smith G. 1997. Microtopographic Heterogeneity and Floristic Diversity in Experimental Wetland Communities. Journal of Ecology, 85 (1), 71-82. https://doi.org/10.2307/2960628

Viviroli D, Dürr H, Messerli B, Meybeck M, Weingartner R. 2007. Mountains of the world, water towers for humanity: Typology, mapping, and global significance. Water Resources Research, 43 (7), W07447

Walker TW and Adams AFR. 1958. Studies on soil organic matter: 1. Soil Sci., 85, 307-318

Walker TW and Adams AFR. 1959. Studies on soil organic matter: 2. Soil Sci., 87, 1-10

Walker TW and Syers JK. 1976. The fate of phosphorus during pedogenesis. Geoderma, 15 (1), 1-19

Walker TW. 1964. The significance of phosphorus in pedogenesis, Hallsworth EG, Crawford DV (Eds.), Experimental Pedology, Butterworths, London, 295-315

Walling DE and He Q. 1992. Interpretation of caesium-137 profiles in lacustrine land other sediments: the role of catchment-derived inputs. Hydrobiologia, 235/236, 219-230

Walling DE and He Q. 1994. Rates of overbank sedimentation on the flood plains of several British rivers during the past 100 years. Variability in Stream Erosion and Sediment Transport (Proceedings of the Canberra Symposium), IAHS Publication No. 224, 203-210.

Walling DE and He Q. 1996. Interpreting particle size effects in the adsorption of 137Cs and unsupported 210Pb by mineral soils and sediments. Journal of Environmental Radioactivity, 30 (2), 117-137

Walling DE and He Q. 1996. Use of fallout Pb-210 measurements to investigate longer-term rates and patterns of overbank sediment deposition on the floodplains of lowland rivers. Earth surface processes and landforms, 21 (2), 141-154

Walling DE and He Q. 1997. Investigating spatial patterns of overbank sedimentation on river floodplains. Water, Air, and Soil Pollution, 99, 9-20

Walling DE and He Q. 1997. Use of fallout 137Cs in investigations of overbank sediment deposition on river floodplains. Catena, 29 (3-4), 263-282

Walling DE and He Q. 1998. The spatial variability of overbank sedimentation on river floodplains. Geomorphology, 24 (2–3), 209–223. Available from: https://doi.org/10.1016/S0169-555X(98)00017-8

Walling DE and He Q. 1999. Using fallout lead-210 measurements to estimate soil erosion on cultivated land. Soil Science Society of America Journal, 63 (5), 1404-1412

Walling DE and Moorehead PW. 1989. The particle size characteristics of fluvial suspended sediment: an overview. Sediment/Water Interactions: Proceedings of the Fourth International Symposium. Springer Netherlands, 125-149

Walling DE and Owens PN. 2003. The role of overbank floodplain sedimentation in catchment contaminant budgets. Hydrobiologia, 494 (1-3), 83–91. Available from: https://doi.org/10.1023/A:1025489526364

Walling DE and Quine TA. 1992. The use of caesium-137 measurements in soil erosion surveys. In: Erosion and sediment transport monitoring programmes in River Basins (Proceedings of the Oslo Symposium. August 1992). IAHS Publ. no. 210, 143–152

Walling DE and Quine TA. 1993. Using Chernobyl-derived fallout radionuclides to investigate the role of downstream conveyance losses in the suspended sediment budget of the River Severn, United Kingdom. Physical Geography, 14 (3), 239–253. Available from: https://doi.org/10.1080/02723646.1993.10642478

Walling DE, Collins AL, Jones PA, Leeks GJL, Old G. 2006. Establishing fine-grained sediment budgets for the Pang and Lambourn LOCAR catchments, UK. Journal of hydrology, 330 (1-2), 126-141

Walling DE, Collins AL, Stroud RW. 2008. Tracing suspended sediment and particulate phosphorus sources in catchments. Journal of Hydrology, 350 (3-4), 274-289

Walling DE, Collins AL. 2005. Suspended sediment sources in British rivers. Sediment budgets. IAHS Press Wallingford, 1 (291), 2005123-33

Walling DE, He Q, Blake WH. 2000. River flood plains as phosphorus sinks. IAHS Publication (International Association of Hydrological Sciences), 263, 211-218

Walling DE, He Q, Nicholas AP. 1996. Floodplains as suspended sediment sinks: in Anderson MG, Walling DE and Bates PD (Eds), Floodplain Processes, Wiley, Chichester, 399-440.

Walling DE, He Q, Quine T. 1996. Use of fallout radionuclide measurements in sediment budget investigations. Geomorphologie: relief, processus, environment, 2 (3), 17-27

Walling DE, Owens PN and Leeks GJ. 1998. The role of channel and floodplain storage in the suspended sediment budget of the River Ouse, Yorkshire, UK. Geomorphology, 2 2(3–4), 225–242. Available from: https://doi.org/10.1016/S0169-555X(97)00086-X

Walling DE, Owens PN and Leeks GJ. 1999. Rates of contemporary overbank sedimentation and sediment storage on the floodplains of the main channel systems of the Yorkshire Ouse and River Tweed, UK. Hydrological Processes, 13 (7), 993–1009. Available from: https://doi.org/10.1002/(SICI)1099-1085(199905)13:7<993::AIDHYP786>3.0.CO;2-C

Walling DE, Owens PN, Carter J, Leeks GJL, Lewis S, Meharg AA, Wright J. 2003. Storage of sediment-associated nutrients and contaminants in river channel and floodplain systems. Applied Geochemistry., 18 (2), 195–220. https:// doi.org/ 10. 1016/ S0883- 2927(02) 00121-X

Walling DE, Webb B, Russell MA. 1997. Sediment-associated nutrient transport in UK rivers. IAHS Publications-Series of Proceedings and Reports-International Association Hydrological Sciences 243:69–84

Walling DE, Zhang Y, He Q. 2011. Models for deriving estimates of erosion and deposition rates from fallout radionuclide (caesium-137, excess lead-210 and beryllium-7) measurements and the development of

user-friendly software for model implementation. In Impact of Soil Conservation Measures on Erosion Control and Soil Quality, IAEA, Vienna, 11-33

Walling DE. 1983. The sediment delivery problem. Journal of hydrology, 65 (1-3), 209-237

Walling DE. 1996. Erosion and sediment yield in a changing environment. Geological Society, London, Special Publications, 115 (1), 43-56

Walling DE. 1999. Linking land use, erosion and sediment yields in river basins. Hydrobiologia, 410, 223–240

Walling DE. 2005. Tracing suspended sediment sources in catchments and river systems. Science of the total environment, 134 (1-3), 159-184

Wallinga J, Hobo N, Cunningham AC, Versendaal AJ, Middelkoop H, Makaske B. 2010. Sedimentation rates on embanked floodplains determined through quartz optical dating. Quaternary Geochronology, 5 (2–3), 170–175. https:// doi.org/ 10. 1016/j. quageo. 2009. 01. 002

Walsh CJ, Fletcher TD, Burns MJ. 2012. Urban Stormwater Runoff: A New Class of Environmental Flow Problem. PLoS ONE, 7 (9). e45814. https://doi.org/10.1371/journal.pone.0045814

Walsh EA, Kirkpatrick JB, Pockalny R, Sauvage J, Spivack AJ, Murray RW, Sogin ML, D'Hondt S. 2016. Relationship of Bacterial Richness to Organic Degradation Rate and Sediment Age in Subseafloor Sediment. Applied and environmental microbiology, 82 (16), 4994-4999. doi: 10.1128/AEM.00809-16. PMID: 27287321; PMCID: PMC4968545

Wang F, Zhou B, Xu J, Song L, Wang X. 2009. Application of neural network and MODIS 250m imagery for estimating suspended sediments concentration in Hangzhou Bay, China. Environmental Geology, 56, 1093-1101.

Wang GP, Liu JS, Tang H. 2004. The long-term nutrient accumulation with respect to anthropogenic impacts in the sediments from two freshwater marshes (Xianghai Wetlands, Northeast China). Water research, 38 (20), 4462-4474

Wang X, Xiao X, Zou Z, Chen B, Ma J, Dong J, Doughty RB, Zhong Q, Qin Y, Dai S, Li X, Zhao B, Li B. 2020. Tracking annual changes of coastal tidal flats in China during 1986–2016 through analyses of Landsat images with Google Earth Engine. Remote Sensing of Environment, 238. https:// doi. org/ 10. 1016/j. rse. 2018. 11. 030

Ward JV, Tockner K, Schlemer F. 1999. Biodiversity of floodplain river ecosystems: ecotones and connectivity. Regulated Rivers: Research & Management, 15 (1-3), 125-139. https://doi.org/10.1002/(SICI)1099-1646(199901/06)15:1/3<125::AID-RRR523>3.0.CO;2-E

Warner RF. 1987. Spatial adjustment to temporal variations in flood regime in some Australian Rivers, In Richards, K.S. (ed), River Channel Changes, Environment and Process, Basil Blackwell, Oxford, 14-40

Warner RF. 1997. Floodplain stripping: another form of adjustment to secular hydrologic regime change in Southeast Australia. Catena, 30 (4), 263-282. https://doi.org/10.1016/S0341-8162(97)00014-3

Weigelhofer G, Hein T, Bondar-Kunze E. 2018. Phosphorus and Nitrogen Dynamics in Riverine Systems: Human Impacts and Management Options. In: Schmutz, S., Sendzimir, J. (eds) Riverine Ecosystem Management. Aquatic Ecology Series, 8. Springer, Cham. https://doi.org/10.1007/978-3-319-73250-3_10

Weis DA, Callaway JC, Gersberg RM. 2001. Vertical Accretion Rates and Heavy Metal Chronologies in Wetland Sediments of the Tijuana Estuary. Estuaries, 24 (6), 840–850. https://doi.org/10.2307/1353175

Wemple BC, Jones JA. 2003. Runoff production on forest roads in a steep, mountain catchment. Water Resources Research, 39 (8). https://doi.org/10.1029/2002WR001744

Wentworth CK. 1922. A scale of grade and class terms for clastic sediments. The Journal of Geology, 30(5), 377–392. Available from: https://doi.org/10.1086/622910

Wiener KD, Schlegel PK, Grenfell SE and van der Waal B. 2022. Contextualising sediment trapping and phosphorus removal regulating services: a critical review of the influence of spatial and temporal variability in geomorphic processes in alluvial wetlands in drylands. Wetlands Ecology and Management, 4 (4), 1–34. Available from: https://doi.org/10.1007/s11273-022-09861-9

Wigginton JD, Lockaby GB, Trettin CC. 2000. Soil organic matter formation and sequestration across a forested floodplain chronosequence. Ecological Engineering, 15, 141-155. SO925-SS74(99)00080-4

Wilkinson SN, Olley JM, Prosser IP, Read AM. 2005. Targeting erosion control in large river systems using spatially distributed sediment budgets, Geomorphological Processes and Human Impacts in River Basins. International Association of Hydrological Sciences Publication No. 299 IAHS Press, Wallingford, UK, 56–64

Williams EG and Saunders WMH. 1956. Distribution of phosphorus in profiles and particle-size fractions of some Scottish soils. Journal Soil Science, 7, 90-108

Williams GP and Wolman MG. 1984. Downstream effects of dams on alluvial rivers. Professional Paper 1286, USGS, 10.3133/pp1286

Wilson CG, Kuhnle RA, Bosch DD, Steiner JL, Starks PJ, Tomer MD, Wilson GV. 2008. Quantifying relative contributions from sediment sources in CEAP watersheds. Journal of Soil Water Conservation, 63, 639–649

Wissmar RC and Bisson PA (eds). 2003. Strategies for restoring river ecosystems: sources of variability and uncertainty in natural and managed systems. American Fisheries Society, Bethesda, Maryland

Wohl E, Bledsoe BP, Jacobson RB, Poff NL, Rathburn SL, Walters DM, et al. 2015. The natural sediment regime in rivers: Broadening the foundation for ecosystem management. Bioscience, 65 (4), 358–371. Available from: https://doi.org/10.1093/biosci/biv002

Wohl E, Lininger K, Scott DN. 2018. River beads as a conceptual framework for building carbon storage and resilience to extreme climate events into river management. Biogeochemistry, 141 (3), 365-383. 10.1007/s10533-017-0397-7

Wohl E. 2021. An Integrative Conceptualization of Floodplain Storage. Reviews of Geophysics, 59 (2). https://doi.org/10.1029/2020RG000724

Wolf S, Esser V, Lehmkuhl F, Schüttrumpf H. 2022. Long-time impact of a large dam on its downstream river's morphology: determined by sediment characteristics, pollutants as a marker, and numerical modelling. Journal Sediment Environment. https://doi.org/10.1007/s43217-022-00103-9

Wolman MG and Leopold L B. 1957. River floodplains: some observations on their formation, US Geological Survey Professional Paper 282-C, 109

Wolman MG and Miller JP. 1960. Magnitude and Frequency of Forces in Geomorphic Processes. The Journal of Geology, 68 (1). https://doi.org/10.1086/626637

Woodward J and Foster I. 1997. Erosion and Suspended Sediment Transfer in River Catchments: Environmental Controls, Processes and Problems. Geography, 353-376

Woodyer KD.1975. Concave bank benches on the Barwon River N.S.W. Australia. Australian Geographer, 13, 36-40

Wren DG, Davidson GR, Walker WG, Galicki SJ. 2008. The evolution of an oxbow lake in the Mississippi alluvial floodplain, Journal of Soil and Water Conservation, 63, 129-135, https://doi.org/10.2489/jswc.63.3.129, 2008

Wren DG, Taylor JM, Rigby JR, Locke MA, Yasarer LMW. 2019. Short term sediment accumulation rates reveal seasonal time lags between sediment delivery and deposition in an oxbow lake. Agriculture, Ecosystems and Environment, 281, 92-99

Xu J. 1998. Naturally and anthropogenically accelerated sedimentation in the lower Yellow River, China, over the past 13,000 years. Geografiska Annaler Series A, 80, 67–77. https:// doi. org/ 10. 1111/j. 0435- 3676. 1998. 00027.x

Yang SL, Belkin LM, Belkina AI, Zhao QY, Zhu J, Ding XD. 2003. Delta response to decline in sediment supply from the Yangtze River: evidence of the recent four decades and expectations for the next half-century. Estuarine, Coastal and Shelf Science, 57, 589-599

Yang SL, Milliman JD, Xu KH, Dena B, Zhang XY, Luo XX. 2014. Downstream sedimentary and geomorphic impacts of the Three Gorges Dam on the Yangtze River. Earth-Science Reviews, 138, 469-486

Yarbro LA, Carlson PR, Fisher TR, Chanton JP, Kemp WM. 1983. A sediment budget for the Choptank River estuary in Maryland, USA. Estuarine, Coastal and Shelf Science, 17 (5), 555-570

Young EO, Ross DS, Alves C, Villars T. 2012. Soil and landscape influences on native riparian phosphorus availability in three Lake Champlain Basin stream corridors. Journal of soil and water conservation, 67 (1), 1-7

Zedler JB and Kercher S. 2005. Wetland resources: Status, trends, ecosystem services and restorability. Annual Review of Environment and Resources, 30, 39–74. https:// doi. org/ 10. 1146/ annur ev. energy. 30.050504. 144248

Zheng F. 2006. Effect of vegetation changes on soil erosion on the Loess Plateau. Pedosphere, 16 (4), 420-427. https://doi.org/10.1016/S1002-0160(06)60071-4

Ziegler CK and Nisbet BS. 1995. Long-Term Simulation of Fine-Grained Sediment Transport in Large Reservoir. Journal of Hydraulic Engineering, 121 (11)

Zinger JA, Rhoads BL, Best JL, Johnson KK. 2013. Flow structure and channel morphodynamics of meander bend chute cutoffs: A case study of the Wabash River, USA, Journal of Geophysical Research: Earth Surface, 118, 2468–2487. doi:10.1002/jgrf.20155

Zinger JA, Rhoads BL, Best JL. 2011. Extreme sediment pulses generated by bend cutoffs along a large meandering river. Nature Geoscience, 4 (10), 675-678

APPENDIX 1- CHAPTER 4 MAPS

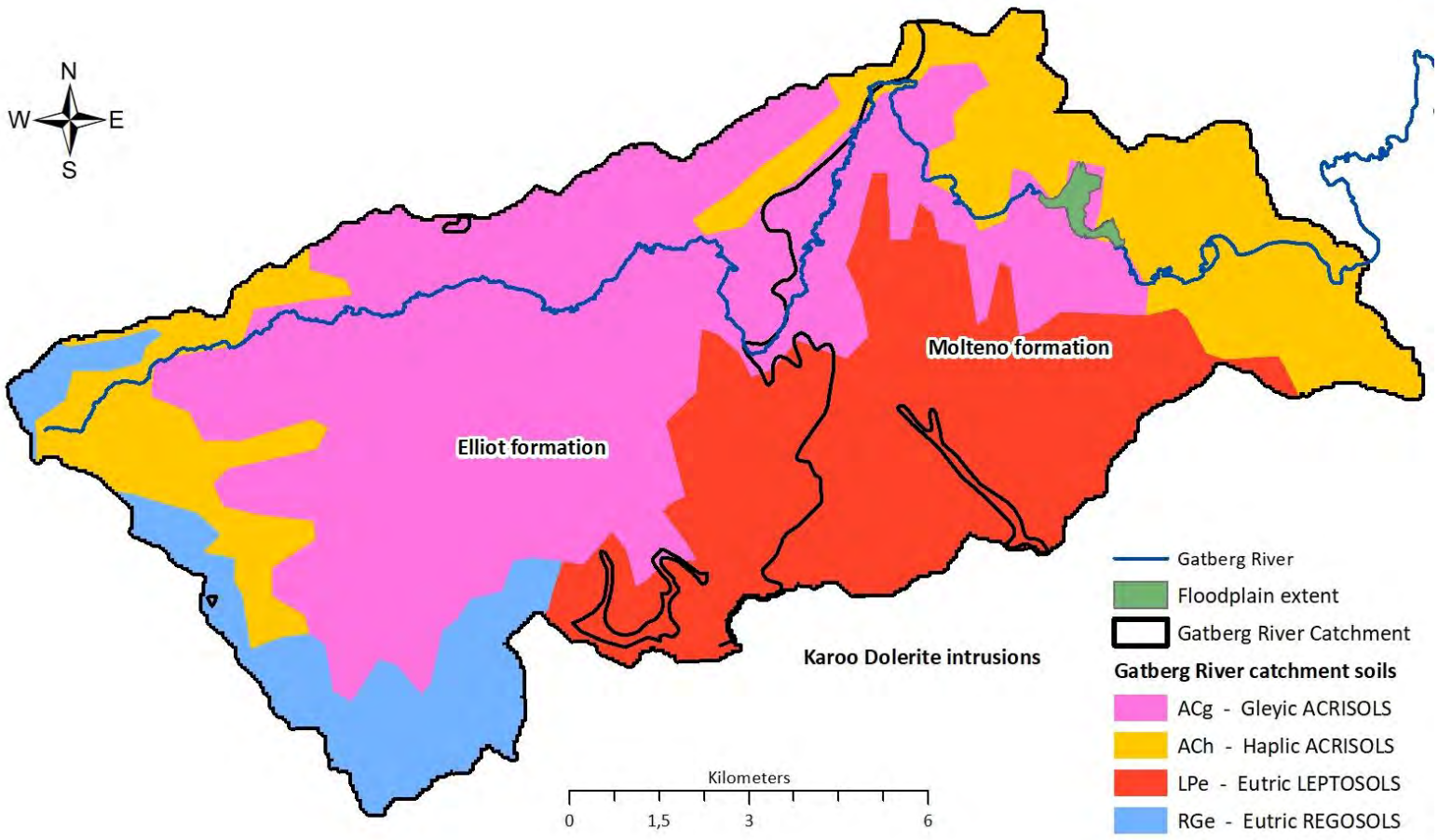

Soil properties for the Gatberg River catchment (spatial dataset from Dijkshoorn et al. 2008)

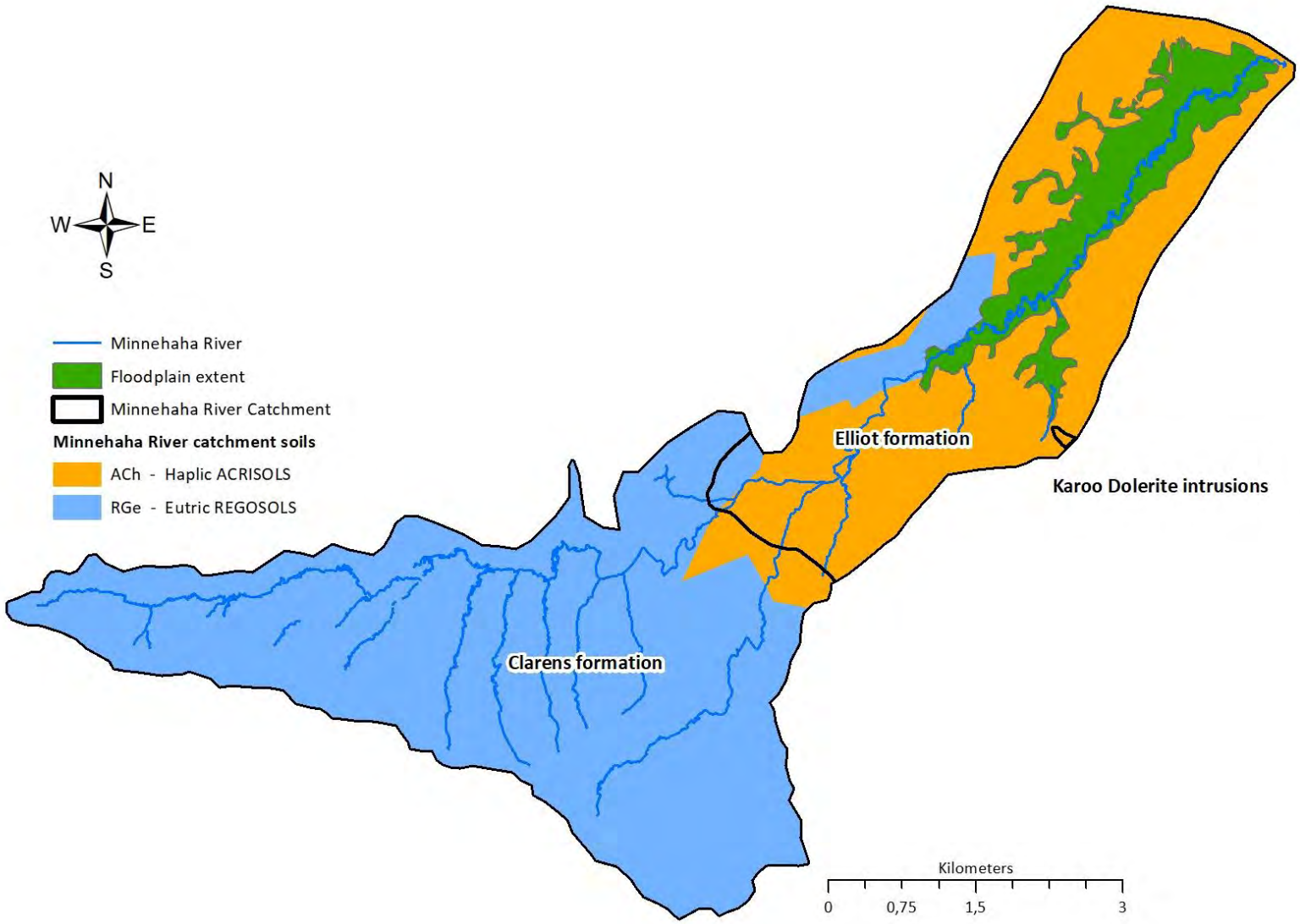

Soil properties for the Minnehaha River catchment (spatial dataset from Dijkshoorn et al. 2008)

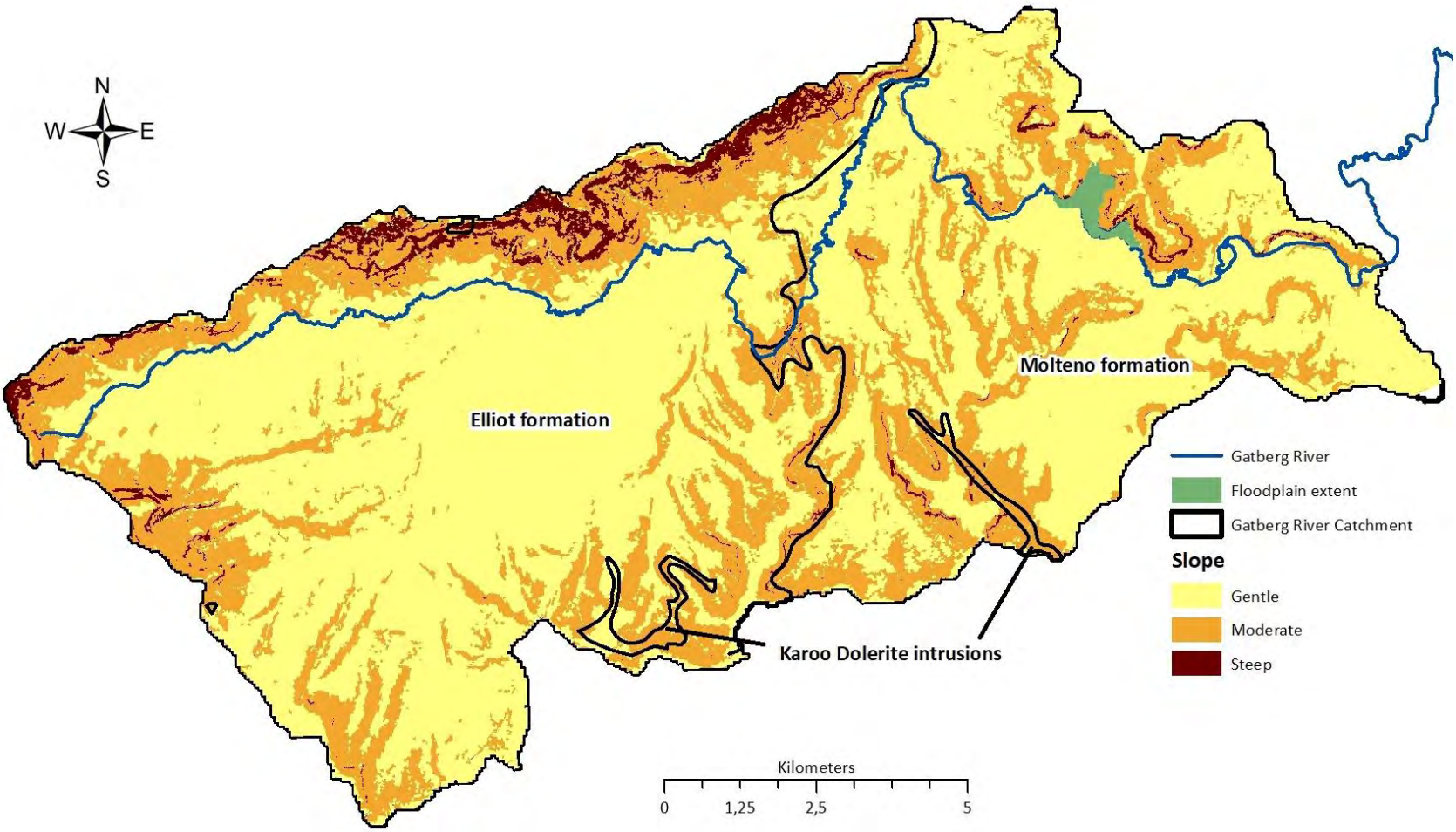

A slope map indicating gentle (< 5), moderate (5-20) and steep (> 20) slopes for the Gatberg River catchment. Also indicated are the geological provinces.

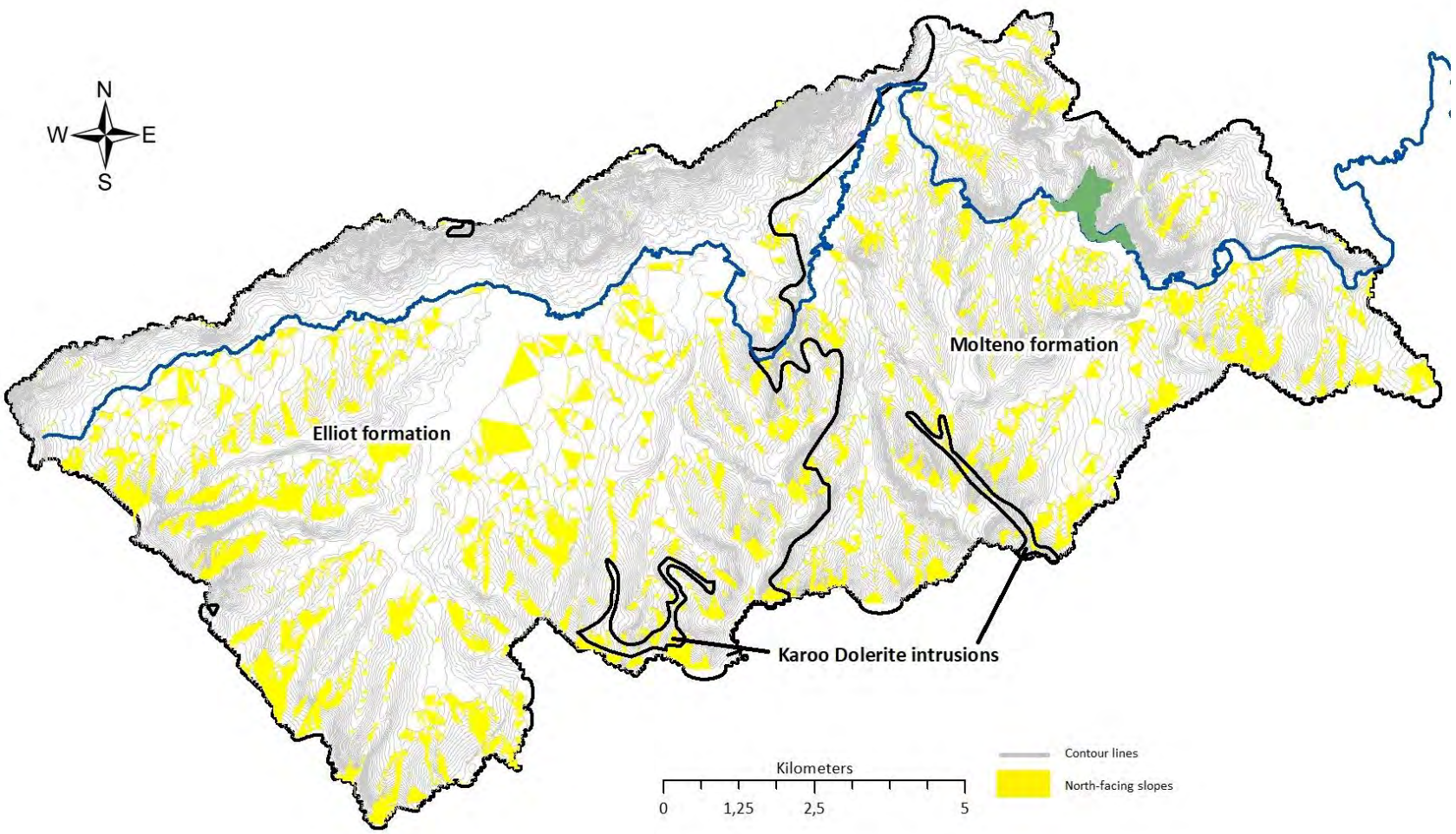

The potential sediment and phosphorus source maps of the Gatberg River catchment are displayed indicating north-facing slopes. Also indicated are the geological provinces.

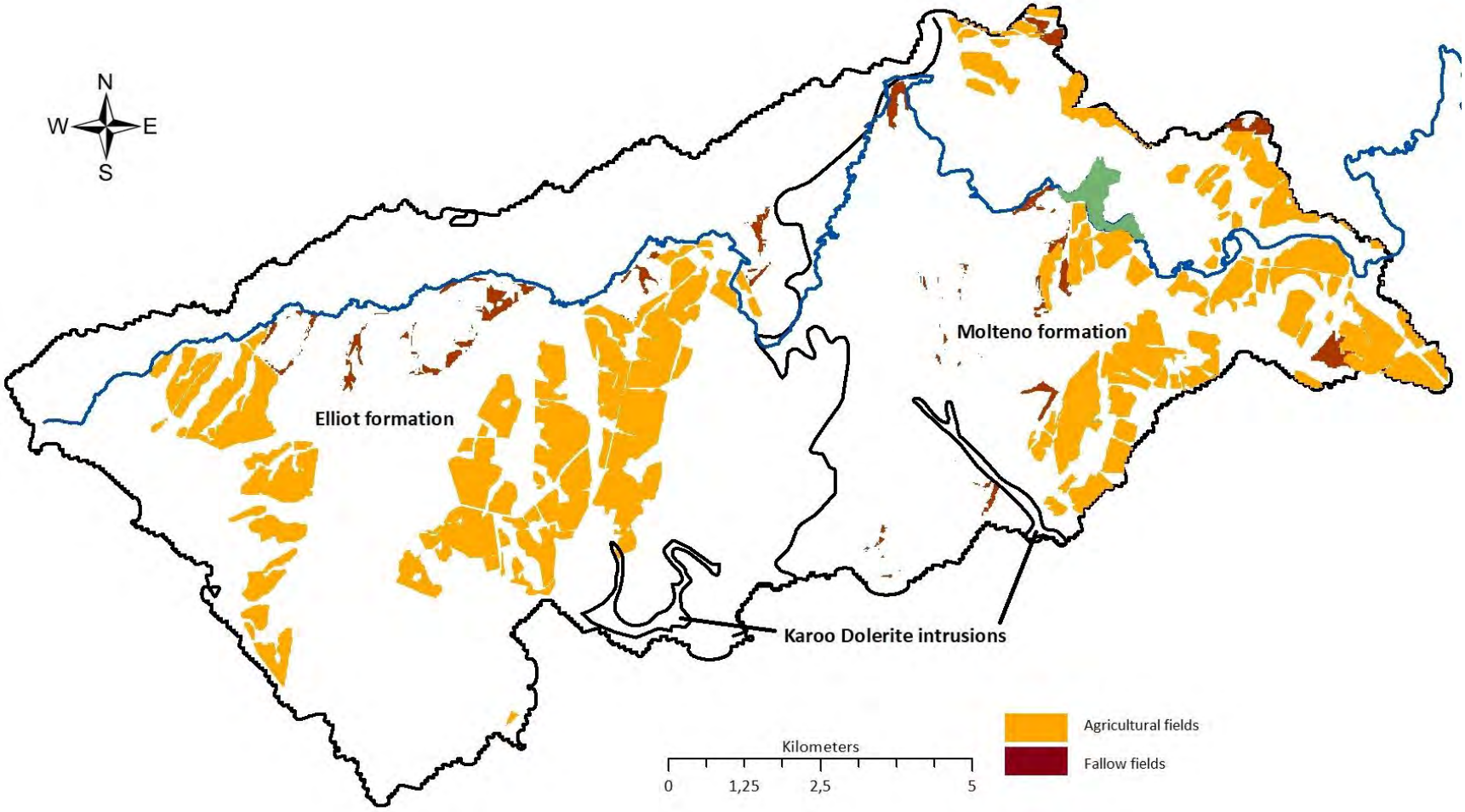

The potential sediment and phosphorus source maps of the Gatberg River catchment are displayed indicating the cultivated fields (currently and previously) and fallow land. Also indicated are the geological provinces.

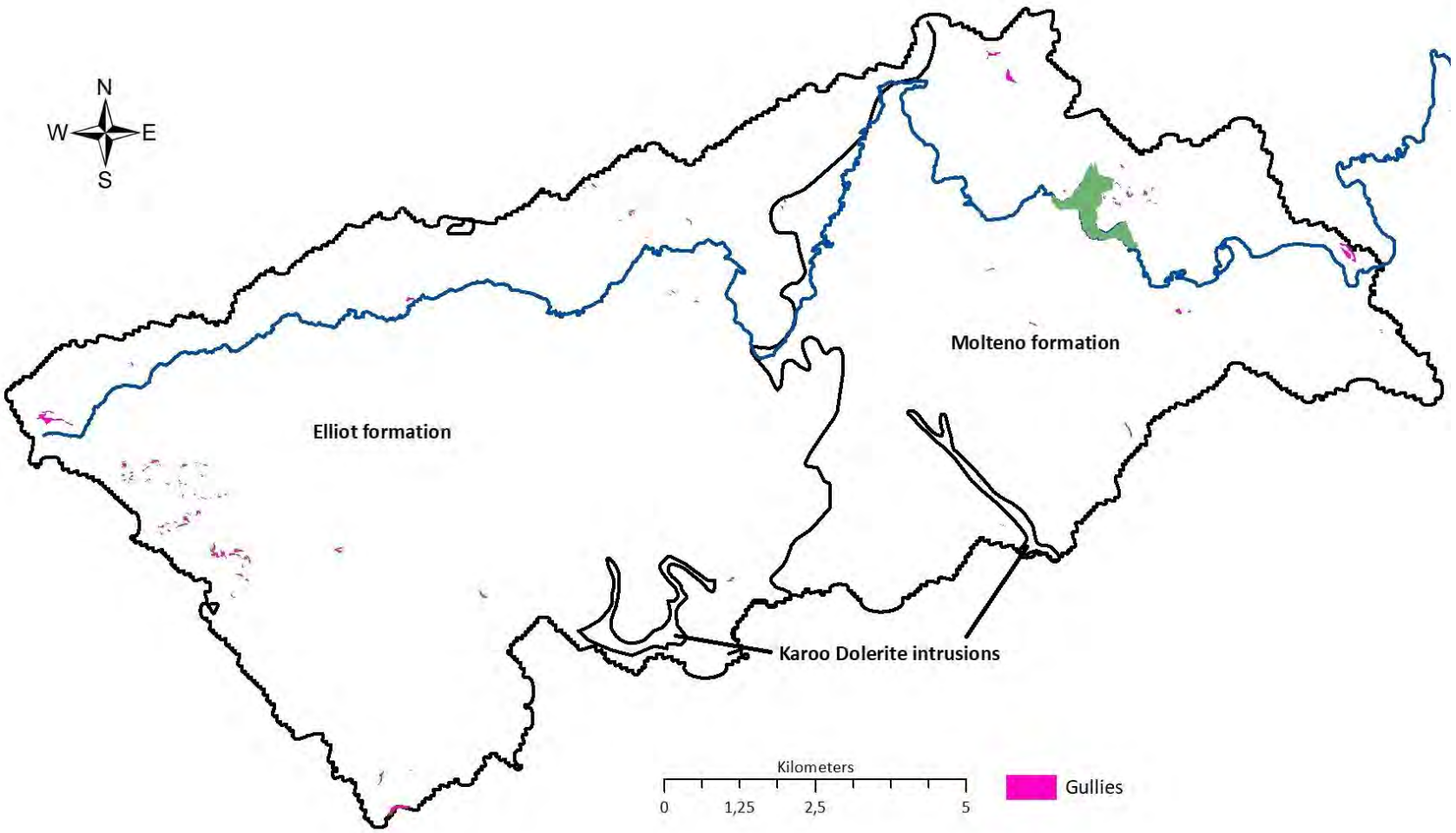

The potential sediment and phosphorus source maps of the Gatberg River catchment are displayed indicating the erosional gullies. Also indicated are the geological provinces.

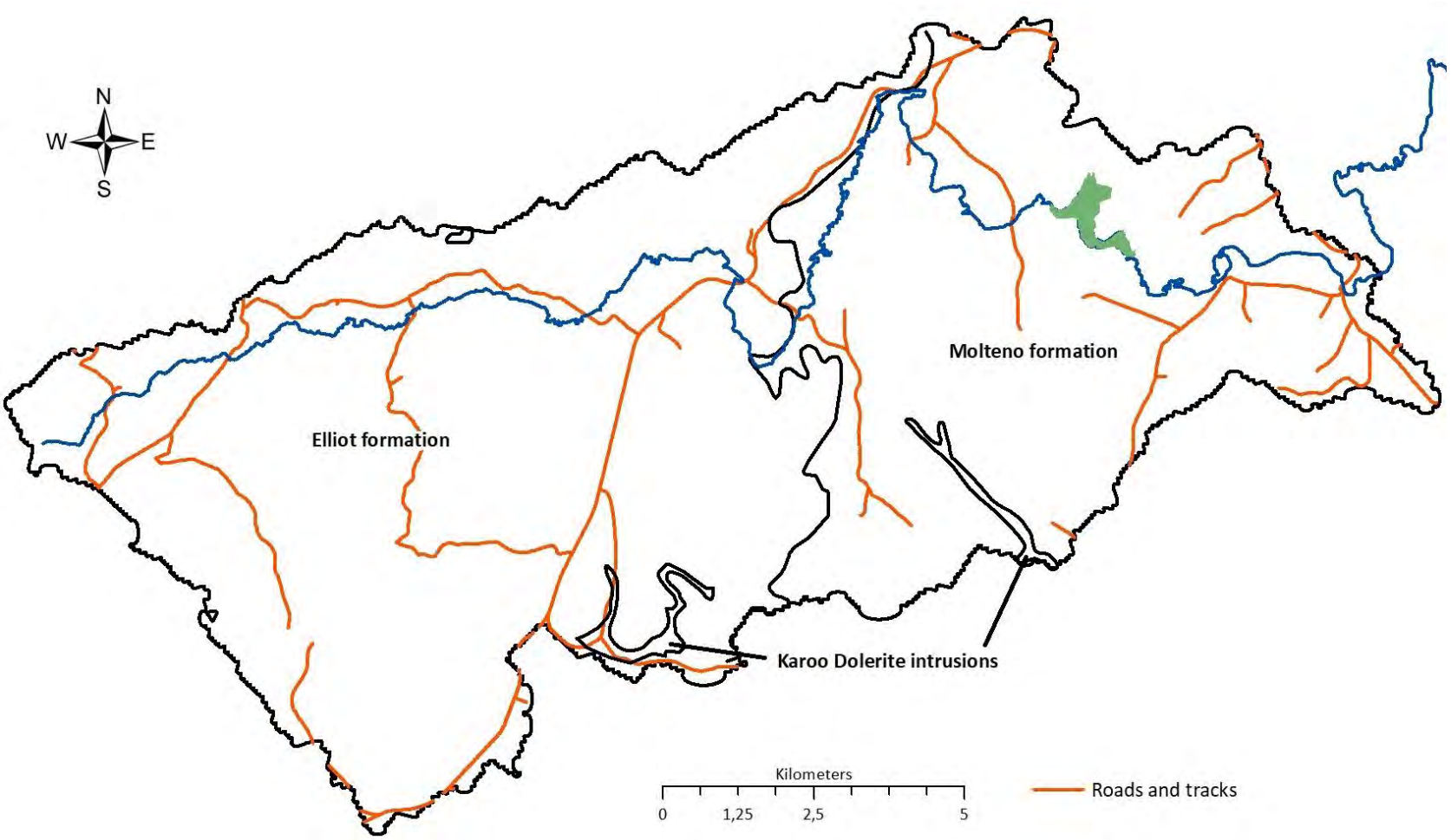

The potential sediment and phosphorus source maps of the Gatberg River catchment are displayed indicating the roads. Also indicated are the geological provinces.

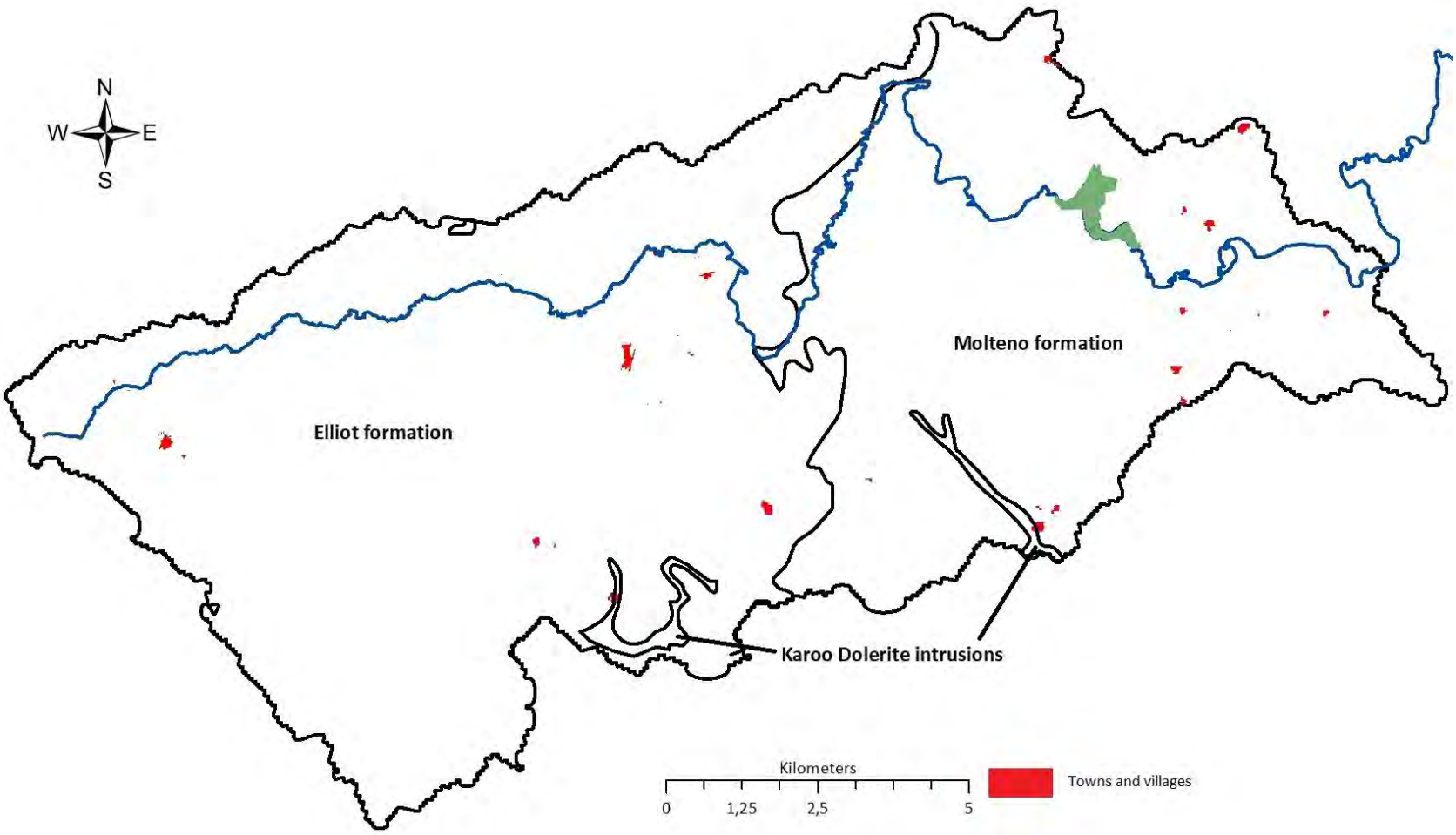

The potential sediment and phosphorus source maps of the Gatberg River catchment are displayed indicating towns and villages. Also indicated are the geological provinces.

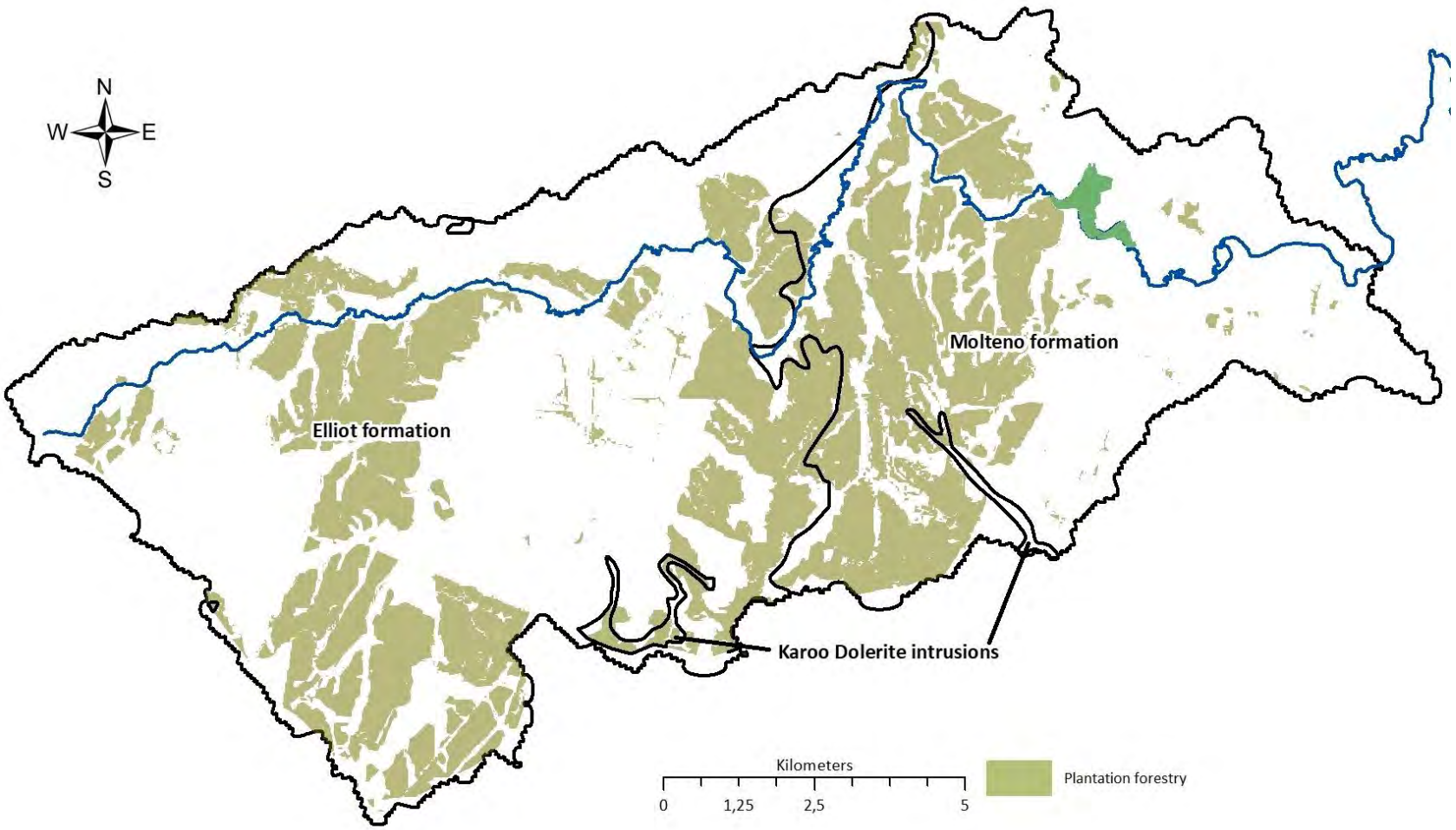

The potential sediment and phosphorus source maps of the Gatberg River catchment are displayed indicating commercial forestry. Also indicated are the geological provinces.

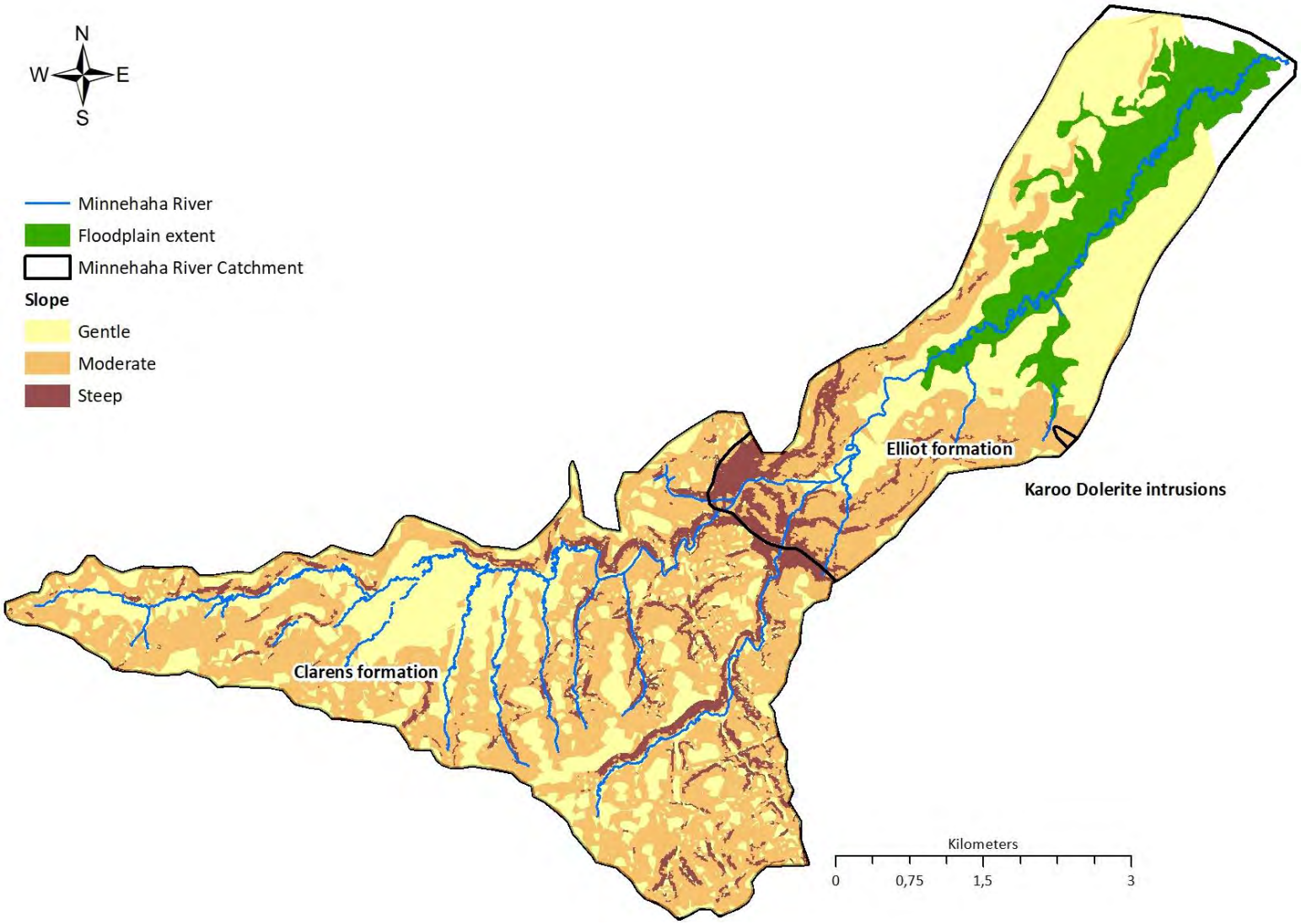

A slope map indicating gentle (< 5), moderate (5-20) and steep (> 20) slopes for the Minnehaha River catchment. Also indicated are the geological provinces.

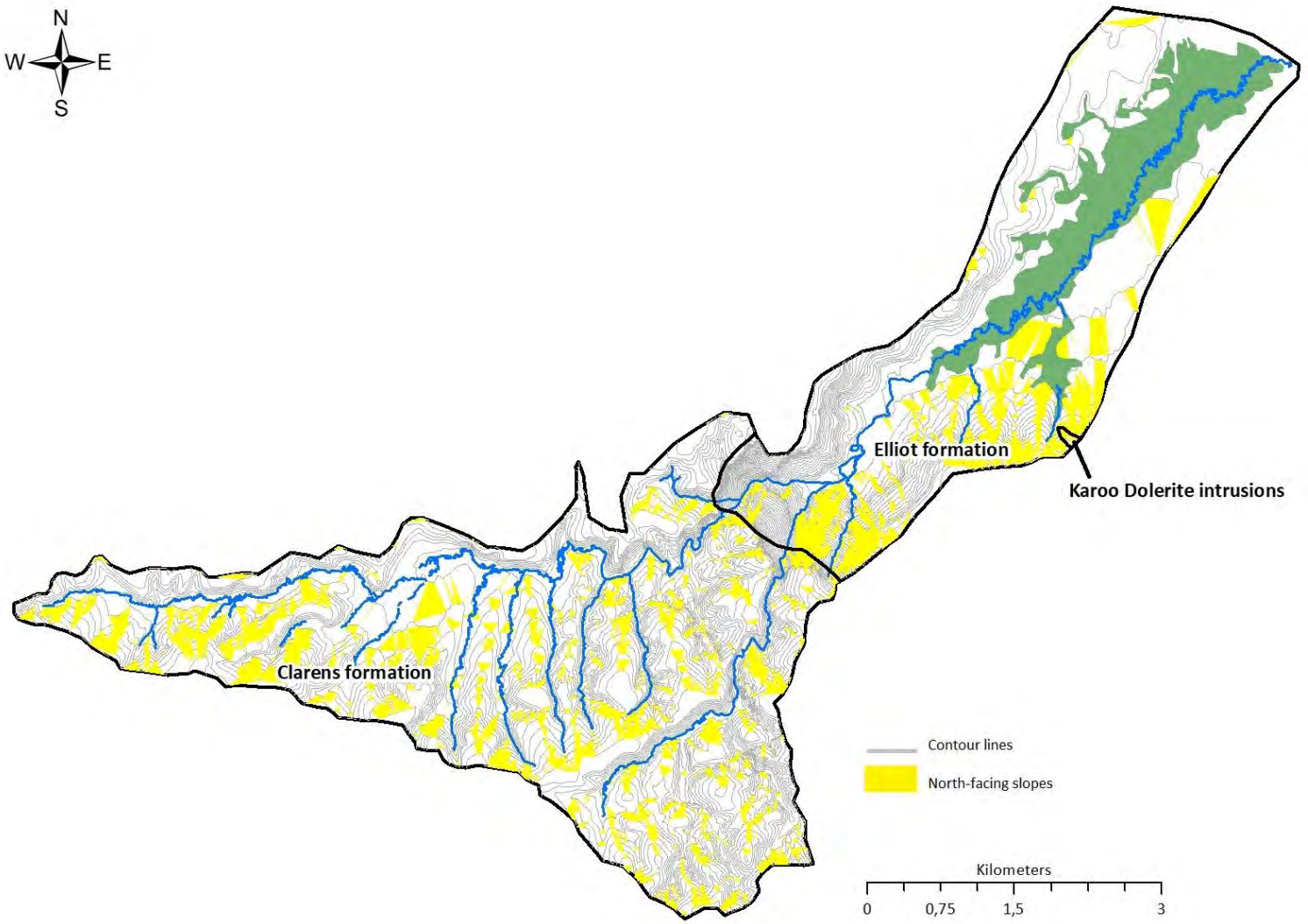

The north-facing slopes in the Minnehaha River catchment. Also indicated are the geological provinces.

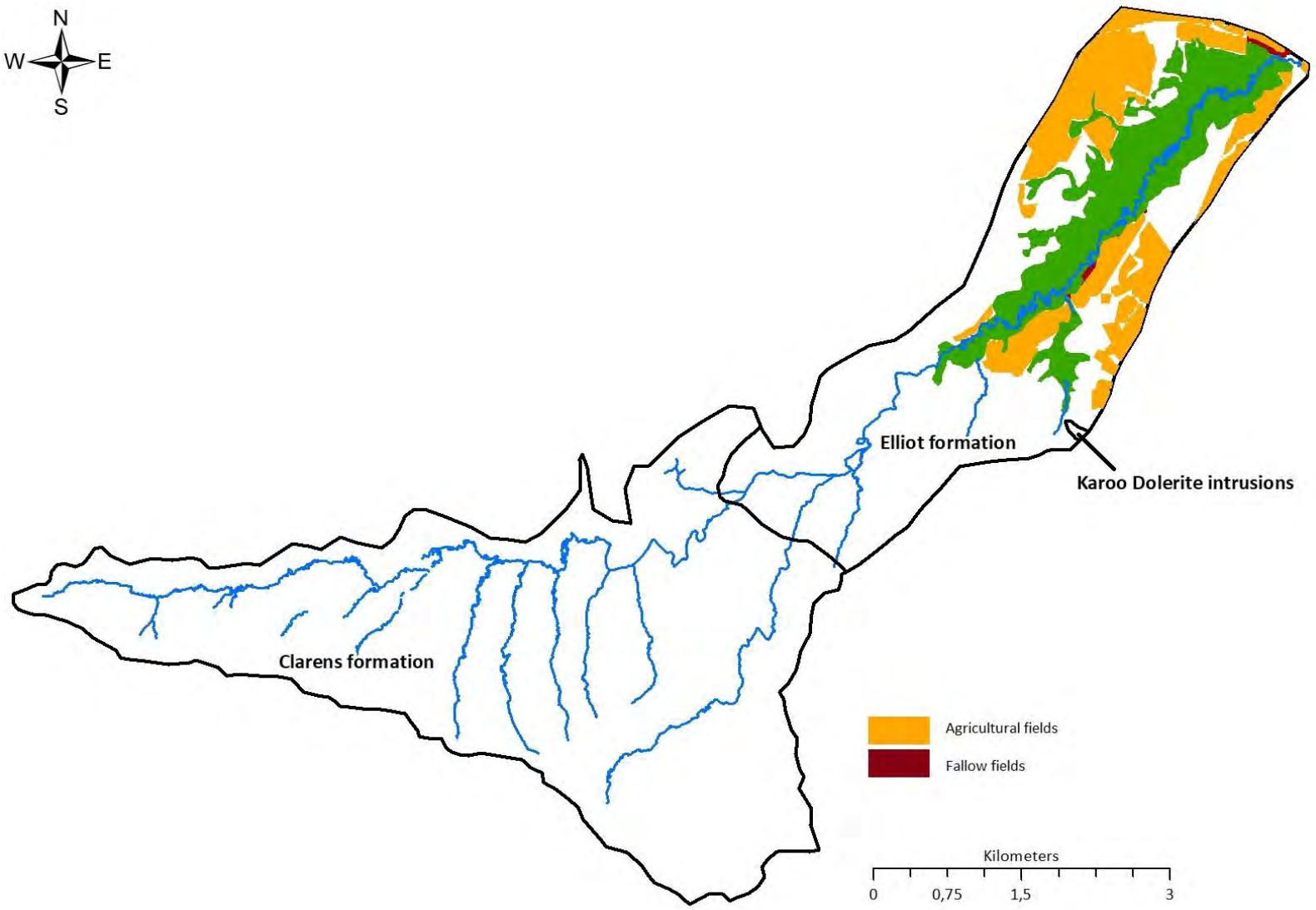

The cultivated fields (currently and previously) and fallow land in the Minnehaha River catchment. Also indicated are the geological provinces.

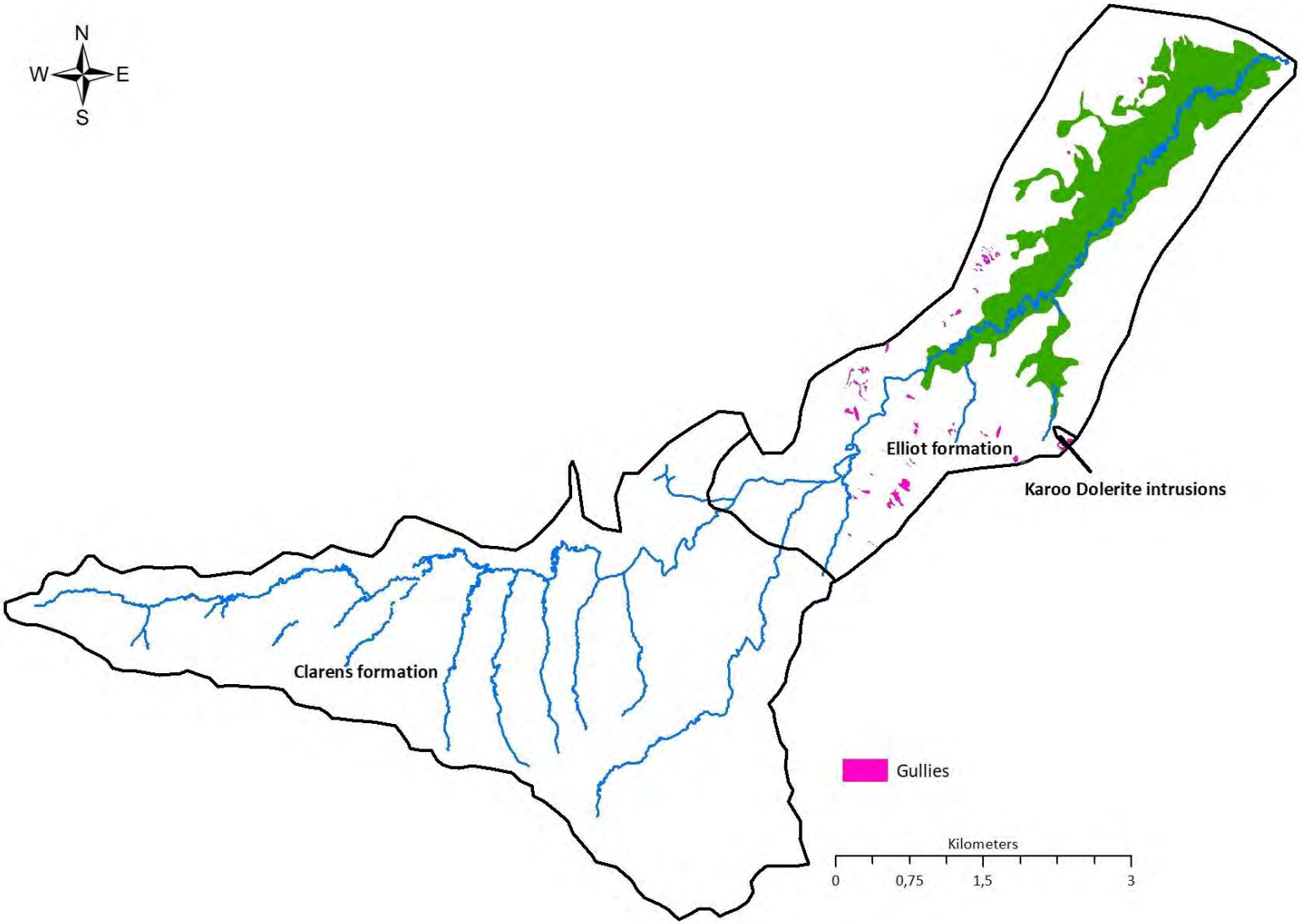

The erosional gullies in the Minnehaha River catchment. Also indicated are the geological provinces.

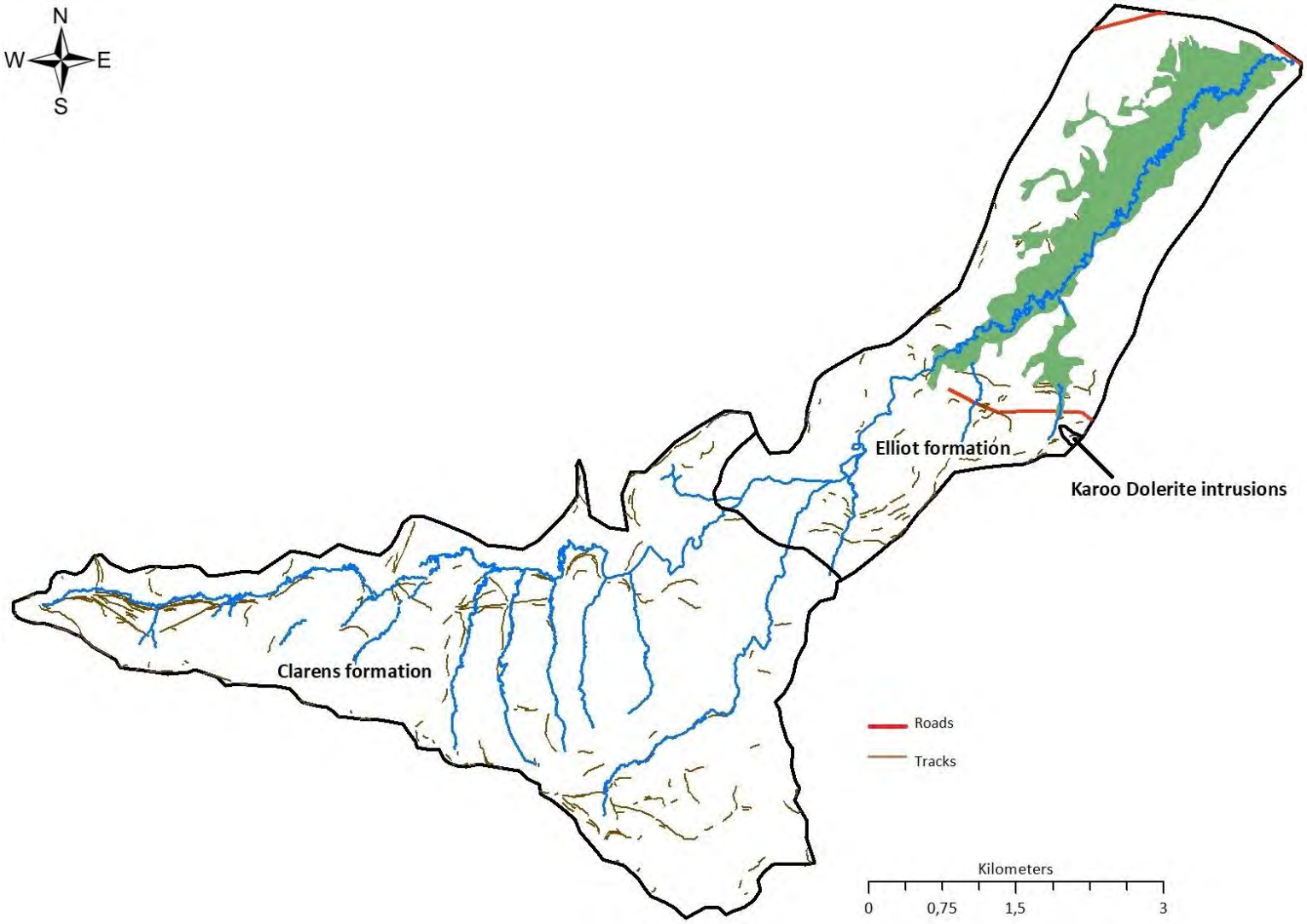

The roads and livestock tracks in the Minnehaha River catchment. Also indicated are the geological provinces.

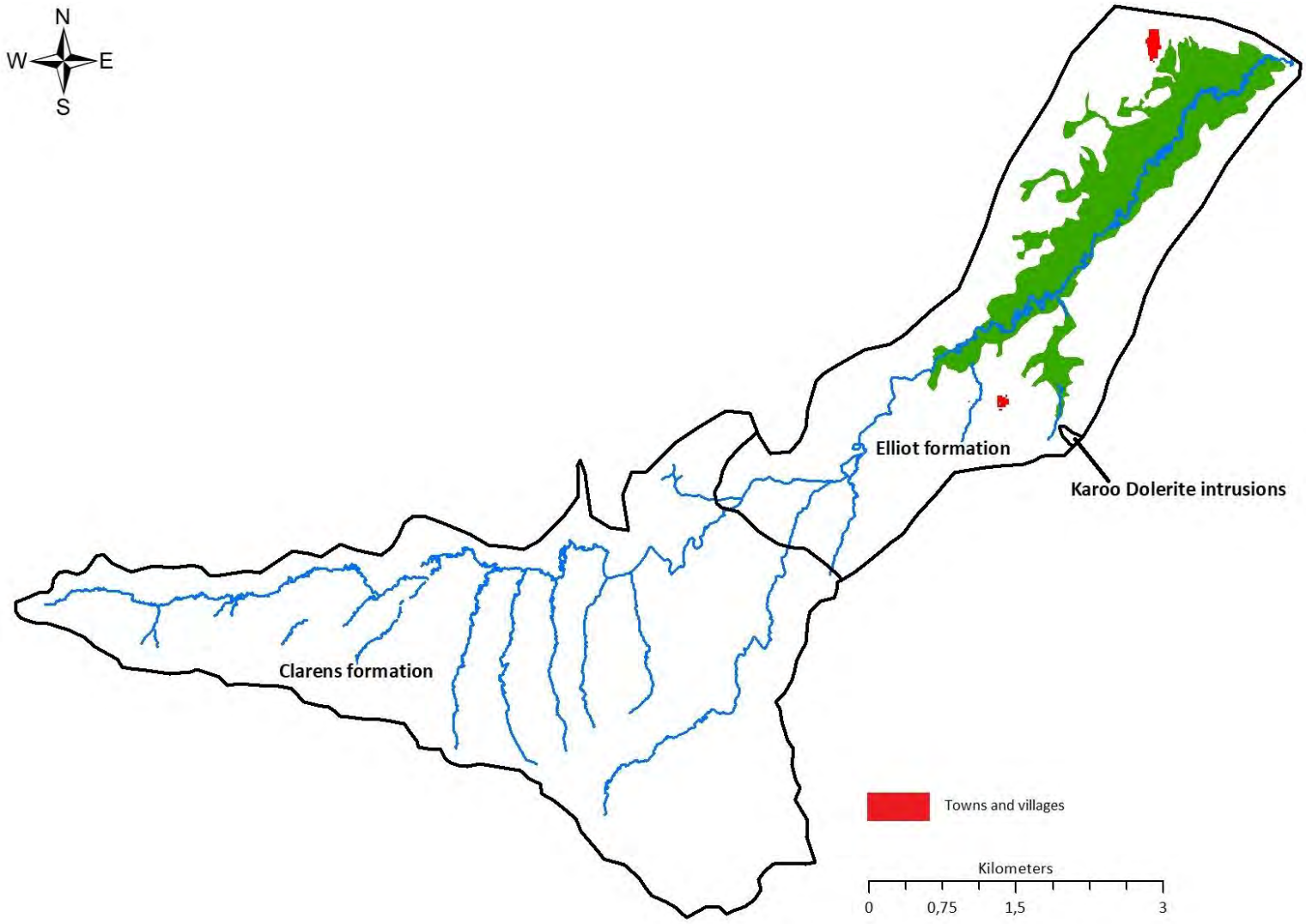

The towns, villages, and residential buildings in the Minnehaha River catchment. Also indicated are the geological provinces.

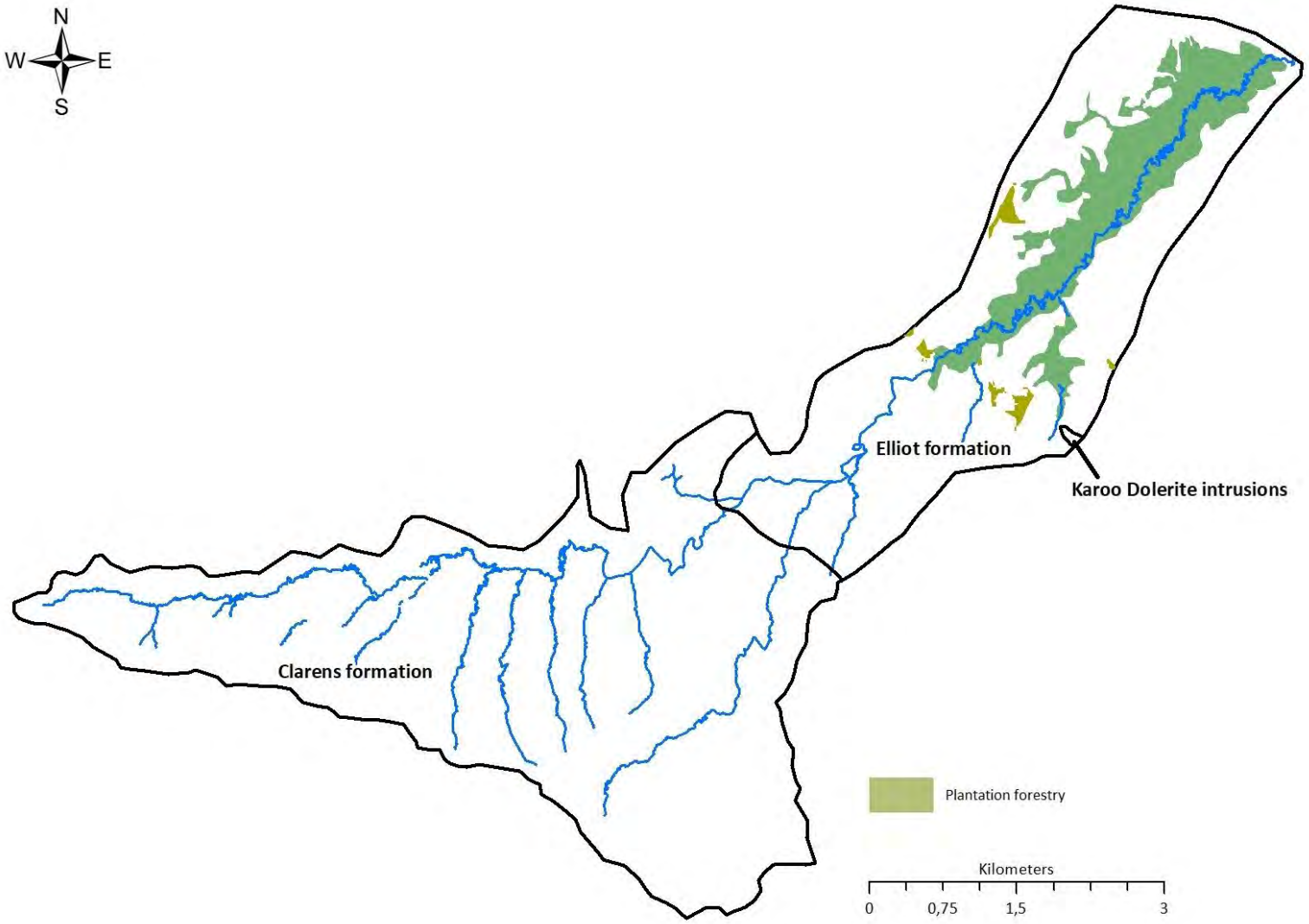

The commercial forestry in the Minnehaha River catchment. Also indicated are the geological provinces.

APPENDIX 2- CHAPTER 5 FLOODPLAIN SEDIMENT STATISTICS

Comprehensive analysis showing the trend analysis (R^2 values), to explore the relationships between sediment properties and the morphological and geometrical properties of the Gatberg floodplain surface samples

	Dependent variable										
Independent variable	**D_{16} (µm)**	**D_{50} (µm)**	**D_{84} (µm)**	**Sand fraction (%)**	**Clay and silt fraction (%)**	**Clay fraction (%)**	**OMC (%)**	**TP (g kg^{-1})**	**Fe (g kg^{-1})**	**Al (g kg^{-1})**	**Mg (g kg^{-1})**
Vegetation density per m^2	0.0	0.0	0.0	0.0	0.0	0.0	0.1	0.2	0.0	0.0	0.1
Vegetation height (m)	0.1	0.2	0.2	0.1	0.1	0.1	0.2	0.4	0.1	0.0	0.0
Vegetation stem diameter (m)	0.1	0.1	0.1	0.1	0.1	0.0	0.1	0.1	0.2	0.0	0.0
Distance from channel (m)	0.2	0.3	0.2	0.1	0.1	0.2	0.2	0.0	0.0	0.1	0.0
Distance downstream (m)	0.1	0.2	0.1	0.1	0.1	0.2	0.0	0.0	0.0	0.1	0.0
Relative elevation (m.a.s.l)	0.3	0.3	0.3	0.2	0.2	0.3	0.1	0.1	0.2	0.1	0.0
Floodplain perpendicular slope (%)	0.2	0.3	0.3	0.2	0.2	0.2	0.3	0.1	0.1	0.1	0.0
Floodplain downstream slope (%)	0.2	0.2	0.1	0.1	0.1	0.2	0.0	0.0	0.0	0.2	0.0
Floodplain width (m)	0.1	0.0	0.0	0.0	0.0	0.1	0.0	0.0	0.0	0.2	0.0
Floodplain width/ channel width ratio	0.1	0.0	0.0	0.0	0.0	0.1	0.0	0.0	0.0	0.2	0.0
Channel slope (%)	0.0	0.0	0.0	0.0	0.0	0.0	0.0	0.1	0.0	0.0	0.0
Sinuosity	0.0	0.0	0.0	0.0	0.0	0.0	0.0	0.0	0.0	0.0	0.0
D_{16} particle size (µm)							0.2	0.1	0.1	0.2	0.0
D_{50} particle size (µm)							0.4	0.3	0.2	0.3	0.0
D_{84} particle size (µm)							0.5	0.3	0.1	0.4	0.1
Organic matter content (%)								0.5	0.5	0.3	0.0
Sand fraction (%)							0.4	0.3	0.1	0.4	0.1
Clay and silt fraction (%)							0.4	0.3	0.1	0.4	0.1
Clay fraction (%)							0.3	0.1	0.1	0.2	0.0
Total phosphorus concentration (g kg^{-1})									0.3	0.3	0.0

Comprehensive analysis showing the trend analysis (R^2 values), to explore the relationships between sediment properties and the morphological and geometrical properties of the Minnehaha floodplain surface samples

	Dependent variable												
Independent variable	**D_{16} (µm)**	**D_{50} (µm)**	**D_{84} (µm)**	**Sand fraction (%)**	**Clay and silt fraction (%)**	**Clay fraction (%)**	**OMC (%)**	**TP (g kg^{-1})**	**Bioavailable TP (g kg^{-1})**	**Ca (g kg^{-1})**	**Fe (g kg^{-1})**	**Al (g kg^{-1})**	**Mg (g kg^{-1})**
Vegetation density per m^2	0.1	0.1	0.1	0.1	0.1	0.1	0.0	0.0	0.0	0.0	0.0	0.2	0.0
Vegetation height (m)	0.0	0.0	0.0	0.0	0.0	0.1	0.0	0.0	0.0	0.0	0.0	0.0	0.1
Vegetation stem diameter (m)	0.2	0.2	0.2	0.3	0.3	0.2	0.0	0.1	0.1	0.0	0.1	0.2	0.0
Distance from channel (m)	0.3	0.2	0.1	0.0	0.0	0.3	0.1	0.3	0.0	0.3	0.3	0.2	0.2
Distance downstream (m)	0.0	0.0	0.0	0.0	0.0	0.0	0.0	0.0	0.1	0.0	0.0	0.1	0.0
Relative elevation (m.a.s.l)	0.1	0.1	0.0	0.0	0.0	0.1	0.1	0.0	0.1	0.0	0.0	0.2	0.0
Floodplain perpendicular slope (%)	0.0	0.0	0.0	0.0	0.0	0.0	0.0	0.0	0.0	0.0	0.0	0.0	0.0
Floodplain downstream slope (%)	0.0	0.0	0.0	0.0	0.0	0.0	0.0	0.0	0.0	0.0	0.0	0.0	0.0
Floodplain width (m)	0.0	0.0	0.0	0.0	0.0	0.0	0.0	0.0	0.0	0.0	0.0	0.0	0.0
Floodplain width/ channel width ratio	0.0	0.0	0.0	0.0	0.0	0.0	0.0	0.0	0.1	0.0	0.0	0.1	0.0
Channel slope (%)	0.1	0.1	0.1	0.1	0.1	0.1	0.0	0.0	0.0	0.0	0.0	0.1	0.0
Sinuosity	0.0	0.0	0.0	0.0	0.0	0.1	0.0	0.0	0.1	0.0	0.0	0.1	0.0
D_{16} particle size (µm)							0.0	0.2	0.1	0.2	0.2	0.1	0.1
D_{50} particle size (µm)							0.0	0.1	0.0	0.1	0.2	0.1	0.0
D_{84} particle size (µm)							0.0	0.1	0.0	0.0	0.1	0.0	0.0
Organic matter content (%)								0.5	0.1	0.4	0.2	0.2	0.4
Sand fraction (%)							0.0	0.1	0.0	0.0	0.1	0.0	0.0
Clay and silt fraction (%)							0.0	0.1	0.0	0.0	0.1	0.0	0.0
Clay fraction (%)							0.0	0.2	0.1	0.2	0.3	0.1	0.1
Total phosphorus concentration (g kg^{-1})									0.3	0.5	0.6	0.4	0.4

APPENDIX 3- CHAPTER 7 OXBOW AND MEANDER BEND STATISTICS

Oxbows identified on the Gatberg River floodplain

Oxbow number	Distance from channel (m)	Area (m²)	Length (m)	Average bankfull width (m)	Diversion angle (°)	Radius of curvature (m)
1	46	210	25	5	80	8
2	47	1864	189	9	60	24
3	90	1564	176	10	70	22
4	33	191	34	8	82	8
5	37	3291	46	6	85	32
6	59	356	60	9	90	11
7	90	556	89	13	75	13
8	145	950	165	12	94	17
9	28	166	49	6	90	7
10	70	233	119	7	83	9
11	45	435	25	5	90	12
12	57	1281	70	6	80	20
13	53	1353	91	7	80	21
14	46	594	65	9	85	14
15	21	303	34	8	92	10
16	54	562	65	9	70	13
17	65	1147	97	9	95	19
18	39	459	50	10	90	12
19	84	688	80	5	75	15
20	39	1356	165	9	85	21
21	32	242	56	9	94	9
22	50	483	101	9	100	12
23	18	166	36	7	87	7
24	26	998	30	5	89	18
25	58	633	43	9	90	14
26	13	378	44	8	100	11
27	38	605	45	8	82	14
28	71	210	52	7	87	8
29	103	777	76	9	98	16
30	23	236	63	9	80	9
31	64	1989	33	9	79	25
32	42	544	130	10	80	13
33	87	528	27	6	79	13
34	61	2600	104	8	78	29
35	56	305	144	10	85	10
36	23	202	34	7	89	8
37	25	896	43	5	80	17
38	72	429	64	6	86	12
39	29	922	37	10	88	17

40	20	128	124	7	105	6
41	37	1889	20	6	78	25
42	73	358	131	12	92	11

Oxbows identified on the Minnehaha River floodplain

Oxbow number	Distance from channel (m)	Area (m^2)	Length (m)	Average bankfull width (m)	Diversion angle (^{o})	Radius of curvature (m)
1	38	10279	430	8	90	57
2	53	4961	175	7	94	40
3	50	665	131	7	95	15
4	45	3208	118	6	100	32
5	39	4536	303	12	102	38
6	36	4106	322	10	94	36
7	19	936	52	9	90	17
8	19	1075	443	9	105	19
9	114	484	50	6	120	12
10	57	2078	65	7	80	26
11	31	926	78	8	82	17
12	17	991	74	11	85	18
13	24	1563	116	8	75	22
14	31	2002	72	11	70	25
15	43	2451	197	13	72	28
16	27	2248	83	7	80	27
17	20	2724	189	13	83	29
18	7	1192	123	8	65	19
19	10	236	44	8	85	9
20	32	575	55	6	115	14
21	17	1052	128	9	70	18
22	11	1028	86	8	90	18
23	7	1381	113	9	90	21
24	13	3393	320	5	90	33
25	12	1407	143	6	110	21
26	41	1574	79	8	105	22
27	36	921	91	8	75	17
28	15	790	109	10	90	16
29	22	3526	109	12	105	34
30	33	680	174	11	80	15
31	56	384	47	13	105	11
32	6	463	84	6	98	12
33	11	327	59	6	95	10
34	5	4929	203	9	45	40

35	14	5788	240	6	80	43
36	9	2173	125	6	90	26
37	30	1698	76	7	80	23
38	5	2722	100	6	80	29
39	56	837	138	7	90	16
40	26	2396	161	6	90	28
41	21	2219	110	6	87	27
42	9	168	40	6	80	7
43	9	322	47	5	92	10
44	17	3608	152	5	100	34
45	22	1250	84	4	95	20
46	7	592	62	5	90	14
47	36	1137	98	9	90	19
48	9	692	78	6	80	15
49	30	780	82	6	85	16
50	13	761	74	6	75	16
51	66	1718	119	6	90	23
52	14	396	59	8	100	11
53	8	2597	119	7	105	29
54	39	1667	204	5	62	23
55	108	259	48	5	95	9
56	27	2009	192	5	82	25
57	92	701	69	6	105	15
58	20	180	38	4	90	8
59	23	1440	93	7	120	21
60	14	895	140	7	90	17
61	199	8335	320	8	80	52
62	33	464	140	7	70	12
63	8	254	39	5	65	9
64	28	968	97	5	70	18
65	27	897	233	6	80	17
66	40	572	40	4	110	13
67	30	1282	87	5	80	20
68	37	1143	101	7	100	19
69	8	126	24	4	50	6
70	13	772	149	6	80	16
71	20	1007	149	6	102	18
72	8	107	36	6	85	6
73	9	386	48	6	78	11

Measurements of the meander bends found in the Gatberg River system

Meander bend number	Area (m^2)	Wavelength (m)	Bend length (m)	Meander bend neck width (m)	chute ratio	Amplitude (m)	radius of curvature (m)	Mean bankfull width (m)	Tightness of bend	Type of meander bend (Frascati and Lanzoni 2009)	Models of meander bend change (Hooke 1977)
1	493	148	54	28	2	29	13	6	2.1	Upstream-skewed	Extension and rotation
2	361	129	55	43	1	27	11	7	1.5	Downstream-skewed	Extension, expansion, and rotation
3	122	80	37	24	2	31	6	5	1.2	Upstream-skewed	Extension and rotation
4	328	78	44	34	1	27	10	5	2.0	Upstream-skewed	Extension and rotation
5	292	67	30	26	1	24	10	7	1.4	Symmetrical	Extension
6	269	66	26	23	1	14	9	7	1.3	Symmetrical	
7	202	193	93	40	2	61	8	7	1.1	Compound	Extension and rotation
8	104	54	23	20	1	14	6	7	0.8	Symmetrical	
9	106	48	17	16	1	13	6	7	0.8	Symmetrical	
10	207	71	37	25	1	25	8	8	1.0	Upstream-skewed	Extension and rotation
11	391	82	41	38	1	19	11	6	1.9	Symmetrical	
12	231	78	36	19	2	37	9	6	1.4	Upstream-skewed	Extension and rotation
13	236	127	74	21	4	59	9	7	1.2	Upstream-skewed	Extension and rotation
14	62	141	19	18	1	10	4	7	0.6	Symmetrical	
15	153	179	72	34	2	37	7	7	1.0	Upstream-skewed	Extension and rotation
16	705	191	82	39	2	73	15	7	2.1	Compound	Extension, expansion, and rotation
17	233	113	34	28	1	15	9	7	1.2	Symmetrical	
18	398	97	42	23	2	25	11	6	1.9	Downstream-skewed	Extension and rotation
19	163	173	99	33	3	71	7	6	1.2	Compound	Extension, expansion, and rotation
20	410	175	58	39	1	29	11	6	1.9	Upstream-skewed	Extension and rotation
21	1134	121	55	44	1	29	19	7	2.7	Symmetrical	Expansion
22	283	89	23	19	1	20	9	6	1.6	Downstream-skewed	Extension and rotation
23	359	68	37	20	2	28	11	7	1.5	Upstream-skewed	Extension and rotation

24	339	98	32	29	1	20	10	7	1.5	Symmetrical		
25	249	148	45	27	2	21	9	6	1.5	Symmetrical		Extension
26	569	217	82	28	3	82	13	7	1.9	Compound		Extension and rotation
27	483	187	64	33	2	31	12	8	1.5	Compound		Extension and rotation
28	403	74	32	21	2	24	11	8	1.4	Symmetrical		
29	501	47	23	20	1	13	13	5	2.5	Symmetrical		
30	182	58	22	17	1	14	8	7	1.1	Symmetrical		Extension
31	232	73	22	18	1	11	9	7	1.2	Symmetrical		
32	927	142	88	41	2	47	17	6	2.9	Compound		Extension and rotation
33	196	157	26	23	1	12	8	6	1.3	Symmetrical		
34	173	153	69	34	2	36	7	6	1.2	Downstream-skewed		Extension and rotation
35	436	136	58	38	2	28	12	5	2.4	Upstream-skewed		Rotation
36	496	108	48	38	1	18	13	7	1.8	Upstream-skewed		Rotation
37	300	98	43	32	1	23	10	5	2.0	Upstream-skewed		Rotation
38	246	90	50	31	2	24	9	7	1.3	Downstream-skewed		Extension and rotation
39	612	100	42	28	2	33	14	6	2.3	Symmetrical		
40	595	139	70	37	2	50	14	7	2.0	Compound		Extension and rotation
41	1157	113	68	48	1	30	19	6	3.2	Compound		Rotation
42	206	76	28	24	1	15	8	7	1.2	Upstream-skewed		Rotation
43	464	76	35	25	1	17	12	7	1.7	Symmetrical	Multiple loops	
44	491	70	36	31	1	17	12	6	2.1	Downstream-skewed		Rotation
45	347	83	33	26	1	22	11	6	1.8	Upstream-skewed		Rotation
46	515	117	54	33	2	41	13	7	1.8	Downstream-skewed		Extension and rotation
47	587	121	70	39	2	44	14	6	2.3	Compound		Extension and rotation
48	602	147	67	47	1	33	14	6	2.3	Upstream-skewed		Extension and rotation
49	934	177	89	45	2	43	17	7	2.5	Downstream-skewed		Extension and rotation
50	238	111	30	25	1	14	9	7	1.2	Downstream-skewed		Extension and rotation
51	401	73	36	27	1	22	11	6	1.9	Symmetrical		

52	634	83	48	31	2	33	14	6	2.4	Symmetrical		Extension and expansion
53	320	71	34	21	2	24	10	7	1.4	Symmetrical		
54	445	89	41	27	2	29	12	8	1.5	Symmetrical		
55	698	131	76	42	2	34	15	7	2.1	Upstream-skewed	Compound	Extension and expansion
56	547	145	56	40	1	25	13	4	3.3	Symmetrical		
57	684	171	126	35	4	61	15	7	2.1	Compound		Extension and expansion
58	261	132	30	27	1	13	9	6	1.5	Downstream-skewed		Rotation
59	257	46	16	16	1	10	9	6	1.5	Symmetrical		
60	336	72	26	22	1	19	10	7	1.5	Downstream-skewed		Extension and expansion
61	301	191	102	31	3	57	10	5	2.0	Compound		Extension
62	337	206	50	44	1	14	10	8	1.3	Symmetrical		Extension

Measurements of the meander bends found in the Minnehaha River system

Meander bend number	Wavelength (m)	Bend length (m)	Meander bend neck width (m)	chute ratio	Amplitude (m)	Angle of curvature (^{o})	radius of curvature (m)	Mean bankfull width (m)	Tightness of bend	Type of meander bend (based on Frascati and Lanzoni 2009	Models of meander bend change (Hooke 1977)
1	417	107	84	1	98	16	53	17	3	Downstream-skewed	Extension
2	450	149	129	1	39	15	45	14	3	Symmetrical	Extension
3	435	60	40	2	27	10	22	14	2	Downstream-skewed	Extension and rotation
4	326	34	33	1	10	10	12	6	2	Symmetrical	
5	149	31	31	1	10	8	11	5	2	Symmetrical	Expansion
6	104	45	30	2	28	30	15	5	3	Symmetrical	
7	125	67	33	2	41	20	12	6	2	Compound downstream-skewed	Extension and rotation
8	56	31	30	1	18	30	15	5	3	Symmetrical	
9	87	43	24	2	21	40	12	6	2	Symmetrical	Extension
10	133	44	22	2	22	10	9	4	2	Symmetrical	
11	130	53	42	1	15	28	16	4	4	Symmetrical	Extension
12	106	45	24	2	41	20	12	5	2	Compound downstream-skewed	Extension and rotation
13	88	36	18	2	19	21	8	4	2	Upstream-skewed	Extension and rotation
14	75	15	13	1	8	10	8	3	3	Symmetrical	Extension
15	97	33	31	1	15	23	12	4	3	Compound	Extension
16	160	27	16	2	42	25	6	5	1	Downstream-skewed	Extension and rotation
17	193	153	79	2	71	50	52	4	13	Compound	Extension and expansion
18	134	39	23	2	18	6	8	5	2	Symmetrical	
19	209	40	25	2	29	20	15	5	3	Downstream-skewed	Extension and rotation
20	193	43	21	2	18	15	11	3	4	Downstream-skewed	Extension and rotation
21	46	18	16	1	7	15	6	3	2	Symmetrical	

Multiple loops

Multiple loops

22	27	12	12	1	6	12	6	3	2	Symmetrical		
23	27	11	10	1	5	8	4	2	2	Symmetrical		
24	50	20	11	2	11	16	6	3	2	Symmetrical		
25	57	32	21	2	23	21	10	3	3	Downstream-skewed		Extension and rotation
26	67	14	11	1	9	15	7	2	3	Downstream-skewed	Multiple loops	Extension and rotation
27	81	29	22	1	18	25	7	3	2	Downstream-skewed		Extension and rotation
28	68	21	14	2	14	20	9	4	2	Downstream-skewed		Extension and rotation
29	50	19	16	1	17	12	9	4	2	Downstream-skewed		Extension and rotation
30	49	24	21	1	21	16	9	5	2	Upstream-skewed		Extension and rotation
31	50	25	14	2	20	15	5	5	1	Symmetrical		Extension
32	66	23	22	1	17	18	7	3	2	Downstream-skewed		Extension and rotation
33	88	23	24	1	18	15	10	4	2	Symmetrical		Extension
34	96	28	27	1	8	20	11	2	6	Symmetrical		
35	80	33	17	2	22	25	8	4	2	Symmetrical		Extension
36	107	25	19	1	20	20	9	2	4	Symmetrical	Multiple loops	
37	125	46	26	2	23	22	10	3	3	Symmetrical		Extension
38	70	20	15	1	17	20	8	2	4	Symmetrical		Extension
39	63	20	15	1	9	15	8	3	3	Symmetrical		
40	78	42	30	1	31	40	11	4	3	Compound	Multiple loops	Extension, expansion, and rotation
41	59	26	22	1	12	20	9	3	3	Symmetrical		
42	83	23	15	2	12	20	9	3	3	Symmetrical		Extension
43	104	82	41	2	62	70	26	5	5	Compound		Extension and rotation
44	56	18	12	2	10	10	6	3	2	Symmetrical	Multiple loops	Extension
45	69	17	17	1	9	15	4	2	2	Symmetrical		Extension
46	86	50	42	1	29	40	15	4	4	Compound		Extension and expansion
47	108	47	12	4	26	40	7	3	2	Compound		Extension and expansion

48	161	49	30	2	30	30	15	4	4	Symmetrical	Multiple loops	Extension
49	145	54	18	3	36	40	11	4	3	Compound		Extension
50	81	30	20	2	16	15	10	4	2	Downstream-skewed		Extension and rotation
51	71	21	18	1	11	15	9	4	2	Symmetrical	Multiple loops	
52	65	23	19	1	9	15	9	5	2	Symmetrical		
53	69	19	15	1	6	15	6	4	2	Symmetrical		
54	77	19	16	1	4	10	5	3	2	Symmetrical		
55	83	26	12	2	15	15	6	5	1	Symmetrical		Extension
56	51	19	16	1	8	20	9	3	3	Symmetrical		
57	60	34	23	1	23	20	9	4	2	Symmetrical		Extension
58	80	14	11	1	7	10	7	4	2	Downstream-skewed		Extension and rotation
59	57	21	15	1	15	15	7	3	2	Downstream-skewed		Extension and rotation
60	105	14	14	1	9	10	6	4	1	Symmetrical		
61	133	25	13	2	11	11	8	4	2	Symmetrical		
62	61	26	17	2	17	30	7	4	2	Symmetrical	Multiple loop	
63	55	29	17	2	22	22	7	3	2	Symmetrical		
64	81	44	19	2	33	26	7	3	2	Symmetrical		
65	97	46	21	2	37	25	9	4	2	Symmetrical		
66	82	36	33	1	7	22	19	4	5	Symmetrical		
67	63	28	13	2	23	26	6	5	1	Symmetrical		Extension
68	96	45	24	2	24	24	9	4	2	Upstream-skewed		Extension and rotation
69	119	54	32	2	41	30	16	4	4	Compound		Extension, rotation, and expansion
70	69	14	8	2	12	16	6	5	1	Downstream-skewed		Extension and rotation
71	67	20	15	1	24	30	7	4	2	Compound		Extension and rotation
72	157	60	19	3	38	30	10	7	1	Compound		Extension and rotation
73	168	49	30	2	31	45	14	9	2	Symmetrical		Extension and expansion

74	144	53	22	2	31	30	12	6	2	Upstream-skewed		Extension and rotation
75	134	48	27	2	32	32	11	6	2	Compound		Extension, rotation, and expansion
76	235	32	10	3	25	28	6	4	2	Downstream-skewed		Extension and rotation
77	222	48	46	1	26	40	13	4	3	Compound		Expansion
78	162	54	26	2	23	30	10	4	3	Compound		Extension, rotation, and expansion
79	169	38	20	2	18	30	9	5	2	Upstream-skewed		Extension and rotation
80	78	29	19	2	29	30	9	4	2	Upstream-skewed		Extension and rotation
81	53	25	15	2	16	25	7	6	1	Upstream-skewed		Extension and rotation
82	77	34	28	1	25	33	11	5	2	Symmetrical		Expansion
83	90	55	21	3	39	50	10	5	2	Compound		Extension, rotation, and expansion
84	96	35	26	1	18	26	10	4	3	Upstream-skewed		Extension and rotation
85	128	73	32	2	49	40	11	6	2	Upstream-skewed		Extension and rotation
86	321	54	33	2	34	10	13	5	3	Compound		Extension, rotation, and expansion
87	275	55	28	2	27	45	14	6	2	Symmetrical		Extension and expansion
88	52	20	13	2	14	28	12	5	2	Symmetrical		Extension
89	49	32	30	1	14	23	9	4	2	Symmetrical		
90	200	26	21	1	13	10	7	4	2	Symmetrical		Extension
91	230	40	14	3	42	18	8	4	2	Symmetrical		Extension
92	83	54	19	3	28	40	10	5	2	Compound	Multiple loops	Extension, rotation, and expansion
93	67	20	11	2	14	22	7	4	2	Symmetrical		
94	80	35	21	2	24	25	8	5	2	Downstream-skewed		Extension and rotation
95	92	42	31	1	16	20	10	4	3	Symmetrical	Compound	
96	97	38	34	1	15	27	10	4	2	Symmetrical		
97	73	23	23	1	8	20	7	3	2	Symmetrical		

98	47	25	17	1	14	14	7	4	2	Symmetrical		
99	48	27	20	1	11	20	9	3	3	Symmetrical		
100	99	40	21	2	29	30	7	4	2	Upstream-skewed		Extension and rotation
101	106	53	30	2	31	27	10	4	2	Downstream-skewed		Extension and rotation
102	67	27	20	1	18	20	10	5	2	Downstream-skewed	Multiple loops	Extension and rotation
103	53	34	12	3	19	30	9	6	1	Compound		Extension and rotation
104	73	16	16	1	6	10	7	2	3	Symmetrical		
105	84	30	24	1	20	20	11	3	4	Symmetrical		
106	73	32	21	2	24	30	11	5	2	Upstream-skewed		Extension and rotation
107	132	45	33	1	35	30	15	5	3	Symmetrical		
108	122	38	28	1	17	23	14	5	3	Downstream-skewed		Extension and rotation
109	104	31	16	2	19	22	9	4	2	Symmetrical		Extension and expansion
110	97	31	27	1	16	17	12	5	2	Symmetrical	Compound	Extension
111	62	30	22	1	18	14	13	5	3	Downstream-skewed		Extension and expansion
112	94	23	18	1	15	12	7	4	2	Symmetrical		Extension
113	85	23	18	1	14	16	9	4	2	Upstream-skewed		Extension and expansion
114	51	31	16	2	27	24	7	4	2	Upstream-skewed		Extension and expansion
115	62	15	12	1	8	12	7	3	2	Symmetrical		
116	59	38	26	1	26	22	11	4	3	Downstream-skewed		Extension and expansion
117	67	43	22	2	25	24	10	5	2	Upstream-skewed		Extension and expansion
118	59	21	18	1	15	20	10	5	2	Symmetrical		
119	64	39	27	1	35	34	13	4	3	Compound		Extension and expansion
120	80	30	24	1	14	16	10	4	2	Symmetrical		
121	57	32	23	1	23	20	8	4	2	Downstream-skewed		Extension and expansion
122	49	25	19	1	15	28	7	5	1	Symmetrical		
123	77	33	20	2	22	26	7	4	2	Downstream-skewed		Extension and expansion
124	170	66	19	3	40	18	8	3	3	Compound		Extension and expansion

125	192	28	25	1	10	12	12	3	4	Symmetrical		
126	100	48	26	2	33	38	11	5	2	Symmetrical		
127	85	19	15	1	13	20	8	4	2	Symmetrical		Extension
128	70	31	23	1	25	35	10	6	2	Symmetrical		Extension
129	122	22	17	1	14	20	10	4	2	Symmetrical		
130	159	61	33	2	47	40	12	4	3	Compound		Extension and expansion
131	100	51	27	2	34	30	10	5	2	Downstream-skewed		Extension and expansion
132	96	35	22	2	29	35	10	4	2	Downstream-skewed		Extension and expansion
133	159	40	27	1	30	40	9	4	2	Compound		Extension, rotation, and expansion
134	221	110	30	4	53	50	16	5	3	Compound		Extension
135	221	64	35	2	31	35	11	4	3	Compound		Extension
136	177	104	31	3	41	50	17	5	3	Symmetrical		Extension
137	135	43	16	3	21	20	7	3	2	Upstream-skewed		Extension and rotation
138	93	44	26	2	26	38	12	5	2	Compound	Multiple loops	Extension
139	69	28	23	1	12	21	9	4	2	Symmetrical		
140	108	41	29	1	16	30	11	4	3	Symmetrical		
141	148	64	27	2	34	33	11	6	2	Downstream-skewed	Compound	Extension and rotation
142	106	59	27	2	29	28	9	4	2	Downstream-skewed		Extension and rotation
143	55	21	17	1	15	20	10	3	3	Symmetrical		
144	54	28	16	2	19	18	8	3	3	Symmetrical		Extension
145	126	35	19	2	22	20	9	4	2	Upstream-skewed		Extension and rotation
146	131	36	23	2	30	22	10	5	2	Upstream-skewed		Extension and rotation
147	66	26	22	1	11	16	9	4	2	Symmetrical		
148	62	25	21	1	12	21	9	4	2	Symmetrical		
149	65	32	23	1	19	35	10	3	3	Symmetrical		
150	80	54	15	4	25	40	8	3	3	Symmetrical		Extension

151	95	31	19	2	20	32	8	3	3	Upstream-skewed		Extension and rotation
152	91	57	20	3	26	45	9	4	2	Compound		Extension and rotation
153	74	26	18	1	8	23	9	3	3	Symmetrical	Multiple loops	
154	76	41	29	1	16	30	8	4	2	Compound		Extension and rotation
155	125	36	19	2	17	20	8	3	3	Upstream-skewed		Extension and rotation
156	127	40	24	2	20	20	8	3	3	Upstream-skewed		Extension and rotation
157	92	34	28	1	16	14	9	3	3	Symmetrical		Extension
158	82	32	20	2	17	20	6	3	2	Downstream-skewed		Extension and rotation
159	78	37	24	2	22	24	8	3	3	Compound		Extension and rotation
160	96	40	18	2	23	18	9	3	3	Upstream-skewed		Extension and rotation
161	100	42	32	1	21	26	11	3	4	Symmetrical		Extension
162	110	62	40	2	38	45	18	3	6	Downstream-skewed		Extension and rotation
163	136	80	30	3	31	45	14	4	3	Compound		Extension and rotation
164	122	60	30	2	35	34	15	4	4	Compound		Extension and rotation
165	95	38	13	3	25	35	7	4	2	Upstream-skewed		Extension and rotation
166	84	51	39	1	26	40	20	4	5	Symmetrical		Extension
167	60	28	13	2	24	23	6	3	2	Upstream-skewed		Extension and rotation
168	109	42	27	2	25	25	10	4	3	Compound upstream skewed		Extension and rotation
169	134	38	14	3	21	30	8	3	3	Upstream-skewed		Extension and rotation
170	124	64	27	2	32	55	13	3	4	Upstream-skewed		Extension and rotation
171	100	26	16	2	18	20	9	4	2	Symmetrical		Extension and expansion
172	74	32	13	2	26	30	7	3	2	Symmetrical		Extension
173	98	39	24	2	22	30	8	4	2	Compound		Extension and expansion
174	99	64	16	4	32	45	8	3	3	Compound		Extension
175	96	51	22	2	25	40	11	5	2	Compound		Extension
176	86	31	12	3	15	28	7	3	2	Symmetrical		
177	96	56	26	2	20	45	10	4	3	Compound		Extension and expansion

178	90	35	24	1	17	15	8	4	2	Downstream-skewed	Multiple loops	Extension and expansion
179	72	29	17	2	16	30	8	4	2	Symmetrical		Extension
180	65	33	22	2	15	40	9	3	3	Compound		Extension and rotation
181	53	17	13	1	6	15	8	3	3	Symmetrical		
182	62	38	21	2	17	20	6	4	2	Symmetrical		Extension
183	150	48	24	2	21	24	9	3	3	Upstream-skewed		Extension and rotation
184	162	69	7	10	29	20	10	3	3	Compound		Extension and rotation
185	96	38	20	2	20	21	9	3	3	Compound		Extension and rotation
186	81	33	22	2	16	25	8	4	2	Downstream-skewed		Extension and rotation
187	99	45	29	2	22	30	13	4	3	Compound		Extension and rotation
188	119	82	35	2	32	23	14	3	5	Compound		Extension and rotation
189	89	30	25	1	19	20	12	3	4	Compound		Extension and rotation
190	60	35	15	2	23	17	8	2	4	Downstream-skewed		Extension and rotation
191	81	30	16	2	15	14	6	3	2	Symmetrical		Extension
192	77	29	26	1	8	24	12	3	4	Symmetrical		Extension